PO Box 2345, Beijing 100023, China
www.wjgnet.com
wjg@wjgnet.com

ELSEVIER

World J Gastroenterol 2005;11(38):5915-5919
World Journal of Gastroenterology ISSN 1007-9327

inhibitory effects of extracellular adenosine triphosphate on growth of esophageal carcinoma cells

Ming-Xia Wang, Lei-Ming Ren, Bao-En Shan

Ming-Xia Wang, Bao-En Shan, the Fourth Affiliated Hospital of Hebei Medical University, Shijiazhuang 050011, Hebei Province, China
Lei-Ming Ren, School of Pharmacy, Hebei Medical University, Shijiazhuang 050017, Hebei Province, China
Supported by the Science and Technology Development Project of Hebei Province, No. 032761192
Correspondence to: Lei-Ming Ren, MD, PhD, School of Pharmacy, Hebei Medical University, Shijiazhuang 050017, Hebei Province, China. ren-leiming@263.net
Telephone: +86-311-6034579 Fax: +86-311-6077634
Received: 2004-12-28 Accepted: 2005-03-24

Key words: Extracellular adenosine triphosphate; Esophageal carcinoma cells; Apoptosis; Growth inhibition

Wang MX, Ren LM, Shan BE. inhibitory effects of extracellular adenosine triphosphate on growth of esophageal carcinoma cells. *World J Gastroenterol* 2005; 11(38): 5915-5919
http://www.wjgnet.com/1007-9327/11/5915.asp

Abstract

AIM: To study the growth inhibitory effects of ATP on TE-13 human squamous esophageal carcinoma cells *in vitro.*

METHODS: MTT assay was used to determine the inhibition of proliferation of ATP or adenosine (ADO) on TE-13 cell line. The morphological changes of TE-13 cells induced by ATP or ADO were observed under fluorescence light microscope by acridine orange (AO)/ethidium bromide (EB) double stained cells. The internucleosomal fragmentation of genomic DNA was detected by agarose gel electrophoresis. The apoptotic rate and cell cycle after treatment with ATP or ADO were determined by flow cytometry.

RESULTS: ATP and ADO produced inhibitory effects on TE-13 cells at the concentration between 0.01 and 1.0 mmol/L. The IC_{50} of TE-13 cells exposed to ATP or ADO for 48 and 72 h was 0.71 or 1.05, and 0.21 or 0.19 mmol/L, respectively. The distribution of cell cycle phase and proliferation index (PI) value of TE-13 cells changed, when being exposed to ATP or ADO at the concentrations of 0.01, 0.1, and 1 mmol/L for 48 h. ATP and ADO inhibited the cell proliferation by changing the distribution of cell cycle phase via either G_0/G_1 phase (ATP or ADO, 1 mmol/L) or S phase (ATP, 0.1 mmol/L) arrest. Under light microscope, the tumor cells exposed to 0.3 mmol/L ATP or ADO displayed morphological changes of apoptosis. A ladder-like pattern of DNA fragmentation was obtained from TE-13 cells treated with 0.1-1 mmol/L ATP or ADO in agarose gel electrophoresis. ATP and ADO induced apoptosis of TE-13 cells in a dose-dependent manner at the concentration between 0.03 and 1 mmol/L. The maximum apoptotic rate of TE-13 cells exposed to ATP or ADO for 48 h was 16.63% or 16.9%, respectively.

CONCLUSION: ATP and ADO inhibit cell proliferation, arrest cell cycle, and induce apoptosis of TE-13 cell line.

INTRODUCTION

Extracellular ATP and adenosine (ADO) are important signaling molecules in both intracellular and extracellular microenvironments of cells. Though the regulatory control is exerted by ectonucleotidases, which maintain its low physiologic concentrations, extracellular ATP may reach high concentrations when released exocytotically from various cell types such as neurons, platelets, basophils, and mast, or when released nonexocytotically from damaged cells[1]. Since the pioneering work of Rapaport and Fontaine[2,3] showing the anticancer activities of extracellular adenine nucleotides on tumor, inhibitory effects of extracellular ATP have been described in the majority of cells and tissues studied so far, including human histiocytic leukemia cell line U-937[4], macrophages[5], mouse neuroblastoma cell line N1E-115[6], pancreatic cancer cells[7], endothelial cells[8], pulmonary artery endothelial cells[9], colorectal carcinoma cells[10], prostate carcinoma cells[11], murine dendritic cells, etc.[12-16]. But in other cell lines, such as human ovarian tumor cells and breast tumor cells, ATP shows opposite effects[17,18]. Recently, Maaser *et al*.[19], reported that extracellular nucleotides inhibit growth of moderately differentiated human esophageal cancer cells. However, the effects of ATP on poorly differentiated esophageal cancer cells have not been reported. In this study, we observed the growth inhibitory and apoptotic effects of ATP and its final metabolite, ADO, on poorly-differentiated human TE-13 esophageal cancer cells.

MATERIALS AND METHODS

Drugs and reagents

ATP, ADO, acridine orange (AO), ethidium bromide (EB), 3-(4,5-dimethyiazol-2-yl)-2, 5-diphenyl tetrazolium bromide (MTT) were purchased from Sigma. RNase, SDS, proteinase K, trypsin and agarose were from Sino-American Biotec Co., RPMI 1640 medium was from GIBCO, and fetal bovine serum (FBS) was from Hangzhou Sijiqing Biotec Co. ATP and ADO were dissolved in sterile PBS, and stored at -20 ℃.

Cell culture

Human esophageal carcinoma TE-13 cells, obtained from Japanese Cancer Cell Database, were cultured in RPMI 1640 medium supplemented with 100 mL/L FBS, 100 U/mL penicillin, and 100 μg/mL streptomycin at 37 ℃ in a humidified CO_2-controlled (50mL/L) incubator.

MTT assays

The cell viability was determined by MTT assay[20]. TE-13 cells in exponential phase of growth were harvested and seeded in 96-well plates (Costar, USA) at a density of 10 000 cells/well, and cultured for 24 h. ATP or ADO (0.01, 0.03, 0.1, 0.3, and 1 mmol/L), and control (PBS) were added into the wells and incubated continuously for 48 or 72 h at 37 ℃ with 50 mL/L CO_2. The drugs were added daily and replaced with fresh medium every 2 d. A 20-μL sample of MTT solution (5 g/L dissolved in PBS) was added to each well and the plates were incubated at 37 ℃ for 4 h. The supernatant was discarded and 150 μL dimethylsulfoxide was added to dissolve the blue insoluble MTT formazan produced by mitochondrial succinate dehydrogenase. The absorbance was measured at 492 nm in a spectrophotometer (Zhengzhou Bosai Biotech Co., ht2010), and the negative control well contained only the medium. The percentage of viable cells was calculated as the relative ratio of their absorbances to the control. All determinations were performed in quadruplicate and each experiment was repeated at least thrice.

Morphological assessment of apoptotic cells induced by ATP or ADO

Morphological assessment of apoptotic cells was performed using the AO/EB double staining method[21]. TE-13 cells in exponential phase of growth were harvested and seeded in a 25-mL cultured flask. The cells were incubated for 24 h at 37 ℃ with 50 mL/L CO_2, and then treated with 0.3 mmol/L ATP or ADO for 48 h. Freshly isolated TE-13 cells (1×10^6) were harvested in an Ependorf centrifuge tube, centrifuged for 5 min at 1 000 r/min and suspended in PBS containing fluorescence dye AO/EB (both AO and EB were at the concentration of 100 mg/L in PBS). The cells were prepared, and dropped on slides. The morphology of the cells was observed under fluorescence light microscope (UFX-II; Nikon, Japan) and photographed.

Agarose gel electrophoresis of DNA[22]

After treatment with ATP or ADO (0.1, 0.3, and 1 mmol/L) for 72 h, TE-13 cells (1×10^6) were harvested in an Ependorf centrifuge tube and washed twice with PBS. The cells were resuspended in a cell lysis buffer (50 mmol/L Tris-HCl buffer, 20 mmol/L EDTA, pH 8.0, 1% SDS) and then mixed by vortexing briefly. After the cells stood for 30 min on ice, proteinase K was added at a final concentration of 0.25 g/L. The cell lysates were incubated at 37 ℃ overnight in a water bath, and RNase was added at a final concentration of 0.5 g/L and incubated at 37 ℃ for 1 h. The lysates were mixed with an equal volume of Tris-saturated phenol–chloroform (1:1, v/v) and mildly shaken for 30 min, and the mixture was centrifuged at 3 000 r/min for 10 min at room temperature to separate the aqueous phase from the organic phase. Extraction of each aqueous phase was repeated using the Tris-saturated phenol-chloroform-isopropanol (25:24:1, v/v/v) mixture, and the aqueous phase was further extracted with an equal volume of chloroform. Mixing with 2 volumes of ice-cold ethanol and 0.1 volume of 3 mol/L NaAc precipitated DNA in the final aqueous phase. At this point, the mixture could be stored overnight. DNA was recovered by centrifugation at 13 000 *g* for 20 min in an Ependorf centrifuge tube. The supernatant was discarded, the DNA pellet was washed once with 70% ethanol, air-dried, and then redissolved in an appropriate volume of deionized distilled water and electrophoresed for 3 h at a constant voltage of 60 mV on an 1.8% agarose gel containing 0.5 mg/L EB, using an electrophoresis buffer (40 mmol/L Tris/acetate buffer, 1 mmol/L EDTA, pH 8.0). Each DNA sample contained bromophenol blue as a front-running dye. Ladder formation of oligonucleosomal DNA was made visible by an ultraviolet transillumination and photographed using a gel imaging system (PE Co., USA).

Determination of apoptosis by flow cytometric analysis

After the cells were incubated with different concentrations of ATP or ADO for 48 h, they were harvested by centrifugation, washed with ice-cold PBS once and fixed in 70% ethanol at 4 ℃ overnight. The cells were then washed once with ice-cold PBS and resuspended in PBS (pH 7.4) containing 0.5% pepsin, 5 mg/L EB and RNase at room temperature for 30 min. Finally, cells were analyzed by flow cytometry on a FACS420 (Becton Dickinson Corporation, USA), equipped with an argon ion laser (488 nm), using the HP-300 Consort 30 software to determine percentage of the apoptotic cells and the proportion of cells in G_0/G_1, S, G_2/M phases of cell cycle. The proliferation index (PI) of cells was calculated by the following formula:

$$PI\ (\%) = ([S+G_2/M]/[G_0/G_1+S+G_2/M])\times100\%.$$

Statistical analysis

The data shown were mean values of at least three independent experiments and expressed as mean±SD. Statistical comparisons were made by ANOVA. $P<0.05$ was considered statistically significant.

RESULTS

Inhibitory effects of ATP or ADO on TE-13 cell proliferation

The proliferation of TE-13 cells was significantly inhibited in a dose- and time-dependent manner, by 0.01-1.0 mmol/L of ATP or 0.3-1.0 mmol/L of ADO for 48 h of incubation, as well as 0.01-1.0 mmol/L of ADO for 72 h of incubation. The inhibitory fraction of TE-13 cells exposed to ATP and ADO for 48 and 72 h was 59.6% and 46.5%, and 80.5% and 74%, respectively (Figures 1A and B). The IC_{50} of TE-13 cells exposed to ATP or ADO for 48 and 72 h was 0.71 or 1.05 mmol/L, and 0.21 or 0.19 mmol/L, respectively.

Effects of ATP or ADO on cell cycle and proliferation index (PI) of TE-13 cells

The cell cycle phase and PI value of TE-13 cells changed when exposed to ATP or ADO at the concentrations of 0.01, 0.1, 1 mmol/L for 48 h. The proportion of cells in

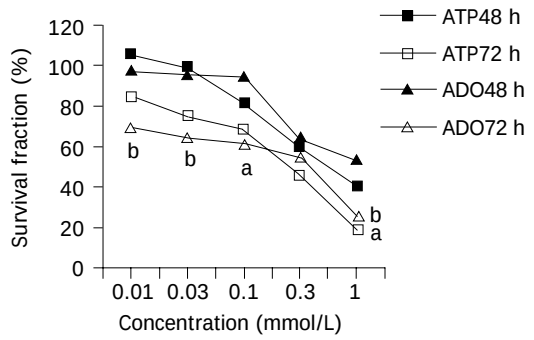

Figure 1 Effects of various concentrations of ATP or ADO on survival fraction of TE-13 cells. [a]*P*<0.05, [b]*P*<0.01 *vs* 48 h groups.

the S phase of cell cycle significantly increased, and that of the G_0/G_1, G_2/M phases and PI value did not alter after sustained incubation of TE-13 cells with ATP (0.1 mmol/L). In contrast, when exposed to ATP or ADO at the concentration of 1 mmol/L, the proportion of cells in the G_0/G_1 phase of cell cycle significantly increased, while that in the S phase of cell cycle and PI value significantly decreased. In accordance with cell proliferation results, neither the cell cycle phase nor PI value changed when exposed to ATP or ADO at the concentration of 0.01 mmol/L. The proportion of cells in G_2/M phase when exposed to ATP at various concentrations did not alter, but that significantly decreased when exposed to ADO at the concentration of 1 mmol/L. These results showed that ATP and ADO inhibited the cell proliferation by changing the distribution of cell cycle phase via either S phase delay (ATP, 0.1 mmol/L) or G_0/G_1 phase delay (ATP and ADO, 1 mmol/L, Table 1 and Figures 2A and B).

Table 1 Effects of ATP or ADO on PI value of TE-13 cells (*n* = 3, mean±SD)

Concentration (mmol/L)		PI (%)
ATP	0	37.57±2.02
	0.01	39.17±3.65
	0.1	31.24±1.04[a]
	1.0	28.69±1.33[a]
ADO	0	36.85±1.15
	0.01	29.91±1.78
	0.1	32.34±3.39
	1.0	21.76±5.20[b]

[a]*P*<0.05, [b]*P*<0.01 *vs* control group.

Morphological changes of TE-13 cells induced by ATP or ADO

Under fluorescence light microscope, the tumor cells exposed to 0.3 mmol/L ATP or ADO displayed morphological changes of apoptosis by AO/EB double staining, such as cell shrinkage, chromatin condensation, cell nuclear fragmentation, cell nucleolus disappearance, increased nuclei fluorescence or labeled orange or red-orange color (Figures 3A-C).

Agarose gel electrophoresis results of TE-13 cells induced by ATP or ADO

By agarose gel electrophoresis, a ladder-like pattern of DNA fragmentation was obtained from TE-13 cells treated with 0.1-1 mmol/L ATP or ADO, indicating that ATP or ADO induced apoptosis of TE-13 tumor cells (Figures 4A and B).

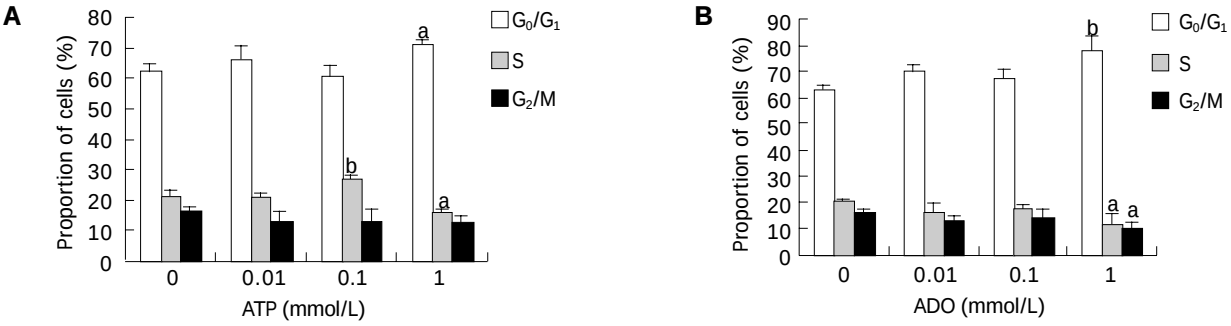

Figure 2 Effects of ATP (A) and ADO (B) on cell cycle of TE-13 cells (*n* = 3). [a]*P*<0.05, [b]*P*<0.01 *vs* 0 mmol/L.

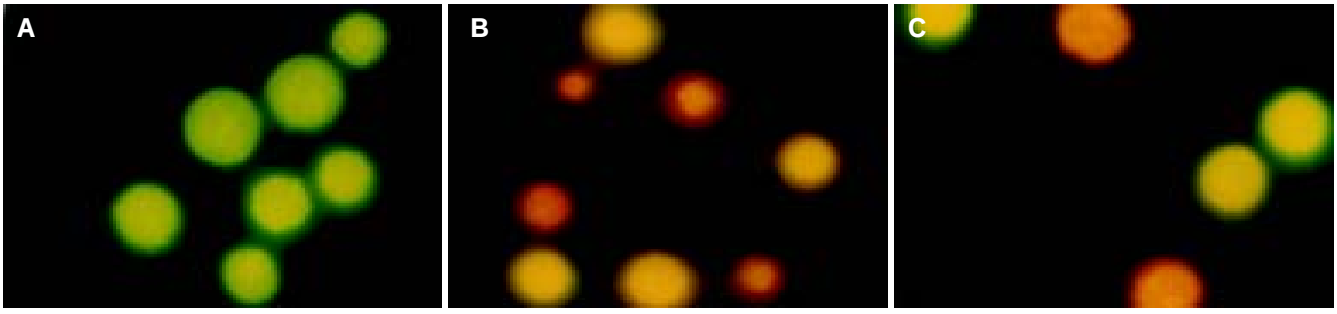

Figure 3 Fluorescence micrographs of TE-13 cells incubated for 48 h without treatment (A) and treated with ATP (B) or ADO (C) (×400).

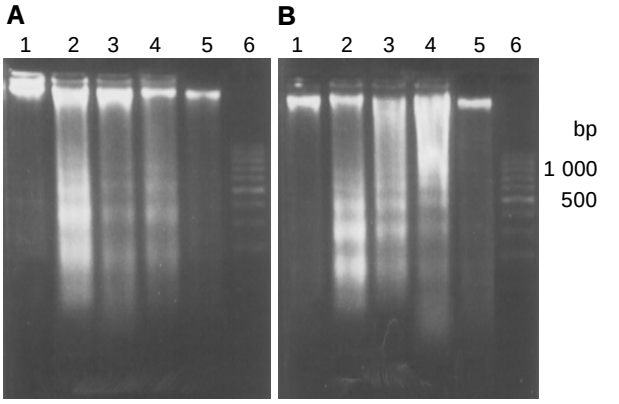

Figure 4 Agarose gel electrophoresis of DNA extracted from apoptotic TE-13 cells treated with ATP (A) or ADO (B) for 72 h. Lane 1: control; lanes 2-5: 1, 0.3, 0.1, and 0.03 mmol/L, respectively; lane 6: marker.

Apoptotic rate of TE-13 cells induced by ATP or ADO

ATP or ADO induced apoptosis of TE-13 cells in a dose-dependent manner at the concentration between 0.03 and 1 mmol/L for 48 h. The apoptotic rate of TE-13 cells treated with ATP or ADO was markedly higher than that of the control. The maximum apoptotic rate of TE-13 cells exposed to ATP or ADO (1 mmol/L) for 48 h was (16.6±1.1)% or (16.9±1.2)%, respectively (Table 2 and Figures 5A-C).

Table 2 Apoptosis of TE-13 cells induced by extracellular ATP or ADO (n = 3, mean±SD)

Concentration (mmol/L)		Apoptotic rate (%)
ATP	0	1.35±0.07
	0.03	3.89±0.29
	0.1	7.73±0.57[a]
	0.3	12.40±0.61[b]
	1.0	16.60±1.10[a]
ADO	0	2.43±0.85
	0.03	6.75±0.49[a]
	0.1	9.73±1.70[d]
	0.3	13.10±0.53[d]
	1.0	16.90±1.20[d]

[a]P<0.05, [b]P<0.01, and [d]P<0.001 *vs* control (0 mmol/L).

DISCUSSION

ATP and related compounds are widespread transmitters for extracellular communication in many cell types. By coupling to specific purinergic receptors, ATP is involved in a large variety of cellular functions. Receptors for purines and pyrimidines (P receptor) are divided into two major classes termed as ADO or P1 receptors at which ADO is the principal natural ligand, and P2 receptors at which ATP, ADP, UTP, and UDP are the principal natural ligands. To date four P1 receptor subtypes have been identified (A1, A2a, A2b, and A3), all of them are coupled to G proteins with distinct tissue distribution and pharmacological properties. The P2 receptors are divided into two families: the ligand-gated ion channels (P2X) and the G protein-coupled receptors (P2Y)[23-25]. ATP can inhibit cancer growth, induce apoptosis in various tumor models[26-30]. Both growth inhibition and programmed cell death are mediated by ionotropic P2-receptors and metabotropic P2-receptors[10,19]. Here we provide evidence that extracellular ATP induces apoptosis and causes cell cycle arrest in poorly differentiated human squamous cancer cells of the esophagus, and ADO plays an important role in them.

Recently, Maaser *et al*.[19], studied the effects of ATP and ADO on moderately differentiated esophageal cancer Kyse-140 cells, and found that ATP (100-500 μmol/L) inhibits cell growth, causes a delay in the S phase of cell cycle, and induces apoptosis. However, ADO has no contribution to the antiproliferative and apoptotic action of Kyse-140 cells. In our study, both ATP (0.1-1 mmol/L) and ADO (0.03-1 mmol/L) inhibited growth of TE-13 cells, caused cell cycle arrest in S phase (ATP, 0.1 mmol/L) or in G_0/G_1 phase (ATP or ADO, 1 mmol/L). The reasons why our results did not accord with those of Maaser *et al*.[19], may be due to the different kinds of esophageal cancer cell line and different concentrations of ATP used in our study. Additionally, a positive correlation between S-phase fraction and the response to anticancer agents has recently been documented[31]. Hence, in addition to the antiproliferative action of ATP on its own, possible synergistic effects of ATP and anticancer drugs should be investigated.

Besides its cell cycle interfering effects, ATP or ADO was shown to induce apoptosis in esophageal cancer TE-13 cells as assessed simultaneously by morphological study, agarose gel electrophoresis, and flow cytometry analysis. After being exposed to various concentrations of ATP or ADO for 48 or 72 h, TE-13 cells displayed a series of apoptotic vents, such as chromatin condensation, fragment nuclei, apoptotic body, apoptotic peak in the flow cytometry imaging

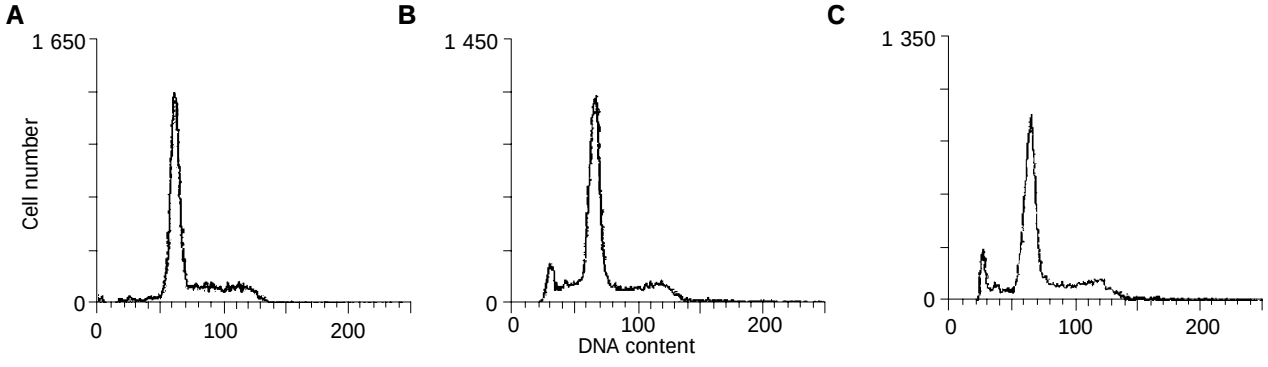

Figure 5 ATP- or ADO-induced apoptosis of TE-13 cells detected by flow cytometry in control (A) and treated with ADO (B) and ATP (C) for 48 h, respectively.

as well as DNA ladder. ADO is the final metabolite of ATP, and the result of ADO contributing to the growth inhibition and apoptosis suggests that the above effects of ATP might be partially related to its metabolite, ADO.

In conclusion, extracellular ATP inhibits cell growth, causes cell cycle arrest, and induces apoptosis. These actions might be partially related to its metabolite, ADO. Although the average concentration of nucleosides in plasma and other extracellular fluids is generally in the range of 0.4-6 μmol/L, these values can increase at sites of vascular inflammation and platelet degranulation[32]. Taken together, to further investigate the effects of ATP on tumor cells may provide an innovative treatment strategy for esophageal cancer.

REFERENCES

1 **Nihei OK**, de Carvalho AC, Savino W, Alves LA. Pharmacologic properties of P(2Z)/P2X(7) receptor characterized in murine dendritic cells: role on the induction of apoptosis. *Blood* 2000; **96**: 996-1005

2 **Rapaport E**, Fontaine J. Anticancer activities of adenine nucleotides in mice are mediated through expansion of erythrocyte ATP pools. *Proc Natl Acad Sci USA* 1989; **86**: 1662-1666

3 **Rapaport E**, Fontaine J. Generation of extracellular ATP in blood and its mediated inhibition of host weight loss in tumor-bearing mice. *Biochem Pharmacol* 1989; **38**: 4261-4266

4 **Schneider C**, Wiendl H, Ogilvie A. Biphasic cytotoxic mechanism of extracellular ATP on U-937 human histiocytic leukemia cells: involvement of adenosine generation. *Biochim Biophys Acta* 2001; **1538**: 190-205

5 **Coutinho-Silva R**, Perfettini JL, Persechini PM, Dautry-Varsat A, Ojcius DM. Modulation of P2Z/P2X$_7$ receptor activity in macrophages infected with Chlamydia psittaci. *Am J Physiol Cell Physiol* 2001; **280**: C81-C89

6 **Schrier SM**, Florea BI, Mulder GJ, Nagelkerke JF, Ijzerman AP. Apoptosis induced by extracellular ATP in the mouse neuroblastoma cell line N1E-115: studies on involvement of P2 receptors and adenosine. *Biochem Pharmacol* 2002; **63**: 1119-1126

7 **Yamada T**, Okajima F, Akbar M, Tomura H, Narita T, Yamada T, Ohwada S, Morishita Y, Kondo Y. Cell cycle arrest and the induction of apoptosis in pancreatic cancer cells exposed to adenosine triphosphate *in vitro*. *Oncol Rep* 2002; **9**: 113-117

8 **von-Albertini M**, Palmetshofer A, Kaczmarek E, Koziak K, Stroka D, Grey ST, Stuhlmeier KM, Robson SC. Extracellular ATP and ADP activate transcription factor NF-kappa B and induce endothelial cell apoptosis. *Biochem Biophys Res Commol* 1998; **248**: 822-829

9 **Rounds S**, Yee WL, Dawicki DD, Harrington E, Parks N, Cutaia MV. Mechanism of extracellular ATP- and adenosine-induced apoptosis of cultured pulmonary artery endothelial cells. *Am J Physiol* 1998; **275**(2 Pt1): L379-L388

10 **Hopfner M**, Maaser K, Barthel B, von Lampe B, Hanski C, Riecken EO, Zeitz M, Scherübl H. Growth inhibition and apoptosis induced by P2Y$_2$ receptors in human colorectal carcinoma cells: involvement of intracellular calcium and cyclic adenosine monophosphate. *Int J Colorectal Dis* 2001; **16**: 154-166

11 **Janssens R**, Boeynaems JM. Effects of extracellular nucleotides and nucleosides on prostate carcinoma cells. *Br J Pharmacol* 2001; **132**: 536-546

12 **Macino B**, Zambon A, Milan G, Cabrelle A, Ruzzene M, Rosato A, Mandruzzato S, Quintieri L, Zanovello P, Collavo D. CD45 regulates apoptosis induced by extracellular adenosine triphosphate and cytotoxic T lymphocytes. *Biochem Biophys Res Commol* 1996; **226**: 769-776

13 **Bronte V**, Macino B, Zambon A, Rosato A, Mandruzzato S, Zanovello P, Collavo D. Protein tyrosine kinases and phosphatases control apoptosis induced by extracellular adenosine 5′-triphosphate. *Biochem Biophys Res Commol* 1996; **218**: 344-351

14 **Sun AY**, Chen YM. Extracellular ATP-induced apoptosis in PC12 cells. *Adv Exp Med Biol* 1998; **446**: 73-83

15 **Schulze-Lohoff E**, Hugo C, Rost S, Arnold S, Gruber A, Brune B, Sterzel RB. Extracellular ATP causes apoptosis and necrosis of cultured mesangial cells via P2Z/P2X$_7$ receptors. *Am J Physiol* 1998; **275**(6 Pt2): F962-F971

16 **Nakamura N,** Wada Y. Properties of DNA fragmentation activity generated by ATP depletion. *Cell Death Differ* 2000; **7**: 477-484

17 **Dixon CJ**, Bowler WB, Fleetwood P, Ginty AF, Gallaghe JA, Carron JA. Extracellular nucleotides stimulate proliferation in MCF-7 breast cancer cells via P2-purinoceptors. *Br J Cancer* 1997; **75**: 34-39

18 **Popper LD** , Batra S. Calcium mobilization and cell proliferation activated by extracellular ATP in human ovarian tumor cells. *Cell Calcium* 1993; **14**: 209-218

19 **Maaser K**, Hopfner M, Kap H, Sutter AP, Barthel B, von Lampe B, Zeitz M, Scherübl H. Extracellular nucleotides inhibit growth of human oesophageal cancer cells via P2Y$_2$-receptors. *Br J Cancer* 2002; **86**: 636-644

20 **Situ ZQ**, Wu JZ. *Cell Culture*. Xi'an: *World Book's Publishing Company* 1996: 186-188

21 **Wang CY**, Sheng RL, Wang F, Ding XJ, Qiu NL. Fluorescence method of apoptotic morphology studying by acridine orange and ethidium bromide double stained cells. *Zhongguo Bingli Shengli Zazhi* 1998; **14**: 104-106

22 **Kim KT**, Yeo EJ, Choi H, Park SC. The effect of pyrimidine nucleosides on adenosine-induced apoptosis in HL-60 cells. *J Cancer Res Clin Oncol* 1998; **124**: 471-477

23 **Fredholm BB**, Abbracchio MP, Burnstock G, Daly JW, Harden TK, Jacobson KA, Leff P, Williams M. Nomenclature and classification of purinoceptors. *Pharmacol Rev* 1994; **46**: 143-156

24 **Burnstock G**. Purinergic signaling and vascular cell proliferation and death. *Arterioscler Thromb Vasc Biol* 2002; **22** 364-373

25 **Vandewalle B**, Hornez L, Revillion F, Lefebvre J. Effect of extracellular ATP on breast tumor cell growth, implication of intracellular calcium. *Cancer Lett* 1994; **85**: 47-54

26 **Ferraria D**, Los M, Bauer MK, Vandenabeele P, Wesselborg S, Schulze-Osthoff K. P2Z purinoreceptor ligation induces activation of caspases with distinct roles in apoptotic and necrotic alterations of cell death. *FEBS Lett* 1999; **447**: 71-75

27 **Peng L**, Bradley CJ, Wiley JS. P2Z purinoceptor, a special receptor for apoptosis induced by ATP in human leukemic lymphocytes. *Chin Med J* 1199; **112**: 356-362

28 **Fujita N**, Kakimi M, Ikeda Y, Hiramoto T, Suzuki K. Extracellular ATP inhibits starvation-induced apoptosis via P2X$_2$ receptors in differentiated rat pheochromocytoma PC12 cells. *Life Sci* 2000; **66**: 1849-1859

29 **Katzur AC**, Koshimizu T, Tomic M, Schultze-Mosgau A, Ortmann O, Stojilkovic SS. Expression and responsiveness of P2Y$_2$ receptors in human endometrial cancer cell lines. *J Clin Endocrinol Metab* 1999; **84**: 4085-4091

30 **Dawicki DD**, Chatterjee D, Wyche J, Rounds S. Extracellular ATP and adenosine cause apoptosis of pulmonary artery endothelial cells. *Am J Physiol* 1997; **273**(2 Pt1): L485-L494

31 **Kolfschoten GM**, Hulscher TM, Pinedo HM, Boven E. Drug resistance features and S-phase fraction as possible determinants for drug response in a panel of human ovarian cancer xenografts. *Br J Cancer* 2000; **83**: 921-927

32 **Traut TW**. Physiological concentrations of purines and pyrimidines. *Mol Cell Biochem* 1994; **140**: 1-22

Science Editor Wang XL and Guo SY **Language Editor** Elsevier HK

PO Box 2345, Beijing 100023, China
www.wjgnet.com
wjg@wjgnet.com

ELSEVIER

World J Gastroenterol 2005;11(38):5920-5925
World Journal of Gastroenterology ISSN 1007-9327

• *GASTRIC CANCER* •

Prognostic implication of isolated tumor cells and micrometastases in regional lymph nodes of gastric cancer

Hye Seung Lee, Min A Kim, Han-Kwang Yang, Byung Lan Lee, Woo Ho Kim

Hye Seung Lee, Department of Pathology, Seoul National University Bundang Hospital, Gyeonggi 463-707, Korea
Min A Kim, Woo Ho Kim, Department of Pathology and Cancer Research Institute, Seoul National University College of Medicine, Seoul 110-799, Korea
Han-Kwang Yang, Department of Surgery and Cancer Research Institute, Seoul National University College of Medicine, Seoul, Korea
Byung Lan Lee, Department of Anatomy, Seoul National University College of Medicine, Seoul, Korea
Supported by a grant (FG03-11-02) from the 21C Frontier Functional Human Genome Project from the Ministry of Science and Technology of Korea
Correspondence to: Dr. Woo Ho Kim, Department of Pathology, Seoul National University College of Medicine, 28 Yongon-dong, Chongno-gu, Seoul 110-799, Korea. woohokim@snu.ac.kr
Telephone: +82-2-7408269 Fax: +82-2-7655600
Received: 2005-02-24 Accepted: 2005-05-12

ABSTRACT

AIM: To determine the prognostic significance of isolated tumor cells (ITCs) and lymph node micrometastases in gastric cancer.

METHODS: Hematoxylin and eosin-stained slides of lymph node dissections of 632 consecutive gastric cancers were reviewed. Cytokeratin immunostaining was performed in 280 node-negative cases and 5 cases indefinite for lymph node metastases. Lymph node metastases were divided into ITCs, micrometastases, or macrometastases, according to the sizes of tumor deposits in largest dimension. ITCs were further classified into four groups according to metastasis pattern.

RESULTS: Lymph node metastases were identified by immunostaining in 58 of 280 node-negative cases (20.7%) and were not significantly associated with patient survival (P = 0.3460). After cytokeratin immunostaining, 196 cases were classified as pN1, which consisted of 20 cases with micrometastases detected by immunostaining (pN1mi(i+)), 34 cases with only micrometastases (pN1mi), and 142 cases with pN1 with one or more macrometastases (pN1). Cases with pN1mi and pN1mi(i+) had a significantly better prognosis than the cases with pN1 (P = 0.0037). ITCs were found in 38 of these 58 cases, and could be divided into four groups: 12 cases with only a single cell pattern, 7 cases with multiple individual cells, 5 cases with single small cluster, and 14 cases with multiple small clusters. Among these four groups, cases with ITCs of multiple individual cell pattern showed the worst survival (median survival: 28 mo, P<0.0001).

CONCLUSION: Both size and pattern of lymph node metastases can give prognostic information on the survival of gastric cancer patients.

Key words: Immunohistochemistry; Cytokeratin; Patient survival; Lymph node metastasis

Lee HS, Kim MA, Yang HK, Lee BL, Kim WH. Prognostic implication of isolated tumor cells and micrometastases in regional lymph nodes of gastric cancer. *World J Gastroenterol* 2005; 11(38): 5920-5925
http://www.wjgnet.com/1007-9327/11/5920.asp

INTRODUCTION

The most important prognostic factor in patients with gastric cancer is the presence of a regional lymph node metastasis[1]. Some patients with histologically node-negative gastric cancer will die as a result of local or distant tumor recurrence, even though their primary tumor is curatively resected. Adjuvant chemotherapy benefits some patients with node-negative gastric cancer, but the treatment of all node-negative patients is unnecessary, as most node-negative patients will never have recurrence after surgery. Therefore, additional markers would be helpful for predicting patients at risk of a poor prognosis.

For the above purpose, histological evaluations of multiple serial sections of lymph nodes at many levels have been undertaken by several investigators[2,3]. Although serial sectioning can increase the detection of occult lymph node metastases, it is also labor-intensive and expensive for routine diagnostic practice. Furthermore, a single cell or minute cluster cannot be detected even by an expert pathologist. Recent advances in immunohistochemistry and molecular biology allow the identification of discrete and occult tumor cells, which are undetectable by standard hematoxylin and eosin (HE) staining, in the lymph nodes of patients with breast[4,5], esophageal[6,7], and colorectal cancers[8,9]. Many investigators have correlated patient prognosis with the presence of metastases detected by immunostaining, but controversy remains over the importance of single cell or cluster of cancer cells in regional lymph nodes.

Recently, regional lymph node metastasis was further classified into isolated tumor cells (ITCs), micrometastases, or macrometastases according to the size of tumor deposits in largest dimension in patients with breast cancers[10]. ITCs are defined as single cells or small clusters not greater than 0.2 mm in largest dimension, usually with no histologic

evidence of malignant activity. Cases with only ITCs are designated as pN0(i+) and categorized into pN0 by AJCC[10]. Single cells and small ill-defined clusters in lymph node metastasis, classified as ITCs, are not uncommon in gastric cancer, since cancer cells in diffuse type cancer frequently loose intercellular adhesion molecules, which represents a critical event of the metastatic cascade[11-13]. However, the clinical importance of size or pattern of metastatic tumor deposits in lymph node metastases is not defined in gastric cancer patients. To clarify the prognostic impact of ITCs and micrometastases on regional lymph nodes, we investigated 632 consecutive gastric cancers resected during one year in the aspect of number, size, and patterns of lymph node metastases and examined their clinical significance.

MATERIALS AND METHODS

Specimens

The files of 659 surgically resected primary gastric cancer cases examined at the Department of Pathology, Seoul National University College of Medicine over a period of 1 year (January 1, 1995-December 31, 1995) were examined in order to evaluate their lymph node metastasis status. Of these 659 cases, 632 cases (95.9%) were available for slide review and immunohistochemical staining of lymph nodes. The series consisted of 280 cases of pN0 stage, 183 cases of pN1 stage, 113 cases of pN2 stage and 56 cases of pN3 stage. Mean age of the patients was 54.5 years, and 92.9% of the patients had undergone curative resection (R0 according to the AJCC guideline). The study included 409 advanced gastric carcinomas and 223 early gastric carcinomas. No patient had received preoperative chemo- or radiotherapy. Glass slides were reviewed to determine histologic types according to WHO classification[11]. The clinical outcomes of the patients were followed from the date of surgery to either the date of death or December 1, 2000, resulting in a follow-up period ranging from 1 to 72 mo (mean: 55 mo). Those cases who lost their follow-up and those who ended in death due to a cause other than gastric cancer were regarded as censored data during survival rate analysis.

Review of HE-stained slides of lymph node dissection

HE-stained slides of lymph node dissection of 632 consecutive gastric cancers (31 421 lymph nodes) were reviewed. In contrast to original report, metastatic nodules in the fat adjacent to a gastric carcinoma without evidence of residual lymph node tissue were regarded as regional lymph node metastases by the AJCC guideline. Lymph node metastases were subdivided into three groups according to the AJCC guidelines using the maximum size of tumor deposit, i.e., ITCs are not greater than 0.2 mm in diameter, micrometastases are greater than 0.2 mm but not greater than 2 mm in diameter, and macrometastases are greater than 2 mm in diameter[10]. Lymph nodes with ITCs were not regarded as lymph node metastases, and cases with only micrometastases (not greater than 2 mm in diameter) were classified as pN1mi.

Immunohistochemistry

Immunohistochemical staining was performed on 280 gastric cancer cases (9 604 lymph nodes) without regional lymph node metastasis (pN0) by conventional HE staining, and on an additional 5 cases, who were originally reported as pN1 but were indefinite for metastasis by reviewing HE-stained slides. A single serial section (4 μm) was cut from each paraffin block, deparaffinized and dehydrated. Immunostaining with antibodies against cytokeratin (mAb anti-human cytokeratin clone MNF116, DAKO, Glostrup, Denmark) at 1:100 dilution was performed using a streptavidin peroxidase procedure after an antigen retrieval process using microwaves. Cells were considered to be occult lymph node metastases, if they were immunoreactive mainly in their cytoplasmic membranes, were found within the substance of the lymph nodes and were morphologically consistent with cancer cells. Immunohistochemically detected lymph node metastases were also subdivided into three groups: ITCs, micrometastases, or macrometastases, according to the size of tumor deposits in the largest dimension. Tumor deposits in lymph nodes with histologic evidence of malignant activity, such as gland formation or stromal reaction, were defined as micrometastases even if they were smaller than 0.2 mm in maximum dimension. ITCs were subdivided into four groups according to metastasis pattern (single cell, multiple individual cells, single cluster and multiple clusters, Figure 1). The number of lymph nodes containing tumors and the total number of tumor cells or clusters in a lymph node were recorded.

Statistical analysis

Either the χ^2 test or Fisher's exact test (two-sided) was performed to determine the correlation between lymph node metastasis and clinicopathologic parameters. Survival curves were estimated using the Kaplan-Meier product-limit method, and the significance of differences between survival curves was determined using the log-rank test. Results were considered to be statistically significant when *P* values were less than 0.05. All statistical analyses were conducted using the SPSS 11.0 statistical software program (SPSS, Chicago, IL, USA).

RESULTS

Reclassified pN stage after immunohistochemistry and reviewing HE-stained slides

Occult lymph node metastases were identified by cytokeratin immunostaining in 58 (20.7%) of 280 cases or in 157 of 9 604 lymph nodes (1.63%), which were originally reported as pN0. Of the 58 cases with positive occult lymph node metastasis, macrometastasis was found in one case, micrometastases in 19 cases (pN1mi(i+)), and ITCs in 38 cases (pN0(i+)). Four cases, who were originally reported as pN1, were reclassified as pN0, and one case was reclassified as pN1mi(i+) after cytokeratin immunostaining.

The pN stage, after immunostaining for cytokeratin and reviewing HE-stained slides, was reclassified as pN0 in 264 cases, pN1 in 196 cases, pN2 in 113 cases, and pN3 in 59 cases. The reclassified pN stage was found to be significantly associated with patient survival (Figure 2A).

Subgroups of pN1

One hundred and ninety-six cases with pN1 were subdivided

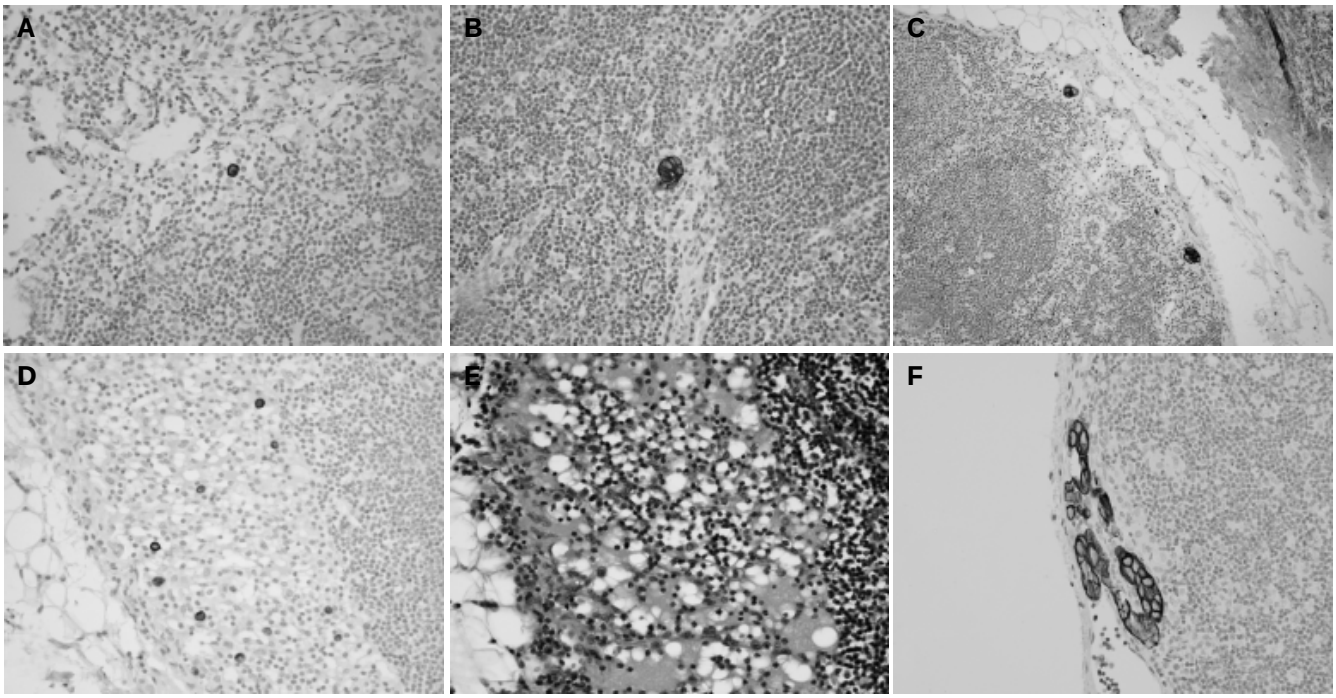

Figure 1 Immunohistochemical staining against cytokeratin. A: Single cell only (×400); B: single small cluster (×400); C: multiple small clusters (×200); D: multiple individual cells (×400); E: HE-stained slides of multiple individual tumor cells in lymph nodes (the same area of D, ×400); F: micrometastasis (×400).

into three groups: 20 cases with pN1mi(i+), 34 cases with pN1mi, and 142 cases with pN1 with one or more macrometastases. Cases with pN1mi, including pN1mi(i+), showed a significantly better prognosis than the 142 cases with macrometastases ($P = 0.0037$, Figure 2B). Furthermore, pN1mi detected by HE staining only was significantly associated with better survival than macrometastases ($P = 0.0218$, Figure 2C). No significant difference was observed between the survival of cases with pN1mi(i+) and pN1mi ($P = 0.3305$, Figure 2B). When compared to pN0(i-) cases, pN1mi cases showed significantly poorer survival ($P = 0.0104$, Figure 2C), but pN1mi (i+) and pN0(i-) cases did not show a survival difference ($P = 0.6738$).

Isolated tumor cells (ITCs)

Cases with lymph node metastases detected by immunohistochemistry (pN0(i+) and pN1(i+)) did not show a different survival when compared to cases without lymph node metastases ($P = 0.3460$, Figure 2D). Patients with immunohistochemically detected metastases had poorly differentiated adenocarcinomas more frequently than those without metastases ($P = 0.019$, Table 1).

Four groups of ITCs included 12 cases with a single cell pattern, 7 cases with multiple individual cells, 5 cases with a single cluster and 14 cases with multiple clusters. Among them, cases with multiple individual cells showed the poorest survival (median survival: 28 mo, $P<0.0001$, Figure 2E),

Table 1 Pathologic findings according to the size and pattern of lymph node metastasis after cytokeratin staining in pN0 cases on initial examination

	Negative	ITCs				Micro meta-stases	Macro meta-stases	*P*
		Single cell	Multiple cells	Single cluster	Multiple clusters			
WHO (%)								0.019
[1]W/D, M/D	112 (50.5)	6 (50.0)	0 (0)	1 (20)	6 (42.9)	8 (42.1)	0 (0)	
[2]P/D	54 (24.3)	4 (33.3)	7 (100)	2 (40)	5 (35.7)	8 (42.1)	1 (100)	
Mucinous	9 (4.0)	0 (0)	0 (0)	1 (20)	0 (0)	2 (10.5)	0 (0)	
[3]SRC	47 (21.2)	2 (16.7)	0 (0)	1 (20)	3 (21.4)	1 (5.3)	0 (0)	
Depth (%)								<0.001
Mucosa	97 (43.7)	4 (33.3)	0 (0)	2 (40)	1 (7.1)	3 (15.8)	0 (0)	
[4]SM	72 (32.4)	2 (16.7)	1 (14.4)	1 (20)	4 (28.7)	5 (26.3)	1 (100)	
[5]PM	21 (9.5)	1 (8.3)	0 (0)	0 (0)	1 (7.1)	2 (10.5)	0 (0)	
Subserosa	28 (12.6)	5 (41.7)	3 (42.8)	2 (40)	7 (50)	4 (21.1)	0 (0)	
Serosa	4 (1.8)	0 (0)	3 (42.8)	0 (0)	1 (7.1)	5 (26.3)	0 (0)	
Total (%)	222 (100)	12 (100)	7 (100)	5 (100)	14 (100)	19 (100)	1 (100)	

[1]Well and moderately differentiated tubular adenocarcinoma, [2]poorly differentiated tubular adenocarcinoma, [3]signet-ring cell carcinoma, [4]submucosa, [5]proper muscle.

and had poorly differentiated non-solid type adenocarcinomas with infiltrative border. Lymphatic invasion was not found in these cases. Histologically, cytokeratin-positive individual cells were found in the sinus of lymph nodes, and these could not be recognized by routine HE staining (Figure 1). In four of seven cases with multiple individual cells, the maximum number of tumor cells in a single lymph node exceeded 20 (Table 2), and prognosis was grave especially in these four cases. By Cox regression analysis, the pattern of metastasis was found to be a significant prognostic factor independent of pT stage and histologic type (P = 0.018, Table 3). Two of the seven patients with multiple individual cells had stage IV disease, and the pattern of multiple individual cells was associated with poor survival even after the patients with stage IV disease were deleted (P = 0.0018, Figure 2F).

Thirty-five of thirty-eight cases with ITCs had one to five positive metastatic nodes. The remaining cases had six or more positive metastatic nodes (9, 11, and 19 metastatic lymph nodes, respectively). Cases with ITCs in six or more lymph nodes showed a significantly poorer prognosis than those with ITCs in 1-5 lymph nodes (P<0.0001, Figure 2G).

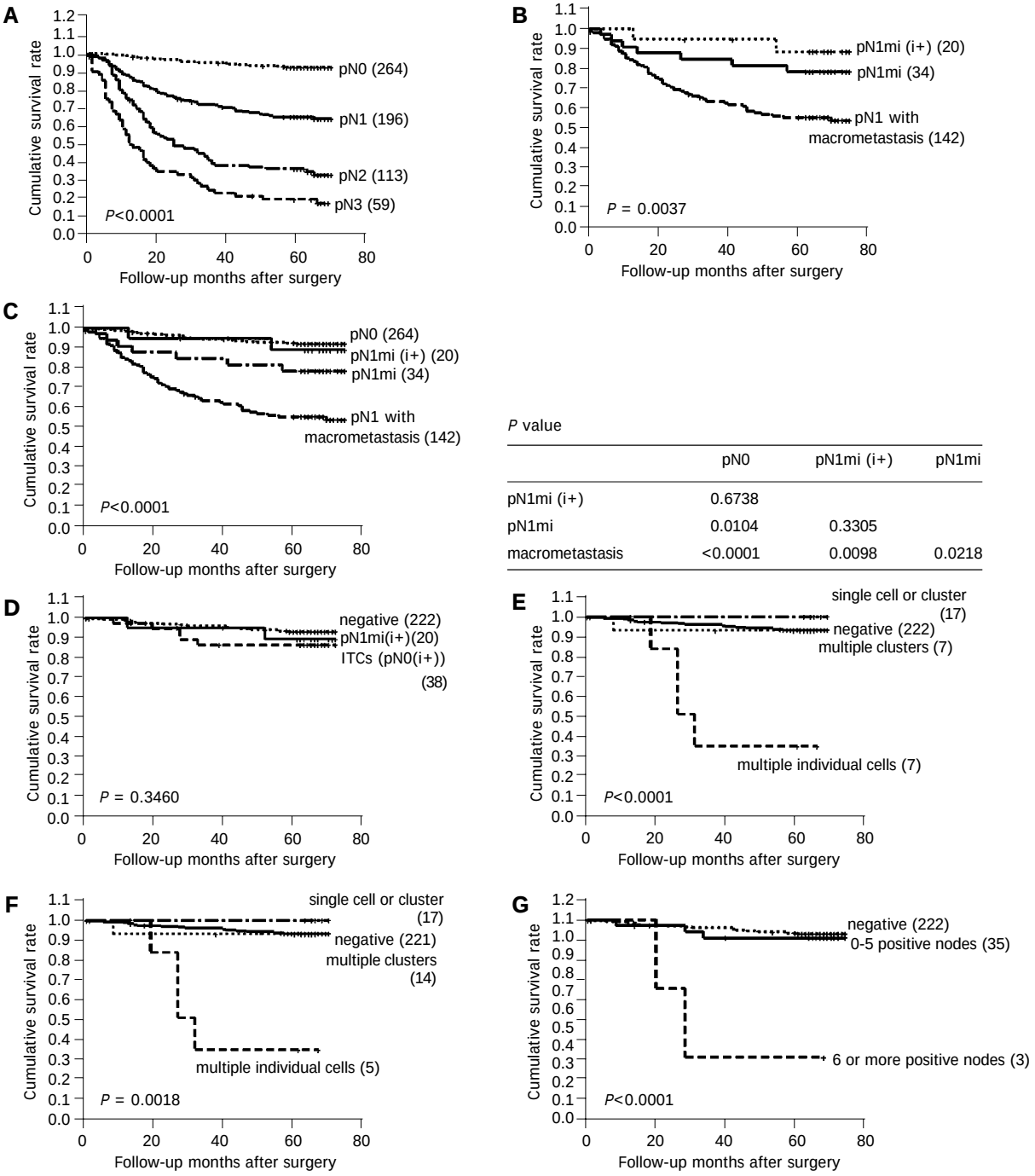

P value

	pN0	pN1mi (i+)	pN1mi
pN1mi (i+)	0.6738		
pN1mi	0.0104	0.3305	
macrometastasis	<0.0001	0.0098	0.0218

Figure 2 Survival curves using the Kaplan-Meier method. A: Patient survival according to reclassified pN stage; B: survival curve of cases with pN1 with one or more macrometastases, pN1mi, and pN1mi(i+); C: survival curve of the cases with pN0 stage, pN1mi(i+), pN1mi, and pN1; D: prognostic impact of lymph node metastases as detected by immunostaining; E: survival curves according to the pattern of ITCs; F: survival curves according to the pattern of ITCs deleting patients with stage IV disease; G: survival curves according to the number of positive nodes.

Table 2 Clinicopathologic findings in seven cases with ITC with multiple scattered single cell pattern

Case	[1]F/U	[1]F/U months	Sex	Age (yr)	Tumor size (cm)	WHO	Depth	Stage	Number of positive nodes	Number of tumor cells in a lymph node
202	Alive	14	[2]M	67	2.0	[4]P/D	[5]SM	Ia	4	2
409	Alive	69	M	40	4.5	P/D	[6]SS	Ib	1	4
437	Died	20	[3]F	35	6.0	P/D	SS	Ib	19	>50
726	Died	33	F	40	14.0	P/D	[7]SE	II	3	>30
737	Died	28	F	30	3.0	P/D	SE	IV	9	>20
829	Died	28	M	46	6.0	P/D	SE	IV	2	45
850	Alive	63	M	49	5.0	P/D	SS	Ib	1	8

[1]Follow-up, [2]male, [3]female, [4]poorly differentiated tubular adenocarcinoma, [5]submucosa, [6]subserosa, [7]serosa.

Table 3 Multivariate analysis of predictive factors for survival in pN0 using Cox regression model

Prognostic factor	Hazard ratio (95%CI)	*P*
Pattern of ITCs		0.018
Multiple individual cells *vs* others	4.09 (1.28–13.10)	
PT stage		<0.001
II–IV *vs* I	8.77 (2.89–26.32)	
Lauren's classification		0.276
Diffuse *vs* intestinal	1.73 (0.65–4.61)	

DISCUSSION

When examining gastric cancer and related material, the pathologist aims to achieve as simply and reliably as possible, a comprehensive diagnosis and prognosis of therapeutic relevance. The routine histologic examination of lymph nodes has long been the gold standard for identifying metastases to regional lymph nodes resected as part of the staging procedure for tumors in diverse locations, including the stomach. However, this method has an inherent limitation, the potential for sampling error. Serial sectioning has been employed to scrutinize metastases[14], but it is impractical for routine surgical pathology practice. In this study, we performed immunohistochemical staining against cytokeratin on routine sections in the cases with original diagnosis of pN0. We found that micrometastases or macrometastases were overlooked in 20 of 280 node-negative cases (7.14%), and ITCs were found in 38 cases (13.6%).

The prognostic impact of lymph node metastases detected by immunohistochemistry remains controversial in gastric cancer. Some authors have reported an insignificant correlation between lymph node metastasis detected by immunostaining and patient survival[15-17], but others have reported a significant impact on patient survival[18-21]. In contrast to previous reports, we subdivided lymph node metastases according to the size of tumor deposits, and then subdivided cases with ITCs into four groups according to the pattern of tumor deposits. In this large scale study, lymph node metastases as detected by immunostaining were not significantly associated with patient survival.

Ishida *et al*.[21], have classified lymph node metastases into five groups according to the pattern of metastasis (single cell *vs* cluster), but did not analyze the implications on patient survival. Fukagawa *et al*.[17], demonstrated that the pattern of micrometastases (single cell *vs* cluster) does not affect the survival curve. In the present study, ITCs were classified into four groups: single cell, multiple individual cells, single cluster, and multiple clusters. Among ITCs, only cases with multiple individual cells comprised the poor prognosis group. Tumors with a pattern of multiple individual cells showed non-solid poorly differentiated type adenocarcinoma and had infiltrative border. Although the pattern of multiple individual cells was very uncommon (7 of 280 pN0, 2.5%), this pattern had a significant impact on patient survival and showed a distinct histologic feature. Therefore, cytokeratin immunostaining is recommended in node-negative gastric cancers especially in non-solid poorly differentiated type adenocarcinoma with infiltrative border, to identify occult metastasis with multiple individual cell pattern.

According to the cancer staging of AJCC, micrometastases are defined when the size of tumor deposits in largest dimension is greater than 0.2 mm and not greater than 2 mm in diameter, and cases in which only micrometastases are detected are defined as pN1mi in breast cancer. However, in previous reports on gastric cancer[17-21], micrometastases are defined as lymph node metastases detected by immunohistochemistry, not according to the size of tumor deposits. In the present study, micrometastases were defined according to cancer staging method recommended by AJCC. Cases with pN1mi including pN1mi(i+) showed a significantly better prognosis than cases with pN1 with macrometastases ($P = 0.0037$), and pN1mi by only HE staining was also significantly associated with better survival than macrometastases ($P = 0.0218$). Therefore, we recommend that pN1mi should be defined in gastric cancer as is currently done in breast cancer. Furthermore, the survival of patients with pN1mi(i+) was not significantly different from that of patients with pN0. Therefore, we also recommend classifying pN1mi(i+) separately from pN1mi.

Several lines of evidence support the interpretation that keratin-positive cells in lymph nodes represent metastatic carcinoma, though occasional normal constituents of lymph nodes may be stained positively for cytokeratin. Other than cancer cells, undesirable cytokeratin has been reported both in plasma cells[22,23] and in interstitial reticulum cells[22,24]. Cytokeratin-positive metastatic cells have an epithelial morphology, in contrast to the dendritic process appearance of keratin-positive reticulum cells. Plasma cells show weak and cytoplasmic expression of cytokeratin and have their characteristic features. Cells are considered as occult node metastases only when they show strong and membranous expression of cytokeratin, reside within the substance of the lymph nodes, and exhibit epithelial morphology.

In conclusion, immunohistochemical staining against cytokeratin can detect occult metastases in regional lymph nodes of patients with gastric cancer, and the presence of immunohistochemically detected ITCs does not affect patient survival, except for a subset of cases with metastasis of multiple individual cells. pN1mi or pN1mi(i+) is distinct from pN0 or pN1 in the aspect of patient survival. Therefore, the size and pattern of lymph node metastases can provide prognostic information in gastric cancer.

References

1 **Adachi Y,** Kamakura T, Mori M, Baba H, Maehara Y, Sugimachi K. Prognostic significance of the number of positive lymph nodes in gastric carcinoma. *Br J Surg* 1994; **81**: 414-416

2 **Isozaki H,** Okajima K, Fujii K. Histological evaluation of lymph node metastasis on serial sectioning in gastric cancer with radical lymphadenectomy. *Hepatogastroenterology* 1997; **44**: 1133-1136

3 Prognostic importance of occult axillary lymph node micrometastases from breast cancers. International (Ludwig) Breast Cancer Study Group. *Lancet* 1990; **335**: 1565-1568

4 **Cote RJ,** Peterson HF, Chaiwun B, Gelber RD, Goldhirsch A, Castiglione-Gertsch M, Gusterson B, Neville AM. Role of immunohistochemical detection of lymph-node metastases in management of breast cancer. International Breast Cancer Study Group. *Lancet* 1999; **354**: 896-900

5 **Dowlatshahi K,** Fan M, Snider HC, Habib FA. Lymph node micrometastases from breast carcinoma: reviewing the dilemma. *Cancer* 1997; **80**: 1188-1197

6 **Glickman JN,** Torres C, Wang HH, Turner JR, Shahsafaei A, Richards WG, Sugarbaker DJ, Odze RD. The prognostic significance of lymph node micrometastasis in patients with esophageal carcinoma. *Cancer* 1999; **85**: 769-778

7 **Doki Y,** Ishikawa O, Mano M, Hiratsuka M, Sasaki Y, Kameyama M, Ohigashi H, Murata K, Yamada T, Miyashiro I, Yokoyama S, Ishiguro S, Imaoka S. Cytokeratin deposits in lymph nodes show distinct clinical significance from lymph node micrometastasis in human esophageal cancers. *J Surg Res* 2002; **107**: 75-81

8 **Liefers GJ,** Cleton-Jansen AM, van de Velde CJ, Hermans J, van Krieken JH, Cornelisse CJ, Tollenaar RA. Micrometastases and survival in stage II colorectal cancer. *N Engl J Med* 1998; **339**: 223-228

9 **Nicholson AG,** Marks CG, Cook MG. Effect on lymph node status of triple levelling and immunohistochemistry with CAM 5.2 on node negative colorectal carcinomas. *Gut* 1994; **35**: 1447-1448

10 American Joint Committee on Cancer. AJCC cancer staging manual 6th ed. New York: Springer-Verlag, 2002

11 International Agency for Research on Cancer (IARC). World Health Organization Classification of Tumors; pathology and genetics of tumors of the digestive system. Lyon: IARC Press, 2000

12 **Woo DK,** Kim HS, Lee HS, Kang YH, Yang HK, Kim WH. Altered expression and mutation of beta-catenin gene in gastric carcinomas and cell lines. *Int J Cancer* 2001; **95**: 108-113

13 **Kumar V,** Abbas AK, Fausto N. Robbins and Cotran pathologic basis of disease 7th ed. Philadelphia: Elsevier, 2004

14 **Pickren JW.** Significance of occult metastases. A study of breast cancer. *Cancer* 1961; **14**: 1266-1271

15 **Morgagni P,** Saragoni L, Scarpi E, Zattini PS, Zaccaroni A, Morgagni D, Bazzocchi F. Lymph node micrometastases in early gastric cancer and their impact on prognosis. *World J Surg* 2003; **27**: 558-561

16 **Choi HJ,** Kim YK, Kim YH, Kim SS, Hong SH. Occurrence and prognostic implications of micrometastases in lymph nodes from patients with submucosal gastric carcinoma. *Ann Surg Oncol* 2002; **9**: 13-19

17 **Fukagawa T,** Sasako M, Mann GB, Sano T, Katai H, Maruyama K, Nakanishi Y, Shimoda T. Immunohistochemically detected micrometastases of the lymph nodes in patients with gastric carcinoma. *Cancer* 2001; **92**: 753-760

18 **Yasuda K,** Adachi Y, Shiraishi N, Inomata M, Takenchi H, Kitano S. Prognostic effect of lymph node micrometastasis in patients with histologically node-negative gastric cancer. *Ann Surg Oncol* 2002; **9**: 771-774

19 **Lee E,** Chae Y, Kim I, Choi J, Yeom B, Leong AS. Prognostic relevance of immunohistochemically detected lymph node micrometastasis in patients with gastric carcinoma. *Cancer* 2002; **94**: 2867-2873

20 **Nakajo A,** Natsugoe S, Ishigami S, Matsumoto M, Nakashima S, Hokita S, Baba M, Takao S, Aikou T. Detection and prediction of micrometastasis in the lymph nodes of patients with pN0 gastric cancer. *Ann Surg Oncol* 2001; **8**: 158-162

21 **Ishida K,** Katsuyama T, Sugiyama A, Kawasaki S. Immunohistochemical evaluation of lymph node micrometastases from gastric carcinomas. *Cancer* 1997; **79**: 1069-1076

22 **Xu X,** Roberts SA, Pasha TL, Zhang PJ. Undesirable cytokeratin immunoreactivity of native nonepithelial cells in sentinel lymph nodes from patients with breast carcinoma. *Arch Pathol Lab Med* 2000; **124**: 1310-1313

23 **Greenson JK,** Isenhart CE, Rice R, Mojzisik C, Houchens D, Martin EW Jr. Identification of occult micrometastases in pericolic lymph nodes of Duke's B colorectal cancer patients using monoclonal antibodies against cytokeratin and CC49. Correlation with long-term survival. *Cancer* 1994; **73**: 563-569

24 **Gould VE,** Bloom KJ, Franke WW, Warren WH, Moll R. Increased numbers of cytokeratin-positive interstitial reticulum cells (CIRC) in reactive, inflammatory and neoplastic lymphadenopathies: hyperplasia or induced expression? *Virchows Arch* 1995; **425**: 617-629

Science Editor Wang XL and Guo SY **Language Editor** Elsevier HK

PO Box 2345, Beijing 100023, China
www.wjgnet.com
wjg@wjgnet.com

ELSEVIER

World J Gastroenterol 2005;11(38):5926-5930
World Journal of Gastroenterology ISSN 1007-9327

Overexpression of decoy receptor 3 in hepatocellular carcinoma and its association with resistance to Fas ligand-mediated apoptosis

Hong-Wei Shen, Shun-Liang Gao, Yu-Lian Wu, Shu-You Peng

Hong-Wei Shen, Shun-Liang Gao, Yu-Lian Wu, Shu-You Peng, Department of Surgery, 2nd Affiliated Hospital of Medical College, Zhejiang University, Hangzhou 310009, Zhejiang Province, China
Correspondence to: Hong-Wei Shen, Department of Surgery, 2nd Affiliated Hospital of Medical College, Zhejiang University, Hangzhou 310009, Zhejiang Province, China. shenhongwei2002@yahoo.com
Telephone: +86-571-87783585 Fax: +86-571-87022776
Received: 2004-03-26 Accepted: 2004-04-13

ABSTRACT

AIM: To characterize the expression and genomic amplification of decoy receptor 3 (DcR3) in hepatocellular carcinoma (HCC) and to evaluate the role of DcR3 in apoptosis.

METHODS: We examined 48 cases of HCC for DcR3 expression by RT-PCR and DcR3 gene amplification by quantitative genomic PCR. DcR3 protein was detected by immunohistochemistry. Terminal deoxynucleotidyl transferase-mediated dUTP digoxigenin nick and labeling (TUNEL) was used to identify the apoptosis cells in tissues. Primary hepatoma cell culture and MTT test were used to evaluate the protection against FasL- and chemical-induced apoptosis by DcR3 expression.

RESULTS: DcR3 mRNA overexpression was detected in 60% HCC (29/48) patients. The occurrence of HCC was not associated with amplification of the gene. One sample base substitution was found in three sites as a sequence in Genbank. The expression of DcR3 in HCC was associated with the apoptotic index (0.067±0.04 *vs* 0.209±0.12, $P<0.01$), size of mass, stage, and infiltration or metastasis (41.2% *vs* 71.0%, 40% *vs* 75%, 51.8% *vs* 84.6%, $P<0.05$). DcR3 expression could protect hepatoma cells against apoptosis induced by FasL, but not by chemicals.

CONCLUSION: These data suggest that in addition to gene amplification there may be another mechanism underlying DcR3 overexpression. The effect of overexpression of DcR3 on the apoptosis of cancer cells may have direct therapeutic implications for the management of HCC.

Key words: DcR3; Hepatocellular carcinoma; Apoptosis

Shen HW, Gao SL, Wu YL, Peng SY. Overexpression of decoy receptor 3 in hepatocellular carcinoma and its association with resistance to Fas ligand-mediated apoptosis. *World J Gastroenterol* 2005; 11(38): 5926-5930
http://www.wjgnet.com/1007-9327/11/5926.asp

INTRODUCTION

DcR3, a member of the tumor necrosis factor receptor superfamily, is amplified and overexpressed in various human cancers as a negative regulator of Fas-mediated apoptosis[1-3]. It was reported that DcR3 can bind to LIGHT and FasL[4-8]. Therefore, DcR3 may act as an inhibitor of LIGHT-induced tumor cell death by blocking LIGHT interaction with its receptors. DcR3 is characterized by a soluble cognate receptor for both LIGHT and FasL/CD95L[9,10]. LIGHT and FasL mediate apoptosis, which is the most common physiological form of cell death and occurs during embryonic development, tissue remodeling, immune regulation, and tumor regression. Abnormalities in FasL and LIGHT system can result in a number of human pathological conditions such as tumor. The cause of DcR3 overexpression in human cancers remains unclear, but its value in tumor escaping from apoptosis and immune surveillance of organism is worthy of special remark.

In contrast, no data are available regarding the expression and amplification of DcR3 gene in HCC. We found that there was a high DcR3 protein level in serum of patients with HCC. In the present study, we examined 48 cases of HCC for DcR3 gene expression by RT-PCR and DcR3 gene amplification by quantitative genomic PCR. The expression of DcR3 protein was detected by immunohistochemistry. *In situ* TUNEL was used to identify the apoptosis cells in tissues of HCC. Primary hepatoma cell culture and MTT test were used to evaluate the role of DcR3 expression in protection against FasL and chemical-induced cell death. The findings in our study suggest that in addition to gene amplification there may be another mechanism underlying DcR3 gene expression. The effect of overexpression of DcR3 on the apoptosis of cancer cells may have direct therapeutic implications for the management of HCC, which remains a major unsolved health problem throughout the world.

MATERIALS AND METHODS

Quantitative genomic PCR

Quantitative genomic PCR was performed as previously described[2,11]. Genomic DNA was isolated from fresh tissues of HCC. Quantitative PCR was carried out by a lightcycler. Primers for DcR3 were designed using an intron sequence to avoid amplification from DcR3 mRNA. The DcR3-specific primers were 5'-CTTCTTCGCGCACGCTG-3' (sense) and 5'-ATCACGCCGGCACCAG-3' (antisense), and the fluorogenic probe was 5'-FAM-ACACGATGCGTGC-TCCAAGCAGAA-TAMARA-3'. The beta-globin primers were 5'-ACCCTTAGGCTGCTGGTGG-3' (sense) and 5'-GGAGTGGACAGATCCCCAAA-3' (antisense), and the

fluorogenic probe was 5'-FAM-CTACCCTTGGACCCA-GAGGTTCTTTGAGTC-TAMARA-3'. For each run, DNA isolated from normal matched tissues was used for comparison.

RT-PCR analysis

For RT-PCR analysis, total RNA was isolated using Trizol (Life Technologies, Inc.) from the tumor and its adjacent normal tissues of 48 HCC cases. RNA was converted to cDNA by reverse transcription and amplified for 35 cycles by PCR. Primers used for amplification of the DcR3 fragment were according to the RNA sequence of DcR3. Beta-actin was used as an internal control for RNA integrity. The DcR3-specific primers were 5'-TCCACCGCGCCACTACAC-3' (sense) and 5'-ACGGCACGCTCACACTCC-3' (antisense). The beta-actin specific primers were 5'-TTCCAGCCT-TCCTTCCTGG-3' (sense) and 5'-TTGCGCTCAGG-AGGAGCA AT-3'(antisense). PCR products were run on 2% agarose gel, stained with ethidium bromide, and visualized by UV illumination. RT-PCR product of one sample was sequenced to show reliability of the reaction.

Immunohistochemistry

HCC tissues were obtained from the Surgical Department of the Second Affiliated Hospital of Zhejiang University. Four micrometer-thick formalin-fixed and paraffin-embedded sections were deparaffinized and treated in microwave with citrate buffer, pH 6.0 (three times each for 5 min) for antigen retrieval and incubated for 15 min in 30 mL/L H_2O_2 Tris-buffered saline (TBS), pH 7.4 to block endogenous peroxidase activities. The sections were then incubated for 10 min at room temperature with blocking solution. Each section was incubated with anti-DcR3 antibody diluted 1:5000 for 30-60 min at room temperature. Bound antibodies were detected with the peroxidase-labelled streptavidin-biotin method, and stained with diaminobenzidine. Counterstaining was performed with Mayer's heamatoxylin, and the sections were mounted.

As a negative control for DcR3 protein expression, the primary antibody was replaced by normal non-immune rabbit serum. There were no known normal tissues expressing DcR3 protein, and no positive control was set up in the DcR3 immunostaining.

In situ TUNEL

HCC tissues were obtained from the Surgical Department of the Second Affiliated Hospital of Zhejiang University. Four micrometer-thick formalin-fixed and paraffin-embedded sections were deparaffinized and treated in microwave with citrate buffer, pH 6.0 (three times each for 5 min) for antigen retrieval and incubated for 15 min in 30 mL/L H_2O_2 TBS, pH 7.4 to block endogenous peroxidase activities. Each section was incubated with TUNEL reaction solution (Roche) for 60 min at 37 ℃, and washed three times with PBS. The signal translation solution was added to the slides for 30 min at 37 ℃. After being washed three times with PBS, each section was stained with freshly prepared diaminobenzidine. Counterstaining was performed with Mayer's heamatoxylin, and the sections were mounted.

As a negative control for *in situ* TUNEL, the TUNEL reaction solution was replaced by TBS. As a positive control, a slide (Roche) in the kit was used together with the samples.

FasL-induced apoptosis and drug-induced cell death of hepatoma cells

Hepatoma cells were obtained from patients with HCC who underwent surgery for tumor resection. After tumor removal, the tissues were placed immediately in petri dishes, minced mechanically, and digested by collagenase (3 h, 37 ℃). Subsequently, the dissociated cells were filtered through 100 μm of cell strainers to remove tissue debris. After centrifugation and lysis of erythrocytes by treatment with hypotonic water, the hepatoma cells were washed and resuspended in full medium (CAM).

The hepatoma cells were cultured with serum-free CAM in 96-well plates. A total 5×10^4 cells were seeded per well. Then 3 ng/mL FasL and ADM, MMC, and GEMZAR of 4-, 1- and 0.25-fold drug concentrations respectively were used to detect the cytotoxic effect on primary hepatoma cells. Each concentration and blank control were put in three parallel wells. The hepatoma cells were co-cultured with FasL or drugs in serum-free CAM for 5 d. The survival rate of the cells was detected with MTT method.

Statistical analysis

Results were expressed as mean±SE. Differences between groups were examined for statistical significance using analysis of variance (ANOVA) and *t*-test. $P<0.05$ was considered statistically significant.

[redacted]

We report that DcR3 mRNA is overexpressed in a substantial percentage of HCC, and that this overexpression can occur in the absence of detectable DcR3 gene amplification. In a case of sequence analysis, three base differences in the DcR3 gene of HCC were identified. The expression of DcR3 in HCC shows a relationship with the apoptosis index of the tissues of cancer. We also demonstrate that the hepatoma cells expressed DcR3 are protected from FasL-induced apoptotic cell death, but not the cell death induced by chemicals.

Relationship between clinical data and DcR3 mRNA expression

The mean age of cancer patients was 58.3±14 years. The clinical and pathological features of the total 48 cases were collected and summarized. The relationship between the DcR3 mRNA expression and the clinical and pathological features was analyzed. DcR3 mRNA expression in HCC showed a relationship with size of the mass, TNM stage and infiltration or metastasis of the tumor ($P<0.05$), but no relationship with membrane of the tumor, cancer embolus, and number of the tumor nodes (Table 1).

Overexpression of DcR3 mRNA and protein in HCC

Twenty-nine of 48 HCC cases were positive for DcR3 mRNA expression (Figure 1A). The ratio of positive expression was 60.4% (29/48). No positive expression was detected in adjacent normal tissues. As the level of DcR3 mRNA appeared to be elevated in HCC, we investigated

Table 1 Relationship between DcR3 mRNA expression and clinical and pathological features of HCC (n = 48)

Features	n	DcR3 mRNA expression (%)	P
Size of mass			
≤5 cm	17	41.2 (7/17)	<0.05
>5 cm	31	71.0 (22/31)	
Number of node			
Single	32	53.1 (17/32)	>0.05
Multiple	16	75 (12/16)	
Membrane of the mass			
Intact	14	50 (7/14)	>0.05
Not intact	34	64.7 (22/34)	
Cancer embolus			
Negative	38	60.5 (23/38)	>0.05
Positive	10	60 (6/10)	
TNM stage			
Stage I, II	20	40 (8/20)	<0.05
Stage III, IV	28	75 (21/28)	
Infiltration or metastasis			
Negative	35	51.4 (18/35)	<0.05
Positive	13	84.6 (11/13)	

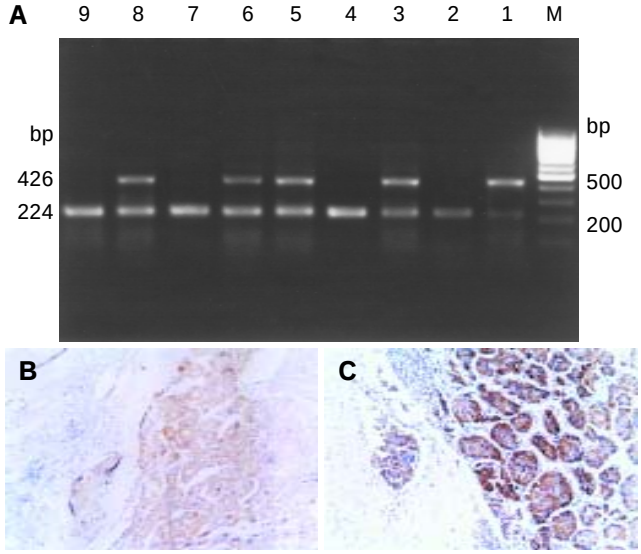

Figure 1 DcR3 gene expression in nine representative HCC samples. A: DcR3 gene mRNA expression detected by RT-PCR. Lanes 1,3,5,6, and 8: positive mRNA expression; lanes 2,4,7 and 9: negative expression. B, C: DcR3 protein expression detected by immunohistochemistry. (Magnification 100×).

whether it was true for DcR3 at the protein level. The expression of DcR3 protein was detected in five cases of HCC by immunohistochemistry. An obvious positive staining signal of DcR3 protein was detected in three out of five HCC cases (Figures 1B, and C). RT-PCR showed positive signals only in cancer cells. Furthermore, we found a high DcR3 protein level in serum of HCC patients by ELISA with anti-DcR3 antibody.

DcR3 overexpression without DcR3 gene amplification

DcR3 gene amplification was proposed to be the mechanism for DcR3 overexpression to promote tumor survival in lung and colon cancer. To determine whether DcR3 overexpression was due to gene amplification, quantitative PCR was carried out on genomic DNA from all the patients, with the relative number DcR3 gene copies determined by normalization of the beta-globin gene. Unexpectedly, the amplification was 2-fold higher only in 7 of 48 tumors patients than that in 29 of 48 tumors patients with positive DcR3 mRNA expression. Among the 29 HCC cases with postive DcR3 mRNA expression, the amplification was 2-fold higher only in six cases. From the result of sequence analysis, we found accidentally that there were three bases different from the DcR3 mRNA sequence in GenBank (Figure 2).

Table 2 Survival rate of hepatoma cells cultured in chemicals with different concentration (mean±SE)

	ADM	P	MMC	P	GENZAR	P
4×	51±0.2		44.6±0.19		52.2±0.17	
1×	72.7±0.18	<0.01	64.8±0.16	<0.01	66.7±0.17	<0.01
0.25×	82.6±0.17		81.8±0.16		77.9±0.18	

Apoptosis index and DcR3 mRNA expression in HCC

In situ TUNEL was used to identify the apoptosis cells in 29 tissue specimens of HCC. The apoptosis index was calculated by counting the positive cells in five visual fields under light microscope at 400-fold magnification. DcR3 mRNA positive expression was detected in 19 out of 29 HCC cases. The apoptosis index of the 29 HCC cases ranged from 0.021 to 0.362. The apoptosis index of the 19 patients with positive DcR3 mRNA expression was significantly lower than that (0.067±0.04) of the 10 patients with negative DcR3 mRNA expression (0.209±0.12) (P<0.01).

Expression of DcR3 protected hepatoma cells from FasL-induced apoptosis

Hepatoma cells of 19 HCC cases were studied. After treatment with FasL, the cell survival rate (CSR) of 10 HCC cases with DcR3 mRNA expression (83.7%±0.18) was significantly higher than that of another eight HCC cases without DcR3 expression (62.2%±0.16) (P<0.01).

From 0.25- to 4-fold drug concentrations, the hepatoma cell death induced by ADM, MMC, and GEMZAR had a positive relationship with the drug concentration (Table 2, P<0.01). But the effect of three drugs between hepatoma cells with positive and negative DcR3 mRNA expression had no significant difference (Table 3, P>0.05).

[illegible]

DcR3 gene is mapped on chromosome 20q13.3, a region known to be associated with gene amplification and rearrangement in human cancer[12,13]. Numerous reports have shown genomic amplifications of 20q13 in breast[14], gastric[15], colon, and lung[12] tumors and neuroblastomas[16]. Pitti *et al*.[1], found that the DcR3 gene is amplified in approximately half of human lung tumors and human colon adenocarcinomas and that DcR3 receptor overexpression might also occur, conferring growth advantage on tumor cells by blocking FasL-induced cell death. In this paper, we demonstrated DcR3 mRNA and protein overexpression in HCC. From the result our data, we found that there were only 20.7% (6/29) genomic amplifications in HCC with positive DcR3 mRNA

Table 3 Comparision of hepatoma cell death induced by chemicals between groups with negative and positive DcR3 expression (mean±SE)

	Survival rate of hepatoma cells					
	4-fold	*P*	1-fold	*P*	0.25-fold	*P*
ADM						
DcR3 negative	41.8±0.18	>0.05	65.9±0.17	>0.05	74.5±0.19	>0.05
DcR3 positive	58.4±0.19		78.1±0.17		89.1±0.12	
MMC						
DcR3 negative	36.2±0.07	>0.05	58.6±0.12	>0.05	77.9±0.18	>0.05
DcR3 positive	51.3±0.23		69.7±0.18		85±0.15	
GENZAR						
DcR3 negative	45.7±0.16	0.146	62.8±0.17	0.396	73.1±0.18	0.332
DcR3 positive	57.4±0.16		69.8±0.17		81.8±0.19	

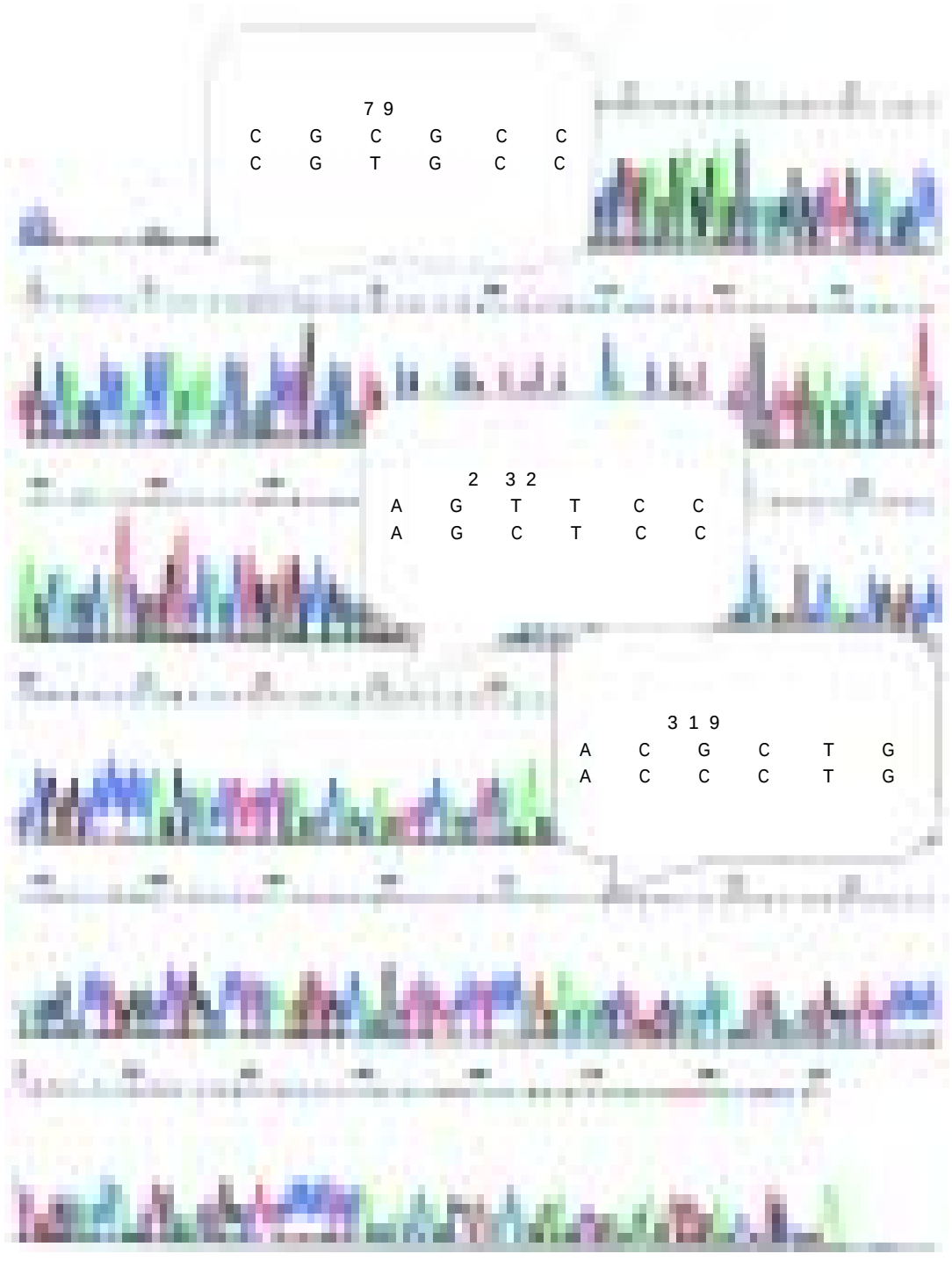

Figure 2 Sequence of DcR3 gene mRNA in HCC detected by sequencing RT- PCR product.

expression, suggesting that overexpression of DcR3 gene occurs without genomic amplification. Bai *et al*.[2], examined DcR3 genomic DNA, mRNA, and protein levels in a series of human gastrointestinal tract tumors and found that DcR3 gene is overexpressed in a substantial number of tumors in which gene amplification could not be detected by fluorescence *in situ* hybridization or quantitative genomic PCR. The identification of tumors with high-level DcR3 overexpression but no significant gene amplification raises the possibility that DcR3 protein overexpression might be an early event in oncogenesis, possibly driving selection of gene amplification. The cause of nongenomic DcR3 overexpression remains unclear. From the result of sequence analysis, we found accidentally that there were three bases different from the DcR3 mRNA sequence in GenBank. The base difference might represent a point mutation or a gene polymorphism in HCC. The meaning and mechanism of the base differences in HCC remain unclear and still need further work.

Since DcR3 is a soluble protein, it can be easily detected in serum with DcR3 antibody. The protein overexpression is likely to be the eventual choice of diagnostic method for DcR3. We found a high DcR3 protein level in serum of the HCC patients by ELISA with anti-DcR3 antibody. Although the diagnostic value of DcR3 protein still needs an overall evaluation, at least it can be used as an auxiliary diagnostic method in combination with other methods for HCC.

Fas-induced apoptosis plays a role in the hepatic pathology of Wilson's disease, in which Fas and FasL are induced in hepatocytes overloaded with copper[17,18]. Bai *et al*.[2,19-21], used an model of copper-induced hepatocellular injury to test whether expression of DcR3 could protect cells from apoptosis and found that DcR3 might indeed plays a physiologically important role in the regulation of apoptosis. In this study, we found that DcR3 mRNA expression in HCC showed a significant relationship with the apoptosis index. Patients with a positive DcR3 mRNA expression had a low apoptosis index compared to those with a negative expression. The difference in apoptosis index between positive and negative DcR3 mRNA expression groups showed a statistic significance. suggesting that DcR3 protein on apoptosis shows its therapeutic value of down-regulating DcR3 overexpression by genetic or immunotherapeutic means.

□□□□□□□□□□

1 **Pitti RM**, Marsters SA, Lawrence DA, Roy M, Kischkel FC, Dowd P, Huang A, Donahue CJ, Sherwood SW, Baldwin DT, Godowski PJ, Wood WI. Genomic amplification of a decoy receptor for Fas ligand in lung and colon cancer. *Nature* 1998; **396**: 699-703

2 **Bai C**, Connolly B, Metzker ML, Hilliard CA, Liu X, Sandig V, Soderman A, Galloway SM, Liu Q, Austin CP, Caskey CT. Overexpression of M68/DcR3 in human gastrointestinal tract tumors independent of gene amplification and its location in a four-gene cluster. *Proc Natl Acad Sci USA* 2000; **97**: 1230-1235

3 **Roth W**, Isenmann S, Nakamura M, Platten M, Wick W, Kleihues P, Bahr M, Ohgaki H, Ashkenazi A, Weller M. Soluble decoy receptor 3 is expressed by malignant gliomas and suppresses CD95 ligand-induced apoptosis and chemotaxis. *Cancer Res* 2001; **61**: 2759-2765

4 **Yu KY**, Kwon B, Ni J, Zhai Y, Ebner R, Know BS. A newly identified member of tumor necrosis factor receptor superfamily (TR6) suppresses LIGHT-mediated apoptosis. *J Biol Chem* 1999; **274**: 13733-13736

5 **Ohshima K**, Haraoka S, Sugihara M, Suzumiya J, Kawasaki C, Kanda M, Kikuchi M. Amplification and expression of a decoy receptor for fas ligand (DcR3) in virus (EBV or HTLV-I) associated lymphomas. *Cancer Lett* 2000; **160**: 89-97

6 **Otsuki T**, Tomokuni A, Sakaguchi H, Aikoh J, Matsuki T, Isozaki Y, Hyodoh F, Ueki H, Kusaka M, Kita S, Ueki A. Over-expression of the decoy receptor 3 (DcR3) gene in peripheral blood mononuclear cells (PBMC) derived from silicosis patients. *Clin Exp Immunol* 2000; **119**: 323-327

7 **Ibrahim SM**, Ringel J, Schmidt C, Ringel B, Muller P, Koczan D, Thiesen HJ, Lohr M. Pancreatic adenocarcinoma cell lines show variable susceptibility to TRAIL-mediated cell death. *Pancreas* 2001; **23**: 72-79

8 **Shen HW**, Wu YL, Peng SY. Overexpression and genomic amplification of decoy receptor 3 in hepatocellular carcinoma and significance. *Zhonghua Yixue Zazhi* 2003; **83**: 744-747

9 **Wu Y**, Han B, Shen H. Clinical significance of detecting elevated serum DcR3/TR6/M68 in malignant tumor patients. *Int J Cancer* 2003; **105**: 724-732

10 **Tsuji S**, Hosotani R, Yonehara S. Endogenous decoy receptor 3 blocks the growth inhibition signals mediated by Fas ligand in human pancreatic adenocarcinoma. *Int J Cancer* 2003; **106**: 17-25

11 **Chen J**, Zhang L, Kim S. Quantification and detection of DcR3, a decoy receptor in TNFR family. *J Immunol Methods* 2004; **285**: 63-70

12 **Muleris M**, Almeida A, Gerbault-Seureau M, Malfoy B, Dutrillaux B. Identification of amplified DNA sequences in breast cancer and their organization within homogeneously staining regions. *Genes Chromosomes Cancer* 1995; **14**: 155-163

13 **Shinomiya T**, Mori T, Ariyama Y, Sakabe T, Fukuda Y, Murakami Y, Nakamura Y, Inazawa J. Comparative genomic hybridization of squamous cell carcinoma of the esophagus: the possible involvement of the DPI gene in the 13q34 amplicon. *Genes Chromosomes Cancer* 1999; **24**: 337-344

14 **Schwendel A**, Richard F, Langreck H, Kaufmann O, Lage H, Winzer KJ, Petersen I, Dietel M. Chromosome alterations in breast cancer carcinomas: frequent involvement of DNA losses including chromosomes 4q and 21q. *Br J Cancer* 1998; **78**: 806-811

15 **Sakakura C**, Mori T, Sakabe T, Ariyama Y, Shinomiya T, Date K, Hagiwara A, Yamaguchi T, Takahashi T, Nakamura Y, Abe T, Inazawa J. Gains, losses, and amplifications of genomic materials in primary gastric cancers analyzed by comparative genomic hybridization. *Genes Chromosomes Cancer* 1999; **24**: 299-305

16 **Altura RA**, Maris JM, Li H, Boyett JM, Brodeur GM, Look AT. Novel regions of chromosomal loss in familial neuroblastoma by comparative genomic hybridization. *Genes Chromosomes Cancer* 1997; **19**: 176-184

17 **Kondo T**, Suda T, Fukuyama H, Adachi M, Nagata S. Essential roles of the Fas ligand in the development of hepatitis. *Nat Med* 1997; **3**: 409-413

18 **Strand S**, Hofmann WJ, Grambihler A, Hug H, Volkmann M, Otto G, Wesch H, Mariani SM, Hack V, Stremmel W, Krammer PH, Galle PR. Hepatic failure and liver cell damage in acute Wilson's disease involve CD95 (APO-1/Fas) mediated apoptosis. *Nat Med* 1998; **4**: 588-593

19 **Wu Y**, Han B, Luo H. DcR3/TR6 effectively prevents islet primary nonfunction after transplantation. *Diabetes* 2003; **52**: 2279-2286

20 **Shi G**, Wu Y, Zhang J. Death decoy receptor TR6/DcR3 inhibits T cell chemotaxis *in vitro* and *in vivo*. *J Immunol* 2003; **171**: 3407-3414

21 **Yang CR**, Hsieh SL, Teng CM. Soluble decoy receptor 3 induces angiogenesis by neutralization of TL1A, a cytokine belonging to tumor necrosis factor superfamily and exhibiting angiostatic action. *Cancer Res* 2004; **64**: 1122-1129

Science Editor Wang XL **Language Editor** Elsevier HK

PO Box 2345, Beijing 100023, China
www.wjgnet.com
wjg@wjgnet.com

ELSEVIER

World J Gastroenterol 2005;11(38):5931-5937
World Journal of Gastroenterology ISSN 1007-9327

Expressions of inducible nitric oxide synthase and matrix metalloproteinase-9 and their effects on angiogenesis and progression of hepatocellular carcinoma

Min-Hua Sun, Xi-Chun Han, Ming-Ku Jia, Wei-Dong Jiang, Min Wang, Hong Zhang, Gang Han, Yi Jiang

Min-Hua Sun, Xi-Chun Han, Ming-Ku Jia, Wei-Dong Jiang, Min Wang, Hong Zhang, Gang Han, Yi Jiang, Department of General Surgery, Second Hospital, Jilin University, Changchun 130041, Jilin Province, China
Correspondence to: Professor Xi-Chun Han, Department of General Surgery, Second Hospital, Jilin University, Changchun 130041, Jilin Province, China. hanxichun@medmail.com.cn
Telephone: +86-431-8796988 Fax: +86-431-8934741
Received: 2005-03-12 Accepted: 2005-04-02

Abstract

AIM: To determine the expressions of inducible nitric oxide synthase (iNOS) and matrix metalloproteinase-9 (MMP-9) in hepatocellular carcinoma (HCC) and to investigate the relationship between iNOS and MMP-9 expression and their effects on angiogenesis and progression of HCC.

METHODS: In this study, we examined iNOS, MMP-9, and CD34 expression in specimens surgically removed from 32 HCC patients and 7 normal liver tissues by immunohistochemical staining. Meanwhile, microvessel density (MVD) was determined as a marker of angiogenesis by counting CD34-positive cells.

RESULTS: The positive rates of iNOS and MMP-9 expression were 71.88% (23/32) and 78.13% (25/32) in HCC. MMP-9 expression was significantly correlated with tumor size, capsule status, TNM stage, and risk of HCC recurrence ($P = 0.032$, $P = 0.033$, $P = 0.007$, and $P = 0.001$, respectively). There was also a significant relationship between iNOS expression and capsule status and risk of HCC recurrence ($P = 0.049$ and $P = 0.004$, respectively), but no correlation between iNOS expression and tumor size and TNM stage. There was a positive association between MVD and TNM stage and risk of HCC recurrence ($P = 0.037$ and $P = 0.000$, respectively). The count of MVD was significantly different in different iNOS and MMP-9 immunoreactivity groups ($F = 17.713$ and 17.097, $P = 0.000$ and $P = 0.000$, respectively). The examination of Spearman's rank correlation coefficient showed that there was a significant positive correlation between MVD and iNOS, MMP-9 immunoreactivity ($r = 0.754$ and 0.751, $P = 0.000$ and $P=0.000$, respectively). There was also a significant association between MMP-9 and iNOS expression in HCC ($P = 0.010$).

CONCLUSION: Nitric oxide (NO) produced by iNOS could modulate MMP-9 production and therefore contribute to tumor cell angiogenesis and invasion and metastasis in HCC. The strong expression of iNOS and MMP-9 in HCC may be helpful in evaluating the recurrence of HCC, predicting poor prognosis. For patients with strong expression of MMP-9 and iNOS, the optimal treatment scheme needs to be selected.

Key words: Inducible nitric oxide synthase; Matrix metalloproteinase-9; Angiogenesis; Hepatocellular carcinoma

Sun MH, Han XC, Jia MK, Jiang WD, Wang M, Zhang H, Han G, Jiang Y. Expressions of inducible nitric oxide synthase and matrix metalloproteinase-9 and their effects on angiogenesis and progression of hepatocellular carcinoma. *World J Gastroenterol* 2005; 11(38): 5931-5937
http://www.wjgnet.com/1007-9327/11/5931.asp

INTRODUCTION

Hepatocellular carcinoma (HCC) is a highly vascular tumor characterized by a propensity for vascular invasion and distant metastasis. Angiogenesis is a prerequisite for tumor growth and metastasis[1]. In the process of invasion and metastasis of tumor cells, destruction of the extracellular matrix (ECM) is an essential initial step. Among the enzymes responsible for ECM degradation, several studies have shown a critical role played by matrix metalloproteinases (MMPs)[2]. MMP-9 (gelatinase B, 92-ku type IV collagenase) is capable of degrading the main components of the ECM, types IV and V collagen and gelatin[3-6]. Thus, its activities are closely related to the angiogenesis and invasiveness and metastasis of tumor cells[7,8]. However, it is secreted by cells as an inactive form, proMMP-9, which is then activated through an enzymatic cascade involving the generation of plasmin by urokinase-type plasminogen activator (u-PA)[9-12].

Nitric oxide (NO) is an important bioactive agent and a signaling molecule and may contribute to the pathogenesis of cancer[13]. Three distinct isoforms of NOS catalyze the formation of NO. Endothelial nitric oxide synthase (eNOS) and neuronal nitric oxide synthase (nNOS) are constitutively expressed in different tissues, whereas inducible nitric oxide synthase (iNOS) is related to a high-output pathway and is responsible for various pathological processes[14]. Although overexpression of iNOS has been demonstrated in various human neoplasms, such as colorectal cancer[15], pancreatic

cancer[16], and breast cancer[17], its exact function in tumor biology is complex and remains to be fully defined. During the initiation of tumor growth, natural killer cells and macrophages kill tumor cells by a NO-mediated mechanism[18]. However, NO may also suppress the antitumor defense, promote tumor angiogenesis and blood flow in the tumor neovasculature, and enhance tumor growth, invasion and metastasis[18]. Recently, investigators have tended to attribute NO-mediated stimulation of invasiveness to an alteration in the balance between the productions of MMPs and TIMPs[19-21]. Since NO has been assessed for the ability to upregulate u-PA in endothelial cells of post capillary venules during the process of NO-mediated stimulation of angiogenesis[22], the u-PA can convert plasminogen to plasmin, which can activate numerous MMPs.

There is evidence that NO produced by iNOS enhances the activity of MMP-9[19-21]. Both iNOS and MMP-9 expression have been reported to be increased in bone and joint disease and cardiovascular disease[23-25]. However, the relationship between them in tumors has been very seldom studied. To determine the role of iNOS and MMP-9 in HCC, we compared their expressions by the immunohistochemical method.

□□□□□□□□□ □□□ □□□□□□□

Materials

Thirty-two patients (24 males and 8 females, ranging in age from 16 years to 69 years, mean 53 years) who had undergone curative hepatectomy for HCC at the Second Hospital, Jilin University, and Tumor Hospital, Jilin Province, between May 2001 and October 2002 were involved in this study. As controls, seven normal adult liver specimens were wedge biopsies obtained during surgeries from patients with rupture of liver and cavernous hemangioma of liver. Of the 32 patients, 21 were positive for hepatitis B surface antigen (HBsAg), while 11 were infected with neither hepatitis C virus nor HBV. Five patients showed tumor thrombi in the portal vein, 3 patients showed lymph node metastasis in the porta hepatis, 14 patients showed microsatellite nodules. The patients were regarded as a high-risk group for HCC recurrence, if any one of the following factors existed: lymph node metastasis of the porta hepatis; tumor thrombi in the portal vein; surrounding the primary tumor two or more microsatellite tumor nodules were present in the same lobe of liver, or the microsatellite tumor nodules scattered over the two or more liver lobes. Eighteen cases were in high recurrence-risk group and 14 cases in low recurrence-risk group. The histological grade of malignancy was classified according to the criteria of World Health Organization. There were 17 cases of G1, 9 cases of G2, and 6 cases of G3. The degree of TNM classification was decided according to the general rules for the clinical and pathological study of primary liver tumor. One patient was staged I, 15 patients were staged II, and 16 patients were staged III. None of our patients received preoperative treatments, such as chemotherapy or embolization therapy. The resected surgical specimens were fixed in 10% buffered formalin and embedded in paraffin. Four-micrometer-thick sections were prepared for H&E and immunohistochemical staining.

Methods

Immunohistochemistry Immunostaining was performed according to the avidin-biotin-peroxidase complex method. Sections were dewaxed in xylene, and dehydrated in ethanol, and then heated at 98 ℃ in EDTA-retrieved solution for the antigens. Endogenous peroxidase was blocked by 3% hydrogen peroxide for 60 min at room temperature. The samples were incubated for 20 min at room temperature with a protein-blocking solution containing 5% normal horse serum and 1% normal goat serum. Subsequently, slides were incubated with primary anti-iNOS rabbit polyclonal antibody (Boster Bio, Wuhan) at 1:200 dilution for 60 min at room temperature, mouse anti-human MMP-9 mAb (Maixin Bio, Fuzhou) at 1:200 dilution overnight at 4 ℃, rat anti-mouse CD34 mAb (Maixin Bio, Fuzhou) at 1:100 dilution for 2 h at room temperature. Slides were then treated with a biotin-conjugated secondary antibody for 30 min followed by incubation with peroxidase-conjugated streptavidin for 60 min at room temperature. All steps were followed by washing in PBS. Finally, the sections were stained with a freshly prepared diaminobenzidine solution for 5 min and then counterstained with Mayer's hematoxylin. For CD34 staining, counterstaining was not done. As a negative control, PBS was used instead of the primary antibody. Known immunostaining-positive slides were used as positive controls.

Evaluation of iNOS and MMP-9 expression

Two independent observers screened all sections as semiqu-antitative evaluation of iNOS and MMP-9 immunostaining. The immunoreactive score was determined by the sum of intensity and extension of staining[26]. The intensity of staining was scored on a scale of 0-3, in which 0, negative staining; 1, weakly positive staining; 2, moderately positive staining; and 3, strongly positive staining. The extent of distribution of positive cells was estimated on a scale of 0-3, in which 0, negative or positive staining in 1-5% of cells; 1, positive staining in 6-25% of cells; 2, positive staining in 26-50% of cells; 3, positive staining in 51-100% of cells. The combined staining score (intensity+extension) $\geqslant$2 was considered as positive staining. The diagnosed grades accorded to the sum of two scores, -: 0-1; +: 2; ++: 3-4; and +++: >5.

Quantification of MVD

Microvessel density (MVD) was evaluated by two independent observers who were blinded to the patients' clinicopathologic data after sections were immunostained with anti-CD34 antibodies according to the procedure described by Weidner *et al*.[27]. In all tumors collected, the density of microvessels was higher in the peripheral tumor tissue close to the margin than in the central areas. Therefore, the peripheral tissue sections were used for counting of microvessels. Any brown-stained endothelial cells or endothelial cell clusters that was clearly separated from adjacent microvessels, tumor cells, or other stromal cells were counted as one microvessel. For MVD estimation, at low power magnification (×40 and ×100), the tissue sections were screened and five areas with the highest vessel density (hot spots) were selected. Microvessel counts of these areas were performed at a high power field (×200, the surface area of every vision

field being 0.708 mm^2) and the maximum microvessel count of the five richest vascular areas was taken as the MVD.

Statistical analysis

Qualitative data were expressed as the number of cases and quantitative data as mean±SD. These data were analyzed with the SPSS (version11.5) software. The qualitative data were compared using χ^2 test and Fisher's exact test, and the quantitative data were compared using one-way analysis of variance and independent sample *t*-test. Correlation between factors was evaluated using the Spearman's rank correlation coefficient. $P<0.05$ was considered statistically significant.

RESULTS

Correlation between MMP-9 and clinicopathologic parameters in HCC

The incidence of positive MMP-9 expression in cases with their tumor being more than 5 cm, their tumor capsules being not integral or their tumor without capsules was significantly higher than that in those with their tumor measured either less than or equal to 5 cm in diameter and their tumor capsules being integral ($\chi^2 = 5.283$ and $\chi^2 = 5.258$, $P = 0.032$ and $P = 0.033$, respectively). The incidence of MMP-9 expression was also significantly higher in high-risk group for HCC recurrence and TNM III stage group than in low-risk group for HCC recurrence and TNM I-II stage group ($\chi^2 = 11.160$ and $\chi^2 = 8.680$, $P = 0.001$ and $P = 0.007$, respectively). At the same time no significant correlation was demonstrated between the expression of MMP-9 and other parameters, such as sex, age, ascites, hepatitis B, cirrhosis of liver, value of AFP, and grade of histology (Table 1).

Correlation between iNOS and clinicopathologic parameters in HCC

The positive immunohistochemical staining for iNOS in cases with their tumor capsules being not integral or their tumors without capsules was significantly higher than that in those with their tumor capsules being integral ($\chi^2 = 4.652$, $P = 0.049$). The iNOS immunoreactivity was significantly higher in high-risk group for HCC recurrence than in low-risk group ($\chi^2 = 10.043$, $P = 0.004$). But there was no significant difference between iNOS expression and each of the parameters such as sex, age, value of AFP, TNM stage, tumor size, grade of histology, hepatitis B, cirrhosis

Table 1 Correlation between clinicopathologic parameters and MMP-9, iNOS expression and MVD in HCC

Variables	*n* (*n*=32)	MMP-9		*P*	iNOS		*P*	MVD	*P*
		+[1] (*n* = 25)	– (*n* = 7)		+ (*n* = 23)	– (*n* = 9)		(mean±SD)	
Sex									
Male	24	20	4		17	7		68.50±17.38	
Female	8	5	3	NS[2]	6	2	NS	80.64±29.51	NS
Age (yr)									
>50	19	17	2		16	3		76.11±18.86	
≤50	13	8	5	NS	7	6	NS	64.86±23.35	NS
Size of HCC (cm)									
>5.0	21	19	2		17	4		74.48±18.16	
≤5.0	11	6	5	0.032	6	5	NS	62.91±20.63	NS
Tumor capsule									
Present integrally	15	9	6		8	7		67.73±25.72	
Absent or not integral	17	16	1	0.033	15	2	0.049	74.88±16.31	NS
HbsAg[3]									
+	21	18	3		16	5		75.48±19.02	
–	11	7	4	NS	7	4	NS	64.00±23.96	NS
Cirrhosis									
+	19	16	3		15	4		72.79±16.30	
–	13	9	4	NS	8	5	NS	64.46±15.95	NS
Ascites									
+	6	4	2		3	3		64.83±22.73	
–	26	21	5	NS	20	6	NS	73.08±20.99	NS
Serum AFP[4] (μg/L)									
≤400	13	10	3		11	2		68.84±21.77	
>400	19	15	4	NS	12	7	NS	75.46±20.53	NS
Histological grade									
G1	17	12	5		11	6		65.94±19.14	
G2	9	7	2		6	3		73.56±20.97	
G3	6	6	0	NS	6	0	NS	84.33±24.48	NS
TNM stage									
I–II	16	9	7		9	7		63.81±21.78	
III	16	16	0	0.007	14	2	NS	79.25±18.08	0.037
Risk of recurrence									
High-risk group	18	18	0		17	1		82.56±17.29	
Low-risk group	14	7	7	0.001	6	8	0.004	57.36±17.19	0.000

[1]Score≥2: positive staining (+); [2]NS: not significant; [3]HBsAg: hepatitis B surface antigen; [4]AFP: serum α-fetoprotein.

of liver, and ascites in HCC (Table 1).

CD34 expression and its relationship to clinicopathologic parameters in HCC

No CD34 staining was found in the sinusoids of seven healthy liver tissues. In HCC tissues from 32 cases, sinusoid-like tumor vessels reacted intensively with anti-CD34 (mean±SD, 71.53±21.19; range, 31-126), and the positive staining of CD34 distributed with a diffuse pattern or an intensive cluster pattern and was defined as the buffy zonale staining on the cell membrane (Figure 1). In nonmalignant tissue, anti-CD34 stainings were confined to vessels of the portal triad with weak staining in few of the sinusoids at the periportal area in case of cirrhosis or chronic hepatitis. There was a significant difference in MVD between TNM III stage group (79.25±18.08) and TNM I-II stage group (63.81±21.78, t = 2.182, P = 0.037). There was also a significant difference in MVD between high-risk group for HCC recurrence (82.56±17.29) and low-risk group (57.36±17.19, t = 4.100, P = 0.000). But no significant association was noted between MVD and other clinicopathologic features (Table 1).

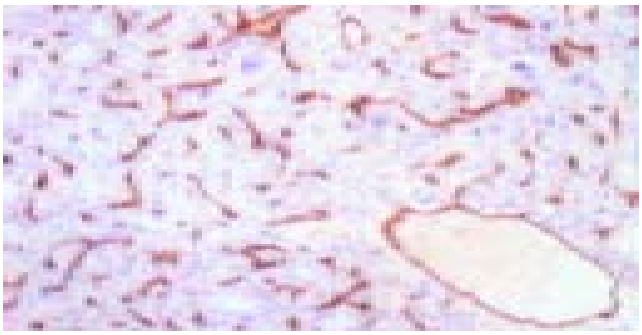

Figure 1 Immunohistochemical staining for CD34 in HCC (×100).

Relationship between iNOS, MMP-9 and MVD in HCC

As shown in Table 2, tumors were divided into three groups based on the degree of immunoreactivity. Along with the increase of immunoreactivity grades, the incidence of iNOS and MMP-9 expression enhanced gradually. The count of MVD was significantly different in different iNOS and MMP-9 immunoreactivity groups (F = 17.713 and 17.097, P = 0.000 and P = 0.000, respectively). The examination of Spearman's rank correlation coefficient showed that there was a significant positive correlation between iNOS, MMP-9 immunoreactivity and MVD (r = 0.754 and 0.751, P = 0.000 and P = 0.000, respectively).

Table 2 Relationship between MVD and MMP-9, iNOS staining intensity in HCC (mean±SD)

Degree of staining	n	iNOS	n	MMP-9
–	9	49.33±11.24	7	48.57±14.62
++	11	71.82±15.06[b]	8	62.50±11.98
+++	12	87.92±16.49[b]	17	85.24±16.02[b,d]

[b]P<0.01 *vs* degree of staining (–), [d]P<0.01 *vs* degree of staining (++).

Correlation between MMP-9 and iNOS expression in 32 HCC tissues

There was no MMP-9 staining in the normal liver tissue. MMP-9 immunoreactivity was detected in 25 (78.13%) of 32 HCCs. MMP-9 was mainly localized in cytoplasm and cytoplasmic membranes and its staining was detected in vascular endothelial cells, bile ducts, HCC cells, and stromal fibroblasts (Figures 2A and B). iNOS was expressed weakly in healthy liver tissue and mainly localized in tumor

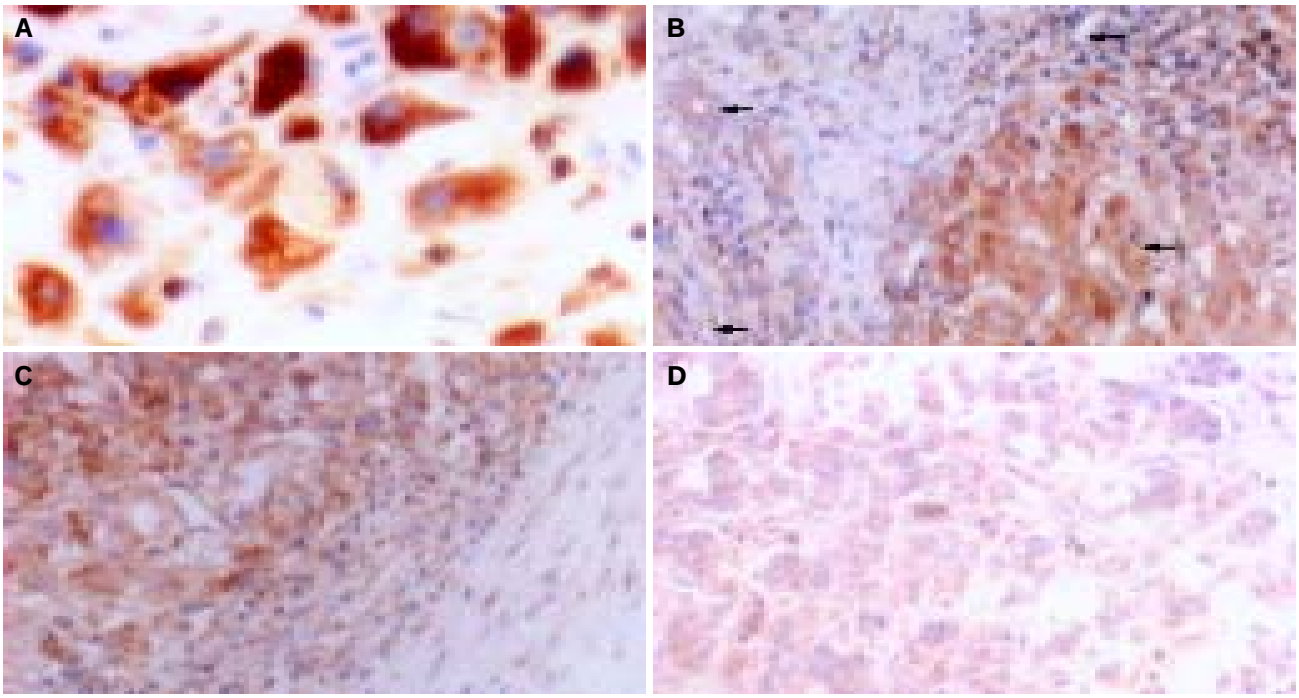

Figure 2 Immunohistochemical staining for MMP-9. A: MMP-9 in cytoplasm and cytoplasmic membranes in HCC (×400); B: MMP-9 in vascular endothelial cells, bile ducts, HCC cells, and stromal fibroblasts (arrow heads from top to bottom) within HCC (×200); C: MMP-9 expression in neighboring capsule of HCC (×200); and D: weak expression of MMP-9 in central areas of HCC tissues (×200).

cytoplasm with a diffuse distribution pattern and a granular pattern. It was also found in cell membranes occasionally. There was no expression of iNOS in tumor nuclei or interstitial cells (Figure 3A). The common characteristics of MMP-9 and iNOS expression were that their stainings were more frequent in tumor cells localized in the anterior borders of invasion or neighboring capsules of tumor tissues (Figures 2C and 3B) than in those cells in central areas (Figures 2D and 3C) and that they displayed various degrees of intensities and inter-tumor heterogeneity. There was a significant correlation between MMP-9 and iNOS expression ($\chi^2 = 8.052$, $P = 0.010$, Table 3).

Table 3 Correlation between MMP-9 and iNOS expression in 32 HCC tissues

iNOS	MMP-9		Total	*P*
	+	–		
+	21	2	23	
–	4	5	9	0.010
Total	25	7	32	

DISCUSSION

HCC is the fifth most common malignant disease in the world, causing almost one million deaths annually[28]. Surgical resection is the only proven cure for HCC, yet over 80%[29] of patients with HCC undergoing hepatectomy develop new tumors in the residual livers within 2 years. Further investigation of the pathological and biological factors of HCC in relation to recurrence and metastasis using molecular biology techniques will provide promising strategies for treatment and prevention of cancer invasion.

MMP-9 plays a key role in cancer invasion and metastasis by digesting native type IV collagen, which is a major structural component of basement membranes, since increased MMP-9 levels have been observed in various tumors such as HCC[30], bladder carcinoma[33], head, and neck cancer[19]. There is a trend toward a higher proportion of active MMP-9 with an increasing invasiveness of tumor cells. Our immunohistochemical study showed that the expression of MMP-9 was negative in the 7 normal liver tissues, and positive in 25 (78.13%) of 32 HCC tissues, suggesting that MMP-9 is produced by tumor cells. The strong staining in the marginal areas of tumor tissues suggests the close involvement of MMP-9 in the digestion of ECM. Moreover, positive staining of some fibroblasts and endothelial cells with anti-MMP-9 antibody suggests a participation of these cells in degradation of the ECM. The incidence of MMP-9 expression was significantly higher in high-risk group for HCC recurrence and TNM III stage group than in low-risk group and TNM I-II stage group, suggesting that overexpression of MMP-9 plays an important role in the progress of HCC, and that MMP-9 protein may serve as a marker for invasiveness and metastasis of HCC. These results are similar to the results reported by Arii *et al*.[30], and Hayasaka *et al*.[31]. In contrast to their study, there was also a significant correlation between MMP-9 expression and tumor size and capsule status of HCC. Both MMP-9 mRNA and activation of latent type of MMP-9 are significantly correlated with capsular infiltration of tumor[32]. Durkan *et al*.[33], reported that MMP-9 staining is associated with tumor size. Therefore, the above data further indicate that MMP-9 plays an important role in the dispersion of HCC cells and may accelerate the growth of tumors by enhancing angiogenesis of tumors.

MVD is an important indicator to reflect the level of tumor angiogenesis[34]. The result of our study revealed that there was a positive association between the extent of neovascularization and the clinicopathologic characteristics related to aggressiveness, such as TNM stage and risk of recurrence, indicating that the MVD reflects the potentiality for HCC recurrence and metastasis. We also found that the MVD was statistically different in different MMP-9 immunoreactivity groups. There was a significant positive relationship between MMP-9 and MVD, the higher the MMP-9 expression, the higher the MVD. MMP-9 plays a vital role in the turnover of basement membrane collagen types IV and I, which exert a crucial effect on the formation of new capillary sprouts and neoangiogenesis. Based on the above facts, we speculate that MMP-9 expression may initiate angiogenesis and promote vascularization.

A large body of clinical and experimental data suggest that NO plays a promoting role in tumor progression and metastasis[35-37], though a few reports indicate that the presence of NO in tumor cells or their microenvironment may exert deleterious effects on the tumor cell survival and consequently their metastatic ability[13]. In the current study, we found that iNOS was expressed weakly in healthy

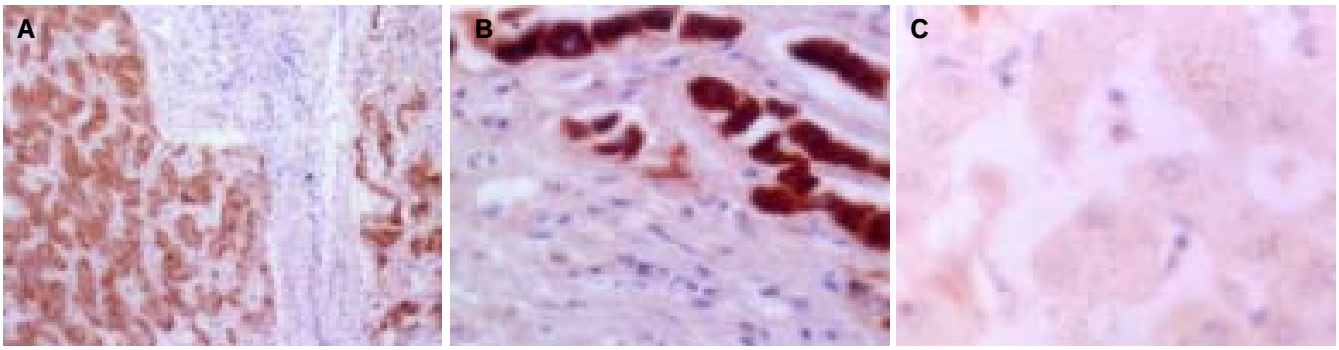

Figure 3 Immunohistochemical staining for iNOS. A: iNOS expression in tumor cytoplasm (×100); B: strong expression of iNOS in neighboring capsule of HCC tissues (×400); and C: weak expression of iNOS in central areas of HCC tissues (×400).

liver tissues, suggesting that iNOS is associated with the physiological function of normal liver tissues. The expression of iNOS showed strong cytoplasmic staining in cancerous cells but not in tumor nuclei and interstitial cells, suggesting that NO is produced by HCC cells and directly or indirectly influences the fate of HCC cells. Here, we also demonstrated that the rate of iNOS expression in cases with their tumor capsules being not integral or their tumors without capsules was significantly higher than that in those with their tumor capsules being integral. The expression of iNOS in high recurrence-risk group was significantly higher than that in low recurrence-risk group, indicating that iNOS positivity is upregulated along with the biological aggressiveness of HCC lesions. It seems more likely that iNOS may increase the viability and infiltrative potential of HCC.

In this study, the count of MVD was statistically different in different iNOS immunoreactivity groups, the higher the iNOS expression the higher the MVD. NO has been implicated in all processes of angiogenesis in a manner consistent with a pre-angiogenic phenotype[38]. iNOS-transfected human colon adenocarcinoma DLD-1 cells have a higher vessel density and a higher growth rate *in vivo* than parental cells in mammary tumor model, suggesting that NO is a key mediator of C3L5 tumor-induced angiogenesis in NOS inhibitor-treated mice[39]. Therefore, the above data further indicate that local NO production by iNOS in HCC cells is able to enhance angiogenesis. It was reported that MMP-9 can also facilitate angiogenesis[40]. In this study, we found that there was a significant association between MMP-9 and iNOS. Both MMP-9 and iNOS positive expressions were more frequent in tumor cells localized in the anterior borders of invasion or neighboring capsules of tumor tissues and were associated with the capsule status and the risk of HCC recurrence, demonstrating that the effect of iNOS on angiogenesis can promote metastatic potential as well as tumor invasiveness by inducing HCC cells to produce MMP-9. To evaluate the mechanism, further investigations are needed.

In conclusion, there is a significant positive correlation between MMP-9 and iNOS expression, suggesting that NO produced by iNOS modulates MMP-9 production and therefore contributes to tumor cell angiogenesis, invasion, and metastasis in HCC. The strong expression of iNOS and MMP-9 in HCC may be helpful in evaluating the recurrence of HCC, predicting poor prognosis. For patients with strong expression of MMP-9 and iNOS, the optimal treatment scheme needs to be selected.

REFERENCES

1 **Folkman J.** What is the evidence that tumors are angiogenesis dependent? *J Natl Cancer Inst* 1990; **82**: 4-6
2 **Stetler-Stevenson WG,** Liotta LA, Kleiner DE Jr. Extracellular matrix 6: role of matrix metalloproteinases in tumor invasion and metastasis. *FASEB J* 1993; **7**: 1434-1441
3 **Westermarck J,** Kahari VM. Regulation of matrix metalloproteinase expression in tumor invasion. *FASEB J* 1999; **13**: 781-792
4 **Curran S,** Murray GI. Matrix metalloproteinases: molecular aspects of their roles in tumor invasion and metastasis. *Eur J Cancer* 2000; **36**: 1621-1630
5 **Yoshizaki T,** Sato H, Furukawa M. Recent advances in the regulation of matrix metalloproteinase 2 activation: from basic research to clinical implication. *Oncol Rep* 2002; **9**: 607-611
6 **Mott JD,** Werb Z. Regulation of matrix biology by matrix metalloproteinases. *Curr Opin Cell Biol* 2004; **16**: 558-564
7 **Ramos-DeSimone N,** Hahn-Dantona E, Sipley J, Nagase H, French DL, Quigley JP. Activation of matrix metalloproteinase-9 (MMP-9) via a converging plasmin/stromelysin-1 cascade enhances tumor cell invasion. *J Biol Chem* 1999; **274**: 13066-13076
8 **Kallakury BV,** Karikehalli S, Haholu A, Sheehan CE, Azumi N, Ross JS. Increased expression of matrix metalloproteinases 2 and 9 and tissue inhibitors of metalloproteinases 1 and 2 correlate with poor prognostic variables in renal cell carcinoma. *Clin Cancer Res* 2001; **7**: 3113-3119
9 **Lee KH,** Hyun MS, Kim JR. Growth factor-dependent activation of the MAPK pathway in human pancreatic cancer: MEK/ERK and p38 MAP kinase interaction in uPA synthesis. *Clin Exp Metastasis* 2003; **20**: 499-505
10 **Legrand C,** Polette M, Tournier JM, de Bentzmann S, Huet E, Monteau M, Birembaut P. uPA/plasmin system-mediated MMP-9 activation is implicated in bronchial epithelial cell migration. *Exp Cell Res* 2001; **264**: 326-336
11 **Mazzieri R,** Masiero L, Zanetta L, Monea S, Onisto M, Garbisa S, Mignatti P. Control of type IV collagenase activity by components of the urokinase-plasmin system: a regulatory mechanism with cell-bound reactants. *EMBO J* 1997; **16**: 2319-2332
12 **Koolwijk P,** Miltenburg AM, van Erck MG, Oudshoorn M, Niedbala MJ, Breedveld FC, van Hinsbergh VW. Activated gelatinase-B (MMP-9) and urokinase-type plasminogen activator in synovial fluids of patients with arthritis. Correlation with clinical and experimental variables of inflammation. *J Rheumatol* 1995; **22**: 385-393
13 **Holian O,** Wahid S, Atten MJ, Attar BM. Inhibition of gastric cancer cell proliferation by resveratrol: role of nitric oxide. *Am J Physiol Gastrointest Liver Physiol* 2002; **282**: 809-816
14 **Michel T,** Feron O. Nitric oxide synthases: which, where, how, and why? *J Clin Invest* 1997; **100**: 2146-2152
15 **Cianchi F,** Cortesini C, Fantappie O, Messerini L, Sardi I, Lasagna N, Perna F, Fabbroni V, Di Felice A, Perigli G, Mazzanti R, Masini E. Cyclooxygenase-2 activation mediates the proangiogenic effect of nitric oxide in colorectal cancer. *Clin Cancer Res* 2004; **10**: 2694-2704
16 **Franco L,** Doria D, Bertazzoni E, Benini A, Bassi C. Increased expression of inducible nitric oxide synthase and cyclooxygenase-2 in pancreatic cancer. *Prostaglandins Other Lipid Mediat* 2004; **73**: 51-58
17 **Oktem G,** Karabulut B, Selvi N, Sezgin C, Sanli UA, Uslu R, Yurtseven ME, Omay SB. Differential effects of doxorubicin and docetaxel on nitric oxide production and inducible nitric oxide synthase expression in MCF-7 human breast cancer cells. *Oncol Res* 2004; **14**: 381-386
18 **Lala PK,** Orucevic A. Role of nitric oxide in tumor progression: lessons from experimental tumors. *Cancer Metastasis Rev* 1998; **17**: 91-106
19 **Franchi A,** Santucci M, Masini E, Sardi I, Paglierani M, Gallo O. Expression of matrix metalloproteinase 1, matrix metalloproteinase 2, and matrix metalloproteinase 9 in carcinoma of the head and neck. *Cancer* 2002; **95**: 1902-1910
20 **Eberhardt W,** Beeg T, Beck KF, Walpen S, Gauer S, Bohles H, Pfeilschifter J. Nitric oxide modulates expression of matrix metalloproteinase-9 in rat mesangial cells. *Kidney Int* 2000; **57**: 59-69
21 **Egi K,** Conrad NE, Kwan J, Schulze C, Schulz R, Wildhirt SM. Inhibition of inducible nitric oxide synthase and superoxide production reduces matrix metalloproteinase-9 activity and restores coronary vasomotor function in rat cardiac allografts. *Eur J Cardiothorac Surg* 2004; **26**: 262-269
22 **Vincent VA,** Lowik CW, Verheijen JH, de Bart AC, Tilders FJ, Van Dam AM. Role of astrocyte-derived tissue-type plasminogen activator in the regulation of endotoxin-stimulated nitric oxide production by microglial cells. *Glia* 1998; **22**: 130-137

23 **Marcet-Palacios M,** Graham K, Cass C, Befus AD, Mayers I, Radomski MW. Nitric oxide and cyclic GMP increase the expression of matrix metalloproteinase-9 in vascular smooth muscle. *J Pharmacol Exp Ther* 2003; **307**: 429-436

24 **Johanning JM,** Armstrong PJ, Franklin DP, Han DC, Carey DJ, Elmore JR. Nitric oxide in experimental aneurysm formation: early events and consequences of nitric oxide inhibition. *Ann Vasc Surg* 2002; **16**: 65-72

25 **Sasaki K,** Hattori T, Fujisawa T, Takahashi K, Inoue H, Takigawa M. Nitric oxide mediates interleukin-1-induced gene expression of matrix metalloproteinases and basic fibroblast growth factor in cultured rabbit articular chondrocytes. *J Biochem* 1998; **123**: 431-439

26 **Koomagi R,** Volm M. Expression of Fas (CD95/APO-1) and Fas ligand in lung cancer, its prognostic and predictive relevance. *Int J Cancer* 1999; **84**: 239-243

27 **Weidner N,** Semple JP, Welch WR, Folkman J. Tumor angiogenesis and metastasis correlation in invasive breast carcinoma. *N Engl J Med* 1991; **324**: 1-8

28 **Yu AS,** Keeffe EB. Management of hepatocellular carcinoma. *Rev Gastroenterol Disord* 2003; **3**: 8-24

29 Primary liver cancer in Japan. Clinicopathologic features and results of surgical treatment. Liver cancer study group of Japan. *Ann Surg* 1990; **211**: 277-287

30 **Arii S,** Mise M, Harada T, Furutani M, Ishigami S, Niwano M, Mizumoto M, Fukumoto M, Imamura M. Overexpression of matrix metalloproteinase 9 gene in hepatocellular carcinoma with invasive potential. *Hepatology* 1996; **24**: 316-322

31 **Hayasaka A,** Suzuki N, Fujimoto N, Iwama S, Fukuyama E, Kanda Y, Saisho H. Elevated plasma levels of matrix metalloproteinase-9 (92-kd type IV collagenase/gelatinase B) in hepatocellular carcinoma. *Hepatology* 1996; **24**: 1058-1062

32 **Hollingsworth HC,** Kohn EC, Steinberg SM, Rothenberg ML, Merino MJ. Tumor angiogenesis in advanced stage ovarian carcinoma. *Am J Pathol* 1995; **147**: 33-41

33 **Durkan GC,** Nutt JE, Marsh C, Rajjayabun PH, Robinson MC, Neal DE, Lunec J, Mellon JK. Alteration in urinary matrix metalloproteinase-9 to tissue inhibitor of metalloproteinase-1 ratio predicts recurrence in nonmuscle-invasive bladder cancer. *Clin Cancer Res* 2003; **9**: 2576-2582

34 **Zolota V,** Gerokosta A, Melachrinou M, Kominea A, Aletra C, Scopa CD. Microvessel density, proliferating activity, p53 and bcl-2 expression in *in situ* ductal carcinoma of the breast. *Anticancer Res* 1999; **19**: 3269-3274

35 **Feng CW,** Wang LD, Jiao LH, Liu B, Zheng S, Xie XJ. Expression of p53, inducible nitric oxide synthase and vascular endothelial growth factor in gastric precancerous and cancerous lesions: correlation with clinical features. *BMC Cancer* 2002; **2**: 8

36 **Yagihashi N,** Kasajima H, Sugai S, Matsumoto K, Ebina Y, Morita T, Murakami T. Increased in situ expression of nitric oxide synthase in human colorectal cancer. *Virchows Arch* 2000; **436**: 109-114

37 **Thomsen LL,** Miles DW. Role of nitric oxide in tumour progression: lessons from human tumours. *Cancer Metastasis Rev* 1998; **17**: 107-118

38 **Nicolson GL.** Tumor and host molecules important in the organ preference of metastasis. *Semin Cancer Biol* 1991; **2**: 143-154

39 **Jenkins DC,** Charles IG, Thomsen LL, Moss DW, Holmes LS, Baylis SA, Rhodes P, Westmore K, Emson PC, Moncada S. Roles of nitric oxide in tumor growth. *Proc Natl Acad Sci USA* 1995; **92**: 4392-4396

40 **Zhang Y,** Wu XH, Cao GH, Li S. Relationship between expression of matrix metalloproteinase-9 (MMP-9) and angiogenesis in renal cell carcinoma. *Aizheng* 2004; **23**: 326-329

Science Editor Wang XL and Guo SY **Language Editor** Elsevier HK

PO Box 2345, Beijing 100023, China
www.wjgnet.com
wjg@wjgnet.com

ELSEVIER

World J Gastroenterol 2005;11(38):5938-5943
World Journal of Gastroenterology ISSN 1007-9327

Anti-hepatoma effect of arsenic trioxide on experimental liver cancer induced by 2-acetamidofluorene in rats

Bing Tan, Jie-Fei Huang, Qun Wei, Hong Zhang, Run-Zhou Ni

Bing Tan, Jie-Fei Huang, Qun Wei, Hong Zhang, Run-Zhou Ni, Department of Digestive Medicine, Affiliated Hospital of Nantong Medical College, Nantong 226001, Jiangsu Province, China
Co-first-authors: Bing Tan
Correspondence to: Dr. Jie-Fei Huang, Department of Digestive Medicine, Affiliated Hospital of Nantong Medical College, Nantong 226001, Jiangsu Province, China
Telephone: +86-513-5806629
Received: 2004-06-08 Accepted: 2004-08-05

Abstract

AIM: To study the anti-hepatoma efficiency of arsenic trioxide (As_2O_3) in the treatment of experimental rat hepatocellular carcinoma (HCC) induced by 2-acetamidofluorene (2-FAA) and to elucidate the possible mechanisms.

METHODS: SD rats (2 mo old) had been fed with 2-FAA for 8 wk to induce HCC, and then they were treated with As_2O_3 or matrine. On d 29, the rats were killed and the liver was weighed and liver tumors were counted. The histological changes of liver tissue were observed under microscope, and the cellular dynamic parameters were studied by flow cytometry. Immunohistochemistry (two-step method) was used to observe the expression of vascular endothelial growth factor (VEGF) and micro-vessel density (MVD) on consecutive sections. The pathological parameters were also analyzed, the levels of serum aspartate aminotransferase (AST), alanine aminotransferase (ALT), total bilirubin (TBi), and direct bilirubin (DBi).

RESULTS: The number of liver tumors decreased significantly in groups treated with As_2O_3, especially in medium-dose (1 mg/kg) group (t = 2.80, P<0.01). As_2O_3 caused HCC cell death via apoptosis; necrosis was seen and apoptosis was common when the dose was 1 mg/kg. Proliferation index decreased sharply in medium-dose (1 mg/kg) group (7.87±4.11 *vs* 24.46±6.49, t = 2087, P<0.01), but not in 0.2 mg/kg group. However, S-phase fraction decreased dramatically in both groups, it reached the bottom level only when the dose was 1 mg/kg compared with control (0.40±0.13 *vs* 3.01±0.51, t = 2.97, P<0.01), and it was obviously accompanied with accumulation of cells in G_0/G_1 (G_0/G_1 restriction). The expressions of VEGF and MVD in medium-dose (1 mg/kg) group were significantly lower than normal saline group (0.63±0.74 *vs* 2.44±0.88, P<0.05; 15.75±3.99 *vs* 47.44±13.41, t = 2.80, P<0.01). Compared with normal saline group, medium- and low-dose groups As_2O_3 and matrine lowered the levels of ALT in serum (61.46±9.46, 63.75±20.40, 61.18±13.00 *vs* 108.98±29.86, t = 2.14, P<0.05), but had no effect on the level of serum AST, TBi, and DBi.

CONCLUSION: As_2O_3 had inhibitory effect on growth of experimental HCC in rats induced by 2-FAA, but had no obvious effect on normal hepatic cells. The mechanisms may involve decrease of cell division, accumulation of cells in G_0/G_1 phase, apoptosis of tumor cells, and inhibitory effect on angiogenesis through blocking VEGF.

Key words: Arsenic trioxide; Liver cancer; Cell proliferation

Tan B, Huang JF, Wei Q, Zhang H, Ni RZ. Anti-hepatoma effect of arsenic trioxide on experimental liver cancer induced by 2-acetamidofluorene in rats. *World J Gastroenterol* 2005; 11(38): 5938-5943
http://www.wjgnet.com/1007-9327/11/5938.asp

INTRODUCTION

Hepatocellular carcinoma (HCC), with the highest malignancy and worst prognosis, is a common digestive tumor[1]. In recent years, there have been many clinical drugs for the therapy of HCC patients who cannot tolerate operation, such as tamoxifen[2], flutamide[3], lipiodol for embolism[4], but the results were so far unsatisfactory. Arsenic trioxide (As_2O_3) has been extensively used for many malignant leukemia tumors and was proved to be effective[5]. Zhang found As_2O_3 inhibited growth of experimental HCC by inducing apoptosis of tumor cells[6]. Si applied matrine for late HCCs and noticed growth inhibition and apoptosis of malignant cells[7]. To elucidate the antineoplastic mechanisms of As_2O_3, we treated experimental HCC in rats induced by 2-acetamidofluorene (2-FAA) with As_2O_3, counted liver tumors, examined liver histological changes under microscope, examined expression of vascular endothelial growth factor (VEGF) and micro-vessel density (MVD) of tumor with immunohistochemistry, studied cellular dynamic parameters by flow cytometry, and also investigated the levels of serum aspartate aminotransferase (AST), alanine aminotransferase (ALT), total bilirubin (TBi), and direct bilirubin (DBi).

MATERIALS AND METHODS

Establishment of HCC rat models

Seventy SD rats from blocked population, about 2-mo old, weighing 140-180 g (supplied by the Experimental Animal

Center of Nantong Medical College), were fed with granules mixed by 0.05% (w/w) carcinogen 2-FAA (from Sigma Company, USA), and kept in constant environment (20 ℃, moisture content 50%). During the 3rd-5th wk, some rats died; 4 wk later some visible gray nodes appeared on the liver surface of the dead by autopsy. Moreover, the number and size of these nodes had an increasing tendency. At the end of the 8th wk, 34 rats were still alive, and they were then fed with normal granules.

Grouping of animals Thirty-four HCC rats were divided randomly into four groups: two groups were injected intraperitoneally with As_2O_3 (produced by Haerbing Yida Pharma AG), diluted with four volumes of normal saline before injection, including medium-dose (1 mg/kg per d) and small-dose (0.2 mg/kg per d) groups; the third group was injected with matrine (4.2 g/kg per d) in the same way; the last was injected with normal saline (1.5 mL/kg per d) similarly. Treatment effects in all groups were observed: group A (with medium-dose As_2O_3 for 4 wk, n = 8); group B (with small-dose for 4 wk, n = 9); group C (with matrine for 8 wk, n = 8); group D (with saline for 4 wk, n = 9). During the experiment, we weighed the rats and then adjusted the dosage each week.

Sampling of liver and serum specimens At the end of the treatment, 34 rats were killed under diethyl ether anesthesia. Blood (4-5 mL) was drawn from heart and serum sample was collected after blood clotting and stored at 20 ℃ until assay. Whole liver was taken out and weighed immediately after rats were killed. After recording the distribution, size, and number of neoplastic nodes on the liver surface, we fixed part of liver tissue in 10% neutral formaldehyde for pathological examination.

Histopathologic and immunohistochemical examination Formaldehyde-fixed liver tissue was embedded in paraffin, cut into 4-μm-thick sections, some were stained with routine hematoxylin and eosin (HE) to observe liver neoplasia and morphological apoptosis under microscope; the others were examined with the immunohistochemical method. Polyclonal antibodies of VEGF and FVIIIRAg were obtained from the Beijing Zhongshan Biotechnology Company Limited. The two-step staining method consisted of the following main procedures: paraffin section was dewaxed and hydrated; tissue antigens were retrieved with microwave; the first antigen was dropped on tissue section, subsequently, which was incubated in a wet box at 37 ℃ for 1 h. After addition of envision reagent, these sections were put into a wet box again at room temperature for 30 min. Between the above-mentioned steps, tissue sheets were washed thrice in Tris-buffered saline (TBS, 0.01 mol/L, pH 7.4). After that, these tissue samples were colored with dolichos bifows agglutinin, cellular nuclei were redyed with hematoxylin and then sealed. In the negative control group, TBS was used as the first antibody, while the positive controls were from confirmed positive tissue specimens.

Buffy granules in cytoplasm were indicative of positive VEGF expression. According to Wang's standards[8], the median percentage of VEGF-positive-stained cells in 10 high power fields (200×) was counted. These medians were divided into five classes: less than 10% was negative (-); equivalent to or more than 10% was positive: 10-25% was +, 26-50% was ++, 51-75% was +++, and 76% or above were ++++. The five classes were respectively graded as 0-4.

MVD count was in accordance with Weidner's method (ref no.). First under low power microscope, the most intensive micro-vessel area in tumor tissues was identified, and then counted under high power (400×). Any buffy-stained endothelial cell or cell tuft, as well as any structure-unconnected micro-vessel branch, which was distinct from the surrounding tumor cells and connective tissues, was regarded as one "micro-vessel", excluding those vessels with muscular layers or a cavity with more than eight RBCs. The average of three counts was MVD of a liver tissue sample, which was checked by two pathological doctors with double-blind method.

Flow cytometric study Single-cell suspension, about 0.2 g, was prepared from fresh liver neoplasm tissue, first washed twice in PBS, cut into fragments with a clipper, and then filtered twice through a 35-μm-pore nylon filter. Cell count ranged from 3×10^5 to 10×10^5 cells/mL per sample. The suspension was spun by centrifugation at the rate of 1 000 r/min for 5 min, and washed in PBS twice. The obtained pellet was fixed by 70% cold ethanol, and then stored at -20 ℃ for 12-18 h. After being spun and washed again as previously described, the fixed single-cell suspension was pipetted into 0.01% RNase solution (Becton Dickinson Corporation) 200 μL, vortex-mixed and incubated continuously at 4 ℃ for 30 min, stained with 50 μg/mL propidium iodide 200 μL (Becton Dickinson Corporation), and then placed in the dark at 4 ℃ for 10 min. The sample was analyzed from 30 min to 3 h after addition of propidium iodide. Flow cytometric analysis was performed with an FACS Caliber flow cytometer (Becton Dickinson Corporation), which was equipped with a 5 W argon-ion laser. The fluorescence intensity of propidium iodide-stained nuclei, excited by blue laser light (488 nm) with 200 mW of light-regulated power, was quantified after filtering through a 457-502 nm nylon blocking filter. Percent coefficient of variation (%CV) was adjusted to less than 4% with glutaral-fixed chicken erythrocyte nuclei (CEN). Two-micron beads function to verify instrument alignment. The modifier for color compensation was corrected with a fluorescence microsphere. A minimum of 1×10^4 stained nuclei was examined through the flow cytometer, and the data were saved in a computer. DNA data were acquired using CELLQuest, and analyzed with ModFit LT™. Normal peripheral blood lymphocytes and normal SD rat liver cells were used as the control samples to identify the staining efficiency of propidium iodide and the channel of diploid cells (G_0/G_1 phase cells). With the G_0/G_1 peak of CEN as an internal standard, both G_0/G_1 and G_2/M peaks of analyzed samples were determined, and then the DNA quantity was calculated. Cell cycle percentages were derived from DNA histograms. The peak of hypodiploid, anterior to the G_0/G_1 peak, was the apoptosis peak. Proliferative index (PI) was equal to the sum percentage of S-phase and G_2/M-phase nuclei to all; the S-phase fraction (SPF) was determined and calculated with the area under the curve between G_0/G_1 and G_2/M peaks.

Serum enzyme determination Serum AST, ALT, TBi,

and DBi total activity were measured by the direct method of nitrobenzenamine.

Statistical analysis

Experimental data were shown as mean±SD. Student's *t*-test, and rank sum test were performed to assess potentially significant differences between individual groups, with STATA 7.0 statistical analysis software. A P value of <5% was regarded as significant when comparing various groups.

RESULTS

General observation during treatment

During the 1st wk, several As_2O_3-administrated SD rats had a short-term sinus tachycardia, which self-recovered after 1 or 2 d. Skin induration could be avoided if injection sites were changed daily. Whether by As_2O_3 or matrine treatment, there was no significant difference between the treatment group and the control, in terms of body weight gain and the weight ratio of liver to body (Table 1).

Table 1 Changes of body and liver weights in SD rats (mean±SD)

Groups	Body weight	Weight gain	Liver weight	Liver weight /body weight
A	272.25±35.51	74.25±20.71	12.475±1.9	3.49±0.40
B	247.56±63.94	58.44±16.99	13.11±3.15	4.42±0.60
C	253.00±28.63	58.25±24.01	12.54±1.132	4.08±0.50
D	258.22±49.99	40.44±40.15	11.89±1.59	4.24±1.00

Morphological changes In contrast to the normal, HCC rat liver was gray, and hard, both volume and weight increased; slight hemorrhage and necrosis could be found on liver cross section; multiple nodes were distributed unevenly on liver surface, mostly 1-6 mm in diameters, one 9 mm-diameter node was found in the control group; the nodes were widespread on part of liver lobes, more evidently in the saline group; bulky tumor nodes appeared more frequently in the control groups. On the contrary, less node-widespread liver lobes and smaller tumor nodes were found in As_2O_3-treated rats (Table 2).

At the end of 4-wk treatment, five rats in group A and three rats in group B had no visible liver tumor nodes; while in the control group, all rats had widespread nodes on liver lobes and only one had sparsely distributed nodes on liver lobes (Figures 1A and B). Visible neoplastic nodes and node-widespread liver lobes in group A were less than those in groups B (P<0.05) and C (P<0.01), there was no significant difference between groups B and C.

Table 2 The number and distribution of tumor nodes on rat liver

Groups	*n*	2–4 mm diameter nodes	>4 mm diameter nodes	Liver lobes with diffuse nodes
A	8	0 (0)	1 (0.125)	0 (0)
B	9	50 (5.56)	9 (1)	17.5 (1.94)
C	8	137 (15.22)	13 (1.44)	29 (3.22)
D	9	223 (24.778)	49 (5.444)	39 (4.333)

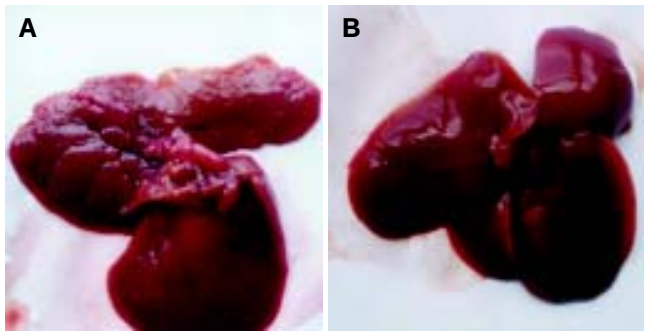

Figure 1 Gross changes of rat's liver after treatment. A: The control group (4 wk after NS injection); B: The treatment group (4 wk after medium-dose As_2O_3 injection).

Pathological examination Under microscope, all 2-FAA-induced HCC rat liver tissues had hepatic cell degeneration, oval cell proliferation, and inflammatory cell infiltration. There were more extensive infiltrations of inflammatory cells in control groups. Whereas in group A, these pathological changes were comparatively slight: there were fewer infiltrating inflammatory cells, more regenerated nodes, partly abnormal differentiated cells, and fewer carcinoma nodes (Figure 2A). There were more apoptotic cells in As_2O_3-treated tumor tissues, which were shrunk and separated from other surrounding cells, round or oval in shape, and had complete cellular membrane; chromatin of apoptotic cells was condensed, edge-gathered or broken, and formed into intra-cellular nucleosomes of different sizes; acidophilia of shrunk cytoplasm was raised; no infiltrating inflammatory cells were seen near apoptotic cells (Figure 2B).

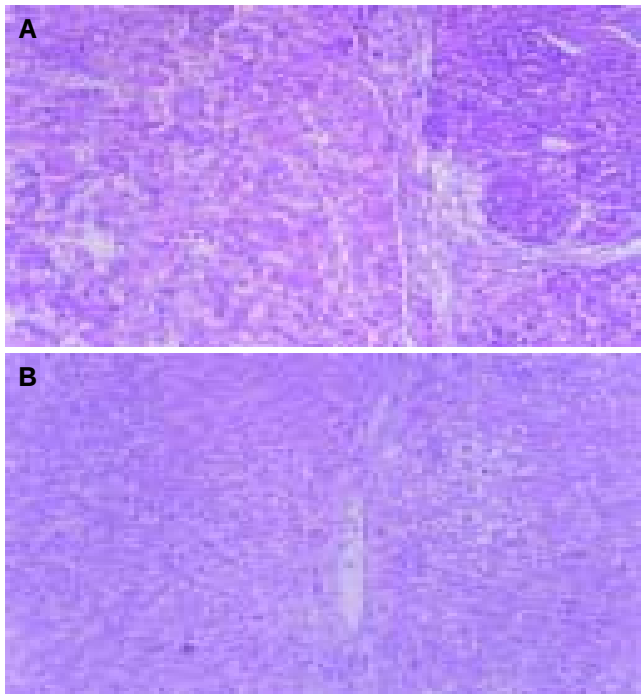

Figure 2 Pathological changes after treatment. A: The control group (4 wk after NS injection, HE×20); B: The treatment group (4 wk after medium-dose As_2O_3 injection, apoptotic cell observed).

Distribution of cell cycle phases The mean percentages of SPF, G_2/M phase, and PI of the 4-wk As_2O_3 group were less than those of the control ($P<0.05$), while G_0/G_1 phase mean ratio increased insignificantly ($P>0.05$, Table 3, Figures 3A and B).

The apoptotic rate in liver tumor tissues By means of DNA content assay, an obvious hypodiploid peak, before the G_0/G_1 peak, was called the apoptotic peak (Figures 3A and B). There was a significant increase in the apoptotic rate of the 4-wk As_2O_3-treated group compared with that of the control ($P<0.01$).

Levels of serum enzymes Compared with the control, serum ALT level of the 4-wk-treated groups was decreased ($P<0.05$), while AST, TBi, and DBi activity differed insignificantly ($P>0.05$, Table 4).

Immunohistochemical staining results Widespread brown cytoplasmic granules were VEGF positive, chiefly distributed inside tumor tissues and near the vessel endothelial cells (Figure 4A). In group A, more rats showed + to ++ degree VEGF signals, while four of eight rats were VEGF negative; in the control groups, more signals were from ++ to +++, with no negative expression (Figure 4B). There was a weakened intensity of VEGF in group A rats in comparison with the control and C groups ($P<0.05$, Table 5), but the difference was insignificant in all treatment groups ($P>0.05$), except for group A.

Vessel endothelial cells of tumor tissues, exhibited by FVIIIAg staining, formed into irregular micro-vessels, in the shapes of cluster and germination, which distributed unevenly, more intensively at the edge of tumor tissues (Figure 5A). As_2O_3 administration obviously inhibited neovascularization of liver tumor (Table 5, Figure 5B).

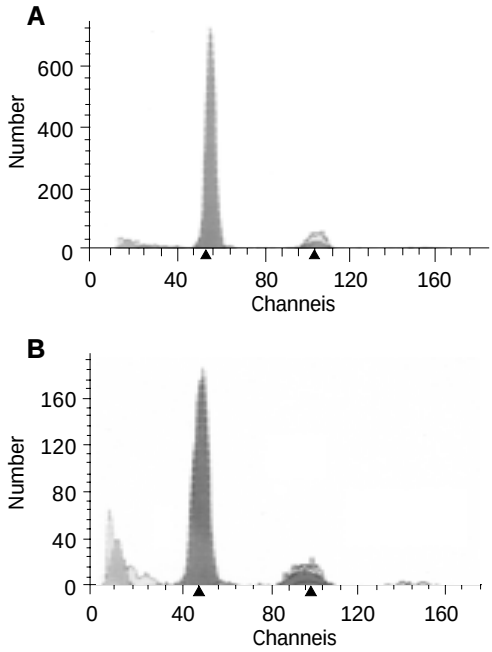

Figure 3 Changes of cell cycle phases after treatment. A: the control group (4 wk after NS injection); B: The treatment group (4 wk after medium-dose As_2O_3 injection, obvious hypodiploid peak).

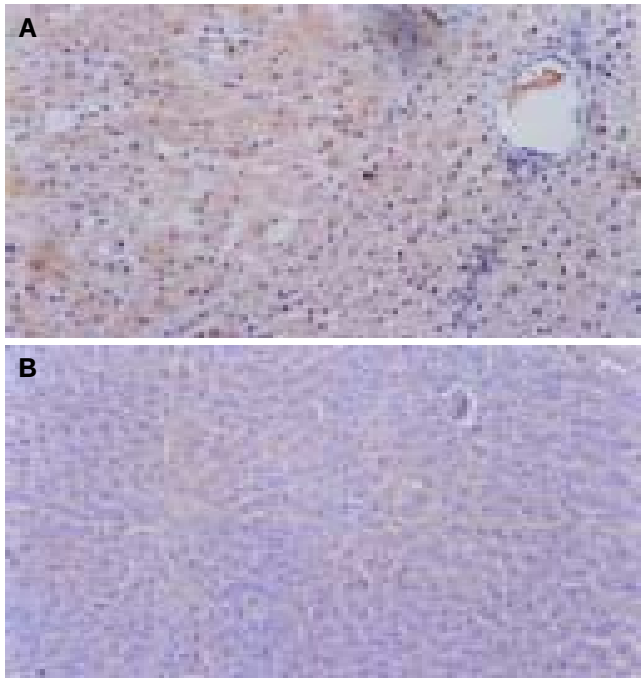

Figure 4 VEGF-positive signals after treatment. A: the control group (4 wk after NS injection, ×20); B: The treatment group (4 wk after medium-dose As_2O_3 injection, ×20).

Table 3 The percentages of cell cycle phases and PI

Groups	G_0/G_1 (%)	S (%)	G_2/M (%)	PI (%)
A	93.31±3.01[b]	0.40±0.13[b,d,f]	6.28±3.26[a]	7.87±4.11[b,d]
B	88.99±2.63	1.58±0.60[b]	9.43±2.29	17.14±6.08
C	87.34±4.75	2.05±0.62	10.61±4.33	20.77±5.28
D	84.26±2.53	3.01±0.51	12.73±2.40	24.46±6.49

[a]$P<0.05$, [b]$P<0.01$ *vs* group D; [d]$P<0.01$ *vs* group C; [f]$P<0.01$ *vs* group B.

Table 4 The levels of serum enzymes

Groups	AST (μ/L)	ALT (μ/L)	TBi (μmol/L)	DBi (μmol/L)
A	61.46±9.46[a]	31.65±9.25	0.52±0.11	0.35±0.15
B	63.75±20.40[a]	34±12.58	0.62±0.27	0.40±0.24
C	61.18±13.00[a]	33.45±16.44	0.51±0.14	0.30±0.12
D	108.98±29.86	40±16.12	0.47±0.13	0.60±0.28

[a]$P<0.05$ *vs* group D. AST: aspartate aminotransferase, ALT: alanine aminotransferase, TBi: total bilirubin, DBi: direct bilirubin.

Table 5 Expression intensity of VEGF and count of MVD in rat liver tumor tissues

Groups	*n*	VEGF					MVD	Marks
		–	+	++	+++	++++		
A	8	4	3	1	0	0	0.63±0.74[a]	15.75±3.99[b,d]
B	9	1	5	2	1	0	1.33±0.87	28.22±9.28[b]
C	8	1	1	3	3	0	2.00±1.07	41.13±7.70
D	9	0	1	4	3	1	2.44±0.88	47.44±13.41

[a]$P<0.05$, [b]$P<0.01$ *vs* group D; [d]$P<0.01$ *vs* group C.

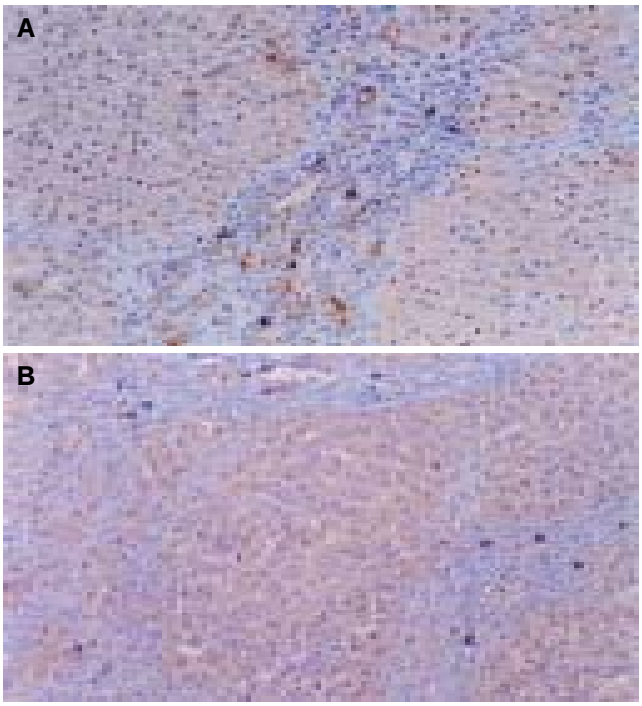

Figure 5 Micro-vessels by FVIIIAg staining after treatment, ×20. A: The control group (4 wk after NS injection); B: The treatment group (4 wk after medium-dose As_2O_3 injection).

DISCUSSION

The antineoplastic mechanisms of As_2O_3 are not yet clear. There are probably five major pathways: (1) inducing apoptosis of tumor cells[6,9-11]; (2) restraining the metastasis of HCC[12]; (3) effecting immunity of liver tumor cells[13]; (4) inhibiting angiogenesis through blocking VEGF; (5) having synergistic anti-hepatoma effect combined with chemical drugs.

PI and SPF often indicate the proliferation of tumor cells. In our study, the distribution of cell cycle phases showed cell proliferation tended to be inhibited after 4-wk of As_2O_3 administration. SPF, G_2/M phase, and PI all decreased ($P<0.05$), whereas G_0/G_1 phase increased insignificantly. More cells were blocked in G_0/G_1 phase. It is implied that As_2O_3 is able to prevent cells transisting from G_0/G_1 phase to S-phase, inhibiting the growth of tumor cells. In addition, apoptosis of tumor cells promoted by As_2O_3 occurred mainly at 1 mg/kg dose. PI decreased sharply in medium-dose (1 mg/kg) group ($P<0.01$), but not in the other (0.2 mg/kg) group ($P>0.05$). However, SPF decreased dramatically in both groups, suggesting 0.2 mg/kg dose also apparently inhibited synthesizing of DNA of tumor cells, but it was weaker. Therefore, antineoplastic mechanisms of As_2O_3 for HCC may involve the following two ways: inhibition of proliferation and induction of apoptosis of tumor cells.

In recent years, much importance has been attached to the relationship between angiogenesis and neoplasm. It has been confirmed that, solid carcinoma, once its diameter is over 2 mm, has to depend on neovascularization for its growth. It is through the blood vessel network that sufficient oxygen and nutrition are transported to meet the needs of high metabolism and fast proliferation of tumor cells. To some extent, the ability of inducing angiogenesis reflects tumor biological behaviors[14].

Various vessel growth factors act as the media to neovascularization, and VEGF is one of the most important one. Flt-1 and KDR/Flk-1, two receptors of VEGF, only exist in vessel endothelial cells, so VEGF promotes the proliferation of endothelial cells with a high specificity. VEGF can obviously improve the vessel permeability, which play an important role in tumor infiltration and metastasis[14,15]. It is necessary to find an objective and accurate indicator for the neovascularization. Thus, MVD count, which is for this purpose, has become a hot spot. In our study, VEGF and MVD were chosen to reflect the activity of tumor neovascularization. Our experiment showed that inhibitive effect of As_2O_3 on the angiogenesis was through inhibition of VEGF.

Morphological improvement by As_2O_3 in HCC rats could also be explained with its effects on cytokinetics. The number and distribution of liver tumor nodes decreased significantly in the As_2O_3-treated than in the controls, especially in medium-dose (1 mg/kg) group ($P<0.01$). As_2O_3 also lowered VEGF expression and MVD count in rat liver tumor tissues.

Compared with normal saline group, administration of As_2O_3 or matrine lowered the levels of AST in serum ($P<0.05$), but had no effect on the amount of serum AST, TBi, and DBi ($P>0.05$), indicating As_2O_3 has no obvious effect on normal hepatic cells.

In summary, through effective inhibition of proliferation, inducement of apoptosis, and restrain of neovascularization of tumor, As_2O_3 can serve as a new alternative for HCC treatment without serious adverse effects.

REFERENCES

1 **Lee JH,** Ku JL, Park YJ, Lee KU, Kim WH, Park JG. Establishment and characterization of four human hepatocellular carcinoma cell lines containing hepatitis B virus DNA. *World J Gastroenterol* 1999; **5**: 289-295
2 **Manesis EK,** Giannoulis G, Zoumpoulis P, Vafiadou I, Hadziyannis SJ. Treatment of hepatocellular carcinoma with combined suppression and inhibition of sex hormones: a randomized controlled trial. *Hepatology* 1995; **21**: 1535-1542
3 **Chao Y,** Chan WK, Huang YS, Teng HC, Wang SS, Lui WY, Whang-Peng J, Lee SD. Phase II study of flutamide in the treatment of hepatocellular carcinoma. *Cancer* 1996; **77**: 635-639
4 **Ram AM,** Bhattacharya S, Novell JR, Dick R, Winslet MC, Hobbs KEF. Intra-arterial radiotherapy with 131 iodinelipiodol for irresectable hepatocellular carcinoma. *Gut* 1996; **38** (Suppl 1): A17
5 **Dia J,** Weinberg RS, Waxman S, Jing Y. Malignant cells can be sensitized to undergo growth inhibition and apoptosis by arsenic trioxide through modulation of the glutathione redox system. *Blood* 1999; **93**: 268-277
6 **Zhang C,** Wang SS, Qi QH. The morphplogical and cellular dynamic changes in Arsenic Trioxide-treated rat liver cancer. *Zhongliu* 2001; **21**: 101-105
7 **Si WK,** Zhang GY, Ma WK, Kang GF. Effect of Matrine on the prolideration of $HepG_2$ cell line. *Disan Junyi Daxue Xueba* 2000; **22**: 451
8 **Wang Y,** Yang SQ, Wang ZG, Tang S, Sun WG, Liu GZ. Expressive meaning of ras p21, C-erbB-2 and P16 protein in Hepatocellular carcinoma. *Shijie Huaren Xiaohua Zazhi* 1999; **7**: 808-809

9 **Shen ZY,** Shen J, Cai WJ. The alteration of mitochondria is an early event of arsenic trioxide induced apoptosis in esophageal carcinoma cells. *Int J Mol Med* 2000; **5**: 155
10 **Liu LX,** Jiang HC, Zhuan AL, Zhou J, Wang XQ, Wu W. Arsenic trioxide induces apoptosis in hepatocellular carcinoma cells and to elucidate the possible mechanism. *Zhonghua Yixue Zazhi* 2001; **18**: 1526-1527
11 **Chen GQ,** Zhu J, Shi XG, Ni GH, Zhong HJ, Si GY, Jin XL, Tang W, Li XS, Xong SM, Shen ZC, Sun GL, Ma J, Zhang P, Zhang TD, Gazin C, Naoe T, Chen SJ, Wang ZY, Chen Z. *In vitro* studies on cellular and molecular mechanisms of arsenic trioxide (As2O3)in the treatment of acute promyelocytic leukemia: As2O3 induces NB4 cell apoptosis with downregulation of Bcl-2 expression and modulation of PML-RAR alpha/PML proteins. *Blood* 1996; **88**: 1052-1061
12 **Liu TF,** Cheng BL, Guan YG, Liang T. Study on relationship between expressions of CD44 and inhibition effect of arsenic trioxide on carcinoma. *Haerbing Yikedaxue Xuebao* 2001; **35**: 111-112
13 **Tang YH,** Liu TF. Effect of arsenic trioxide on the Immuni of H_{22} hepatocarcinoma rats. *Zhonghua Weishengwuxue He Mianyixue Zazhi* 2001; **21**: 63
14 **Kong HL,** Crystal RG. Gene therapy strategies for tumor antiangiogenesis. *J Natl Cancer Inst* 1998; **90**: 273-286
15 **Ng IO,** Poon RT, Lee JM, Fan ST, Ng M, Tso WK. Microvessel density, vascular endothelial growth factor and its receptors Flt-1 and Flk-1/KDR in hepatocellular carcinoma. *Am J Clin Pathol* 2001; **116**: 838-845

Science Editor Zhu LH and Guo SY **Language Editor** Elsevier HK

PO Box 2345, Beijing 100023, China
www.wjgnet.com
wjg@wjgnet.com

ELSEVIER

World J Gastroenterol 2005;11(38):5944-5950
World Journal of Gastroenterology ISSN 1007-9327

Excess body weight, liver steatosis, and early fibrosis progression due to hepatitis C recurrence after liver transplantation

Pierluigi Toniutto, Carlo Fabris, Claudio Avellini, Rosalba Minisini, Davide Bitetto, Elisabetta Rossi, Carlo Smirne, Mario Pirisi

Pierluigi Toniutto, Carlo Fabris, Davide Bitetto, Elisabetta Rossi, Liver Transplantation Unit, Department of Pathology and Medicine Experimental and Clinical (DPMSC), University of Udine, Udine, Italy
Claudio Avellini, Pathology, University of Udine, Udine, Italy
Rosalba Minisini, Carlo Smirne, Mario Pirisi, Department of Medical Sciences, University of Eastern Piedmont "A. Avogadro", Novara, Italy
Correspondence to: Dr. Pierluigi Toniutto, Clinica di Medicina Interna, Università degli Studi, Piazzale Santa Maria della Misericordia, 1, Udine 33100, Italy. pierluigi.toniutto@uniud.it
Telephone: +39-432-559824 Fax: +39-432-42097
Received: 2004-12-22 Accepted: 2005-04-18

Abstract

AIM: To investigate how weight gain after OLT affects the speed of fibrosis progression (SFP) during recurrent hepatitis C virus (HCV) infection of the graft.

METHODS: Ninety consecutive patients (63 males, median age 53 years; 55 with HCV-related liver disease), transplanted at a single institution, were studied. All were followed for at least 2 years after OLT and had at least one follow-up graft biopsy, performed not earlier than 1 year after the transplant operation. For each biopsy, a single, experienced pathologist gave an estimate of both the staging according to Ishak and the degree of hepatic steatosis. The SFP was quantified in fibrosis units/month (FU/mo). The lipid metabolism status of patients was summarized by the plasma triglycerides/cholesterol (T/C) ratio. Body mass index (BMI) was measured before OLT, and 1 and 2 years after it.

RESULTS: In the HCV positive group, the highest SFP was observed in the first post-OLT year. At that time point, a SFP $\leqslant$0.100 FU/mo was observed more frequently among recipients who had received their graft from a young donor and had a pre-transplant BMI value >26.0 kg/m^2. At completion of the first post-transplant year, a BMI value >26.5 kg/m^2 was associated with a T/C ratio $\leqslant$1. The proportion of patients with SFP >0.100 FU/mo descended in the following order: female recipients with a high T/C ratio, male recipients with high T/C ratio, and recipients of either gender with low T/C ratio. Hepatic steatosis was observed more frequently in recipients who, in the first post-transplant year, had increased their BMI $\geqslant$1.5 kg/m^2 in comparison to the pre-transplant value. Hepatic steatosis was inversely associated with the staging score.

CONCLUSION: Among HCV positive recipients, excess weight gain post-OLT does not represent a factor favoring early liver fibrosis development and might even be protective against it.

Key words: Liver transplantation; Hepatitis C infection; Liver fibrosis; Liver steatosis; Body mass index

Toniutto P, Fabris C, Avellini C, Minisini R, Bitetto D, Rossi E, Smirne C, Pirisi M. Excess body weight, liver steatosis, and early fibrosis progression due to hepatitis C recurrence after liver transplantation. *World J Gastroenterol* 2005; 11(38): 5944-5950

http://www.wjgnet.com/1007-9327/11/5944.asp

INTRODUCTION

Re-infection by hepatitis C virus (HCV) after liver transplantation (OLT) for HCV-related liver disease is almost universal, but the degree of necro-inflammatory damage and fibrosis deposition in the liver graft varies[1]. In the majority of cases, recurrent hepatitis C is mild. In up to one-third of OLT recipients with recurrent hepatitis C, however, a more severe course is observed, with progression to frank cirrhosis in less than 5 years[2]. The mechanisms associated with early fibrosis progression in this setting are actively investigated but remain poorly understood.

After liver transplantation, most patients gain weight[3], partly because of better health and freedom from pre-transplant dietary restrictions. As a result, within 2 years after the transplant operation, 60% of liver transplantation recipients are either overweight or obese. The role of excess weight post-transplant as a cardiovascular and metabolic risk factor has been widely addressed[4]: whether it may also contribute to graft damage, however, is unclear. Specifically, it is unknown if, in recipients with recurrent hepatitis C, fibrosis occurs earlier and is more severe when the patient is overweight or obese. This is conceivable, though, since data in immune-competent patients with chronic hepatitis C demonstrate that excess body weight leads to steatosis[5-7], acts as a cofactor for fibrosis progression[5,8,9] and represents an independent risk factor for non-response to antiviral treatment[10]. Independently of HCV infection, obesity may cause non-alcoholic steatohepatitis, a disease potentially capable of evolving toward cirrhosis and end-stage liver disease[11-13].

The present retrospective, longitudinal study aimed to investigate the possibility of a relationship between pre- and post-transplant body mass and fibrosis progression during recurrent hepatitis C. The study population included both

HCV positive and negative OLT recipients, in whom the value of body mass index (BMI) evaluated pre transplant and in the first 2 years post-transplant was related to the staging score measured in follow-up liver biopsies, taking into account other factors (pertaining to donor and host) which might have influenced the progression of recurrent hepatitis C.

MATERIALS AND METHODS

Patients

A total of 194 patients received a liver graft from a cadaveric donor between March 1996 and December 2002, at our institution. Insufficient data were available for 53 patients, who died either in the early post-transplant period or were lost to follow-up. Of the remaining 141 patients, 90 consecutive OLT recipients had a minimum follow-up of 2 years after OLT and had been subjected to at least one liver biopsy obtained not earlier than 1 year after OLT, and were included in the present study. Table 1 shows the demographic and clinical characteristics of the studied population. All were maintained in an immunosuppressive regimen that was either cyclosporine- or tacrolimus-based, associated, in the first few months, to corticosteroids. Cyclosporine dosage was calculated to obtain serum levels (measured 2 h after the drug administration) ranging from 800 to 1 200 μg/L in the first 6 wk after transplant and from 600 to 800 μg/L thereafter. Tacrolimus dosage was calculated to obtain pre-dose serum levels ranging from 10 to 15 μg/L in the first 6 wk after transplant and from 5 to 10 μg/L thereafter. Corticosteroid tapering was completed in 8 mo after the transplant in all except six patients (four HCV positive and two HCV negative). Thirty-two out of fifty-five HCV positive patients received antiviral treatment with interferon plus ribavirin due to recurrence of HCV hepatitis, defined as detectable serum HCV-RNA, serum alanine-aminotransferase (ALT) levels above the upper normal limit, Ishak grading score $\geqslant$2 and no evidence of rejection. Therapy was intended to be maintained for 12 mo. Antiviral treatment was started at a median time of 11.4 mo (range 0.7-75.9) after OLT and was completed in 17 patients. In the remaining 15 patients antiviral therapy had to be stopped prematurely due to adverse effects. Body weight was measured to the nearest 0.1 kg and height to the nearest 1 cm, with study participants wearing only underwear and no shoes. BMI was calculated as weight in kilograms divided by the square of the height in meters; it was measured pre transplant and one and 2 years after transplantation. In patients with ascites, pre-OLT BMI was calculated subtracting from the body weight the amount of ascitic fluid calculated on the basis of an ultrasound evaluation.

Liver histology In follow-up liver biopsies, grading and staging were scored according to the method of Ishak[14]. Fibrosis progression was evaluated annually in the first 4 years after OLT. It was based on the staging score at the corresponding "per protocol" liver biopsy, or, when unavailable, on the closest "on demand" liver biopsy. The speed of fibrosis progression (SFP), expressed in fibrosis units per month (FU/mo), was calculated for each 1-year time interval after OLT. It was obtained dividing the change observed in the fibrosis score at the end of the pertinent interval of time, with respect to either the transplant operation (for the first post-transplant year) or the previous liver biopsy (for the following years), by the number of months elapsed. The sum of micro- and macro-vesicular liver steatosis was calculated in each liver biopsy and graded as absent, $\leqslant$10% or >10%. All histological studies were performed by a single experienced histopathologist (CA).

Table 1 Clinical and demographic characteristics of the studied population

Recipient male gender, *n* (%)	63 (70.0)
Donor male gender, *n* (%)	53 (58.9)
Recipient age at transplantation (yr), median (range)	53 (23-66)
Donor age (yr), median (range)	41 (17-77)
Etiology of liver disease, *n* (%)	
HCV infection	55 (61.1)
HBV infection	12 (13.3)
Alcohol abuse	13 (14.5)
Other, unknown	10 (11.1)
Child–Pugh score pre-transplantation, median (range)	8 (5-14)
Immunosuppressive regimen, *n* (%)	
Tacrolimus-based	69 (76.7)
Cyclosporine-based	21 (23.3)
Antiviral therapy in HCV positive, *n* (%)	32 (58.2)

Categorical variables are expressed as frequencies (%); continuous variables as median (range). HCV: hepatitis C virus.

Statistical analysis

Statistical analysis of data was performed by means of the biomedical statistical software package BMDP Dynamic, Rel. 7.0 (Statistical Solutions, Cork, Ireland). Comparisons of continuous variables from two groups were explored by means of the Mann-Whitney's test. Correlations between continuous variables were performed either using the Spearman rank correlation coefficient or the Pearson product moment after logarithmic transformation of the values. Analysis of variance for repeated measures was employed to ascertain the significance of BMI increase post-OLT with respect to pre-OLT values. Wilcoxon matched pairs signed rank sum test was employed to evaluate modifications of fibrosis progression 2 and 3 years post-OLT in comparison to 1 year post-OLT. The associations between categorical variables were explored by means of the Pearson χ^2 test (in selected cases, with comparison of cross product ratios); if appropriate, the χ^2 test for linear trend was applied. Time-to-event analysis was performed to test whether the function to reach a staging score >2, in HCV positive patients, differed according to gender and BMI recorded pre- and 1 year post-OLT. Stepwise logistic regression analysis with a forward approach was used to evaluate the variables independently associated with a high one year post-OLT SFP. A level of 0.05 (two tailed) was chosen to indicate statistical significance.

RESULTS

BMI pre and post-OLT

BMI values, recorded before OLT, as well as 1 and 2 years post-OLT, are expressed in kg/m^2 and presented as medians (25-75th percentiles). For the entire study population, values were 25.0 (23.0-27.1), 25.4 (23.5-27.5) and 26.0 (23.7-28.4),

respectively (ANOVA for repeated measures, $P<0.05$). Among HCV positive recipients, the corresponding values were 24.7 (23.0-26.6), 25.1 (23.3-27.1) and 25.4 (23.4-28.1), respectively. Among HCV negative recipients, the corresponding values were 25.9 (23.0-28.4), 26.0 (24.0-28.0) and 26.6 (24.2-28.9), respectively. A BMI value $\geqslant$35 kg/m^2 (the limit indicating grade two obesity) was recognized before transplant operation in one HCV positive male recipient, who had a value of 38.4 kg/m^2. While 1 year after OLT, none of the recipients reached a BMI value $\geqslant$35 kg/m^2, 2 years after transplant, one HCV positive recipient had a BMI value of 36.5 kg/m^2 and one HCV negative patient a BMI value of 37.8 kg/m^2. The BMI values recorded pre-OLT and 1 and 2 years post-OLT were not statistically different between HCV positive and negative recipients. Among recipients belonging to both groups, no association was found between the pre-OLT BMI values and the severity of liver disease, calculated as the Child-Pugh score. Similarly, 1 and 2 years post-OLT BMI values did not differ considering the kind of immunosuppressive regimen in use (cyclosporine- or tacrolimus-based) or the rate of corticosteroid tapering (withdrawal completed before or after 90 d from OLT).

Liver histology

The histological follow-up lasted a median of 48 mo (range, 12-102 mo) in the HCV positive group and 30 mo (range, 12-78 mo) in the HCV negative group. A total of 465 follow-up liver biopsies were performed. In the group of HCV positive patients, the liver biopsies performed in a total of 315 patients, with a median number of five biopsies (range, 1-13) for each patient; protocol biopsies were 106/315 (median: two for each patient). In the group of HCV negative recipients, the liver biopsies performed were in a total of 150 patients, with a median number of four biopsies (range, 1-9) for each patient; protocol biopsies were 51 (median: one for each patient). In a median of 27 mo of follow up after OLT (range, 12-66mo), eight patients (8.8%; 6/8 were HCV positive) developed histological cirrhosis. The causes of cirrhosis in the two HCV negative patients were severe *de novo* autoimmune hepatitis and *de novo* HBV infection, respectively. At completion of the first post-transplant year, the median SFP was significantly faster in HCV positive in comparison to HCV-negative recipients: 0.083 (range, 0-0.455) *vs* 0.059 (range, 0-0.250) FU/mo ($P<0.02$). Table 2 shows the associations observed between 1 year post-OLT SFP >0.100 FU/mo and clinical and demographic characteristics of patients. Older donor age and lower BMI value pre-OLT were both significantly associated with faster fibrosis progression in HCV positive but not in HCV-negative recipients.

Figure 1 shows the fibrosis progression rates calculated at 1-4 years after OLT in the HCV-positive recipients. The fastest rate of fibrosis progression was observed during the 1st year after OLT. Later biopsies demonstrated a decrease in SFP with a non linear logarithmic trend ($r = 0.436$, $F = 37.1$, $P<0.0001$). Starting with the 3rd year after OLT, the SFP stabilized. Among the variables reported in Table 2, only a BMI value 1 year post-OLT >27.5 kg/m^2 was significantly associated with fibrosis progression <0.050 FU/mo (8/8 *vs* 18/35; $P<0.02$) in the 2nd year post-OLT. There was no difference in the SFP at 1 and 2 years post-OLT between patients that completed antiviral therapy as scheduled in comparison to those that either were untreated or terminated early interferon plus ribavirin treatment.

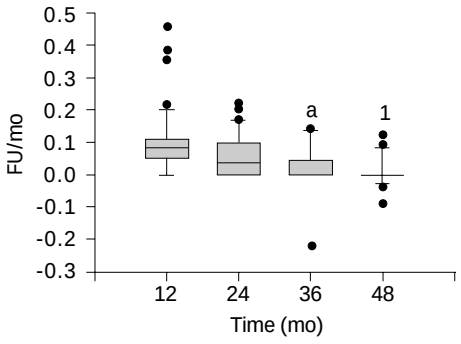

Figure 1 Vertical box plots of fibrosis progression rates in HCV-positive recipients, expressed as FU/mo, at different time points after the transplant operation. Median values, 10th, 25th, 75th, and 90th percentile are reported. Dots indicate outliers. [a]$P<0.005$ in comparison to FU/mo at 12 mo (Wilcoxon matched pairs signed rank sum test), [1]$P = 0.0001$ in comparison to FU/mo at 12 mo (Wilcoxon matched pairs signed rank sum test).

To further explore the relationship between gender and BMI, on the one hand, and fibrosis progression, on the other,

Table 2 Frequencies of patients with a SFP$\leqslant$0.100 FU/mo in the 1st year post-OLT, in relationship with a selection of demographic and clinical variables

	All patients ($n = 90$) FU/mo$\leqslant$0.100 $n = 70$	HCV-positive patients ($n = 55$) FU/mo$\leqslant$0.100 $n = 39$	HCV-negative patients ($n = 35$) FU/mo$\leqslant$0.100 $n = 31$
Recipient male gender ($n = 63$)	53[a]	29	24
Donor male gender ($n = 53$)	40	19	21
Recipient age $\leqslant$55 yr ($n = 54$)	42	19	23
Donor age $\leqslant$45 yr ($n = 54$)	47[d]	29[f]	18
Pre-OLT BMI >26.0 kg/m^2 ($n = 35$)	32[b]	16[c]	16
Tacrolimus therapy ($n = 69$)	56	31	25
Corticosteroid tapering >90 d ($n = 47$)	39	25	14
Diabetes mellitus ($n = 24$)	17	10	7

FU/mo: fibrosis units per month, HCV: hepatitis C virus, BMI: body mass index, [a]$P<0.05$ *vs* recipient female gender, [b]$P<0.02$ *vs* pre-OLT BMI $\leqslant$26 kg/m^2, [d]$P<0.01$ *vs* donor age >45 yr; [c]$P<0.05$ *vs* pre-OLT BMI $\leqslant$26 kg/m^2, [f]$P<0.001$ *vs* donor age >45 yr. P value refers to χ^2.

Table 3 Degree of hepatic steatosis in 105 biopsies performed between 12 and 36 mo after the transplant operation (HCV-positive recipients only), in relationship with a selection of variables

	Steatosis			
	Absent (n = 34)	≤10% (n = 60)	>10% (n = 11)	P
Ishak staging score≤2 (n = 79)	19	49	11	<0.005
Recipient male gender (n = 72)	20	42	10	<0.05
Recipient age≤55 yr (n = 50)	15	28	7	NS
Donor age≤45 yr (n = 65)	19	39	7	NS
BMI increase <1.5 kg/m^2 (n = 76)	29	41	6	<0.05
Recurrent hepatitis C≤1 yr post-OLT (n = 79)	31	41	7	<0.02
Diabetes mellitus (n = 31)	10	18	3	NS

BMI: body mass index, OLT: orthotopic liver transplantation, BMI increase: difference between BMI value 1 yr post-OLT and BMI value pre-OLT. P value refers to χ^2 for linear trend.

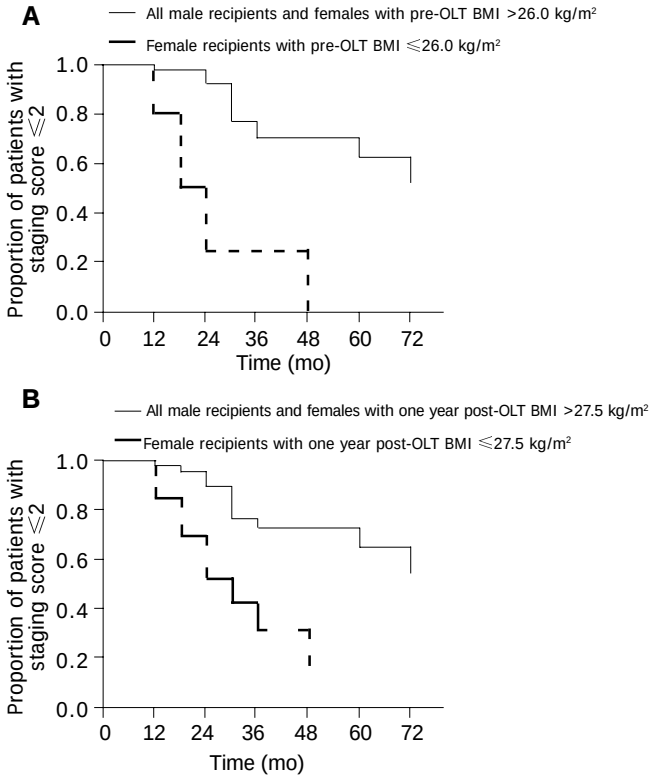

Figure 2 A: Time-to-event analysis to reach a staging score >2. HCV-positive recipients were divided as follows: all the male recipients and those females with pre-OLT BMI value >26.0 kg/m^2 (n = 45, continuous line); females with pre-OLT BMI value ≤26.0 kg/m^2 (n = 10, dotted line). B: Time-to-event analysis to reach a staging score >2. HCV-positive recipients were divided as follows: all the male recipients and those females with 1 year post-OLT BMI value >27.5 kg/m^2 (n = 42, continuous line); females with 1 year post-OLT BMI value ≤27.5 kg/m^2 (n = 13, dotted line).

we categorized OLT recipients as follows: females with BMI pre-OLT ≤26.0 kg/m^2 (group A^{pre}) or ≤27.5 kg/m^2 1 year post-OLT (group A^{post}); males with pre-OLT BMI value ≤26.0 kg/m^2 (group B^{pre}) or ≤27.5 kg/m^2 1 year post-OLT (group B^{post}); recipients of either gender and pre-OLT BMI >26.0 kg/m^2 (group C^{pre}) or >27.5 kg/m^2 1 year post-OLT (group C^{post}). Group A^{pre} showed the fastest SFP 1 year post-OLT, in comparison to group B^{pre} and group C^{pre} (7/10 *vs* 7/27 *vs* 16/18; P<0.002 for linear trend); a similar trend also was found considering 1 year post-OLT BMI and 2 years post-OLT fibrosis progression (A^{post} 6/10 *vs* B^{post} 11/25 *vs* C^{post} 8/8; P<0.02 for linear trend). Time-to-event analysis showed that, in females with lower BMI, the probability to reach a staging score >2 was the highest in comparison to all other recipients; this observation held true either considering BMI values pre-OLT (Figure 2A, Mantel-Cox, P<0.0001) or BMI values 1 year after OLT (Figure 2B, Mantel-Cox, P = 0.0005). Stepwise logistic regression analysis was performed among the predictive variables that, at univariate analysis, were associated, with a P value <0.10, to faster SFP (donor age, recipient gender, type of immunosuppressive therapy, and pre-OLT BMI). A SFP in the 1st year post-OLT >0.100 FU/mo was independently associated with older donor age (improvement of χ^2 11.63, P = 0.001), female recipient gender (improvement of χ^2 5.09, P<0.05) and lower pre-OLT BMI value (improvement of χ^2 4.26, P<0.05).

Post-OLT BMI, blood lipids, and liver steatosis One year post-OLT, having a BMI >26.5 kg/m^2, was found to be associated with a triglycerides/cholesterol (T/C) ratio ≤1 (14/15 *vs* 26/40, P<0.05). In relationship to the recipient gender, a low T/C ratio, i.e., higher serum levels of cholesterol than of triglycerides, was associated both to a delayed (>1 year) hepatitis C recurrence and to a slower post-OLT SFP. Female recipients with a high T/C ratio had the highest proportion of early hepatitis C recurrence and 1 year SFP >0.100 FU/mo, followed by male recipients with high T/C ratio and patients of either gender with low T/C ratio: 4/4 *vs* 11/11 *vs* 28/40 (P<0.05 for linear trend), and 4/4 *vs* 3/11 *vs* 9/40 (P<0.01 for linear trend), respectively.

One-hundred and five liver biopsies were performed in HCV-positive patients along the period of time elapsed between 12 and 36 mo post-OLT. Table 3 shows the relationship between hepatic steatosis and a selection of variables, including the Ishak fibrosis score. Male gender, delayed hepatitis C recurrence, and body weight gain post-OLT were positively associated with steatosis; on the contrary, progression to significant fibrosis was less frequent in the presence of hepatic steatosis.

[redacted]

Post-OLT fibrosis progression in patients transplanted for HCV-related liver cirrhosis has been recently reported to behave not linearly[15], reaching, a sharp increase in the first

2 years, a plateau at the 3rd year after OLT. In the present paper, we confirmed this observation, showing that fibrosis progression during the 1st year after OLT is faster than that observed in the longer follow-up, when the process tends to slow down. Furthermore, early fibrosis progression in the grafts of HCV recipients is confirmed to be related to factors pertaining both to the donor and to the host. First and most importantly, fibrosis progression is affected by the age of donors, in agreement with previous work by several authors who considered an aged donor as the strongest predictor of fibrosis progression in patients with post-OLT HCV recurrence[16]. Second, a novel finding and the focus of the present investigation, early fibrosis progression after OLT appears to be related to the BMI value measured either pre-OLT or post-OLT. The association is not direct, as one might expect, but inverse: the higher the BMI value, the lower is the degree of early fibrosis development. This association is peculiar to HCV-positive patients and was not observed in HCV-negative recipients. Third, the presence of steatosis in the graft, which occurs in association with the increase in BMI, does not predict, as reported in immune-competent patient, a higher fibrosis score. To reconcile these findings with the existing literature, the elements that need to be considered in detail concern the differences that exist between the natural history of HCV infection in immune-competent *vs* OLT patients, and the putative molecular mechanisms of HCV re-infection.

Obesity[5,8,9] and liver steatosis[6,17,18] are recognized factors of liver fibrosis progression in HCV-positive immune-competent patients. Some authors have hypothesized a direct steatogenic effect of HCV, supported by several lines of evidence: the development of progressive hepatic steatosis in transgenic mice expressing the HCV core gene[19], the inhibition of very low density lipoprotein (VLDL) secretion in a transgenic murine model expressing HCV core protein[20], the close relationship between intra-hepatic HCV RNA and development of steatosis[21], and the correlation between hepatic steatosis and hepatic HCV replication in patients infected with HCV genotype 3[22]. Others have investigated the mechanisms involved in the progression of liver fibrosis due to the concomitant presence of steatosis and HCV infection, suggesting that steatosis might contribute to fibrosis through a steatohepatitis-like pathway involving stellate cell activation and peri-sinusoidal fibrosis production[23]. In OLT patients, however, the situation is different. A recent report[24], while confirming that body weight is the best predictor of liver steatosis 12 mo post-OLT, demonstrated that allograft steatosis does not predict the severity of HCV recurrence in HCV-infected patients within the first 12 mo after OLT. The present results converge in the same direction, and suggest, for the first time, that overweight, while facilitates liver steatosis, on the other hand may protect the liver graft, during an initial phase, from the damage due to HCV recurrence. Further data outline the need to be cautious when transposing the information concerning the natural history of HCV in immune-competent patients to the natural history of HCV recurrence post-OLT. For example, female gender, known to be protective against fibrosis in immune-competent patients[25], is on the contrary a negative prognostic factor in the post-OLT setting[26]. The present data showed that, among the patients with the lowest BMI values, female recipients had a SFP faster than the corresponding males. Therefore, one might hypothesize that the stronger susceptibility of female recipients to HCV recurrence could be related, at least in part, to factors affected by the interrelationship between gender and BMI variations, for example the lipid profile.

According to recent studies, several aspects of HCV infection are connected with lipid metabolism and lipid profile modifications. Binding of HCV to cell membrane of hepatocytes is thought to occur via two putative HCV receptors: CD81, a cellular surface protein belonging to the tetraspanin protein super-family, and the low density lipoprotein receptor (LDL-r)[27-29]. The HCV envelope glycoprotein E2 may interact with the CD81 molecule, while HCV or HCV-LDL complexes interact preferentially with the LDL-r[30]. HCV circulates in blood in association with different lipoproteins: early in the course of the infection, the preferential association is with LDL, while later on the association is with high-density lipoproteins (HDL). In accordance, patients with immune-deficiencies present higher HCV RNA titers in the LDL and HDL fractions than the immune-competent counterparts[31]. During the early viremic phase of experimental HCV infection, several genes associated with lipid metabolism are upregulated; interestingly, the fatty acid synthesizing gene is expressed at higher levels among chimpanzees that attain sustained clearance of the virus[32]. Binding and internalization of HCV RNA containing particles seem strictly regulated by lipoproteins: an increase of LDL and other lipoproteins decreases the LDL-r HCV particles interaction[28,33,34] while an upregulation of the LDL-r increases the internalization of HCV[35]. According to a recently proposed model, virions are released by liver cells and may infect other liver cells via LDL-r; free β-lipoproteins may regulate the rate of the infection of liver cells by competing with the virus[29]. Considering altogether these observations, it is tempting to speculate that a particular lipid profile could be associated with a slower kinetic of HCV infection of the hepatocytes and as a consequence a lesser fibrosis progression of the graft. We calculated the ratio between serum triglycerides and serum cholesterol as a proxy index of the balance between VLDL and LDL in the circulation. An association was found between a low T/C ratio and a higher BMI 1 year post-OLT. As previously observed considering the association between BMI and fibrosis progression, the relationships between the value of T/C ratio and both the timing of hepatitis C recurrence and the 1 year fibrosis progression rate were gender-related: females with higher T/C ratio were found to present the fastest SFP. Following this line, one might hypothesize that a low BMI, especially for female patients, could be associated with a lipid profile characterized by reduced serum LDL/VLDL levels. In fact, the relationship between increasing body weight and blood lipid profile is stricter in men than in women[36-38]. Furthermore, we have previously found that recipient's carriage of at least one ε4 allele of the apo-lipoprotein E (an allelic variant associated with higher cholesterol levels) was associated with better histological outcome of recurrent hepatitis C in male, but not in female recipients[39]. An unfavorable lipoprotein profile could possibly enhance HCV infectivity through an

upregulation of LDL-r[40], or decreased interference of LDL at the level of the interaction between HCV and LDL-r[29].

In conclusion, post-OLT overweight in HCV-positive recipients does not represent a factor favoring early liver fibrosis development and could even be protective against it. The explanation of this unexpected finding might reside on the peculiar lipid profile of patients with excess body weight post-OLT, capable to modulate the severity of HCV recurrence and hence the speed at which liver fibrosis develops.

REFERENCES

1 **McCaughan GW**, Zekry A. Pathogenesis of hepatitis C virus recurrence in the liver allograft. *Liver Transpl* 2002; **8**: S7-13
2 **Berenguer M**. Natural history of recurrent hepatitis C. *Liver Transpl* 2002; **8**: S14-18
3 **Mazuelos F**, Abril J, Zaragoza C, Rubio E, Moreno JM, Turrion VS, Cuervas-Mons V. Cardiovascular morbidity and obesity in adult liver transplant recipients. *Transplant Proc* 2003; **35**: 1909-1910
4 **Nair S**, Verma S, Thuluvath PJ. Obesity and its effect on survival in patients undergoing orthotopic liver transplantation in the United States. *Hepatology* 2002; **35**: 105-109
5 **Hourigan LF**, Macdonald GA, Purdie D, Whitehall VH, Shorthouse C, Clouston A, Powell EE. Fibrosis in chronic hepatitis C correlates significantly with body mass index and steatosis. *Hepatology* 1999; **29**: 1215-1219
6 **Adinolfi LE**, Gambardella M, Andreana A, Tripodi MF, Utili R, Ruggiero G. Steatosis accelerates the progression of liver damage of chronic hepatitis C patients and correlates with specific HCV genotype and visceral obesity. *Hepatology* 2001; **33**: 1358-1364
7 **Monto A**, Alonzo J, Watson JJ, Grunfeld C, Wright TL. Steatosis in chronic hepatitis C: relative contributions of obesity, diabetes mellitus, and alcohol. *Hepatology* 2002; **36**: 729-736
8 **Ortiz V**, Berenguer M, Rayon JM, Carrasco D, Berenguer J. Contribution of obesity to hepatitis C-related fibrosis progression. *Am J Gastroenterol* 2002; **97**: 2408-2414
9 **Friedenberg F**, Pungpapong S, Zaeri N, Braitman LE. The impact of diabetes and obesity on liver histology in patients with hepatitis C. *Diabetes Obes Metab* 2003; **5**: 150-155
10 **Bressler BL**, Guindi M, Tomlinson G, Heathcote J. High body mass index is an independent risk factor for nonresponse to antiviral treatment in chronic hepatitis C. *Hepatology* 2003; **38**: 639-644
11 **Poonawala A**, Nair SP, Thuluvath PJ. Prevalence of obesity and diabetes in patients with cryptogenic cirrhosis: a case-control study. *Hepatology* 2000; **32**: 689-692
12 **Clark JM**, Diehl AM. Nonalcoholic fatty liver disease: an underrecognized cause of cryptogenic cirrhosis. *Jama* 2003; **289**: 3000-3004
13 **Ioannou GN**, Weiss NS, Kowdley KV, Dominitz JA. Is obesity a risk factor for cirrhosis-related death or hospitalization? A population-based cohort study. *Gastroenterology* 2003; **125**: 1053-1059
14 **Ishak K**, Baptista A, Bianchi L, Callea F, De Groote J, Gudat F, Denk H, Desmet V, Korb G, MacSween RN. Histological grading and staging of chronic hepatitis. *J Hepatol* 1995; **22**: 696-699
15 **Neumann UP**, Berg T, Bahra M, Seehofer D, Langrehr JM, Neuhaus R, Radke C, Neuhaus P. Fibrosis progression after liver transplantation in patients with recurrent hepatitis C. *J Hepatol* 2004; **41**: 830-836
16 **Machicao VI**, Bonatti H, Krishna M, Aqel BA, Lukens FJ, Nguyen JH, Rosser BG, Satyanarayana R, Grewal HP, Hewitt WR, Harnois DM, Crook JE, Steers JL, Dickson RC. Donor age affects fibrosis progression and graft survival after liver transplantation for hepatitis C. *Transplantation* 2004; **77**: 84-92
17 **Serfaty L**, Poujol-Robert A, Carbonell N, Chazouilleres O, Poupon RE, Poupon R. Effect of the interaction between steatosis and alcohol intake on liver fibrosis progression in chronic hepatitis C. *Am J Gastroenterol* 2002; **97**: 1807-1812
18 **Castera L**, Hezode C, Roudot-Thoraval F, Bastie A, Zafrani ES, Pawlotsky JM, Dhumeaux D. Worsening of steatosis is an independent factor of fibrosis progression in untreated patients with chronic hepatitis C and paired liver biopsies. *Gut* 2003; **52**: 288-292
19 **Moriya K**, Yotsuyanagi H, Shintani Y, Fujie H, Ishibashi K, Matsuura Y, Miyamura T, Koike K. Hepatitis C virus core protein induces hepatic steatosis in transgenic mice. *J Gen Virol* 1997; **78**(Pt 7): 1527-1531
20 **Perlemuter G**, Sabile A, Letteron P, Vona G, Topilco A, Chretien Y, Koike K, Pessayre D, Chapman J, Barba G, Brechot C. Hepatitis C virus core protein inhibits microsomal triglyceride transfer protein activity and very low density lipoprotein secretion: a model of viral-related steatosis. *Faseb J* 2002; **16**: 185-194
21 **Fujie H**, Yotsuyanagi H, Moriya K, Shintani Y, Tsutsumi T, Takayama T, Makuuchi M, Matsuura Y, Miyamura T, Kimura S, Koike K. Steatosis and intrahepatic hepatitis C virus in chronic hepatitis. *J Med Virol* 1999; **59**: 141-145
22 **Rubbia-Brandt L**, Quadri R, Abid K, Giostra E, Male PJ, Mentha G, Spahr L, Zarski JP, Borisch B, Hadengue A, Negro F. Hepatocyte steatosis is a cytopathic effect of hepatitis C virus genotype 3. *J Hepatol* 2000; **33**: 106-115
23 **Clouston AD**, Jonsson JR, Purdie DM, Macdonald GA, Pandeya N, Shorthouse C, Powell EE. Steatosis and chronic hepatitis C: analysis of fibrosis and stellate cell activation. *J Hepatol* 2001; **34**: 314-320
24 **Machicao VI**, Krishna M, Bonatti H, Aqel BA, Nguyen JH, Weigand SD, Rosser BG, Hughes C, Dickson RC. Hepatitis C recurrence is not associated with allograft steatosis within the first year after liver transplantation. *Liver Transpl* 2004; **10**: 599-606
25 **Poynard T**, Ratziu V, Benmanov Y, Di Martino V, Bedossa P, Opolon P. Fibrosis in patients with chronic hepatitis C: detection and significance. *Semin Liver Dis* 2000; **20**: 47-55
26 **Forman LM**, Lewis JD, Berlin JA, Feldman HI, Lucey MR. The association between hepatitis C infection and survival after orthotopic liver transplantation. *Gastroenterology* 2002; **122**: 889-896
27 **Agnello V**, Abel G, Elfahal M, Knight GB, Zhang QX. Hepatitis C virus and other flaviviridae viruses enter cells via low density lipoprotein receptor. *Proc Natl Acad Sci USA* 1999; **96**: 12766-12771
28 **Germi R**, Crance JM, Garin D, Guimet J, Lortat-Jacob H, Ruigrok RW, Zarski JP, Drouet E. Cellular glycosaminoglycans and low density lipoprotein receptor are involved in hepatitis C virus adsorption. *J Med Virol* 2002; **68**: 206-215
29 **Monazahian M**, Bohme I, Bonk S, Koch A, Scholz C, Grethe S, Thomssen R. Low density lipoprotein receptor as a candidate receptor for hepatitis C virus. *J Med Virol* 1999; **57**: 223-229
30 **Wunschmann S**, Medh JD, Klinzmann D, Schmidt WN, Stapleton JT. Characterization of hepatitis C virus (HCV) and HCV E2 interactions with CD81 and the low-density lipoprotein receptor. *J Virol* 2000; **74**: 10055-10062
31 **Pumeechockchai W**, Bevitt D, Agarwal K, Petropoulou T, Langer BC, Belohradsky B, Bassendine MF, Toms GL. Hepatitis C virus particles of different density in the blood of chronically infected immunocompetent and immunodeficient patients: Implications for virus clearance by antibody. *J Med Virol* 2002; **68**: 335-342
32 **Su AI**, Pezacki JP, Wodicka L, Brideau AD, Supekova L, Thimme R, Wieland S, Bukh J, Purcell RH, Schultz PG, Chisari FV. Genomic analysis of the host response to hepatitis C virus infection. *Proc Natl Acad Sci USA* 2002; **99**: 15669-15674
33 **Triyatni M**, Saunier B, Maruvada P, Davis AR, Ulianich L, Heller T, Patel A, Kohn LD, Liang TJ. Interaction of hepatitis C virus-like particles and cells: a model system for studying

viral binding and entry. *J Virol* 2002; **76**: 9335-9344

34 **Enjoji M**, Nakamuta M, Kinukawa N, Sugimoto R, Noguchi K, Tsuruta S, Iwao M, Kotoh K, Iwamoto H, Nawata H. Beta-lipoproteins influence the serum level of hepatitis C virus. *Med Sci Monit* 2000; **6**: 841-844

35 **Andre P**, Komurian-Pradel F, Deforges S, Perret M, Berland JL, Sodoyer M, Pol S, Brechot C, Paranhos-Baccala G, Lotteau V. Characterization of low- and very-low-density hepatitis C virus RNA-containing particles. *J Virol* 2002; **76**: 6919-6928

36 **Brown CD**, Higgins M, Donato KA, Rohde FC, Garrison R, Obarzanek E, Ernst ND, Horan M. Body mass index and the prevalence of hypertension and dyslipidemia. *Obes Res* 2000; **8**: 605-619

37 **Heitmann BL**. The effects of gender and age on associations between blood lipid levels and obesity in Danish men and women aged 35-65 years. *J Clin Epidemiol* 1992; **45**: 693-702

38 **Wilsgaard T**, Arnesen E. Change in serum lipids and body mass index by age, sex, and smoking status: the Tromso study 1986-1995. *Ann Epidemiol* 2004; **14**: 265-273

39 **Toniutto P**, Fabris C, Fumo E, Apollonio L, Caldato M, Mariuzzi L, Avellini C, Minisini R, Pirisi M. Carriage of the apolipoprotein E-epsilon4 allele and histologic outcome of recurrent hepatitis C after antiviral treatment. *Am J Clin Pathol* 2004; **122**: 428-433

40 **Olson RE**. Discovery of the lipoproteins, their role in fat transport and their significance as risk factors. *J Nutr* 1998; **128**: S439-443

Science Editor Guo SY **Language Editor** Elsevier HK

PO Box 2345, Beijing 100023, China
www.wjgnet.com
wjg@wjgnet.com

ELSEVIER

World J Gastroenterol 2005;11(38):5951-5957
World Journal of Gastroenterology ISSN 1007-9327

• *BASIC RESEARCH* •

Upregulation of cathepsin W-expressing T cells is specific for autoimmune atrophic gastritis compared to other types of chronic gastritis

Doerthe Kuester, Michael Vieth, Ulrich Peitz, Stefan Kahl, Manfred Stolte, Albert Roessner, Ekkehard Weber, Peter Malfertheiner, Thomas Wex

Doerthe Kuester, Michael Vieth, Albert Roessner, Institute of Pathology, Otto-von-Guericke University Magdeburg, Leipziger Str. 44, Magdeburg D-39120, Germany
Ulrich Peitz, Stefan Kahl, Peter Malfertheiner, Thomas Wex, Department of Gastroenterology, Hepatology and Infectious Diseases, Otto-von-Guericke University Magdeburg, Leipziger Str. 44, Magdeburg D-39120, Germany
Manfred Stolte, Institute of Pathology, Klinikum Bayreuth GmbH, Preuschwitzerstr 101, Bayreuth D-95445, Germany
Ekkehard Weber, Institute of Physiological Chemistry, Medical Faculty, Martin-Luther University Halle-Wittenberg, Holly Str. 1, Halle D-06097, Germany
Supported by the "Deutsche Forschungsgemeinschaft", Germany (We2170/3-1) and the NBL-3 program of the "Bundesministerium für Forschung und Technik" (NBL3/01ZZ0407/PFG1)
Correspondence to: Dr. Thomas Wex, Department of Gastroenterology, Hepatology and Infectious Diseases, Otto-von-Guericke University, Magdeburg, Leipziger Str. 44, Magdeburg D-39120, Germany. thomas.wex@medizin.uni-magdeburg.de
Telephone: +49-391-6713106 Fax: +49-391-6713105
Received: 2005-03-04 Accepted: 2005-04-30

Abstract

AIM: To investigate a pathophysiological role of cathepsin W (CatW), a putative thiol-dependent cysteine protease, which is specifically expressed in cytotoxic lymphocytes, in different types of chronic inflammation of the gastric mucosa.

METHODS: Gastric and duodenal biopsies of patients with *Helicobacter pylori* (*H pylori*)-associated active gastritis (*Hp*, $n = 19$), chemically induced reactive gastritis (CG, $n = 17$), autoimmune atrophic gastritis (AIG, $n = 20$), lymphocytic corpus gastritis (LG, $n = 29$), celiac disease (CD, $n = 10$), and corresponding controls ($n = 24$) were analyzed by immunohistochemistry for the expression of CatW and CD45. Furthermore, immunohistochemical double staining with anti-CD3 and anti-cathepsin was performed for the samples of AIG.

RESULTS: Median values of CatW-expressing cells among CD45-positive immune cells were between 2% and 6% for normal gastric mucosa, CG, and LG, whereas the corresponding value was significantly increased for AIG (24.7%, $P<0.001$) and significantly decreased for HP (0.7%, $P<0.05$). Double staining with anti-CD3 and anti-CatW antibodies revealed that >90% of CatW-expressing cells in gastric mucosa of AIG were T cells. Duodenal mucosa had significantly more CatW/CD45-positive cells than normal gastric mucosa (median: 17.8% *vs* 2%, $P<0.01$). The corresponding proportion of CatW/CD45-positive cells was decreased in CD compared to duodenal mucosa (median: 2.1% *vs* 17.8%, $P<0.05$).

CONCLUSION: The opposite findings regarding the presence of CatW-positive cells in AIG (increase) and CD (decrease) reflects the different cellular composition of immune cells involved in the pathogenesis of these diseases.

Key words: Cathepsin W; Inflammation; Gastritis; Immunohistochemistry; NK cells

Kuester D, Vieth M, Peitz U, Kahl S, Stolte M, Roessner A, Weber E, Malfertheiner P, Wex T. Upregulation of cathepsin W-expressing T cells is specific for autoimmune atrophic gastritis compared to other types of chronic gastritis. *World J Gastroenterol* 2005; 11(38): 5951-5957
http://www.wjgnet.com/1007-9327/11/5951.asp

INTRODUCTION

Gastritis, by definition, is a histopathological entity characterized by the chronic and active inflammation of the gastric mucosa. The classification of gastritis, according to the updated Sydney system[1], is organized along traditional lines with active and chronic gastritis and includes specific forms of chronic gastritis defined by topography, morphology, and etiology and is graded with the help of a semiquantitative visual scale. The discovery of *Helicobacter pylori* (*H pylori*) has dramatically altered the etiological concepts of several gastric diseases. *H pylori* is the major cause of gastritis, gastric ulcer and has been classified as a definite human carcinogen playing a key role in the pathogenesis of gastric cancer and MALT lymphoma[2,3]. The host response to *H pylori* and its bacterial products is composed of T-, B-lymphocytes and plasma cells defined as chronicity of the gastritis. The infiltration of the lamina propria and gastric epithelium by polymorph nuclear leukocytes (mostly neutrophil granulocytes) reflects the activity of the inflammation.

NSAID-associated or bile-induced chemical reactive gastritis, causing 20-30% of gastritis, as well as autoimmune and lymphocytic gastritis (LG) are distinct entities. The presence

of atrophy in the gastric corpus with diffuse atrophy of parietal and chief cells are the main characteristics of autoimmune atrophic gastritis (AIG) together with a hyperplasia of ECL cells. This disease is associated with serum anti-parietal and anti-intrinsic factor (IF) antibodies that cause IF deficiency, which can lead eventually to pernicious anemia in some patients. It has been shown that AIG is associated with infiltration of $CD4^+$ T lymphocytes into the gastric mucosa, where they contribute to tissue destruction and gastric atrophy[4].

Chemically induced reactive gastritis (CG), caused by the use of nonsteroidal anti-inflammatory agents (NSAIDs) or bile reflux, is characterized by regenerative processes that lead to foveolar hyperplasia, mucosal edema, hemorrhage, capillary ectasia, proliferation of ascending smooth muscle fibers, and apical fibrosis. Usually, these lesions exhibit a slight superficial infiltration of lymphocytes and plasma cells. NSAIDs might additionally cause epithelial damage such as erosions and ulcers[1].

LG is a rare form of gastritis. The essential diagnostic feature is the presence of increased intraepithelial lymphocytes (mostly T cells), at least 25 lymphocytes per 100 epithelial cells. In the lamina propria, there are often additional neutrophil granulocytes among lymphocytes and plasma cells at the surface epithelium and within foveolar epithelium[5-7]. LG is believed to represent a special form of Helicobacter-mediated gastritis, mostly found in the corpus and fundus, although *H pylori* is only rarely found morphologically[6,7]. Three different types of LG can be distinguished depending on the endoscopic appearance: LG without typical endoscopic findings, the varioliform gastritis with thickened rugal folds, and Ménétriers disease with prominent rugal folds.

In human beings, the group of thiol-dependent cathepsins comprises 11 different cysteine proteases that are mostly localized in the lysosomal compartment[8]. During the last decade, it has become evident that most of these enzymes in addition to their role in lysosomal protein degradation[9] can mediate or regulate specific processes in various tissues and cell types. These functions include 'limited proteolysis' leading to the activation of granzymes[10], the maturation of hormones[11,12] and the regulation of antigen presentation[13]. As today, there is limited knowledge concerning the role of thiol-dependent cathepsins in gastric physiology and related disorders. Notably, cathepsins B and L were found to be associated with the carcinogenesis and metastasis of gastric and esophageal cancer[14-16]. Furthermore, cathepsins X and K were found to be specifically expressed in gastric epithelium[17], whereas cathepsin W (CatW) was found to be specifically expressed in lymphocyte-like cells within the gastric and intestinal tissue[18]. This finding was in line with the restricted expression pattern of CatW, which is expressed in NK cells and in cytotoxic T cells[19-21]. Although, its enzymatic activity and major function has not been characterized, there are some data supporting a regulatory role of this putative protease in the cytotoxic process for the NK-92 cell model[22]. However, cells from CatW-deficient mice were not affected in their cell-mediated cytotoxicity *in vitro*[23]. The specific association between CatW and cytotoxic cells and the potential involvement of these cells in chronic inflammation, prompted us to investigate the expression of CatW in different types of gastritis.

MATERIALS AND METHODS

Materials

A total of 119 formalin-fixed, paraffin-embedded biopsy specimens from patients suffering from different gastrointestinal disorders were retrieved from the archives of the institutes of Pathology Bayreuth and Magdeburg. The selection was based on clinical and histological evidence of the corresponding diagnosis including *H pylori*-associated chronic active gastritis (n = 19), CG (n = 17), AIG (n = 20), lymphocytic corpus gastritis without endoscopic findings (n = 29) as well as samples of duodenal mucosa of 10 patients with celiac disease (CD). Furthermore, healthy controls of both gastric (n = 14) and duodenal (n = 10) mucosa were examined immunohistochemically. Histological diagnosis was made by hematoxylin-eosin and Warthin-Starry stainings.

Methods

Detection of cathepsin W and CD45 by immunohistochemistry After the removal of paraffin by xylol, two sets of serial sections of all tissue specimens were subsequently dehydrated using increasing concentrations of ethanol. In order to demask the antigens, the samples were boiled thrice in 0.01 mol/L sodium citrate buffer (pH 6.0) for 10 min in a microwave (600 W), and incubated for 30 min at room temperature in 1×staining buffer containing 5% RPMI, 5% FCS, and 0.05% sodium azide in aqua dest (pH 7.4-7.6). The subsequent staining procedure on each one serial slide was performed using the monoclonal anti-CatW antibody CW-401B1 (1:1 000 in 1×staining buffer, 1 h at room temperature) and the Vectastain ABC-AP Kit (Vector, Burlingame) following the manufacturer's instructions. In addition, a matching set of serial sections was stained with anti-CD45 (LCA, DakoCytomation, Glostrup, Denmark). The used antibody is a mixture of two mAbs (2B11 and PD7/26) representing all isoforms (2B11) and the isoform CD45R0 (PD7/26). Immunostaining was performed as described elsewhere[24]. All samples were counterstained with hematoxylin, dehydrated and mounted using DEPEX™ (Serva, Heidelberg, Germany).

Detection of cathepsin W and CD3 by double immunohistochemistry in autoimmune atrophic gastritis To distinguish between CatW-positive-stained natural killer cells and cytotoxic T lymphocytes, a third series of sections of the above used tissue specimens with AIG was pretreated and stained with the anti-CatW antibody and detected with Vectastain ABC-AP Kit as described above. After washing the slides thoroughly in PBS, subsequent staining with the anti-CD3-antibody (1:100; anti-human CD3, A 0452; DakoCytomation, Hamburg, Germany) was performed; marking the CD3-complex of T cells.

For revealing positive immunohistochemical reaction, the iVIEW™ DAB Detection Kit (Ventana, Germany) was used as chromogen substrate, and then specimens were counterstained with hematoxylin and mounted with DEPEX™.

For all immunohistochemical analyses, two persons counted the numbers of stained cells in three independent high-power fields. Mann-Whitney U test was used for group comparison. For all statistical analyses, $P<0.05$ was considered to indicate statistical significance.

Generally, a consistent staining pattern exhibiting CatW-positive cells with a lymphocytic phenotype was obtained in all samples. The tissue specimens of the different chronic gastrointestinal disorders contained various amounts of CatW-expressing cells. In normal gastric mucosa, CatW-expressing cells were rarely detected (0.5±1 cells/field), whereas the different forms of gastritis revealed higher absolute numbers of 4.1-41 cells per observation field (Figure 2). Other immune cells including polymorph nuclear neutrophils, macrophages, and plasma cells as well as epithelial and stroma cells did not express CatW. AIG showed extensive mucosal atrophy, replacement of the oxyntic glands by intestinal metaplastic epithelium and mononuclear infiltrate within the lamina propria with approximately 25% of $CD45^+$ cells expressing CatW (Figure 1C). CD with subtotal villous atrophy and dense inflammatory infiltrate revealed a fraction of about 5% $CatW^+/CD45^+$ cells (Figure 1D). In chronic *H pylori* gastritis, the gastric mucosa contained high absolute numbers of $CatW^+$ cells among the dense infiltrate consisting of $CD45^+$ lymphocytes, macrophages, plasma cells as well as neutrophils (Figure 1E).

Notably, the relative proportion of CatW-expressing cells among the infiltrating leukocytes, determined by CD45, differed remarkably for the investigated types of chronic inflammation (Figure 2). The highest proportion of CatW-expressing $CD45^+$ cells was found in AIG reaching 24.7% (ranging from 8% to 70%). Normal gastric mucosa, which comprised samples without gastritis, revealed a fraction of 2% (ranging from 1% to 5%). The difference between both groups was found to be significant ($P<0.001$). Surprisingly, for CD as another autoimmune-triggered intestinal disease investigated in this study, a significant reduction of the relative number of CatW-expressing cells was observed compared to healthy duodenal mucosa (2.1% *vs* 17.8%, $P<0.05$, Figure 2). Normal duodenal mucosa contained significantly more CatW-positive cells than normal gastric mucosa ($P<0.01$). Furthermore, the proportion of $CatW^+/CD45^+$ cells was analyzed in the specimens with *H pylori*-associated chronic active gastritis. Here, a significant decreased proportion of 0.7% (ranging from 0.5% to 2%, $P<0.05$) compared to normal gastric mucosa was detected (Figure 2).

For the other two chronic gastric disorders (CG and LG) analyzed in this study, the proportions of $CatW^+/CD45^+$ cells were not changed and similar to normal gastric mucosa (Figure 2). CatW was identified in about 6% and 2.2% of the $CD45^+$ cells in CG and LG, respectively.

As exemplarily shown in Figure 3, the double staining permitted a clear classification of the lymphocyte-like infiltrate of the lamina propria in AIG. The great majority (>90%) of CatW-expressing cells represented $CD3^+$ T lymphocytes, whereas $CatW^+$ NK cells ($CD3^-$) were rarely detected. Whereas $CatW^-/CD3^+$ positive T cells were abundantly seen in the samples of AIG, a high proportion of CatW-expressing cytotoxic T cells (CTL) was detected, too. $CatW^+$ NK cells (NK) were only rarely spotted in the lamina propria.

This study revealed two new and important findings. First, it provides evidence that the elevated number of CatW-expressing cells in AIG is a rather specific event for this disease and does not just represent a general phenomenon of mucosal inflammation. Second, data provide evidence that the cellular distribution of CatW is different in peripheral blood and mucosal compartment[25,26].

The elevated number of CatW-positive cells in AIG supports a pathophysiological role of these cells in this type of gastritis as discussed previously[18]. The specific expression pattern of CatW[19-21] and its potential involvement in cytotoxic processes[22] imply an involvement of CatW in Th1-mediated inflammation like AIG. According to the current model of AIG, first, self-antigen-reactive Th1 cells, which express IFN-γ, IL-2 and are capable for transendothelial migration, are activated by self-antigens of gastric mucosa and participate in tissue destruction and resulting inflammation. Second, Th2 cells, being sessile in the draining lymph nodes and activated by the self-antigens released from tissue destruction, support autoantibody production and might develop into memory cells[27]. Although, IFN-γ, which is mainly released by NK cells is one of the predominant cytokines increased in AIG[28-30], there are data implying that NK cells are dispensable for the onset of AIG. In mice models with neonatal thymectomy and subsequent depletion of NK cells, the disease incidence was not changed suggesting that other cells such as $CD8^+$ T cells are the primary source of IFN-γ[31]. Furthermore, it has been shown by several groups that in the experimental mouse model, CD4-positive T cells are mainly responsible for the development of gastric lesions[32-34]. Interestingly, the predominant role of CD4-positive T cells has not been fully confirmed. D'Elios and co-workers showed an association between AIG and Th1-differentiated T cells that possessed cytotoxic activity[35]. Other studies investigating patient-derived samples identified an upregulation of $CD16^+$ and $CD8^+$ cells suggesting a potential role of these cytotoxic cells in human AIG[36,37]. Based on these reports, an interaction of the $CD4^+$ cells with autoreactive $CD8^+$ effector cells might lead to the development of autoimmune gastritis that involves also regulatory T cells[38,39]. Taking into consideration the data from the human disease that showed a predominant involvement of T cells in AIG[35,36], the higher proportion of $CD8^+$ T cell in mucosal compartments[26] and the specific expression pattern of CatW in cytotoxic T and NK cells[21], we assume that in AIG mostly $CD8^+$ T cells contribute to the high proportion of $CatW^+/CD45^+$ cells. By performing double staining immunohistochemistry, we were able to confirm this hypothesis by showing a very low proportion of $CatW^+$ NK cells, whereas the number of CatW-expressing cytotoxic T lymphocytes was increased significantly. This observation supports a specific role of CTLs in the pathophysiological processes of AIG. For comparison, tissue samples of CD, another prototype of T-cell mediated autoimmune disease, were also investigated. Surprisingly, a decrease of the $CatW^+/CD45^+$ cells was determined in CD. This phenomenon is presumably caused by the massive increase of CatW-negative $CD4^+$ T cells, which make up the majority of infiltrating immune cells in this disease[39,40]. The observation, that the absolute number of CatW-expressing cells is significantly higher in normal intestinal samples compared to gastric samples, is in line with the distribution

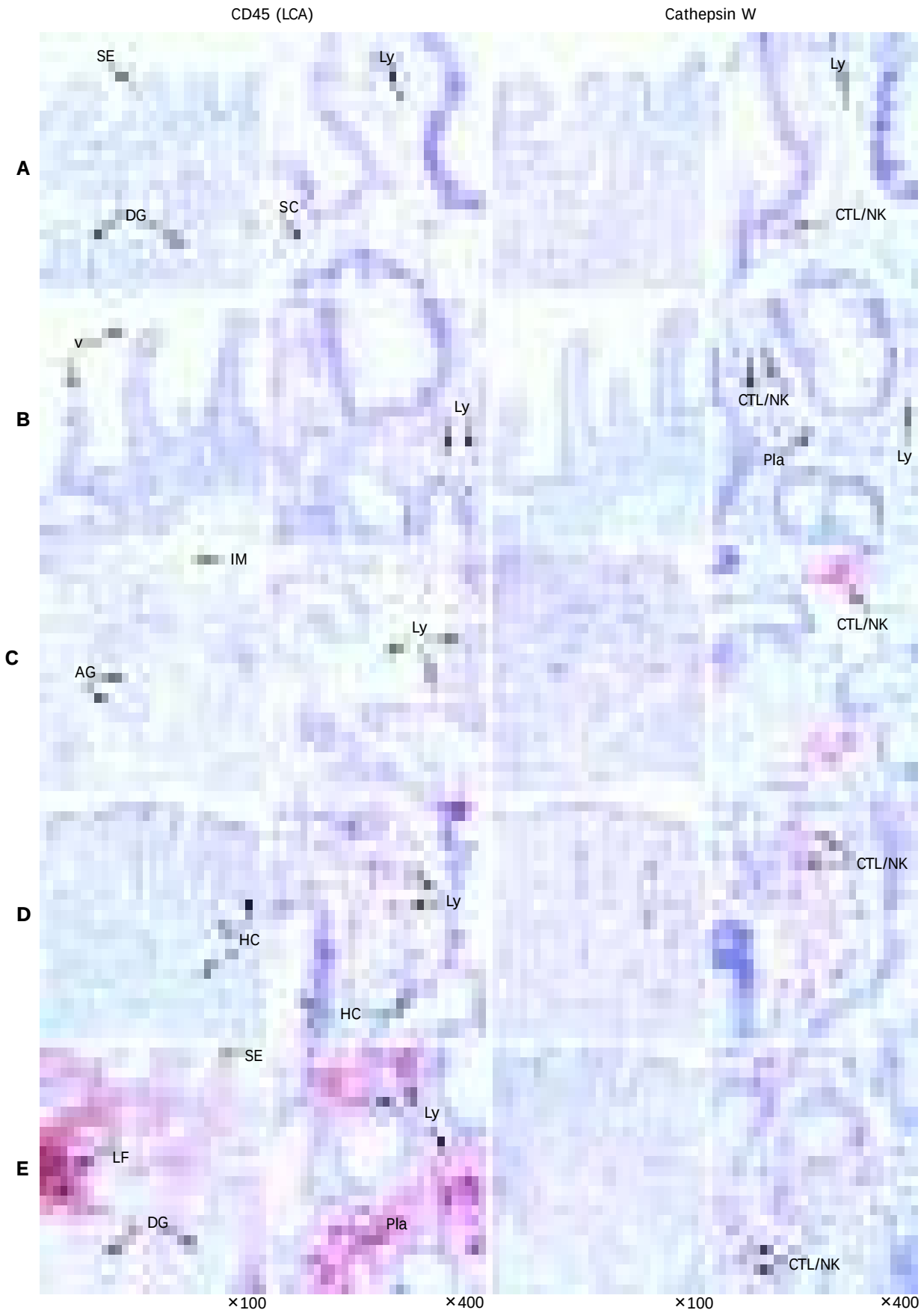

Figure 1 Immunohistochemical detection of CatW in gastrointestinal tissue specimens. The cellular distribution of CatW expression is presented by red staining, whereas the nuclei are counterstained with hematoxylin (blue). The distribution of CD45 (LCA) is shown as brownish staining. The negative controls (using isotype controls) did not reveal any signals (not shown). The tissue samples were as follows: normal gastric mucosa (A), duodenum (B), AIG (C), CD (D) and *H pylori* gastritis (E). AG: Atrophic glands, CTL: cytotoxic T-lymphocyte, DG: deep gastric glands, HC: hyperplastic crypts, IM: intestinal metaplasia, LF: lymph follicle, Ly: lymphocyte, Pla: plasma cell, NK: natural killer cell, SC: stroma cells, SE: surface epithelium, T-Ly: T lymphocyte, and V: duodenal villi.

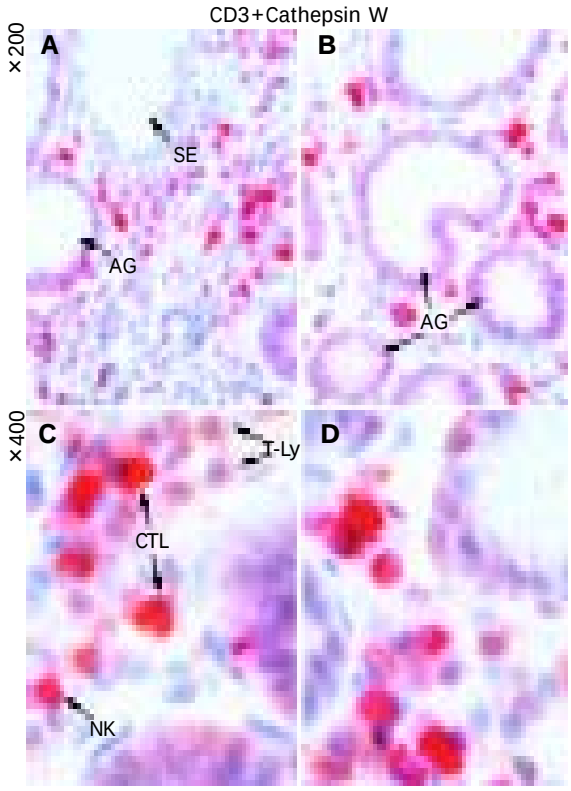

Figure 2 Detection of CatW and CD3$^+$ T cells in tissue specimens of AIG. The immunohistochemical double staining allowed a differentiation of both CatW-expressing cell types as well as a separation of CTLs from the other T cells (T-Ly) among the infiltrating cells of the lamina propria: Whereas CatW$^-$/CD3$^+$ positive T cells could be clearly distinguished by the brownish staining and were abundantly seen in the samples of AIG, an additional cytoplasmic red staining detected the CatW-expressing CTL. The exclusively red staining marked the CatW$^+$ NK cells, which were only rarely spotted in the lamina propria.

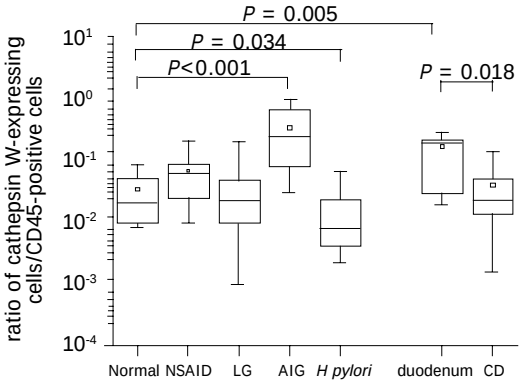

Figure 3 Presence of CatW-expressing cells among infiltrating immune cells in samples of patients with gastritis. The distribution of CatW- and LCA (leukocyte common antigen, CD45)-expressing cells was separately analyzed by immunohistochemistry in serial sections of tissue specimens. The number of CD45-positive cells was considered as 100% presented as a ratio of 1 at the Y-axis. The ratio of CatW$^+$/LCA$^+$ cells illustrates the proportion of CatW-expressing cells among leukocytes present in the gastric/duodenal mucosa. Data are shown as box plot for each group (antral mucosa: normal; chemically induced gastritis: NSAID; lymphocytic gastritis: LG; autoimmune gastritis: AIG; *H pylori*-induced gastritis: *H pylori*; normal duodenum: duodenum; celiac disease: CD). Boxes represent the 25th, 50th, and 75th percentile values (horizontal lines of the box) and means (squares). Mean values of absolute numbers of CatW-expressing cells per observation field were 0.5, 4.1, 4.2, 10.7, and 41 for normal antral mucosa, *H pylori* gastritis, NSAID-associated gastritis, LG and AIG, respectively. Tissue specimens from normal duodenum revealed 16 CatW-expressing cells per field, while samples from patient with CD had 6.3 CatW-positive cells in average per field.

of immune cells in these compartments.

It is well known that *H pylori* leads to an infiltration of neutrophils and a predominant Th1-dominated immune response[41]. The analysis of lymphocytic subsets in chronic gastritis revealed that most of the infiltrating lymphocytes were found to be CD4$^+$ T cells[42], whereas neutrophils and cytotoxic T cells seem to play an important role with respect to the activity of *H pylori* gastritis[43,44]. Furthermore, a significant increase of IL-2 receptor positive cells, including NK cells, was reported in chronic gastritis[44]. Taking into consideration the involvement of different subsets of immune cells in *H pylori*-mediated gastritis, the relative decrease of CatW-expressing cells can be attributed to the massive infiltration of CD45$^+$ leukocytes (CD4$^+$ T cells, B cells, and granulocytes). Although, there is no doubt that these cells in general participate in the immunological response by the secretion of cytokines and mediating cytotoxic effects, the lower numbers of CatW-expressing cells compared to AIG implies that they do not play a predominant role in the pathogenesis of *H pylori* gastritis[17].

No differences in the CatW$^+$/CD45$^+$ proportions for the CG and LG were detected compared to healthy controls. These findings are in line with the pathogenesis of both types of gastritis. NSAIDs, as the most common cause of CG, lead primarily to an inhibition of cyclooxygenases that subsequently leads to lower levels of prostaglandins and thromboxane and less lymphocytic infiltration compared to *H pylori* gastritis and AIG[45,46]. Therefore, CG showed normal numbers or only a minor increase of inflammatory cells, mostly being lymphocytes and plasma cells, in the mucosa[1]. Since the typical histological picture includes only a slight amount of inflammatory cells, the minimal presence of CatW-expressing cells, comparable to healthy gastric mucosa, is in concordance with these studies.

As the name implies, LG is characterized by the presence of large numbers of mature lymphocytes infiltrating the surface and foveolar epithelium[7]. Based on the guidelines, 25-40 intraepithelial lymphocytes per 100 epithelial cells are necessary for this diagnosis. Intraepithelial lymphocytes comprise mostly suppressor T cells showing cytotoxic ability through production of TIA1 and granzyme B[7,47]. The unchanged CatW$^+$/CD45$^+$ proportion in LG obviously corresponds to the normal fraction of CatW-expressing cells among the physiological infiltrate of inflammatory cells in gastric mucosa. It is notable that LG is thought to be related to *H pylori* infection, as shown by their improvement after eradication[6], indicating that LG may represent an atypical host immune response to this infection, even if *Helicobacter* is only rarely found morphologically[5,6].

The numeric differences of CatW-expressing cells and the differences of the relative portion of CatW-expressing cells among infiltrating CD45$^+$ leukocytes in the investigated types of chronic gastroduodenal inflammation imply a distinct involvement of cytotoxic cells expressing CatW in the pathogenesis among these diseases. Whereas CatW-expressing CTLs seem to contribute to the pathogenesis of AIG and to a lesser extent in *H pylori*-associated gastritis, the low

absolute and relative numbers of CatW-positive cells in the inflammatory infiltrate in CG and LG suggest that CatW-expressing cells do not play a major role in these diseases.

The identification of CTL as the predominant CatW-expressing cell type in gastric mucosa, as shown for AIG, supports the idea that the CatW-expression pattern might differ between certain subpopulations of cytotoxic cells. This hypothesis is further supported by the recent finding that cytotoxic cells of gastric mucosa can express an alternatively spliced isoform that has not been detected in peripheral NK cells so far[48].

ACKNOWLEDGMENTS

The authors thank Ursula Stolz, Claudia Miethke, and Carola Kügler for their skilful technical assistance while performing immunohistochemical procedures.

REFERENCES

1 **Dixon MF**, Genta RM, Yardley JH, Correa P. Classification and grading of gastritis. The updated Sydney System. International Workshop on the Histopathology of Gastritis, Houston 1994. *Am J Surg Pathol* 1996; **20**: 1161-1181
2 **Parsonnet J**, Friedman GD, Vandersteen DP, Chang Y, Vogelman JH, Orentreich N, Sibley RK. *Helicobacter pylori* infection and the risk of gastric carcinoma. *N Engl J Med* 1991; **325**: 1127-1131
3 **Asaka M**, Takeda H, Sugiyama T, Kato M. What role does *Helicobacter pylori* play in gastric cancer? *Gastroenterology* 1997; **113**: S56-60
4 **Toh BH**, van Driel IR, Gleeson PA. Pernicious anemia. *N Engl J Med* 1997; **337**: 1441-1448
5 **Dixon MF**, Wyatt JI, Burke DA, Rathbone BJ. Lymphocytic gastritis: relationship to Campylobacter pylori infection. *J Pathol* 1998; **154**: 125-132
6 **Müller H**, Volkholz H, Stolte M. Healing of Lymphocytic Gastritis by Eradication of *Helicobacter pylori*. *Digestion* 2001; **63**: 14-19
7 **Haot J**, Hamichi L, Wallez L, Mainguet P. Lymphocytic gastritis: a newly described entity: a retrospective endoscopic and histological study. *Gut* 1998; **29**: 1258-1264
8 **Turk V**, Turk B, Turk D. Lysosomal cysteine proteases: facts and opportunities. *EMBO J* 2001; **20**: 4629-4633
9 **Kirschke H**, Barrett AJ, Rawlings ND. Proteinases 1: lysosomal cysteine proteinases. *Protein Profile* 1995; **2**: 1581-1643
10 **Pham CT**, Ley TJ. Dipeptidyl peptidase I is required for the processing and activation of granzymes A and B *in vivo*. *Proc Natl Acad Sci USA* 1999 **96**: 8627-8632
11 **Yasothornsrikul S**, Greenbaum D, Medzihradszky KF, Toneff T, Bundey R, Miller R, Schilling B, Petermann I, Dehnert J, Logvinova A, Goldsmith P, Neveu JM, Lane WS, Gibson B, Reinheckel T, Peters C, Bogyo M, Hook V. Cathepsin L in secretory vesicles functions as a prohormone-processing enzyme for production of the enkephalin peptide neurotransmitter. *Proc Natl Acad Sci USA* 2003; **100**: 9590-9595
12 **Friedrichs B**, Tepel C, Reinheckel T, Deussing J, von Figura K, Herzog V, Peters C, Saftig P, Brix K. Thyroid functions of mouse cathepsins B, K, and L. *J Clin Invest* 2003; **111**: 1733-1745
13 **Honey K**, Rudensky AY. Lysosomal cysteine proteases regulate antigen presentation. *Nat Rev Immunol* 2003; **3**: 472-482
14 **Hughes SJ**, Glover TW, Zhu XX, Kuick R, Thoraval D, Orringer MB, Beer DG, Hanash S. A novel amplicon at 8p22-23 results in overexpression of cathepsin B in esophageal adenocarcinoma. *Proc Natl Acad Sci USA* 1998; **95**: 12410-12415
15 **Lauritzen C**, Pedersen J, Madsen MT, Justesen J, Martensen PM, Dahl SW. Active recombinant rat dipeptidyl aminopeptidase I (cathepsin C) produced using the baculovirus expression system. *Protein Expr Purif* 1998; **14**: 434-442
16 **Dohchin A**, Suzuki JI, Seki H, Masutani M, Shiroto H, Kawakami Y. Immunostained cathepsins B and L correlate with depth of invasion and different metastatic pathways in early stage gastric carcinoma. *Cancer* 2000; **89**: 482-487
17 **Buhling F**, Peitz U, Kruger S, Kuster D, Vieth M, Gebert I, Roessner A, Weber E, Malfertheiner P, Wex T. Cathepsins K, L, B, X and W are differentially expressed in normal and chronically inflamed gastric mucosa. *Biol Chem* 2004; **385**: 439-445
18 **Buhling F**, Kellner U, Guenther D, Kahl S, Bromme D, Weber E, Malfertheiner P, Wex T. Characterization of novel anti-cathepsin W antibodies and cellular distribution of cathepsin W in the gastrointestinal tract. *Biol Chem* 2002; **383**: 1285-1289
19 **Linnevers C**, Smeekens SP, Bromme D. Human cathepsin W, a putative cysteine protease predominantly expressed in CD8+ T-lymphocytes. *FEBS Lett* 1997; **405**: 253-259
20 **Brown J**, Matutes E, Singleton A, Price C, Molgaard H, Buttle D, Enver T. Lymphopain, a cytotoxic T and natural killer cell-associated cysteine proteinase. *Leukemia* 1998; **12**: 1771-1781
21 **Wex T**, Buhling F, Wex H, Gunther D, Malfertheiner P, Weber E, Bromme D. Human cathepsin W, a cysteine protease predominantly expressed in NK cells, is mainly localized in the endoplasmic reticulum. *J Immunol* 1998; **167**: 2172-2178
22 **Wex T**, Wex H, Hartig R, Wilhelmsen S, Malfertheiner P. Functional involvement of cathepsin W in the cytotoxic activity of NK-92 cells. *FEBS Lett* 2003; **552**: 115-119
23 **Ondr JK**, Pham CT. Characterization of murine cathepsin W and its role in cell-mediated cytotoxicity. *J Biol Chem* 2004; **279**: 27525-27533
24 **Borscheri N**, Roessner A, Rocken C. Canalicular immunostaining of neprilysin (CD10) as a diagnostic marker for hepatocellular carcinomas. *Am J Surg Pathol* 2001; **25**: 1297-1303
25 **Hayday A**, Theodoridis E, Ramsburg E, Shires J. Intraepithelial lymphocytes: exploring the Third way in immunology. *Nat Immunol* 2001; **2**: 997-1003
26 **Neutra MR**, Mantis NJ, Kraehenbuhl JP. Collaboration of epithelial cells with organized mucosal lymphoid tissues. *Nat Immunol* 2001; **2**: 1004-1009
27 **Katakai T**, Mori KJ, Masuda T, Shimizu A. Differential localization of Th1 and Th2 cells in autoimmune gastritis. *Int Immunol* 1998; **10**: 1325-1334
28 **Barrett SP**, Gleeson PA, de Silva H, Toh BH, van Driel IR. Interferon-gamma is required during the initiation of an organ-specific autoimmune disease. *Eur J Immunol* 1996; **26**: 1652-1655
29 **Chen H**, Paul WE. Cultured NK1.1+ CD4+ T cells produce large amounts of IL-4 and IFN-gamma upon activation by anti-CD3 or CD1. *J Immunol* 1997; **159**: 2240-2249
30 **Romagnani S**. Induction of TH1 and TH2 responses: a key role for the 'natural' immune response? *Immunol Today* 1992; **13**: 379-381
31 **La Gruta NL**, van Driel IR, Toh BH, Gleeson PA. The role of natural killer cells in the induction of autoimmune gastritis. *Autoimmunity* 2001; **34**: 147-154
32 **De Silva HD**, Van Driel IR, La Gruta N, Toh BH, Gleeson PA. CD4+ T cells, but not CD8+ T cells, are required for the development of experimental autoimmune gastritis. *Immunology* 1998; **93**: 405-408
33 **Martinelli TM**, van Driel IR, Alderuccio F, Gleeson PA, Toh BH. Analysis of mononuclear cell infiltrate and cytokine production in murine autoimmune gastritis. *Gastroenterology* 1996; **110**: 1791-1802
34 **Alderuccio F**, Toh BH, Gleeson PA, van Driel IR. A novel method for isolating mononuclear cells from the stomachs of mice with experimental autoimmune gastritis. *Autoimmunity* 1995; **21**: 215-221
35 **D'Elios MM**, Bergman MP, Azzurri A, Amedei A, Benagiano M, De Pont JJ, Cianchi F, Vandenbroucke-Grauls CM, Romagnani S, Appelmelk BJ, Del Prete G. H(+),K(+)-atpase (proton pump) is the target autoantigen of Th1-type cytotoxic T cells in autoimmune gastritis. *Gastroenterology* 2001; **120**: 377-386

36 **Vargas JA**, Alvarez-Mon M, Manzano L, Albillos A, Fernandez-Corugedo A, Albarran F, Durantez A. Functional defect of T cells in autoimmune gastritis. *Gut* 1995; **36**: 171-175
37 **Mitomi H**, Tanabe S, Igarashi M, Katsumata T, Arai N, Kikuchi S, Kiyohashi A, Okayasu I. Autoimmune enteropathy with severe atrophic gastritis and colitis in an adult: proposal of a generalized autoimmune disorder of the alimentary tract. *Scand J Gastroenterol* 1998; **33**: 716-720
38 **Shevach EM**, McHugh RS, Piccirillo CA, Thornton AM. Control of T-cell activation by CD4+ CD25+ suppressor T cells. *Immunol Rev* 2001; **182**: 58-67
39 **Shan L**, Molberg O, Parrot I, Hausch F, Filiz F, Gray GM, Sollid LM, Khosla C. Structural basis for gluten intolerance in celiac sprue. *Science* 2002; **297**: 2275-2279
40 **Maiuri L**, Ciacci C, Ricciardelli I, Vacca L, Raia V, Auricchio S, Picard J, Osman M, Quaratino S, Londei M. Association between innate response to gliadin and activation of pathogenic T cells in coeliac disease. *Lancet* 2003; **362**: 30-37
41 **Mohammadi M**, Czinn S, Redline R, Nedrud J. *Helicobacter* specific cell-mediated immune responses display a predominant Th1 phenotype and promote a delayed-type hypersensitivity response in the stomachs of mice. *J Immunol* 1996; **156**: 4729-4738
42 **Raptopoulou-Gigi M**, Polyzonis M, Orphanou-Koumerkeridou H, Agorastos J, Vacolas J, Gigis P. Immunohistological phenotyping of the stomach infiltrating lymphocytes in chronic gastritis. *Allergol Immunopathol* 1990; **18**: 87-89
43 **Fiocca R**, Villani L, Luinetti O, Gianatti A, Perego M, Alvisi C, Turpini F, Solcia E. *Helicobacter* colonization and histopathological profile of chronic gastritis in patients with or without dyspepsia, mucosal erosion and peptic ulcer: a morphological approach to the study of ulcerogenesis in man. *Virchows Arch A Pathol Anat Histopathol* 1992; **420**: 489-498
44 **Ohtani N**, Ohtani H, Nakayama T, Naganuma H, Sato E, Imai T, Nagura H, Yoshie O. Infiltration of CD8+ T cells containing RANTES/CCL5+ cytoplasmic granules in actively inflammatory lesions of human chronic gastritis. *Lab Invest* 2004; **84**: 368-375
45 **Wallace JL**, Zamuner SR, McKnight W, Dicay M, Mencarelli A, del Soldato P, Fiorucci S. Aspirin, but not NO-releasing aspirin (NCX-4016), interacts with selective COX-2 inhibitors to aggravate gastric damage and inflammation. *Am J Physiol Gastrointest Liver Physiol* 2004; **286**: G76-81
46 **Tomisato W**, Tsutsumi S, Hoshino T, Hwang HJ, Mio M, Tsuchiya T, Mizushima T. Role of direct cytotoxic effects of NSAIDs in the induction of gastric lesions. *Biochem Pharmacol* 2004; **67**: 575-585
47 **Oberhuber G**, Bodingbauer M, Mosberger I, Stolte M, Vogelsang H. High proportion of granzyme B-positive (activated) intraepithelial and lamina propria lymphocytes in lymphocytic gastritis. *Am J Surg Pathol* 1998; **22**: 450-458
48 **Meinhardt C**, Peitz U, Treiber G, Wilhelmsen S, Malfertheiner P, Wex T. Identification of a novel isoform predominately expressed in gastric tissue and a triple-base pair polymorphism of the cathepsin W gene. *Biochem Biophys Res Commun* 2004; **321**: 975-980

Science Editor Guo SY **Language Editor** Elsevier HK

PO Box 2345, Beijing 100023, China
www.wjgnet.com
wjg@wjgnet.com

ELSEVIER

World J Gastroenterol 2005;11(38):5958-5965
World Journal of Gastroenterology ISSN 1007-9327

• *BASIC RESEARCH* •

Ischemic preconditioning inhibits development of edematous cerulein-induced pancreatitis: Involvement of cyclooxygenases and heat shock protein 70

Zygmunt Warzecha, Artur Dembinski, Piotr Ceranowicz, Stanislaw J Konturek, Marcin Dembinski, Wieslaw W Pawlik, Romana Tomaszewska, Jerzy Stachura, Beata Kuşnierz-Cabala, Jerzy W Naskalski, Peter C Konturek

Zygmunt Warzecha, Artur Dembiński, Piotr Ceranowicz, Stanisław J Konturek, Marcin Dembiński, Wiesław W Pawlik, Department of Physiology, Jagiellonian University Medical College, Kraków, Poland
Romana Tomaszewska, Jerzy Stachura, Department of Pathology, Jagiellonian University Medical College, Kraków, Poland
Beata Kuśnierz-Cabała, Jerzy W Naskalski, Department of Clinical Biochemistry, Jagiellonian University Medical College, Kraków, Poland
Peter C Konturek, Department of Internal Medicine I, University of Erlangen-Nuremberg, Erlangen, Germany
Correspondence to: Professor Artur Dembiński, MD, PhD, Department of Physiology, Jagiellonian University Medical College, ul. Grzegórzecka 16, Kraków 31-531, Poland. mpdembin@cyf-kr.edu.pl
Telephone: +48-12-4211006 Fax: +48-12-4225478
Received: 2004-12-17 Accepted: 2005-03-21

Abstract

AIM: To determine whether ischemic preconditioning (IP) affects the development of edematous cerulein-induced pancreatitis and to assess the role of cyclooxygenase-1 (COX-1), COX-2, and heat shock protein 70 (HSP 70) in this process.

METHODS: In male Wistar rats, IP was performed by clamping of celiac artery (twice for 5 min at 5-min intervals). Thirty minutes after IP or sham operation, acute pancreatitis was induced by cerulein. Activity of COX-1 or COX-2 was inhibited by resveratrol or rofecoxib, respectively (10 mg/kg).

RESULTS: IP significantly reduced pancreatic damage in cerulein-induced pancreatitis as demonstrated by the improvement of pancreas histology, reduction in serum lipase and poly-C ribonuclease activity, and serum concentration of pro-inflammatory interleukin (IL)-1β. Also, IP attenuated the pancreatitis-evoked fall in pancreatic blood flow and pancreatic DNA synthesis. Serum level of anti-inflammatory IL-10 was not affected by IP. Cerulein-induced pancreatitis and IP increased the content of HSP 70 in the pancreas. Maximal increase in HSP 70 was observed when IP was combined with cerulein-induced pancreatitis. Inhibition of COXs, especially COX-2, reduced the protective effect of IP in edematous pancreatitis.

CONCLUSION: Our results indicate that IP reduces pancreatic damage in cerulein-induced pancreatitis and this effect, at least in part, depends on the activity of COXs and pancreatic production of HSP 70.

Key words: Acute pancreatitis; Ischemic preconditioning; Cyclooxygenase-2; Interleukin-1β; Heat shock protein-70

Warzecha Z, Dembinski A, Ceranowicz P, Konturek SJ, Dembinski M, Pawlik WW, Tomaszewska R, Stachura J, Kuśnierz-Cabala B, Naskalski JW, Konturek PC. Ischemic preconditioning inhibits development of edematous cerulein-induced pancreatitis: Involvement of cyclooxygenases and heat shock protein 70. *World J Gastroenterol* 2005; 11 (38): 5958-5965
http://www.wjgnet.com/1007-9327/11/5958.asp

INTRODUCTION

Various organs including the heart[1], brain[2], kidney[3], liver[4], skeletal muscle[5], and stomach[6] respond to brief exposure to ischemia with an increase in resistance to severe ischemia, and this phenomenon is called ischemic preconditioning (IP). Also, the protective effect of IP has been found in the pancreas against ischemia/reperfusion-induced pancreatitis[7]. However, no study so far has been undertaken to determine whether IP is also able to prevent the acute pancreatic damage induced by other primary non-vascular factors.

Cyclooxygenase (COX), the key enzyme for prostaglandin synthesis, exists in two isoforms as COX-1 and COX-2[8]. COX-1 is constitutively expressed in most tissues and has been suggested to mediate the synthesis of prostaglandins required for physiological functions and maintenance of organ integrity. COX-2 is undetectable in most tissues in normal condition, but is highly inducible by cytokines, mitogens, and endotoxins, and is responsible for an increased production of prostaglandins during inflammation[8]. However, it was reported that both COXs contribute to gastric mucosal defense[9]. Inhibition of COXs activity by nonselective nonsteroidal anti-inflammatory drugs leads to induction of gastric ulcers and delays the healing of gastric mucosa[10,11], while the selective inhibition of COX-2 delays gastric ulcer healing[12]. The role of COX-2 in pancreatic pathology is unclear. Studies performed by Song *et al*.[13], and Ethridge *et al*.[14], with mice have shown that pharmacological inhibition of COX-2 or

COX-2 gene disruption reduces the severity of pancreatitis and pancreatitis-associated lung injury. On the other hand, our own study has shown that inhibition of COX-2 abolishes the protective effect of hepatocyte growth factor (HGF) against cerulein-induced pancreatitis[15].

Heat shock proteins (HSPs) are cytoprotective molecules that help to maintain the metabolic and structural integrity of cells. HSPs are induced by a variety of stresses, including heat, free radicals, and toxins[16]. In the pancreas, HSPs have been shown to provide the protection against cerulein-[17,18] and arginine-induced[19] acute pancreatitis. However, it is not investigated whether IP interacts with HSPs and what is the biological consequence of this potential interaction in the development of cerulein-induced pancreatitis.

The present study was to determine the effect of IP on the development of acute cerulein-induced pancreatitis, to evaluate the role of COX-1 and COX-2 in pancreatic IP, and to assess the effect of IP on the pancreatic synthesis of HSP 70.

[illegible]

Animals and treatment

Studies were performed on male Wistar rats weighing 180-220 g and following the experimental protocol approved by the Committee for Research and Animal Ethics of Jagiellonian University. Rats were fasted for 18 h before final experiment, but they had free access to drinking water. Animals were housed in cages with wire mesh bottoms at normal room temperature in 12-h light–dark cycle.

Experiments were carried out in the following experimental groups (10 animals in each group); (1) sham-operated control group; (2) IP group; (3) sham-operated group treated with resveratrol (Cayman Chemicals, Ann Arbor, MI, USA, 10 mg/kg, intragastrically (i.g.) 1 h before sham operation); (4) sham-operated group treated with rofecoxib (Vioxx, Merck Sharp & Dohme Idea Inc., Glattbrugg, Switzerland, 10 mg/kg, i.g. 1 h before sham operation); (5) sham-operated group with cerulein-induced pancreatitis; (6) IP group with cerulein-induced pancreatitis; (7) sham-operated group with cerulein-induced pancreatitis and treated with resveratrol (10 mg/kg, i.g. 1 h before sham operation); (8) cerulein-induced pancreatitis group treated with rofecoxib (10 mg/kg, i.g. 1 h before sham operation); (9) IP group with cerulein-induced pancreatitis and treated with resveratrol (10 mg/kg, i.g. 1 h before IP); (10) IP group with cerulein-induced pancreatitis and treated with rofecoxib (10 mg/kg, i.g. 1 h before IP).

IP of the pancreas was performed under ketamine anesthesia (50 mg/kg i.p., Bioketan, Biowet, Gorzów Wlkp., Poland). After longitudinal laparotomy, the celiac artery was clamped twice for 5 min at 5-min intervals. In sham-operated rats, longitudinal laparotomy and mobilization of the pancreas without the clamping of any artery was performed.

Thirty minutes after IP or sham operation, acute pancreatitis was induced by cerulein (Takus, Pharmacia & Upjohn GmbH, Erlangen, Germany) i.p. five times at 1-h intervals at a dose 10 μg/kg per injection. Animals without induction of acute pancreatitis were treated with 0.9% NaCl i.p. at the same time as cerulein.

Determination of pancreatic blood flow

After the last injection of cerulein or saline, animals were anesthetized with ketamine and the abdomen was opened. The pancreas was exposed for the measurement of pancreatic blood flow by a laser Doppler flowmeter using PeriFlux 4001 Master monitor (Perimed AB, Järfälla, Sweden), as described previously[20]. Pancreatic blood flow was measured in five different portions of the pancreas. The area of laser emission of the probe was about 1 mm^2, while the depth of measurement reached about 3 mm. Data were presented as percent change from control value obtained in sham-operated rats injected with saline.

Determination of serum lipase activity and serum interleukin-1β and interleukin-10 concentration

Immediately after measurement of pancreatic blood flow, the abdominal aorta was exposed and blood was taken for determination of serum lipase activity and serum interleukin-1β (IL-1β) and IL-10 concentration. Serum lipase activity was determined with a Kodak Ectachem DT II System analyzer (Eastman Kodak Company, Rochester, NY, USA) using Lipa DT slides (Vitros DT Chemistry System, Johnson & Johnson Clinical Diagnostic, Inc., Rochester, NY, USA). Serum lipase activity was expressed as units per liter. Serum IL-1β and IL-10 concentrations were measured in duplicate, using appropriate BioSource Cytoscreen rat kits based on a solid phase sandwich ELISA (BioSource International, Camarillo, CA, USA). Concentration of IL was determined from standard curves for recombinant IL-1β or IL-10, respectively. Serum IL-1β or IL-10 concentration was expressed as picogram per milliliter.

Determination of serum poly-C specific ribonuclease activity

Poly-C specific ribonuclease activity was determined using Warsaw and Lee's procedure[21], employing polycytydylic acid (poly-C) as a ribonuclease substrate, as described previously in detail[22]. Poly-C specific ribonuclease activity was expressed in units per liter.

Protein extraction and analysis of pancreatic HSP 70 expression by Western blot analysis

Shock-frozen tissue from rat pancreas was homogenized in a lysis buffer (100 mmol/L Tris-HCl, pH 7.4, 15% glycerol, 2 mmol/L EDTA, 2% sodium dodecyl sulfate (SDS), 100 mmol/L D,L-dithiothreitol) by the addition of 1:20 dilution of aprotinin and 1:50 dilution of 100 mmol/L phenylmethylsulfonyl fluoride. Insoluble materials were removed by centrifugation at 12 000 *g* for 15 min. Approximately 50 μg of the total protein extract was loaded on SDS-polyacrylamide gels and run 40 mA, followed by transfer on nitrocellulose membrane (Protran, Schleicher & Schuell, Germany) by electroblotting. Bovine serum albumin (30 g/L, Sigma-Aldrich, Germany) in Tris buffered saline (TBS)-Tween-20 buffer (137 mmol NaCl, 20 mmol Tris-HCl, pH 7.4, 0.1% Tween-20) was used to block filters for at least 1 h at room temperature. Specific primary antibody against HSP 70 (mouse monoclonal, 1:200 dilution; Stressgen Biotechnologies Corp., Canada) or β-actin (mouse monoclonal, dilution 1:5 000; Sigma-Aldrich, Germany) was added to the membrane, followed by an anti-mouse-IgG or anti-mouse IgG horseradish

peroxidase-conjugated secondary antibody (dilution 1:20 000; Promega, WI, USA) dissolved in 1% non-fat milk in TBS-Tween-20 buffer. Incubation of primary antibody was followed by washing thrice with TBS-Tween-20 buffer for 10 min. Incubation of the secondary antibody was followed by five washes for 10 min. Immunocomplexes were detected by the SuperSignal West Pico chemiluminescent kit (Pierce, USA). Thereafter, the developed membrane was exposed to an X-ray film (Kodak, Wiesbaden, Germany). Comparison between different treatment groups was made by determining the HSP 70/β-actin ratio of the immunoreactive area by densitometry.

Determination of pancreatic DNA synthesis

The rate of DNA synthesis in samples of pancreatic tissue was determined as described previously[23]. Briefly, the minced pancreatic tissue was incubated at 37 ℃ for 45 min in 2 mL of medium containing 8 μCi/mL of [^{3}H]thymidine ([6-^{3}H] thymidine, 20-30 Ci/mmol; Institute for Research, Production and Application of Radioisotopes, Prague, Czech Republic). The incorporation of [^{3}H]thymidine into DNA was measured by counting DNA containing solution in a liquid scintillation system. DNA synthesis was expressed as [^{3}H]thymidine disintegrations per minute per microgram DNA (dpm/μg DNA).

Histological examination

Samples of pancreatic tissue for histological examination were fixed in 40 g/L formaldehyde, embedded in paraffin and sections were sliced and stained with hematoxylin and eosin. Slides were examined by two experienced pathologists without the knowledge of the treatment given (four slides per animal). The histological grading of edema was made using our scale ranging from 0 to 3: 0 = no edema, 1 = interlobular edema, 2 = interlobular and moderate intralobular edema, and 3 = severe interlobular and intralobular edema. Hemorrhage was graded: 0 = absent, 1 = 1-2 foci per slide, 2 = 3 to 5 foci per slide, 3 = more than 5 foci per slide. Leukocyte infiltration was graded: 0 = absent, 1 = scare perivascular infiltration, 2 = moderate perivascular and scare diffuse infiltration, 3 = abundant diffuse infiltration. Acinar necrosis was graded: 0 = absent, 1 = less than 15% of cells involved, 2 = 15–35% of cells involved, 3 = more than 35% of cells involved. Grading of vacuolization was based on the percentage of cells involved: 0 = absent, 1 = less than 25%, 2 = 25-50% and 3 = more than 50%.

Statistical analysis

Results were expressed as mean±SE. Statistical analysis was carried out by one-way analysis of variance followed by Tukey's multiple comparison test using GraphPadPrism (GraphPad Software, San Diego, CA, USA). $P<0.05$ was considered statistically significant.

[illegible]

Morphological features of pancreatic tissue

The pancreas of saline-treated sham-operated rats showed no tissue alteration macroscopically and at light microscopic level (Table 1). Exposure to IP combined with treatment with saline caused the mild interlobular edema and minimal vacuolization of acinar cells in cases 4 and 5, respectively. Rest of the animals exposed to IP and treated with saline did not show any histological alterations. Administration of the COX-1 inhibitor - resveratrol - in saline-treated animals did not affect pancreatic tissue morphology. Treatment with combination of the COX-2 inhibitor - rofecoxib - plus saline had no effect on pancreatic histology or caused mild interlobular edema. Administration of cerulein caused acute edematous pancreatitis in all rats that were tested (Table 1). The pancreas was grossly swollen and enlarged with a visible collection of edematous fluid. At light microscopic level, moderate or severe interlobular and intralobular edema was accompanied with moderate perivascular and scare diffuse inflammatory leukocyte infiltration. Vacuolization was observed in 25-50% of acinar cells. Additionally, in few cases, one or two foci of hemorrhages per slide were found. IP applied prior to cerulein-induced pancreatitis reduced histological signs of pancreatic damage such as pancreatic edema, inflammatory infiltration, and vacuolization of acinar cells. Also, administration of resveratrol or rofecoxib in combination with cerulein slightly reduced the cerulein-evoked pancreatic damage. In animals with IP applied prior to cerulein, inhibition of COXs abolished the beneficial effect of IP. This effect was especially pronounced after administration of rofecoxib and pancreatic damage was similar to that in animals treated with cerulein alone (Table 1).

Effect of ischemic preconditioning, resveratrol, and rofecoxib on serum lipase activity in rats without or with cerulein-induced pancreatitis

In sham-operated saline-treated rats, serum lipase activity reached 61.5±3.5 U/L (Figure 1A). IP, applied without

Table 1 Morphological features of pancreatic tissue of animals exposed to IP or sham-operated and treated with saline, resveratrol, rofecoxib or cerulein alone or in combination

	Edema	Inflammatory infiltration	Vacuolization	Hemorrhages	Necrosis
Sham-operation+saline (control)	0	0	0	0	0
IP+saline	0/1	0	0/1	0	0
Resveratrol+sham operation+saline	0	0	0	0	0
Rofecoxib+sham operation+saline	0/1	0	0	0	0
Sham-operation+cerulein	2/3	2	2	0/1	0
IP+cerulein	2	1	1	0	0
Resveratrol+sham operation+cerulein	2	1	2	0	0
Rofecoxib+sham operation+cerulein	2	1	2	0/1	0
Resveratrol+IP+cerulein	2	1/2	2	0	0
Rofecoxib+IP+cerulein	2/3	2	2	0/1	0

Numbers represent the predominant histological grading in each group.

induction of acute pancreatitis, did not affect serum lipase activity. Also, administration of the COX-1 inhibitor - resveratrol - or the COX-2 inhibitor - rofecoxib - had no effect on serum lipase activity in rats treated with saline. Administration of cerulein caused more than sevenfold increase in serum lipase activity, when compared to that of saline-treated control rats. IP markedly reduced the cerulein-evoked increase in serum lipase activity by 37% ($P<0.001$). Also, administration of resveratrol or rofecoxib reduced serum lipase activity in animals with cerulein-induced pancreatitis ($P<0.01$ or $P<0.05$, respectively). The effect of these blockers of COX on serum lipase activity was weaker than the effect of IP, but was still statistically significant. In contrast, administration of resveratrol or rofecoxib in combination with IP significantly abolished the IP-evoked reduction in serum lipase activity in animals with cerulein-induced pancreatitis ($P<0.001$). However, serum lipase activity in these animals was still lower than that in animals with cerulein-induced pancreatitis and treated with resveratrol or rofecoxib alone (Figure 1A).

Effect of ischemic preconditioning, resveratrol, and rofecoxib on serum concentration of IL-1β and IL-10 in rats without or with cerulein-induced pancreatitis

In control sham-operated rats treated with saline, the serum IL-1β concentration was 69.9±3.1 pg/mL (Figure 1B). IP or treatment with resveratrol or rofecoxib alone had no effect on serum IL-1β in rats without induction of acute pancreatitis. In sham-operated rats, cerulein caused more than threefold increase in serum IL-1β concentration and this increase was significantly diminished by IP ($P<0.001$). Lower but still significant reduction of serum IL-1β was also observed when administration of cerulein was combined with pretreatment with resveratrol ($P<0.05$). Administration of rofecoxib alone tended to reduce the cerulein-evoked increase in serum IL-1β concentration, but this effect was not statistically significant. Pretreatment with resveratrol or rofecoxib in animals with IP significantly reversed the

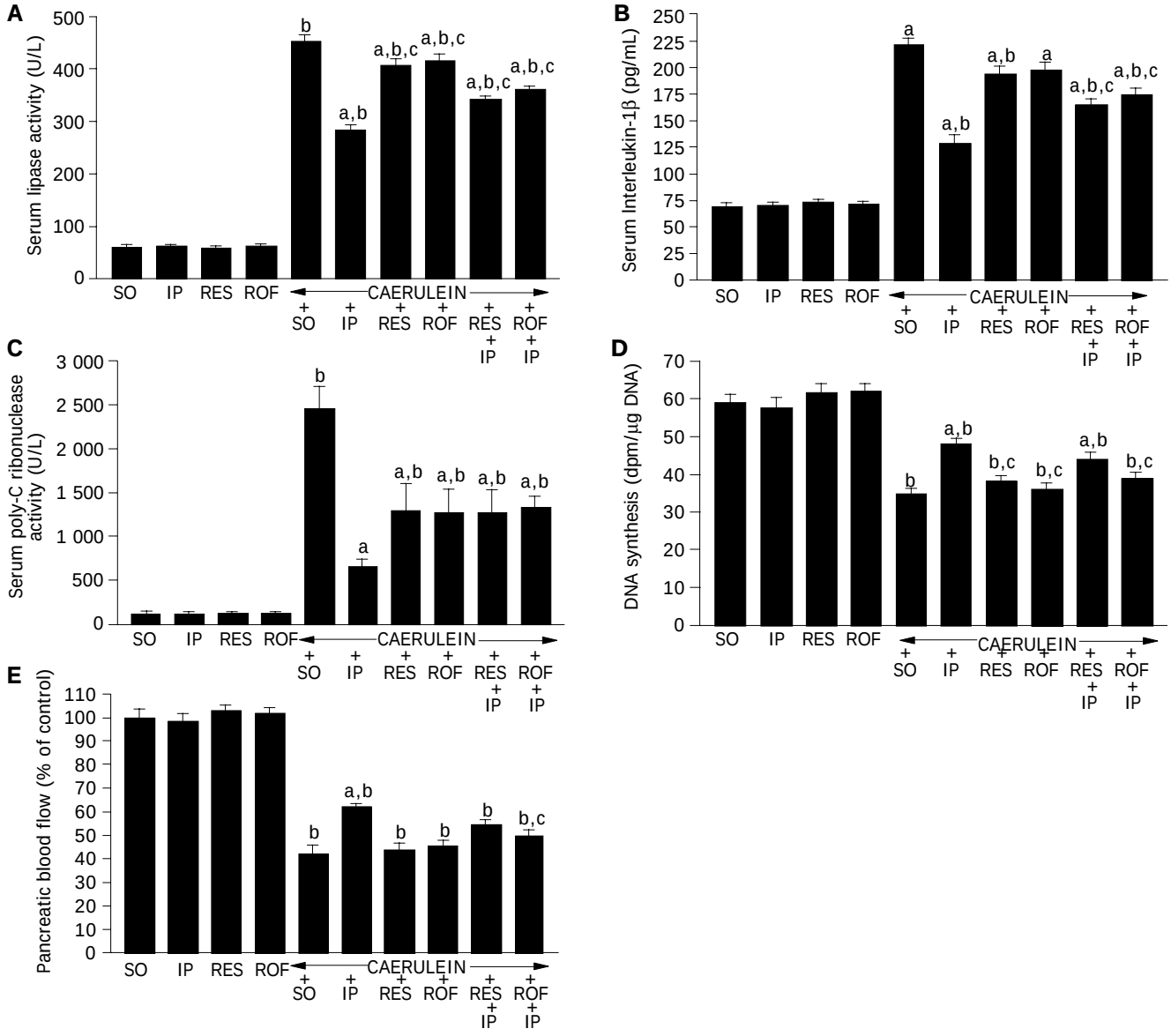

Figure 1 Effect of sham operation (SO), IP, resveratrol (RES) or rofecoxib (ROF) applied alone or in combination on serum lipase activity (A), IL-1β (B), poly-C ribonuclease (C), pancreatic DNA synthesis (D), and pancreatic blood flow (E) in rats with or without cerulein-induced pancreatitis. [a]$P<0.05$ *vs* sham-operated rats treated with cerulein alone, [b]$P<0.001$ *vs* sham-operated saline-treated control (SO), [c]$P<0.05$ *vs* rats exposed to IP and treated with cerulein.

IP-evoked decrease in serum IL-1β concentration in animals with cerulein-induced pancreatitis (P<0.001, Figure 1B).

In control sham-operated rats treated with saline, the serum IL-10 level reached 73.0±5.0 pg/mL (data not shown). Neither IP nor resveratrol or rofecoxib or cerulein applied alone or in their combination significantly affected the serum IL-10 concentration.

Effect of ischemic preconditioning, resveratrol, and rofecoxib on serum activity of poly-C ribonuclease in rats without or with cerulein-induced pancreatitis

In saline-treated sham-operated control rats, serum poly-C ribonuclease activity reached 125±25 U/L (Figure 1C). IP or administration of resveratrol or rofecoxib did not affect serum poly-C ribonuclease activity in animals without induction of acute pancreatitis. Cerulein-induced pancreatitis caused nearly 20-fold increase in serum poly-C ribonuclease activity and this effect was strongly and significantly inhibited by IP (P<0.001). Also administration of resveratrol or rofecoxib reduced the cerulein-induced increase in serum activity of poly-C ribonuclease, but the effect of these blockers of COX was weaker than that of IP (P<0.001). Combination of resveratrol or rofecoxib plus IP decreased the serum poly-C ribonuclease activity in cerulein-treated rats to the similar values as administration of resveratrol or rofecoxib in sham-operated rats with cerulein-induced pancreatitis (Figure 1C).

Effect of ischemic preconditioning, resveratrol, and rofecoxib on pancreatic DNA synthesis in rats without or with cerulein-induced pancreatitis

In saline-treated sham-operated control rats, pancreatic DNA synthesis reached 59.0±2.3 dpm/μg DNA (Figure 1D). IP as well as administration of resveratrol or rofecoxib did not affect pancreatic DNA synthesis in animals without induction of acute pancreatitis. In animals with cerulein-induced pancreatitis, pancreatic DNA synthesis was significantly reduced, reaching 34.7±1.6 dpm/μg DNA (P<0.001). IP significantly attenuated the pancreatitis-related reduction in pancreatic DNA synthesis (P<0.001). Resveratrol or rofecoxib given alone did not affect pancreatic DNA synthesis in animals treated with cerulein. Pretreatment with resveratrol tended to reduce the pancreatic DNA synthesis in animals treated with a combination of IP plus cerulein, but this effect was not statistically significant. In contrast, pretreatment with rofecoxib significantly reduced the pancreatic DNA synthesis in animals treated with IP plus cerulein (P<0.05).

Effect of ischemic preconditioning, resveratrol, and rofecoxib on pancreatic blood flow in rats without or with cerulein-induced pancreatitis

IP or treatment with resveratrol or rofecoxib did not affect pancreatic blood flow in rats without administration of cerulein (Figure 1E). Administration of cerulein for 5 h significantly reduced pancreatic blood flow by 58% when compared to that of saline-treated sham-operated control rats (P<0.001). Exposure to IP significantly reversed the cerulein-induced fall in pancreatic blood flow (P<0.001), whereas resveratrol or rofecoxib given alone had no effect on pancreatic blood flow in animals with cerulein-induced pancreatitis. Pretreatment with rofecoxib significantly abolished the IP-induced improvement of pancreatic blood flow in animals with pancreatitis (P<0.05).

Effect of ischemic preconditioning and cerulein-induced pancreatitis on synthesis of HSP 70 detected by Western blot

Figure 2 shows the effect of IP and cerulein-induced pancreatitis on the production of HSP 70 in the pancreatic tissue. In sham-operated control animals with an intact pancreas, the synthesis of HSP 70 was weak and the ratio of HSP 70 over β-actin reached a value of 0.11±0.01. IP or induction of acute pancreatitis by cerulein significantly increased the ratio of HSP 70 over β-actin in pancreatic tissue reaching 0.31±0.01 and 0.74±0.02, respectively (P<0.05 and P<0.001, respectively). The highest ratio of HSP 70 to β-actin in pancreatic tissue was observed in animals treated with combination of IP plus cerulein.

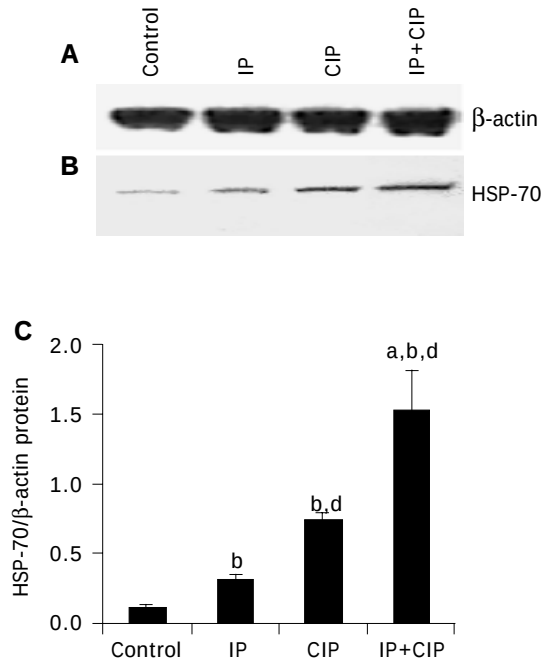

Figure 2 Representative Western blot analysis of β-actin protein (A) and HSP 70 (B), and the ratio of HSP 70 over β-actin protein (C) in pancreatic tissue of sham-operated control rats (lane 1), rats exposed to IP (lane 2), sham-operated rats with cerulein-induced pancreatitis (CIP, lane 3), and rats with IP applied prior to cerulein-induced pancreatitis (IP+CIP, lane 4). [b]P<0.001 *vs* sham-operated rats treated with cerulein alone (CIP), [a]P<0.05 *vs* sham-operated saline-treated control, [d]P<0.001 *vs* rats exposed to IP without induction of acute pancreatitis (CIP).

DISCUSSION

Our present study showed for the first time that: (1) IP could reduce the pancreatic damage in cerulein-induced acute pancreatitis; (2) IP and cerulein-induced pancreatitis could increase synthesis of HSP 70 in the pancreas and combination of these two factors could stimulate the production of HSP 70 to the highest extent; (3) inhibition of COXs, especially COX-2, could reduce the pancreatoprotective effect of IP against cerulein-induced pancreatitis.

Protective effect of IP against pancreatic damage evoked by cerulein was manifested by improvement of the biochemical and histological parameters. Exposure to IP prior to induction of acute pancreatitis significantly reduced the cerulein-evoked increase in serum lipase and poly-C ribonuclease activity, and serum concentration of pro-inflammatory IL-1β. A close relationship was found between the IP-evoked decrease in biochemical signs of pancreatitis and the improvement of pancreatic DNA synthesis, and pancreatic blood flow, as well as the reduction in histological score of pancreatic damage. Morphological features showed a decrease in pancreatic edema, vacuolization of acinar cells, and leukocyte infiltration of pancreatic tissue.

The increase in serum lipase activity is a well known manifestation of acute pancreatitis with high sensitivity and specificity[24]. Pancreatic-type poly-C specific ribonuclease is one of the few direct markers of severe pancreatic injury and pancreatic necrosis[21,25]. In our present study, acute pancreatitis was evoked by stimulation of pancreatitis by overdose of cerulein. This procedure leads to the development of mild edematous acute pancreatitis without pancreatic necrosis[26,27]. However, also in this case, we observed increase in serum activity of poly-C specific ribonuclease, suggesting that serum activity of pancreatic-type poly-C ribonuclease is not specific for severe pancreatic injury and pancreatic necrosis, and that serum activity of this enzyme increases in all types of acute pancreatitis, whereas severity of acute pancreatitis affects only the degree of poly-C ribonuclease activity in the serum. This discrepancy between our data and reports of Warshaw and Lee[21] or Naskalski *et al.*[25], may also be a result of species differences. On the other hand, our finding that IP applied before induction of acute pancreatitis reduced serum poly-C ribonuclease activity provides an additional support for the protective effect of IP on the pancreas in cerulein-induced pancreatitis.

In our present study, IP applied alone did not significantly affect pancreatic DNA synthesis. Induction of acute pancreatitis by cerulein caused a reduction in the pancreatic DNA synthesis, which is in agreement with previous observations[28,29] and may be considered as an index of pancreatic damage. In rats with induction of pancreatitis, IP attenuated the pancreatitis-evoked fall in pancreatic DNA synthesis. This observation brings the additional support for the concept that IP enhances resistance of the pancreas against tissue damage.

Our present observation that IP reduced pancreatic damage in cerulein-induced pancreatitis confirms and extends our previous finding that exposure to IP could protect the pancreas against damage evoked by severe ischemia followed by reperfusion[7]. These data suggest that IP, causing a mild damage, enhances resistance against pancreatic damage independently to the etiology of acute pancreatitis. This hypothesis is also supported by the observation that exposure to other mild damaging factors such as bacterial lipopolysaccharides[30], grapefruit-seed extract[22], or low doses of capsaicin[31] exhibits protective effect against acute pancreatitis.

The role of COX-2 in acute pancreatitis is unclear. Previous experimental studies on mice[13,14] have shown that pharmacological inhibition of COX-2 or COX-2 gene disruption ameliorates the severity of pancreatitis and the pancreatitis-associated lung injury. In contrast, in the rat model of pancreatitis, Foitzik *et al.*[32], have found some beneficial systemic effects of COX-2 inhibition on acute pancreatitis, such as an improvement of renal and respiratory function, but they have not observed any significant effect of COX-2 inhibition on histological score of pancreatic damage or plasma level of trypsinogen activation peptides. In our present study, blockade of COX-1 or COX-2 significantly reduced serum lipase and serum poly-C ribonuclease activity, as well as decreased pancreatic edema and inflammatory infiltration in morphological features in animals with cerulein-induced pancreatitis. The new and important finding of the present study is that inhibition of COXs, especially COX-2, reduces the protective effect of IP against pancreatic damage evoked by cerulein. This observation indicates that activity of COX-2 is necessary for the beneficial effect of IP. The involvement of COX-2 in IP effects on the pancreas is similar to that observed after treatment with HGF. Serum concentration of HGF is increased in patients with acute pancreatitis, and the HGF level reflects the clinical severity of pancreatitis and organ dysfunction[33,34]. Also experimental studies have shown the increase in plasma HGF level and tissue HGF overexpression in acute pancreatitis[35,36]. On the other hand, administration of antibodies that neutralize HGF aggravates the organ dysfunction and increases apoptosis in the course of acute pancreatitis[35], whereas treatment with HGF reduces pancreatic damage in cerulein-induced pancreatitis[37]. These data indicate that HGF is not a pro-inflammatory factor, but a result of pancreatic damage in acute pancreatitis and the elevation of HGF level plays a role of self-defense mechanism, limiting the intensity of inflammatory process. It was reported that inhibition of COX-2 abolishes the protective effect of HGF against acute pancreatitis[15]. Our present study showed that inhibition of COXs, especially COX-2, reduced the protective effect of IP against damage evoked by cerulein. These findings taken together suggest that pancreatoprotective effects evoked by IP and HGF involve similar but not strictly the same mechanisms. In contrast to the administration of HGF[37], exposure to IP did not increase the serum level of anti-inflammatory IL-10.

Another finding of our present study is the observation that cerulein-induced pancreatitis and IP increased pancreatic synthesis of HSP 70 and these two factors applied together caused maximal induction of HSP 70 synthesis in the pancreas. HSPs are highly conserved cytoprotective proteins that are induced by a variety of stresses including hyper- and hypothermia, toxin, heavy metals, and free radicals[16]. Previous studies demonstrated that both thermal and non-thermal stresses protect against cerulein-induced pancreatitis and prevent trypsinogen activation in the pancreas and this effect is mediated by HSP 70[38]. HSPs have also been shown to provide the protection against arginine-[19] and taurocholate-induced[39] pancreatitis. The potential protective mechanisms of HSPs on pancreas include stabilization and refolding of damaged proteins, resistance of cells to apoptosis or necrosis, decrease in the level of pro-inflammatory cytokines, antioxidant effects and interference with intra-acinar zymogen activation[16,38,40]. Our present results are consistent with the

previous studies showing an increase of HSP 70 at the mRNA and protein level after induction of cerulein-induced pancreatitis[41]. The major finding is, however, the observation of the further increase in HSP 70 synthesis in rats with IP, which indicates that the protective effects of IP could be mediated via this HSP.

In conclusion, exposure to IP reduces pancreatic damage in cerulein-induced acute pancreatitis and this protective effect of IP, at least in part, depends on COXs activity and production of HSP 70.

REFERENCES

1 **Murry CE**, Jennings RB, Reimer KA. Preconditioning with ischemia: a delay of lethal cell injury in ischemic myocardium. *Circulation* 1986; **74**; 1124-1136
2 **Kato H**, Liu Y, Kogure K, Kato K. Induction of 27-kDa heat shock protein following cerebral ischemia in a rat model of ischemic tolerance. *Brain Res* 1994; **634**: 235-244
3 **Turman MA**, Bates CM. Susceptibility of human proximal tubular cells to hypoxia: effect of hypoxic preconditioning and comparison to glomerular cells. *Ren Fail* 1997; **19**: 47-60
4 **Kume M**, Yamamoto Y, Saad S, Gomi T, Kimoto S, Shimabukuro T, Yagi T, Nakagami M, Takada Y, Morimoto T, Yamaoka Y. Ischemic preconditioning of the liver in rats: implications of heat shock protein induction to increase tolerance of ischemia-reperfusion injury. *J Lab Clin Med* 1996; **128**: 251-258
5 **Mounsey RA**, Pang CY, Boyd JB, Forrest C. Augmentation of skeletal muscle survival in the latissimus dorsi porcine model using acute ischemic preconditioning. *J Otolaryngol* 1992; **21**: 315-320
6 **Pajdo R**, Brzozowski T, Konturek PC, Kwiecien S, Konturek SJ, Sliwowski Z, Pawlik M, Ptak A, Drozdowicz D, Hahn EG. Ischemic preconditioning, the most effective gastroprotective intervention: involvement of prostaglandins, nitric oxide, adenosine and sensory nerves. *Eur J Pharmacol* 2001; **427**: 263-276
7 **Dembiñski A**, Warzecha Z, Ceranowicz P, Tomaszewska R, Dembinski M, Pabiañczyk M, Stachura J, Konturek SJ. Ischemic preconditioning reduces the severity of ischemia/reperfusion-induced pancreatitis. *Eur J Pharmacol* 2003; **473**: 207-216
8 **Smith WL**, Garavito RM, DeWitt DL. Prostaglandin endoperoxide H synthases (cyclooxygenases)-1 and 2. *J Biol Chem* 1996; **271**: 33157-33160
9 **Peskar BM**. Role of cyclooxygenase isoforms in gastric mucosal defence. *J Physiol Paris* 2001; **95**: 3-9
10 **Konturek SJ**, Piastucki I, Brzozowski T, Radecki T, Dembinska-Kiec A, Zmuda A, Gryglewski R. Role of prostaglandins in the formation of aspirin-induced gastric ulcers. *Gastroenterology* 1981; **80**: 4-9
11 **Wang JY**, Yamasaki S, Takeuchi K, Okabe S. Delayed healing of acetic acid-induced gastric ulcers in rats by indomethacin. *Gastroenterology* 1989; **96**: 393-402
12 **Mizuno H**, Sakamoto C, Matsuda K, Wada K, Uchida T, Noguchi H, Akamatsu T, Kasuga M. Induction of cyclooxygenase 2 in gastric mucosal lesions and its inhibition by the specific antagonist delays healing in mice. *Gastroenterology* 1997; **112**: 387-397
13 **Song AM**, Bhagat L, Singh VP, van Acker GGD, Steer ML, Saluja AK. Inhibition of cyclooxygenase-2 ameliorates the severity of pancreatitis and associated lung injury. *Am J Physiol Gastrointest Liver Physiol* 2002; **283**: G1166-1174
14 **Ethridge RT**, Chung DH, Slogoff M, Ehlers RA, Hellmich MR, Rajaraman S, Saito H, Uchida T, Evers BM. Cyclooxygenase-2 gene disruption attenuates the severity of acute pancreatitis and pancreatitis-associated lung injury. *Gastroenterology* 2002; **123**: 1311-1322
15 **Warzecha Z**, Dembinski A, Ceranowicz P, Konturek SJ, Tomaszewska R, Stachura J, Nakamura T, Konturek PC. Inhibition of cyclooxygenase-2 reduces the protective effect of hepatocyte growth factor in experimental pancreatitis. *Eur J Pharmacol* 2004; **486**: 107-119
16 **Rakonczay Z Jr**, Takacs T, Boros I, Lonovics J. Heat shock proteins and the pancreas. *J Cell Physiol* 2003; **195**: 383-391
17 **Wagner AC**, Weber H, Jonas L, Nizze H, Strowski M, Fiedler F, Printz H, Steffen H, Goke B. Hyperthermia induces heat shock protein expression and protection against cerulein-induced pancreatitis in rats. *Gastroenterology* 1996; **111**: 1333-1342
18 **Kubisch C**, Dimagno MJ, Tietz AB, Welsh MJ, Ernst SA, Brandt-Nedelev B, Diebold J, Wagner AC, Goke B, Williams JA, Schafer C. Overexpression of heat shock protein Hsp27 protects against cerulein-induced pancreatitis. *Gastroenterology* 2004; **127**: 275-286
19 **Tashiro M**, Ernst SA, Edwards J, Williams JA. Hyperthermia induces multiple pancreatic heat shock proteins and protects against subsequent arginine-induced acute pancreatitis in rats. *Digestion* 2002; **65**: 118-126
20 **Konturek SJ**, Szlachcic A, Dembinski A, Warzecha Z, Jaworek J, Stachura J. Nitric oxide in pancreatic secretion and hormone-induced pancreatitis in rats. *Int J Pancreatol* 1994; **15**: 19-28
21 **Warshaw AL**, Lee KH. Serum ribonuclease elevations and pancreatic necrosis in acute pancreatitis. *Surgery* 1979: **86**: 227-234
22 **Dembiñski A**, Warzecha Z, Konturek SJ, Ceranowicz P, Dembinski M, Pawlik WW, Kucœnierz-Cabała B, Naskalski JW. Extract of grapefruit-seed reduces acute pancreatitis induced by ischemia/reperfusion in rats; Possible implication of tissue antioxidants. *J Physiol Pharmacol* 2004; **55**: 799-809
23 **Warzecha Z**, Dembinski A, Ceranowicz P, Jaworek J, Konturek PC, Dembiñski M, Bilski J, Konturek SJ. Influence of leptin administration on the course of acute ischemic pancreatitis. *J Physiol Pharmacol* 2002; **53**: 775-790
24 **Dervenis C**, Johnson CD, Bassi C, Bradley E, Imrie CW, McMahon MJ, Modlin I. Diagnosis, objective assessment of severity, and management of acute pancreatitis. Santorini consensus conference. *Int J Pancreatol* 1999; **25**: 195-210
25 **Naskalski JW**, Kucœnierz-Cabała B, Panek J, Kędra B. Poly-C specific ribonuclease activity correlates with increased concentrations of IL-6, IL-8 and sTNFR55/sTNFR75 in plasma of patients with acute pancreatitis. *J Physiol Pharmacol* 2003; **54**: 439-448
26 **Watanabe O**, Baccino FM, Steer ML, Meldolesi J. Supramaximal caerulein stimulation and ultrastructure of rat pancreatic acinar cell: early morphological changes during development of experimental pancreatitis. *Am J Physiol* 1984; **246**: G457-G467
27 **Konturek SJ**, Dembinski A, Konturek PJ, Warzecha Z, Jaworek J, Gustaw P, Tomaszewska R, Stachura J. Role of platelet activating factor in pathogenesis of acute pancreatitis in rats. *Gut* 1992; **33**: 1268-1274
28 **Dembiñski A**, Warzecha Z, Konturek PC, Ceranowicz P, Konturek SJ, Tomaszewska R, Stachura J. Adaptation of pancreas to repeated caerulein-induced pancreatitis in rats. *J Physiol Pharmacol* 1996; **47**: 455-467
29 **Warzecha Z**, Dembinski A, Ceranowicz P, Konturek SJ, Tomaszewska R, Stachura J, Konturek PC. IGF-1 stimulates production of interleukin-10 and inhibits development of caerulein-induced pancreatitis. *J Physiol Pharmacol* 2003; **54**: 575-590
30 **Jaworek J**, Jachimczak B, Tomaszewska R, Konturek PC, Pawlik WW, Sendur R, Hahn EG, Stachura J, Konturek SJ. Protective action of lipopolysaccharides in rat caerulein-induced pancreatitis: role of nitric oxide. *Digestion* 2000; **62**: 1-13
31 **Warzecha Z**, Dembinski A, Ceranowicz P, Stachura J, Tomaszewska R, Konturek SJ. Effect of sensory nerves and CGRP on the development of caerulein-induced pancreatitis and pancreatic recovery. *J Physiol Pharmacol* 2001; **52**: 679-704
32 **Foitzik T**, Hotz HG, Hotz B, Witting F, Buhr HJ. Selective inhibition of cyclooxygenase-2 (COX-2) reduces prostaglandin E_2 production and attenuates systemic disease sequelae in experimental pancreatitis. *Hepatogastroenterology* 2003; **50**:

1159-1162
33 **Ueda T**, Takeyama Y, Toyokawa A, Kishida S, Yamamoto M, Saitoh Y. Significant elevation of serum human hepatocyte growth factor levels in patients with acute pancreatitis. *Pancreas* 1996; **12**: 76-83
34 **Ueda T**, Takeyama Y, Hori Y, Nishikawa J, Yamamoto M, Saitoh Y. Hepatocyte growth factor in assessment of acute pancreatitis: Comparison with C-reactive protein and interleukin-6. *J Gastroenterol* 1997; **32**: 63-70
35 **Ueda T**, Takeyama Y, Hori Y, Shinkai M, Takase K, Goshima M, Yamamoto M, Kuroda Y. Hepatocyte growth factor increases in injured organs and functions as an organotrophic factor in rats with experimental acute pancreatitis. *Pancreas* 2000; **20**: 84-93
36 **Menke A**, Yamaguchi H, Giehl K, Adler G. Hepatocyte growth factor and fibroblast growth factor 2 are overexpressed after cerulein-induced acute pancreatitis. *Pancreas* 1999; **18**: 28-33
37 **Warzecha Z**, Dembinski A, Konturek PC, Ceranowicz P, Konturek SJ, Tomaszewska R, Schuppan D, Stachura J, Nakamura T. Hepatocyte growth factor attenuates pancreatic damage in caerulein-induced pancreatitis in rats. *Eur J Pharmacol* 2001; **430**: 113-121
38 **Frossard JL**, Bhagat L, Lee HS, Hietaranta AJ, Singh VS, Song AM, Steer ML, Saluja AK. Both thermal and non-thermal stress protect against caerulein induced pancreatitis and prevent trypsinogen activation in the pancreas. *Gut* 2002; **50**: 78-83
39 **Rakonczay Z Jr**, Takacs T, Ivanyi B, Mandi Y, Papai G, Boros I, Varga IS, Jost K, Lonovics J. The effects of hypo- and hyperthermic pretreatment on sodium taurocholate-induced acute pancreatitis in rats. *Pancreas* 2002; **24**: 83-89
40 **Takayama S**, Reed JC, Homma S. Heat-shock proteins as regulators of apoptosis. *Oncogene* 2003; **22**: 9041-9047
41 **Weber CK**, Gress T, Muller-Pillasch F, Lerch MM, Weidenbach H, Adler G. Supramaximal secretagogue stimulation enhances heat shock protein expression in the rat pancreas. *Pancreas* 1995; **10**: 360-367

Science Editor Wang XL and Guo SY **Language Editor** Elsevier HK

PO Box 2345, Beijing 100023, China
www.wjgnet.com
wjg@wjgnet.com

ELSEVIER

World J Gastroenterol 2005;11(38):5966-5972
World Journal of Gastroenterology ISSN 1007-9327

• *BASIC RESEARCH* •

Role of nuclear receptor CAR in carbon tetrachloride-induced hepatotoxicity

Yuichi Yamazaki, Satoru Kakizaki, Norio Horiguchi, Hitoshi Takagi, Masatomo Mori, Masahiko Negishi

Yuichi Yamazaki, Satoru Kakizaki, Norio Horiguchi, Hitoshi Takagi, Masatomo Mori, Department of Medicine and Molecular Science, Gunma University Graduate School of Medicine, Maebashi, Gunma 371-8511, Japan
Masahiko Negishi, Pharmacogenetics Section, Laboratory of Reproductive and Developmental Toxicology, National Institute of Environmental Health Sciences, National Institutes of Health, Research Triangle Park, NC 27709, USA
Supported by a Grant-in Aid for Scientific Research, No. 15790337 from the Ministry of Education, Science, Sports and Culture of the Japanese Government
Correspondence to: Satoru Kakizaki, MD, PhD, Department of Medicine and Molecular Science, Gunma University Graduate School of Medicine, 3-39-15 Showa-machi, Maebashi 371-8511, Japan. kakizaki@showa.gunma-u.ac.jp
Telephone: +81-27-220-8127 Fax: +81-27-220-8136
Received: 2005-03-25 Accepted: 2005-04-30

Abstract

AIM: To investigate the precise roles of CAR in CCl_4-induced acute hepatotoxicity.

METHODS: To prepare an acute liver injury model, CCl_4 was intraperitoneally injected in $CAR^{+/+}$ and $CAR^{-/-}$ mice.
RESULTS: Elevation of serum alanine aminotransferase and extension of centrilobular necrosis were slightly inhibited in $CAR^{-/-}$ mice compared to $CAR^{+/+}$ mice without PB. Administration of a CAR inducer, PB, revealed that CCl_4-induced liver toxicity was partially inhibited in $CAR^{-/-}$ mice compared with $CAR^{+/+}$ mice. On the other hand, androstanol, an inverse agonist ligand, inhibited hepatotoxicity in $CAR^{+/+}$ but not in $CAR^{-/-}$ mice. Thus, CAR activation caused CCl_4 hepatotoxicity while CAR inhibition resulted in partial protection against CCl_4-induced hepatotoxicity.There were no differences in the expression of CYP2E1, the main metabolizing enzyme for CCl_4, between $CAR^{+/+}$ and $CAR^{-/-}$ mice. However, the expression of other CCl_4-metabolizing enzymes, such as CYP2B10 and 3A11, was induced by PB in $CAR^{+/+}$ but not in $CAR^{-/-}$ mice. Although the main pathway of CCl_4-induced acute liver injury is mediated by CYP2E1, CAR modulates its pathway via induction of CYP2B10 and 3A11 in the presence of activator or inhibitor.

CONCLUSION: The nuclear receptor CAR modulates CCl_4-induced liver injury via induction of CCl_4-metabolizing enzymes in the presence of an activator. Our results suggest that drugs interacting with nuclear receptors such as PB might play critical roles in drug-induced liver injury or drug-drug interaction even though such drugs themselves are not hepatotoxic.

Key words: CAR; Phenobarbital; Cytochrome P450; CCl_4; Drug-induced liver injury

Yamazaki Y, Kakizaki S, Horiguchi N, Takagi H, Mori M, Negishi M. Role of nuclear receptor CAR in carbon tetrachloride-induced hepatotoxicity. *World J Gastroenterol* 2005; 11 (38): 5966-5972
http://www.wjgnet.com/1007-9327/11/5966.asp

INTRODUCTION

Drug-induced liver injury is a clinical-relevant problem[1-3], and investigation of mechanisms of drug-induced liver injury is therefore of pharmacological and clinical importance. Animals induce drug-metabolizing enzymes to detoxify xenochemicals, including therapeutic drugs[4-6]. However, paradoxically, this can often result in bioactivation of toxic drugs and cause liver injury[4-6]. Thus, drug-metabolizing enzymes are a two-edge blade and have very crucial roles in drug-induced liver injury.

Recent studies indicate that the nuclear receptor constitutive androstane receptor (CAR) is a key regulator of drug-metabolizing enzymes such as cytochrome P450 (CYP)[7-9], UDP-glucuronosyltransferase (UGT)[10,11] and multidrug resistance-associated protein (MRP)[12,13]. CAR has also been reported as a key regulator for bile acid[14] and bilirubin liver injury[11,15,16]. As a cellular defense mechanism against toxicity and carcinogenicity, induction of and metabolism by CYPs usually leads to increased detoxification and elimination of xenobiotics[4-6]. The nuclear receptor CAR is implicated as an essential factor that mediates this inducible activation of drug-metabolizing enzymes[7-9]. CAR, acting as a heterodimer with the retinoid X receptor, binds to a nuclear receptor-binding site NR1 within the 51-bp phenobarbital-responsive enhancer module and activates genes such as CYP2B in response to phenobarbital (PB)-type inducers[7-9]. Expression analysis of hepatic genes in $CAR^{-/-}$ mice has also revealed that CAR is a key regulator of a group of xenochemical-metabolizing enzymes that include the CYP2B and CYP3A subfamilies[17]. Thus, CAR is closely associated with the regulation of drug-metabolizing enzymes. Because of its regulating roles for drug-metabolizing enzymes, CAR is thought to play an important role in the development of drug-induced liver injury.

Carbon tetrachloride (CCl_4) was once used widely as a solvent cleaner, anesthetic agent, and degreaser both for industrial and home use[18-20]. However, the high incidence of liver and renal problems following administration led to

discontinuation of its use. CCl_4 is used as a model drug for the study of hepatotoxicity in acute and chronic liver failure[18-20]. CCl_4 is metabolized by CYP2E1, CYP2B, and possibly CYP3A, to form the trichloromethyl radical, CCl_3*[18-20]. CCl_3* can bind to cellular molecules (nucleic acid, protein, and lipid), impairing crucial cellular processes. This radical can also react with oxygen to form the trichloromethylperoxy radical CCl_3OO*, a highly reactive species. Thus, the metabolites of CCl_4 cause the hepatic injury in the CCl_4 acute liver injury model. Inducers of drug-metabolizing enzymes, such as PB or dichlorodiphenyltrichloroethane, are also known to cause severe liver toxicity with CCl_4[18-20].

The nuclear receptor CAR has recently been shown to mediate the effects of PB and other PB-like inducers[21] and to act as a key regulator of drug-metabolizing enzymes[21-23]. However, the precise relationship between CAR and CCl_4-induced liver injury is not fully understood. We investigated the mechanism of CCl_4-induced acute liver injury and the roles of CAR in drug-induced liver injury using $CAR^{-/-}$ mice *in vivo*.

MATERIALS AND METHODS

Materials

PB was purchased from Sigma Chemicals Co. (St. Louis, MO, USA). 5α-Androstan-3δ-ol (androstanol) was purchased from Steraloids (Newport, RI, USA). CCl_4 was purchased from Kanto Chemistry (Tokyo, Japan). The total glutathione quantification kit was purchased from Dojindo Molecular Technologies Inc. (Gaithersburg, MD, USA).

Animals and treatment

$CAR^{-/-}$ and $CAR^{+/+}$ mice used in this study were generated as described previously[24]. The background strain contained 98% of the C3H/HeNCrlBR markers by microsatellite analysis[24]. All mouse work was performed in accordance with the guidelines for animal care and use established by Gunma University Graduate School of Medicine. Germline transmission of the disrupted allele was detected by PCR[17]. Mice were injected intraperitoneally with the indicated concentration of CCl_4 dissolved in olive oil at 8-10 wk of age and were killed, and their sera and livers were collected at specified time points. PB was administered in H_2O at a dose of 100 mg/kg body weight for 12 and 36 h before CCl_4 administration. Androstanol was administered in olive oil at a dose of 100 mg/kg body weight for 1 h before CCl_4 administration. For control mice, 100 μL of H_2O or olive oil per 25 g of body weight was injected. Serum alanine aminotransferase (ALT), total bilirubin, and blood urea nitrogen (BUN) levels were measured with an auto-analyzer at each point. Liver tissues were fixed in 40 g/L formaldehyde, embedded in paraffin and stained with hematoxylin-eosin. At a magnification of ×40, 10 areas of centrilobular necrosis were measured in a blinded fashion for each group using NIH Image 1.62 software (National Institute of Health, MD, USA). The index of centrilobular necrosis was scored as follows: area of centrilobular necrosis divided by whole area.

Reverse transcription-polymerase chain reaction

Total RNA extraction from liver and subsequent synthesis of first-strand cDNA were performed using TRIzol reagent (Invitrogen, Carlsbad, CA, USA) and SuperScript™ preamplification system (Invitrogen, Carlsbad, CA, USA), respectively. cDNAs were amplified using the following sets of primers: CYP2B10 mRNA, 5'-AAAGTCCCGTGGCAACTTCC-3' and 5'-CATCCCAAAGTCTCTCATGG-3'; CYP3A11 mRNA, 5'-CTCAATGGTGTGTATATCCCC-3' and 5'-CCGATGTTCTTAGACACTGCC-3'; GSTpi, 5'-CTTGCTCAAGCCCACTTGTC-3' and 5'-ATGGGACGGTTCACATGTTC-3'; CYP2E1, 5'-GGATGAATATGCCCTACATG-3' and 5'-TGATGGGCAGCAGGTCTCAT-3'. β-actin mRNA level was also measured as an internal control. One-twentieth of each cDNA synthesized from 5 μg of RNA was subjected to PCR. PCR was performed using Taq DNA polymerase (Promega, Madison, WI, USA) with TaqStart antibody (Clontech, Palo Alto, CA, USA) at 95 ℃ for 60 s, 55 ℃ for 60 s, and 72 ℃ for 60 s. The amplified DNA was separated on a 1.5% agarose gel and visualized with staining by ethidium bromide. The expected sizes of the amplified cDNA were 340, 423, 468, and 486 bp for CYP2B10, CYP3A11, CYP2E1, and GSTPi, respectively.

Hepatic glutathione concentration

Total hepatic reduced glutathione concentration was determined by the total glutathione quantification kit (Dojindo Molecular Technologies Inc.). Each liver was excised and homogenized with 5% trichloroacetic acid, and centrifuged at 4 ℃, 2 000 r/min for 15 min. The supernatant was used for total glutathione assay using the total glutathione quantification kit according to the manual provided by the manufacturer.

Statistical analysis

All experimental data are shown as mean±SD. Differences in serum ALT levels and the index of centrilobular necrosis were determined by one-way factorial analysis of variance for each group. The level of significance for all statistical analyses was set at $P<0.05$.

RESULTS

Phenobarbital pretreatment induces CCl_4 toxicity in $CAR^{+/+}$ mice

$CAR^{+/+}$ and $CAR^{-/-}$ mice were administered a 25-mg/kg dose of CCl_4 by intraperitoneal injection ($n = 6$ per treatment group) and the ALT level was measured at 24 h (Figure 1A). The serum levels of ALT increased following CCl_4 administration in both groups ($P<0.001$). The level of ALT was slightly higher in $CAR^{+/+}$ mice than in $CAR^{-/-}$ mice ($P<0.001$). There were no significant changes in the serum levels of total bilirubin and BUN in both groups (data not shown). $CAR^{+/+}$ and $CAR^{-/-}$ animals pretreated with PB (12 and 36 h before CCl_4 administration) were then administered the same dose of CCl_4. PB pretreatment caused marked elevation of ALT in $CAR^{+/+}$ mice. The $CAR^{-/-}$ mice showed some elevation of ALT with PB pretreatment, but the level was less than that in wild-type mice. The difference of ALT levels became clear between $CAR^{+/+}$ and $CAR^{-/-}$ mice with pre-treatment by PB ($P<0.001$). PB alone and control mice did not show such an elevation of ALT.

Histological changes associated with CCl_4 toxicity

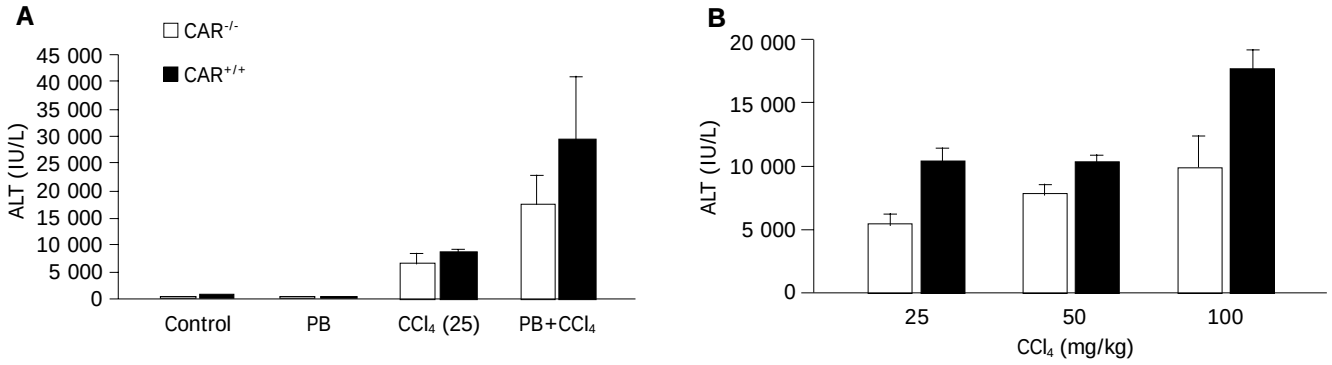

Figure 1 A: PB pretreatment induced CCl_4 toxicity. $CAR^{+/+}$ or $CAR^{-/-}$ mice were administered a 25-mg/kg dose of CCl_4 by intraperitoneal injection with or without PB pretreatment (n = 6 per treatment group). Serum was collected and ALT levels were measured after 24 h. The ALT level was slightly higher in $CAR^{+/+}$ mice than in $CAR^{-/-}$ mice with CCl_4 treatment (P<0.001). The difference in ALT levels became clearer between $CAR^{+/+}$ and $CAR^{-/-}$ mice with pre-treatment by PB (P<0.001). B: Dose dependency of CCl_4 toxicity. $CAR^{+/+}$ and $CAR^{-/-}$ mice were given 25-, 50-, or 100-mg/kg doses of CCl_4. Blood samples were collected 24 h later, and serum ALT levels were measured (n = 4). $CAR^{-/-}$ animals were significantly less sensitive than $CAR^{+/+}$ mice to CCl_4 toxicity (P<0.001). Data are mean±SD.

$CAR^{+/+}$ or $CAR^{-/-}$ mice were administered a 25-mg/kg dose of CCl_4 by intraperitoneal injection with or without pretreatment with PB (n = 6 per treatment group). Liver sections from each treatment were examined by hematoxylin and eosin staining. Liver samples from all treated animals were analyzed but representative histology is presented in Figure 2A showing marked centrilobular necrosis. The extent of the necrotic area with CCl_4 in the $CAR^{+/+}$ liver was slightly larger than that in $CAR^{-/-}$ mice. PB pretreatment caused extensive centrilobular necrosis in $CAR^{+/+}$ mice compared with $CAR^{-/-}$ mice. The indices of centrilobular necrosis (Figure 2B) in $CAR^{+/+}$ mice and $CAR^{-/-}$ mice treated with CCl_4 alone were 17.44±1.02 and 13.11±1.41, respectively (P<0.001). The indices of centrilobular necrosis in $CAR^{+/+}$ mice and $CAR^{-/-}$ mice treated with PB plus CCl_4 were 39.08±2.10 and 26.33±2.33, respectively (P<0.001).

Dose dependency and time course of CCl_4 toxicity

$CAR^{+/+}$ or $CAR^{-/-}$ mice were treated with 25-, 50-, or 100-mg/kg CCl_4 by intraperitoneal injection (n = 4 per treatment group). Five and twenty-four hours later, the mice were killed and blood samples were collected (Figure 1B).

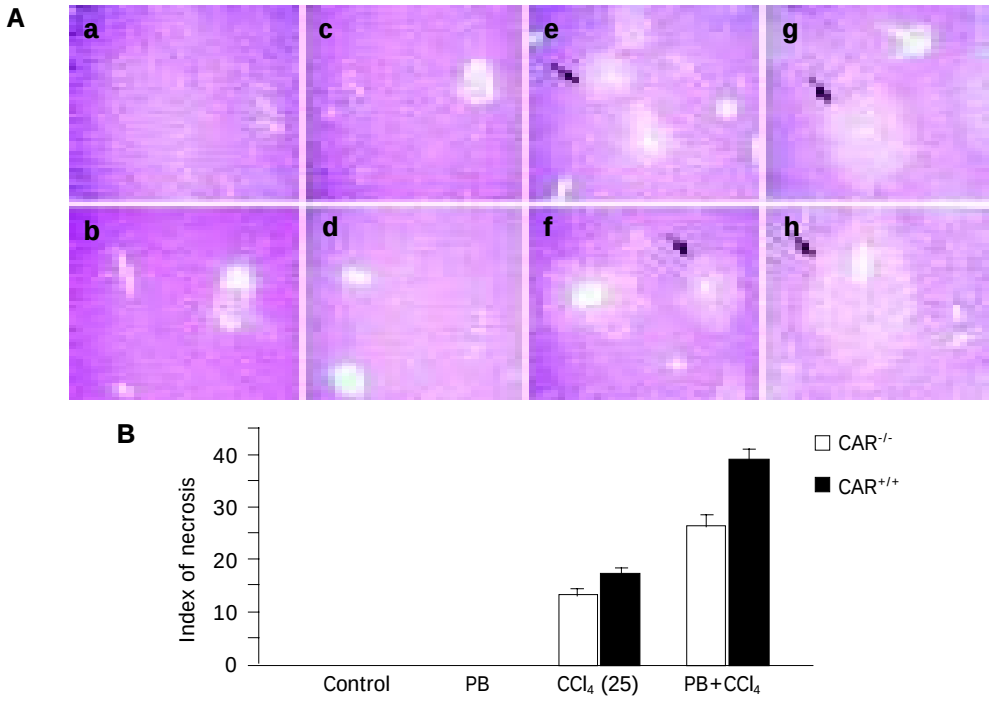

Figure 2 Histological changes associated with CCl_4 toxicity. A: Histological findings in the liver; (a) $CAR^{-/-}$ mice, control; (b) $CAR^{+/+}$ mice, control; (c) $CAR^{-/-}$ mice, PB; (d) $CAR^{+/+}$ mice, PB; (e) $CAR^{-/-}$ mice, CCl_4; (f) $CAR^{+/+}$ mice, CCl_4; (g) $CAR^{-/-}$ mice, PB plus CCl_4; and (h) $CAR^{+/+}$ mice, PB plus CCl_4. Liver sections from each treatment were examined by hematoxylin and eosin staining. Liver samples from all treated animals were analyzed, but only representative histology is presented. The extent of the necrotic area in the $CAR^{+/+}$ liver was larger than that in $CAR^{-/-}$ mice. PB pretreatment caused extensive centrilobular necrosis in $CAR^{+/+}$ mice. The arrows indicate centrilobular necrosis. Magnification, ×100. B: The indices of centrilobular necrosis in $CAR^{+/+}$ mice and $CAR^{-/-}$ mice. The indices of centrilobular necrosis were higher in $CAR^{+/+}$ mice than that in $CAR^{-/-}$ mice with PB pretreatment. The index in $CAR^{+/+}$ mice treated with CCl_4 plus PB was significantly increased. The index of centrilobular necrosis was scored as follows: area of centrilobular necrosis divided by whole area. Data are mean±SD.

No elevation of ALT was observed at 5 h (data not shown). At 24 h, ALT was significantly elevated and dose dependency was observed in CCl_4 toxicity in both groups of mice. The serum ALT concentrations of $CAR^{-/-}$ mice were lower than those of the $CAR^{+/+}$ mice ($P<0.001$). Thus, $CAR^{+/+}$ mice were apparently more sensitive to CCl_4 liver toxicity compared with $CAR^{-/-}$ mice.

Hepatic mRNA levels of CCl_4-metabolizing enzymes

CCl_4 is reported to be metabolized and activated by CYP2E1, CYP2B, and possibly CYP3A, to form the trichloromethyl radical, CCl_3*[18-20]. To evaluate the relationship between CAR and CCl_4-metabolizing enzymes, $CAR^{+/+}$ or $CAR^{-/-}$ animals were treated with a 100-mg/kg PB intraperitoneally ($n = 6$ per treatment group, Figure 3). There were no differences in the basal expression of CYP2E1, the main metabolizing enzyme of CCl_4, between $CAR^{+/+}$ and $CAR^{-/-}$ mice. Among the genes associated with CCl_4 metabolism, PB treatment did not influence CYP2E1 mRNA levels but induced CYP2B10, CYP3A11 mRNAs in $CAR^{+/+}$ mice. On the other hand, no induction of the enzymes CYP2E1, CYP2B10, and CYP3A11 was observed in $CAR^{-/-}$ mice. Thus, PB activated CCl_4-metabolizing enzymes, CYP2B10 and CYP3A11, via CAR. Because CAR is reported to regulate GSTPi, the enzyme that enhances glutathione depletion in acetaminophen toxicity[18-21], GSTPi mRNA, was also measured. GSTPi mRNA was induced by PB in $CAR^{+/+}$ mice stronger than in $CAR^{-/-}$ mice.

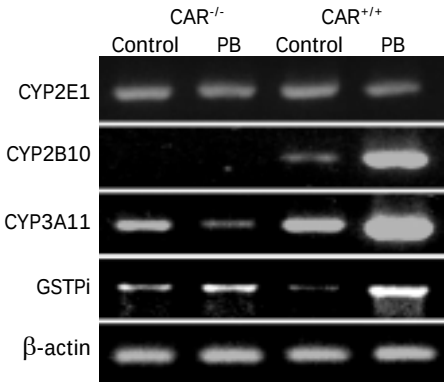

Figure 3 Hepatic mRNA level of drug-metabolizing enzymes with PB treatment. Total liver RNA was prepared from $CAR^{+/+}$ or $CAR^{-/-}$ animals treated with a 100-mg/kg dose of PB by intraperitoneal injection ($n = 6$ per treatment group). Total liver RNA was prepared 12 h after PB treatment and subjected to PCR analysis with the indicated primers in Materials and methods. β-Actin mRNA level was also measured as an internal control. The amplified DNA was separated on a 1.5% agarose gel and visualized with staining by ethidium bromide. The expected sizes of the amplified cDNA are described in Materials and methods.

Hepatic glutathione level

For detoxification, metabolites of CCl_4 such as CCl_3* decreased the amount of reduced glutathione. A decrease of glutathione in the liver reflects increased production of CCl_4 metabolites. Liver samples treated with CCl_4 and/or PB were collected 24 h after each treatment and glutathione levels were measured ($n = 6$ per treatment group, Figure 4). Hepatic glutathione levels in the PB plus CCl_4-treated $CAR^{+/+}$ mice were significantly different from those of the $CAR^{-/-}$ mice ($P<0.001$). $CAR^{+/+}$ mice treated with PB plus CCl_4 showed about a 50% decrease in hepatic glutathione level compared with $CAR^{-/-}$ mice.

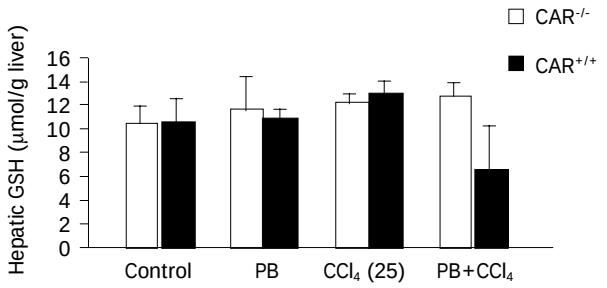

Figure 4 Hepatic glutathione (GSH) level. Liver samples treated with the indicated chemicals were collected 24 h after each treatment and glutathione levels were measured ($n = 6$ per treatment group) using the total glutathione quantification kit. Hepatic glutathione levels in the PB plus CCl_4 treated $CAR^{+/+}$ mice significantly decreased, compared with those of the $CAR^{-/-}$ mice ($P<0.001$). Data are mean±SD.

Androstanol reduced CCl_4-induced hepatotoxicity in $CAR^{+/+}$ mice to the level of $CAR^{-/-}$ mice

$CAR^{+/+}$ or $CAR^{-/-}$ mice were treated with 100-mg/kg CCl_4 intraperitoneally, with or without pretreatment with androstanol (100 mg/kg). Serum ALT levels were measured 24 h later ($n = 6$ per treatment group, Figure 5). Without androstanol, $CAR^{+/+}$ mice treated with CCl_4 showed significantly higher ALT concentrations than did $CAR^{-/-}$ mice ($P<0.0001$). Surprisingly, androstanol reduced the ALT concentration of $CAR^{+/+}$ mice to the level of $CAR^{-/-}$ mice. Liver sections from the same animals, as indicated, were stained with hematoxylin and eosin (Figure 5B). Androstanol pretreatment reduced the hepatic centrilobular necrosis (Figure 5C) of $CAR^{+/+}$ mice to the level of $CAR^{-/-}$ mice. The indices of centrilobular necrosis of $CAR^{+/+}$ mice and $CAR^{-/-}$ mice treated with CCl_4 alone were 33.39±5.04 and 26.49±2.87, respectively ($P<0.001$). With androstanol treatment, the indices of centrilobular necrosis in $CAR^{+/+}$ mice and $CAR^{-/-}$ mice decreased to 23.64±1.89 and 25.15±2.36, respectively ($P = 0.15$). Thus, androstanol, the inverse agonist of CAR, reduced the CCl_4-induced hepatotoxicity of $CAR^{+/+}$ mice to the level of $CAR^{-/-}$ mice.

To evaluate the effect of androstanol on CCl_4-metabolizing enzymes, hepatic mRNA levels were determined with RT-PCR. Androstanol treatment did not influence CYP2E1 mRNA levels but slightly repressed CYP3A11 mRNA in $CAR^{+/+}$ mice as previously reported[25]. Because of low basal expression of CYP2B10 mRNA, the repression of CYP2B10 mRNA by androstanol could not be demonstrated with RT-PCR in $CAR^{+/+}$ mice. However, androstanol was reported to repress the basal promoter activity of CYP2B10 by luciferase reporter assay[26]. On the other hand, no induction or repression of the enzymes CYP2E1, CYP2B10, and CYP3A11 was observed in $CAR^{-/-}$ mice. Thus, androstanol repressed basal expression of CCl_4-metabolizing enzymes, CYP3A11 and may be CYP2B10, via CAR. Androstanol

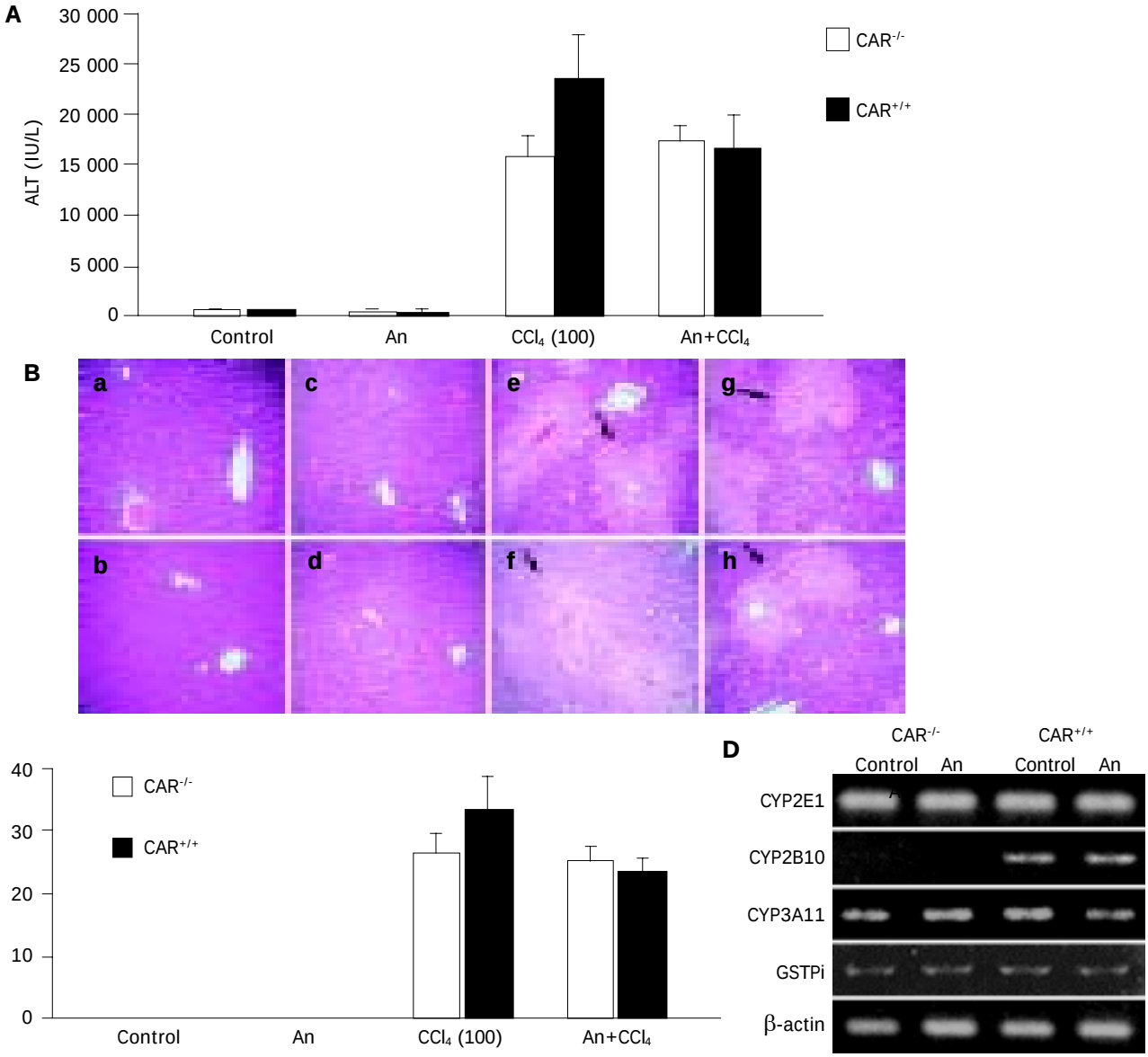

Figure 5 Androstanol prevented CCl_4-induced hepatotoxicity. A: $CAR^{+/+}$ or $CAR^{-/-}$ mice were given a 100-mg/kg dose of CCl_4 by intraperitoneal injection, with or without pretreatment with androstanol (100 mg/kg). Serum ALT levels were measured 24 h later (n = 6 per treatment group). Androstanol-pretreatment reduced the ALT level of $CAR^{+/+}$ mice to the level of $CAR^{-/-}$ mice. An: androstanol. B: Liver sections from the same animals 24 h after different treatments, as indicated, were stained with hematoxylin and eosin. (a) $CAR^{-/-}$ mice, control; (b) $CAR^{+/+}$ mice, control; (c) $CAR^{-/-}$ mice, androstanol; (d) $CAR^{+/+}$ mice, androstanol; (e) $CAR^{-/-}$ mice, CCl_4; (f) $CAR^{+/+}$ mice, CCl_4; (g) $CAR^{-/-}$ mice, androstanol plus CCl_4; and (h) $CAR^{+/+}$ mice, androstanol plus CCl_4. Androstanol pretreatment reduced the hepatic centrilobular necrosis in $CAR^{+/+}$ mice. Arrows indicate areas of hepatic necrosis. C: The indices of centrilobular necrosis in $CAR^{+/+}$ mice and $CAR^{-/-}$ mice. Androstanol-pretreatment reduced hepatic centrilobular necrosis of $CAR^{+/+}$ mice to the level of $CAR^{-/-}$ mice. Data in (A) and (C) are mean±SD. (D) Hepatic mRNA level of drug-metabolizing enzymes with androstanol treatment. Total liver RNA was prepared from $CAR^{+/+}$ or $CAR^{-/-}$ animals treated with a 100-mg/kg dose of androstanol by intraperitoneal injection (n = 6 per treatment group) and subjected to PCR analysis with the indicated primers in Materials and methods. β-actin mRNA level was also measured as an internal control. The amplified DNA was separated on a 1.5% agarose gel and visualized with staining by ethidium bromide. The expected sizes of the amplified cDNA are described in Materials and methods.

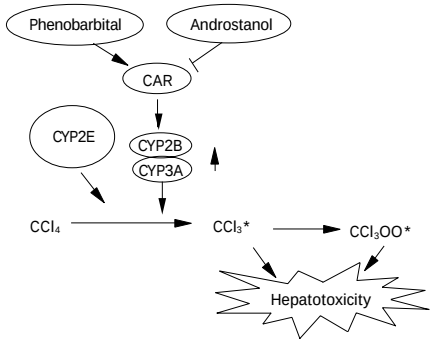

Figure 6 Schematic representation of CAR-mediated CCl_4 hepatotoxicity.

treatment did not influence GSTPi mRNA levels in $CAR^{+/+}$ and $CAR^{-/-}$ mice by RT-PCR.

DISCUSSION

In this study, we showed that CAR partially modulates the CCl_4 toxicity that is associated with induction of some CCl_4-metabolizing enzymes in the presence of agonist. The loss of CAR function results in partial resistance to CCl_4 toxicity. However, the CCl_4 liver toxicity is not fully inhibited in $CAR^{-/-}$ mice and differences between $CAR^{+/+}$ and $CAR^{-/-}$ mice were small in the absence of an inducer, PB. Metabolites of CCl_4 such as CCl_3* and CCl_3OO* are known to cause the

hepatic injury associated with CCl_4[18-20]. CCl_4 is metabolized by CYP2E1, CYP2B, and possibly CYP3A, to form the trichloromethyl radical, CCl_3*[18-20]. The main CCl_4-metabolizing enzyme is CYP2E1 and it is expressed in $CAR^{+/+}$ and $CAR^{-/-}$ mice in the same way. Therefore, CCl_4 liver toxicity occurs despite an absence of CAR. Thus, CYP2B or CYP3A may only have supplementary roles in CCl_4 metabolism in the absence of PB. On the other hand, in the presence of CAR inducers, it results in the induction of CYP2B and CYP3A, and CCl_4 liver toxicity is severe, as seen in $CAR^{+/+}$ mice. Inducers of drug-metabolizing enzymes including PB have long been known to cause severe liver toxicity with CCl_4[18-20]. In this study, we showed that PB activated CYP2B10 and 3A11 via receptor CAR and that it caused the severe CCl_4 liver toxicity (Figure 6). Thus, the xenobiotic receptor CAR will have a mean with the presence of its agonist/antagonist. PB treatment resulted in enhanced CCl_4 liver toxicity in $CAR^{-/-}$ mice although to a lesser degree than that in $CAR^{+/+}$ mice. PB may impact on pathways distinct from CAR to cause CCl_4 liver toxicity. Indeed, cDNA microarray analysis of $CAR^{-/-}$ mice showed CAR-independent genes in response to PB treatment[17]. A total of 138 genes were detected to be either induced or repressed in response to PB treatment, of which about half were not under CAR regulation[17]. Enzymes such as amino levulinate synthase 1 and squalene epoxidase displayed CAR-independent induction by PB[17]. CYP4A10 and CYP4A14 represented the group of genes induced by PB only in $CAR^{-/-}$ mice, indicating that CAR may be a transcription blocker that prevents these genes from being induced by PB[17]. The enzymes having CCl_4-metabolizing activity may be included in these CAR-independent PB response genes.

CAR was also identified as a key regulator of acetaminophen metabolism and hepatotoxicity[27]. CAR regulates GSTPi, the enzyme that enhances glutathione depletion and so promotes acetaminophen toxicity[27-29]. In this study, CAR also induced GSTPi with PB treatment. The metabolites of CCl_4 such as CCl_3* and CCl_3OO* induce hepatotoxicity and expend glutathione and cause a decrease of hepatic glutathione level. In addition, induction of GSTPi expression may cause further depletion of glutathione and severe toxicity in CCl_4-treated mice.

Although CAR acted as a hepatotoxic regulator in this study, CAR could act as a protective manner in other situations[30,31]. PB is a well-established therapy for hyperbilirubinemia in Crigler-Najjar type II patients[30]. CAR has the ability to activate expression of known components of the bilirubin pathway including UGT1A1, OATP2, MRP2, and GSTA1[15]. It was also reported that paralysis by the muscle relaxant zoxazolamine was avoided by pretreatment with CAR activators but was prolonged in $CAR^{-/-}$ mice[21]. Thus, CAR coordinates the induction of metabolic activity and increases elimination of the drugs in a protective manner in some cases.

Transactivation of target genes by CAR can be blocked by the inverse agonist androstanol[32]. Androstanol is reported to not only prevent induction but also to decrease basal expression of CAR target genes including CYP3A11[25]. Androstanol reduced the liver toxicity of $CAR^{+/+}$ mice to the level of $CAR^{-/-}$ mice in this study. This effect of androstanol may result in decrease of the basal expression of CAR target genes including CYP3A11. Androstanol treatment was also reported to decrease the toxicity of acetaminophen[24].

The nuclear receptor CAR has only a small role in CCl_4 toxicity without its agonist/antagonist. However, because of its nature as a xenobiotic sensor, CAR exhibits its ability to the full in the presence of agonist/antagonist. Since some kinds of CAR inducers such as PB and phenytoin are used clinically, CAR may have an important clinical role in drug-induced liver injury or drug-drug interaction. Nuclear receptors regulating drug-metabolizing enzymes such as CAR are a two-edge blade in animals. In some cases, activation of CAR increases production of drug-metabolizing enzymes and increases toxicity. Thus, CAR inverse agonists such as androstanol may have potential for treatment of these kinds of drug-induced liver injury. On the other hand, activation of CAR by appropriate inducers acts in a hepato-protective manner in some cases such as bilirubin toxicity. Conversely, induction of CAR activity reduced the liver injury in these cases.

Thus, a nuclear receptor that regulates drug-metabolizing enzymes is a key factor in drug-induced liver injury. Regulation of CAR activity may be an important clinical strategy for treatment of drug-induced liver injury. Both CAR and nuclear receptor regulating drug-metabolizing enzymes such as pregnane X receptor and peroxisome proliferator activated receptors are thought to be associated with drug-induced liver injury. Activating or inverse agonists for nuclear receptors may provide a clinically useful means to treat drug-induced liver injury.

REFERENCES

1 **Sgro C**, Clinard F, Ouazir K, Chanay H, Allard C, Guilleminet C, Lenoir C, Lemoine A, Hillon P. Incidence of drug-induced hepatic injuries: a French population-based study. *Hepatology* 2002; **36**: 451-455

2 **Chitturi S**, Farrell GC. Drug-induced cholestasis. *Semin Gastrointest Dis* 2001; **12**: 113-124

3 **Ibanez L**, Perez E, Vidal X, Laporte JR. Grup d'Estudi Multicenteric d'Hepatotoxicitat Aguda de Barcelona (GEMHAB). Prospective surveillance of acute serious liver disease unrelated to infectious, obstructive, or metabolic diseases: epidemiological and clinical features, and exposure to drugs. *J Hepatol* 2002; **37**: 592-600

4 **Guengerich FP**, Liebler DC. Enzymatic activation of chemicals to toxic metabolites. *Crit Rev Toxicol* 1985; **14**: 259-307

5 **Guengerich FP**, Shimada T. Oxidation of toxic and carcinogenic chemicals by human cytochrome P-450 enzymes. *Chem Res Toxicol* 1991; **4**: 391-407

6 **Zhou S**, Gao Y, Jiang W, Huang M, Xu A, Paxton JW. Interactions of herbs with cytochrome P450. *Drug Metab Rev* 2003; **35**: 35-98

7 **Honkakoski P**, Moore R, Washburn K, Negishi M. Activation by diverse xenochemicals of the 51-base pair phenobarbital-responsive enhancer module in the CYP2B10 gene. *Mol Pharmacol* 1998; **53**: 597-601

8 **Honkakoski P**, Zelko I, Sueyoshi T, Negishi M. The nuclear orphan receptor CAR-retinoid X receptor heterodimer activates the phenobarbital-responsive enhancer module of the CYP2B gene. *Mol Cell Biol* 1998; **18**: 5652-5658

9 **Sueyoshi T**, Kawamoto T, Zelko I, Honkakoski P, Negishi M. The repressed nuclear receptor CAR responds to phenobarbital in activating the human CYP2B6 gene. *J Biol Chem* 1999; **274**: 6043-6046

10 **Sugatani J**, Kojima H, Ueda A, Kakizaki S, Yoshinari K, Gong QH, Owens IS, Negishi M, Sueyoshi T. The phenobarbital response enhancer module in the human bilirubin UDP-

glucuronosyltransferase UGT1A1 gene and regulation by the nuclear receptor CAR. *Hepatology* 2001; **33**: 1232-1238

11 **Xie W**, Yeuh MF, Radominska-Pandya A, Saini SP, Negishi Y, Bottroff BS, Cabrera GY, Tukey RH, Evans RM. Control of steroid, heme, and carcinogen metabolism by nuclear pregnane X receptor and constitutive androstane receptor. *Proc Natl Acad Sci USA* 2003; **100**: 4150-4155

12 **Kast HR**, Goodwin B, Tarr PT, Jones SA, Anisfeld AM, Stoltz CM, Tontonoz P, Kliewer S, Willson TM, Edwards PA. Regulation of multidrug resistance-associated protein 2 (ABCC2) by the nuclear receptors pregnane X receptor, farnesoid X-activated receptor, and constitutive androstane receptor. *J Biol Chem* 2002; **277**: 2908-2915

13 **Cherrington NJ**, Hartley DP, Li N, Johnson DR, Klaassen CD. Organ distribution of multidrug resistance proteins 1, 2, and 3 (Mrp1, 2, and 3) mRNA and hepatic induction of Mrp3 by constitutive androstane receptor activators in rats. *J Pharmacol Exp Ther* 2002; **300**: 97-104

14 **Saini SP**, Sonoda J, Xu L, Toma D, Uppal H, Mu Y, Ren S, Moore DD, Evans RM, Xie W. A novel constitutive androstane receptor-mediated and CYP3A-independent pathway of bile acid detoxification. *Mol Pharmacol* 2004; **65**: 292-300

15 **Huang W**, Zhang J, Chua SS, Qatanani M, Han Y, Granata R, Moore DD. Induction of bilirubin clearance by the constitutive androstane receptor (CAR). *Proc Natl Acad Sci USA* 2003; **100**: 4156-4161

16 **Huang W**, Zhang J, Moore DD. A traditional herbal medicine enhances bilirubin clearance by activating the nuclear receptor CAR. *J Clin Invest* 2004; **113**: 137-143

17 **Ueda A**, Hamadeh HK, Webb HK, Yamamoto Y, Sueyoshi T, Afshari CA, Lehmann JM, Negishi M. Diverse roles of the nuclear orphan receptor CAR in regulating hepatic genes in response to phenobarbital. *Mol Pharmacol* 2002; **61**: 1-6

18 **Weber LW**, Boll M, Stampfl A. Hepatotoxicity and mechanism of action of haloalkanes: carbon tetrachloride as a toxicological model. *Crit Rev Toxicol* 2003; **33**: 105-136

19 **Jones IW**. Chloroform anaesthesia in Liverpool. *Anaesthesia* 1983; **38**: 578-580

20 **Clawson GA**. Mechanisms of carbon tetrachloride hepatotoxicity. *Pathol Immunopathol Res* 1989; **8**: 104-112

21 **Wei P**, Zhang J, Egan-Hafley M, Liang S, Moore DD. The nuclear receptor CAR mediates specific xenobiotic induction of drug metabolism. *Nature* 2000; **407**: 920-923

22 **Wang H**, LeCluyse EL. Role of orphan nuclear receptors in the regulation of drug-metabolising enzymes. *Clin Pharmacokinet* 2003; **42**: 1331-1357

23 **Moore LB**, Parks DJ, Jones SA, Bledsoe RK, Consler TG, Stimmel JB, Goodwin B, Liddle C, Blanchard SG, Willson TM, Collins JL, Kliewer SA. Orphan nuclear receptors constitutive androstane receptor and pregnane X receptor share xenobiotic and steroid ligands. *J Biol Chem* 2000; **275**: 15122-15127

24 **Yamamoto Y**, Moore R, Goldsworthy TL, Negishi M, Maronpot RR. The orphan nuclear receptor CAR is essential for liver tumor promotion by phenobarbital in mice. *Cancer Res* 2004; **64**: 7197-7200

25 **Wei P**, Zhang J, Dowhan DH, Han Y, Moore DD. Specific and overlapping functions of the nuclear hormone receptors CAR and PXR in xenobiotic response. *Pharmacogenomics J* 2002; **2**: 117-126

26 **Tzameli I**, Chua SS, Cheskis B, Moore DD. Complex effects of rexinoids on ligand dependent activation or inhibition of the xenobiotic receptor, CAR. *Nucl Recept* 2003; **1**: 2

27 **Zhang J**, Huang W, Chua SS, Wei P, Moore DD. Modulation of acetaminophen-induced hepatotoxicity by the xenobiotic receptor CAR. *Science* 2002; **298**: 422-424

28 **Morel F**, Fardel O, Meyer DJ, Langouet S, Gilmore KS, Meunier B, Tu CP, Kensler TW, Ketterer B, Guillouzo A. Preferential increase of glutathione S-transferase class alpha transcripts in cultured human hepatocytes by phenobarbital, 3-methylcholanthrene, and dithiolethiones. *Cancer Res* 1993; **53**: 231-234

29 **Hayes JD**, Pulford DJ. The glutathione S-transferase supergene family: regulation of GST and the contribution of the isoenzymes to cancer chemoprotection and drug resistance. *Crit Rev Biochem Mol Biol* 1995; **30**: 445-600

30 **Berk PD**, Martin JF, Blaschke TF, Scharschmidt BF, Plotz PH. Unconjugated hyperbilirubinemia. Physiologic evaluation and experimental approaches to therapy. *Ann Intern Med* 1975; **82**: 552-570

31 **Guo GL**, Lambert G, Negishi M, Ward JM, Brewer HB Jr, Kliewer SA, Gonzalez FJ, Sinal CJ. Complementary roles of farnesoid X receptor, pregnane X receptor, and constitutive androstane receptor in protection against bile acid toxicity. *J Biol Chem* 2003; **278**: 45062-45071

32 **Forman BM**, Tzameli I, Choi HS, Chen J, Simha D, Seol W, Evans RM, Moore DD. Androstane metabolites bind to and deactivate the nuclear receptor CAR-beta. *Nature* 1998; **395**: 612-615

Science Editor Guo SY **Language Editor** Elsevier HK

PO Box 2345, Beijing 100023, China
www.wjgnet.com
wjg@wjgnet.com

ELSEVIER

World J Gastroenterol 2005;11(38):5973-5977
World Journal of Gastroenterology ISSN 1007-9327

• *BASIC RESEARCH* •

Damaging effects of gliadin on three-dimensional cell culture model

Ersilia Dolfini, Luca Elli, Leda Roncoroni, Barbara Costa, Maria Pia Colleoni, Vito Lorusso, Simona Ramponi, Paola Braidotti, Stefano Ferrero, Maria Letizia Falini, Maria Teresa Bardella

Ersilia Dolfini, Leda Roncoroni, Department of Biology and Genetics for Health Sciences, University of Milan, Milan, Italy
Luca Elli, Maria Teresa Bardella, Department of Gastroenterology, University of Milan, Ospedale Maggiore Policlinico, Mangiagalli e Regina Elena IRCCS, Milan, Italy
Barbara Costa, Department of Biotechnology and Bioscience, University of Milan-Bicocca, Milan, Italy
Maria Pia Colleoni, Department of Pharmacology, Chemotherapy and Toxicology, University of Milan, Milan, Italy
Vito Lorusso, Simona Ramponi, Bracco Imaging SpA, Milan Research Centre, Milan, Italy
Paola Braidotti, Stefano Ferrero, Department of Medicine, Surgery and Dentistry, S. Paolo Hospital and Ospedale Maggiore Policlinico, Mangiagalli e Regina Elena IRCCS, Milan, Italy
Maria Letizia Falini, Department of Agrifood Molecular Science, University of Milan, Milan, Italy
Supported by the San Paolo Foundation grant to "Centro per lo Studio della Celiachia"
Correspondence to: Maria Teresa Bardella, MD, Department of Gastroenterology, Ospedale Maggiore Policlinico, Mangiagalli e Regina Elena IRCCS, Via F. Sforza 35, Milan 20122, Italy. mariateresa.bardella@unimi.it
Telephone: +39-2-55033384 Fax: +39-2-50320403
Received: 2004-11-18 Accepted: 2005-01-26

Abstract

AIM: To evaluate the effects of gliadin on the oxidative environment in the "*in vivo*-like" model of a three-dimensional cell culture system.

METHODS: LoVo cell line (intestinal adenocarcinoma) multicellular spheroids were treated with digested gliadin (with albumin used as a control). Spheroid volumes, cell viability and morphology, lactate dehydrogenase (LDH) release, content of reduced glutathione (GSH) and activity of GSH-related enzymes were examined. The data were statistically analyzed using the Student's *t*-test ($P<0.05$). was considered statistically significant.

RESULTS: Gliadin reduced cell viability (from 20% to 60%) and led to morphological alterations characterized by apoptotic findings and cytoskeletal injuries. LDH activity increased. The content of GSH reduced (-20% *vs* controls), and activity of GSH-related enzymes was significantly inhibited.

CONCLUSION: Gliadin treatment induces an imbalance in the antioxidative mechanism of cells cultured by the three-dimensional technique. This alteration may explain the cell damage directly caused by gliadin and the subsequent morphological abnormalities.

Key words: Gliadin; Celiac disease; Cytotoxicity; Multicellular spheroids

Dolfini E, Elli L, Roncoroni L, Costa B, Colleoni MP, Lorusso V, Ramponi S, Braidotti P, Ferrero S, Falini ML, Bardella MT. Damaging effects of gliadin on three-dimensional cell culture model. *World J Gastroenterol* 2005; 11(38): 5973-5977
http://www.wjgnet.com/1007-9327/11/5973.asp

INTRODUCTION

Since Hudson *et al*.[1], first observed the inhibited growth and morphological modifications in different human cell lines induced by gliadin exposure, a number of *in vitro* studies have confirmed the cytotoxicity of the peptide. Gliadin has agglutinating activity on K562 cells (human chronic myeloid leukemia), reduces F-actin content in intestine 407 cells, inhibits cell growth, induces apoptosis and alters redox equilibrium in Caco-2 cells (human intestinal adenocarcinoma), and causes a rearrangement of the cytoskeleton through the zonulin pathway and the loss of tight junction permeability in IEC-6 cells[2].

Three-dimensional cell cultures (multicellular tumor spheroids, MCTSs) were first introduced by Sutherland *et al*.[3], in the early 1970s, and are now considered as an interesting model in biomedical research[4]. Unlike conventional monolayer cell culture systems, MCTSs maintain the specific morphological and biochemical properties of the corresponding *in vivo* tissue, and remain in a differentiated and functionally active state for many weeks, thus making it possible to study the long-term effects of various xenobiotics[5]. We have recently used MCTSs from the LoVo cell line to test gliadin, and have shown that it has a direct cytotoxic effect on cell growth and morphology[6].

Redox equilibrium plays a pivotal role in cell homeostasis, and can affect biological functions[7,8]. Glutathione (GSH), which consists of L-glutamine, L-cysteine and glycine, is the most important low-molecular-weight peptide involved in redox equilibrium. It has a reductive action on the cell environment and neutralizes the reactive oxygen compounds and free radicals formed during metabolism. GSH depletion induces low thiol protein stores, a determinant of cell homeostasis, and triggers cytotoxicity[9,10]. GSH depletion has also been shown in a number of human diseases

(alcoholic liver disease, HIV infection, acute respiratory distress syndrome, and inflammatory bowel disease), and it has been shown that depressed intracellular GSH levels in liver and mammary tissues promote carcinogenesis[11].

The aim of this study was to evaluate the content of reduced GSH and the activity of GSH-related enzymes in LoVo MCTSs treated with gliadin.

[illegible]

Protein digestion

Gliadin was purified from *Triticum aestivum* flour (Hereward cultivar) according to Capelli *et al*.[12]. Bovine serum albumin (BSA) used as a control was purchased from Sigma (Milan, Italy). Pepsin was supplied by Sigma (Milan, Italy) and pancreatin by Merck (Milan, Italy). All the chemicals were of analytical grade. Digestion was performed as previously described[6]: briefly, gliadin was first incubated with pepsin at 37 ℃ for 24 h, and then with pancreatin at 37 ℃ for 3 h, adjusting to pH 8.0.

The digested proteins were analytically controlled by reverse-phase HPLC, size-exclusion HPLC and SDS-PAGE before being freeze-dried and stored.

Cell culture, treatment, volumetric analysis and viability test

LoVo human colon adenocarcinoma cell line (ATCC, Rockville, USA) was maintained in exponential monolayer growth and routinely checked for mycoplasma contamination as previously described[6].

MCTSs were initiated according to Dolfini *et al*.[6], by seeding 2×10^5 cells/mL in 25 mL of complete medium in polycarbonate Erlenmeyer flasks (Corning, Milan, Italy), and incubated in a gyratory rotation incubator. MCTS volumes were evaluated according to Chignola *et al*.[13].

On the 7th d, MCTSs (mean±SD: 220±70 μm) were exposed to digested gliadin (PT-gliadin, 500 μg/mL) or BSA (PT-BSA, 500 μg/mL) in completely renewed medium for further 5 d, and subsequently taken for the evaluation of lactate dehydrogenase (LDH) release, GSH content and GSH-related enzyme activity, and morphological analysis.

MCTS viability was tested (colony-forming assay) by plating a cell suspension obtained after trypsin disaggregation of MCTSs (on the 5th d of treatment at PT-gliadin concentrations of 125, 500, 750, and 1 000 μg/mL, and a PT-BSA concentration of 1 000 μg/mL) in triplicate in six-well plates (500 cells/well). The surviving cell fraction was calculated after 10 d and compared with the plating efficiency of the controls.

Lactate dehydrogenase activity

LDH released from damaged cells was measured in free aliquots of medium from the cell cultures, and cell-free complete medium was included as a negative control.

Briefly, 50 μL of the aliquots of cell supernatants was mixed with 25 μL of LDH reagent (Sigma, Milan, Italy) and incubated at room temperature for 30 min. LDH activity was calculated by measuring the increase in absorbance at 490 nm according to Legrand *et al*.[14], and related to the protein content of MTCSs[15]. LDH activity was reported as percentages of control values.

GSH content and GSH-related enzyme activity

MTCSs were washed with PBS (Sigma, Milan, Italy), and then sonicated and centrifuged. The cytosolic supernatant was used to measure GSH content and activity of the GSH-related enzymes, namely reductase (GSR), peroxidase (GPOX) and GSH-*S*-transferase (GST).

GSH content and enzyme activity were analyzed according to previously described methods[16], and expressed as percentages of control values.

Light and electron microscopy

LoVo cell line MCTS samples were prepared as previously described[6], fixed in 2.5% glutaraldehyde in a phosphate buffer, and then washed in the same buffer. In order to avoid injury or loss of spheroids, they were encapsulated in a solidifying agar solution and small spheroid-containing cubes were routinely processed for transmission electron microscopy (TEM)[17]. The semi-thin (0.5 μm) sections used for light microscopy analysis were stained with toluidine blue, the ultra-thin sections (50-70 nm) used for the ultrastructural study were counterstained with uranyl acetate and lead citrate. The MCTSs were studied for the presence of microvilli and intercellular junctions, and the appearance of nuclei, cytoplasm and intracytoplasmic organelles.

Scanning electron microscopy (SEM) was performed using a Philips mod. XL20 scanning electron microscope. MCTSs were washed twice with PBS, and then fixed in 2.5% glutaraldehyde in a phosphate buffer at 4 ℃ for a minimum of 24 h. At the time of analysis, a representative spheroid sample was recovered, immediately placed on a filter paper, and observed in low vacuum modality at a high voltage of 10 kV.

Statistical analysis

Each experiment was repeated four times. All the data were expressed as mean±SD and analyzed using the two-tailed Student's *t*-test. $P<0.05$ was considered statistically significant.

[illegible]

Volume, viability, and LDH activity in medium

The untreated and control MCTSs (treated with PT-BSA) did not show any statistical difference in terms of diameter ($27\pm7\times10^{-3}$ mm^3 *vs* $26\pm10\times10^{-3}$ mm^3), viability (98% of the colonies formed by untreated MCTSs), LDH release (102% of the activity of untreated MCTSs), or microscopic appearance (data not shown). The volumes of MCTSs treated with PT-gliadin were similar to those of the untreated or control MCTSs (Figure 1), but their viability was 20-50% less than that of the controls and inversely related to PT-gliadin concentrations (Figure 2A). LDH activity in the medium of treated MCTSs was significantly increased by about 30% (Figure 2B).

GSH content and GSH-related enzyme activity

As shown in Figure 3A, the GSH content of treated MCTSs was about 20% less than that observed in the controls ($P<0.05$). The activity of GSH-related enzymes (GSR, GST, and GPOX) was also significantly decreased (by respectively 56%, 34%, and 27%, Figure 3B).

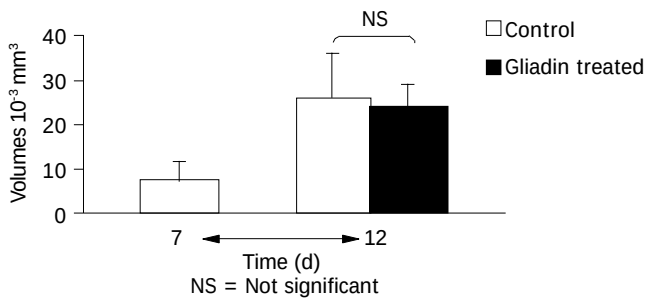

Figure 1 Volumes of MCTSs treated with PT-gliadin.

Morphological analysis

At light microscopy, both the treated and control MCTSs were spherical or oval in shape, but the control cells grew in a solid manner (with pseudoglandular differentiation, and without necrosis or apoptosis), whereas those in PT-gliadin-treated MCTSs showed nucleic displacement, a foamy cytoplasm and loss of cell adhesion: 20-50% had pycnotic nuclei and condensed chromatin (Figures 4A and B).

TEM showed that the control MCTSs had microvilli on their external surface and normal nuclei, cytoplasmatic organelles (rough endoplasmic reticulum, mitochondria,

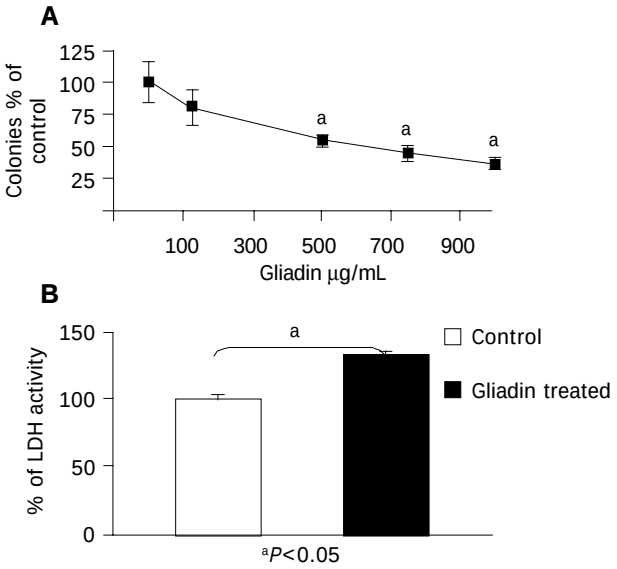

Figure 2 Viability test of MCTSs after treatment with different doses of digested gliadin (A) and lactate dehydrogenase (LDH) activity after gliadin treatment (B).

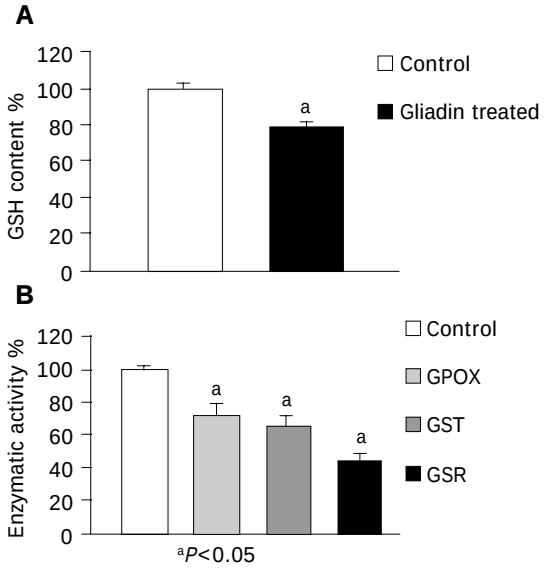

Figure 3 Content of reduced GSH (A) and GSH-related enzyme activity (B) in MCTSs treated with PT-gliadin.

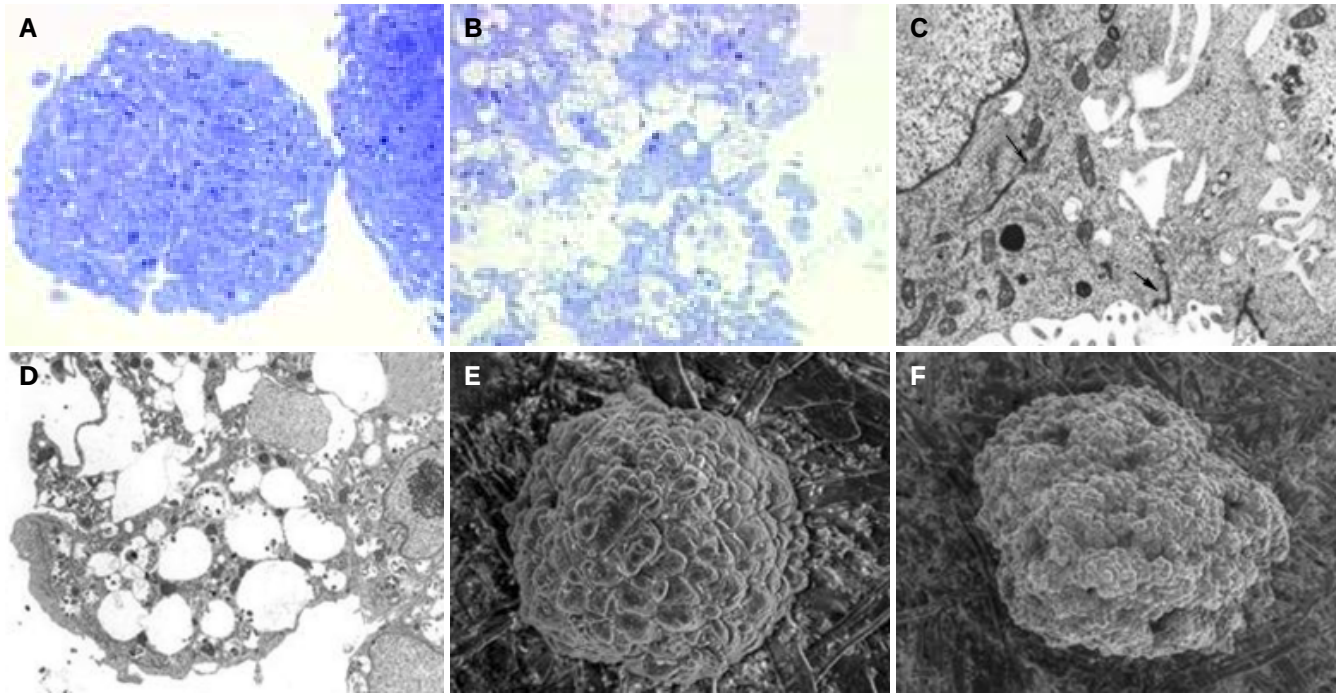

Figure 4 Microscopic analysis of MCTSs treated with digested gliadin or untreated. (A and B) Untreated and gliadin-treated MCTSs with cytoplasmatic vacuoles, (C and D) images of untreated and treated MCTSs, and (E) no holes and blebs on untreated controls, (F) holes and blebs on the surface of treated MCTSs.

Golgi complex, and lysosomes), and cytokeratin tonofilaments. The cells were joined by complexes of tight, intermediate and desmosome junctions. In the treated MCTSs, microvilli disappeared from the cell surface and there were cytoskeletal and tight junction injuries. The cytoplasm contained electron-dense material in numerous phagosomes and frequent vacuoles of various sizes. Some cells showed cytoplasmatic lipid-like droplets and cannibalism (Figures 4C and D).

SEM of the control MCTSs revealed an ovoid or spherical shape with compact cells, which were densely organized and tightly packed together, but clearly distinguishable from each other. The treated MCTSs were irregular in shape with loosely packed cells, and the external surface was focally interrupted by irregularly distributed holes and blebs (Figures 4E, F, and 5).

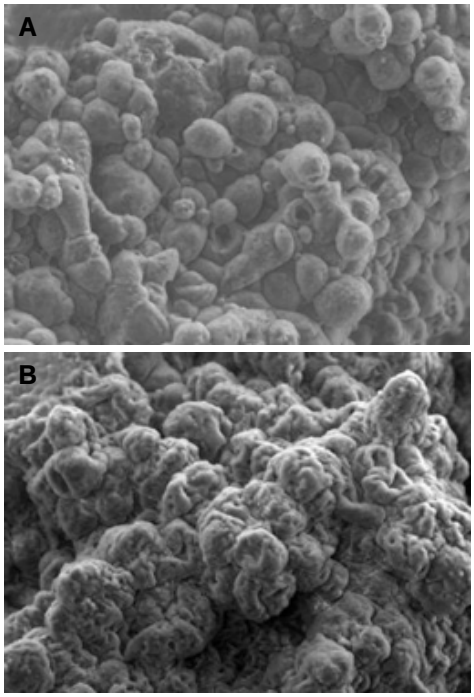

Figure 5 Smooth surface of untreated MCTS (A) and bleb on surface of MCTS treated with digested gliadin (B).

DISCUSSION

Our findings show that gliadin had significant functional and morphological cytotoxic effects on intestinal adenocarcinoma cell line (LoVo) cultured in a three-dimensional model.

Gliadin is a protein characterized by a particularly high proline and glutamine content (respectively 15% and 35% of the residues) that forms a kink in the polypeptide structure that prevents peptidase attack[18].

Over the last few years, a number of studies based on the *in vitro* two-dimensional cell culture system have investigated the cellular effects of gliadin in order to clarify its role in the pathogenetic "puzzle" of celiac disease (CD)[19]. Gliadin alters the cytoskeleton through the network of actin filaments, and damages tight junctions (TJ) by creating leaks in intercellular spaces, and these effects may be responsible for the loss of epithelial permeability and the changes in cell-cell signaling associated with CD[20]. Furthermore, gliadin also has a pro-apoptotic and agglutinating effect, inhibits cell growth and viability[2], and modifies the redox status of Caco-2 cells, thus causing a loss in reductive potential and an increase in the levels of reactive oxygen species[21].

Oxidative balance plays a pivotal role in cell homeostasis, and it has been suggested that its imbalance may be involved in various human diseases (liver diseases, HIV infection, pulmonary diseases, tumors, Parkinson's disease, myocardial ischemia, and inflammatory bowel disease)[9,11]. GSH and its enzymatic machinery represent one of the most important cellular defenses against oxidative agents and harmful xenobiotics. Three enzymes are mainly involved in the GSH cycle: GPOX, which converts peroxides into less dangerous fatty acids, water, and GSH disulfide (GSSG); GSR, which reduces GSSG to GSH in NADPH-dependent reaction; and GST, which is involved in detoxification from xenobiotic compounds[22]. GSH has also been implicated in other cell functions: apoptosis, cell differentiation, prostaglandin synthesis, DNA repair, amino acid transport, enhanced immune response, and enzymatic activation[23].

The reduced GSH content and GSH-related enzyme activity observed in our gliadin-treated MCTSs confirm the dangerous effect of this peptide in an experimental model that maintains some of the biochemical and morphological features of the corresponding *in vivo* tissue[5], and support the hypothesis that relates a deficiency in an oxidable substrate[24]. The disturbed redox equilibrium is associated with the reduced cell viability in treated MCTSs and the alteration in the integrity of plasma membrane, as demonstrated by the leakage of large molecules such as LDH into the medium[25].

These functional alterations affect the morphology of MCTSs and their cells, whose clearly foamy cytoplasm and peripherally displaced nuclei, together with the fact that many are pycnotic with marginally condensed chromatin, support the presence of apoptotic processes[26]. TEM confirmed cell injury by revealing the presence of numerous phagosomes and frequent vacuoles of different sizes in the cytoplasm, as well as intra-cytoplasmic lipid-like droplets. The external ring normally consisting of columnar cells with serrated intercellular TJs and surface microvilli resembling normal enterocyte epithelia was altered in our treated MCTSs, which showed disrupted TJs and microvilli (Figure 4). SEM also showed that the treatment causes a loss of organization in cells contained in the external layer of spheroid, with the formation of hole-like structures and an abundant presence of apoptotic blebs[27].

Although our data cannot explain whether the redox imbalance is due to a resource-consuming mechanism, decreased nuclear expression or protein synthesis (an effect previously associated with gliadin exposure[28]), they clearly demonstrate that gliadin has a direct damaging effect on human intestinal cells. Furthermore, we have confirmed that the three-dimensional cell culture system is a good experimental model for investigating the effects of different peptides, and can therefore be added to the techniques used to study CD.

ACKNOWLEDGMENTS

The authors would like to thank the "Centro per lo Studio

della Celiachia", University of Milan, for its logistic support and Kevin Smart (LINK Srl, Milan) for his help in preparing the manuscript.

References

1 **Hudson DA,** Purdham DR, Cornell HJ, Rolles CJ. Non specific cytotoxicity of wheat gliadin components towards cultured human cells. *Lancet* 1976; **1**: 339-341

2 **Elli L,** Dolfini E, Bardella MT. Gliadin cytotoxicity and *in vitro* cell cultures. *Toxicol Lett* 2003; **146**: 1-8

3 **Sutherland RM,** Inch WR, McCreide JA, Kruuv J. A multicomponent radiation survival curve using an *in vitro* tumor model. *Int J Radiat Biol Relat Stud Phys Chem Med* 1970; **18**: 491-495

4 **Kunz-Schughart LA,** Kreutz M, Knuechel R. Multicellular spheroids: a three-dimensional *in vitro* culture system to study tumor biology. *Int J Exp Pathol* 1998; **79**: 1-23

5 **Kunz-Schughart LA.** Multicellular tumor spheroids: intermediates between monolayer culture and *in vivo* tumor. *Cell Biol Int* 1999; **23**: 157-161

6 **Dolfini E,** Elli L, Ferrero S, Braidotti P, Roncoroni L, Dasdia T, Falini ML, Forlani F, Bardella MT. Bread wheat gliadin cytotoxicity: a new three-dimensional cell model. *Scand J Clin Lab Inv* 2003; **63**: 135-142

7 **Burdon RH.** Superoxide and hydrogen peroxide in relation to mammalian cell proliferation. *Free Rad Biol Med* 1995; **18**: 775-794

8 **Halliwell B.** Free radicals, antioxidants, and human disease: curiosity, cause or consequence? *Lancet* 1994; **344**: 721-724

9 **Burg D,** Mulder G. Glutathione conjugates and their synthetic derivatives as inhibitors of glutathione dependent enzymes involved in cancer and drug resistance. *Drug Met Rev* 2002; **34**: 821-863

10 **Ketterer B.** Protective role of glutathione and glutathione transferases in mutagenesis and carcinogenesis. *Mutation Res* 1988; **202**: 343-361

11 **Lomaestro BM,** Malone M. Glutathione in health and disease: pharmacotherapeutic issue. *Ann Pharmacol* 1995; **29**: 1263-1272

12 **Capelli L,** Forlani F, Perini F, Guerrieri N, Cerletti P, Righetti PG. Wheat cultivar discrimination by capillary electrophoresis of gliadins in isoelectric buffer. *Electrophoresis* 1998; **19**: 1-8

13 **Chignola R,** Schenetti A, Chiesa E, Forini R, Sartoris S, Brendolan A, Tridente G, Andrighetto G, Liberati D. Oscillating growth patterns of multicellular tumor spheroids. *Cell Prolif* 1999; **32**: 39-48

14 **Legrand C,** Bour JM, Jacob C, Capiaumont J, Martial A, Marc A, Wudtke M, Kretzmer G, Demangel C, Duval D. Lactate dehydrogenase (LDH) activity of the cultured eukaryotic cells as marker of the number of dead cells in the medium. *J Biotechnol* 1992; **25**: 231-243

15 **Lowry OH,** Rosebrough NJ, Farr AL, Randall RJ. Protein measurement with the folin phenol reagent. *J Biol Chem* 1951; **193**: 265-275

16 **Dolfini E,** Elli L, Dasdia T, Bufardeci B, Colleoni MP, Costa B, Floriani I, Falini ML, Guerrieri N, Forlani F, Bardella MT. *In vitro* cytotoxic effect of bread wheat gliadin on Lovo human adenocarcinoma cell line. *Toxicol In vitro* 2002; **16**: 331-337

17 **Ryter A,** Kellemberg E. Encapsulating methods for isolated cells. In: Glauter AM, ed. Fixation, dehydration and embedding of biological specimens, 3rd ed. *Oxford: North Holland Publishing Company* 1998: 95

18 **Dewar D,** Pereira SP, Ciclitira P. The pathogenesis of coeliac disease. *Int J Biochem Cell Biol* 2004; **36**: 17-24

19 **Elli L,** Dolfini E, Bardella MT. Direct gliadin cytotoxicity as a cofactor in the pathogenesis of celiac disease. *Int Arch All Immunol* 2004; **134**: 88

20 **Clemente MG,** De Virgiliis S, Kang JS, Macatagney R, Musu MP, Di Pierro MR, Drago S, Congia M, Fasano A. Early effects of gliadin on enterocyte intracellular signalling involved in intestinal barrier function. *Gut* 2003; **52**: 218-223

21 **Rivabene R,** Mancini E, De Vincenzi M. *In vitro* cytotoxic effect of wheat gliadin-derived peptides on Caco 2 intestinal cell line is associated with intracellular oxidative imbalance: implications for coeliac disease. *Biochim Biophys Acta* 1999; **1453**: 152-160

22 **Sies H.** Strategies of antioxidative defence. *Eur J Biochem* 1993; **215**: 213-219

23 **Peterson JD,** Herzenberg LA, Vasquez K, Waltenbaugh C. Glutathione levels in antigen-presenting cells modulate Th1 versus Th2 response patterns. *Proc Natl Acad Sci USA* 1998; **95**: 3071-3076

24 **Toborek M,** Hennig B. Fatty acid-mediated effects on the glutathione redox cycle in cultured endothelial cells. *Am J Clin Nutr* 1994; **59**: 60-65

25 **Gissel H,** Clausen T. Excitation-induced Ca^{2+} influx and skeletal muscle cell damage. *Acta Physiol Scand* 2001; **171**: 327-334

26 **Ashkenazi A,** Dixit VM. Death receptors: signaling and modulation. *Science* 1998; **281**: 1305-1308

27 **Hentze H,** Latta M, Kunstle G, Dhakshinamoorthy S, Yomg P, Porter AG, Wendel A. Topoisomerase inhibitor camptothecin sensitizes mouse hepatocytes *in vitro* and *in vivo* to TNF-mediated apoptosis. *Hepatology* 2004; **39**: 1311-1320

28 **Giovannini C,** Mancini E, De Vincenzi M. Inhibition of the cellular metabolism of Caco-2 cells by prolamin peptides from cereals toxic for coeliacs. *Toxicol In vitro* 1996; **10**: 533-538

Science Editor Wang XL and Guo SY **Language Editor** Elsevier HK

PO Box 2345, Beijing 100023, China
www.wjgnet.com
wjg@wjgnet.com

ELSEVIER

World J Gastroenterol 2005;11(38):5978-5983
World Journal of Gastroenterology ISSN 1007-9327

• *BASIC RESEARCH* •

Insulin promotes sinusoidal endothelial cell proliferation mediated by upregulation of vascular endothelial growth factor in regenerating rat liver after partial hepatectomy

Jian-Guo Qiao, Long Wu, Dao-Xiong Lei, Lu Wang

Jian-Guo Qiao, Long Wu, Dao-Xiong Lei, Lu Wang, Department of General Surgery, Zhongnan Hospital Affiliated to Wuhan University, Wuhan 430071, Hubei Province, China
Co-first-authors: Jian-Guo Qiao and Long Wu
Correspondence to: Jian-Guo Qiao, Department of General Surgery, Zhongnan Hospital Affiliated to Wuhan University, Wuhan 430071, Hubei Province, China. jian_guoqiao@yahoo.com
Telephone: +86-27-67812959 Fax: +86-27-87307622
Received: 2004-12-28 Accepted: 2005-03-24

Abstract

AIM: To determine whether insulin could promote sinusoidal endothelial cell (SEC) proliferation mediated by upregulation of vascular endothelial growth factor (VEGF) in regenerating rat liver after partial hepatectomy (PHx).

METHODS: Adult male Sprague-Dawley rats undergoing 70% PHx were injected with insulin (300 MU/kg) or saline via the tail veins every 8 h after surgery for 7 d and killed at 0, 24, 48, 72, 96, 120, 144, and 168 h after surgery. Proliferation of both hepatocytes and SECs was monitored by evaluating the proliferating cell nuclear antigen (PCNA) labeling index (LI). The expression of VEGF protein was evaluated by immunohistochemistry. The mRNA expressions of VEGF and its receptors Flt-1 and Flk-1 were evaluated by semi-quantitative reverse transcription-PCR.

RESULTS: Insulin markedly increased the expression of VEGF mRNA between 24 and 120 h after hepatectomy compared to controls. Similarly, insulin significantly increased the expression of Flt-1 between 24 and 96 h. However, insulin had no significant effect on Flk-1. Furthermore, the immunohistochemical staining revealed that expression of VEGF protein increased in the insulin groups. Insulin significantly increased the PCNA LI of hepatocytes and SECs compared to controls.

CONCLUSION: Exogenous insulin may promote SEC proliferation with an enhanced expression of VEGF and its receptor Flt-1 in regenerating rat liver after PHx.

Key words: Insulin; Sinusoidal endothelial cell; VEGF

Qiao JG, Wu L, Lei DX, Wang L. Insulin promotes sinusoidal endothelial cell proliferation mediated by upregulation of vascular endothelial growth factor in regenerating rat liver after partial hepatectomy. *World J Gastroenterol* 2005; 11 (38): 5978-5983
http://www.wjgnet.com/1007-9327/11/5978.asp

INTRODUCTION

Hepatic regeneration is a key step in the recovery process that occurs after various forms of liver injury, including partial hepatectomy (PHx)[1]. The exact mechanism of liver regeneration remains unclear. Several important cytokines and growth factors are involved in the regulation of hepatocyte proliferation[2-6]. Angiogenesis is a fundamental course required for wound healing and regeneration[5]. The liver microvasculature consists of large vessels such as portal and central venules and hepatic arterioles lined with continuous endothelial cells, and sinusoids lined with sinusoidal endothelial cells (SECs) expressing undiaphragmed fenestrations[6]. SECs are the second largest number of resident liver cells, and are vital in supplying nutrients and growth factors to proliferating hepatocytes by the formation of new blood vessels during liver regeneration[5]. Vascular endothelial growth factor (VEGF) is a potent angiogenic factor stimulating the proliferation and migration of endothelial cells, and is also known as a vascular permeability factor[7-9]. The effects of VEGF are mediated through at least two specific receptors, Flt-1 and Flk-1, expressed on the endothelial cell surface[7]. Recent studies have revealed that VEGF stimulates endothelial cell proliferation and plays an important role in the supply of blood to the newly replicating hepatocytes during regeneration[5,7]. Moreover, it is reported that exogenous VEGF can stimulate liver cell proliferation following PHx[5,7,10].

Insulin is a hepatocyte growth modulator, which is essential in liver regeneration, and is transported into the liver during the process of liver regeneration[11]. There is evidence that treatment with insulin contributes to the normal regeneration of liver by decreasing hepatocellular injury and by increasing hepatocyte proliferative capacity[11-13]. In addition, insulin therapy has also been shown epidemiologically as an independent risk factor for the progression of intraocular neovascularization in diabetic retinopathy[13,14]. Yamagishi *et al*.[13], have demonstrated that insulin stimulates the growth and tube formation of human microvascular endothelial cells through autocrine VEGF *in vitro*. Nevertheless the effect of insulin on blood vessels during regeneration after PHx in rats is still unknown.

Based on these studies, we believe that insulin promotes SECs and subsequently liver regeneration by accelerating the expression of VEGF. In the present study, we investigated the expression of VEGF and its receptors, Flt-1 and Flk-1, as well as the expression of proliferating cell nuclear antigen (PCNA) during rat liver regeneration after 70% PHx.

[illegible]

Animals

Adult male Sprague-Dawley rats aged 7-8 wk (180-200 g; from the Center of Animal Laboratory, Wuhan University) were used for all experiments. The rats were maintained in temperature-controlled rooms in a 12-h light/dark cycle with free access to food (standard laboratory chow) and water. Seventy percent PHx was performed by the standard two-thirds PHx under light anesthesia with ether. The animals were randomly divided into two groups: PHx group was injected with insulin (300 MU/kg) in saline via the tail vein of rats every 8 h after PHx for a week, while control group was given saline alone. Five rats in each group were used at each of the eight time points (0, 24, 48, 72, 96, 120, 144, and 168 h after surgery, with a total of 80 animals). All surgeries were performed between 08:30 and 11:30 a.m..

Immunohistochemical examination of VEGF

Anti-VEGF antibody (Santa Cruz Biotechnology Inc., Delaware, CA, USA) was used for the immunohistochemical staining of VEGF on formalin-fixed and paraffin-embedded liver tissue. Briefly, liver tissues excised at designated times after surgery were fixed in 40 g/L formaldehyde solution and embedded in paraffin wax. Sections were cut at 4 μm, mounted on poly-L-lysine-coated glass slides, air dried overnight at room temperature, dehydrated in graded alcohols, and cleared in xylene. The three-step immunoperoxidase method using a LSAB kit (Dako, Copenhagen, Denmark) was performed according to the manufacturer's instructions. Anti-VEGF antibody used was diluted at 1:100 and incubated overnight at 4 ℃.

PCNA labeling index

Immunohistochemical staining of the PCNA was performed using an indirect two-step labeling technique with peroxidase-conjugated IgG (Amersham NA 931, Amersham Life Science, NY, USA). The monoclonal anti-PCNA antibodies were purchased from Amersham Life Science (PC-10). The sections were deparaffinized in xylene and dehydrated by passage through graded alcohol. Endogenous peroxidase was blocked by incubation of the slides with 3% H_2O_2 in methanol for 30 min. After being washed in PBS, 10% normal goat serum (Amersham Life Science) in PBS was applied for 20 min at room temperature. Slides were incubated overnight with monoclonal anti-PCNA antibodies and subsequently exposed to prediluted peroxidase-conjugated IgG for 40 min at room temperature. The peroxidase reaction was developed by incubation in 0.005% H_2O_2 and 0.02% 3,3'-diaminobenzidine tetrachloride. The proliferative activity in the remnant liver was expressed as the labeling index (LI). The LI was the ratio of the number of PCNA positive nuclei of either hepatocytes or SECs to the total number of cells counted. In each liver, the hepatocytes and SECs in 200 consecutive high power fields were counted. In this study, the spindle-shaped sinusoid-lining cells in the open sinusoids were regarded as SECs.

RNA extraction, cDNA synthesis and PCR amplification of different angiogenic factors

About 20 mg liver tissues was immediately flash frozen in liquid nitrogen and stored at -70 ℃ after excision for RNA isolation. Total RNA was extracted with the RNeasy® Mini kit (Qiagen Cat. No. 74104) according to the manufacturer's protocol and eluted in 25 μL RNase-free water. Single-stranded cDNA was synthesized from 8 μL of RNA by the RevertAid™ first strand cDNA synthesis kit (MBI Cat. No. K1621) with random hexamer primers and 3 μL of the product was used for PCR.

The PCR primer pairs are listed in Table 1. Thirty cycles of DNA amplification using a Taq DNA polymerase (recombinant, MBI Cat. No. EP0404) was performed under the following conditions: denaturation at 94 ℃ for 1 min, annealing (β-actin, 52 ℃; VEGF, 60 ℃; Flt-1, 53 ℃; Flk-1, 52 ℃) for 1 min, extension at 72 ℃ for 1 min. Negative controls (cDNA-free solutions) were included in each reaction. β-actin, a house-keeping gene equally expressed in most eukaryotic cells, was used as an external standard and amplified in parallel with different angiogenic factors in all PCR samples.

Table 1 Oligonucleotides used as primers in RT-PCR procedure

Primer	Nucleotide sequence	PCR product lengths (bp)
Rat VEGF	Sense: 5′-ACTGGACCCTGGCTTTACTG-3′	256
Antisense:	5′-ACGCACTCCAGGGCTTCATC-3′ GenBank NM031836	
Rat Flt-1	Sense: 5′-AGGAGAGGACCTGAAACTGTCTT-3′ Antisense: 5′-ATTCCTGGGCTCTGCAGGCATAG-3′[10]	214
Rat Flk-1	Sense: 5′-GTGATTGCCATGTTCTTCTGGC-3′ Antisense: 5′-TCAGACATGAGAGCTCGATGCT-3′ GenBank U93306	337
Rat β-actin	Sense: 5′-TTCCACACACACCAGCTTCG-3′ Antisense: 5′-GGGGTGGTGTGGAGATTTAG-3′ GenBank NM031144	366

Semi-quantification of PCR products

After PCR amplification from 50 μL reaction volume, 10 μL was electrophoresed on 1.5% agarose gel in 1× TBE buffer. The amplified bands were detected by ethidium bromide staining. The intensity of ethidium bromide fluorescence was measured by the Photo Documentation and Imaging System (Bio-1D, VL, France). For quantification of the PCR products from all samples, the samples were evaluated by comparing the PCR product to β-actin.

Statistical analysis

The results were expressed as mean±SD. Statistical analysis was performed for the unpaired data using SPSS11.0 for Windows (SPSS Inc., Chicago, IL, USA). $P<0.05$ was considered statistically significant.

Hepatic VEGF, Flt-1 and Flk-1 mRNA expression

The changes in hepatic VEGF, Flt-1 and Flk-1 mRNA following surgery are shown in Figures 1 and 2. The expression of VEGF mRNA increased after 24 h of 70% PHx, with a peak from 48 to 72 h. Insulin significantly increased VEGF mRNA from 24 to 120 h after hepatectomy compared to controls ($P<0.01$; Figures 1C, D and 2A). Similarly, hepatic Flt-1 mRNA expression increased after hepatectomy. Insulin significantly increased Flt-1 mRNA from 24 to 96 h after hepatectomy compared to controls ($P<0.01$; Figures 1E, F and 2B). Insulin had no significant effect on Flk-1 when compared to controls (Figures 1G, H and 2C).

PCNA labeling index

The PCNA LI was lower than 5% in both hepatocytes and SECs before hepatectomy. However, liver cell proliferation was evident as early as 24 h postoperation. Insulin significantly promoted hepatocyte proliferation from 24 to 120 h compared to controls ($P<0.01$, Figure 3).

Immunohistochemical staining of VEGF protein in remnant liver

Before hepatectomy, there were very few VEGF-positive

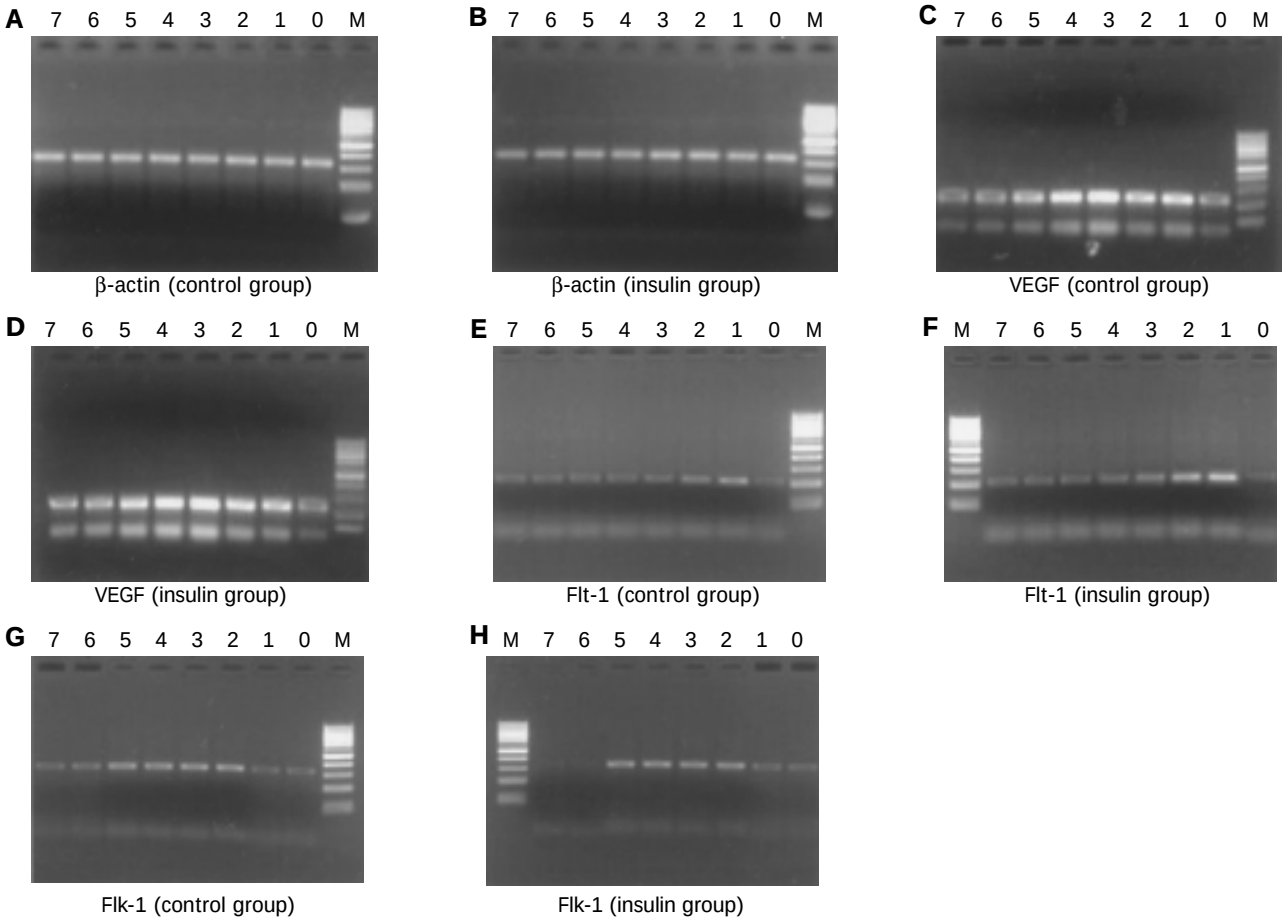

Figure 1 RT-PCR results of VEGF, Flt-1, and Flk-1 mRNA expressions in liver of different groups. M: 100-bp DNA ladder (upper to lower: 1 000, 900, 800, 700, 600, 500, 400, 300, 200, and 100 bp); lane 0: 0 h; lane 1: 24 h; lane 2: 48 h; lane 3: 72 h; lane 4: 96 h; lane 5: 120 h; lane 6: 144 h; lane 7: 168 h.

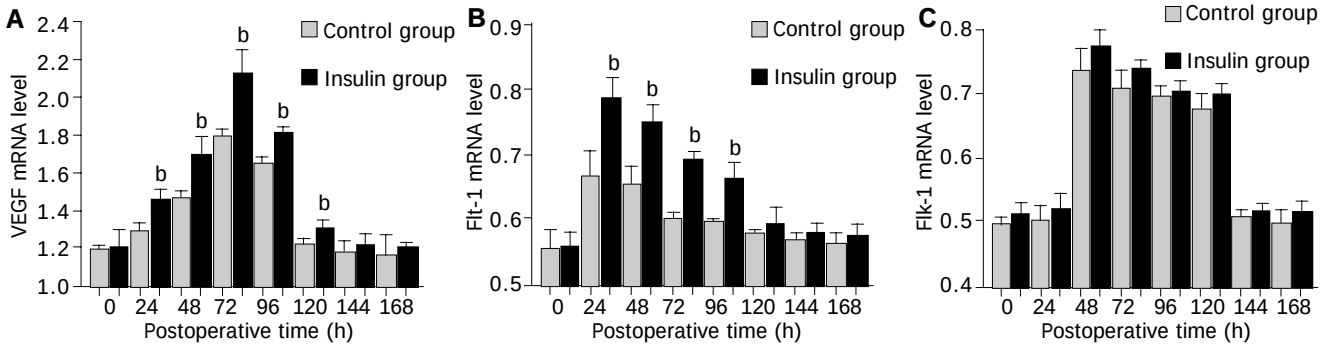

Figure 2 VEGF (A), Flt-1 (B), and Flk-1 (C) mRNA expressions after 70% hepatectomy in rats by RT-PCR.

cells, but increased expression of VEGF was observed 24 h after surgery (P<0.01, Figure 4A). Insulin increased the expression of VEGF, with a peak at 72 h (P<0.01, Figure 4D).

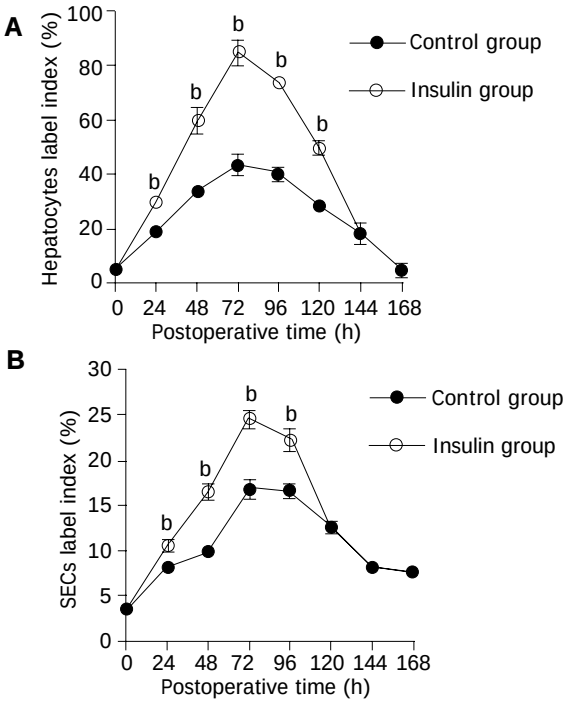

Figure 3 PCNA LI of hepatocytes (A) and SECs (B) after 70% hepatectomy in rats.

DISCUSSION

Liver remodeling following PHx comprises a complex set of events including activation and secretion of numerous factors, cell proliferation, thus finally re-establishing liver architecture[15-19]. Angiogenesis is the integrated process of endothelial cell division, vascular sprouting, and migration from pre-existing cells[20], indicating that SEC proliferation is strongly associated with hepatocyte proliferation during liver regeneration. Liver regeneration involves two processes: liver architecture remodeling and liver cell proliferation. In our study, SECs influenced the regenerative capacity of liver following PHx. Rebuilding the network of blood supply is necessary in liver regeneration. SECs play an important role in the formation of a complex network of blood vessels for remodeling liver architecture following liver resection. Additionally, SECs surround avascular clusters of hepatocytes, subsequently re-establish normal vascular architecture and directly supply nutrition and growth factors to liver cells[6].

The role of VEGF in liver regeneration has been reported[20-25]. SECs have a unique response to growth factors[6-8,18]. Information on the association of angiogenic factors with liver regeneration is available[5,6,18]. VEGF isoform signal has several receptors, including Flt-1 and Flk-1[26-30]. These receptors can operate in a paracrine and cooperative manner with VEGF produced by hepatocytes in regulating SEC growth and subsequent vascularization of the liver[13]. The receptors are structurally similar to members of the platelet-derived growth factor receptor family and consist of an extracellular domain composed of seven immunoglobulin-like motifs, a transmembrane domain, a juxtamembrane domain, a tyrosine kinase that is split by a kinase insert region, and a C-terminal tail. It is uncertain what role each VEGF receptor actually plays in cell signaling during liver revascularization. In some studies, Flk-1/KDR and Flt-1 have been shown to act in unique capacities[6]. These studies have determined that Flk-1/KDR can activate both mitogenicity and motility pathways, whereas

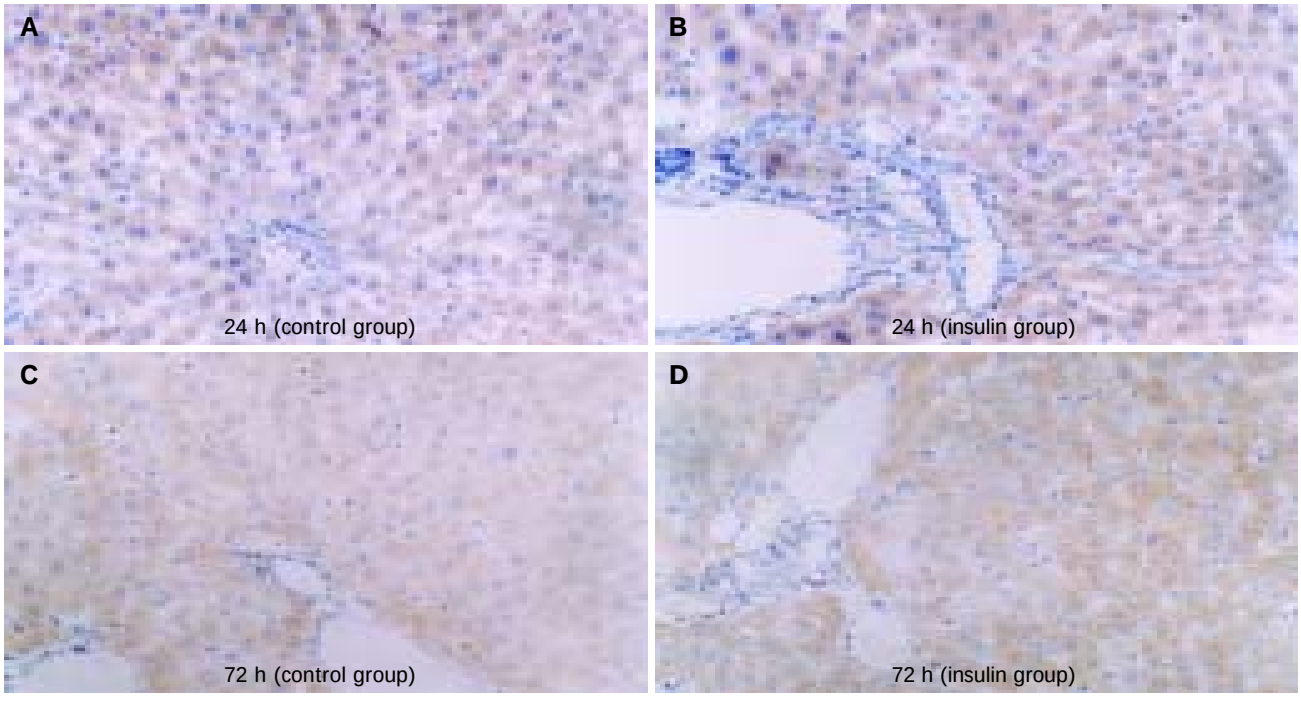

Figure 4 Expression of VEGF protein at 24 h in control group (A) and insulin group (B), at 72 h in control group (C), and insulin group (D).

Flt-1 appears to mediate actin reorganization[6]. Moreover, Flt-1 is induced by hypoxia, which emerges during regeneration, whereas Flk-1/KDR is not[6]. Exogenous $VEGF_{165}$ can stimulate liver cell proliferation following PHx and antibodies to VEGF significantly inhibit hepatocyte proliferation following PHx[5,29]. However, $VEGF_{165}$ does not induce either a motogenic or a mitogenic response in isolated hepatocytes, though Flt-1 is phosphorylated[6,29], indicating that VEGF may stimulate liver cell proliferation by acting on surrounding SECs, which influence hepatocytes by improving nutrient availability or through vascular permeability.

The present study demonstrated that exogenous insulin could stimulate SECs following PHx in rats. Insulin can induce a host of effects on glucose transport and utilization, protein synthesis, and cell proliferation, *etc*.[12].

However, the effect of insulin on blood vessels during regeneration after PHx in rats is still unknown. It has been reported that vascular abnormalities and pathologies are commonly associated with diabetes[31,32]. Jiang *et al*.[25], demonstrated that insulin can stimulate several signaling cascades in endothelial cells and vascular smooth muscle cells by phosphorylating both insulin receptor substrate-1 and -2. The vascular-specific action of insulin may be attributed to the growth factors, especially VEGF, and cytokines of which the expression is regulated by insulin. The exact mechanism underlying insulin-induced VEGF mRNA upregulation in microvascular EC is currently unknown. It was reported that insulin-induced VEGF expression is mediated through the activation of phosphatidylinositol (PI) 3-kinase/Akt being downstream to the insulin receptors[33,34]. It was reported that the activation of PI 3-kinase/Akt pathway can upregulate the expression of hypoxia-inducible factor-1α, a principal factor that causes angiogenesis[34]. Insulin may upregulate the VEGF mRNA through a nuclear factor-κB-mediated pathway, and mAb against VEGF can completely neutralize the proliferation and tube formation of endothelial cells induced by insulin[11,33].

In conclusion, insulin induces expression of VEGF and its receptor after PHx, and promotes liver regeneration besides the traditional metabolic action on hepatocytes.

ACKNOWLEDGMENTS

The authors thank Ms. Ou, Mr. Zhang, Mr. Gao, and Mr. Yu for their technical assistance.

REFERENCES

1 **Michalopoulos GK,** DeFrances MC. Liver regeneration. *Science* 1997; **276**: 60-66
2 **Kim I,** Kim HG, Kim H, Kim HH, Park SK, Uhm CS, Lee ZH, Koh GY. Hepapatic expression, synthesis and secretion of a novel fibrinogen/angiopoietin-related protein that prevents endothelial-cell apoptosis. *Biochem J* 2000; **346**(Pt 3): 603-610
3 **Mirpuri E,** Garcia-Trevijano ER, Castilla-Cortazar I, Berasain C, Quiroga J, Rodriguez-Ortigosa C, Mato JM, Prieto J, Avila MA. Altered liver gene expression in CCL_4-cirrhotic rats is partially normalized by insulin-like growth factor-I. *Int J Biochem Cell Biol* 2002; **34**: 242-252
4 **Rastegar M,** Lemaigre FP, Rousseau GG. Control of gene expression by growth hormone in liver: key role of a network transcription. *Mol Cell Endocrinol* 2000; **164**: 1-4
5 **Kraizer Y,** Mawasi N, Seagal J, Paizi M, Assy N, Spira G. Vascular endothelial growth factor and angiopoietin in liver regeneration. *Biochem Biophs Res Commun* 2001; **287**: 209-215
6 **Ross MA,** Sander CM, Kleeb TB, Watkins SC, Stolz DB. Spatiotemporal expression of angiogenesis growth factor receptors during the revascularization of regenerating rat liver. *Hepatology* 2001; **34**: 1135-1148
7 **Mustonen T,** Alitalo K. Endothelial receptor tyrosine kinases involved in angiogenesis. *J Cell Biol* 1995; **129**: 895-898
8 **Neufeld G,** Cohen T, Gengrinovitch S, Poltorak Z. Vascular endothelial growth factor (VEGF) and its receptors. *FASEB J* 1999; **13**: 9-22
9 **Stouffer RL,** Martinez-Chequer JC, Molskness TA, Xu F, Hazzard TM. Regulation and action of angiogensic factors in the primate ovary. *Arch Med Res* 2001; **32**: 567-575
10 **Sato T,** El-Assal ON, Ono T, Yamanoi A, Dhar DK, Nagasue N. Sinusoidal endothelial cell proliferation and expression of angiopoietin/Tie family in regenerating rat liver. *J Hepatol* 2001; **34**: 690-698
11 **Jiang ZY,** He Z, King BL, Kuroki T, Opland DM, Suzuma K, Suzuma I, Ueki K, Kulkarni RN, Kahn CR, King GL. Characterization of multiple signaling pathways of insulin in the regulation of vascular endothelial growth factor expression in vascular cells and angiogenesis. *J Biol Chem* 2003; **278**: 31964-31971
12 **Klein D,** Schubert T, Horch RE, Jauch KW, Jeschke MG. Insulin treatment improves hepatic morphology and function through modulation of hepatic signals after severe trauma. *Ann Surg* 2004; **240**: 340-349
13 **Yamagishi S,** Kawakami T, Fujimori H, Yonekura H, Tanaka N, Yamamoto Y, Urayama H, Watanabe Y, Yamamoto H. Insulin stimulates the growth and tube formation of human microvascular endothelial cells through autocrine vascular endothelial growth factor. *Microvasc Res* 1999; **57**: 329-339
14 **Sasso FC,** Carbonara O, Persico E, D'Ambrosio R, Coppola L, Nasti R, Campana B, Moschella S, Torella R, Cozzolino D. Increased vascular endothrlial growth factor mRNA expression in the heart of streptozotocin-induced diabetic rats. *Metabolism* 2003; **52**: 675-678
15 **Mitchell C,** Nivison M, Jackson LF, Fox R, Lee DC, Campbell JS, Fausto N. HB-EGF links hepatocyte priming with cell cycle progression during liver regeneration. *J Biol Chem* 2005; **280**: 2562-2568
16 **White P,** Brestelli JE, Kaestner KH, Greenbaum LE. Identification of transcriptional networks during liver regeneration. *J Biol Chem* 2005; **280**: 3715-3722
17 **Tracy TF Jr,** Fox ES. Molecular and cellular control points in pediatric liver injury and repair. *Semin Pediatr Surg* 1996; **5**: 175-181
18 **LeCouter J,** Moritz DR, Li B, Phillips GL, Liang XH, Gerber HP, Hillan KJ, Ferrara N. Angiogenesis-independent endothelial protection of liver: role of VEGFR-1. *Science* 2003; **299**: 890-893
19 **Leu JI,** Crissey MA, Craig LE, Taub R. Impaired hepatocyte DNA synthetic response posthepatectomy in insulin-like growth factor binding protein 1-deficient mice with defects in C/EBP beta and mitogen-activated protein kinase/extracellular signal-regulated kinase regulation. *Mol Cell Biol* 2003; **23**: 1251-1259
20 **Grosskreutz CL,** Anand-Apte B, Duplaa C, Quinn TP, Terman BI, Zetter B, D'Amore PA. Vascular endothelial growth factor-induced migration of vascular smooth muscle cells *in vitro*. *Microvasc Res* 1999; **58**: 128-136
21 **Unsoeld AS,** Junker B, Mazitschek R, Martin G, Hansen LL, Giannis A, Agostini HT. Local injection of receptor tyrosine kinase inhibitor MAE 87 reduces retinal neovascularization in mice. *Mol Vis* 2004; **10**: 468-475
22 **Manley PW,** Bold G, Bruggen J, Fendrich G, Furet P, Mestan J, Schnell C, Stolz B, Meyer T, Meyhack B, Stark W, Strauss A, Wood J. Advances in the structural biology, design and clinical development of VEGF-R kinase inhibitors for the treatment of angiogenesis. *Biochim Biophys Acta* 2004; **1697**: 17-27
23 **Sigrist S,** Mechine-Neuville A, Mandes K, Calenda V, Legeay

G, Bellocq JP, Pinget M, Kessler L. Induction of angiogenesis in omentum with vascular endothelial growth factor: influence on the viability of encapsulated rat pancreatic islets during transplantation. *J Vasc Res* 2003; **40**: 359-367

24 **Carmeliet P,** Storkebaum E. Vascular and neuronal effects of VEGF in the nervous system: implications for neurological disorders. *Semin Cell Dev Biol* 2002; **13**: 39-53

25 **Jiang ZY,** Lin YW, Clemont A, Feener EP, Hein KD, Igarashi M, Yamauchi T, White MF, King GL. Characterization of selective resistance to insulin signaling in the vasculature of obese zucker (fa/fa) rats. *J Clin Invest* 1999; **104**: 447-457

26 **Nakagawa M,** Kaneda T, Arakawa T, Morita S, Sato T, Yomada T, Hanada K, Kumegawa M, Hakeda Y. Vascular endothelial growth factor (VEGF) directly enhances osteoclastic bone resorption and survival of mature osteoclasts. *FEBS Lett* 2000; **473**: 161-164

27 **Tarnawski AS,** Chai J, Pai R, Chiou SK. Rebamipide activates genes encoding angiogenic growth factors and Cox2 and stimulates angiogensis: a key to its ulcer healing action? *Dig Dis Sci* 2004; **49**: 202-209

28 **Kraneburg O,** Gebbink MF, Voest EE. Stimulation of angiogensis by Ras proteins. *Biochim Biophys Acta* 2004; **1654**: 23-37

29 **Assy N,** Spira G, Paizi M, Shenkar L, Kraizer Y, Cohen T, Neufeld G, Dabbah B, Enat R, Baruc Y. Effect of vascular endothelial growth factor on hepatic regenerative activity following partial hepatectomy in rats. *J Hepatol* 1999; **30**: 911-915

30 **Shimizu H,** Miyazaki M, Wakabayashi Y, Mitsuhashi N, Kato A, Ito H, Nakagawa K, Yoshidome H, Kataoka M, Nakajima N. Vascular endothelial growth factor secreted by replicating hepatocytes induces sinusoidal endothelial cell proliferation during regeneration after partial hepatectomy in rats. *J Hepatol* 2001; **34**: 683-689

31 **Carrillo MC,** Favre C, Monti JA, Alvarez ML, Carnovale CE. Insulin hyperresponsiveness in partially hepatectomized diabetic rats. *Life Sci* 2001; **68**: 1417-1426

32 **Chiarelli F,** Santilli F, Mohn A. Role of growth factors in the development of diabetic complications. *Horm Res* 2000; **53**: 53-67

33 **Stiehl DP,** Jelkmann W, Wenger RH, Hellwig-Burgel T. Normoxic induction of the hypoxia-inducible factor 1alpha by insulin and interleukin-1beta involves the phosphatidylinositol 3-kinase pathway. *FEBS Lett* 2002; **512**: 157-162

34 **Poulaki V,** Qin W, Joussen AM, Hurlbut P, Wiegand SJ, Rudge J, Yancopoulos GD, Adamis AP. Acute intensive insulin therapy exacerbates diabetic blood-retinal barrier breakdown via hypoxia-inducible factor-1alpha and VEGF. *J Clin Invest* 2002; **109**: 805-815

Science Editor Wang XL and Guo SY **Language Editor** Elsevier HK

PO Box 2345, Beijing 100023, China
www.wjgnet.com
wjg@wjgnet.com

ELSEVIER

World J Gastroenterol 2005;11(38):5984-5987
World Journal of Gastroenterology ISSN 1007-9327

• *CLINICAL RESEARCH* •

Sealing of the hepatic resection area using fibrin glue reduces significant amount of postoperative drain fluid

Frank Eder, Frank Meyer, Gerd Nestler, Zuhir Halloul, Hans Lippert

Frank Eder, Frank Meyer, Gerd Nestler, Zuhir Halloul, Hans Lippert, Department of Surgery, University Hospital, Magdeburg D-39120, Germany
Correspondence to: Frank Eder, MD, Department of Surgery, University Hospital, Leipziger Strasse 44, Magdeburg D-39120, Germany. frank.eder@medizin.uni-magdeburg.de
Telephone: +49-391-6715500 Fax: +49-391-6715570
Received: 2005-03-22 Accepted: 2005-04-18

ABSTRACT

AIM: To investigate whether the routine use of fibrin glue applied onto the hepatic resection area can diminish postoperative volume of bloody or biliary fluids drained via intraoperatively placed perihepatic tubes and can thus lower the complication rate.

METHODS: Two groups of consecutive patients with a comparable spectrum of recent hepatic resections were compared: (1) 13 patients who underwent application of fibrin glue immediately after resection of liver parenchyma; (2) 12 patients who did not. Volumes of postoperative drainage fluid were determined in 4-h intervals through 24 h indicating the intervention caused bloody and biliary segregation.

RESULTS: Through the first 8 h postoperatively, there was a tendency of higher amounts of fluids in patients with no additional application of fibrin glue while through the following intervals, a significant increase of drainage volumes was documented in comparison with the first two 4-h intervals, e.g., after 12 h, 149.6 mL +/-110 mL *vs* 63.2 mL +/-78 mL. Using fibrin glue, postoperative fluid amounts were significantly lower through the postoperative observation period of 24 h (851 mL +/-715 mL *vs* 315 mL +/-305 mL).

CONCLUSION: For hepatic resections, the use of fibrin glue appears to be advantageous in terms of a significant decrease of surgically associated segregation of blood or bile out of the resection area. This might result in a better outcome.

Key words: Fibrin glue; Hepatic resection

Eder F, Meyer F, Nestler G, Halloul Z, Lippert H. Sealing of the hepatic resection area using fibrin glue reduces significant amount of postoperative drain fluid. *World J Gastroenterol* 2005; 11(38): 5984-5987
http://www.wjgnet.com/1007-9327/11/5984.asp

INTRODUCTION

Hepatic resections are considered as a standard intervention in abdominal surgery. Despite this, there is still a remarkable complication rate. In addition to patient-dependent factors, aspects of the surgical technique play a major role, in particular, with regard to the occurrence of postoperative bleeding and bile leakages. A precise dissection is as important as supplements such as hemostatics and tissue glue for the daily surgical practice to avoid complications, e.g., bleeding and biliary segregation from the resection area of the liver.

The aim of the study was to investigate, whether the sealing of the hepatic resection area using biocompatible glue leads to a significant decrease of postoperative release of blood and/or biliary fluid volume, which was measured in the local drainage(s).

MATERIALS AND METHODS

In a pilot study, a comparative non-randomized study of two case series, all consecutive patients with hepatic resections were enrolled with prospective data documentation over a defined observational period until the planned number of individuals was reached (n = 12 per group). Patients were retrospectively (to avoid a study bias) subdivided into two groups with or without sealing of the hepatic resection area using fibrin glue. Patient characteristics are listed in Table 1A.

Hepatic resections were carried out according to standardized technique following anatomically adequate resection margins (segmental resection, bi-/tri-segmental resection or hemihepatectomy) or as atypical hepatic resection with a tumor-free resection margin of minimally 5 mm ("wedge" resection).

Perioperative prophylaxis with antibiotics was performed (2 g of Cefotiam iv., Spizef®, Grünthal GmbH, Aachen, Germany). After explorative laparotomy, definitely exclusion of extrahepatic tumor manifestation and exploration of the hepatic tumor lesion needs to be approached (if necessary including intraoperative ultrasound of liver parenchyma). The liver was mobilized in a typical manner at the "Ligg. triangularia" and "falciforme", a tourniquet loop was placed around the hepatoduodenal ligament. After marking the resection margins, dissection of liver parenchyma was carried out using cavitron ultrasonic surgical aspirator (CUSA) technology. The intraparenchymatic vessels and ducts of the biliary tree were clipped and cut. Bleeding control at the hepatic resection area was achieved by bi- and/or mono-polar electrocoagulation. During the dissection,

Pringle's maneuver (temporary cessation of the blood flow in hepatic artery and portal vein) of maximally 20-min periods was executed to minimize the intraoperative blood loss. Bigger vessels and biliary ducts were ligated. After completion of the hepatic resection, the resection area was repeatedly coagulated (bi- or mono-polar electrocoagulation or infrared coagulation). Depending on the size of the resection area, one (or two) drain (s) was (were) placed into the subhepatic (and subphrenic) space.

According to the aim of the study, the hepatic resection area of the patients was sealed with fibrin glue (Tissucol or Tachocomb seal) or not.

For thrombosis prophylaxis heparin (low dose, low molecular heparin-derivative) was not given for 24 h postoperatively whereas antithrombosis socks were obligatory.

Patients were monitored at the surgical ICU for 24 h postoperatively.

Table 1 Comparison of patient groups with hepatic resection

(A) Patient characteristics.

		Fibrin glue	
		Without	With
Sex ratio			
Patients (*n*)	Male	8	7
	Female	4	6
Mean age (range) (yr)			
	Male	65 (37–77)	68 (41–75)
	Female	55 (44–70)	62 (46–75)

(B) Diagnosis

Diagnosis	Number of patients (sealing with fibrin glue)	
	Without	With
Hepatocellular carcinoma	5	2
Cholangiocellular carcinoma		
Liver metastases	5	9
Adenoma/FNH	2	2

(C) Types of resections

Type of resections	No. of patients (sealing with fibrin glue)	
	Without	With
Hemihepatectomy	4	1
Segmental resection (more than one segment)	4 (3 bisegmental resections)	10 (2 trisegmental and 5 bisegmental resections)
Atypical resection	4	2

(D) Values of significance

Postoperative time interval (h)	Value of significance (one side)
4	0.0094
8	0.0129
12	0.0059
16	0.0054
20	0.0026
24	0.0028

[a]*P*<0.05 *vs* no sealing, [b]*P*<0.01 *vs* no sealing, [c]*P*<0.005 *vs* no sealing, [d]*P*<0.001 *vs* no sealing.

Sealing with fibrin glue

Tissucol® (Baxter Deutschland GmbH, Heidelberg, Germany) was applied by spraying it on the hepatic resection area. Tachocomb seal (Tachocomb®, fibrin glue on a collagen fleece, Nycomed, Ismaning, Germany) was applied on the hepatic resection area after moistening it.

In the group of the patients with fibrin glue sealing, 13 patients (6 females and 7 males; mean age 62 years) with hepatic resections enrolled (Table 1A), were compared with a group of 12 subjects (4 females and 8 males; mean age, 60 years) with no fibrin glue application who were enrolled in the same study period.

The diagnoses and types of resections of both groups are listed in Tables 1B and C.

The fluid volumes drained via the intra-abdominally placed drains were documented in 4-h periods in a separate (Table 1D) and additive manner (Figure 1), in total through a time period of 24 h.

Informed consent for hepatic resection was obtained from each patient.

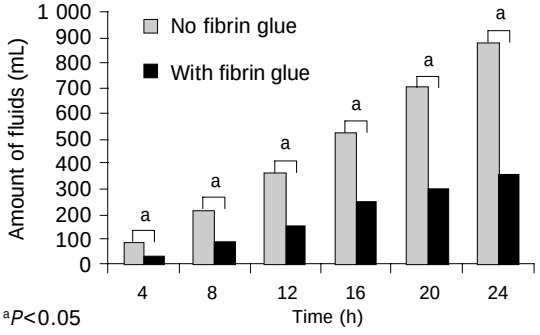

Figure 1 Time course of the mean of the added drain volumes depending on the application of fibrin glue. There was a significant reduction of the segregated amount of fluids in the group of patients in whom sealing with fibrin glue was used. [a]*P*<0.05 *vs* no sealing.

Statistical analysis

In addition to the descriptively statistical presentation of the results (SPSS 10.0 for Windows), fluid volumes of the drains in both patient groups with and without sealing with fibrin glue after hepatic resection were compared by a non-parametric test according to Mann-Whitney (*U* test) as appropriate. A value of $P<0.05$ was considered statistically significant.

RESULTS

The mean age and sex ratio of both patient groups appeared to be comparable. The spectrum and surgical extension of hepatic resections in both groups were similar.

The listed diagnoses demonstrate the patient profile, which is treated in our center of hepatobiliary surgery and varies from primary liver tumors, cholangio- and hepatocellular carcinomas ($n = 2$ and $n = 5$ in the group with and without fibrin glue, respectively), FNH ($n = 2$; no fibrin glue) or hepatocellular adenoma ($n = 2$; no fibrin glue), to metastases of colorectal ($n = 8$ in the group with

fibrin glue *vs* $n = 5$ without) or gastric carcinomas ($n = 1$; with fibrin glue, Table 1B). All patients showed an acceptable preoperative liver function, and no patient showed a postoperative decompensation of liver function.

In the spectrum of resections, there were one right hemihepatectomy, 10 segmental resections (trisegmental resections, $n = 2$; bisegmental resections, $n = 5$; one segment, $n = 3$) and two atypical resections in the patient group with no fibrin glue application *vs* four hemihepatectomies, four segmental resections (bisegmental resections, $n = 3$; one segment, $n = 1$) and four atypical resections in the comparison group with fibrin glue (Table 1C, Figure 2).

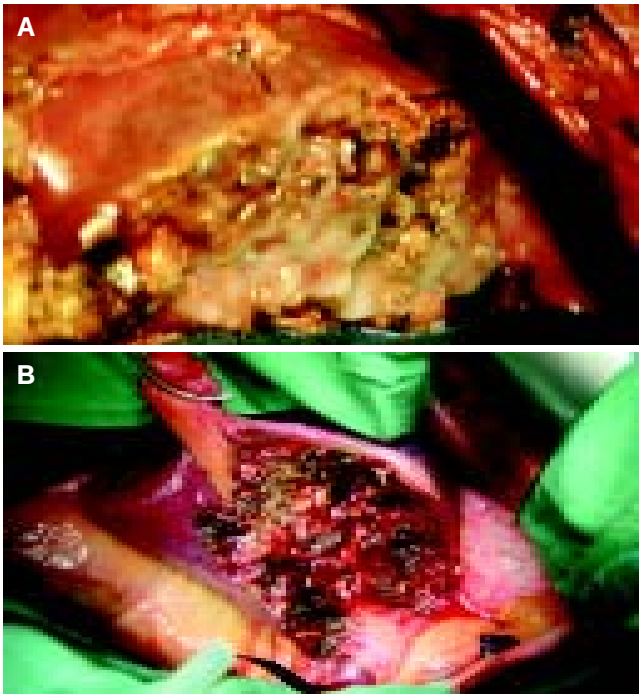

Figure 2 Hepatic resection area after segmental resection. A: With fibrin glue (sealing with Tissucol®). B: Without fibrin glue.

For sealing the hepatic resection area with fibrin glue, Tissucol® was used in 11 patients whereas in two further cases, Tachocomb® was chosen (data not shown).

In none of the patients included in the study, a severe postoperative complication occurred neither as acute nor intermediate problem. The drain fluid was either of serous or bloody-serous nature or serous quality with slight bile impurity. The comparison of the single drain volumes of both groups including the *P* values is shown in Table 1D.

Through the first 8 h postoperatively, there was a tendency of a higher drain fluid volume in the patient group with no fibrin glue, which was indicated by the single (of each 4-h time period) as well as the added amounts of fluids (total volume at specific time points during the postoperative course). Through the following time periods, the segregation increased significantly in this group compared with the first two time periods of 4 h each, resulting in the fact that a significant reduction of the segregated volumes via the drains in the patient group with fibrin glue was observed after 12 h ($P = 0.0059$). This difference became even more distinct through the following time periods up to 24 h ($P = 0.0028$). Figure 1 shows the comparison of the added postoperative amount of fluids drained postoperatively from the hepatic resection area. While the summation of the single drain volumes of the patients with fibrin glue through the 24-h time period shows a linear curve, the curve in the comparison group (no fibrin glue) shows an exponential increase.

Using fibrin glue, a significant reduction of the postoperative drain volume of segregated fluids out of the hepatic resection area was found during the study period of 24 postinterventional hours.

[redacted]

By means of a pilot study, two patient groups with similar demographic and treatment characteristics were compared to investigate whether the application of fibrin glue on the hepatic resection area has a significant impact on the postoperative segregation of fluids via the drains. Using a precise surgical technique with accurate dissection of liver parenchyma, in particular, according to the anatomic margins of the liver segments, with CUSA and a subtle control of bleeding, the complication rate in hepatic resections can be kept low.

The hypothesis was that, by the mean of an additive sealing the hepatic resection area with fibrin glue, the rate of local complications such as postoperative bleeding and biliary fistulas can be reduced. As a first step to prove this hypothesis, the amounts of segregated fluid via the drain(s) was compared between the groups of patients with or without application of fibrin glue on the hepatic resection area despite complete control of bleeding and biliary excretion occurred immediately after accomplishing the resection. It showed a significant difference with lower volumes of segregated fluids after 24 h, indicating a further possible reduction of the surgical risk and complication rate, which can be achieved by the use of fibrin glue. However, the main result of this pilot study needs to be confirmed in a currently ongoing study, in which more patients are being included.

The possible impact of a heparin medication was excluded by the department-specific standard since the continuation of the preoperatively initiated heparin administration for antithrombotic prophylaxis was postponed by 24 h postoperatively according to the duration of the study period[1]. In addition, acetylsalicylic acid-based medication was stopped a couple of days prior to the admission. The pathophysiological background to use postinterventional sealing with fibrin glue is as follows: hepatic resection can lead to an activation of fibrinolysis. Even in the case of a perfect hepatic resection from a technical point of view, postoperative bleeding and segregations of fluids can occur though the resection that was accomplished by leaving a dry hepatic resection area[2]. By the mean of fibrin application, the hepatic resection area can be sealed and, thus, smallest microlesions can be closed. In addition, the fibrin excess can avoid early fibrinolysis.

One limitation of the study might be the possibly varying size of the hepatic resection area but which is, because of the similar spectrum of different types of hepatic resections, almost comparable. In addition, the underlying liver disease

might affect the drain volume, which cannot be satisfyingly clarified in this study, which included only a limited number of patients. Furthermore, following studies need to focus on the composition of the segregated fluid with regard to the content of hemoglobin and bilirubin and the discrimination between the various types of sealing (Tissucol *vs* Tachocomb), which has not been the main focus and can be considered as an acceptable approximation in this pilot study.

From a technical point of view, the fast availability of the fibrin-coated collagen fleece seems to be advantageous as compared with the fibrin glue, which needs to be thawed[3].

There is a varying opinion on the additive use of fibrin glue in several surgical departments. In a Japanese study, 231 hospitals were asked about their routine use in hepatic resections. While in 203 hospitals, CUSA was used for resection (87%), only 135 (60%) applied fibrin glue on the hepatic resection area after the resection[4]. Comparison studies on the use of fibrin glue in hepatic resections were undertaken using animal experiments. The difficulty in the judgment of the fibrin effect was the usage of various additional agents, the different experimental designs, and varying animal strains and species. Davidson showed the advantage of a sealing with fibrin glue and cellulose gauze application after hepatic resections with regard to a tendency of a lower rate of postoperative bleeding using a pig model[5].

Turner has described the advantage of a composition consisting of thrombin and autologous plasma for control of bleeding after hepatic resections in sheep[6]. In addition, Martis has reported the benefit of Tachocomb in hepatic resections of dogs[7].

In conclusion, the presented pilot study in a clinical setting supports the thesis that an additional application of fibrin glue can contribute to the safe postoperative outcome as shown by the impressive statistically significant reduction of the postoperative volumes of segregated fluids via the perihepatic drain (s). Following studies using a prospective randomized study design, in a greater number of patients, and on various aspects such as the postoperative complication rate in patients with and without fibrin glue on the hepatic resection area may result in further facts and arguments for the impact and the beneficial effect of this additional tool.

ACKNOWLEDGEMENTS

We are grateful to Dr. Kropf, Institute for Biometry and Medical Informatics, University Hospital, Magdeburg, for appropriate statistical advice. For critical prereview of the manuscript, we thank M Reymond.

REFERENCES

1 **Lippert H,** Scheele J. Lebertumoren. In: Lippert H (ed.) Praxis der Chirurgie, Allgemein- und Viszeralchirurgie. 1st ed. *Stuttgart, New York: Thieme* 1998: 549-562
2 **Köckerling F,** Schneider C, Scheidbach H, Hohenberger W. Stellenwert der Fibrinklebung in der Leberchirurgie. In: Köckerling F (ed.) Leberchirurgie. 1st ed. Heidelberg, Leipzig: *Johann Ambrosius Barth* 1999: 103-108
3 **Ringe B.** Gewebeklebung in der hepatobiliären und Transplantationschirurgie. In: Ringe B (ed.) Gewebeklebung in der Chirurgie: Grundlagen und Anwendung. 1st ed. *Stuttgart, New York: Thieme* 2001: 63-75
4 **Nakajima Y,** Shimamura T, Kamiyama T, Matsushita M, Sato N, Todo S. Control of intraoperative bleeding during liver resection: analysis of a questionnaire sent to 231 Japanese hospitals. *Surg Today* 2002; **32**: 48-52
5 **Davidson BR,** Burnett S, Javed MS, Seifalian A, Moore D, Doctor N. Experimental study of a novel fibrin sealant for achieving haemostasis following partial hepatectomy. *Br J Surg* 2000; **87**: 790-795
6 **Turner AS,** Parker D, Egbert B, Maroney M, Armstrong R, Powers N. Evaluation of a novel hemostatic device in an ovine parenchymal organ bleeding model of normal and impaired hemostasis. *J Biomed Mater Res* 2002; **63**: 37-47
7 **Martis G,** Miko I, Szendroi T, Kathy S, Kovacs J, Hajdu Z. Results with collagen fleece coated with fibrin glue (TachoComb). A macroscopical and histological experimental study. *Acta Chir Hung* 1997; **36**: 221-222

Science Editor Guo SY **Language Editor** Elsevier HK

PO Box 2345, Beijing 100023, China
www.wjgnet.com
wjg@wjgnet.com

ELSEVIER

World J Gastroenterol 2005;11(38):5988-5992
World Journal of Gastroenterology ISSN 1007-9327

• *CLINICAL RESEARCH* •

Low circulating levels of gastrin-17 in patients with Barrett's esophagus

Pentti Sipponen, Matti Vauhkonen, Timo Helske, Ilpo Kääriäinen, Matti Härkönen

Pentti Sipponen, Division of Pathology, Department of Pathology, HUSLAB, Helsinki University Central Hospital (HUCH), Jorvi Hospital, Espoo 02740, Finland
Matti Vauhkonen, Timo Helske, Ilpo Kääriäinen, Department Internal Medicine, Helsinki University Central Hospital (HUCH), Jorvi Hospital, Espoo 02740, Finland
Matti Härkönen, Department of Clinical Chemistry, Helsinki University Central Hospital (HUCH), Meilahti Hospital, Helsinki 00290, Finland
Correspondence to: Dr. Pentti Sipponen, Department of Pathology, HUSLAB, Jorvi Hospital, Espoo 02740, Finland. pentti.sipponen@hus.fi
Telephone: +358-9-8612671 Fax: +358-9-8615912
Received: 2004-11-30 Accepted: 2005-01-26

Abstract

AIM: To examine whether the fasting levels of serum gastrin-17 (G-17) are lower in Barrett's esophagus (BE) patients than in non-Barrett controls.

METHODS: Nineteen patients with BE (presenting with a tubular segment ⩾2 cm long in lower esophagus and intestinal metaplasia of incomplete type ("specialized columnar epithelium") in endoscopic biopsies from the tubular segment below the squamocolumnar junction were collected prospectively from outpatients referred to diagnostic gastroscopy. The controls comprised 199 prospectively collected dyspeptic outpatients without BE or any endoscopically visible lesions in the upper GI tract. Fasting levels of serum G-17 (G-17fast) were assayed with an EIA test using a Mab highly specific to amidated G-17. None of the patients and controls received therapy with PPIs or other antisecretory agents.

RESULTS: The mean and median levels of G-17fast in serum were significantly lower (P = 0.001) in BE patients than in controls. The positive likelihood ratios (LR+) of low G-17fast to predict BE in the whole study population at G-17fast levels <0.5, <1, or <1.5 pmol/L were 3.5, 3.0, and 2.8, respectively. Among patients and controls with healthy stomach mucosa, the LR+ were 5.6, 3.8, and 2.6, respectively. In the whole study population, serum G-17 was below 2 pmol/L in 15 of 19 BE patients (79%). The corresponding prevalence was 66 of 199 (33%) in controls (P<0.001). The G-17fast was 5 pmol/L or more in only one of the 19 BE patients (5%). In controls, 76 of the 199 patients (38%) had such high serum G-17fast levels (P<0.01).

CONCLUSION: Serum levels of G-17fast tend to be lower in native patients with BE than in healthy controls.

Key words: Gastrin-17; Barrett's esophagus; Chronic gastritis; Atrophic gastritis; Diagnostics

Sipponen P, Vauhkonen M, Helske T, Kääriäinen I, Härkönen M. Low circulating levels of gastrin-17 in patients with Barrett's esophagus. *World J Gastroenterol* 2005; 11(38): 5988-5992
http://www.wjgnet.com/1007-9327/11/5988.asp

INTRODUCTION

High intragastric acidity inhibits the release of gastrin into circulation from antral G cells, and conversely, low acidity and high intragastric pH enhance this release[1,2]. Amidated gastrin-17 (G-17) is the biologically active main gastrin fragment, and G-17 is a gastrin compound secreted nearly entirely from the antral G cells[3-5]. It is conceivable that fasting levels of G-17 (G-17fast) in serum or plasma reflect indirectly the intragastric acidity. Correspondingly, it is conceivable that low serum levels of G-17 occur particularly in patients with acid-related diseases.

Gastroesophageal reflux disease is one of the most important acid-related diseases[6]. Patients with Barrett's esophagus (BE) are a subgroup of reflux patients in whom the refluxed acid gastric juice is a factor causing mucosal damages in the lower esophagus, and at the esophagogastric junction[7-9]. Some studies indicate that the prevalence of BE ranges from 0.5% to 5.0% in patients undergoing upper-GI endoscopy for dyspepsia, and from 12% to 15% in patients with gastroesophageal reflux disease and reflux symptoms[10-13].

In the present study, we investigated whether the serum levels of G-17 are lower in patients with BE than in non-BE controls.

MATERIALS AND METHODS

Patient and control series were collected prospectively in 2002 in Helsinki University Central Hospital (HUCH), Jorvi Hospital, Espoo, Finland, from patients who were referred to diagnostic gastroscopy for dyspeptic or reflux-type symptoms.

Patient series

The patient series consisted of 19 subjects with a BE diagnosed by endoscopy and histology. All had a Barrett's segment 2 cm or more in length in the lower columnar, tubular esophagus.

Of the available 19 patients, 14 were males and 5 females. The mean age was 60±12 years. Three of the nineteen BE patients (16%) had *Helicobacter pylori* (*H pylori*)-related gastritis. In one of these three patients, gastritis was strongly antrum dominant, and this patient showed moderate atrophy and intestinal metaplasia in the antrum. The histopathology was evaluated by biopsies from antrum and corpus (at least two biopsies from each site), and by the principles of the updated Sydney System. The biopsy specimens were stained with HE and Alcian blue (pH 2.5)-PAS methods and modified Giemsa for *H pylori*.

Control series

The control series consisted of 199 patients without any visible endoscopic lesions in the upper GI tract. Of the 199 patients, 71 were males and 128 females. The mean age was 54±15 years. Altogether, 94 patients (47%) had chronic *H pylori*-related or autoimmune chronic gastritis, or atrophic gastritis. The rest had normal and healthy gastric mucosa in gastric biopsies (no chronic gastritis, no *H pylori*, no intestinal metaplasia or atrophy). Of the total number of patients with chronic gastritis, 48 had atrophic gastritis of some grade and type. Advanced (moderate or severe) atrophic gastritis in corpus was found in 23 patients.

Inclusions and exclusions

A patient in the Barrett series was included if he/she had a segment of Barrett's mucosa 2 cm or more in length that was verified by endoscopy and histology of the biopsies taken below the squamocolumnar junction (*z*-line). The biopsies had to show the presence of intestinal metaplasia of incomplete type ("specialized columnar epithelium"), i.e. intestinal metaplasia of type II or III in the Alcian blue (pH 2.5)-PAS-stained sections[14]. In incomplete type of intestinal metaplasia, both goblet cells and columnar epithelium between the goblet cells showed secretory mucins that were stained blue with Alcian blue (pH 2.5)-PAS.

The following patients were excluded: patients with a short segment Barrett (the presence of "specialized columnar epithelium" in biopsies from a segment that is less than 2 cm long); patients with erosive esophagitis, ulcers, or polyps, or those with any endoscopically visible local lesions in stomach or esophagus.

Use of PPIs

Patients and controls with a long-term use of PPIs were excluded from the study, and none of the patients or controls was recorded having used PPI at the time of the diagnosis (information obtained from the patient at endoscopy). Thus, the present BE patients represented the native cases of dyspeptic subjects in whom BE was accidentally diagnosed in a diagnostic endoscopy, and in the subjects who did not receive any effective treatment.

Endoscopy

Diagnostic upper-GI endoscopy was done in all patients and controls. In both patient and control series, two groups were formed: the whole study population that included all patients and controls, and a subgroup of patients and controls in which the histology showed normal and healthy gastric mucosa (updated Sydney criteria) in both antrum and corpus biopsies (no gastritis, no atrophy, no intestinal metaplasia, nor *H pylori*). In the Barrett series, 16 of 19 patients (84%) were classified into the subgroup 2 (subjects with healthy and normal gastric mucosa). In controls, 105 of 199 (53%) subjects were classified into the subgroup 2.

Assay of amidated gastrin-17

G-17 was determined using specific EIA tests (G-17 EIA test kit Cat. No. 601 030, Biohit Plc, Helsinki, Finland) performed in batches of 40 samples on a microwell plate according to the instructions of the manufacturer. The EIA technique was based on measuring the absorbance after a peroxidation reaction at 450 nm. Between the reaction steps the plates were washed in a BW50 microplate strip washer (Biohit Plc, Helsinki, Finland). The absorbances were measured using a microplate reader (BP800 Microplate Reader, Biohit Plc, Helsinki, Finland). For determination of G-17 values, a 2nd order fit on standard concentrations was used to interpolate/extrapolate unknown sample concentrations automatically with the help of the BP800 in-built software (Biohit Plc, Helsinki, Finland).

The monoclonal antibody (Mab) of G-17 in the EIA tests was highly specific. The G-17 antibody used detected only amidated G-17, but no other gastrin molecules or fragments (e.g., glycine extended G-17, a kind gift from Prof. Jens F Rehfeld, Copenhagen, Denmark; human synthetic gastrin-34, G-5024, Sigma; human synthetic gastrin-13, G-0267, Sigma; or cholecystokinin fragment 26-33 amide, C-2901, Sigma) were detected. In immunohistochemistry (formalin-fixed, paraffin-embedded specimens: dilutions up to 10 000), the G-17 antibody stained only antral G cells and glands, not other cells or tissues in stomach, duodenum, small or large bowel, or pancreas. The G-17 EIA results correlated well with those of the G-17 RIA (by the courtesy of Prof. Jens F Rehfeld and Dr. Jens-Peter Gotze, Copenhagen, Denmark).

The G-17 assays from serum samples were done first after an overnight fast (G-17fast) and 20 min after a drink of a glass of a protein-rich juice (Biohit Plc, Helsinki, Finland) in which the protein content corresponded to that in an ordinary beef.

Specificity of G-17 antibody

The specificity of the antibody to G-17 secreted from antral G cells alone has been recently verified[15]. The G-17 assay measured only amidated G-17, and not other gastrin fragments.

Invasive and non-invasive tests for gastritis and atrophic gastritis

In addition to endoscopy and histology, the patient and control series were also classified into those with normal and healthy stomach or into those with non-atrophic or atrophic gastritis by serological tests which applied assays of *H pylori* antibodies, pepsinogens I (PGI) and II (PGII) and postprandial G-17 in serum (GastroPanel, Biohit Plc, Helsinki, Finland). The patients without *H pylori* antibodies and with PGI 50 microg/L, or more or above, were considered to have normal and healthy stomach mucosae.

Ethics

The study was approved by the Ethical Committee of the

Helsinki District University Hospital (HUCH), Helsinki, Finland. The purpose of the study was explained to all patients before taking blood samples, and all patients signed a written consent before enrolment into the study.

Statistical analysis

Non-parametric tests (Wilcoxon-Mann-Whitney test; χ^2 test; SPSS 10.1 Software) were used in the calculations of the significance between the groups. In order to examine the clinical value of low serum G-17 in the diagnosis of BE, the likelihood ratio (LR+) of the positive test result (low G-17fast or G-17prand) between the cases and controls was calculated at arbitrary cut-off levels of G-17. The LR+ indicates a factor by which the pre-test odds of BE has to be multiplied to obtain the post-test odds and, further, the post-test probability of the disease.

[illegible]

The mean and median values of serum G-17fast were significantly lower in patients with long-segment BE than in controls. This was the case both in males and females, or when the analysis was done in the whole study population (all patients and controls), or if the analysis was limited to subgroups of patients and controls with histologically normal and healthy gastric mucosa. The results in the whole study population and among those with healthy stomach mucosa are shown in Figures 1 and 2 in a box-plot form.

In contrast to G-17fast, the serum levels of postprandial G-17 (G-17prand) were significantly lower in BE patients than in controls in the whole study population only but not in the subjects with normal and healthy stomach mucosae (Figure 2).

The positive LR+ of low serum G-17 to predict odds of BE in the whole study population below the arbitrary cut-off levels of G-17fast are presented in Table 1. The corresponding results in the subgroups of cases and controls with histologically normal, healthy gastric mucosa are shown in Table 2. It appears that the LR+ gradually increased with a decreasing concentration of G-17fast. The sensitivity and specificity of low serum G-17fast (<1 pmol/L) to indicate BE in the whole study population were 47% and 89%, respectively.

The study population was also classified into those with normal and healthy stomach mucosae (16 BE patients and 108 controls) and those with gastritis or atrophic gastritis (3 BE patients and 91 controls) by applying the serological tests (GastroPanel, Biohit Plc, Helsinki, Finland). By these tests, the stomach mucosa was healthy when *H pylori* antibodies were not present and the serum pepsinogen I was 50 μg/L, or more. Among the patients diagnosed to have a healthy stomach mucosa by these tests, the LR+s of BE are presented in Table 3. The sensitivity and specificity of low serum G-17fast (<1 pmol/L) to indicate BE were 50% and 82%,

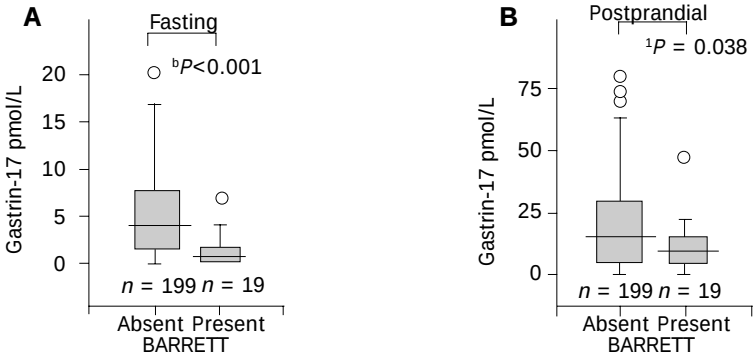

Figure 1 Fasting (A) and postprandial (B) serum G-17 levels in patients with or without long-segment BE in the whole study population. A box plot presentation. The boxes show the central 50% of the cases. The length of the box shows the range within which the center 50% of the values fell. The whiskers show the range of values that fall within 1.5×difference of the values of median from the two hinges of the box. Differences: ^bP<0.001; ^1P = 0.038; non-parametric test (Mann-Whitney *U*). To make the figure clear, the very most extreme outliers are not shown in the pictures.

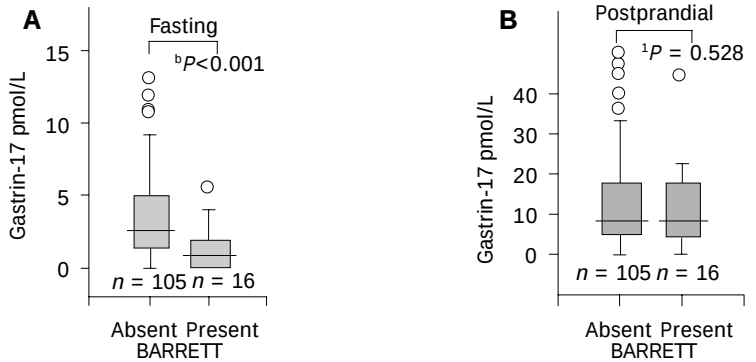

Figure 2 Fasting (A) and postprandial (B) serum G-17 levels in patients with or without long-segment BE among patients and controls with normal and healthy stomach mucosae (no gastritis, no *H pylori*, and no atrophy). A box plot presentation (see Figure 1). Differences: ^bP<0.001; ^1P = 0.528; non-parametric test (Mann-Whitney *U*). To make the figure clear, the very most extreme outliers are not shown in the pictures.

Table 1 LR+ of low serum level of fasting G-17 in whole study population

G-17fast pmol/L	Barrett *n*	Controls *n*	LR+(95%CI)
<0.5	7	21	3.5 (1.3-9.3)
<1	9	31	3.0 (1.3-7.3)
<1.5	13	48	2.8 (1.3-6.1)
<2	15	66	2.4 (1.1-4.9)
<3	17	89	2.0 (1.0-4.0)
<5	18	123	1.5 (0.8-3.0)
All	19	199	1

Table 2 LR+ of low serum level of fasting G-17 in patients and controls (males and females) with normal and healthy gastric mucosae (histology)

G-17fast pmol/L	Barrett *n*	Controls *n*	LR+(95%CI)
<0.5	6	7	5.6 (1.7-19)
<1	7	12	3.8 (1.3-11)
<1.5	10	25	2.6 (1.1-6.5)
<2	12	42	1.9 (0.8-4.3)
<3	14	61	1.5 (0.7-3.3)
<5	15	79	1.2 (0.6-2.7)
All	16	105	1

Table 3 LR+ of low serum level of fasting G-17 in patients and controls with healthy gastric mucosa, no *H pylori* antibodies and serum pepsinogen I ⩾50 μg/L

G-17fast pmol/L	Barrett *n*	Controls *n*	LR+(95%CI)
<0.5	6	13	3.1 (1.0-9.4)
<1	8	19	2.8 (1.1-7.6)
<1.5	11	34	2.2 (0.9-5.1)
<2	13	49	1.8 (0.8-4.0)
<3	15	65	1.6 (0.7-3.4)
<5	15	81	1.3 (0.6-2.7)
All	16	108	1

respectively, and at the cut-off level <2 pmol/L 81% and 55%, respectively. The corresponding overall accuracies were 77% and 55%, respectively.

In the whole study population, the G-17fast was very low (<0.5 pmol/L) in 7 of the 19 BE (37%) and 15 of the 199 controls (8%). Correspondingly, the G-17fast was lower than 2 pmol/L in 15 of 19 BE patients (79%) and in 66 of 199 controls (33%, $P<0.001$; χ^2). The G-17fast was 5 pmol/L or more in 1 of 19 BE patients (5%) but in 76 of 199 controls (38%, $P<0.01$; χ^2). In this BE patient, the G-17fast was 5.4 pmol/L.

Three BE patients had *H pylori*-positive chronic gastritis in the biopsy specimens from antrum and corpus. In one of these patients, gastritis was strongly antrum dominant and showed intestinal metaplasia of moderate grade in the antral biopsy specimens. In spite of the presence of gastritis, all three of these BE patients had a low serum level of G-17fast (0.02, 0.6, and 1.4 pmol/L).

Among controls with normal and healthy stomach mucosae (antrum and corpus mucosae were histologically healthy), age and serum G-17fast did not correlate (Pearson correlation 0.05; $P = 0.587$); neither was there any difference in the serum G-17fast between males and females (mean±SD: 4.7±5.7 and 4.1±5.4 pmol/L, respectively).

[redacted]

The present data indicate that the mean and median levels of serum G-17fast tend to be lower in patients with "native" (without previous or ongoing medication, nor previous knowledge of the disease) BE than in controls among outpatients referred to diagnostic endoscopy for dyspeptic symptoms. The BE is associated inversely with the serum level of G-17fast.

An inverse association between the likelihood of BE and serum level of G-17 was seen among the subjects with healthy stomach mucosa (normal gastric histology) and in the whole study population including subjects with gastritis and *H pylori* infection. Several earlier studies have shown that gastric inflammation (gastritis) tends to raise the serum levels of gastrin and other gastric peptides[4,16-18]. In accordance with this, the serum G-17fast levels were higher in the non-BE patients with gastritis than in those without. However, a surprise was that gastritis did not clearly raise the G-17fast concentrations in the present BE patients. Three of the nineteen BE patients had chronic *H pylori* gastritis and all had low serum G-17fast levels that did not differ from those in BE patients without gastritis.

The observations suggest that the inverse relationship between G-17fast and BE is a genuine characteristic of the Barrett's disease itself, and is not a result from gastric inflammation or atrophy, or *H pylori*. The low mean and median levels of G-17fast in BE patients are best explained by assuming that the basal intragastric acidity (basal acid output, BAO) tends to be higher in BE patients than in ordinary dyspeptic patients referred to diagnostic endoscopy. High intragastric acidity may, on the other hand, inhibit the release of G-17 from stomach mucosa, resulting thereby in low serum levels of fasting G-17. In other words, the BE patients may frequently have BAO levels that inhibit the release of G-17 from antral G cells. In two earlier studies, an elevated BAO has been shown to be a characteristic of patients with BE when compared to healthy controls[19,20].

Gastrins themselves have been linked to the pathogenesis of BE in some studies. Gastrins may have direct influences on growth and replication of the metaplastic Barrett epithelium[21], and may impair the esophageal motility and the function of the lower esophageal sphincter[22]. The present study indicates, however, that a low G-17fast in the circulation is a characteristic of BE, and that serum levels of G-17fast above 5 pmol/L are quite rare in BE patients.

Postprandial serum G-17 did not differ between BE and non-BE groups when investigated among subjects with healthy gastric mucosa. This may indicate that the post-stimulation level of serum G-17 does not reflect the intragastric acidity similarly as the fasting level of G-17 (G-17fast). Instead, the G-17prand may merely indicate the number of G cells in the antral mucosa, similarly as the peak acid output and maximal acid output (MAO) are measures of the number and mass of parietal cells in the oxyntic mucosa. Supporting this conclusion, atrophic antral gastritis results in a loss of antral G cells and, consequently, the serum G-17prand levels are low in these patients[23,24].

It was reported that the serum levels of total gastrin are similar in BE patients and controls even though the BAO and MAO are significantly increased[20]. Total serum gastrin was not assayed in the present study. Total immunoreactive gastrin consists of several gastrin fragments of which one-third are G-17 molecules under fasting conditions[25]. The fasting levels of G-17 tend to be very low in normal, healthy subjects in general, and these low G-17 concentrations may be easily eclipsed by other gastrin compounds.

In summary, the present investigation suggests that the serum level of G-17fast tends to be low in native BE patients who are not under PPI medication.

□□□□□□□□□□

1 **Hirschowitz BI**, Molina E. Relation of gastric acid and pepsin secretion to gastrin levels in dogs given bombesin and gastrin-17. *Am J Physiol* 1983; **244**: G546-551
2 **Muller J**, Kirchner T, Muller-Hermelink HK. Gastric endocrine cell hyperplasia and carcinoid tumors in atrophic gastritis type A. *Am J Surg Pathol* 1987; **11**: 909-917
3 **Malmström J**, Stadil F. Gastrin content and gastrin release. Studies on the antral content of gastrin and its release to serum during stimulation by food. *Scand J Gastroenterol* 1976; **37**: 71-76
4 **Petersen B**, Andersen BN. Increased concentrations of the NH2-terminal fragment of gastrin-17 in acute duodenal ulcer and acute gastritis. *Scand J Gastroenterol* 1983; **18**: 635-641
5 **Stepan V**, Sugano K, Yamada T, Paerk J, Dickson CJ. Gastrin biosynthesis in canine G cells. *Am J Physiol Gastrointest Liver Physiol* 2002; **282**: 766-775
6 **Spechler SJ**. Barrett´s esophagus and esophageal adenocarcinoma: pathogenesis, diagnosis, and therapy. *Med Clin North Am* 2002; **86**: 1423-1445
7 **Fitzgerald RC**. Significance of acid exposure in Barrett´s esophagus. *Am J Gastroenterol* 2003; **98**: 699-700
8 **Falk GW**. Barrett´s esophagus. *Gastroenterology* 2002; **122**: 1569-1591
9 **Zaninotto G**, Portale G, Parenti A, Lanza C, Costantini M, Molena D, Ruol A, Battaglia G, Costantino M, Epifani M, Nicoletti L. Role of acid and bile reflux in development of specialized metaplasia in distal oesophagus. *Dig Liver Dis* 2002; **34**: 251-257
10 **Cameron AJ**. Epidemiology of columnar-lined esophagus and adenocarcinoma. *Gastroenterol Clin North Am* 1997; **26**: 487-494
11 **Romero Y**, Cameron AJ, Schaid DJ, McDonnell SK, Burgart LJ, Hardtke CL, Murray JA, Locke GR 3rd. Barrett's esophagus: prevalence in symptomatic relatives. *Am J Gastroenterol* 2002; **97**: 1127-1132
12 **Gerson LB**, Shetler K, Triadafilopoulos G. Prevalence of Barrett's esophagus in asymptomatic individuals. *Gastroenterology* 2002; **123**: 636-639
13 **Bersentes K**, Fass R, Padda S, Johnson C, Sampliner RE. Prevalence of Barrett's esophagus in Hispanics is similar to Caucasians. *Dig Dis Sci* 1998; **43**: 1038-1041
14 **Spechler SJ**. Columnar-lined epithelium. Definitions. *Chest Surg Clin N Am* 2002; **12**: 1-13
15 **Goetze JP**, Paloheimo LI, Linnala A, Sipponen P, Hanssen CP, Rehfeld JF. Gastrin-17 specific antibodies are too specific for gastrinoma but stain G-cells. *Scand J Gastroenterol* 2005; 40: 596-598
16 **Mulholland G**, Ardill JE, Fillmore D, Chittajallu RS, Fullarton GM, McColl KE. *Helicobacter pylori* related hypergastrinaemia is the result of a selective increase in gastrin 17. *Gut* 1993; **34**: 757-761
17 **Beardshall K**, Moss S, Gill J, Levi S, Ghosh P, Playford RJ, Calam J. Suppression of *Helicobacter pylori* reduces gastrin releasing peptide stimulated gastrin release in duodenal ulcer patients. *Gut* 1992; **33**: 601-603
18 **Laheij RJ**, Van Rossum LG, De Boer WA, Jansen JB. Corpus gastritis in patients with endoscopic diagnosis of reflux oesophagitis and Barrett's oesophagus. A*liment Pharmacol Ther* 2002; **16**: 887-891
19 **Collen MJ**, Johnson DA. Correlation between basal acid output and daily ranitidine dose required for therapy in Barrett's esophagus. *Dig Dis Sci* 1992; **37**: 570-576
20 **Mulholland MW**, Reid BJ, Levine DS, Rubin CE. Elevated gastric acid secretion in patients with Barrett's metaplastic epithelium. *Dig Dis Sci* 1989; **34**: 1329-1334
21 **Haigh CR**, Attwood SE, Thompson DG, Jankowski JA, Kirton CM, Pritchard DM, Varro A, Dimaline R. Gastrin induces proliferation in Barrett's metaplasia through activation of the CCK2 receptor. *Gastroenterology* 2003; **124**: 615-625
22 **Straathof JW**, Lamers CB, Masclee AA. Effect of gastrin-17 on lower esophageal sphincter chracteristics in man. *Dig Dis Sci* 1997; **42**: 2547-2551
23 **Sipponen P**, Ranta P, Helske T. Kääriäinen I, Mäki T, Linnala A, Suovaniemi O, Alanko A, Härkönen M. Serum level of amidated gastrin-17 and pepsinogen I in atrophic gastritis; an observational case-control study. *Scand J Gastroenterol* 2002; **37**: 785-791
24 **Väänänen H**, Vauhkonen M, Helske T, Kääriäinen I, Rasmussen M, Tunturi-Hihnala H, Koskenpato J, Sotka M, Turunen M, Sandström R, Ristikankare M, Jussila A, Sipponen P. Non-endoscopic diagnosis of atrophic gastritis with a blood test. Correlation between gastric histology and blood levels of gastrin-17 and pepsinogen I: a multicentre study. *Eur J Gastroenterol Hepatol* 2003; **15**: 885-891
25 **Rehfeld JF**, Christiansen LA, Malmström J, Schwartz T, Stadil F. The heterogeneity of gastrin, with reference to conversion of gastrin-17. *Clin Endocrinol* 1976: **5**(Suppl): 185S-193S

Science Editor Wang XL and Guo SY **Language Editor** Elsevier HK

PO Box 2345, Beijing 100023, China
www.wjgnet.com
wjg@wjgnet.com

ELSEVIER

World J Gastroenterol 2005;11(38):5993-5996
World Journal of Gastroenterology ISSN 1007-9327

• *BRIEF REPORTS* •

Expression profiling of gastric cancer samples by oligonucleotide microarray analysis reveals low degree of intra-tumor variability

Karolin Trautmann, Christine Steudel, Dana Grossmann, Daniela Aust, Gerhard Ehninger, Stephan Miehlke, Christian Thiede

Karolin Trautmann, Christine Steudel, Dana Grossmann, Gerhard Ehninger, Stephan Miehlke, Christian Thiede, Medical Department I, University of Dresden, Dresden, Germany
Daniela Aust, Department of Pathology, University of Dresden, Dresden, Germany
Supported by a MeDDrive grant From the University of Dresden 2003 and by a grant from the Dr. Mildred Scheel Stiftung No. 70-2923
Correspondence to: Dr. Christian Thiede, Medical Department I, Fetscherstr. 74, 01307 Dresden,
Germany. thiede@mk1.med.tu-dresden.de
Telephone: +49-351458-4680 Fax: +49-351458-5362
Received: 2004-10-04 Accepted: 2004-12-23

Abstract

AIM: Gene expression profiling provides an unique opportunity to gain insight into the development of different types of gastric cancer. Tumor sample heterogeneity is thought to decrease the sensitivity and tumor specificity of microarray analysis. Thus, microdissection and preamplification of RNA is frequently performed. However, this technique may also induce considerable changes to the expression profile. To assess the effect of gastric tumor heterogeneity on expression profiling results, we measured the variation in gene expression within the same gastric cancer sample by performing a gene chip analysis with two RNA preparations extracted from the same tumor specimen.

METHODS: Tumor samples from six intestinal T2 gastric tumors were dissected under liquid nitrogen and RNA was prepared from two separate tumor fragments. Each extraction was individually processed and hybridized to an Affymetrix U133A gene chip covering approximately 18 000 human gene transcripts. Expression profiles were analyzed using Microarray Suite 5.0 (Affymetrix) and GeneSpring 6.0 (Silicon Genetics).

RESULTS: All gastric cancers showed little variance in expression profiles between different regions of the same tumor sample. In this case, gene chips displayed mean pair wise correlation coefficients of 0.94±0.02 (mean±SD), compared to values of 0.61±0.1 for different tumor samples. Expression of the variance between the two expression profiles as a percentage of "total change" (Affymetrix) revealed a remarkably low average value of 1.18±0.78 for comparing fragments of the same tumor sample. In contrast, comparison of fragments from different tumors revealed a percentage of 24.4±4.5.

CONCLUSION: Our study indicates a low degree of expression profile variability within gastric tumor samples isolated from one patient. These data suggest that tumor tissue heterogeneity is not a dominant source of error for microarray analysis of larger tumor samples, making total RNA extraction an appropriate strategy for performing gene chip expression profiling of gastric cancer.

Key words: Gastric cancer; Microarray analysis; Tissue heterogeneity

Trautmann K, Steudel C, Grossmann D, Aust D, Ehninger G, Miehlke S, Thiede C. Expression profiling of gastric cancer samples by oligonucleotide microarray analysis reveals low degree of intra-tumor variability. *World J Gastroenterol* 2005; 11(38): 5993-5996
http://www.wjgnet.com/1007-9327/11/5993.asp

INTRODUCTION

Gastric cancer is one of the most common malignancies, accounting for almost 10% of new cancer cases diagnosed worldwide[1,2]. However, knowledge about the molecular mechanisms underlying tumor development and progression is limited and molecular features of gastric cancer are not commonly used for diagnosis and treatment.

cDNA and oligonucleotide microarrays are capable of profiling gene expression patterns of tens of thousands of genes in a single experiment. They are an ideal tool to study cancer progression and development and to identify new molecular markers for tumor classification and prognosis. Microarrays have been successfully applied to study various tumors, including gastric cancers[3-13].

Like most solid tumors, gastric cancer consists of many different cell types including endothelium, different types of stromal cells and inflammatory cells. Such tissue heterogeneity is thought to decrease the sensitivity and tumor specificity of the microarray analysis[14-16]. One strategy to overcome the problem of tissue heterogeneity is the use of laser capture microdissection (LCM) for isolation of a defined cell population[17,18], followed by amplification of the RNA for subsequent microarray analysis[19,20]. However, amplification-associated bias may induce considerable changes to the expression profile[15,21]. Depending on both the degree of tissue heterogeneity and the robustness of the microarray analysis protocol, it may therefore sometimes be advantageous to avoid RNA amplification and instead extract total RNA directly from a larger tumor sample.

To assess the influence of gastric tumor heterogeneity on the outcome of the microarray analysis, we measured the variation between gene expression profiles derived from

two RNA preparations extracted from the same gastric tumor specimen.

[illegible]

Gastric tumor samples

Tumor samples from six patients who underwent surgery for gastric cancer at the University Hospital of Dresden were used for microarray analysis. Immediately after gastrectomy, a certified pathologist obtained representative samples of 1 cm^3 from the tumor centers. Special care was taken to avoid tumor necrosis. Tumors were snap-frozen in liquid nitrogen and stored at -80 ℃. To ensure consistency of the study population, only tumors classified as intestinal and T2 by pathology were included in the study[22]. Clinical and histopathological tumor characteristics are summarized in Table 1.

Table 1 Clinical data and histopathological features of gastric cancers included in the study

Tumor number	Age/Sex	Site	Lauren	TNM
1	72/Female	Antrum	Intestinal	T2 N2 G3
2	78/Male	Body	Intestinal	T2 N1 G2
3	81/Male	Antrum	Intestinal	T2 N1 G2
4	75/Female	Antrum	Intestinal	T2 N0 G3
5	76/Male	Cardia	Intestinal	T2 N2 G3
6	76/Male	Cardia	Intestinal	T2 N0 G3

RNA preparation

For RNA isolation, tumor samples were fragmented into smaller pieces under liquid nitrogen using a mortar and pestle. Subsequently, total RNA was extracted from two independent, randomly selected tumor fragments using RNAzol reagent according to the manufacturer's instructions (TelTest Inc., Friendswood, TX). Both extractions (extractions A and B) were processed individually until hybridization on two separate microarrays. To determine the influence of experimental variability, RNA was extracted only once from tumor no. 3 and aliquots of the same RNA preparation were used for further processing.

High-density oligonucleotide microarray analysis

Microarray analysis was performed according to the Affymetrix instructions for eukaryotic sample preparation[23]. In summary, double-stranded cDNA was synthesized from 5 μg of total RNA with oligo$(dT)_{24}$ T7 primer (Affymetrix), followed by *in vitro* transcription of cRNA synthesis using Enzo BioArray High Yield RNA Transcript Labeling Kit (Affymetrix) and the biotinylated cRNA was hybridized to Affymetrix U133A gene chip arrays containing 22 253 probe sets (approximately 18 000 human gene transcripts). The hybridized probe array was stained with streptavidin–phycoerythrin conjugate and scanned by the Affymetrix gene chip scanner.

Statistical analysis

Expression profiles were analyzed using Microarray Suite 5.0 (Affymetrix) and GeneSpring 6.0 (Silicon Genetics). We used the Affymetrix software to identify changes in expression levels between fragments of the same tumor specimen using standard protocols recommended by Affymetrix[24]. For normalization, data from each expression array were scaled, so that the overall fluorescence intensity across each chip was equivalent (average target intensity set at 500). Only relative changes equal or greater than twofold level of expression were considered. For a given gene transcript in any chip-to-chip comparison, Microarray Suite Software generates a "change call" parameter ("Increase" or "Decrease") based on a consideration of signal specificity as well as intensity. In other words, the "change call" is based on an evaluation of the intensities of the signals generated from each gene transcript on one chip relative to the corresponding signal intensities on the other chip. Instances where the signal on the higher intensity chip is falsely elevated are called "Increased" in a comparison between two chips derived from the same target preparation. "Decrease" calls represent instances where the signal on the lower intensity array has been falsely elevated. Consequently we define all "Increase" or "Decrease" calls in a comparison between arrays derived from the same target preparation as false positive. According to the Affymetrix specification, a percentage of "total change" up to 2% between two chips derived from the same hybridization cocktail is acceptable. To confirm results derived by Microarray Suite, GeneSpring was used to perform multiple comparisons between arrays and to generate pairwise correlation coefficients (Spearman correlation) for all arrays.

[illegible]

RNA and hybridization quality control parameters

Extracted total RNA was evaluated on a 2% agarose gel for the presence of 28S and 18S rRNA bands, which were clearly visible in all RNA samples. RNA purity was assessed by UV spectrophotometry. An $A_{260/280}$ ratio >1.9 was achieved in all samples. Total RNA was also used for RT-PCR of a housekeeping mRNA species to assess RNA quality. Human GAPDH (Applied Biosystems Inc., Foster City, CA, USA) was robustly amplified in all cases.

We followed the Affymetrix guidelines for efficient hybridization: Among the 22 253 probe sets, there was a consistent percentage of "present" calls for each of the 12 cRNA samples tested with a median of 50.68 (range 42.9-54.7). No array image showed grossly visible artifacts. The ratio of the 3' probe set to the 5' probe set of the GAPDH internal control gene, which acts as an indicator for overall RNA quality was below three in all cases. RNA and gene chip hybridization quality control parameters are summarized in Table 2.

Intra-tumor variability

Expression profiles from five gastric tumors were used to determine the degree of intra-tumor variability. As shown in Table 3, all gastric cancers demonstrated very little variance in expression profiles between different regions of the same tumor sample. In this case, expression arrays displayed mean pairwise correlation coefficients of 0.95±0.02, in contrast to values of 0.61±0.1 when different tumor samples were compared to each other. In accordance, the variance between two expression profiles calculated with the Affymetrix software

Table 2 RNA and hybridization quality control parameters

Extraction /Tumor number	$A_{260/280}$ ratio	GAPDH CT	Present calls (%)	GAPDH 3′5′ ratio
A/1	2.18	15.86	52.5	1.08
B/1	2.18	15.7	52.3	1.26
A/2	2.09	15.8	49.2	0.89
B/2	2.07	15.6	54.4	1.19
A/3	2.1	15.2	53.5	1.09
B/3	2.1	15.2	52.5	1.08
A/4	2.07	15.5	48.8	0.99
B/4	2.08	15.2	49.8	0.96
A/5	2.15	16.07	51.7	1.95
B/5	2.24	16.15	54.7	1.46
A/6	2.19	16.08	42.9	1.58
B/6	2.13	16.2	45.9	1.34

(percentage of "total change") revealed a remarkably low average value of 1.18±0.78 for comparing fragments of the same tumor sample. This result is even more striking in light of the Affymetrix guidelines, which suggest that a percentage of "total change" up to 2% is tolerable for comparing chips derived from the same hybridization cocktail. In contrast, when we compared tumor fragments from different tumors the percentage of "total change" was 24.4±4.5. As an example, Figure 1 illustrates different analyses results for two regions of the same gastric cancer sample (Figure 1A) and for two different gastric cancer samples (Figure 1B). In conclusion, there is a surprisingly low degree of expression profile variability within all gastric tumor samples studied.

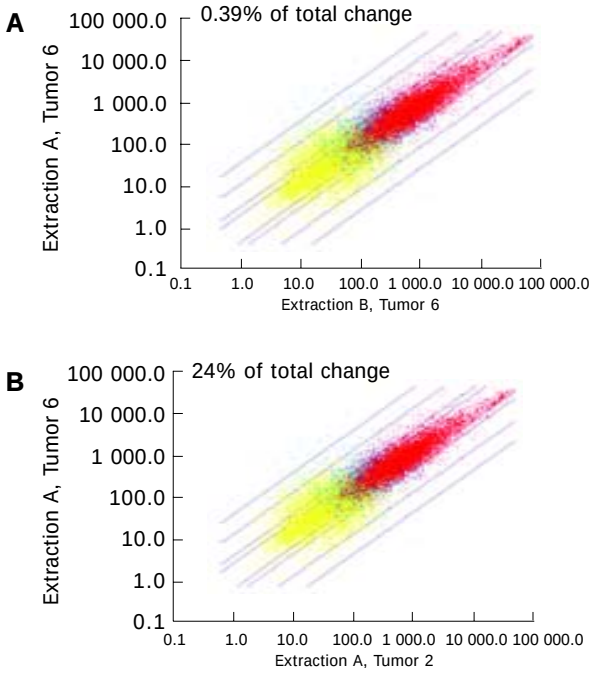

Figure 1 Scatter plots of the expression profiles derived from two different regions of the same gastric cancer sample (extraction A *vs* extraction B from tumor no. 6) (B) and from two different gastric cancer samples (extraction A from tumor no. 6 *vs* extraction A from tumor no. 2). The solid lines indicate 2-, 3-, 10-, and 30-fold expression level differences. Red dots represent gene transcripts detected in both arrays, yellow dots represent gene transcripts undetectable in both arrays, and blue dots represent transcripts detectable in one but undetectable in the other array. Gene transcripts detectable in both arrays (red dots) show a high correlation and thus a low percentage of "total change" for two different regions of the same tumor sample (B), whereas they show a poor correlation and thus a high percentage of "total change" for fragments of different tumors (A).

Experimental variability

During the whole procedure of the microarray experiment, so called experimental variability is generated by multiple factors including chip manufacture, preparation of cRNA, hybridization, washing steps, *etc*. To measure the degree of experimental variability, RNA was extracted only once from tumor no. 3. Subsequently, two aliquots from the same RNA preparation were used for further processing and hybridization on two separate Affymetrix U133A arrays. In this case, gene chip expression profiles differed in only 0.18% of all genes analyzed. Likewise the correlation coefficient was 0.99, respectively. Table 3 summarizes comparison of results from all samples.

Table 3 Comparison results for all tumor samples analyzed

Comparison	Pairwise correlation coefficient	Percentage of "total change"
Tumor 1, extraction A *vs* B	0.96	1.07
Tumor 2, extraction A *vs* B	0.91	2.65
Tumor 3, extraction A *vs* B	0.99	0.08
Tumor 4, extraction A *vs* B	0.96	0.55
Tumor 5, extraction A *vs* B	0.94	1.28
Tumor 6, extraction A *vs* B	0.95	0.39

Tumor no. 3 was used to evaluate experimental variability.

DISCUSSION

Microarray studies on gastric cancer are currently based on two main methods of RNA preparation: the recently developed technique of LCM allows for the isolation of cancer cells and other subpopulations of interest from a heterogeneous piece of tumor tissue. The advantage of microdissection is that it directly focuses on the gastric cancer cells[5,10]. The disadvantage of LCM is at the level of resources and expertise. A certified pathologist is required to select the cells to be microdissected under the microscope, and microdissection itself requires an expensive technology and special training. Furthermore the amount of RNA obtained after LCM is not sufficient for microarray analysis and generally requires amplification. However, the amplification of small amounts of RNA from laser-captured samples is difficult and has been proved to be less reproducible than measurement of unamplified mRNA[15,21]. Even a minor degree of amplification bias might result in a substantial variation to the expression profile.

The approach we used here is based on total RNA extraction with RNA isolated directly from the gastric tumor tissue without the need for subsequent amplification. Hence, the microarray profile reflects all different tissue components present in the tumor. Most gastric cancer microarray studies are based on this method of RNA extraction[3,4,6-9,11-13]. This strategy is less laborious, because it does not require isolation of specific cell types. Moreover, there is usually a sufficient amount of high quality RNA obtained for microarray analysis. However, since the actual proportion of tumor cells in the gastric cancer tissue studied remains unknown, expression profiling based on this strategy may not reliably represent "true" tumor changes. In other words, the level of intra-tumor variability is crucial for the sensitivity and tumor specificity of the microarray experiment. If there is a significant amount of intra-tumor variability, LCM becomes the strategy of choice.

In this study we found an unexpectedly low degree of

expression profile variability within all gastric tumor samples studied. Randomly selected fragments from the same tumor sample displayed a striking similarity in expression profiles, while expression profiles derived from distinct tumor samples differed significantly. These data suggest that tissue heterogeneity is not a dominant source of error for microarray analysis of larger gastric tumor samples, making total RNA extraction an appropriate strategy for performing gene chip expression profiling of gastric cancer.

Our findings are in contrast to a recently published microarray study on human muscle biopsies[25], where tissue heterogeneity was a major source of expression profile variability. This indicates that our results may be exclusive for larger tumor samples and should not be generalized. It might also reflect the influence of study design and appropriate material selection on the outcome of any microarray experiment. We believe that an experienced pathologist who is able to carefully select an appropriate piece of gastric tumor for microarray experiments directly from a large tumor avoiding necrosis and infiltration by normal gastric mucosa is crucial for the quality of our results.

In our study, the degree of experimental variability was only minimal. In the early times of gene chip technology, Mills and Gordon[26] found a substantial level of experimental variability, with an average of 12% increase/decrease calls between the same RNA processed in parallel and hybridized on two Mu11k-A Affymetrix arrays. However, studies using newer, more robust Affymetrix array generations have achieved results consistent with our studies[25,27]. The low degree of experimental variability reflects the inherent advantage of the Affymetrix Gene Chip technology. Due to commercial mass production, they contain a robust series of controls designed to minimize chip-to-chip variation. The availability of standardized protocols together with the use of stringent laboratory quality control parameters also helps to reduce experimental variability.

In conclusion, we assume that gastric tumor expression profiling based on total RNA extraction reliably represents "true" tumor changes. Therefore, total RNA extraction may be the strategy of choice for microarray studies including large gastric cancer samples.

REFERENCES

1 **Neugut AI**, Hayek M, Howe G. Epidemiology of gastric cancer. *Semin Oncol* 1996; **23**: 281-291
2 **Pisani P**, Parkin DM, Bray F, Ferlay J. Estimates of the worldwide mortality from 25 cancers in 1990. *Int J Cancer* 1999; **83**: 18-29
3 **Boussioutas A**, Li H, Liu J, Waring P, Lade S, Holloway AJ, Taupin D, Gorringe K, Haviv I, Desmond PV, Bowtell DD. Distinctive patterns of gene expression in premalignant gastric mucosa and gastric cancer. *Cancer Res* 2003; **63**: 2569-2577
4 **El-Rifai W**, Frierson HF Jr, Harper JC, Powell SM, Knuutila S. Expression profiling of gastric adenocarcinoma using cDNA array. *Int J Cancer* 2001; **92**: 832-838
5 **Hasegawa S**, Furukawa Y, Li M, Satoh S, Kato T, Watanabe T, Katagiri T, Tsunoda T, Yamaoka Y, Nakamura Y. Genome-wide analysis of gene expression in intestinal-type gastric cancers using a complementary DNA microarray representing 23,040 genes. *Cancer Res* 2002; **62**: 7012-7017
6 **Hippo Y**, Yashiro M, Ishii M, Taniguchi H, Tsutsumi S, Hirakawa K, Kodama T, Aburatani H. Differential gene expression profiles of scirrhous gastric cancer cells with high metastatic potential to peritoneum or lymph nodes. *Cancer Res* 2001; **61**: 889-895
7 **Hippo Y**, Taniguchi H, Tsutsumi S, Machida N, Chong JM, Fukayama M, Kodama T, Aburatani H. Global gene expression analysis of gastric cancer by oligonucleotide microarrays. *Cancer Res* 2002; **62**: 233-240
8 **Inoue H**, Matsuyama A, Mimori K, Ueo H, Mori M. Prognostic score of gastric cancer determined by cDNA microarray. *Clin Cancer Res* 2002; **8**: 3475-3479
9 **Kim B**, Bang S, Lee S, Kim S, Jung Y, Lee C, Choi K, Lee SG, Lee K, Lee Y, Kim SS, Yeom YI, Kim YS, Yoo HS, Song K, Lee I. Expression profiling and subtype-specific expression of stomach cancer. *Cancer Res* 2003; **63**: 8248-8255
10 **Mori M**, Mimori K, Yoshikawa Y, Shibuta K, Utsunomiya T, Sadanaga N, Tanaka F, Matsuyama A, Inoue H, Sugimachi K. Analysis of the gene-expression profile regarding the progression of human gastric carcinoma. *Surgery* 2002; **131**: S39-47
11 **Suganuma K**, Kubota T, Saikawa Y, Abe S, Otani Y, Furukawa T, Kumai K, Hasegawa H, Watanabe M, Kitajima M, Nakayama H, Okabe H. Possible chemoresistance-related genes for gastric cancer detected by cDNA microarray. *Cancer Sci* 2003; **94**: 355-359
12 **Tay ST**, Leong SH, Yu K, Aggarwal A, Tan SY, Lee CH, Wong K, Visvanathan J, Lim D, Wong WK, Soo KC, Kon OL, Tan P. A combined comparative genomic hybridization and expression microarray analysis of gastric cancer reveals novel molecular subtypes. *Cancer Res* 2003; **63**: 3309-3316
13 **Liu LX**, Liu ZH, Jiang HC, Qu X, Zhang WH, Wu LF, Zhu AL, Wang XQ, Wu M. Profiling of differentially expressed genes in human gastric carcinoma by cDNA expression array. *World J Gastroenterol* 2002; **8**: 580-585
14 **Liotta L,** Petricoin E. Molecular profiling of human cancer. *Nat Rev Genet* 2000; **1**: 48-56
15 **Alizadeh AA**, Ross DT, Perou CM, van de Rijn M. Towards a novel classification of human malignancies based on gene expression patterns. *J Pathol* 2001; **195**: 41-52
16 **Lakhani SR**, Ashworth A. Microarray and histopathological analysis of tumours: the future and the past? *Nat Rev Cancer* 2001; **1**: 151-157
17 **Simone NL**, Bonner RF, Gillespie JW, Emmert-Buck MR, Liotta LA. Laser-capture microdissection: opening the microscopic frontier to molecular analysis. *Trends Genet* 1998; **14**: 272-276
18 **Emmert-Buck MR**, Bonner RF, Smith PD, Chuaqui RF, Zhuang Z, Goldstein SR, Weiss RA, Liotta LA. Laser capture microdissection. *Science* 1996; **274**: 998-1001
19 **Van Gelder RN**, von Zastrow ME, Yool A, Dement WC, Barchas JD, Eberwine JH. Amplified RNA synthesized from limited quantities of heterogeneous cDNA. *Proc Natl Acad Sci USA* 1990; **87**: 1663-1667
20 **Wang E**, Miller LD, Ohnmacht GA, Liu ET, Marincola FM. High-fidelity mRNA amplification for gene profiling. *Nat Biotechnol* 2000; **18**: 457-459
21 **Nygaard V**, Loland A, Holden M, Langaas M, Rue H, Liu F, Myklebost O, Fodstad O, Hovig E, Smith-Sorensen B. Effects of mRNA amplification on gene expression ratios in cDNA experiments estimated by analysis of variance. *BMC Genomics* 2003; **4**: 11
22 **Sarbia M**, Becker KF, Hofler H. Pathology of upper gastrointestinal malignancies. *Semin Oncol* 2004; **31**: 465-475
23 Gene chip expression analysis technical manual Affymetrix Inc.; 2003
24 GeneChip Expression Analysis Data Analysis Fundamentals Affymetrix Inc.; 2002
25 **Bakay M**, Chen YW, Borup R, Zhao P, Nagaraju K, Hoffman EP. Sources of variability and effect of experimental approach on expression profiling data interpretation. *BMC Bioinformatics* 2002; **3**: 4
26 **Mills JC**, Gordon JI. A new approach for filtering noise from high-density oligonucleotide microarray datasets. *Nucleic Acids Res* 2001; **29**: E72
27 **Unger MA**, Rishi M, Clemmer VB, Hartman JL, Keiper EA, Greshock JD, Chodosh LA, Liebman MN, Weber BL. Characterization of adjacent breast tumors using oligonucleotide microarrays. *Breast Cancer Res* 2001; **3**: 336-341

Science Editor Guo SY **Language Editor** Elsevier HK

PO Box 2345, Beijing 100023, China
www.wjgnet.com
wjg@wjgnet.com

ELSEVIER

World J Gastroenterol 2005;11(38):5997-6002
World Journal of Gastroenterology ISSN 1007-9327

• *BRIEF REPORTS* •

Effect of herpesvirus infection on pancreatic duct cell secretion

Péter Hegyi, Balázs Ördög, Zoltán Rakonczai Jr, Tamás Takács, János Lonovics, Annamária Szabolcs, Réka Sári, András Tóth, Julius G Papp, András Varró, Mária K Kovács, Mike A Gray, Barry E Argent, Zsolt Boldogköi

Péter Hegyi, Zoltán Rakonczai Jr, Tamás Takács, János Lonovics, Annamária Szabolcs, Réka Sári, First Department of Medicine, Faculty of Medicine, University of Szeged, Szeged, Hungary
Péter Hegyi, Zoltán Rakonczai Jr, Mike A Gray, Barry E Argent, School of Cell and Molecular Biosciences, University Medical School, Newcastle upon Tyne NE2 4HH, UK
Balázs Ördög, Mária K Kovács, Zsolt Boldogköi, Department of Biology, Faculty of Medicine, University of Szeged, Szeged, Hungary
András Tóth, Julius G Papp, András Varró, Mária K Kovács, Division of Cardiovascular Pharmacology, Department of Pharmacology and Pharmacotherapy, Faculty of Medicine, Hungarian Academy of Sciences, University of Szeged, Szeged, Hungary
Co-first-authors: Péter Hegyi and Balázs Ördög
Supported by a Wellcome Trust IRDA Grant to P.H. (No. 022618), Hungarian Scientific Research Funds to P.H. and J.L. (No. D42188, T43066), a Wellcome Trust Travelling Fellowship to Z.R. (No. 069470), a Bolyai Postdoctoral Fellowship to P.H. (No. 00276/04) and a National Fund for Scientific Research (OTKA) to Z.B. (No. T049171)
Correspondence to: Zsolt Boldogköi, Department of Biology, Faculty of Medicine, University of Szeged, Somogyi Bela str. 4, H-6720 Szeged, Hungary. boldog@sb4.szote.u-szeged.hu
Telephone: +36-62-545595 Fax: +36-62-545131
Received: 2004-12-09 Accepted: 2005-02-18

AIM: To examine the effect of acute infection caused by herpesvirus (pseudorabies virus, PRV) on pancreatic ductal secretion.

METHODS: The virulent Ba-DupGreen (BDG) and non-virulent Ka-RREp0lacgfp (KEG) genetically modified strains of PRV were used in this study and both of them contain the gene for green fluorescent protein (GFP). Small intra/interlobular ducts were infected with BDG virus (10^7 PFU/mL for 6 h) or with KEG virus (10^{10} PFU/mL for 6 h), while non-infected ducts were incubated only with the culture media. The ducts were then cultured for a further 18 h. The rate of HCO_3^- secretion [base efflux -$J(B^-)$] was determined from the buffering capacity of the cells and the initial rate of intracellular acidification (1) after sudden blockage of basolateral base loaders with dihydro-4,4,-diisothiocyanatostilbene-2,2,-disulfonic acid (500 μmol/L) and amiloride (200 μmol/L), and (2) after alkali loading the ducts by exposure to NH_4Cl. All the experiments were performed in HCO_3^--buffered Ringer solution at 37 ℃ (n = 5 ducts for each experimental condition). Viral structural proteins were visualized by immunohistochemistry. Virally-encoded GFP and immunofluorescence signals were recorded by a confocal laser scanning microscope.

RESULTS: The BDG virus infected the majority of accessible cells of the duct as judged by the appearance of GFP and viral antigens in the ductal cells. KEG virus caused a similarly high efficiency of infection. After blockage of basolateral base loaders, BDG infection significantly elevated -$J(B^-)$ 24 h after the infection, compared to the non-infected group. However, KEG infection did not modify -$J(B^-)$. After alkali loading the ducts, -$J(B^-)$ was significantly elevated in the BDG group compared to the control group 24 h after the infection. As we found with the inhibitor stop method, no change was observed in the group KEG compared to the non-infected group.

CONCLUSION: Incubation with the BDG or KEG strains of PRV results in an effective infection of ductal epithelial cells. The BDG strain of PRV, which is able to initiate a lytic viral cycle, stimulates HCO_3^- secretion in guinea pig pancreatic duct by about four- to fivefold, 24 h after the infection. However, the KEG strain of PRV, which can infect, but fails to replicate, has no effect on HCO_3^- secretion. We suggest that this response of pancreatic ducts to virulent PRV infection may represent a defense mechanism against invasive pathogens to avoid pancreatic injury.

Key words: Pancreas; Hypersecretion; Ductal cells; Infection; Pseudorabies virus

Hegyi P, Ördög B, Rakonczai Z Jr, Takács T, Lonovics J, Szabolcs A, Sári R, Tóth A, Papp JG, Varró A, Kovács MK, Gray MA, Argent BE, Boldogköi Z. Effect of herpesvirus infection on pancreatic duct cell secretion. *World J Gastroenterol* 2005; 11(38): 5997-6002
http://www.wjgnet.com/1007-9327/11/5997.asp

INTRODUCTION

Pseudorabies virus (PRV) is an α-herpesvirus closely related to the herpes simplex virus (HSV), a well-known human pathogen[1,2]. The natural host of PRV is the pig, but it has a very wide host range including several mammalian families, such as carnivores, ungulates and rodents, but humans are resistant to PRV infection[1]. PRV infection is a multistep process initiated by the receptor-mediated attachment of the virus to the cell surface. Upon entering the cells, the PRV nucleocapsid approaches the nuclear membrane and the viral DNA is released into the nuclei by a poorly understood mechanism. The lytic cycle of the virus is controlled by a transcriptional cascade mechanism[2].

Acute pancreatitis is most commonly associated with

biliary stone and alcoholism. Other causes, including infections, drugs, lipid abnormalities, congenital anomalies, trauma, tumors, and idiopathic form, account for at least 10-20% of the total number of cases[3]. The incidence of pancreatitis may even be higher since the diagnosis of acute pancreatitis may go undetected in many patients. Several viruses have been reported to cause acute pancreatitis, including coxsackievirus B3[4] and B4[5], mumpsvirus[6], varicella[7], hepatitis A[8] and B[9], cytomegalovirus[10], varicella-zoster virus[11] and HSV[12].

We have previously shown that hypersecretion can be observed during the early phase of experimental edematous and necrotizing pancreatitis[13]. However, the source and the role of this hypersecretion are unknown. Either acinar cells and/or the ductal epithelium could be responsible for hypersecretion.

Our aim in this study was to examine the effect of acute infection caused by PRV on pancreatic ductal secretion.

□□□□□□□□□ □□□ □□□□□□□

Virus strain

Ba-Dup Green (BDG), a genetically modified replicating strain of PRV, was used in this study. The Bartha virus[14], which is an attenuated live vaccine strain of PRV, was used as the parental virus for the generation of BDG. Two copies of a genetically modified green fluorescent protein (GFP) gene-containing expression cassettes were inserted into the PRV antisense promoter region located in the inverted repeat segment of the virus[15,16]. Ka-EP0lacgfp (KEG) strain of PRV was used as a non-replicating control virus for these experiments. KEG was constructed by deleting the small subunit of ribonucleotide reductase[17] and the early protein 0 (EP0)[18] genes. An expression cassette containing a GFP and a lacZ gene was inserted in place of the EP0 gene[19]. These mutations render the virus incapable of replication in non-dividing cells[19].

Isolation and infection of pancreatic ducts

Small intra/interlobular ducts were isolated from the pancreas of guinea pigs weighing 150-250 g. The guinea pig was humanely killed by cervical dislocation, the pancreas was removed and intra/interlobular ducts were isolated by enzymatic dissociation, microdissection and then cultured at 37 ℃ in 50 mL/L CO_2[20]. Ducts were incubated in McCoy's-based culture medium containing BDG viruses at a dose of 10^7 PFU/mL for 6 h or KEG virus (10^{10} PFU/mL for 6 h), while the non-infected ducts were exposed to culture media only. The ducts were then cultured for a further 18 h as described earlier[20], during which time the ducts seal to form a closed sac that swells due to accumulation of ions and water secretions within the duct lumen[20].

Immunohistochemistry

The immunofluorescent detection of structural viral proteins was performed as follows. Isolated pancreatic ducts were fixed in 40 g/L paraformaldehyde in PBS, pH 7.4 for 1 h at room temperature. Following three rinses in PBS, the ducts were blocked with 10 g/L bovine serum albumin and 1 mL/L Triton X-100 in PBS for 1 h at room temperature. Thereafter, a rabbit polyclonal antiviral antibody (Affinity Bioreagents, Golden, USA) diluted at 1:500 (v/v) in blocking solution was applied for 24 h at 4 ℃. After being washed with PBS, the ducts were incubated with an anti-rabbit antibody conjugated with a red light-emitting dye (Alexa Fluor® 633; Molecular probes, USA) diluted at 1:1 000 (v/v) in a blocking solution for 24 h at 4 ℃. After further washing in PBS, the ducts were mounted on slides using Aqua-Poly/ Mount (Polysciences Inc., Niles, USA). The specificity of immunohistochemical procedure was assessed by simultaneous staining of non-infected ducts. No immunohistochemical labeling was observed in control experiments.

Microscopy

For monitoring virally expressed GFP and immunofluorescence signals, fluorescent images and optical sections of the infected ducts were recorded by a confocal laser scanning microscope (Zeiss, LSM 400).

Measurement of intracellular pH

Cultured ducts were attached, using Cell-Tak, to a coverslip (24 mmol/L) forming the base of a perfusion chamber mounted on a Nikon Diaphot microscope (Nikon UK Ltd, Budapest, Hungary). The ducts were bathed in the standard Hepes solution at 37 ℃ and loaded with the pH-sensitive fluorescent dye 2',7'-bis-(2-carboxyethyl)-5-(and-6)-carboxyfluorescein (BCECF) by exposure to 2 μmol/L BCECF-AM for 20-30 min. After loading, the ducts were continuously perfused with solutions at a rate of 4-5 mL/min. Intracellular pH (pH_i) was measured using a microspectrofluorimeter system (Cairn, Kent, UK). A small area of 5-10 cells was excited with light at wavelengths of 490 and 440 nm, and the 490/440 fluorescence emission ratio was measured at 535 nm. Four pH_i measurements were obtained per second. *In situ* calibration of the fluorescence signal was performed using the high K^+-nigericin technique[21,22]. During calibration, the ducts were bathed in high K^+ HEPES solution and extracellular pH stepped between 5.95 and 8.46.

Determination of base efflux

The intrinsic buffering capacity (β_i) of duct cells was estimated according to the NH_4^+ pre-pulse technique[23,24]. β_i refers to the ability of intrinsic cellular components (excluding HCO_3^-/CO_2) to buffer changes of pH_i. Briefly, pancreatic duct cells were exposed to various concentrations of NH_4Cl, while Na^+ and HCO_3^- were omitted from the solution in order to block the Na^+-dependent pH regulatory mechanisms. β_i was estimated by the Henderson-Hasselbach equation. The total buffering capacity (β_{total}) was calculated from: $\beta_{total} = \beta_i+\beta_{HCO3^-} = \beta_i+2.3\times[HCO_3^-]_i$, where β_{HCO3}- is the buffering capacity of the HCO_3^-/CO_2 system and $[HCO_3^-]_i$ is the intracellular HCO_3^- concentration[24].

Measurement of HCO_3^- efflux

Inhibitor stop method Exposing the ducts to dihydro-4, 4,-diisothiocyanatostilbene-2,2,-disulfonic acid (H_2DIDS, 0.5 mmol/L) and amiloride (0.2 mmol/L) for 5 min caused a marked acidification of pH_i (Figure 2A). This acidification occurred due to inhibition of the basolateral Na^+/HCO_3^- co-transporters and Na^+/H^+ exchangers, which normally

act to transport HCO_3^- into the duct cell from the blood[25,26]. The rate of pH_i acidification after the exposure to H_2DIDS and amiloride could reflect the intracellular buffering capacity and the rate at which HCO_3^- effluxes (i.e., secreted) across the apical membrane via Cl^-/HCO_3^- exchangers and CFTR channels[24,25].

The initial rate of intracellular acidification (dpH/dt), over the first 60 s of exposure to amiloride and H_2DIDS, was calculated by linear regression analysis using 240 data points (four pH_i measurements per second)[24].

Alkali load method Exposing the ducts to 20 mol/L NH_4Cl caused an alkalization of pH_i due to the rapid influx of NH_3 into cells (Figure 3A). Recently, we demonstrated that the recovery of pH_i under these conditions was dependent on the presence of HCO_3^- in the bathing solution, suggesting that it results from HCO_3^- efflux (i.e., secretion) out of the duct cells[24]. In the present study, the initial rate of recovery from alkalosis (dpH/dt) over the first 30 s (120 pH_i measurements) in the continued presence of NH_4Cl was calculated as described previously[24].

The rates of pH_i change measured in these inhibitors stopped and alkali load experiments were converted to transmembrane base flux $J(B^-)$ using the equation: $J(B^-)= dpH/dt \times \beta_{total}$. We denoted base influx as $J(B^-)$ and base efflux (secretion) as $-J(B^-)$.

Solutions and chemicals

The standard Hepes-buffered solution contained (mmol/L) 130 NaCl, 5 KCl, 1 $CaCl_2$, 1 $MgCl_2$, 10 D-glucose, and 10 Na-Hepes. The high K^+ Hepes-buffered solution contained (mmol/L) 130 KCl, 5 NaCl, 1 $CaCl_2$, 1 $MgCl_2$, 10 D-glucose, and 10 Na-Hepes. Hepes-buffered solutions were gassed with 100% O_2 and their pH was set to 7.4 at 37 ℃ with HCl. The standard HCO_3^--buffered solution contained (mmol/L) 115 NaCl, 25 $NaHCO_3$, 5 KCl, 1 $CaCl_2$, 1 $MgCl_2$, and 10 D-glucose. The ammonia pulse solution contained (mmol/L) 95 NaCl, 20 NH_4Cl, 25 $NaHCO_3$, 5 KCl, 1 $CaCl_2$, 1 $MgCl_2$, and 10 D-glucose. HCO_3^--buffered solutions were gassed with 95% O_2/50 mL/L CO_2 to set pH to 7.4 at 37 ℃.

Chromatographically pure collagenase was obtained from Worthington (Lakewood, NJ, USA), culture media from Sigma (Budapest, Hungary). Nigericin (Sigma, Budapest, Hungary) was dissolved in absolute ethanol, H_2DIDS (from Molecular Probes,Eugene, OR, USA) and amiloride in dimethyl sulfoxide (DMSO). CellTak was obtained from Becton Dickinson Labware (Bedford, MA, USA). BCECF-AM was obtained from Molecular Probes (Eugene, OR, USA) and was made up as a 2 mmol/L stock solution using DMSO. The 10-fold concentrated PBS stock solution contained (g/L) 80 NaCl, 2 KCl, 2.4 NaH_2PO_4, 14.4 Na_2HPO_4 (pH 7.2). Chemicals were obtained from Merck (Darmstadt, Germany). Blocking solution contained 10 g/L bovine serum albumin from Sigma (Budapest, Hungary) and 1 mL/L scintillation grade Triton X-100 (BDH Chemicals, Poole, UK).

Statistical analysis

Results were expressed as mean±SE (n = 5 ducts). Statistical analyses were performed using ANOVA. $P<0.05$ was accepted as statistically significant.

Efficacy of viral infection

Two GFP-expressing cassettes were inserted into the PRV genome[15] enabling virus infection to be visualized in both living and fixed cells. Monitoring of GFP expression of BDG was utilized to assess the extent of viral infection of ductal epithelial cells. We observed that BDG virus practically infected all accessible cells of the duct when used at a titer of 10^7 PFU/mL after 24 h (Figure 1A). We used a higher concentration (10^{10} PFU/mL) of KEG virus and found a similarly high efficiency of infection (Figure 1C).

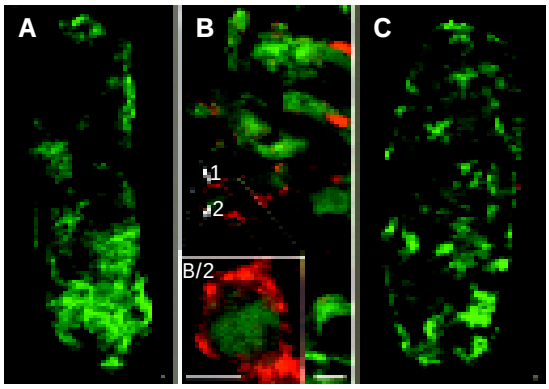

Figure 1 Infection of guinea pig pancreatic ducts with BDG and Ka-EP0lacgfp (KEG). A: Infection of the pancreatic ductal epithelial cells with BDG; B: appearance of viral antigens indicating the productive BDG infection and GFP fluorescence; C: non-virulent KEG strain-produced high efficiency of infection. Scale bars represent 10 μm.

Cytotoxic effect of PRV infection

BDG is a virulent strain; therefore, virus uptake by cells results in the immediate initiation of the lytic viral cycle and the unavoidable death of the infected cells. Productive virus infection was detected in the BDG group by labeling the structural viral proteins by means of immunohistochemistry. The GFP gene was placed under the control of the constitutive human cytomegalovirus immediate early promoter, which conferred a very early expression of the reporter gene. In contrast, viral structural proteins, which are recognized by the anti-PRV antibodies, appeared at a later stage of viral infection[15]; therefore, a shift between the appearance of GFP and immunofluorescence could be observed (Figure 1B). In contrast, in the KEG group, we did not observe any cytopathic effects and could not detect viral antigens. However, GFP expression indicated the presence of the virus within the infected cells (Figure 1C).

Pancreatic ductal bicarbonate secretion

Exposing the ducts to 0.5 mmol/L H_2DIDS and 0.2 mmol/L amiloride caused an acidification of pH_i (Figure 2A), due to inhibition of the basolateral Na^+/HCO_3^- co-transporters and Na^+/H^+ exchangers. The effect of H_2DIDS and amiloride was reversible, removal of the inhibitors caused pH_i to return to the control value. In these series of experiments, we tested whether virus infection affected the net HCO_3^- secretion of pancreatic duct cells. Base efflux was significantly elevated

in the BDG group compared to the non-infected ducts, 24 h after the infection (7.84±1.24 mmol/L B^-/min *vs* 2.2±0.18 mmol/L B^-/min, respectively; $n = 5$). However, no change was observed in the KEG group (2.4±0.32 mmol/L B^-/min; $n = 5$) compared to the non-infected ducts. These data are summarized in Figure 2B.

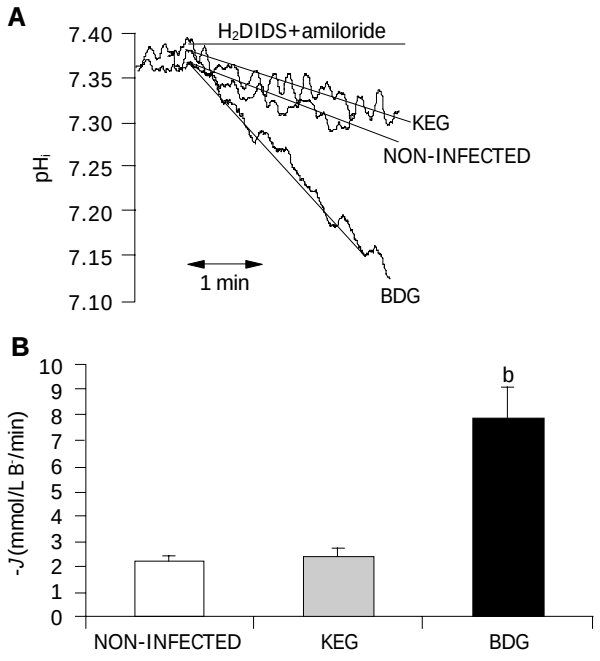

Figure 2 Inhibitor stop method for determining bicarbonate secretion. A: Representative pH_i traces; B: summary of the results obtained using the inhibitory stop method. $^bP<0.001$ *vs* the control (ANOVA).

Exposure of duct cells to 20 mmol/L NH_4Cl induced an immediate rise in pH_i due to the rapid entry of NH_3 into the duct cells (Figure 3A). In this series of experiments, base efflux was significantly elevated in the BDG group compared to the control group 24 h after the infection (160.04±19.16 mmol/L B^-/min *vs* 36.37±1.08 mmol/L B^-/min, respectively; $n = 5$). However, as we found with the inhibitor stop method, no change was observed in the KEG group (39.34±3.49 mmol/L B^-/min, $n = 5$) compared to the non-infected ducts (Figure 3B).

Using the ammonium pulse technique, we also tested whether PRV affected the ability of duct cells to recover from an acid load following removal of NH_4Cl from the superfusate. The transporters most likely to be involved in this process are the Na^+/HCO_3^- co-transporter, the Na^+/H^+ exchanger and the H^+ pump located on the basolateral membrane of the duct cells. No significant change was observed between the PRV infected and non-infected groups (Figure 3A, $n = 5$).

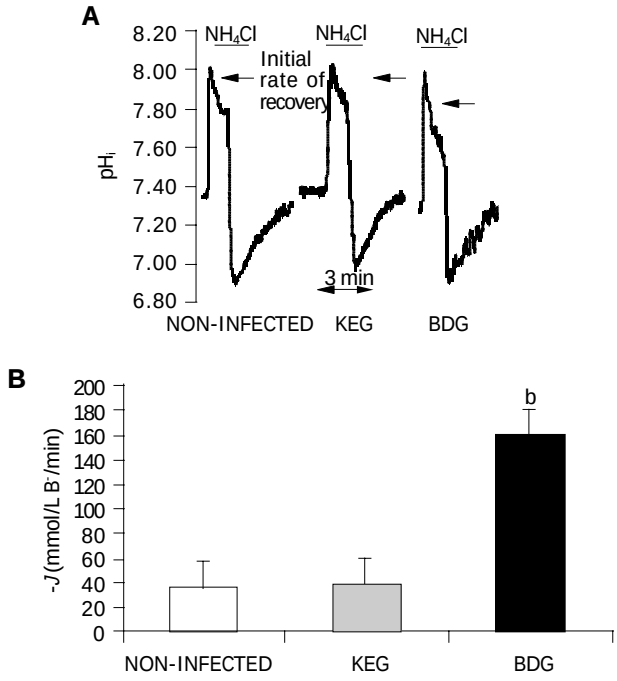

Figure 3 Alkali load method for determining bicarbonate secretion. A: Representative pH_i traces; B: summary of the results obtained using the alkali load method. $^bP<0.001$ *vs* the control (ANOVA).

[redacted]

Though the broad spectrum of etiological factors is involved in acute pancreatitis, the pathophysiology of the disease is less understood. Most investigators believe that acute pancreatitis results from an early intra-acinar cell activation of zymogens[26]. Following this early activation, a trypsin cascade occurs in the gland leading to the auto-digestion of acinar cells[26]. However, a possible pathophysiological role of the ductal epithelium has not been investigated. The permeability of the pancreatic ductal epithelium to HCO_3^- and Cl^- is increased by exposure to various bile salts at concentrations within the range normally found in the duodenum[27]. Moreover, *E. coli*-infected bile causes further increases of the permeability of the ductal epithelium to HCO_3^- and Cl^-[27]. Ethanol could induce fluid hypersecretion from guinea pig pancreatic duct cells. Low concentrations of ethanol directly augment pancreatic ductal fluid secretion stimulated by physiological and pharmacological concentrations of secretin (cAMP pathway) and via Ca^{2+} mobilization[28]. The effects of other etiologic factors for acute pancreatitis on pancreatic ductal HCO_3^- secretion have not been characterized as yet.

Viruses can alter ion transport by epithelial cells. Kunzelmann *et al*.[29], reported that parainfluenza virus I (Sendai virus) produces rapid changes in ion transport across tracheal epithelium. The Sendai virus, at concentrations observed during respiratory infections, activates Cl^- secretion and inhibits Na^+ absorption[29] by triggering the release of ATP, which then acts on apical P2Y receptors to produce changes in ion transport[29]. Bacterial infection (e.g., *Pseudomonas aeruginosa* or *Staphylococcus aureus*) triggers mucus and interleukin production[30,31]. Mucus clearance is a primary innate defense mechanism for mammalian airways[32].

In this study, we developed a model to investigate the effect of acute infection with a herpes virus (PRV) on the pancreatic ductal epithelium. Incubating BDG at a dose of 10^7 PFU/mL for 6 h resulted in the infection of the majority

of accessible epithelial cells within the duct. As expected, the virulent PRV strain resulted in a productive infection of epithelial cells, indicated by the appearance of viral antigens. We used two different measures of HCO_3^- secretion (inhibitor stop and alkali load methods) to study the effect of acute PRV infection on pancreatic ducts. Both methods showed that BDG infection stimulated HCO_3^- secretion in guinea pig pancreatic duct by about four or fivefold. However, BDG had no effect on the pH_i recovery after an acid load, suggesting that neither the basolateral Na^+/HCO_3^- co-transporter nor the basolateral Na^+/H^+ exchanger is involved in the hypersecretory effect. We have previously reported that pancreatic hypersecretion is observed during the early phase of acute necrotizing pancreatitis[33]. Furthermore, the early phase hypersecretion is accompanied with a simultaneous decrease in protein output[34], suggesting that the pancreatic ducts are at least in part involved in the change of secretory pattern. In our study, the genetically engineered control virus (KEG) did not evoke hypersecretion in the ductal cells, indicating that the presence of the virus in the cell is not enough to trigger hypersecretion. Hypersecretion was only induced by the BDG virus, which is able to initiate a lytic viral cycle.

Our finding that BDG stimulates HCO_3^- secretion from pancreatic ducts may represent a defense mechanism against invasive pathogens in order to avoid pancreatic injury. We speculate that the stimulated secretion can wash out activated enzymes, viruses and other toxic factors from the pancreas. Moreover, the high efficiency of PRV infection in the pancreatic ductal epithelium may open the possibility for gene transfer and gene therapy of the duct cells using non-replicating or conditionally replicating PRV variants (KEG)[2,19].

ACKNOWLEDGEMENTS

We would like to thank Dr. János Szabad for his helpful discussions.

REFERENCES

1 **Boldogkoi Z**, Bratincsak A, Fodor I. Evaluation of pseudorabies virus as a gene transfer vector and an oncolytic agent for human tumor cells. *Anticancer Res* 2002**;** **22**: 2153-2159
2 **Boldogkoi Z**, Nogradi A. Gene and Cancer Therapy - Pseudorabies Virus: A Novel Research and Therapeutic Tool? *Curr Gene Ther* 2003; **3**: 155-182
3 **Steer ML**. Etiology and pathophysiology of acute pancreatitis. In: The Exocrine *Pancreas: Biology, Pathobiology and Diseases*. Edited by Go VLW, Dimagno EP, Gardner JD, Lebenthal E, Reber HA, Scheele GA. *Raven Press New York* 1993: 581-593
4 **Vuorinen T**, Kallajoki M, Hyypia T, Vainionpaa R. Coxsackievirus B3-induced acute pancreatitis: analysis of histopathological and viral parameters in a mouse model. *Br J Exp Pathol* 1989; **70**: 395-403
5 **Vella C**, Brown CL, McCarthy DA. Coxsackievirus B4 infection of the mouse pancreas: acute and persistent infection. *J Gen Virol* 1992; **73**: 1387-1394
6 **Imrie CW**, Ferguson JC, Sommerville RG. Coxsackie and mumpsvirus infection in a prospective study of acute pancreatitis. *Gut* 1977; **18**: 53-56
7 **Kirschner S**, Raufman JP. Varicella pancreatitis complicated by pancreatic pseudocyst and duodenal obstruction. *Dig Dis Sci* 1988; **33**: 1192-1195
8 **Khanna S**, Vij JC. Severe acute pancreatitis due to hepatitis A virus infection in a patient of acute viral hepatitis. *Trop Gastroenterol* 2003; **24**: 25-26
9 **de Oliveira LC**, Rezende PB, Ferreira AL, de Freitas AA, de Carvalho AM, Guedes CA, Costa WO. Concurrent acute hepatitis and pancreatitis associated with hepatitis B virus: case report. *Pancreas* 1988; **16**: 559-561
10 **Wilcox CM**, Forsmark CE, Grendell JH, Darragh TM, Cello JP. Cytomegalovirus-associated acute pancreatic disease in patients with acquired immunodeficiency syndrome. Report of two patients. *Gastroenterology* 1990; **99**: 263-267
11 **Pulik M**, Teillet F, Teillet-Thiebaud F, Lionnet F, Genet P, Petitdidier C. Varicella-zoster virus pancreatitis in hematologic diseases (in French). *Ann Med Interne* 1995; **146**: 292-294
12 **Shintaku M**, Umehara Y, Iwaisako K, Tahara M, Adachi Y. Herpes simplex pancreatitis. *Arch Pathol Lab Med* 2003; **127**: 231-234
13 **Hegyi P**, Czako L, Takacs T, Szilvassy Z, Lonovics J. Pancreatic secretory responses in L-arginine-induced pancreatitis: comparison of diabetic and nondiabetic rats. *Pancreas* 1999; **19**: 167-174
14 **Bartha A**. Experimental reduction of virulence of Aujeszky's disease (in Hungarian). *Magy Allatorv Lapja* 1961; **16**: 42-45
15 **Boldogkoi Z**, Reichart A, Toth IE, Sik A, Erdelyi F, Medveczky I, Llorens-Cortes C, Palkovits M, Lenkei Z. Construction of recombinant pseudorabies viruses optimized for labeling and neurochemical characterization of neural circuitry. *Brain Res Mol Brain Res* 2002; **109**: 105-118
16 **Boldogkoi Z**, Sik A, Denes A, Reichart A, Toldi J, Gerendai I, Kovacs KJ, Palkovits M. Novel tracing paradigms-genetically engineered herpesviruses as tools for mapping functional circuits within the CNS: present status and future prospects. *Prog Neurobiol* 2004; **72**: 417-445
17 **Boldogkoi Z**, Medveczky I, Glavits R, Braun A, Fodor I. *In vivo* studies on Aujeszky's disease virus mutants. *Acta Microbiol Immunol Hung* 1996; **43**: 307-318
18 **Boldogkoi Z**, Braun A, Fodor I. Replication and virulence of early protein 0 and long latency transcript deficient mutants of the Aujeszky's disease (pseudorabies) virus. *Microbes Infect* 2000; **2**: 1321-1328
19 **Boldogkoi Z**, Szabo A, Vrbova G, Nogradi A. Pseudorabies virus-based gene delivery to rat embryonic spinal cord grafts. *Hum Gene Ther* 2002; **13**: 719-729
20 **Argent BE**, Arkle S, Cullen MJ, Green R. Morphological, biochemical and secretory studies on rat pancreatic ducts maintained in tissue culture. *Q J Exp Physiol* 1986; **71**: 633-648
21 **Thomas JA**, Buchsbaum RN, Zimniak A, Racker E. Intracellular pH-measurements in Ehrlich ascites tumor cells utilizing spectroscopic probes generated *in situ*. *Biochemistry* 1979; **18**: 2210-2218
22 **Hegyi P**, Rakonczay Z Jr, Gray MA, Argent BE. Measurement of intracellular pH in pancreatic duct cells: A new method for calibrating the fluorescence data. *Pancreas* 2004; **28**: 427-434
23 **Weintraub WH**, Machen TE. pH regulation in hepatoma cells: roles for Na-H exchange, Cl-HCO_3 exchange, and Na-HCO_3 cotransport. *Am J Physiol* 1989; **257**: G317-G327
24 **Hegyi P**, Gray MA, Argent BE. Substance P inhibits bicarbonate secretion from guinea-pig pancreatic ducts by modulating an anion exchanger. *Am J Physiol* 2003; **285**: C268-C276
25 **Szalmay G**, Varga G, Kajiyama F, Yang XS, Lang TF, Case RM, Steward MC. Bicarbonate and fluid secretion by cholecystokinin, bombesin and acetylcholine in isolated guinea-pig pancreatic ducts. *J Physiol* 2001; **535**: 795-807
26 **Lerch MM**, Albrecht E, Ruthenburger M, Mayerle J, Halangk W, Kruger B. Pathophysiology of alcohol-induced pancreatitis. *Pancreas* 2003; **27**: 291-296
27 **Reber HA**, Mosley JG. The effect of bile salts on the pancreatic

duct mucosal barrier. *Br J Surg* 1980; **67**: 59-62

28 **Yamamoto A**, Ishiguro H, Ko SB, Suzuki A, Wang Y, Hamada H, Mizuno N, Kitagawa M, Hayakawa T, Naruse S. Ethanol induces fluid hypersecretion from guinea-pig pancreatic duct cells. *J Physiol* 2003; **551**: 917-926

29 **Kunzelmann K**, Konig J, Sun J, Markovich D, King NJ, Karupiah G, Young JA, Cook DI. Acute effects of parainfluenza virus on epithelial electrolyte transport. *J Biol Chem* 2004; **279**: 48760-48766

30 **McNamara N**, Khong A, McKemy D, Caterina M, Boyer J, Julius D, Basbaum C. ATP transduces signals from ASGM1, a glycolipid that functions as a bacterial receptor. *Proc Natl Acad Sci USA* 2001; **98**: 9086-9091

31 **Ratner AJ**, Bryan R, Weber A, Nguyen S, Barnes D, Pitt A, Gelber S, Cheung A, Prince A. Cystic fibrosis pathogens activate Ca2+-dependent mitogen-activated protein kinase signaling pathways in airway epithelial cells. *J Biol Chem* 2001; **276**: 19267-19275

32 **Knowles MR**, Boucher RC. Mucus clearance as a primary innate defense mechanism for mammalian airways. *J Clin Invest* 2002; **109**: 571-577

33 **Hegyi P**, Rakonczay Z Jr, Sari R, Gog C, Lonovics J, Takacs T, Czako L. L-arginine induced experimental pancreatitis. *World J Gastroenterol* 2004; **10**: 2003-2009

34 **Czako L**, Yamamoto M, Otsuki M. Exocrine pancreatic function in rats after acute pancreatitis. *Pancreas* 1997; **15**: 83-90

Science Editor Wang XL and Guo SY **Language Editor** Elsevier HK

PO Box 2345, Beijing 100023, China
www.wjgnet.com
wjg@wjgnet.com

ELSEVIER

World J Gastroenterol 2005;11(38):6003-6008
World Journal of Gastroenterology ISSN 1007-9327

• *BRIEF REPORTS* •

Haplotype of prostaglandin synthase 2/cyclooxygenase 2 is involved in the susceptibility to inflammatory bowel disease

David G Cox, J Bart A Crusius, Petra HM Peeters, H Bas Bueno-de-Mesquita, A Salvador Peña, Federico Canzian

David G Cox, International Agency for Research on Cancer, Lyon, France (Current address: Molecular Epidemiology, Harvard School of Public Health, Boston, MA, USA)
J Bart A Crusius, Laboratory of Immunogenetics, VU University Medical Center, Amsterdam, The Netherlands
Petra HM Peeters, Julius Center for Health Sciences and Primary Care, University Medical Center, Utrecht, The Netherlands
H Bas Bueno-de-Mesquita, Department of Epidemiology, National Institute of Public Health and Environmental Protection, Bilthoven, The Netherlands
A Salvador Peña, Laboratory of Immunogenetics and Department of Gastroenterology, VU University Medical Center, Amsterdam, The Netherlands
Federico Canzian, International Agency for Research on Cancer, Lyon, France (Current address: German Cancer Research Center, Heidelberg, Germany)
Supported by The Grants from the International Agency for Research on Cancer (Special Training Award to DGC), the French Association for Research on Cancer (grant #7478), and the Crohn's and Colitis Foundation of America (to ASP)
Correspondence to: Federico Canzian, PhD, German Cancer Research Centre (DKFZ), Im Neuenheimer Feld 280, D-69120 Heidelberg, Germany. f. canzian@dkfz.de
Telephone: +49-6221-421791 Fax: +49-6221-421810
Received: 2005-01-21 Accepted: 2005-02-18

Abstract

AIM: Prostaglandin G/H synthase 2 (PTGS2 or COX2) is one of the key factors in the cellular response to inflammation. PTGS2 is expressed in the affected intestinal segments of patients with inflammatory bowel diseases (IBD). In IBD patients, non-steroidal anti-inflammatory drugs, which have been shown to reduce both the production and activity of PTGS2, may activate IBD and aggravate the symptoms. We aimed at examining genetic variants of *PTGS2* that may be risk factors for IBD.

METHODS: We genotyped 291 individuals diagnosed with IBD and 367 controls from the Dutch population for the five most frequent polymorphisms of the *PTGS2* gene. Clinical data were collected on all patients. DNA was extracted via normal laboratory methods. Genotyping was carried out using multiplex PCR followed by the Invader Assay and the 5' exonuclease assay (TaqMan). New polymorphism screening was performed by pre-screening with denaturing high-performance liquid chromatography, followed by fluorescent sequencing.

RESULTS: Allele 5209G was weakly associated with Crohn's disease (odds ratio [OR] 1.63, 95% confidence interval [CI] 1.03-2.57), and allele 8473T with ulcerative colitis (OR 1.50, 95%CI 1.00-2.27). The haplotype including both alleles showed a strong association with IBD (OR 13.15, 95%CI 3.17-116.15). This haplotype, while rare (-0.3%) in the general population, is found more frequently in patients (3.5%).

CONCLUSION: Our data suggest that this haplotype of *PTGS2* contributes to the susceptibility of IBD.

Key words: Inflammatory bowel disease; Prostaglandin G/H synthase; Cyclooxygenase; SNP; Haplotype

Cox DG, Crusius JBA, Peeters PHM, Bueno-de-Mesquita HB, Peña AS, Canzian F. Haplotype of prostaglandin synthase 2/cyclooxygenase 2 is involved in the susceptibility to inflammatory bowel disease. *World J Gastroenterol* 2005; 11(38): 6003-6008
http://www.wjgnet.com/1007-9327/11/6003.asp

INTRODUCTION

Risk factors for inflammatory bowel diseases (IBD) include several environmental and genetic exposures. Diet, tobacco smoking, and childhood diseases or poor hygiene have been identified as risk factors for IBD, with some important differences between ulcerative colitis (UC) and Crohn's disease (CD)[1-3]. Caucasians have been shown to be at higher risk than non-Caucasians, with North-South gradients seen in Europe[4,5].

Familial aggregation of IBD suggests a genetic component in the susceptibility to IBD. One major locus of susceptibility to IBD has been mapped by linkage analysis to chromosome 16, at the *CARD15/NOD2* gene[6-8], which has a role in inflammatory responses, through activation of nuclear factor NF-κB. Two more susceptibility genes have recently been identified[9,10]. Population-based association studies focused on polymorphisms of inflammatory genes, such as genes of the interleukin-1β pathway. Few showed significant associations with some degree of contradiction between studies[11-15].

Key genes involved in the regulation of the inflammatory processes, such as prostaglandin G/H synthase/cyclooxygenase (PTGS/COX), are obvious candidates to look for variants predisposing to IBD. One of the two PTGS isoforms, PTGS2/COX2, is expressed in epithelial cells and mononuclear cells in IBD[4], and it is induced in response to pro-inflammatory cytokines, including interleukin-1β[16-18]. PTGS2 is the rate-

limiting enzyme in the production of prostaglandins. Prostaglandins are thought to be essential in the process of wound healing in the gastrointestinal tract[19]. The use of non-steroidal anti-inflammatory drugs (NSAIDs), which inhibit both the transcription and activity of PTGS2, exacerbates the symptoms in UC[20] and may even activate quiescent IBD[21]. Thus, the expression of PTGS2 in the inflamed intestine might be a protective response within the wound-healing process[22]. Consequently, polymorphisms that change the amount of prostaglandins produced in inflamed cells could cause susceptibility to IBD.

To address this hypothesis, we have studied 145 UC patients, 146 CD patients, and 367 controls from the Dutch Caucasian population, which has a high incidence of IBD[23]. The present study was to search for associations between IBD and common single nucleotide polymorphisms (SNPs) in the *PTGS2* gene.

[illegible]

Samples

The recruitment of cases took place at the Department of Gastroenterology of the VU University Medical Center (VUmc), a referral center for IBD, between April 1992 and September 2000. Patients with indeterminate colitis were excluded from this study. Seventy-five UC patients were females and seventy males, with a median age of 46 years (range 19-89 years). The gender repartition of CD patients was 101 females and 45 males, with a median age of 40 years (range 15-80 years). The control population consisted of 175 healthy individuals who were students or staff at the VUmc, with a median age of 51 years (range 24-88 years). All subjects were unrelated Dutch Caucasians. Genomic DNA was extracted using the DNAzol procedure (Invitrogen).

In order to ensure that the control group was representative of the general population, a second control group was also used, consisting of 192 Dutch subjects (96 males and 96 females). These samples were selected from the European Prospective Investigation on Cancer (EPIC) cohort[24] to provide information on the genetic background in the overall Dutch population. These samples were selected to provide a similar age distribution and sex ratio as the original control group. DNA was extracted from buffy coat using Puregene chemistry (Gentra Systems, Minneapolis, MN, USA). This population-based sample was indistinguishable from the VUmc controls from the point of view of frequencies of *PTGS2* alleles and genotypes (data not shown). We take this as confirmation that both groups were drawn from the general Dutch population, at least from the genetic point of view.

Patient classification

Diagnosis and assessment of maximal extent of IBD were based on endoscopic, histopathological, and radiological criteria[25]. Patients with indeterminate colitis were not included in this study, as they can be categorized as UC or CD only at a later stage. UC patients were subdivided into three groups: proctitis, limited to the rectum (12 cases), left-sided colitis with disease activity up to the splenic flexure (72 cases), and pancolitis (61 cases), extending beyond the splenic flexure. In addition, the patients with UC were subdivided into one group with their colon *in situ* (116 cases), and a second group in which (procto)colectomy had to be performed during the course of disease (29 cases), indicative of severe or intractable disease (i.e., unresponsive to medical therapy). No patient was operated on prophylactic indication. In CD, patients were subdivided according to the Vienna classification[26]. This classification subdivides patients with CD according to age at onset (<40 years [125 cases] or ⩾40 years [21 cases]), disease behavior (non-stricturing, non-penetrating [51 cases], stricturing [63 cases], penetrating [32 cases]) and location of disease (terminal ileum [50 cases], colon [32 cases], ileocolonic [62 cases], or upper gastrointestinal tract [2 cases]). Anatomical classification is defined as the maximal extent of the disease prior to the first surgical procedure, while behavior is assessed at any time during the course of the disease.

SNP selection and genotyping

SNPs were selected from our previously collected data[27] to include those SNPs with a prevalence of greater than 5% in Caucasians. Among the SNPs we studied, the only one with a proven functional role is a SNP located in the promoter of *PTGS2*, at position 926 of GenBank entry D28235 (dbSNP rs20417), which has been shown to affect the expression of *PTGS2* mRNA[28].

The order of samples of patients and controls was randomized in the PCR plates, so that a uniform number of patients and controls could be analyzed simultaneously in each run. EPIC samples were genotyped separately.

Three SNPs were genotyped with the Invader Assay[29]. PCR for the Invader assay (Third Wave Technologies, Madison, WI, USA) was carried out in 25 μL reactions, using the following concentrations: 20 ng DNA, 20 μmol/L dNTPs, 1×Taq Platinum buffer, 1.5 mmol/L $MgCl_2$, 1.25 U Taq Platinum polymerase (Life Technologies, Inc., Gaithersburg, MD, USA), 0.5 μmol/L of each primer. The primers used were as follows (nomenclature of SNPs refers to base numbers in GenBank entry D28235):

PTGS2.401 (rs689465)
401F: AAG GAC TTA GGA CAT AAC TGA ATT TTC
401R: ATG GGT AGT GCT CAG GGA GGA G
PTGS2.3050 (rs5277)
3050F: CGT TGT GAA TAA CAT TCC CTT
3050R: ATT TTT CTT TGA GAA GGC TAA AA
PTGS2.5209 (rs20432)
5209F: ATG ATG TAT GCC ACA ATC TGG CTG
5209R: TTG TCT GGA ACA ACT GCT CAT CAC.

This multiplex reaction was then carried out in a Tetrad DNA Engine PCR machine (MJ Research, Waltham, MA, USA), with the following cycling conditions: 96 ℃ for 5 min, then 30 cycles of 96 ℃ for 30 s, 50 ℃ for 60 s, and 72 ℃ for 10 s, with a final extension of 72 ℃ for 5 min. PCR volumes were then brought up to 150 μL, and Invader reactions were carried out as per manufacturer's instructions. Plates were read in a fluorometer with excitation and emission spectra as recommended by Third Wave.

The SNPs *PTGS2*.926 and *PTGS2*.8473 were tested using the TaqMan assay with MGB chemistry (Applied Biosystems,

Foster City, CA, USA). The assay was carried out in a 10 μL reaction, with 20 ng DNA, 1×TaqMan master mix (Applied Biosystems), 0.1 μmol/L of each primer, and 0.2 μmol/L of each probe. Primer and probe sequences are as follows:
PTGS2.926 (rs20417)
926F: TTA ACT ATT TAC AGG GTA ACT GCT TAG G
926R: CTT CAC CCC CTC CTT GTT TC
926VIC: CCT TTC CCG CCT CT
926FAM: CTT TCC CCC CTC TC
PTGS2.8473 (rs5275)
8473F: ATG CAC TGA TAC CTG TTT TTG TTT G
8473R: GTT TCC AAT GCA TCT TCC ATG A
8473VIC: TGA CAG AAA AAT AAC CAA AA
8473FAM: TGA CAG AAA AAT GAC CAA A

The cycling conditions for these PCR reactions were as follows: 95 ℃ for 10 min, then 35 cycles of 95 ℃ for 15 s, and 60 ℃ (58 ℃ for *PTGS2*.926) for 60 s. Plates were then read in the ABI 7900HT sequence detection system.

Data analysis

For genotype data from the Invader assay, raw intensity counts were corrected with a negative control, and the ratio between the two signals (one color for each allele) was used to call each genotype. For the TaqMan assay, groups of genotypes (homozygote common, heterozygote, and homozygote rare) were determined manually within the SDS software (Applied Biosystems). Each SNP was tested in the control group to ensure that it does not deviate from Hardy-Weinberg equilibrium. Linkage disequilibrium tests were performed using macros developed by the authors in conjunction with the PHASE program[30] to reconstruct haplotype frequencies. Odds ratios (OR) and 95% confidence interval (CI) were calculated in Stata 7.0, using logistic regressions correcting for sex and age in analyzing genotypes at single SNPs. Simple OR were calculated when data consisted of frequencies of alleles or haplotypes in the population. All *P* values reported are two sided. SNPs were tested for effects on splicing using the Delila Server (http://www.lecb.ncifcrf.gov/-toms/delilaserver.html) at the Laboratory of Experimental and Computational Biology of the National Cancer Institute[31].

New polymorphism screening

Individuals termed "at risk" based on association testing (i.e., the 19 cases carrying the haplotype, which includes the two alleles showing increase in risk at SNPs 5 209 and 8 473) were screened for novel polymorphisms using denaturing high-performance liquid chromatography (DHPLC) via the WAVE system (Transgenomic, Omaha, NE, USA). The areas studied were the promoter region, exons 6 and 10, and the 3' UTR. The protocols followed were as published previously[27].

Figure 1 shows a graphical representation of the structure of the *PTGS2* gene. The five major SNPs as well as the polymorphisms discovered as part of this study are depicted. The allele frequencies of the five major SNPs in the control group were 11.4% (*PTGS2*.401), 13.4% (*PTGS2*.926), 14.6% (*PTGS2*.3050), 13.5% (*PTGS2*.5209), and 33.9% (*PTGS2*.8473). All SNPs, except *PTGS2*.3050, were in Hardy-Weinberg equilibrium in the control group. Table 1 shows the genotype counts of the SNPs studied, among cases and controls. The SNP at position 5 209 shows an increase in the carriers of the G allele in cases as compared to controls, with a weak but significant association was found only in CD (OR = 1.63, 95%CI 1.03-2.57, $P = 0.04$). The SNP at position 8 473 shows an increase in the frequency of the T/T homozygote genotype in cases as compared to controls, with an association of borderline significance found only in UC (OR = 1.50, 95%CI 1.00-2.27, $P = 0.05$). No association was seen with the SNPs at position 401, 926, or 3 050, although it should be noted that there is a lack of homozygous rare genotypes at bp 3 050 in the control group, which is the reason for its departure from Hardy-Weinberg equilibrium.

We analyzed differences in genotype counts among the different clinical variables for CD and UC. No statistically significant differences between classification levels were observed (data not shown).

Significant levels of linkage disequilibrium were seen among the most common SNPs in the *PTGS2* gene (data not shown). Table 2 shows the frequencies of haplotypes of the *PTGS2* gene in both IBD patients and controls. The SNP at bp 3 050 was not included in haplotype analysis, as it was not in Hardy-Weinberg equilibrium in the control population, and this has been shown to affect the accuracy of haplotype reconstruction methods[32]. All individuals were genotyped for the SNP at bp 3 050, eliminating the risk that its lack of Hardy-Weinberg equilibrium is caused by bias due to the genotyping technique missing preferentially one genotype. Haplotype frequencies were calculated using all four valid SNPs, and all data are shown. There were no differences in haplotype frequency between the two groups of IBD patients and the controls, except for haplotype AGGT, which shows an OR of 11.9 (95%CI 2.83-105.76, $P<0.00005$, for UC and CD combined). Interestingly, this haplotype includes the two alleles showing an increase in risk at SNPs 5 209 and 8 473. If we consider the haplotype including the 5209.G and 8473.T alleles (by lumping haplotypes

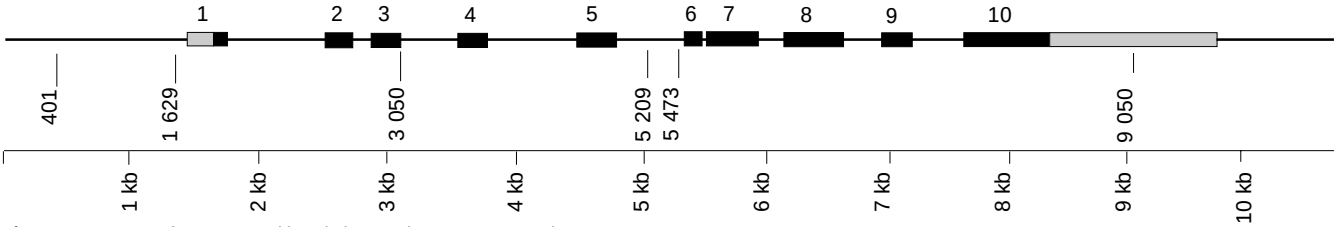

Figure 1 Structure of *PTGS2*. Positions in base pairs as per GenBank sequence D28235. Exons are shown as dark boxes, untranslated regions as light boxes. Vertical lines represent SNPs, with their positions in the sequence indicated.

Table 1 Genotype frequencies and OR for UC and CD of *PTGS2* SNPs

Genotype	Controls		UC			CD		
	n[1]	%	*n*[1]	%	OR (95%CI)[2]	*n*[1]	%	OR (95%CI)[2]
PTGS2.401								
A/A	277	79	115	82	1.00	107	77	1.00
A/G	66	19	24	17	0.82 (0.48-1.39)[3]	30	22	1.17 (0.70-1.94)[3]
G/G	7	2	1	1		1	1	
Total	350	100	140	100		138	100	
PTGS2.926								
G/G	256	75	112	81	1.00	106	76	1.00
G/C	75	22	23	17	0.77 (0.47-1.28)[3]	31	22	1.06 (0.65-1.73)[3]
C/C	8	2	4	3		3	2	
Total	339	100	139	100		140	100	
PTGS2.3050								
G/G	250	71	109	75	1.00	102	71	1.00
G/C	99	28	32	22	0.83 (0.52-1.32)[3]	38	26	0.97 (0.62-1.53)[3]
C/C	1	1	4	3		4	3	
Total	350	100	145	100		144	100	
PTGS2.5209								
T/T	265	75	110	76	1.00	95	66	1.00
T/G	81	23	30	21	1.00 (0.62-1.61)[3]	46	33	1.63 (1.03-2.57)[3]
G/G	7	2	5	3		2	1	
Total	353	100	145	100		143	100	
PTGS2.8473								
C/C	44	13	18	14	1.00[3]	21	15	1.00[3]
T/C	147	42	49	34		54	38	
T/T	155	45	78	54	1.50 (1.00-2.27)	68	47	1.10 (0.72-1.68)
Total	346	100	145	100		143	100	

[1]Numbers may not sum up to the totals of controls or cases due to genotyping failure. All samples that did not give a reliable result in the first round of genotyping were resubmitted to up to three additional rounds of genotyping. Data points that were still not filled up after this procedure were left blank. [2]All ORs are adjusted for sex and age. [3]Heterozygotes and homozygotes for the rare allele have been grouped in order to improve statistical power.

Table 2 *PTGS2* haplotype frequencies and OR for IBD

Haplotype[1]	Controls	UC cases		CD cases		UC+CD cases[2]	
	n (%)	*n* (%)	OR (95%CI)	*n* (%)	OR (95%CI)	*n* (%)	OR (95%CI)[3]
AGTT	471 (64.7)	193 (65.6)	1.00 (ref.)	183 (62.7)	1.00 (ref.)	376 (64.2)	1.00 (ref.)
AGTC	147 (20.2)	55 (18.7)	0.91 (0.64-1.30)	54 (18.5)	0.95 (0.66-1.35)	109 (18.6)	0.93 (0.69-1.24)
GCGC	64 (8.8)	22 (7.5)	0.84 (0.50-1.39)	27 (9.2)	1.09 (0.67-1.75)	49 (8.4)	0.96 (0.63-1.45)
ACGC	25 (3.4)	8 (2.7)	0.78 (0.35-1.73)	7 (2.4)	0.72 (0.31-1.66)	15 (2.6)	0.75 (0.36-1.51)
AGGT	2 (0.3)	10 (3.4)	12.2 (2.97-inf.)	9 (3.1)	11.58 (2.79-inf.)	19 (3.2)	11.9 (2.83-105.76)
Rare[4]	19 (2.6)	6 (2.0)	0.77 (0.31-1.90)	12 (4.1)	1.63 (0.78-3.37)	18 (3.1)	1.19 (0.61-2.29)

[1]The order of SNPs in the haplotypes is *PTGS2*.401, *PTGS2*.926, *PTGS2*.5209, and *PTGS2*.8473. [2]UC and CD combined. [3]ORs are not corrected as they are based on population level haplotype frequencies and are relative to the most common haplotype (AGTT). [4]Rare haplotypes (frequency ≤1% in both cases and controls).

AGGT and GCGT), we observe an increase in its frequency in patients with IBD (0.035, UC and CD combined) as compared to controls (0.003). This increase in frequency yields an OR of 13.15 (95%CI 3.17-116.15, $P<0.00005$, for UC and CD combined).

In order to test the possibility that these positive associations are in reality indicative of linkage disequilibrium with yet undiscovered nearby polymorphisms, we studied by DHPLC the 19 cases who could carry the risk haplotype. Regions of *PTGS2* surrounding the three SNPs, and in addition the promoter region, exon 1 and the UTRs were analyzed. No novel polymorphisms were discovered in the coding sequence of the gene. One SNP was discovered at bp 9 850 (A-G), with a minor allele frequency of lower than 2%. Therefore, we considered it unlikely that polymorphisms other than 5 209 or 8 473 could explain the observed associations.

[redacted]

PTGS2 is a critical enzyme involved in the production of prostaglandins, which are essential in the process of healing bowel wounds. The use of NSAIDs, which inhibit both the translation and activity of PTGS2, can induce a flare-up[21] and actually exacerbate the symptoms of IBD[20]. We hypothesized that polymorphisms in *PTGS2* might influence prostaglandin production in inflamed cells, thus affecting susceptibility to IBD. In this study, we have found a slightly increased risk of IBD associated to *PTGS2*.5209 and *PTGS2*.8473, and a strong association with a haplotype including alleles of these two SNPs.

PTGS2.5209 is in intron 5 of *PTGS2*. *In silico* analysis

of this SNP for splice site mutations[31] reveals that the T-G substitution creates a new splicing acceptor sequence with nearly the same strength as that found in normal splice sites. While this is most probably not enough of a change to exclude completely the normal splicing of exons 5-6, it could cause some "leaking", reducing the amount of normal *PTGS2* mRNA. *PTGS2*.8473, being in the 3' untranslated region (UTR), could affect the stability of *PTGS2* mRNA[33]. In fact, the unusually long 3' UTR plays an important role in determining the half-life of the mRNA. Various proteins bind to it and cause either acceleration or protection of the degradation of the mRNA[34,35].

The associations we have found between CD and *PTGS2*.5209 G/G, and UC and *PTGS2*.8473 T/T are statistically significant, but of moderate importance. We propose that it is the combination of the G allele at *PTGS2*.5209 with the T allele at *PTGS2*.8473, on the same chromosome (GT haplotype), that would have the most influence on disease status.

The association between IBD and the GT haplotype could be due to linkage disequilibrium with another polymorphism that lies nearby. To test this hypothesis, we have analyzed subjects who carry the GT haplotype for the presence of novel functional polymorphisms of *PTGS2*, but this search has not yielded any additional candidates. Linkage disequilibrium with polymorphisms in neighboring genes is not a likely explanation either, as there is no gene mapping of at less than 100 kbp on either side of *PTGS2*.

We are inclined to think that this association is not a finding by chance. First of all, we have found a higher level of linkage disequilibrium between alleles at bp 5 209 and 8 473 in controls than in cases. This could mean that natural selection has exerted pressure toward the disappearance of the GT haplotype, i.e. this haplotype might negatively affect the fitness of individuals carrying it. Additionally, we have observed that this haplotype is virtually absent not only in the Dutch population, but in other Northern European populations as well (Cox *et al*., unpublished data).

These results are the first linking of *PTGS2* to IBD. While the GT haplotype of *PTGS2* is rare, the two alleles that compose it are much more frequent, they both show a modest association with the disease, and could therefore be important for a large proportion of the population. Future steps are to replicate these findings by independent studies, to determine experimentally the extent to which *PTGS2* polymorphisms alter the expression or function of the gene, and to discover genetic or environmental factors that may alter the risk of IBD interacting with *PTGS2* alleles.

ACKNOWLEDGEMENTS

The authors thank Pietro Ferrari (Nutrition and Cancer Group, IARC) for discussion on statistical issues, Stéphanie Monnier (Genome Analysis Team, IARC) for bioinformatic support and AA van Bodegraven MD, PhD for facilitating the clinical database of the IBD patients at the VUmc.

REFERENCES

1 **Van Kruiningen HJ**, Freda BJ. A clustering of Crohn's disease in Mankato, Minnesota. *Inflamm Bowel Dis* 2001; **7**: 27-33
2 **Mahmud N**, Weir DG. The urban diet and Crohn's disease: is there a relationship? *Eur J Gastroenterol Hepatol* 2001; **13**: 93-95
3 **Koutroubakis I**, Manousos ON, Meuwissen SG, Pena AS. Environmental risk factors in inflammatory bowel disease. *Hepatogastroenterology* 1996; **43**: 381-393
4 **Farrokhyar F**, Swarbrick ET, Irvine EJ. A critical review of epidemiological studies in inflammatory bowel disease. *Scand J Gastroenterol* 2001; **36**: 2-15
5 **Karlinger K**, Gyorke T, Mako E, Mester A, Tarjan Z. The epidemiology and the pathogenesis of inflammatory bowel disease. *Eur J Radiol* 2000; **35**: 154-167
6 **Ogura Y**, Bonen DK, Inohara N, Nicolae DL, Chen FF, Ramos R, Britton H, Moran T, Karaliuskas R, Duerr RH, Achkar JP, Brant SR, Bayless TM, Kirschner BS, Hanauer SB, Nunez G, Cho JH. A frameshift mutation in NOD2 associated with susceptibility to Crohn's disease. *Nature* 2001; **411**: 603-606
7 **Hugot JP**, Chamaillard M, Zouali H, Lesage S, Cezard JP, Belaiche J, Almer S, Tysk C, O'Morain CA, Gassull M, Binder V, Finkel Y, Cortot A, Modigliani R, Laurent-Puig P, Gower-Rousseau C, Macry J, Colombel JF, Sahbatou M, Thomas G. Association of NOD2 leucine-rich repeat variants with susceptibility to Crohn's disease. *Nature* 2001; **411**: 599-603
8 **Hampe J**, Cuthbert A, Croucher PJ, Mirza MM, Mascheretti S, Fisher S, Frenzel H, King K, Hasselmeyer A, MacPherson AJ, Bridger S, van Deventer S, Forbes A, Nikolaus S, Lennard-Jones JE, Foelsch UR, Krawczak M, Lewis C, Schreiber S, Mathew CG. Association between insertion mutation in NOD2 gene and Crohn's disease in German and British populations. *Lancet* 2001; **357**: 1925-1928
9 **Peltekova VD**, Wintle RF, Rubin LA, Amos CI, Huang Q, Gu X, Newman B, Van Oene M, Cescon D, Greenberg G, Griffiths AM, St George-Hyslop PH, Siminovitch KA. Functional variants of OCTN cation transporter genes are associated with Crohn disease. *Nat Genet* 2004; **36**: 471-475
10 **Stoll M**, Corneliussen B, Costello CM, Waetzig GH, Mellgard B, Koch WA, Rosenstiel P, Albrecht M, Croucher PJ, Seegert D, Nikolaus S, Hampe J, Lengauer T, Pierrou S, Foelsch UR, Mathew CG, Lagerstrom-Fermer M, Schreiber S. Genetic variation in DLG5 is associated with inflammatory bowel disease. *Nat Genet* 2004; **36**: 476-480
11 **Watts DA**, Satsangi J. The genetic jigsaw of inflammatory bowel disease. *Gut* 2002; **50**(Suppl 3): III31-III36
12 **Nemetz A**, Nosti-Escanilla MP, Molnar T, Kope A, Kovacs A, Feher J, Tulassay Z, Nagy F, Garcia-Gonzalez MA, Pena AS. IL1B gene polymorphisms influence the course and severity of inflammatory bowel disease. *Immunogenetics* 1999; **49**: 527-531
13 **Tagore A**, Gonsalkorale WM, Pravica V, Hajeer AH, McMahon R, Whorwell PJ, Sinnott PJ, Hutchinson IV. Interleukin-10 (IL-10) genotypes in inflammatory bowel disease. *Tissue Antigens* 1999; **54**: 386-390
14 **Heresbach D**, Alizadeh M, Dabadie A, Le Berre N, Colombel JF, Yaouanq J, Bretagne JF, Semana G. Significance of interleukin-1beta and interleukin-1 receptor antagonist genetic polymorphism in inflammatory bowel diseases. *Am J Gastroenterol* 1997; **92**: 1164-1169
15 **Klein W**, Tromm A, Griga T, Fricke H, Folwaczny C, Hocke M, Eitner K, Marx M, Runte M, Epplen JT. The IL-10 gene is not involved in the predisposition to inflammatory bowel disease. *Electrophoresis* 2000; **21**: 3578-3582
16 **Kujubu DA**, Fletcher BS, Varnum BC, Lim RW, Herschman HR. TIS10, a phorbol ester tumor promoter-inducible mRNA from Swiss 3T3 cells, encodes a novel prostaglandin synthase/cyclooxygenase homologue. *J Biol Chem* 1991; **266**: 12866-12872
17 **Maier JA**, Hla T, Maciag T. Cyclooxygenase is an immediate-early gene induced by interleukin-1 in human endothelial cells. *J Biol Chem* 1990; **265**: 10805-10808
18 **Masferrer JL**, Seibert K, Zweifel B, Needleman P. Endogenous glucocorticoids regulate an inducible cyclooxygenase enzyme. *Proc Natl Acad Sci USA* 1992; **89**: 3917-3921

19 **Wallace JL**. Prostaglandin biology in inflammatory bowel disease. *Gastroenterol Clin North Am* 2001; **30**: 971-980
20 **Eberhart CE**, Dubois RN. Eicosanoids and the gastrointestinal tract. *Gastroenterology* 1995; **109**: 285-301
21 **Kaufmann HJ**, Taubin HL. Nonsteroidal anti-inflammatory drugs activate quiescent inflammatory bowel disease. *Ann Intern Med* 1987; **107**: 513-516
22 **Singer II**, Kawka DW, Schloemann S, Tessner T, Riehl T, Stenson WF. Cyclooxygenase 2 is induced in colonic epithelial cells in inflammatory bowel disease. *Gastroenterology* 1998; **115**: 297-306
23 **Russel MG**, Dorant E, Volovics A, Brummer RJ, Pop P, Muris JW, Bos LP, Limonard CB, Stockbrugger RW. High incidence of inflammatory bowel disease in The Netherlands: results of a prospective study. The South Limburg IBD Study Group. *Dis Colon Rectum* 1998; **41**: 33-40
24 **Bingham S**, Riboli E. Diet and cancer-the European Prospective Investigation into Cancer and Nutrition. *Nat Rev Cancer* 2004; **4**: 206-215
25 **Lennard-Jones JE**. Classification of inflammatory bowel disease. *Scand J Gastroenterol Suppl* 1989; **170**: 2-6
26 **Gasche C**, Scholmerich J, Brynskov J, D'Haens G, Hanauer SB, Irvine EJ, Jewell DP, Rachmilewitz D, Sachar DB, Sandborn WJ, Sutherland LR. A simple classification of Crohn's disease: report of the Working Party for the World Congresses of Gastroenterology, Vienna 1998. *Inflamm Bowel Dis* 2000; **6**: 8-15
27 **Cox D**, Boillot C, Canzian F. Data mining: Efficiency of using sequence databases for polymorphism discovery. *Hum Mutat* 2001; **17**: 141-150
28 **Papafili A**, Hill MR, Brull DJ, McAnulty RJ, Marshall RP, Humphries SE, Laurent GJ. Common promoter variant in cyclooxygenase-2 represses gene expression: evidence of role in acute-phase inflammatory response. *Arterioscler Thromb Vasc Biol* 2002; **22**: 1631-1636
29 **Mein CA**, Barratt BJ, Dunn MG, Siegmund T, Smith AN, Esposito L, Nutland S, Stevens HE, Wilson AJ, Phillips MS, Jarvis N, Law S, de Arruda M, Todd JA. Evaluation of single nucleotide polymorphism typing with invader on PCR amplicons and its automation. *Genome Res* 2000; **10**: 330-343
30 **Stephens M**, Smith NJ, Donnelly P. A new statistical method for haplotype reconstruction from population data. *Am J Hum Genet* 2001; **68**: 978-989
31 **Rogan PK**, Faux BM, Schneider TD. Information analysis of human splice site mutations. *Hum Mutat* 1998; **12**: 153-171
32 **Single RM**, Meyer D, Hollenbach JA, Nelson MP, Noble JA, Erlich HA, Thomson G. Haplotype frequency estimation in patient populations: the effect of departures from Hardy-Weinberg proportions and collapsing over a locus in the HLA region. *Genet Epidemiol* 2002; **22**: 186-195
33 **Rodriguez-Pascual F**, Hausding M, Ihrig-Biedert I, Furneaux H, Levy AP, Forstermann U, Kleinert H. Complex contribution of the 3'-untranslated region to the expressional regulation of the human inducible nitric-oxide synthase gene. Involvement of the RNA-binding protein HuR. *J Biol Chem* 2000; **275**: 26040-26049
34 **Nabors LB**, Gillespie GY, Harkins L, King PH. HuR, a RNA stability factor, is expressed in malignant brain tumors and binds to adenine- and uridine-rich elements within the 3' untranslated regions of cytokine and angiogenic factor mRNAs. *Cancer Res* 2001; **61**: 2154-2161
35 **Sheng H**, Shao J, Dixon DA, Williams CS, Prescott SM, Dubois RN, Beauchamp RD. Transforming growth factor-beta1 enhances Ha-ras-induced expression of cyclooxygenase-2 in intestinal epithelial cells via stabilization of mRNA. *J Biol Chem* 2000; **275**: 6628-6635

Science Editor Guo SY **Language Editor** Elsevier HK

PO Box 2345, Beijing 100023, China
www.wjgnet.com
wjg@wjgnet.com

ELSEVIER

World J Gastroenterol 2005;11(38):6009-6013
World Journal of Gastroenterology ISSN 1007-9327

• *BRIEF REPORTS* •

Helicobacter pylori antibiotic resistance in Iran

Marjan Mohammadi, Delaram Doroud, Nazanin Mohajerani, Sadegh Massarrat

Marjan Mohammadi, Delaram Doroud, Nazanin Mohajerani, Biotechnology Research Center, Pasteur Institute of Iran, Tehran, Iran
Sadegh Massarrat, Gastroenterology Department, Shariati Hospital, Tehran University of Medical Sciences, Tehran, Iran
Supported by a Research Grant From the Pasteur Institute of Iran, No. 198
Co-first-authors: Marjan Mohammadi and Delaram Doroud
Correspondence to: Marjan Mohammadi, Biotechnology Research Center, Pasteur Institute of Iran, Tehran, Iran. marjan@institute.pasteur.ac.ir
Telephone: +98-21-6480780 Fax: +98-21-6480780
Received: 2004-11-16 Accepted: 2005-01-26

ABSTRACT

AIM: To examine the frequency of antibiotic resistance in Iranian *Helicobacter pylori* (*H pylori*) strains isolated from two major hospitals in Tehran.

METHODS: Examination of antibiotic resistance was performed on 120 strains by modified disc diffusion test and PCR-RFLP methods. In addition, in order to identify the possible causes of the therapeutic failure in Iran, we also determined the resistance of these strains to the most commonly used antibiotics (metronidazole, amoxicillin, and tetracycline) by modified disc diffusion test.

RESULTS: According to modified disc diffusion test, 1.6% of the studied strains were resistant to amoxicillin, 16.7% to clarithromycin, 57.5% to metronidazole, and there was no resistance to tetracycline. Of the clarithromycin resistant strains, 73.68% had the A2143G mutation in the *23S rRNA* gene, 21.05% A2142C, and 5.26% A2142G. None of the sensitive strains were positive for any of the three point mutations. Of the metronidazole resistant strains, deletion in *rdxA* gene was studied and detected in only 6 (5%) of the antibiogram-based resistant strains. None of the metronidazole sensitive strains possessed *rdxA* gene deletion.

CONCLUSION: These data show that despite the fact that clarithromycin has not yet been introduced to the Iranian drug market as a generic drug, nearly 20% rate of resistance alerts toward the frequency of macrolide resistance strains, which may be due to the widespread prescription of erythromycin in Iran. *rdxA* gene inactivation, if present in Iranian *H pylori* strains, may be due to other genetic defects rather than gene deletion.

Key words: *H pylori*; Clarithromycin; Metronidazole; Resistance; Iran

Mohammadi M, Doroud D, Mohajerani N, Massarrat S. *Helicobacter pylori* antibiotic resistance in Iran. *World J Gastroenterol* 2005; 11(38): 6009-6013
http://www.wjgnet.com/1007-9327/11/6009.asp

INTRODUCTION

Helicobacter pylori (*H pylori*) infects the majority of the adult population in developing countries including Iran. The rate of infection in Iranian adults according to serology data is up to 80%[1]. The outcomes include gastritis, peptic ulcers and gastric adenocarcinomas, which are highly prevalent in Iran[2]. Patient compliance with the prescribed medications, presence of pre-existing resistance to the key anti-*H pylori* antibiotics (clarithromycin and metronidazole), final duration of therapy and prescribed dose of antibiotics are all the factors which influence the effectiveness of therapy[3]. Host genetic polymorphisms, i.e. IL-1-511 and CYP450 and CYP2C19, may affect the efficiency of the therapy as well [4]. Antibiotic resistance varies geographically and there is a great need for local studies.

Clarithromycin is recommended as a key component in anti-*H pylori* eradication[5]. In different geographic locations, resistance to clarithromycin differs. In countries with a higher use of macrolides, the rate of resistance to clarithromycin is reported to be proportionally higher[6]. The basis of the resistance is the presence of defined mutations in the *23S rRNA* gene, which results in a decrease in the antibiotic binding to the bacterial ribosome[7-9]. Mutations in the form of A-G transition at nucleotide positions 2143, 2144, and A-C at nucleotide position 2142 have been found to confer clarithromycin resistance in *H pylori* strains[10]. Recently in *H pylori* isolates from northeast China, three new mutation points (G2224A, C2245T, and T2289C) were found to be related to the clarithromycin resistance[11]. Several different PCR-based methods have been developed for the detection of the above-mentioned mutations in order to amplify part of the V domain of *23Sr RNA* gene[12]. The amplified fragments are digested by restriction enzymes, indicating mutations in the positions 2143 and 2144 which yield a high level clarithromycin resistance[10,13]. A2142C is reported to be less frequent and is detectable by PCR using 3'-mismatched specific primers[14,15].

Though most countries include clarithromycin in the prescribed anti-*H pylori* treatment regimens, this drug is infrequently prescribed in Iran due to its high cost.

As regards to metronidazole, the basis of resistance in *H pylori* has been partly associated with inactivation of *rdxA*, the gene encoding an oxygen-insensitive NADPH nitroreductase may be enhanced by mutations in *frxA* gene

encoding a NAD(P)H-flavin oxidoreductase[16].

This study presents the first documented report from Iran on the *rdxA* gene deletion. Frameshift mutations in *frxA* gene were not studied as their frequent occurrence has questioned its reliability as a resistance marker[17].

We have used modified disc diffusion test for primary analysis followed by the described molecular assays to examine resistance among Iranian *H pylori* strains with particular emphasis on clarithromycin and metronidazole.

MATERIALS AND METHODS

Bacterial strains and growth conditions

Gastric antral biopsies were taken from 120 non-*H pylori* pretreated patients (52 males and 68 females, aged 42±20 years) with epigastralgia referring to gastric endoscopy (during 2001-2002) followed by rapid urease test. These patients did not undergo any prior treatment. Urease positive samples were cultured on brucella agar (Merck) supplemented with 5% sheep blood, (6 mg/L) vancomycin (Fluka BioChemika), (5 mg/L) trimethoprim (Fluka BioChemika) and (2 mg/L) amphotericin-B (Gibco) under microaerophilic conditions (85% N_2, 100 mL/L CO_2, 5% O_2) at 37 ℃ for 3-5 d. Single colonies of *H pylori* were then isolated and confirmed for identity according to colony morphology, wet mount, microscopic observation after Gram staining and biochemical analysis (urease and catalase tests).

Disc diffusion susceptibility test

Bacterial resistance to clarithromycin[18], metronidazole[19], amoxicillin, and tetracycline[20] was determined using modified Kirby-Bauer procedure as previously described[21,22]. Suspensions of 4-d-old cultures were prepared in sterile saline to opacity of No. 4 (108 CFU/mL) McFarland standard. Muller-Hinton agar plates supplemented with 5% sheep blood were then inoculated with a swab from the prepared suspension. House-made discs containing 2 μg clarithromycin, 5 μg metronidazole, 10 μg amoxicillin, and 30 μg tetracycline were placed separately on the culture plates for each strain. Plates were then incubated at 37 ℃ for 72 h under microaerophilic conditions generated by Gas Pak jars. The disc diffusion tests were made thrice for each strain. The inhibition zone diameters were measured in millimeters with a ruler. If similar results were observed in two experiments out of three, the isolates were considered susceptible or resistant but as mixed populations. A *H pylori* control strain susceptible to metronidazole (Sydney strain, ss1) was used. The breakpoints with the Mueller-Hinton agar for the inhibition diameters are described in Table 3, briefly: 20 mm for tetracycline, 11 mm for amoxicillin, for metronidazole zones areas; <16 mm resistant, 16-21 mm intermediate and >21 mm susceptible (but in this study isolates in the intermediate and resistant zone were both considered as resistant), for clarithromycin development of any size zone is considered resistant[23].

DNA extraction and PCR assays

Genomic DNA was extracted as previously described[10]. PCR primers used for this study were chosen from published reports with the implementation of the same PCR cycles[10] (Table 1). Primer sets 1 and 2 were designed to detect point mutations in the *23S rRNA* gene responsible for clarithromycin resistance. Set 1 was used to amplify a 1 400-bp PCR fragment following digestion with *Bsa*I produced three fragments of 700, 400, and 300 bp, if the A2143G mutation was present. *Mbo*II digestion of the 1 400-bp fragment produced two 700-bp fragments, if A2142G mutation was present. A 750 and a 850 bp were produced, if A2144G mutations existed[10]. Set 2 was used in 3'-mismatched PCR to obtain a 700-bp-amplified fragment, an indication of the A2141C mutation[15].

For detection of *rdxA* gene deletion, set 3 was used. In this case, the native gene yielded a 850-bp PCR product and its deletion resulted in a 650-bp fragment[24].

Table 1 Primer sets used in this study

Gene	Primers	Expected fragment (bp)	References
23S rRNA	CLA 18: 5″-AGTCGGGAC CTAAGGCGAG-3″	1 400	10
(set 1)	CLA 21: 5″-TTCCCGCTTA GATGCTTTCAG-3″		
23S rRNA	CLA 18: 5″-AGTCGGGACC TAAGGCGAG-3″	700	15
(set 2)	CLA 3: 5″-AGGTCCACGGG GTCTTG-3″		
RdxA	RdxA1: 5″-AATTTGAGCATG GGGCAGA-3″	850	24
(set 3)	RdxA2: 5″-GAAACGCTTGAA AACACCCCT-3″		

Statistical analysis

Data were analyzed by SPSS version 11.0. The Pearson χ^2 test and Fisher's exact test were used to assess the relationships between the results of disc diffusion and PCR/RFLP methods. Standard error of mean for each frequency was determined accordingly.

RESULTS

Primary antibiotic resistance by disc diffusion

According to the disc diffusion test, all 120 strains were sensitive to tetracycline. Of these, 2 strains (1.6%) were resistant to amoxicillin, 20 (16.7%) to clarithromycin and 69 (57.5%) to metronidazole. Five of the one hundred and twenty (4.2% of the strains) showed dual resistance to metronidazole and clarithromycin. Table 2 presents the frequency of single and multiple resistances to the tested antibiotics.

Detection of 23S rRNA mutations via PCR-RFLP

All the DNA samples were positive by the PCR assay for the amplification of the 1 400 bp of *23S rRNA* gene. RFLP analysis pattern showed that 19 out of 120 (15.8%) strains were mutated (Table 2). In this group, 73.68% had the A2143G mutation and 5.26% the A2142G mutations. Moreover, none of the clarithromycin resistant samples showed the A2144G mutation, 21.05% of the samples were positive for the 3'-mismatched PCR, revealing the presence

of the A2142C mutation. Among the 20 clarithromycin resistant strains, only one did not show any of these mutations. None of the sensitive strains were positive for any of the mentioned mutations.

PCR detection of rdxA gene deletion

Among the 69 metronidazole resistant strains (based on antibiograms), only 6 (5% of total) demonstrated 200 bp deletion in the *rdxA* gene (Table 2).

According to the data analysis by the SPSS program, there were no relations between the *23S rRNA* mutations, *rdxA* deletion and antibiotic resistance with age, gender, and cagA status.

Table 2 Frequency of single and multi-drug resistance based on listed methods of detection

Antibiotics	Method of detection					
	Disc diffusion		*23S rRNA* PCR-RFLP		*rdxA* gene deletion	
	n	%	*n*	%	*n*	%
Amoxicillin only	1/120	0.8				
Amoxicillin and metronidazole	1/120	0.8				
Clarithromycin only	15/120	12.5	19/120	15.8		
Clarithromycin and metronidazole	5/120	4.2				
Metronidazole only	63/120	52.5			6/120	5
Metronidazole and amoxicillin	1/120	0.8				
Metronidazole and clarithromycin	5/120	4.2				
Tetracycline	0/120	0				

Table 3 Susceptibility rates of 120 isolates to selected antibiotics by modified disk diffusion method

Antibiotics	Disc content (μg)	Zone size breakpoint (resistance) (mm)	Resistant isolates (%)
Metronidazole	5	16	34.2 resistant 23.3 intermediate
Clarithromycin	2	Any zone	16.7
Amoxicillin	10	11	1.6
Tetracycline	30	20	0

DISCUSSION

Several studies comparing the different susceptibility techniques for *H pylori* have been published, but the results are controversial, as *H pylori* is a very slow growing bacterium with particular growth needs[23,25-28]. The oxygen-dependent metabolism of metronidazole in *H pylori* via several nitroreductases possibly results in great difference in MIC when isolates are tested repeatedly. Nevertheless, strains continue to be classified as resistant or susceptible[25].

As regards to culture-based antimicrobial susceptibility testing (especially to metronidazole), routine methods of agar dilution, disc diffusion, and *E*-test seem to be poorly standardized[29]. Though time consuming agar dilution is accepted as the gold standard and is reported to be highly reproducible in several studies[23,30,31], nowadays, *E*-test is used most frequently as a substitute as it is easier to perform and relatively reproducible[32]. Finally, a cheap and easy way to perform susceptibility testing is via disc diffusion, but no MIC value can be obtained. Recently in UK, susceptibility testing to metronidazole, tetracycline, macrolide, and amoxicillin is performed by the modified disc diffusion method and the results are adequate to determine the resistance rates in a large cohort of patients from a single clinical center whom resistance patterns have been evaluated over time[33]. Then again in a study in France, reproducibility study on randomly selected strains declared that disc diffusion is more reproducible than *E*-test for both clarithromycin and erythromycin[34]. Due to these observations and high cost of *E*-test, modified disc diffusion test was chosen for this study.

Worldwide antibiotic resistance has been carefully reviewed by Megraud[35], and our resistance rate to clarithromycin and metronidazole is comparable to the resistance rate of 50% to metronidazole and 8% to clarithromycin in China[36].

Current regimens for the eradication of *H pylori* in Iran consist of a proton pump inhibitor (omeprazole) or an H_2 receptor blocker (ranitidine), a bismuth salt plus two antibacterial agents, such as amoxicillin, furazolidone/metronidazole or recently clarithromycin[37]. Treatment regimens of 4 or 7 d are unacceptable for *H pylori* infection in Iran, even in the presence of a favorable sensitivity profile[38]. Although the presented data do not support the association with the failure of eradication in our country, according to our results, such rates of resistance to metronidazole and clarithromycin could be the major cause of eradication failure in Iran. For developing countries, the standard triple therapy remains as the best option for the eradication regimen because of its low cost. However, in Iran bismuth triple therapy in the presence of high prevalence of metronidazole resistance has a poor efficacy unless higher doses of metronidazole are prescribed to increase the cure rate of therapy[39].

Our results indicate that making clarithromycin available may not be an effective strategy to improve the eradication rates in Iran, as the level of resistance is already significant. There is a worldwide need for simple and cost effective anti-*H pylori* therapies. Since the effectiveness relates to the level of antibiotic resistance, knowledge of the resistance patterns is essential for choosing empiric therapy. Metronidazole is widely used in Iran because of the prescription in most periodontal and parasitic diseases. Resistance to metronidazole among Iranian patients, as most of the developing countries, is relatively high and this is the major cause of eradication failure in these countries. Thus, the need for a suitable alternative for this drug is highly perceptible and crucial to plan a more effective therapeutic strategy. (OABC) Omeprazole, Amoxicillin, Bismuth, Clarithromycin and (OABF)Omeprazole, Amoxicillin, Bismuth, Furazolidone are both effective in eradicating *H pylori* in countries where metronidazole resistance is a problem. OABF is a good alternative in the face of growing resistance to clarithromycin in developed countries, and is attractive for developing countries where clarithromycin is not readily available and is particularly recommended for Iran[37].

In recent years, *rdxA* gene analysis of the fresh samples showed that the metronidazole resistance is mainly attributed to the mutations in this gene including gene deletion[24]. Antibiogram analysis of our strains demonstrated 57% metronidazole resistance; however, the majority of the metronidazole resistant strains did not show the 200 bp deletion in the *rdxA* gene. One obvious explanation is that the deletion in this gene is not the only defect causing gene inactivation and is not an informative indication of metronidazole resistance in Iranian *H pylori* strains (with ~60% metronidazole resistance). The data are supported by data from Germany[40] and France[16] (with 40-50% metronidazole resistance) and contradicted by data from China[41] and Taiwan[42] (with 50-60% resistance). Due to the reported disparity, it seems that *rdxA* gene mutation is not a suitable marker for molecular prediction of metronidazole resistance. Although *rdxA* gene deletion is not a good resistance indicator, it is only detected in resistant strains and all of the strains with *rdxA* deletion clusterized in specific rapedemes (analyzed by RAPD-PCR), suggesting that they are genetically similar (data not shown). Unlike clarithromycin, metronidazole resistance *in vitro* does not reflect *in vivo* resistance. Other existing genetic defects causing metronidazole resistant phenotypes and the high incurring cost of molecular diagnostic assays lead us to the conclusion that standard culture-based techniques (simple and inexpensive disc diffusion method) remain the recommended method of choice in Iran.

In conclusion, the discovery of such a high rate of resistance to clarithromycin, which is most likely due to the vast consumption of erythromycin in cases of upper respiratory infections, calls for an effective eradication program and disqualifies clarithromycin as an alternative to metronidazole. These results further confirm the essence of continuous monitoring of antibiotic resistance patterns in order to reduce the rate of eradication failure in Iran or any other target population.

ACKNOWLEDGMENTS

The authors would like to thank Dr. David Graham, Digestive Diseases Section, Veterans Affairs Medical Center, Houston, TX, USA, for his kind review of this manuscript.

REFERENCES

1 **Massarrat S,** Saberi-Firoozi M, Soleimani A, Himmelmann GW, Hitzges M, Keshavarz H. Peptic ulcer disease, irritable bowel syndrome and constipation in two populations in Iran. *Eur J Gastroenterol Hepatol* 1995; **7**: 427-433
2 **Sadjadi A,** Malekzadeh R, Derakhshan MH, Sepehr A, Nouraie M, Sotoudeh M, Yazdanbod A, Shokoohi B, Mashayekhi A, Arshi S, Majidpour A, Babaei M, Mosavi A, Mohagheghi MA. Cancer occurrence in Ardabil: results of a population-based cancer registry from Iran. *Int J Cancer* 2003; **107**: 113-118
3 **Perri F,** Villani MR, Festa V, Quitadamo M, Andriulli A. Predictors of failure of *Helicobacter pylori* eradication with the standard 'Maastricht triple therapy. *Aliment Pharmacol Ther* 2001; **15**: 1023-1029
4 **Furuta T,** Shirai N, Xiao F, El-Omar EM, Rabkin CS, Sugimura H, Ishizaki T, Ohashi K. Polymorphism of interleukin-1beta affect the eradication rates of *Helicobacter pylori* by triple therapy. *Clin Gastroenterol Hepatol* 2004; **2**: 22-30
5 **Gisbert JP,** Pajares JM. *Helicobacter pylori* therapy: first-line options and rescue regimen. *Dig Dis* 2001; **19**: 134-143
6 **Grove DI,** Koutsouridis G. Increasing resistance of *Helicobacter pylori* to clarithromycin: is the horse bolting? *Pathology* 2002; **34**: 71-73
7 **Piana A,** Are BM, Maida I, Dore MP, Sotgiu G, Realdi G, Mura I. Genotypic characterization of clarithromycin-resistant *Helicobacter pylori* strains. *New Microbiol* 2002; **25**: 123-130
8 **Perri F,** Qasim A, Marras L, O'Morain C. Treatment of *Helicobacter pylori* infection. *Helicobacter* 2003; **8**: 53-60
9 **Taylor D**E, Ge Z, Purych D, Lo T, Hiratsuka K. Cloning and sequence analysis of two copies of a 23S rRNA gene from *Helicobacter pylori* and association of clarithromycin resistance with 23S rRNA mutations. *Antimicrob Agents Chemother* 1997; **41**: 2621-2628
10 **Versalovic JSD,** Kibler K, Griffy MV, Beyer J, Flamm RK, Tanaka SK, Graham DY, Go MF. Mutations in 23S rRNA are associated with clarithromycin resistance in *Helicobacter pylori*. *Antimicrob Agents Chemother* 1996; **40**: 477-480
11 **Hao Q,** Li Y, Zhang ZJ, Liu Y, Gao H. New mutation points in 23S rRNA gene associated with *Helicobacter pylori* resistance to clarithromycin in northeast China. *World J Gastroenterol* 2004; **1**: 1075-1077
12 **Chisholm SA,** Owen RJ, Teare EL, Savarymuttu S. PCR-based diagnosis of *Helicobacter pylori* infection and real-time determination of clarithromycin resistance directly from human gastric biopsy samples. *J Clin Microbiol* 2001; **39**: 1217-1220
13 **Occhialini AM,** Urdaci M, Doucet-Populaire F, Bebear CM, Lamouliatte H, Megraud F. Macrolide resistance in *Helicobacter pylori*: rapid detection of point mutations and assays of macrolide binding to ribosomes. *Antimicrob Agents Chemother* 1997; **41**: 2724-2728
14 **Menard A,** Santos A, Megraud F, Oleastero M. PCR-restriction fragment length polymorphism can also detect point mutation A2142C in the 23S rRNA gene, associated with *Helicobacter pylori* resistance to clarithromycin. *Antimicrob Agents Chemother* 2002; **46**: 1156-1157
15 **Alarcon T,** Domingo D, Prieto N, Lopez-Brea M. PCR using 3′-mismatched primers to detect A2142C mutation in 23S rRNA conferring resistance to clarithromycin in *Helicobacter pylori* clinical isolates. *J Clin Microbiol* 2000; **38**: 923-925
16 **Marais A,** Bilardi C, Cantet F, Mendz GL, Megraud F. Characterization of the genes *rdxA* and *frxA* involved in metronidazole resistance in *Helicobacter pylori*. *Res Microbiol* 2003; **154**: 137-144
17 **Chisholm SA,** Owen RJ. Frameshift mutations in *frxA* occur frequently and do not provide a reliable marker for metronidazole resistance in UK isolates of *Helicobacter pylori*. *J Med Microbiol* 2004; **53**: 135-140
18 **Grignon B,** Tankovic J, Megraud F, Glupczynski Y, Husson MO, Conroy MC, Emond JP, Loulergue J, Raymond J, Fauchere JL. Validation of diffusion methods for macrolide susceptibility testing of *Helicobacter pylori*. *Microb Drug Resist* 2002; **8**: 61-66
19 **Midolo PD,** Turnidge J, Lambert JR. Validation of a modified Kirby-Bauer disk diffusion method for metronidazole susceptibility testing of *Helicobacter pylori*. *Diagn Micr Infec Dis* 1995; **21**: 135-140
20 **Eltahawy AT.** Prevalence of primary *Helicobacter pylori* resistance to several antimicrobials in a Saudi Teaching Hospital. *Med Princ Pract* 2002; **11**: 65-68
21 **McNulty C,** Owen R, Tompkins D, Hawtin P, McColl K, Price A, Smith G, Teare L. *Helicobacter pylori* susceptibility testing by disc diffusion. *J Antimicrob Chemother* 2002; **49**: 601-609
22 **Debets-Ossenkopp YJ,** Herscheid AJ, Pot RG, Kuipers EJ, Kusters JG, Vandenbroucke-Grauls CM. Prevalence of *Helicobacter pylori* resistance to metronidazole, clarithromycin, amoxycillin, tetracycline and trovafloxacin in The Netherlands. *J Antimicrob Chemother* 1999; **43**: 511-515
23 **Chaves S,** Gadanho M, Tenreiro R, Cabrita J. Assessment of metronidazole susceptibility in *Helicobacter pylori*: statistical validation and error rate analysis of breakpoints determined by the disk diffusion test. *J Clin Microbiol* 1999; **37**: 1628-1631

24 **Debets-Ossenkopp YJ,** Pot RG, van Westerloo DJ, Goodwin A, Vandenbroucke-Grauls CM, Berg DE, Hoffman PS, Kusters JG. Insertion of mini-IS *605* and deletion of adjacent sequences in the nitroreductase (*rdxA*) gene cause metronidazole resistance in *Helicobacter pylori* NCTC11637. *Antimicrob Agents Chemother* 1999; **43**: 2657-2662

25 **Van der Wouden EJ,** de Jong A, Thijs JC, Kleibeuker JH, van Zwet AA. Subpopulations of *Helicobacter pylori* are responsible for discrepancies in the outcome of nitroimidazole susceptibility testing. *Antimicrob Agents Chemother* 1999; **43**: 1448-1456

26 **Piccolomini R,** Di Bonaventura G, Catamo G. Comparative evaluation of the E-test, agar dilution, and broth microdilution for testing susceptibilities of *Helicobacter pylori* strains to 20 antimicrobial agents. *J Clin Microbiol* 1997; **35**: 1842-1846

27 **DeCross AJ,** Marshall BJ, McCallum RW, Hoffman SR, Barrett LJ, Guerrant RL. Metronidazole susceptibility testing for *Helicobacter pylori*: comparison of disk, broth, and agar dilution methods and their clinical relevance. *J Clin Microbiol* 1993; **31**: 1971-1974

28 **Weiss K,** Laverdiere M, Restieri C. Comparison of activity to 10 antibiotics against clinical strains of *H pylori* by three different techniques. *Can J Gastroenterol* 1998; **12**: 181-185

29 **Edwards DI.** Nitroimidazole drugs-action and resistance mechanisms. II. Mechanisms of resistance. *J Antimicrob Chemother* 1993; **31**: 9-20

30 **Knapp CC,** Ludwig MD, W JA. *In vitro* activity of metronidazole against *Helicobacter pylori* as determined by agar dilution and agar diffusion. *Antimicrob Agents Chemother* 1991; **35**: 1230-1231

31 **Hachem CY,** Clarridge JE, Reddy R, Flamm R, Evans DG, Tanaka SK, Graham DY. Antimicrobial susceptibility testing of *Helicobacter pylori*. Comparison of E-test, broth microdilution, and disk diffusion for ampicillin, clarithromycin, and metronidazole. *Diagn Microbiol Infect Dis* 1996; **24**: 37-41

32 **Glupczynski Y,** Broutet N, Cantagrel A, Andersen LP, Alarcon T, Lopez-Brea M, Megraud F. Comparison of the E test and agar dilution method for antimicrobial suceptibility testing of *Helicobacter pylori*. *Eur J Clin Microbiol Infect Dis* 2002; **21**: 549-552

33 **Parsons HK,** Carter MJ, Sanders DS, Winstanley T, Lobo AJ. *Helicobacter pylori* antimicrobial resistance in the United Kingdom: the effect of age, sex and socio-economic status. *Aliment Pharmacol Ther* 2001; **15**: 1473-1478

34 **Grignon B,** Tankovic J, Megraud F, Glupczynski Y, Husson MO, Conroy MC, Emond JP, Loulergue J, Raymond J, Fauchere JL. Validation of diffusion methods for macrolide susceptibility testing of *Helicobacter pylori*. *Microb Drug Resist* 2002; **8**: 61-66

35 **Megraud F.** *H pylori* antibiotic resistance: prevalence, importance, and advances in testing. *Gut* 2004; **53**: 1374-1384

36 **Yakoob J,** Fan X, Hu G, Liu L, Zhang Z. Antibiotic susceptibility of *Helicobacter pylori* in the Chinese population. *J Gastroenterol Hepatol* 2001; **16**: 981-985

37 **Fakheri H,** Malekzadeh RKM, Merat S, Fazel A, Alizadeh BZ, Massarrat S. Clarithromycin *vs* furazolidone in quadruple therapy regimens for the treatment of *Helicobacter pylori* in a population with a high metronidazole resistance rate. *Aliment Pharmacol Ther* 2001; **15**: 411-416

38 **Malekzadeh R,** Merat S, Derakhshan MH, Siavoshi F, Yazdanbod A, Mikaeli J, Sotudemanesh R, Sotude M, Farahvash MJ, Nasseri-Moghaddam S, Pourshams A, Dolatshahi S, Abedi B, Babaei M, Arashi S, Majidpour A. Low *Helicobacter pylori* eradication rate with 4-7 d regimen in an Iranian population. *J Gastroenterol Hepatol* 2003; **18**: 13-17

39 **Roghani HS,** Massarrat S, Pahlewanzadeh MR, Dashti M. Effect of two different doses of metronidazole and tetracycline in bismuth triple therapy on eradication of *Helicobacter pylori* and its resistant strains. *Eur J Gastroenterol Hepatol* 1999; **11**: 709-712

40 **Bereswill S,** Krainick C, Stahler F, Herrmann L, Kist M. Analysis of the *rdxA* gene in high-level metronidazole-resistant clinical isolates confirms a limited use of *rdxA* mutations as a marker for prediction of metronidazole resistance in *Helicobacter pylori*. *FEMS Immunol Med Microbiol* 2003; **36**: 193-198

41 **Dai N,** Zhou G, Yan J. Correlation of *rdxA* gene mutation and metronidazole resistance of *Helicobacter pylori*. *Zhejiang Daxue Xuebao Yixueban* 2003; **32**: 37-40

42 **Yang YJ,** Wu JJ, Sheu BS, Kao AW, Huang AH. The *rdxA* gene plays a more major role than *frxA* gene mutation in high-level metronidazole resistance of *Helicobacter pylori* in Taiwan. *Helicobacter* 2004; **9**: 400-407

Science Editor Wang XL and Guo SY **Language Editor** Elsevier HK

PO Box 2345, Beijing 100023, China
www.wjgnet.com
wjg@wjgnet.com

ELSEVIER

World J Gastroenterol 2005;11(38):6014-6017
World Journal of Gastroenterology ISSN 1007-9327

• *BRIEF REPORTS* •

Receptor-binding cancer antigen expressed on SiSo cells can be detected in metastatic lymph nodes from gastrointestinal cancers

Kawin Leelawat, Surang Engprasert, Supathip Tujinda, Cheepsumon Suthippintawong, Munechika Enjoji, Manabu Nakashima, Takeshi Watanabe, Vijittra Leardkamolkarn

Kawin Leelawat, Department of Surgery, Rajavithi Hospital, Bangkok 10400, Thailand
Kawin Leelawat, Vijittra Leardkamolkarn, Department of Anatomy, Mahidol University, Bangkok 10400, Thailand
Surang Engprasert, Department of Pharmacognosy, Kyushu University, Fukuoka 8128582, Japan
Supathip Tujinda, Cheepsumon Suthippintawong, Department of Pathology, Rajavithi Hospital, Bangkok 10400, Thailand
Munechika Enjoji, Manabu Nakashima, Takeshi Watanabe, Department of Medical Bioregulation, Kyushu University, Fukuoka 8128582, Japan
Supported by the Thailand Research Fund in the Royal Golden Jubilee Program
Correspondence to: Kawin Leelawat, MD, PhD, Department of Surgery, Rajavithi Hospital, Rajavithi Road, Rajathevi, Bangkok 10400, Thailand. kawin@tubtim.cri.or.th
Telephone: +66-2-245-6078 Fax: +66-2-245-6075
Received: 2004-02-02 Accepted: 2004-03-02

Abstract

AIM: To investigate the expression of receptor-binding cancer antigen expressed on SiSo cells (RCAS1) in metastatic lymph nodes from gastrointestinal cancer.

METHODS: Metastatic lymph nodes from gastrointestinal cancer were detected for RCAS1 by immunohistochemical staining and mRNA *in situ* hybridization.

RESULTS: A total of 102 metastatic lymph nodes from bile duct, gastric, colon, and pancreatic cancer were investigated for RCAS1 expression. The immunoreactivity of RCAS1 was identified in 100% of metastatic lymph nodes. Both local and distant metastatic lymph nodes showed RCAS1 expression. On the contrary, specimens of non-cancerous lymph nodes were negative for RCAS1. The result of mRNA *in situ* hybridization was also confirmed by the finding of immunohistochemical staining. RCAS1 mRNA was detected in all tumor cells that metastasized to lymph nodes.

CONCLUSION: All metastatic lymph nodes express RCAS1 in tumor cells at both protein and mRNA levels, and RCAS1 should be used as a complementary factor for identification of metastatic lymph nodes from gastrointestinal cancers.

Key words: RCAS1; Gastrointestinal cancer; Lymph node metastasis

Leelawat K, Engprasert S, Tujinda S, Suthippintawong C, Enjoji M, Nakashima M, Watanabe T, Leardkamolkarn V. Receptor-binding cancer antigen expressed on SiSo cells can be detected in metastatic lymph nodes from gastrointestinal cancers. *World J Gastroenterol* 2005; 11(38): 6014-6017
http://www.wjgnet.com/1007-9327/11/6014.asp

INTRODUCTION

One of the major factors for the poor prognosis of gastrointestinal cancer patients is lymph node metastasis[1-3]. To indicate the lymph node metastasis, pathologists must carefully identify tumor cells spreading to lymph nodes in each serial section of pathological specimens. The suitable method for the identification of tumor cells in lymph nodes is to stain the specimen with antibody, which highly recognizes the tumor antigen. At this time, the antibody to cytokeratin is widely used for detection of lymph node metastasis from breast cancer[4,5]. However,a current study showed that the sensitivity of cytokeratin to lymph node metastasis from gastrointestinal cancer is low[6].

Recently, receptor-binding cancer antigen expressed on SiSo cells (RCAS1) is recognized as type II membrane protein and secreted as a soluble protein[7,8]. This tumor-associated antigen has been demonstrated in several kinds of gastrointestinal cancer by immunohistochemical study using the specific mouse mAb, 22-1-1. The result of RCAS1 expression was evaluated for the percent incidence in various cancers including gall bladder cancer (70%)[9], cholangiocarcinoma (85.9-96.4%)[10,11], gastric cancer (54.3%)[12], pancreatic cancer (100%)[13], and colorectal cancer (100%)[14]. However, until now, there has been no intensive study about the expression of RCAS1 in lymph node metastasis from gastrointestinal cancer. Therefore, the purpose of the present study was to investigate the expression of RCAS1 at both protein and mRNA levels in lymph node metastasis from gastrointestinal cancer.

MATERIALS AND METHODS

Tissue specimens

Fifteen specimens of non-cancerous lymph nodes and 102 specimens of metastatic lymph nodes from different gastrointestinal cancers (surgically resected in Rajavithi Hospital, Bangkok, Thailand) were collected for RNA investigation and immunohistochemical staining. The study was carried out with the approval of the Ethical Committee of Rajavithi Hospital. Pathological diagnosis and evaluation

were routinely performed.

Immunohistochemical staining

The sections (4 μm) were deparaffinized and immunostained for RCAS1 as described previously[14]. Briefly, the sections were incubated overnight at 4 ℃ with 1:1 000 dilution of 22-1-1 mouse mAb (Medical & Biological Laboratories Co., Ltd.). Biotinylated rabbit anti-mouse IgM (DAKO) was applied to the sections followed by avidin-biotin-peroxidase conjugate (ABC Elite, Vector Labs). The immunohistochemical reactions were developed with freshly prepared 3,3'-diaminobenzidine tetrahydrochloride solution (Histofine SAB-PO kit) and counterstained with hematoxylin. As a negative control, primary antibody was replaced with mouse IgM. The positive cell staining in each slide was identified under a high power field (×400) of Olympus BH2 microscope (field width = 0.5 mm).

RCAS1 mRNA in situ hybridization

Fluorescent probe preparation RCAS1 cDNA fragments from metastatic lymph nodes were synthesized by RT-PCR as described previously[14], using forward primer 5'-ACCTTACTGCCCTCCGTCTA-3' and reverse primer 5'-CTTCTTCATTAGCCGTTGTG-3'. The nucleotide sequence was confirmed with a Model 310 genetic analyzer (PE Biosystems) using a BigDye terminator cycle sequencing kit and used for generating fluorescent probes using Gene Images™ random prime labeling kit (Amersham, Biosciences). Twenty nanograms per microliter of denatured RCAS1 cDNA was mixed with 10 μL of nucleotide mix, 5 μL of primer, and 1 μL of 5 U/μL Klenow enzyme solution. The reaction was incubated at 37 ℃ for 1 h and stored at -20 ℃ until used.

***In situ* hybridization** The specimens were deparaffinized in xylene. The sections were treated with proteinase K for 20 min at 37 ℃ then diluted fluorescent-RNA probe (1 ng/mL with hybridization buffer) was applied onto each specimen. The slides were incubated at 55 ℃ for 2 h. The sections were rinsed with TBS and incubated for 15 min with blocking mixture (10% fetal calf serum). For detection of mRNA, the sections were incubated at room temperature for 30 min with anti-FITC/alkaline phosphatase. The immunoreactions were visualized by incubating the sections at room temperature with substrates and immersed in tap water for 5 min. The slides were counterstained with hematoxylin before observation under a light microscope.

Statistical analysis

Statistical analysis for comparing the expression of RCAS1 in the specimens was performed using SPSS 10.0 for Windows. $P<0.05$ was considered statistically significant.

结果

A total of 102 metastatic lymph nodes from various kinds of cancer were investigated for RCAS1 expression as shown in Table 1. The metastatic lymph nodes were divided into two groups (local and distant metastatic nodes) according to the TNM staging systems. The immunostaining pattern for RCAS1 was observed in the cytoplasm of tumor cells but not in lymphocytes (Figure 1). Most metastatic tumor cells showed a high intensity of RCAS1 immunostaining. The staining level was not related with tumor stage or differentiation status. All sections in negative control (non-cancerous lymph nodes) showed no immunoreactivity. RCAS1 was identified in 100% of metastatic lymph nodes. Interestingly, several primary cancers, which identified RCAS1 expression in some parts of tumor tissues, were found to express RCAS1 in most of the metastatic tumor cells in lymph nodes.

The RCAS1 cDNA of metastatic lymph nodes from various gastrointestinal cancers was determined by reverse-transcription-PCR. The 802 bp product was sequenced and its homology was compared with the RCAS1 cDNA sequence databases present at NCBI GenBank (gi: 13528905). This cDNA fragment started from nucleotide 41 to 842 of RCAS1 cDNA. As demonstrated in Figure 2, the cDNA fragment from metastatic lymph nodes revealed a high similarity throughout the 802 bp in the coding region.

To confirm further the expression of RCAS1 in metastatic lymph nodes, RCAS1 mRNA *in situ* hybridization was performed using the cDNA probes showing a high similarity with RCAS1 cDNA. The expression of RCAS1 mRNA was clearly identified in cytoplasm of tumor cells but not in lymphocytes. Figure 3 represents the typical RCAS1 mRNA expression, which could be detected in cytoplasm of tumor cells and represented the negative signal for RCAS1 mRNA in lymphocytes.

Table 1 RCAS1 expression in metastatic lymph nodes from gastrointestinal cancers

Type of cancer	Total no. of lymph nodes		No. of lymph nodes express RCAS1 (%)
	Local metastasis	Distance metastasis	
Bile duct cancer	10	4	14 (100)
Colon cancer	56	6	62 (100)
Pancreatic cancer	12	2	14 (100)
Stomach cancer	10	2	12 (100)

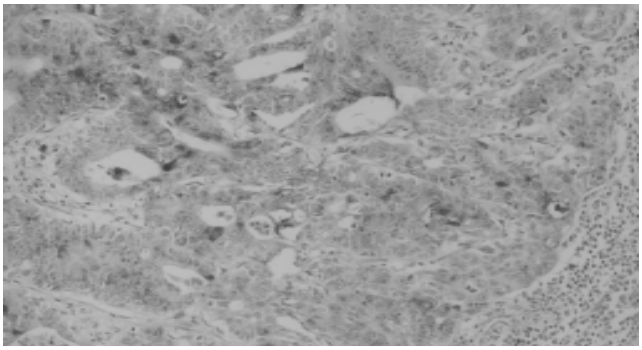

Figure 1 Typical result of immunohistochemical staining of RCAS1 (×200) in metastatic lymph nodes. Expression of RCAS1 was demonstrated both in cytoplasm and on cell membrane of tumor cells.

讨论

RCAS1 expression in lymph node metastasis from various

```
RCAS1     1   cgcagcctcc aaagccgcct tcctcaggga aatttgcgtg  accttactgc  cctccgtcta  60
RT- PCR   1   ---------- ---------- ---------- ----------  accttactgc  cctccgtcta  20
RCAS1     61  caggccttgt acctctccag gccgattttt ccacaattta  aatcccagtt  cacctggtat  120
RT- PCR   21  caggccttgt acctctccag gccgattttt ccacaattta  aatcccagtt  cacctggtat  80
RCAS1     121 ccagctccag caacttagag cgtttcacgt cacgccgggc  gccaggcgtc  ggcttgtata  180
RT- PCR   81  ccagctccag caacttagag cgtttcacgt cacgccgggc  gccaggcgtc  ggcttgtata  140
RCAS1     181 acctgaaaac gctcctgttt ttctcatctg tgcagtgggt  tttgattccc  accatggcca  240
RT- PCR   141 acctgaaaac gctcctgttt ttctcatctg tgcagtgggt  tttgattccc  accatggcca  200
RCAS1     241 tcacccagtt tcggttattt aaattttgta cctgcctagc  aacagtattc  tcattcctaa  300
RT- PCR   201 tcacccagtt tcggttattt aaattttgta cctgcctagc  aacagtattc  tcattcctaa  260
RCAS1     301 agagattaat atgcagatct ggcagaggac ggaaattaag  tggagaccaa  ataactttgc  360
RT- PCR   261 agagattaat atgcagatct ggcagaggac ggaaattaag  tggagaccaa  ataactttgc  320
RCAS1     361 caactacagt tgattattca tcagttccta agcagacaga  tgttgaagag  tggacttcct  420
RT- PCR   321 caactacagt tgattattca tcagttccta agcagacaga  tgttgaagag  tggacttcct  380
RCAS1     421 gggatgaaga tgcacccacc agtgtaaaga tcgaaggagg  gaatgggaat  gtggcaacac  480
RT- PCR   381 gggatgaaga tgcacccacc agtgtaaaga tcgaaggagg  gaatgggaat  gtggcaacac  440
RCAS1     481 aacaaaattc tttggaacaa ctggaacctg actattttaa  ggacatgaca  ccaactatta  540
RT- PCR   441 aacaaaattc tttggaacaa ctggaacctg actattttaa  ggacatgaca  ccaactatta  500
RCAS1     541 ggaaaactca gaaaattgtt attaagaaga gagaaccatt  gaattttggc  atcccagatg  600
RT- PCR   501 ggaaaactca gaaaattgtt attaagaaga gagaaccatt  gaattttggc  atcccagatg  560
RCAS1     601 ggagcacagg tttctctagt agattagcag ctacacaaga  tctgcctttt  attcatcagt  660
RT- PCR   561 ---------- ---------- ---------- ----------  ----------  ----------  620
RCAS1     661 cttctgaatt aggtgactta gatacctggc aggaaaatac  caatgcatgg  gaagaagaag  720
RT- PCR   621 ---------- ---------- ---------- ----------  ----------  ----------  680
RCAS1     721 aagatgcagc ctggcaagca gaagaagttc tgagacagca  gaaactagca  gacagagaaa  780
RT- PCR   681 ---------- ---------- ---------- ----------  ----------  ----------  740
RCAS1     781 agagagcagc cgaacaacaa aggaagaaaa tggaaaagga  agcacaacgg  ctaatgaaga  840
RT- PCR   741 ---------- ---------- ---------- ----------  ----------  ----------  800
RCAS1     841 ag
RT- PCR   801 --
```

Figure 2 Nucleotide sequence alignment of RCAS1 cDNA from databases present at NCBI GenBank (gi: 13528905) and RT-PCR products from metastatic lymph nodes. The residues boxed in black indicate positional identity for both sequences. Numbers of nucleotide sequences are indicated on the left and right margins.

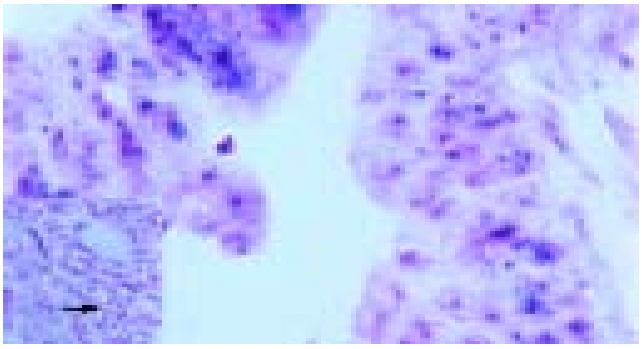

Figure 3 RCAS1 mRNA *in situ* hybridization in metastatic lymph nodes from colon cancer. The positive signal was identified in the cytoplasm of tumor cells. All leukocytes showed negative signal for RCAS1 (as presented in the Figure).

gastrointestinal cancers was first explored at protein level by immunohistochemical staining. The RCAS1 cDNA obtained from metastatic lymph nodes from various gastrointestinal tumors showed high homology with the RCAS1 cDNA sequence databases present at NCBI GenBank (gi: 13528905). This finding increases the reliability of *in situ* hybridization for identification RCAS1 of mRNA expression in metastatic tumor cells.

As suspected, it was expressed in all cases of metastatic lymph nodes. RCAS1 was shown to be a ligand for a putative receptor on immune cells such as T cells and natural killer cells[7-14]. Scientists suggest that RCAS1 may play a protective role in tumor cells against immune surveillance by inhibition of clonal expression and inducing receptor-expressing cell death. It has been previously reported that activated lymphocytes process receptors for RCAS1[7]. Thus, binding interaction between them induces apoptosis of lymphocytes. The mechanism by which tumor cell expressed RCAS1 mediates lymphocyte apoptosis is a main biologic pathway to escape the immune surveillance in both local and distant metastatic lymph nodes.

Although previous results[13,14] have demonstrated the correlation between the staining level and tumor stage or differentiation status, this study did not find any significant correlation between them. Most metastatic tumor cells showed a high intensity of RCAS1 immunostaining. This result may explain why tumor cells expressing RCAS1 metastasize the lymph nodes. The role of RCAS1 in lymph node metastasis needs further study.

Since the expression of RCAS1 is found in gastrointestinal cancers and their metastatic lymph nodes, it can be used as an additional step for identification of the status of lymph nodes.

REFERENCES

1 **Ding YB,** Chen GY, Xia JG, Zang XW, Yang HY, Yang L, Liu YX. Correlation of tumor-positive ratio and number of perigastric lymph nodes with prognosis of patients with surgically-removed gastric carcinoma. *World J Gastroenterol* 2004; **10**: 182-185

2 **Cuschieri A,** Weeden S, Fielding J, Bancewicz J, Craven J, Joypaul V, Sydes M, Fayers P. Patient survival after D1 and D2 resections for gastric cancer: long-term results of the MRC randomized surgical trial. Surgical Co-operative Group. *Br J Cancer* 1999; **79**: 1522-1530

3 **Ichikura T,** Ogawa T, Chochi K, Kawabata T, Sugasawa H, Mochizuki H. Minimum number of lymph nodes that should be examined for the International Union Against Cancer/ American joint committee on cancer TNM classification of gastric carcinoma. *World J Surg* 2003; **27**: 330-333

4 **Lara JF,** Young SM, Velilla RE, Santoro EJ, Templeton SF. The relevance of occult axillary micrometastasis in ductal carcinoma in situ: a clinicopathologic study with long-term follow-up. *Cancer* 2003; **98**: 2105-2113
5 **Euhus DM.** Cytokeratin staining and other sentinel node controversies. *Clin Breast Cancer* 2003; **4**(Suppl 1): S49-54
6 **Mukai M,** Sato S, Nakasaki H, Tajima T, Saito Y, Nishiumi N, Iwasaki M, Tokuda Y, Ogoshi K, Inoue H, Makuuchi H. Occult neoplastic cells in the lymph node sinuses and recurrence of primary breast, lung, esophageal, and gastric cancer. *Oncol Rep* 2004; **11**: 81-84
7 **Nakashima M,** Sonoda K, Watanabe T. Inhibition of cell growth and induction of apoptotic cell death by the human tumor-associated antigen RCAS1. *Nat Med* 1999; **5**: 938-942
8 **Sonoda K,** Nakashima M, Kaku T, Kamura T, Nakano H, Watanabe T. A novel tumor-associated antigen expressed in human uterine and ovarian carcinomas. *Cancer* 1996; **77**: 1501-1509
9 **Oshikiri T,** Hida Y, Miyamoto M, Hashida H, Katoh K, Suzuoki M, Nakakubo Y, Hiraoka K, Shinohara T, Itoh T, Kondo S, Katoh H. RCAS1 as a tumor progression marker: an independent negative prognostic factor in gallbladder cancer. *Br J Cancer* 2001; **85**: 1922-1927
10 **Enjoji M,** Nakashima M, Nishi H, Choi I, Oimomi H, Sugimoto R, Kotoh K, Taguchi K, Nakamuta M, Nawata H, Watanabe T. The tumor-associated antigen, RCAS1, can be expressed in immune-mediated diseases as well as in carcinomas of biliary tract. *J Hepatol* 2002; **36**: 786-792
11 **Suzuoki M,** Hida Y, Miyamoto M, Oshikiri T, Hiraoka K, Nakakubo Y, Shinohara T, Itoh T, Okushiba S, Kondo S, Katoh H. RCAS1 expression as a prognostic factor after curative surgery for extrahepatic bile duct carcinoma. *Ann Surg Oncol* 2002; **9**: 388-393
12 **Fukuda K,** Tsujitani S, Maeta Y, Yamaguchi K, Ikeguchi M, Kaibara N. The expression of RCAS1 and tumor infiltrating lymphocytes in patients with T3 gastric carcinoma. *Gastric Cancer* 2002; **5**: 220-227
13 **Akashi T,** Oimomi H, Nishiyama K, Nakashima M, Arita Y, Sumii T, Kimura T, Ito T, Nawata H, Watanabe T. Expression and diagnostic evaluation of the human tumor-associated antigen RCAS1 in pancreatic cancer. *Pancreas* 2003; **26**: 49-55
14 **Leelawat K,** Watanabe T, Nakajima M, Tujinda S, Suthipintawong C, Leardkamolkarn V. Upregulation of tumor-associated antigen RCAS1 is implicated in high stages of colorectal cancer. *J Clin Pathol* 2003; **56**: 764-768

Science Editor Wang XL and Guo SY **Language Editor** Elsevier HK

PO Box 2345, Beijing 100023, China
www.wjgnet.com
wjg@wjgnet.com

ELSEVIER

World J Gastroenterol 2005;11(38):6018-6021
World Journal of Gastroenterology ISSN 1007-9327

• *BRIEF REPORTS* •

Normal serum alanine aminotransferase activity in uncomplicated obesity

Gianluca Iacobellis, Antonio Moschetta, Maria Cristina Ribaudo, Alessandra Zappaterreno, Concetta Valeria Iannucci, Frida Leonetti

Gianluca Iacobellis, Maria Cristina Ribaudo, Alessandra Zappaterreno, Concetta Valeria Iannucci, Frida Leonetti, Endocrinology, Department of Clinical Sciences, La Sapienza University, Rome, Italy
Gianluca Iacobellis, Center for Human Nutrition, the University of Texas Southwestern Medical Center, Dallas, TX, USA
Antonio Moschetta, Clinica Medica "*Augusto Murri*", Department of Internal and Public Medicine, University of Bari, Italy
Correspondence to: Dr. Gianluca Iacobellis, MD, PhD, Dipartimento Scienze Cliniche,Università La Sapienza,Policlinico I, Viale del Policlinico 155,00161,Roma, Italy, gianluca.iaco@tin.it
Telephone: +39-6-44240932 Fax: +39-6-44240932
Received: 2005-01-12 Accepted: 2005-03-23

AIM: To evaluate serum alanine aminotransferase (ALT) activity in a well-characterized group of uncomplicated obese subjects and its correlation with insulin resistance, plasma adiponectin, and leptin concentrations.

METHODS: One hundred and five uncomplicated obese subjects (87 women, 18 men, age 34.3±9.6 years, BMI 39.9±8.3 kg/m^2) were studied. Serum ALT activity was evaluated. Insulin sensitivity was assessed by euglycemic hyperinsulinemic clamp (M index) and fasting insulin. Plasma leptin and adiponectin levels were also measured.

RESULTS: Serum ALT concentration in the whole group of uncomplicated obese subjects was 17.73±6.33 U/L with none of the subjects presenting ALT levels greater than 43 U/L and only 9 (11%) women and 3 (19%) men showed ALT levels >19 and >30 U/L for women and men, respectively. No significant difference was detected in serum ALT levels between severe obese subjects (BMI >40 kg/m^2) and those with BMI <40 kg/m^2 (18.63±6.25 *vs* 17.26±6.02 U/L). ALT was significantly correlated with fasting insulin (r = 0.485, P = 0.02) and triglycerides (r = 0.358, P = 0.03).

CONCLUSION: Serum ALT activity is practically normal in uncomplicated obese subjects, independently of their obesity degree. These findings suggest the role of obesity-related comorbidities and not of BMI as main risk factors for elevated ALT levels in obese subjects.

Key words: Serum alanine aminotransferase activity; Obesity; Insulin resistance

Iacobellis G, Moschetta A, Ribaudo MC, Zappaterreno A, Iannucci CV, Leonetti F. Normal serum alanine aminotransferase activity in uncomplicated obesity. *World J Gastroenterol* 2005; 11(38): 6018-6021
http://www.wjgnet.com/1007-9327/11/6018.asp

Overweight and obesity have been reported to be major risk factors for elevated serum alanine aminotransferase (ALT) activity[1,2] and non-alcoholic fatty liver disease (NAFLD)[3-6]. High serum ALT levels have also been proposed as a marker of risk for type 2 diabetes[7,8]. A recent atherosclerosis study showed a significant relationship between ALT activity and insulin resistance[7]. In addition, unexplained ALT elevation has been found to be associated with increased visceral adiposity and other features of the metabolic syndrome[9]. Nevertheless, no studies evaluating serum ALT activity in metabolically healthy obese subjects have been performed. Uncomplicated obesity, as previously shown by our group[10], could be a good model to clarify the influence of obesity *per se* on ALT levels, without the confounding effect of the obesity-related comorbidities.

In this study, we sought to evaluate the serum ALT activity in a well-characterized uncomplicated obese subjects and its possible correlation with insulin resistance, plasma adiponectin, and leptin concentrations.

Patients

We selected 105 consecutive Caucasian uncomplicated obese subjects (body mass index [BMI] >30 kg/m^2) from 600 obese subjects who were referred to our Day Hospital from Rome and surrounding areas between January 2001 and June 2004. The selected subjects had the following features: 87 women, 18 men; age, 34.3±9.6 years (range, 20-55 years); BMI, 39.9±8.3 kg/m^2 (range, 30-80.1 kg/m^2); duration of obesity, 15±5 years (range, 10-30 years). Uncomplicated obesity was defined according to the following parameters: no signs, symptoms and history of liver diseases (alcoholic hepatitis, viral hepatitis, positive serum hepatitis B surface antigen, positive serum hepatitis C surface antibody, auto-immune hepatitis, drug-induced hepatitis, familial metabolic disorders, history of fatty liver during pregnancy, portal hypertension, liver cancer, elevated serum transferrin

PO Box 2345, Beijing 100023, China
www.wjgnet.com
wjg@wjgnet.com

ELSEVIER

World J Gastroenterol 2005;11(38):6022-6026
World Journal of Gastroenterology ISSN 1007-9327

• *BRIEF REPORTS* •

Endoscopic treatment and follow-up of gastrointestinal Dieulafoy's lesions

Panagiotis Katsinelos, George Paroutoglou, Kostas Mimidis, Athanasios Beltsis, Basilios Papaziogas, George Gelas, Yiannis Kountouras

Panagiotis Katsinelos, George Paroutoglou, Kostas Mimidis, Athanasios Beltsis, George Gelas, Department of Endoscopy and Motility Unit, "G. Gennimatas" Hospital, Ethnikis Aminis 41, Thessaloniki 54635, Greece
Basilios Papaziogas, 2nd Surgical Clinic, "G.Gennimatas" Hospital, Aristotle University of Thessaloniki, Ethnikis Aminis 41, Thessaloniki 54635, Greece
Yiannis Kountouras, 2nd Department of Internal Medicine, Ippokration Hospital, Aristotle University of Thessaloniki, Greece
Correspondence to: Dr. Panagiotis Katsinelos, Department of Endoscopy and Motility Unit, "G. Gennimatas" Hospital, Ethnikis Aminis 41, Thessaloniki 54635, Greece. pantso@the.forthnet.gr
Telephone: +30-2310-211221 Fax: +30-2310-210401
Received: 2004-11-30 Accepted: 2005-01-26

Abstract

AIM: To investigate retrospectively the clinical and endoscopic features of bleeding Dieulafoy's lesions and to assess the short- and long-term effectiveness of endoscopic treatment.

METHODS: Twenty-three patients who had gastrointestinal bleeding from Dieulafoy's lesions underwent endoscopic therapy. Demographic data, mode of presentation, risk factors for gastrointestinal bleeding, blood transfusion requirements, endoscopic findings, details of endoscopic therapy, recurrence of bleeding, and mortality rates were collected and analyzed retrospectively.

RESULTS: Hemostasis was attempted by dextrose 50% plus epinephrine in 10 patients, hemoclipping in 8 patients, heater probe in 2 patients and ethanolamine oleate in 2 patients. Comorbid conditions were present in 17 patients (74%). Overall permanent hemostasis was achieved in 18 patients (78%). Initial hemostasis was successful with no recurrent bleeding in patients treated with hemoclipping, heater probe or ethanolamine injection. In the group of patients who received dextrose 50% plus epinephrine injection treatment, four (40%) had recurrent bleeding and one (10%) had unsuccessful initial hemostasis. Of the four patients who had rebleeding, three had unsuccessful hemostasis with similar treatment. Surgical treatment was required in five patients (22%) owing to uncontrolled bleeding, recurrent bleeding with unsuccessful retreatment and inability to approach the lesion. One patient (4.3%) died of sepsis after operation during hospitalization. There were no side-effects related to endoscopic therapy. None of the patients in whom permanent hemostasis was achieved presented with rebleeding from Dieulafoy's lesion over a mean long-term follow-up of 29.8 mo.

CONCLUSION: Bleeding from Dieulafoy's lesions can be managed successfully by endoscopic methods, which should be regarded as the first choice. Endoscopic hemoclipping therapy is recommended for bleeding Dieulafoy's lesions.

Key words: Endoscopic treatment; Dieulafoy lesion; Gastrointestinal tract

Katsinelos P, Paroutoglou G, Mimidis K, Beltsis A, Papaziogas B, Gelas G, Kountouras Y. Endoscopic treatment and follow-up of gastrointestinal Dieulafoy's lesions. *World J Gastroenterol* 2005; 11(38): 6022-6026
http://www.wjgnet.com/1007-9327/11/6022.asp

INTRODUCTION

Dieulafoy's lesion was first described by Gallard in 1884 and later fully characterized by French surgeon George Dieulafoy in 1896, as an arterial lesion associated with massive gastric hemorrhage. It is described as a minute defect of the gastrointestinal mucosa with rupture of a large submucosal artery into the lumen. Although usually described in the stomach, Dieulafoy's lesions are also described in the rest of the gastrointestinal tract including esophagus[1-3], duodenum[4], small bowel[5], colon[6], rectum[7], and anus[8].

Until a few years ago, surgical treatment was advocated for such lesions because of the inability to recognize the lesion via endoscopy, or because of massive and recurrent bleeding. However, endoscopic therapy has recently become the treatment of choice by many endoscopists, being effective in the majority of cases[9]. The aim of our study was to assess the short- and long-term effectiveness of endoscopic treatment of Dieulafoy's lesions.

MATERIALS AND METHODS

Between January 1994 and December 2003, 936 patients with acute GI bleeding of non-variceal origin were admitted to our endoscopy unit. After resuscitation with intravenous fluids and blood transfusions, emergency endoscopy without preparation was performed within 24 h of the onset of bleeding, using standard video-endoscopes. If there was fresh blood or clots obscuring bleeding lesion, a lavage with a large bore tube (34F) for upper GI bleeding or rigorous

cleansing of the colon with polyethylene glycol solution was performed. ECG, blood pressure, and oxygen saturation were monitored. Twenty-three patients were diagnosed as having Dieulafoy's lesions.

The endoscopic diagnosis of Dieulafoy's lesions was based on the following established criteria: active arterial spurting or micropulsatile streaming from a minute (<3 mm) mucosal defect, visualization of a protruding vessel with or without active bleeding within a minute mucosal defect or normal surrounding mucosa or densely adherent clot with a narrow point of attachment to a minute mucosal defect or normal-appearing mucosa. To avoid possible inclusion of variceal bleeding at either the index episode of bleeding or an episode of recurrent bleeding, all patients with esophagogastric varices were excluded from the study. If Dieulafoy's lesion was diagnosed at emergency endoscopy according to the criteria outlined above, the choice of the endoscopic method of treatment was left to the endoscopist's discretion.

The therapeutic methods used in the first six years of our study were injection of a solution of dextrose 50% plus epinephrine (1:10 000) and ethanolamine oleate, while heater probe treatment and hemoclipping were used in the last 4 years. In the injection group, 1 mL aliquot was injected via a plastic cannula (23-gauge, 5-mm tip) into and around the Dieulafoy's lesion. A limit of 10 mL of mixture per endoscopic session was set. A 3.2 mm diameter heater probe set at 30 J/pulse was used to coat the bleeding vessel. Hemoclip therapy (HX-3L, 5LR-1; Olympus Optical Co., Ltd, Tokyo, Japan) was performed by mechanical clipping of spurting, oozing or visible vessels.

Therapeutic endoscopy was defined as successful if there was no further bleeding from the Dieulafoy's lesion until the withdrawal of the endoscope. After endoscopic treatment, the patients with Dieulafoy's lesion in the upper GI tract were treated with intravenous administration of a standard dose of PPIs. Follow-up endoscopy was performed within 24 h after the initial procedure and at least once within 5 d. Criteria for recurrent bleeding included fresh hematemesis or hematochezia, fresh blood aspirated through the nasogastric tube, instability of vital signs or a reduction of hemoglobin in excess of 30 g/L within 24 h after endoscopic hemostasis. When recurrent bleeding was suspected, immediate endoscopic retreatment was performed. If bleeding persisted after the second intervention, an operation was performed. In order to determine whether new bleeding episodes occurred after discharge, long-term follow-up was carried out by retrieving the medical records from the files, and when necessary by telephone calls to the patients. The patients who underwent surgery were not subjected to long-term follow-up.

Data including age, gender, comorbidities, mode of presentation, hemodynamic parameters, blood transfusion requirements before and after endoscopic therapy, risk factors for gastrointestinal bleeding (such as coagulopathy, use of aspirin or other non-steroidal anti-inflammatory drugs), endoscopic findings, details of endoscopic therapy, complications, recurrence of bleeding, and 30-d mortality were collected (Table 1).

Informed consent was obtained from the patients and/or their relatives. Because this study was a retrospective review, institutional review board approval was not necessary.

Student's *t*-test was utilized to compare the mean values of continuous variables and Fisher exact test was utilized for the comparison of discrete variables.

[illegible]

The study group consisted of 17 male (74%) and 6 female (26%) patients. The mean age was 70.26 years (range 42-84 years). There was a history of hypertension in nine patients, ischemic heart disease in four, heart failure in six, diabetes in two, gout in two, chronic renal failure in one, BII gastrectomy in two, duodenal ulcer in one, and aorto-iliac bypass in one (Table 1).

Melena was present in 11 patients (47.8%), hematemesis and melena in 9 (39%), and rectal bleeding in the remaining 3 patients (13.2%). Mean hemoglobin concentration was 101 g/L (normal 130-160 g/L). Blood transfusion requirements ranged from 1 to 8 U of packed RBC (mean 2.9 U per patient) during hospitalization. There was no significant difference with respect to coagulation parameters in patients who had recurrent bleeding and those who did not.

The Dieulafoy's lesions were located in the stomach in 18 patients (78%, fundus in 6, body in 9, and antrum in 3), in the colon in 3 (Figure 1), in the jejunum in 1 and in the descending duodenum in 1 (Table 1). Eleven patients (47.8%) had active bleeding (oozing in 7 and spurting in 4) at the initial endoscopy. In the remaining 12 patients (52.2%), a non-bleeding vessel was found (Table 1). In a 84-year-old patient with a medical history of heart failure and aorto-iliac bypass, endoscopy revealed two simultaneous Dieulafoy's lesions in the fundus, 2 cm apart. The initial endoscopy was diagnostic in 69% of patients. The mean number of endoscopies required for diagnosis was 1.7 (range 1-3). Failure to diagnose when the appropriate site was evaluated at endoscopy was due to excessive blood on 11 occasions (47.8%) and a missed lesion on 8 occasions (34.7%).

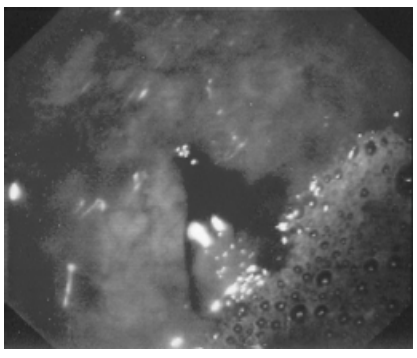

Figure 1 Endoscopic view of Dieulafoy's lesion with oozing in sigmoid.

Ten patients were treated with dextrose 50% plus epinephrine 1:10 000 injection. Mean injection volume was 7.6 mL (range 6-9 mL). Initial hemostasis was achieved in nine patients (90%), but four patients (44%) had rebleeding, which was successfully controlled at repeat endoscopy in one patient, but not in the other three using similar therapy,

Table 1 Clinical characteristics, endoscopic data, and after endoscopic therapy of patients with acute bleeding from Dieulafoy's lesion in GI tract

N	Sex	Age (yr)	Location	Bleeding symptom	Hb g/L	Transfusion (RBC)	Medical history	Endoscopic picture of bleeding	Type of therapy	Hemostasis	Rebleeding	Outcome
1	F	84	Fundus	Melena	98	3	Heart failure, hypertension	Oozing	Dextrose 50%+EPI (7 cm^3)	Successful	No	Discharge
2	F	54	Upper gastric body	Hematemesis /melena	117	1	–	Spurting	Dextrose 50%+EPI (6 cm^3)	Failure	–	Operation
3	F	42	Rectum	Rectal bleeding	121	–	–	Oozing	Dextrose 50%+EPI (7 cm^3)	Successful	No	Discharge
4	M	72	Jejunum	Hematemesis /melena	96	3	Hypertension, angina	Visible vessel	Dextrose 50%+EPI (7 cm^3)	Successful	Yes	Operation /death
5	M	48	Descending duodenum	Melena	117	–	–	Visible vessel	Dextrose 50%+EPI (8 cm^3)	Successful	No	Discharge
6	M	69	Gastric body	Hematemesis /melena	78	8	Angina, BII gastrectomy	Spurting	Dextrose 50%+EPI (9 cm^3)	Successful	Yes	Operation /discharge
7	M	86	Upper gastric body	Melena	104	2	Hypertension, angina	Visible vessel	Dextrose 50%+EPI (7 cm^3)	Successful	No	Discharge
8	F	81	Fundus	Melena	87	4	Hypertension, heart failure	Oozing	Dextrose 50%+EPI (8 cm^3)	Successful	No	Discharge
9	M	82	Fundus	Hematemesis /melena	78	8	Heart failure	Visible vessel	Dextrose 50%+EPI (8 cm^3)	Successful	Yes	Operation /discharge
10	M	83	Gastric body	Hematemesis /melena	96	3	Heart failure	Visible vessel	Dextrose 50%+EPI (8 cm^3)	Successful	Yes	Discharge
11	F	72	Fundus	Melena	77	6	Hypertension	Visible vessel	Ethanolamine oleate (9 cm^3)	Successful	No	Discharge
12	M	66	Upper gastric body	Melena	106	2	Gout, hypertension	Visible vessel	Ethanolamine oleate (6 cm^3)	Successful	No	Discharge
13	M	79	Upper gastric body	Melena	92	4	Hypertension, angina	Visible vessel	EPI+HP (8×30 J)	Successful	No	Discharge
14	M	74	Fundus	Hematemesis /melena	98	3	Renal failure, gout, diabetes	Visible vessel	EPI+HP (6×30 J)	Successful	No	Discharge
15	M	48	Antrum	Melena	110	1	–	Oozing	EPI+3 hemoclips	Successful	No	Discharge
16	M	60	Antrum	Hematemesis /melena	104	3	Duodenal ulcer	Oozing	EPI+4 hemoclips	Successful	No	Discharge
17	M	65	Antrum	Melena	103	2	Diabetes, hypertension	Spurting	EPI+3 hemoclips	Successful	No	Discharge
18	M	67	Sigmoid colon	Rectal bleeding	115	2	Colonic polyps	Oozing	EPI+4 hemoclips	Successful	No	Discharge
19	M	74	Sigmoid	Rectal bleeding	113	2	Angina	Oozing	EPI+3 hemoclips	Successful	No	Discharge
20	M	84	Fundus	Hematemesis /melena	88	4	Heart failure, aorto-iliac bypass	Two visible vessels	4 hemoclips	Successful	No	Discharge
21	F	79	Gastric body	Melena	118	1	Hypertension	Visible vessel	2 hemoclips	Successful	No	Discharge
22	M	75	Gastric body	Melena	103	2	Heart failure	Visible vessel	2 hemoclips	Successful	No	Discharge
23	M	72	Gastric body	Hematemesis /melena	100	3	BII gastrectomy angina	Visible vessel	Inability to approach the visible vessel	–	–	Operation /discharge

EPI, epinephrine solution 1:10 000.

and surgical intervention was required (Table 1). Four patients were treated with injection of ethanolamine oleate and the heater probe respectively, and permanent hemostasis was achieved on a single session (Table 1). The power settings for the heater probe were clearly stated in two patients (30 J in both) and the number of applications ranged from 6 to 8. Among the patients in the hemoclip group, the mean number of hemoclips used was 3.1 (range 2-4). Hemostasis was achieved at the initial endoscopic procedure by hemoclip (Figure 2) in all eight patients. Epinephrine plus normal saline (1:10 000) was used as an useful adjunct when the lesion was oozing or spurting, to slow or stop bleeding prior to hemoclip application or heater probe treatment. Five patients (22%) underwent surgery, four after unsuccessful endoscopic therapy and one because it was impossible to approach the lesion on the posterior wall of the patient's gastrectomized stomach. One patient (4.3%) died of sepsis and multiple organ failure in the postoperative period.

Endoscopic hemoclipping therapy was shown to be generally more effective than injection therapy in terms of the rates of permanent hemostasis (100% *vs* 66.6%, $P<0.01$), recurrent bleeding (0% *vs* 33.3%, $P<0.01$) and surgery (0% *vs* 33.3%, $P<0.01$, Table 2).

In the five patients, who underwent surgery, gastrotomy showed a muscular artery protruding from the mucosa but not ulceration, findings being consistent with Dieulafoy's lesion. Wedge resection was performed and histopathologic examination confirmed the presence of an abnormally large submucosal artery.

None of the patients presented with recurrent gastrointestinal bleeding from Dieulafoy's lesions during a mean long-term follow-up of 29.8 mo (range 2-120 mo). Seven patients died during the follow-up from causes unrelated to the Dieulafoy's lesions or endoscopic procedures.

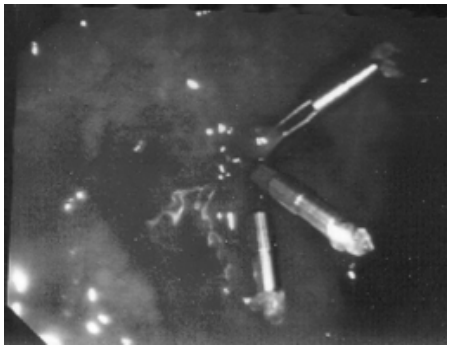

Figure 2 Endoscopic view showing complete closure of a minute mucosal defect with a protruding vessel with three hemoclips.

Table 2 Outcome of endoscopic therapy in injection and mechanical groups, *n* (%)

Parameters	Injection group	Mechanical group	*P*
Initial hemostasis	11 (92.5)	8 (100)	NS
Recurrent bleeding	4 (33.3)	0 (0)	<0.01
Permanent hemostasis	8 (66.6)	8 (100)	<0.01
Operation	4 (33.3)	0 (0)	<0.01

NS, non significant.

DISCUSSION

Dieulafoy's lesion is an uncommon cause of gastrointestinal bleeding, although some authors consider it as an under-recognized entity[1,9]. It is a disease of mainly aged and elderly males[10,11]. Our results with a mean age of 70.3 years and a more pronounced male predominance of 1:3 are consistent with former findings. Though the fact that they have been described in other parts of the gastrointestinal tract, Dieulafoy's lesions are located in the proximal stomach in more than three-fourths of patients[1,2]. Accordingly, in 78% of our patients the lesion was found in the stomach and in 39% in the classic site within 6 cm of the gastroesophageal junction. As in other reports, we identified Dieulafoy's lesions in the colon, jejunum and duodenum. Interestingly, one patient presented two simultaneous Dieulafoy's lesions in the gastric fundus.

The diagnostic yield of the first endoscopy varies from 63% to 92%[9]. Norton *et al*.[12], and Kasapidis *et al*.[13], found that a mean of 1.9 or 1.3 endoscopic sessions is required for diagnosis. In the present study, the diagnosis of Dieulafoy's lesion was established in 69% of patients during the first endoscopy, with a mean of 1.7 endoscopic sessions. A protruding vessel is found in 50% of patients and about two-thirds of patients manifest active bleeding, either as oozing or as spurting[10,11,14,15]. By contrast, in the present study the frequency of active bleeding was low (39%), with the majority of our patients having a non-bleeding visible vessel (61%), though the fact that the comorbid conditions and the mean age of our patients were consistent with former studies.

Some investigators have documented significant diseases in patients with Dieulafoy's lesion[5,10,16,17]. Comorbidity of cardiovascular diseases, diabetes, chronic renal failure and hypertension is present in almost 90% of patients with Dieulafoy's lesion[12]. In more than 40% of patients with Dieulafoy's lesion, the use of medication that influences blood coagulation has also been noted[12,16]. However, other studies have found no association of Dieulafoy's lesion with concomitant disease or the use of medications[14,18]. The results of the present investigation are consistent with the former studies. The significant comorbidity in 17 patients (74%) is likely a reflection of the elderly population studied, since any pathogenic significance remains speculative. Pathologic studies have failed to demonstrate atherosclerosis or aneurismal dilatation of the involved vessel[16,18].

Surgical wedge resection has been the standard treatment of Dieulafoy's lesions in the past[1]. However, its mortality rate is as high as 23%[1]. Since the late 1980s, a variety of endoscopic techniques have been used in the management of Dieulafoy's lesions. Endoscopic hemostatic methods could be divided into three groups: thermal, regional injection and mechanical[9,12,17,19,20]. Each method has both advantages and disadvantages related to the hemostatic mechanism and the technical procedure itself and varying results have been reported. The results of endoscopic hemostatic therapies depend on many and variable factors. The major factors include the level of expertise in performing the endoscopic procedure, coincident clinical risk factors, the use of advanced equipment and the inherent differences in various procedures.

All these factors influence the success of endoscopic outcome, but endoscopic modalities can achieve permanent hemostasis in approximately 95% of patients[9]. The overall lower rate of permanent hemostasis (78%) in our study was due to the low hemostatic effect (60%) of dextrose 50% plus epinephrine injection. It must be emphasized that the osmotic dehydrating and sclerosant effect of hypertonic glucose water (50%) has been reported[21] to be superior than a classic sclerosant agent, like sodium tetradecyl sulfate (15%), in controlling bleeding and rebleeding in patients with advanced liver cirrhosis and gastric variceal bleeding. Therefore, the low rate of hemostasis achieved in our study by dextrose 50% plus epinephrine cannot be explained. A careful search of the MEDLINE database from 1970 to 2003 did not retrieve any report of dextrose 50% plus epinephrine used in the treatment of Dieulafoy's lesions. Thus, the present study seems to be the first report on the use of dextrose 50% plus epinephrine as a therapeutic modality for Dieulafoy's lesions.

In the present investigation, none of the patients treated with heater probe coagulation or ethanolamine oleate injection developed recurrent bleeding. The mechanical method of hemoclips used in our study achieved complete hemostasis in 100% of patients. None of our patients treated with hemoclips had recurrent bleeding, while four patients (33.3%) in the injection group had recurrent bleeding ($P<0.01$, Table 2).

Although the number of patients in our study was small, we believe that the successful management especially by hemostatic clips (Table 2) favors a primary endoscopic approach to Dieulafoy's disease. It must be underscored, however, that an experienced endoscopist is necessary as a Dieulafoy's lesion can easily be overlooked or may be difficult to be approached, as was the case for one of our patients.

Hemoclips are mechanical devices, it must be argued that they cannot eradicate a Dieulafoy's lesion with a large caliber artery as effectively as sclerosant injections or thermal coagulation and that bleeding may recur after this type of treatment. However, in our study no patient had recurrent bleeding after hemoclip treatment during the follow-up period.

In conclusion, endoscopic therapy has become the treatment of choice for Dieulafoy's lesions and the endoscopic hemoclip treatment is effective and appears to be more successful in achieving hemostasis than injection treatment. More definite conclusions require further large controlled studies.

□□□□□□□□□□

1 **Fockens P,** Tytgat GN. Dieulafoy's disease. *Gastroenterol Clin North Am* 1996; **6**: 739-752
2 **Reilly HF,** Al-Kawas FH. Dieulafoy's lesion, diagnosis and management. *Dig Dis Sci* 1991; **36**: 1702-1707
3 **Ertekin C,** Barbaros U, Tavigoglu K, Guloglu R, Kasoglu A. Dieulafoy's lesion of the esophagus. *Surg Endosc* 2002; **16**: 219-221
4 **Goldenberg SP,** DeLuca VJ, Marignani P. Endoscopic treatment of Dieulafoy's lesion of the duodenum. *Am J Gastroenterol* 1990; **85**: 452-454
5 **Gadenstatter M,** Wetscher G, Cookes PF, Mason RJ, Schwab G, Pointner R. Dieulafoy's disease of the large and small bowel. *J Clin Gastroenterol* 1998; **27**: 169-172
6 **Nozoe T,** Kitamura M, Matsumata T, Sugimachi K. Dieulafoy – like lesions of colon and rectum in patients with chronic renal failure on long–term hemodialysis. *Hepatogastroenterology* 1999; **46**: 3121-3133
7 **Kayali Z,** Sangchantz W, Matsumoto B. Lower gastrointestinal bleeding secondary to Dieulafoy–like lesion of the rectum. *J Clin Gastroenterol* 2000; **30**: 328-330
8 **Azimuddin K,** Stasik JJ, Rosen L, Riether RD, Khubchandani IT. Dieulafoy's lesion of the anal canal: a new clinical entity. Report of two cases. *Dis Colon Rectum* 2000; **43**: 423-426
9 **Savides TJ,** Jensen DM. Therapeutic endoscopy for non – variceal gastrointestinal bleeding. *Gastroenterol Clin North Am* 2000; **29**: 465-487
10 **Stark ME,** Gostout CJ, Balm RK. Clinical features and endoscopic management of Dieulafoy's disease. *Gastrointest Endosc* 1992; **38**: 545-550
11 **Schmulewitz N,** Baillie J. Dieulafoy lesion: A review of 6 years of experience at a tertiary referral center. *Am J Gastroenterol* 2001; **96**: 1688-1694
12 **Norton ID,** Petersen BT, Sorbi D, Balm RK, Alexander GL, Gostout CJ. Management and long–term prognosis of Dieulafoy lesion. *Gastrointest Endosc* 1999; **50**: 762-767
13 **Kasapidis P,** Georgopoulos P, Delis V, Balatsos V, Kostantinidis A, Skandalis N. Endoscopic management and long–term follow–up of Dieulafoy's lesions in the upper GI tract. *Gastrointest Endosc* 2002; **55**: 527-531
14 **Veldhuyzen van Zanten SJ,** Bartelsman JF, Schipper ME, Tytgat GN. Recurrent massive hematemesis from Dieulafoy vascular malformations- a review of 101 cases. *Gut* 1986; **27**: 213-222
15 **Mumtaz R,** Shaukat M, Ramirez F. Outcomes of endoscopic treatment of gastrointestinal Dieulafoy's lesion with rubber band ligation and thermal/injection therapy. *J Clin Gastroenterol* 2003; **36**: 310-314
16 **Juler GI,** Labitzke HG, Lamb R, Allen R. The pathogenesis of Dieulafoy's gastric erosion. *Am J Gastroenterol* 1984; **79**: 195-200
17 **Parra-Blanco A,** Takahashi H, Mendez Jerez PV, Kojima T, Aksoz K, Kirihara K, Palmerin J, Takekuma E, Fuijta R. Endoscopic management of Dieulafoy lesions of the stomach: a case study of 26 patients. *Endoscopy* 1997; **29**: 834-839
18 **Katz PO,** Salas L. Less frequent causes of upper gastrointestinal bleeding. *Gastroenterol Clin North Am* 1993; **22**: 875-889
19 **Baettig B,** Haecki W, Lammer F, Jost R. Dieulafoy's disease: endoscopic treatment and follow–up. *Gut* 1993; **34**: 1418-1421
20 **Chung ILK,** Kim EJ, Lee MS, Kim HS, Park SH, Lee MH, Kim SJ, Cho MS. Bleeding Dieulafoy's lesion and the choice of endoscopic method: comparing the hemostatic efficacy of mechanical and injection method. *Gastrointest Endosc* 2000; **52**: 721-724
21 **Chang KY,** Wu CS, Chen PC. Prospective randomized trial of hypertonic glucose water and sodium tetradecyl sulfate for gastric variceal bleeding in patients with advanced liver cirrhosis. *Endoscopy* 1996; **2**: 481-486

Science Editor Wang XL and Guo SY **Language Editor** Elsevier HK

PO Box 2345, Beijing 100023, China
www.wjgnet.com
wjg@wjgnet.com

ELSEVIER

World J Gastroenterol 2005;11(38):6027-6030
World Journal of Gastroenterology ISSN 1007-9327

• *BRIEF REPORTS* •

Manometric assessment of idiopathic megarectum in constipated children

Giuseppe Chiarioni, Giuseppe de Roberto, Alessandro Mazzocchi, Antonio Morelli, Gabrio Bassotti

Giuseppe Chiarioni, Gastroenterological Rehabilitation Division of the University of Verona, Valeggio sul Mincio Hospital, Azienda Ospedaliera of Verona, Valeggio sul Mincio, Verona 37067, Italy
Giuseppe de Roberto, Alessandro Mazzocchi, Antonio Morelli, Gabrio Bassotti, Gastroenterology and Hepatology Section, Department of Clinical and Experimental Medicine, University of Perugia, Perugia 06100, Italy
Correspondence to: Dr. Gabrio Bassotti, Clinica di Gastroenterologia ed Epatologia Via Enrico Dal Pozzo, Padiglione W, Perugia 06100, Italy. gabassot@tin.it
Telephone: +39-75-584-7570
Received: 2005-01-26 Accepted: 2005-04-18

Abstract

AIM: Chronic constipation is a frequent finding in children. In this age range, the concomitant occurrence of megarectum is not uncommon. However, the definition of megarectum is variable, and a few data exist for Italy. We studied anorectal manometric variables and sensation in a group of constipated children with megarectum defined by radiologic criteria. Data from this group were compared with those obtained in a similar group of children with recurrent abdominal pain.

METHODS: Anorectal testing was carried out in both groups by standard manometric technique and rectal balloon expulsion test.

RESULTS: Megarectum patients displayed discrete abnormalities of anorectal variables and sensation with respect to controls. In particular, the pelvic floor function appeared to be impaired in most patients.

CONCLUSION: Constipated children with megarectum have abnormal anorectal function and sensation. These findings may be helpful for a better understanding of the pathophysiological basis of this condition.

Key words: Constipation; Manometry; Megarectum

Chiarioni G, de Roberto G, Mazzocchi A, Morelli A, Bassotti G. Manometric assessment of idiopathic megarectum in constipated children. *World J Gastroenterol* 2005; 11(38): 6027-6030
http://www.wjgnet.com/1007-9327/11/6027.asp

INTRODUCTION

Chronic constipation is a frequently encountered symptom in children[1]. Due to a general belief that childhood constipation gradually disappears before or during puberty, this symptom is often underestimated and scarcely taken into consideration. However, recent evidence suggests that up to one-third of the constipated children followed beyond puberty continue to have severe complaints of constipation[2].

The definition of constipation in childhood is also less standardized than in adults; for the latter, in fact, the Rome II criteria[3,4] seem quite accepted and widespread whereas the criteria for children[5] are believed to be too restrictive, in that they might exclude several children with constipation[6].

For practical purposes, childhood constipation may be grossly divided into two groups, represented by functional fecal retention (FFR, most frequent) and slow transit constipation (STC), which also reflect the main pathophysiological abnormalities[7]. In fact, constipation in children is very rarely caused by a colonic motility disorder, as frequently found in adults[8]. Childhood constipation is mostly due to a maladaptive behavior triggered by an unpleasant defecation that in some subjects led to delay further defecation by withholding the stools. These patients, who were different than those with STC, have normal colonic motility[9].

In chronically constipated children with FFR, the abnormal motor activity is often found in the rectum, which may become so dilated that it is unable to generate enough pressure to propel the stools into the anal canal[9]. This megarectum is found in 30-100% of constipated children, depending on the definition used[10-14]. Thus, no uniform definition of megarectum for constipated children is available, it is unknown whether a large rectum is the result or the cause of constipation, and which underlying mechanism is responsible for fecal impaction[15].

Therefore, purpose of the present study was the assessment of chronically constipated pediatric patients with megarectum defined by radiologic criteria.

MATERIALS AND METHODS

Patients

Fifteen constipated children (11 males and 4 females, age 9±0.6 years) entered the study. Average duration of symptoms was 4 years (range 2-8 years). Patients were recruited when they met at least two of the following criteria[16,17]: (1) less than three defecations per week; (2) soiling and/or encopresis episodes more than twice per week; (3) passage of large amounts of feces once per 7-30 d; and (4) presence of a palpable rectal mass. Moreover, barium enema showed the presence of an enlarged rectum

(diameter more than 6.5 cm in the lateral view, as measured on a line extending perpendicular to S_2[18]) in all patients.

On physical examination, all patients had a large amount of soft stool that filled the rectum. Soiling, defined as the loss of a small amount of loose stool in the underwear[17], was present in 3 (13%) patients and encopresis, defined as the loss of a normal amount of stool in the underwear after the age of 4 years (without an underlying organic disorder)[17], was present in 13 (87%) patients. Before performing manometric and rectal compliance determination, a rectal disimpaction schedule was performed in all patients. This schedule consisted of oral osmotic laxatives (lactitol, 5 g/10 kg body weight in two divided daily doses) and tap water enemas given by the parents for a maximum of 7 d. The last enema was given at least 5 h before physiological assessment was done. Rectal digital examination was performed in all patients, to ascertain that an adequate rectal disimpaction was achieved.

Controls

The control group was represented by 12 children (nine males and three females, age 10±0.7 years) with recurrent abdominal pain (RAP) and without rectal fecal impaction. These patients were recruited on the basis of Rome II criteria for RAP[5]: at least 12 wk of: (1) continuous or nearly continuous abdominal pain in a school-aged child or adolescent; and (2) no or only occasional relation of pain with physiological events (e.g., eating, menses, or defecation); and (3) some loss of daily functions; and (4) the pain is not feigned (e.g., malingering); and (5) the patient had insufficient criteria for other functional gastrointestinal disorders that would explain the abdominal pain. All controls had at least one bowel movement per day, and they did not meet the criteria for constipation as defined above.

Methods

Anorectal manometry and tests of rectal compliance were carried out according to a standard technique. Briefly, a commercially available four-lumen pediatric anorectal catheter with terminal balloon (Menfis bioMedica, Bologna, Italy, type 5R-9-100CB), connected via physiological pressure transducers to a low-compliance infusion pump and to a computerized recording system (Dyno Compact System, Menfis) was used.

After recording the rectoanal pressure profile with stepwise withdrawal (1 cm/30 s), the anal resting tone was recorded for 2-5 min with the catheter fixed at the highest pressure point obtained during two pull-throughs. Then, the rectosphincteric reflex was evaluated by inflating and rapidly deflating the catheter balloon with 10, 20, 30, 50, and 100 mL of air. Finally, the sphincteric response to straining was assessed by asking the patients to strain as if to defecate thrice at 1-min intervals.

To test rectal compliance and sensation, a single-lumen PVC catheter (outer diameter 4 mm) with a 7-cm-long cut terminal unstretched condom was used, connected to the above-mentioned pressure transducer and recorder, as previously described[19]. The balloon was placed with its distal portion about 5 cm from the anal margin and, through a syringe equipped with a three-channel stopcock, inflated with 50 mL of air increments every 60 s until the maximum rectal tolerable volume (MRTV) was reached. Rectal expulsion ability was assessed, with the patient lying on the left side, by inserting a well-lubricated Foley catheter in the rectum, then filling it with 50 mL of water and asking the patient to defecate it[20].

Ethical considerations

After careful explanations about the aims of the study, the parents of the children gave written informed consent, and the studies were carried out in accordance with local ethical guidelines, following the recommendations of the Declaration of Helsinki.

Data analysis

All tracings were analyzed in blind by one of the investigators. For anorectal manometry and test of rectal compliance and sensation, the following variables were taken into account[19,21]: (1) maximum basal pressure of the internal anal sphincter, defined as the mean of the highest resting pressures recorded from each of the four ports during the two pull-throughs[19,21,22]; (2) minimum relaxation volume (MRV), defined as the lower quantity of air inflated in the rectal balloon necessary to elicit the rectoanal inhibitory reflex, a drop in pressure >5 mmHg, which represents relaxation of the internal sphincter[23,24]; (3) defecatory sensation threshold (DST), defined as the smallest volume at which the first desire to defecate was reported by the patient[25,26]; (4) response to straining, evaluated by observing whether straining to defecate caused a decrease in intra-anal pressure (normal response) or a paradoxical increase in intra-anal pressure[27]; (5) MRTV, defined as the maximum volume of air that could be infused into the rectal balloon and responsible either for an intolerable urge to defecate, painful distension, or expulsion of the balloon itself[11]; (6) rectal compliance, defined as the intraballoon pressure at 100 mL when inflated intrarectally minus the intraballoon pressure at 100 mL when inflated in open air[28,29]; and (7) rectal expulsion. Without any time limitation, the test was considered abnormal when the patient was not able to expel the balloon (Foley catheter filled with 50 mL of water) and refused further straining attempts.

Statistical analysis

The Kolmogorov-Smirnov test for normality was applied, and showed that the data were not normally distributed. Therefore, comparisons of data between controls and patients were done by means of nonparametric tests. The Wilcoxon rank sum test (two-tailed) and the χ^2 test were applied, where necessary. Values of P less than 0.05 were chosen for rejection of the null hypothesis. Data are expressed as mean±SE.

RESULTS

No differences between groups were found concerning age (9.6±0.7 years in controls *vs* 9.5±0.6 years in patients, $P = 0.10$). Soiling and/or encopresis was found in none of the controls and in 13/15 (87%) patients ($P<0.0001$). Analysis of anorectal physiological variables showed that

the maximum basal pressure of the anal sphincter was significantly higher in controls with respect to the patients (58±3.4 *vs* 31±3 mmHg, $P<0.001$), whereas the MRV was lower in controls (13.3±1.4 *vs* 39±5.3 mmHg, $P<0.001$). Concerning the DST, this was found to be significantly lower in controls compared to that found in megarectum patients (54±4 mmHg *vs* 130±27 mmHg, $P<0.01$). As expected, controls displayed lower values of MRTV compared to the megarectum patients (171±11 mL *vs* 523±68 mL, $P<0.001$) and higher compliance values (18±1.3 mmHg *vs* 10.5±2 mmHg, $P<0.02$).

The response to straining was abnormal in 1/12 (8.3%) controls and in 9/15 (60%) patients ($P = 0.017$); the rectal expulsion test was abnormal in 1/12 (8.3%) controls and in 15/15 (100%) patients ($P<0.0001$).

DISCUSSION

The term megarectum is frequently employed in children with constipation or fecal impaction without any quantification measure, and there are only a few data obtained in groups with more objective definitions[17]. In the present study, we adopted a validated radiological definition, at least for adults and adolescents: the limit of this definition is due to the fact that lesser degrees of megarectum in the pediatric population may have been excluded. However, we had a well-defined group of patients with objective criteria, and we feel that this is important since to the best of our knowledge there are no such reports from Italy.

The comparison of anorectal parameters between patients and controls showed significant abnormalities in the former that displayed lower basal pressures of the anal sphincter and compliance values, whereas higher values were found for MRV, DST, and MRTV. In addition, most megarectum patients had clinical and instrumental evidence of abnormal pelvic floor function.

These results are in agreement with some previous studies[11,30-33], where others were not able to find such differences[16,17,34]. We are at present unable to explain such discrepancies, although patients' selection, severity of symptoms, and assessment methods may be responsible for these differences between studies.

We feel of interest that this group of children with megarectum shares anorectal abnormalities similar to those we found in adult patients with megarectum[19]. In this rather homogeneous group of pediatric patients, the findings seem consistent with similar mechanisms proposed for adults, i.e. that megarectum may be a mechanism for constipation by outlet obstruction[35], as shown by the impairment of anorectal dynamics in such patients. The rectal function, in fact, seems to be severely deranged, as shown by the MRTV recorded in these children, due to an atonic rectum that sometimes adapted to masses of over 800 mL, too large to be defecated. The MRV and rectal sensation were also impaired, with some of the patients needing higher volumes to relax the sphincter and feeling the defecatory stimulus only at high volumes of distension, thereby enforcing the mechanisms leading to further dilatation of the rectal ampulla.

The clinical significance of a dyssynergic phenomenon in these patients is unclear. Previous studies have proposed this phenomenon as one of the main causes of impaired rectal expulsion in megarectum and megacolon patients[36], but other studies have challenged this hypothesis, since rectal emptying may happen against a contracting pelvic floor[37,38]. However, since fecal consistency is likely to influence the efficiency of rectal emptying[39,40], it is possible that the presence of large, hard stools in a megarectum may elicit a dyssynergic pattern.

In conclusion, we described a group of constipated children with well-defined megarectum, and showed that these patients display important abnormalities of anorectal variables and sensation. We feel these findings may be of some interest for a better understanding of the pathophysiological mechanisms of this condition and, possibly, for a more targeted therapeutic approach.

REFERENCES

1 **Loening-Baucke V.** Chronic constipation in children. *Gastroenterology* 1993; **38**: 1568-1580
2 **van Ginkel R,** Reitsma JB, Buller HA, van Wijk MP, Taminiau JA, Benninga MA. Childhood constipation: longitudinal follow-up beyond puberty. *Gastroenterology* 2003; **125**: 357-363
3 **Thompson WG,** Longstreth GF, Drossman DA, Heaton KW, Irvine EJ, Muller-Lissner SA. Functional bowel disorders and functional abdominal pain. *Gut* 1999; **45**(Suppl 2): II43-II47
4 **Whitehead WE,** Wald A, Diamant NE, Enck P, Pemberton JH, Rao SSC. Functional disorders of the anus and rectum. *Gut* 1999; **45**(Suppl 2): II55-II59
5 **Rasquin-Weber A,** Hyman PE, Cucchiara S, Fleisher DR, Hyams JS, Milla PJ, Staiano A. Childhood functional gastrointestinal disorders. *Gut* 1999; **45**(Suppl 2): II60-II68
6 **Voskuijl WP,** Heijmans J, Heijmans TS, Taminiau JA, Benninga MA. Use of Rome II criteria in childhood defecation disorders: applicability in clinical and research practice. *J Pediatr* 2004; **145**: 213-217
7 **Sutcliffe JR,** King SK, Southwell BR, Hutson JM. Paediatric constipation for adult surgeons–Article 1: targeting the cause. *ANZ J Surg* 2004; **74**: 777-780
8 **Bassotti G,** Iantorno G, Fiorella S, Bustos-Fernandez L, Bilder CR. Colonic motility in man: features in normal subjects and in patients with chronic idiopathic constipation. *Am J Gastroenterol* 1999; **94**: 1760-1770
9 **Di Lorenzo C,** Ciamarra P. Pediatric gastrointestinal motility. In Schuster MM, Crowell MD, Koch KL, eds. *Schuster atlas of gastrointestinal motility*, 2nd edition. *Hamilton, BC Decker Inc.* 2002: 411-428
10 **Liebman WM.** Disorders of defecation in children: evaluation and management. *Postgrad Med* 1979; **66**: 105-108
11 **Meunier P,** Louis D, Jaubert de Beaujeau M. Physiologic investigation of primary chronic constipation in children : comparison with the barium enema study. *Gastroenterology* 1984; **87**: 1351-1357
12 **Loening-Baucke VA,** Cruikshank BM. Abnormal defecation dynamics in chronically constipated children with encopresis. *J Pediatr* 1986; **108**: 562-566
13 **Benninga MA,** Buller HA, Heymans HS, Tytgat GN, Taminiau JA. Is encopresis always the result of constipation? *Arch Dis Child* 1994; **71**: 186-193
14 **Staiano A,** Andreotti MR, Greco L, Basile P, Auricchio S. Long-term follow-up of children with chronic idiopathic constipation. *Dig Dis Sci* 1994; **39**: 561-564
15 **Partin JC,** Hamill SK, Fischel JE, Partin JS. Painful defecation and fecal soiling in children. *Pediatrics* 1992; **89**: 1007-1009
16 **van der Plas RN,** Benninga MA, Buller HA, Bossuyt PM, Akkermans LM, Redekop WK, Taminiau JA. Biofeedback training in treatment of childhood constipation: a randomised controlled study. *Lancet* 1996; **348**: 776-780
17 **van der Plas RN,** Benninga MA, Staalman CR, Akkermans

LMA, Redekop WK, Taminiau JA, Buller HA. Megarectum in constipation. *Arch Dis Child* 2000; **83**: 52-58
18 **Gattuso JM,** Kamm MA. Clinical features of idiopathic megarectum and idiopathic megacolon. *Gut* 1997; **41**: 93-99
19 **Chiarioni G,** Bassotti G, Germani U, Brunori P, Brentegani MT, Minniti G, Calcara C, Morelli A, Vantini I. Idiopathic megarectum in adults. An assessment of manometric and radiologic variables. *Dig Dis Sci* 1995; **40**: 2286-2292
20 **Barnes PR,** Lennard-Jones JE. Balloon expulsion from the rectum in constipation of different types. *Gut* 1985; **26**: 1049-1052
21 **Chiarioni G,** Chistolini F, Menegotti M, Salandini L, Vantini I, Morelli A, Bassotti G. One-year follow-up study on the effects of electrogalvanic stimulation in chronic idiopathic constipation with pelvic floor dyssynergia. *Dis Colon Rectum* 2004; **47**: 346-353
22 **Read NW,** Harford WV, Schmulen AC, Read MG, Santa Ana C, Fortran JS. A clinical study of patients with fecal incontinence and diarrhea. *Gastroenterology* 1979; **76**: 747-756
23 **Dickinson VA.** Maintenance of anal continence. A review of pelvic floor physiology. *Gut* 1978; **19**: 1163-1174
24 **Bassotti G,** Maggio D, Battaglia E, Giulietti O, Spinozzi F, Reboldi G, Serra AM, Emanuelli G, Chiarioni G. Manometric investigation of anorectal function in early and late stage Parkinson's disease. *J Neurol Neurosurg Psych* 2000; **68**: 768-770
25 **Pescatori M,** Parks AG. The sphincteric and sensory components of preserved continence after ileoanal reservoir. *Surg Gynecol Obstet* 1984; **158**: 517-521
26 **Chiarioni G,** Bassotti G, Monsignori A, Menegotti M, Salandini L, Di Matteo G, Vantini I, Whitehead WE. Anorectal dysfunction in constipated women with anorexia nervosa. *Mayo Clin Proceed* 2000; **75**: 1015-1019
27 **Whitehead WE,** Heymen S, Schuster MM. Motility as a therapeutic modality: biofeedback treatment of gastrointestinal disorders. In Schuster MM, Crowell MD, Koch KL, eds. Schuster Atlas of Gastrointestinal Motility, Second edition. *Hamilton, BC Decker Inc* 2002: 381-397
28 **Whitehead WE,** Chaussade S, Corazzieri E, Kumar D. Report of an international workshop on management of constipation. *Gastroenterol Int* 1991; **4**: 99-113
29 **Chiarioni G,** Scattolini C, Bonfante F, Vantini I. Liquid stool incontinence with severe urgency: anorectal function and effective biofeedback therapy. *Gut* 1993; **34**: 1576-1580
30 **Callaghan RP,** Nixon HH. Megarectum: physiological observations. *Arch Dis Child* 1964; **39**: 153-157
31 **Molnar D,** Taitz LS, Urwin OM, Wales JK. Anorectal manometry results in defecation disorders. *Arch Dis Child* 1983; **58**: 257-261
32 **Clayden GS.** Management of chronic constipation. *Arch Dis Child* 1992; **67**: 340-344
33 **Loening-Baucke V,** Yamada T. Is the afferent pathway from the rectum impaired in children with chronic constipation and encopresis? *Gastroenterology* 1995; **109**: 397-403
34 **Benninga MA,** Buller HA, Taminiau JA. Biofeedback training in chronic constipation. *Arch Dis Child* 1993; **68**: 126-129
35 **Verduron A,** Devroede G, Bouchoucha M, Arhan P, Schang JC, Poisson J, Hémond M, Hébert M. Megarectum. *Dig Dis Sci* 1988; **33**: 1164-1174
36 **Barnes PR,** Lennard-Jones JE. Function of the striated anal sphincter during straining in controls subjects and constipated patients with a radiologically normal rectum and idiopathic megacolon. *Int J Colorect Dis* 1988; **3**: 207-209
37 **Jones PN,** Lubowski DZ, Swash M, Path MRC, Henry MM. Is paradoxical contraction of the puborectalis muscle of functional importance? *Dis Colon Rectum* 1987; **30**: 667-670
38 **Miller R,** Duthie GS, Bartolo DCC, Roe AM, Locke-Edmunds J, Mortensen NJ. Anismus in patients with normal and slow transit constipation. *Br J Surg* 1991; **78**: 690-692
39 **Bannister JJ,** Davison P, Timms JM, Gibbons CG, Read NW. Effect of the stool size and consistency on defaecation. *Gut* 1987; **28**: 1246-1249
40 **Ambroze WL,** Pemberton JH, Bell AM, Brown ML, Zinsmeister AR. The effect of stool consistency on rectal and neorectal emptying. *Dis Colon Rectum* 1990; **34**: 1-7

Science Editor Guo SY **Language Editor** Elsevier HK

PO Box 2345, Beijing 100023, China
www.wjgnet.com
wjg@wjgnet.com

ELSEVIER

World J Gastroenterol 2005;11(38):6031-6037
World Journal of Gastroenterology ISSN 1007-9327

• *BRIEF REPORTS* •

Different effects of a CD14 gene polymorphism on disease outcome in patients with alcoholic liver disease and chronic hepatitis C infection

C Meiler, M Mühlbauer, M Johann, A Hartmann, B Schnabl, N Wodarz, G Schmitz, J Schölmerich, C Hellerbrand

C Meiler, M Mühlbauer, B Schnabl, J Schölmerich, C Hellerbrand, Department of Internal Medicine I, University of Regensburg, Regensburg 93042, Germany
M Johann, N Wodarz, Department of Psychiatry, University of Regensburg, Regensburg 93042, Germany
A Hartmann, Department of Pathology, University of Regensburg, Regensburg 93042, Germany
G Schmitz, Institute for Clinical Chemistry and Laboratory Medicine, University of Regensburg, Regensburg 93042, Germany
Supported by grants from the Else Kröner Fresenius-Stiftung to Hellerbrand C and the Deutsche Forschungsgemeinschaft (Schn 620/3-1) to Schnabl B
Co-first-authors: C Meiler and M Mühlbauer
Correspondence to: C Hellerbrand, MD, Department of Internal Medicine I, University of Regensburg, Regensburg D-93042, Germany. claus.hellerbrand@klinik.uni-regensburg.de
Telephone: +49-941-944-7155 Fax: +49-941-944-7154
Received: 2005-03-10 Accepted: 2005-04-09

Abstract

AIM: Clinical and experimental data suggest that gut-derived endotoxins are an important pathogenic factors for progression of chronic liver disease. Recently, a C-T (-159) polymorphism in the promoter region of the CD14 gene was detected and found to confer increased CD14 expression and to be associated with advanced alcoholic liver damage. Here, we investigated this polymorphism in patients with less advanced alcoholic liver disease (ALD) and chronic hepatitis C virus (HCV) infection.

METHODS: CD14 genotyping was performed by PCR-RFLP analysis in (a) 121 HCV patients, (b) 62 patients with alcohol-associated cirrhosis (Alc-Ci), (c) 118 individuals with heavy alcohol abuse without evidence of advanced liver damage (Alc-w/o Ci), and (d) 247 healthy controls. Furthermore, serum levels of soluble CD14 (sCD14) and transaminases were determined.

RESULTS: The TT genotype was significantly more frequent in Alc-Ci compared to Alc-w/o Ci or controls (40.3% *vs* 23.7% or 24.0%, respectively). In Alc-w/o Ci, serum levels of transaminases did not differ significantly between patients with different CD14 genotypes. In HCV patients, TT-homozygotes had significantly higher sCD14 levels and sCD14 serum levels were significantly higher in patients with advanced fibrosis or cirrhosis. However, no association was found between CD14 genotypes and histological staging or grading.

CONCLUSION: Considering serum transaminases as surrogate markers for alcoholic liver damage, the CD14 polymorphism seems to exhibit different effects during the course of ALD. Differences in genotype distribution between cirrhotic HCV patients and alcoholics and the known functional impact of this polymorphism on CD14 expression levels further indicate differences in the pathophysiological role of CD14 and CD14-mediated lipopolysaccharides signal transduction with regard to the stage as well as the type of the underlying liver disease.

Key words: CD14 gene; Alcoholic liver disease; Chronic hepatitis C infection

Meiler C, Mühlbauer M, Johann M, Hartmann A, Schnabl B, Wodarz N, Schmitz G, Schölmerich J, Hellerbrand C. Different effects of a CD14 gene polymorphism on disease outcome in patients with alcoholic liver disease and chronic hepatitis C infection. *World J Gastroenterol* 2005; 11(38): 6031-6037
http://www.wjgnet.com/1007-9327/11/6031.asp

INTRODUCTION

Individuals affected by chronic liver disease show a broad spectrum of responses to the same etiologic agent. As one cause for this finding and increasing evidence indicates that genetic factors influence the natural history of chronic liver disease[1].

In case of alcoholic liver disease (ALD), early studies have focused on polymorphic forms of enzymes involved in alcohol metabolism[2-4]. Recent studies have shown that genetically determined variations in the inflammatory response contribute to different susceptibility for the development of various liver diseases, notably viral hepatitis[5,6] and ALD[7-10]. These findings together with accumulating clinical and experimental data indicate that the extent of the inflammatory response to the etiological agent is crucial in the pathogenesis of chronic hepatitis C virus (HCV) as well as alcoholic and other liver disease.

Several lines of evidence indicate that bacterial products, primarily endotoxins (lipopolysaccharides; LPS) induce and perpetuate hepatic inflammation. Endotoxin levels are correlated with the severity of ALD in experimental models[11] as well as in patients with chronic liver disease[12], and reducing gut endotoxin alleviates hepatic injury[13]. Endogenous LPS are constitutively produced within the gut by the death of Gram-negative bacteria and are absorbed into intestinal capillaries. In low concentrations, LPS can also be demonstrated in the portal venous blood in healthy

humans[14].

Increased LPS levels have been shown in patients with ALD as well as patients with chronic hepatitis C infection[12,15-17]. Several factors promote endotoxemia in this setting, including increased translocation of endotoxins and reduced hepatic clearance[11,18].

Circulating endotoxin is bound mainly to the LPS binding protein. This complex has a high affinity for the CD14 receptor[19]. CD14 is expressed on mature monocytes and macrophages, such as Kupffer cells[20,21]. Furthermore, hepatocytes as well as activated hepatic stellate cells (HSC) get stimulated by LPS via membrane-bound CD14[20,23].

A soluble CD14 (sCD14) is constitutively present in the circulation, and is apparently derived both from secretion of CD14 and from enzymatically cleaved glycosylphosphatidylinositol-anchored tissue CD14[24,25]. sCD14 is believed to play a key role as an intermediate in the neutralization of LPS under physiological conditions. sCD14 accelerates the transfer between LPS micelles and lipoproteins by acting as a carrier. sCD14 also enhances the release of monocyte-bound LPS, transferring LPS into plasma and into lipoproteins[26]. This results in a decreased cellular response to LPS, such as induction of TNF and interleukin-6 synthesis[27].

Recently, a polymorphism of the CD14 gene (C-T transition at bp -159 from the major transcription start site) was described. This polymorphism is located within the Sp1 transcription factor binding site, known to affect CD14 expression. The T allele promotes CD14 gene transcription as shown in *in vitro* on monocytes[28,29].

Functional relevance of the polymorphism has been suggested in several studies finding an association with myocardial infarction[29,30], ulcerative colitis[31], asthma[32], and chronic spondyloarthropathy[33]. Notably, all these diseases have an inflammatory component.

Recently, Järveläinen *et al*., investigated the frequency of this CD14 polymorphism in autopsy series of Finnish patients with ALD[34]. Interestingly, the T allele was associated with advanced ALD, especially with cirrhosis, but not with steatosis or less advanced stages of fibrosis. A subsequent analysis of a relatively small cohort of 30 patients with primary biliary cirrhosis revealed no significant association of the CD14 polymorphism with the severity of the disease and found no differences in the genotype distribution as compared to healthy controls[35]. Poullis *et al*., analyzed the effect of the CD14 polymorphism on liver function tests and found some evidence indicating that the TT genotype, associated with higher serum levels of sCD14, may offer protection from the development of fatty liver disease[36]. This hypothesis is supported by recent studies indicating an association between sCD14 levels and insulin sensitivity[37,38].

As in ALD in HCV patients, elevated serum levels of endotoxin as well as sCD14 have been reported[12,16,39] but the C-T (-159) promotor polymorphism of the CD14 gene had not been investigated in this group of patients so far.

Here we analyzed the association of this CD14 polymorphism with the histological stage of fibrosis and the grade of inflammation in hepatic tissue of HCV patients, and their corresponding sCD14 serum levels, respectively.

Furthermore, the aim of this study was to verify the association of the CD14 polymorphism with the degree of alcoholic liver damage, previously found in the Finnish study[35], in our cohort of patients with ALD from southern Germany.

[illegible]

Patients and controls

The following groups of patients were studied retrospectively: (a) 121 patients (80 males and 41 females; mean age: 37.2±11.5 years) with chronic hepatitis C (positive for HCV-RNA and anti-HCV) consecutively admitted to the medical department of the University of Regensburg. All patients were negative for hepatitis B surface antigen or antibodies to HIV and none of them had evidence of other types of liver disease. Risk factors for acquisition of hepatitis C infection were previous intravenous drug abuse in 25.6%, receipt of blood or blood products before the introduction of donor screening in 15.7%, and other factors or unknown in 58.7%. Liver biopsies were obtained from all patients before initiation of antiviral therapy (naive patients) by percutaneous Menghini-needle biopsy. In these patients fibrosis and inflammation were graded and staged numerically according to a score proposed by Desmet *et al*.[40], by a single pathologist.

The majority of patients received treatment with interferon-α+ribavirin. For 91 patients, data of qualitative HCV-PCR analysis 3 mo after initiation of antiviral therapy were available.

(b) sixty-two patients with alcoholic cirrhosis consecutively admitted to the medical department of the University of Regensburg (49 males and 13 females; mean age: 53.1±8.9 years). Patients were considered to have alcohol-related cirrhosis, if alcohol intake had been in excess of 100 g/d for more than 10 years and if testing for viral, metabolic, and immune etiologies was negative. Liver cirrhosis was diagnosed based on typical clinical, laboratory, ultrasound, and gastroscopical findings.

(c) one hundred and eighteen heavy drinkers without evidence of liver damage (90 males and 28 females; mean age: 42.5±9.1 years). These unrelated individuals of German descent were recruited from an in-patient abstention program at the Department of Psychiatry of the University of Regensburg. Each subject met the criteria of alcohol dependence according to ICD-10[41]. At the day of admission, several serum parameters were analyzed including transaminases (alanine aminotransferase [ALT], AST, and γ-glutamyl transferase [γ-GT]), and anti-HCV- and HBV-antibodies. Previous and current drinking habits, as well as family history of non-ALDs, and potential previous complications of advanced liver damages as ascites or esophageal varices were examined. Furthermore, within 14 d after admission, a clinical and ultrasound examination of the abdomen was performed.

Only alcohol-dependent subjects with an alcohol consumption of at least 80 g/d for more than 5 years were included. Furthermore, clinical or sonomorphological indications for advanced liver damage and serological evidence of HBV or HCV infection were exclusion criteria.

(d)two hundred and forty seven healthy subjects (119

females and 128 males), genotyped already in a previous study[42], served as controls.

Patients and controls were Caucasians and their geographical origin was southern Germany. Informed consent was obtained from all patients and the study was approved by the local ethics committee.

DNA isolation and CD14 genotyping

Genomic DNA specimens were prepared from 200 μL blood using the QIAamp blood kit following the manufacturer's instructions (Qiagen, Hilden, Germany). The C-T polymorphisms at position -159 of the CD14 gene was analyzed by performing PCR and subsequent restriction fragment length polymorphism analysis. PCR was performed under standard conditions (35 cycles, annealing temperature: 55 ℃) in a total reaction volume of 50 μL containing 2 μL of diluted genomic DNA, using the following pair of primers: forward: 5'-CCG AGA TGT TCC CAG CAC AG-3' and reverse: 5'-CTG CTT TGC TTG TGC CTC TT-3'. PCR products were digested by *Hae*III, and the resulting fragments were separated by electrophoresis in a 2% agarose gel and visualized by ethidium bromide staining. With the -159 T polymorphic base, the recognition sequence 5'-GG/CC-3' is modified to 5'-GG/TC-3', which is not cut by *Hae*III.

Serum sCD14 levels

sCD14 concentrations were analyzed in the serum of 97 patients with chronic hepatitis C infection using a sandwich ELISA following the instructor's manual (Biosource Europe, Nivelles, Belgium).

Statistical analysis

Results are expressed as mean±SD (range), median, or percent. Genotype frequencies are reported with their group percentages. Comparisons between clinical subgroups were made using the Student's unpaired *t*-test. A two-sided χ^2 test was used for comparison of qualitative variables. A P value <0.05 was considered statistically significant.

All computations were performed by using the SPSS-10 for Windows statistical computer package (SSPS, Inc., Chicago, IL, USA).

RESULTS

CD14 genotype frequency in patients with chronic alcohol abuse and controls

Initially, we wanted to confirm the finding of the previous Finnish study by Järveläinen *et al*., indicating higher prevalence of the C-159T promotor polymorphism of the CD14 endotoxin receptor in patients with advanced ALD[34].

CD14 genotyping was performed in patients with chronic alcohol abuse and liver cirrhosis (n = 62), or without clinical or sonomorphological signs of liver cirrhosis (n = 118), respectively. Furthermore, 247 healthy controls were genotyped. Results are summarized in Table 1.

Distribution of the individual genotypes in the control group (CC: 64/247 [25.6%], CT 128/247 [51.8%], and TT: 55/247 [22.3%]) was similar as in cohorts of other healthy individuals in previous reports[36,43,44].

Frequency of the C-159T polymorphism did not differ significantly between alcoholics without cirrhosis and controls. However, in accordance to the study by Järveläinen *et al*.[34], the TT genotype was significantly more frequent in alcoholics with cirrhosis (40.3%), compared to alcoholics without cirrhosis (23.7%; P = 0.020) and controls (22.3%; P = 0.006), respectively.

Comparison of ALT and AST levels between TT-homozygotes and alcoholics with genotype CC or CT revealed no significant differences (42.0±61.0 U/L *vs* 33.6±33.8 U/L, and 34.9±27.9 U/L *vs* 28.2±28 U/L, respectively).

Table 1 Frequency of (-159) CD14 genotypes (%) in patients with chronic alcohol abuse and cirrhosis, compared to alcoholics without clinical or sonomorphological signs of cirrhosis and controls

	CD14 genotype frequency		
	CC	CT	TT
Alcoholics with cirrhosis (n = 62)	5 (8.1%)	32 (51.6%)	25 (40.3%)
Alcoholics w/o cirrhosis (n = 118)	32 (27.1%)	58 (49.2%)	28 (23.7%)
Controls (n = 247)	64 (25.6%)	128 (51.8%)	55 (22.3%)

CD14 genotype frequency in patients with chronic hepatitis C infection

Next we wanted to analyze the frequency of the C-159T CD14 polymorphism in patients with a different etiology of chronic liver disease. Genotyping of 121 patients with chronic hepatitis C infection revealed no significant differences compared to healthy controls (CC: 26/121 [21.5%], CT: 66/121 [54.5%], and TT: 29/121 [24.0%]).

Comparing TT-homozygote HCV patients and HCV patients with genotype CC or CT we found no differences in demographic features such as age (38.0±12.3 years *vs* 37.1±11.4 years) and distribution of sexes (58.6% *vs* 68.5% males), and in the frequencies of potential routes of HCV infection (24.1% *vs* 26.1% i.v. drug users; 17.2% *vs* 15.2% recipients of blood transfusions), serum HCV-RNA levels (2.0×10^6 copies/mL *vs* 1.6×10^6 copies/mL) or frequencies of different HCV-genotypes (58.7% *vs* 66.3% type 1; 34.5% *vs* 25.0% type 2, Table 2). The number of initial virological responders to interferon therapy (no HCV-RNA detectable in the serum, 3 mo after initiation of therapy) did not differ between the genotypes (14/21 [66.7%] *vs* 46/70 [65.7%]).

Moreover and in contrast to patients with chronic alcohol abuse, frequency of TT-homozygotes did not differ between HCV patients with different severity of liver damage (Figure 1). TT-homozygotes were similarly frequent in patients with no or only mild, periportal fibrosis (staging 1 or 2) and HCV patients with more advanced septal fibrosis or cirrhosis (staging 3 or 4), respectively (20/85 [23.5%] *vs* 9/36 [25.5%], respectively).

The frequency of the CD14 genotypes was similar in HCV patients with mild or only minimal hepatic inflammation (grading 1 or 2) and patients with more severe hepatic inflammation or necrosis (grading >2): 14/63 [22.2%] *vs* 15/58 [25.9%], respectively. As in patients with chronic alcohol abuse, the comparison of ALT and AST levels between TT-homozygotes and hepatitis C patients with

genotype CC or CT revealed no significant differences (80.4±65.3 U/L *vs* 80.2±78.1 U/L, and 33.9±20.7 U/L *vs* 36.1±28.7 U/L, respectively).

Table 2 Clinical and biological characteristics of 121 patients with chronic hepatitis C infection according to CD14 –159 genotypes (TT *vs* CC and CT)

Clinical and biological characteristics	All patients	CD14 -159 genotype	
		TT	CC or CT
Age (yr; mean±SD)	37.2±11.5	38.0±12.3	37.1±11.4
Male gender (%)	66.1	58.6	68.5
HCV transmission route (%)			
- i.v. drug use	25.6	24.1	26.1
- Post-transfusion	15.7	17.2	15.2
- Other factors or unknown	58.7	58.6	58.7
HCV genotypes (%)			
- Type 1	64.5	58.7	66.3
- Type 3	27.3	34.5	25.0
- Others than type 1 or 3	8.3	6.9	8.7
Viral load			
(10^6 copies/mL; median)	1.7	2.0	1.6
Initial virological response to anti-HCV treatment[1] (%)	65.9	66.7	65.7

[1]HCV-RNA negative, 3 mo after the start of antiviral therapy; data available from 91/121 patients.

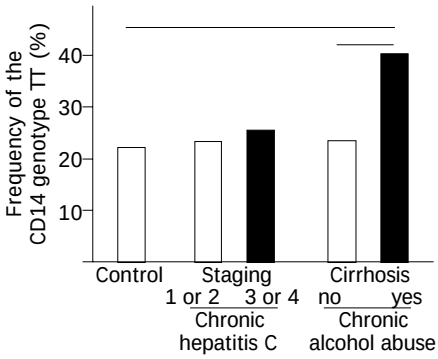

Figure 1 Frequency of the TT genotype at position -159 of the CD14 gene in patients with chronic hepatitis C infection, chronic alcohol abuse, and controls. The TT genotype was significantly more frequent in alcoholics with cirrhosis (25/62; [40.3%]), compared to alcoholics without clinical or sonomorphological signs of cirrhosis (28/118; [23.7%]; $P = 0.020$) and controls (55/247 [22.3%]; $P = 0.006$). In contrast, in HCV patients with no or only mild fibrosis (stage 1 or 2) and patients with prominent fibrosis or cirrhosis (stage 3 or 4) the frequency of the TT genotype was not significantly different (20/85 [23.5%] *vs* 9/36 [25.5%]).

Soluble CD14 serum levels in patients with chronic hepatitis C infection

It has been reported that sCD14 levels were elevated in patients with chronic liver disease[39]. Furthermore, studies investigating sCD14 levels in children recruited from a general population sample or in patients with ulcerative colitis found an association between sCD14 serum levels and CD14 -159 genotypes[28,31].

Therefore, we investigated sCD14 levels in the serum of 87 patients with chronic hepatitis C infection. Mean serum CD14 levels (3.8±0.4 μg/mL) were comparable to previous studies analyzing serum of patients with chronic liver disease[39].

HCV patients with no or only mild, periportal fibrosis, had significantly lower sCD14 serum levels than HCV patients with more advanced septal fibrosis or cirrhosis, respectively (3.5±0.4 μg/mL *vs* 3.8±0.9 μg/mL; $P = 0.004$).

Moreover, TT-homozygote HCV patients ($n = 20$) had significantly higher sCD14 serum levels than HCV patients with -159 CD14 genotype CT or TT ($n = 77$), respectively (3.5±0.4 μg/mL *vs* 3.7±0.7 μg/mL; $P = 0.012$, Figure 2).

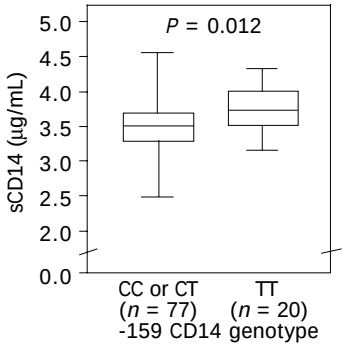

Figure 2 Serum levels of sCD14 comparing TT-homozygote HCV patients and patients with genotypes CC or CT, respectively. Box plots illustrate median values and interquartile distance.

[illegible]

There is a remarkable variation in the course of chronic liver disease in different patients. Recent studies suggest that the natural history of chronic liver disease is influenced by a number of gene polymorphism[1]. These genetic factors could explain the broad spectrum of response of the same etiologic agent seen in these individuals.

Recently, the C-T (-159) polymorphism in the promotor region of the CD14 gene was identified as a risk factor for the development of alcoholic liver cirrhosis in the Finnish population based on autopsy series[34]. The Finnish population has a limited number of founders and is characterized by national and regional isolation[45,46].

The first aim of our study was to re-evaluate the results of this previous study in a cohort of patients with chronic alcohol abuse from southern Germany.

In line with the previous Finnish study[35], the -159 CD14 genotype TT was significantly more frequent in patients with alcoholic liver cirrhosis compared to healthy controls or alcohol-dependent subjects without evidence of advanced liver damage.

Interestingly, serum aminotransferase levels did not vary significantly between patients with different genotypes in the group of alcoholics without evidence of advanced liver damage. Considering serum levels of aminotransferases as surrogate markers for hepatocellular damage, our data are in line with those of Järveläinen *et al*., who also could not find an association between the -159 genotypes and histological steatosis or less advanced stages of fibrosis, respectively[34]. Taken together, these findings indicate that the functional CD14 polymorphism and the associated CD14 expression, respectively, may exhibit different effects during the course of ALD.

On one hand, the CD14 polymorphism has been shown

to affect expression levels of membrane-bound CD14[28,44]. Higher expression levels of membrane-bound CD14 predispose hepatic cells for higher cytokine expression in response to endotoxins and cause increased inflammatory activity[23,47].

On the other hand, the CD14 polymorphism plays a significant role in regulating serum levels of sCD14 as TT-homozygotes have raised levels of sCD14[28,31]. Increased sCD14 can decrease the inflammatory response of monocytes to endotoxin by enhanced clearance[26]. Furthermore, a strong correlation between sCD14 and the endotoxin neutralizing capacity of plasma has been shown[48].

Increased expression of sCD14 in TT-homozygotes may lead to enhanced clearance of portal endotoxin and subsequently low-grade hepatic stimulation. In line with this hypothesis, Poullis *et al*., found the TT polymorphism to be associated with significantly reduced serum levels of ALT and γ-GT[36]. Similarly, Fernandez-Real *et al*., reported an inverse correlation between serum levels of sCD14 and ALT in individuals without known liver disease during routine-checkup visits[38].

These data indicate that the CD14 polymorphism seems to affect two mechanisms with opposite effects on hepatic inflammation by regulating the expression of membrane bound as well as sCD14. During the course of ALD the relative pathophysiological impact of each of these two mechanisms may vary.

Interestingly, there is an association between CD14 expression and the degree of fibrosis[49], and CD14 is *de novo* expressed on HSC during their activation process[23]. These cells are present in acute as well as chronically diseased livers, and there is a positive correlation between the degree of fibrosis and the accumulation of activated HSC[50,51]. Activated HSC synthesize and secrete excessive ECM molecules. In addition, it is recognized that they also play an important role in hepatic inflammation[52], and LPS-mediated NF-κB activation in HSC increases their resistance to apoptosis[23]. Therefore, with progressing liver damage and fibrosis, the number as well as type of CD14-expressing cells varies leading to differences in the LPS effects and CD14-mediated signal transduction.

In summary, the balance between potentially anti-inflammatory effects of sCD14 and proinflammatory effects of mCD14 may shift toward mCD14 during progression of ALD.

This imbalance may be further enhanced by higher endotoxin levels in patients with severe liver damage[11,16,17]. High LPS levels in more advanced liver damage may saturate the scavenger effects of sCD14. Furthermore, higher LPS levels promote hepatic inflammation leading to increased SP1-binding activity[53]. Since the -159 CD14 promotor polymorphism potentially affects binding of the transcription factor SP-1, high LPS levels in more advanced liver disease might promote CD14 expression particularly in carriers of the T-allele.

In summary, this hypothesis could explain that TT genotype promotes fibrosis in late stages of ALD, while in earlier stages pro- and anti-inflammatory mechanisms may be in balance regardless of the genotype.

The second aim of this study was to investigate the role of the -159 CD14 promotor polymorphism in HCV patients.

TT-homozygote HCV patients had significantly higher sCD14 serum levels than HCV patients with -159 CD14 genotype CT or TT, respectively. Moreover, HCV patients with advanced liver fibrosis or cirrhosis had significantly higher sCD14 levels than patients with less advanced stages of liver fibrosis. Similarly, a correlation between sCD14 levels and hepatic fibrosis has been shown previously in patients with ALD[39]. However, in contrast to patients with ALD, liver cirrhosis was not associated with the TT-homozygous state in patients with chronic hepatitis C infection. These findings indicate that the functional CD14 polymorphism and the expression of CD14 may exhibit different effects during the course of ALD and chronic HCV infection.

One explanation for this finding could be different expression patterns of membrane bound and sCD14, respectively, depending on the underlying cause of chronic liver disease. Furthermore, pathophysiological mechanism of viral and ALD may be differently affected by endotoxins, binding of sCD14 or CD14-mediated signal transduction.

It is known that sCD14 reveals inhibitory action on lymphocyte function[54,55]. Hepatic inflammation in HCV patients is characterized by lymphocyte infiltration while in alcoholic hepatitis there is a predominant infiltration with neutrophils. Furthermore, endotoxemia has been shown to exaggerate hepatic inflammation in murine viral infections[56,57] and to be associated with the response to antiviral therapy in HCV patients[58].

The origin of endotoxemia in HCV patients seems to be multifactorial, likely depending on impaired phagocytic functions and reduced T-cell-mediated antibacterial activity[57]. Furthermore, one cannot exclude the passage of LPS from the gut flora to the blood stream, condition owing to altered intestinal permeability, similar as shown in models of ALD[11,18]. In patients with alcoholic cirrhosis, the mean endotoxin concentration was significantly higher than in patients with non-alcoholic cirrhosis and higher endotoxin concentrations were more frequently observed in patients with alcoholic cirrhosis[12]. Therefore, it may be speculated that different LPS levels in patients with ALD and patients with chronic HCV infection may indirectly account for varying pathophysiological effects of CD14-mediated signal transduction.

There are several studies indicating that alcohol potentiates the proinflammatory effects of endotoxins in hepatic diseases. Peripheral blood mononuclear cells or purified monocytes from patients with alcoholic liver cirrhosis, stimulated *in vitro* with LPS, displayed a marked increase of proinflammatory cytokines compared with healthy controls[59]. Furthermore, alcohol was shown to increase the expression of CD14 on Kupffer cells and subsequently increased their responsiveness to endotoxins[60,61]. Interestingly, elegant studies by Järveläinen *et al*., in an animal model indicate that the synergistic effect of endotoxins and alcohol may vary depending on the time of exposure[62].

Finally, as for most genetic association studies, it has to be considered that the single nucleotide polymorphism investigated is in linkage disequilibrium to a different disease-associated genetic variation. Theoretically, this

potential genetic variation may affect particularly the pathophysiology of alcoholics but not viral liver disease. However, the functional relevance of the CD14/-159 polymorphism demonstrated in several studies and the important role of LPS and CD14 signaling in the pathophysiology of chronic liver disease clearly argue against this hypothesis.

In summary, comparison of the frequency of the -159 CD14 genotypes revealed significant differences between the two etiologies of liver diseases investigated in this study. In ALD, the impact of the -159 CD14 polymorphism may vary during the course of the disease, potentially via varying effects of soluble and membrane-bound forms of CD14. It will be interesting to elucidate the importance of this CD14 polymorphism in patients with other underlying liver diseases as non alcoholic fatty or autoimmune liver disease. These studies could potentially lead to therapeutic or prevention strategies selectively for those subgroups of patients that are particularly prone for the pathophysiological effects of gut-derived endotoxins.

[redacted]

1 **Bataller R,** North KE, Brenner DA. Genetic polymorphisms and the progression of liver fibrosis. a critical appraisal. *Hepatology* 2003; **37**: 493-503
2 **Yamauchi M,** Maezawa Y, Mizuhara Y, Ohata M, Hirakawa J, Nakajima H, Toda G. Polymorphisms in alcohol metabolizing enzyme genes and alcoholic cirrhosis in Japanese patients. a multivariate analysis. *Hepatology* 1995; **22**: 1136-1142
3 **Day CP,** Bashir R, James OF, Bassendine MF, Crabb DW, Thomasson HR, Li TK, Edenberg HJ. Investigation of the role of polymorphisms at the alcohol and aldehyde dehydrogenase loci in genetic predisposition to alcohol-related end-organ damage. *Hepatology* 1991; **14**: 798-801
4 **Carr LG,** Hartleroad JY, Liang Y, Mendenhall C, Moritz T, Thomasson H. Polymorphism at the P450IIE1 locus is not associated with alcoholic liver disease in Caucasian men. *Alcohol Clin Exp Res* 1995; **19**: 182-184
5 **Muhlbauer M,** Bosserhoff AK, Hartmann A, Thasler WE, Weiss TS, Herfarth H, Lock G, Scholmerich J, Hellerbrand C. A novel MCP-1 gene polymorphism is associated with hepatic MCP-1 expression and severity of HCV-related liver disease. *Gastroenterology* 2003; **125**: 1085-1093
6 **Yee LJ,** Tang J, Herrera J, Kaslow RA, van Leeuwen DJ. Tumor necrosis factor gene polymorphisms in patients with cirrhosis from chronic hepatitis C virus infection. *Genes Immun* 2000; **1**: 386-390
7 **Takamatsu M,** Yamauchi M, Maezawa Y, Ohata M, Saitoh S, Toda G. Correlation of a polymorphism in the interleukin-1 receptor antagonist gene with hepatic fibrosis in Japanese alcoholics. *Alcohol Clin Exp Res* 1998; **22**: 141-144
8 **Grove J,** Daly AK, Bassendine MF, Gilvarry E, Day CP. Interleukin 10 promoter region polymorphisms and susceptibility to advanced alcoholic liver disease. *Gut* 2000; **46**: 540-545
9 **Grove J,** Daly AK, Bassendine MF, Day CP. Association of a tumor necrosis factor promoter polymorphism with susceptibility to alcoholic steatohepatitis. *Hepatology* 1997; **26**: 143-146
10 **Takamatsu M,** Yamauchi M, Maezawa Y, Saito S, Maeyama S, Uchikoshi T. Genetic polymorphisms of interleukin-1beta in association with the development of alcoholic liver disease in Japanese patients. *Am J Gastroenterol* 2000; **95**: 1305-1311
11 **Nanji AA,** Khettry U, Sadrzadeh SM, Yamanaka T. Severity of liver injury in experimental alcoholic liver disease. Correlation with plasma endotoxin, prostaglandin E2, leukotriene B4, and thromboxane B2. *Am J Pathol* 1993; **142**: 367-373
12 **Fukui H,** Brauner B, Bode JC, Bode C. Plasma endotoxin concentrations in patients with alcoholic and non-alcoholic liver disease: reevaluation with an improved chromogenic assay. *J Hepatol* 1991; **12**: 162-169
13 **Nanji AA,** Khettry U, Sadrzadeh SM. Lactobacillus feeding reduces endotoxemia and severity of experimental alcoholic liver (disease). *Proc Soc Exp Biol Med* 1994; **205**: 243-247
14 **Jacob AI,** Goldberg PK, Bloom N, Degenshein GA, Kozinn PJ. Endotoxin and bacteria in portal blood. *Gastroenterology* 1977; **72**: 1268-1270
15 **Caradonna L,** Mastronardi ML, Magrone T, Cozzolongo R, Cuppone R, Manghisi OG, Caccavo D, Pellegrino NM, Amoroso A, Jirillo E, Amati L. Biological and clinical significance of endotoxemia in the course of hepatitis C virus infection. *Curr Pharm Des* 2002; **8**: 995-1005
16 **Lin RS,** Lee FY, Lee SD, Tsai YT, Lin HC, Lu RH, Hsu WC, Huang CC, Wang SS, Lo KJ. Endotoxemia in patients with chronic liver diseases: relationship to severity of liver diseases, presence of esophageal varices, and hyperdynamic circulation. *J Hepatol* 1995; **22**: 165-172
17 **Chan CC,** Hwang SJ, Lee FY, Wang SS, Chang FY, Li CP, Chu CJ, Lu RH, Lee SD. Prognostic value of plasma endotoxin levels in patients with cirrhosis. *Scand J Gastroenterol* 1997; **32**: 942-946
18 **Rivera CA,** Bradford BU, Seabra V, Thurman RG. Role of endotoxin in the hypermetabolic state after acute ethanol exposure. *Am J Physiol* 1998; **275**: 1252-1258
19 **Wright SD,** Ramos RA, Tobias PS, Ulevitch RJ, Mathison JC. CD14, a receptor for complexes of lipopolysaccharide (LPS) and LPS binding protein. *Science* 1990; **249**: 1431-1433
20 **Matsuura K,** Ishida T, Setoguchi M, Higuchi Y, Akizuki S, Yamamoto S. Upregulation of mouse CD14 expression in Kupffer cells by lipopolysaccharide. *J Exp Med* 1994; **179**: 1671-1676
21 **Tracy TF** Jr, Fox ES. CD14-lipopolysaccharide receptor activity in hepatic macrophages after cholestatic liver injury. *Surgery* 1995; **118**: 371-377
22 **Nanbo A,** Nishimura H, Muta T, Nagasawa S. Lipopolysaccharide stimulates HepG2 human hepatoma cells in the presence of lipopolysaccharide-binding protein via CD14. *Eur J Biochem* 1999; **260**: 183-191
23 **Paik YH,** Schwabe RF, Bataller R, Russo MP, Jobin C, Brenner DA. Toll-Like receptor 4 mediates inflammatory signaling by bacterial lipopolysaccharide in human hepatic stellate cells. *Hepatology* 2003; **37**: 1043-1055
24 **Pugin J,** Heumann ID, Tomasz A, Kravchenko VV, Akamatsu Y, Nishijima M, Glauser MP, Tobias PS, Ulevitch RJ. CD14 is a pattern recognition receptor. *Immunity* 1994; **1**: 509-516
25 **Ulevitch RJ,** Tobias PS. Receptor-dependent mechanisms of cell stimulation by bacterial endotoxin. *Annu Rev Immunol* 1995; **13**: 437-457
26 **Kitchens RL,** Wolfbauer G, Albers JJ, Munford RS. Plasma lipoproteins promote the release of bacterial lipopolysaccharide from the monocyte cell surface. *J Biol Chem* 1999; **274**: 34116-34122
27 **Wurfel MM,** Hailman E, Wright SD. Soluble CD14 acts as a shuttle in the neutralization of lipopolysaccharide (LPS) by LPS-binding protein and reconstituted high density lipoprotein. *J Exp Med* 1995; **181**: 1743-1754
28 **Baldini M,** Lohman IC, Halonen M, Erickson RP, Holt PG, Martinez FD. A Polymorphism* in the 5′ flanking region of the CD14 gene is associated with circulating soluble CD14 levels and with total serum immunoglobulin E. *Am J Respir Cell Mol Biol* 1999; **20**: 976-983
29 **Hubacek JA,** Rothe G, Pit'ha J, Skodova Z, Stanek V, Poledne R, Schmitz G. C(-260)->T polymorphism in the promoter of the CD14 monocyte receptor gene as a risk factor for myocardial infarction. *Circulation* 1999; **99**: 3218-3220
30 **Unkelbach K,** Gardemann A, Kostrzewa M, Philipp M, Tillmanns H, Haberbosch W. A new promoter polymorphism in the gene of lipopolysaccharide receptor CD14 is associated with expired myocardial infarction in patients with low

atherosclerotic risk profile. *Arterioscler Thromb Vasc Biol* 1999; **19**: 932-938
31 **Obana N,** Takahashi S, Kinouchi Y, Negoro K, Takagi S, Hiwatashi N, Shimosegawa T. Ulcerative colitis is associated with a promoter polymorphism of lipopolysaccharide receptor gene, CD14. *Scand J Gastroenterol* 2002; **37**: 699-704
32 **Woo JG,** Assa'ad A, Heizer AB, Bernstein JA, Hershey GK. The -159 C->T polymorphism of CD14 is associated with nonatopic asthma and food allergy. *J Allergy Clin Immunol* 2003; **112**: 438-444
33 **Repo H,** Anttonen K, Kilpinen SK, Palotie A, Salven P, Orpana A, Leirisalo-Repo M. CD14 and TNfa promoter polymorphisms in patients with acute arthritis. Special reference to development of chronic spondyloarthropathy. *Scand J Rheumatol* 2002; **31**: 355-361
34 **Järveläinen HA,** Orpana A, Perola M, Savolainen VT, Karhunen PJ, Lindros KO. Promoter polymorphism of the CD14 endotoxin receptor gene as a risk factor for alcoholic liver disease. *Hepatology* 2001; **33**: 1148-1153
35 **Corpechot C,** Poupon R. Promoter polymorphism of the CD14 endotoxin receptor gene and primary biliary cirrhosis. *Hepatology* 2002; **35**: 242-243
36 **Poullis AP,** Shetty AK, Risley PD, Collinson PO, Mendall MA. Effect of the CD14 promoter polymorphism on liver function tests and its association with alcohol and obesity. *Eur J Gastroenterol Hepatol* 2003; **15**: 1317-1322
37 **Fernandez-Real JM,** Broch M, Richart C, Vendrell J, Lopez-Bermejo A, Ricart W. CD14 monocyte receptor, involved in the inflammatory cascade, and insulin sensitivity. *J Clin Endocrinol Metab* 2003; **88**: 1780-1784
38 **Fernandez-Real JM,** Lopez-Bermejo A, Broch M, Vendrell J, Richart C, Ricart W. Circulating soluble CD14 monocyte receptor is associated with increased alanine aminotransferase. *Clin Chem* 2004; **50**: 1456-1458
39 **Oesterreicher C,** Pfeffel F, Petermann D, Muller C. Increased in vitro production and serum levels of the soluble lipopolysaccharide receptor sCD14 in liver disease. *J Hepatol* 1995; **23**: 396-402
40 **Desmet VJ,** Gerber M, Hoofnagle JH, Manns M, Scheuer PJ. Classification of chronic hepatitis. diagnosis, grading and staging. *Hepatology* 1994; **19**: 1513-1520
41 **Janca A,** Ustun TB, Early TS, Sartorius N. The ICD-10 symptom checklist: a companion to the ICD-10 classification of mental and behavioural disorders. *Soc Psychiatry Psychiatr Epidemiol* 1993; **28**: 239-242
42 **Hubacek JA,** Stuber F, Frohlich D, Book M, Wetegrove S, Rothe G, Schmitz G. The common functional C(-159)T polymorphism within the promoter region of the lipopolysaccharide receptor CD14 is not associated with sepsis development or mortality. *Genes Immun* 2000; **1**: 405-407
43 **Lichy C,** Meiser H, Grond-Ginsbach C, Buggle F, Dorfer C, Grau A. Lipopolysaccharide receptor CD14 polymorphism and risk of stroke in a South-German population. *J Neurol* 2002; **249**: 821-823
44 **Hubacek J,** Pitha J, Skodova Z, Poledne R. Is the CD14 receptor gene a marker for smoking dependence? *Med Sci Monit* 2002; **8**: 172-174
45 **Nevanlinna HR.** The Finnish population structure. A genetic and genealogical study. *Hereditas* 1972; **71**: 195-236
46 **De la Chapelle A.** Disease gene mapping in isolated human populations. the example of Finland. *J Med Genet* 1993; **30**: 857-865
47 **Yin M,** Bradford BU, Wheeler MD, Uesugi T, Froh M, Goyert SM, Thurman RG. Reduced early alcohol-induced liver injury in CD14-deficient mice. *J Immunol* 2001; **166**: 4737-4742
48 **Hiki N,** Berger D, Mimura Y, Frick J, Dentener MA, Buurman WA, Seidelmann M, Kaminishi M, Beger HG. Release of endotoxin-binding proteins during major elective surgery: role of soluble CD14 in phagocytic activation. *World J Surg* 2000; **24**: 499-506
49 **Su GL,** Rahemtulla A, Thomas P, Klein RD, Wang SC, Nanji AA. CD14 and lipopolysaccharide binding protein expression in a rat model of alcoholic liver disease. *Am J Pathol* 1998; **152**: 841-849
50 **Ballardini G,** Degli ES, Bianchi FB, de Giorgi LB, Faccani A, Biolchini L, Busachi CA, Pisi E. Correlation between Ito cells and fibrogenesis in an experimental model of hepatic fibrosis. A sequential stereological study. *Liver* 1983; **3**: 58-63
51 **Knittel T,** Kobold D, Piscaglia F, Saile B, Neubauer K, Mehde M, Timpl R, Ramadori G. Localization of liver myofibroblasts and hepatic stellate cells in normal and diseased rat livers. distinct roles of (myo-) fibroblast subpopulations in hepatic tissue repair. *Histochem Cell Biol* 1999; **112**: 387-401
52 **Marra F.** Hepatic stellate cells and the regulation of liver inflammation. *J Hepatol 1999*; **31**: 1120-1130
53 **Sakuta T,** Matsushita K, Yamaguchi N, Oyama T, Motani R, Koga T, Nagaoka S, Abeyama K, Maruyama I, Takada H, Torii M. Enhanced production of vascular endothelial growth factor by human monocytic cells stimulated with endotoxin through transcription factor SP-1. *J Med Microbiol* 2001; **50**: 233-237
54 **Rey Nores JE,** Bensussan A, Vita N, Stelter F, Arias MA, Jones M, Lefort S, Borysiewicz LK, Ferrara P, Labeta MO. Soluble CD14 acts as a negative regulator of human T cell activation and function. *Eur J Immunol* 1999; **29**: 265-276
55 **Arias MA,** Rey Nores JE, Vita N, Stelter F, Borysiewicz LK, Ferrara P, Labeta MO. Cutting edge: human B cell function is regulated by interaction with soluble CD14: opposite effects on IgG1 and IgE production. *J Immunol* 2000; **164**: 3480-3486
56 **Gut JP,** Schmitt S, Bingen A, Anton M, Kirn A. Probable role of endogenous endotoxins in hepatocytolysis during murine hepatitis caused by frog virus 3. *J Infect Dis* 1984; **149**: 621-629
57 **Jirillo E,** Caccavo D, Magrone T, Piccigallo E, Amati L, Lembo A, Kalis C, Gumenscheimer M. The role of the liver in the response to LPS: experimental and clinical findings. *J Endotoxin Res* 2002; **8**: 319-327
58 **Amati L,** Cozzolongo R, Manghisi OG, Cuppone R, Pellegrino NM, Caccavo D, Jirillo E. The immune responsiveness in hepatitis C virus infected patients: effects of interferon-alfa/ribavirin combined treatment on the lymphocyte response with special reference to B cells. *Curr Pharm Des* 2004; **10**: 2093-2100
59 **Deviere J,** Content J, Denys C, Vandenbussche P, Schandene L, Wybran J, Dupont E. Excessive *in vitro* bacterial lipopolysaccharide-induced production of monokines in cirrhosis. *Hepatology* 1990; **11**: 628-634
60 **Jarvelainen HA,** Oinonen T, Lindros KO. Alcohol-induced expression of the CD14 endotoxin receptor protein in rat Kupffer cells. *Alcohol Clin Exp Res* 1997; **21**: 1547-1551
61 **Kono H,** Wheeler MD, Rusyn I, Lin M, Seabra V, Rivera CA, Bradford BU, Forman DT, Thurman RG. Gender differences in early alcohol-induced liver injury: role of CD14, NF-kappaB, and TNF-alpha. *Am J Physiol Gastrointest Liver Physiol* 2000; **278**: 652-661
62 **Jarvelainen HA,** Fang C, Ingelman-Sundberg M, Lindros KO. Effect of chronic coadministration of endotoxin and ethanol on rat liver pathology and proinflammatory and anti-inflammatory cytokines. *Hepatology* 1999; **29**: 1503-1510

Science Editor Guo SY **Language Editor** Elsevier HK

PO Box 2345, Beijing 100023, China
www.wjgnet.com
wjg@wjgnet.com

ELSEVIER

World J Gastroenterol 2005;11(38):6038-6042
World Journal of Gastroenterology ISSN 1007-9327

• *BRIEF REPORTS* •

Hyperhomocysteinemia in ulcerative colitis is related to folate levels

Petros Zezos, Georgia Papaioannou, Nikolaos Nikolaidis, Themistoclis Vasiliadis, Olga Giouleme, Nikolaos Evgenidis

Petros Zezos, Nikolaos Nikolaidis, Themistoclis Vasiliadis, Olga Giouleme, Nikolaos Evgenidis, Division of Gastroenterology, 2nd Propaedeutic Department of Internal Medicine, Hippokration General Hospital, Aristotle University of Thessaloniki, 49 Konstantinoupoleos Str., Thessaloniki 54642, Greece
Georgia Papaioannou, Department of Haematology, Papageorgiou General Hospital of Thessaloniki, Ring Road Nea Efkarpia, Thessaloniki 56403, Greece
Correspondence to: Associate Professor Nikolaos Evgenidis, Division of Gastroenterology, 2nd Propaedeutic Department of Internal Medicine, Aristotle University of Thessaloniki, Hippokration General Hospital, 49 Konstantinoupoleos Str., Thessaloniki 54642, Greece. zezosp@hol.gr
Telephone: +30-2310-892073 Fax: +30-2310-848354
Received: 2004-12-17 Accepted: 2005-03-21

ABSTRACT

AIM: To study the prevalence and clinical significance of hyperhomocysteinemia (hHcys), an independent factor for arterial and venous thrombosis, in a group of patients with ulcerative colitis (UC).

METHODS: Fasting homocysteine (Hcys), folate, and vitamin B_{12} serum levels were measured in 40 UC patients and 50 healthy controls. Clinical data regarding UC were gathered.

RESULTS: Median serum Hcys levels in UC patients were similar to those in controls (12.26 μmol/L *vs* 12.32 μmol/L), but the prevalence of hHcys was higher in UC patients than in controls (30% *vs* 10%, $P = 0.028$). UC significantly increased the risk of hHcys (adjusted odds ratio: 4.125; 95%CI: 1.26-13.44). Multivariate regression analysis showed that male sex, folate and vitamin B_{12} deficiency or lower serum values were significant independent predictors of higher Hcys levels in UC patients ($r^2 = 0.4$; $P<0.001$).

CONCLUSION: hHcys is common in UC patients and it is related to folate and vitamin B_{12} deficiency or lower serum values. It would be reasonable for patients with UC to receive folate and vitamin B complex supplements as a prophylactic measure.

Key words: Folate; Homocysteine; Hyperhomocysteinemia; Thrombosis; Ulcerative colitis; Vitamin B_{12}

Zezos P, Papaioannou G, Nikolaidis N, Vasiliadis T, Giouleme O, Evgenidis N. Hyperhomocysteinemia in ulcerative colitis is related to folate levels. *World J Gastroenterol* 2005; 11 (38): 6038-6042
http://www.wjgnet.com/1007-9327/11/6038.asp

INTRODUCTION

The risk for thromboembolic complications is increased in patients with inflammatory bowel disease (IBD). The incidence of arterial and venous thromboembolic disease in patients with ulcerative colitis (UC) and Crohn's disease (CD) has been reported between 1% and 8%[1,2], rising to an incidence of 39% in some autopsy studies[3]. Several studies have shown that a hypercoagulable state involving all components of clotting system exists in IBD[4-6]. This hypercoagulable state may be related to an increased tendency for thromboembolic events and may be linked to the disease pathogenesis through promoting microthrombi formation in intestinal microcirculation[7,8]. The etiology and pathogenesis of the hypercoagulable state in IBD have not been fully elucidated but may be induced through a procoagulant effect of proinflammatory cytokines[9-13] in combination with acquired or genetic defects of clotting factors (protein S, protein C, antithrombin, factor V Leiden, prothrombin mutation 20210A, and antiphospholipid antibodies)[14-16]. Recently, the factor V Leiden has been implicated in the increased risk of venous thrombosis in IBD patients[17-19].

Homocysteine (Hcys) is a non-essential, sulfur-containing amino acid formed during the metabolism of methionine. Mild hyperhomocysteinemia (hHcys), which occurs in approximately 5-7% of the general population, has been proved to be thrombogenic and an independent risk factor for coronary artery disease[20], arterial and venous thrombosis[21-26]. Elevated levels of Hcys may result from abnormalities in metabolism pathways due to inherited abnormalities of the enzymes involved or nutrient deficiencies such as insufficiency of folate and vitamins B_2, B_6, and B_{12}[27,28].

The mechanism by which hHcys promotes thrombosis is uncertain, but it may be related to a hypercoagulatory state due to endothelial dysfunction[28-30].

Vitamin B_{12} and folate deficiency are relatively common conditions in IBD (especially in active disease) through malnutrition, malabsorption or antifolate drugs such as methotrexate and sulfasalazine (SASP). Deficiencies of key nutrients/cofactors in Hcys metabolism pathways (B_2, B_6, B_{12}, and folate) might lead to raised Hcys levels in IBD. The association between IBD and hHcys has been shown

in some recent studies, reporting an increased prevalence of hHcys in IBD (both UC and CD)[31-36].

The aim of this study was to evaluate whether Hcys levels were elevated compared to a group of healthy controls and whether Hcys levels were related to vitamin B_{12} and folate serum concentrations, disease activity, disease extent or history of thrombotic complications.

[illegible]

Patients and control population

Forty patients with UC (20 females and 20 males, mean age 41.65±15.21 years, range 17-71 years) were consecutively recruited from our outpatient clinic between February 1999 and February 2000. Diagnosis of UC was based on standard clinical, endoscopic and histological criteria. A detailed clinical history was taken from each patient regarding current symptoms, activity and duration of disease, extraintestinal manifestations, present medication, smoking status, and thrombotic complications. Patients with significant liver or kidney diseases were excluded. Endoscopy was performed in all patients in order to evaluate endoscopic activity, disease extension and histological confirmation and grading. Blood samples from fasting UC patients were collected. Serum Hcys, folate and vitamin B_{12} levels were determined.

Serum Hcys levels were also measured in blood samples from 50 healthy control subjects (HC) with similar age and gender (25 females and 25 males, age 39.96±14.33 years, range 17-72 years), under similar conditions and in the same laboratory. Healthy control subjects were visitors in the outpatient clinic of Hematology Department and had no known diseases, or any clinical or laboratory evidence of metabolic, neoplastic or inflammatory disease. They also had no history of thromboembolic disease. Patients and healthy controls were from the same geographical area (Northern Greece) and had Greek ancestry. Patients and controls reported that they had no daily alcohol intake above 35 g, and no use of drugs affecting Hcys status (phenytoin, theophylline, and vitamin supplements).

Measurements

Total serum Hcys concentrations were measured by the IMx homocysteine assay, which is a fluorescence polarization immunoassay (FPIA, Abbott Laboratories). Reference serum Hcys concentrations for both men and women were <15 μmol/L. Vitamin B_{12} and folate serum levels were measured by enzymatic immunoassays (ELISA). Reference ranges for vitamin B_{12} and serum folate were >223 pg/mL and >2.8 ng/mL respectively.

Statistical analysis

Descriptive statistics for continuous variables (including means and medians) were calculated. Categorical variables were described using proportions. Odds ratios and the 95%CI for the risk of hHcys in UC patients, as compared to healthy controls, were calculated. Multivariate logistic regression was used to adjust these crude odds for confounding differences in sex. Comparisons of continuous variables between the two groups were made by Student's *t*-test for normally distributed data or by Mann-Whitney *U*-test when data were not normally distributed. Fisher's exact test was used for the comparison of proportions. Pearson's correlation coefficient was calculated to describe the relationship between variables. Multiple linear regression analysis was performed in order to study the influence of individual factors on Hcys levels (treated as continuous variable). Since the concentrations of Hcys, folate and B_{12} were not normally distributed, correlation and regression analysis were performed with log-transformed data. Statistical analysis was performed using the SPSS for Windows package (version 11.0, SPSS, Chicago, IL, USA).

[illegible]

Demographics

The baseline characteristics of the patients and controls are shown in Table 1. There were no significant differences in age between healthy controls and patients, or between sexes or between study groups. There were also no significant differences in duration of disease, disease activity, endoscopic score, disease extent, smoking, and use of medication between sexes in UC group.

Table 1 Epidemiological and clinical data of study subjects

	UC patients (95%CI)	Healthy controls (95%CI)
Subjects (*n*)	40	50
Gender (female/male)	20/20	25/25
Mean age (yr±SD)(range)	41.65±15.21	39.96±14.33
	[36.78–46.52]	[35.89–44.03]
	(17–71)	(17–72)
Mean disease duration (mo±SD)	56.65±63.18	
(range)	[36.44–76.86]	
	(3–216)	
Current smoking (%)	9 (22.5)	
Extent of UC (%)		
Rectum/sigmoid	9 (22.5)	
Left colitis	22 (55.5)	
Pancolitis	9 (22.5)	
Activity of UC (%)		
Active	28 (70)	
Inactive	12 (30)	
Extraintestinal complications (%)	6 (15)	
Thrombotic complications (%)	2 (5)	
Medical treatment		
None	1 (2.5)	
5-ASA	35 (87.5)	
SASP	1 (2.5)	
Steroids	17 (42.5)	
Immunosuppressors (AZA/6-MP)	11 (27.5)	

Homocysteine determination and associations

The median serum levels of Hcys in UC patients were similar to those in controls (12.26 μmol/L [range 7.15-35.8 μmol/L] *vs* 12.32 μmol/L [range 5.97-22.06 μmol/L], $P = 0.518$), but hHcys was more prevalent in UC patients (30% [12/40] *vs* 10% [5/50], $P = 0.028$) than in controls. Male sex had higher median serum levels of Hcys both in HC and in UC groups (Table 2). Logistic regression analysis showed an odds ratio of 3.857 [95%CI: 1.22-12.12] for hHcys in the UC group as compared to healthy controls. Advanced age and

male sex were associated with higher Hcys levels, and there was not any difference in age and sex, but males had significant higher Hcys values in both study groups and we believe that sex might be a significant confounder. The adjusted odds ratio for the sex difference was 4.125 (95%CI: 1.26-13.44).

Table 2 Serum Hcys levels in male and female subjects in study groups

	Hcys (μmol/L)		*P*
	Male	Female	
Controls	13.7 (8.17–22.06)	11.94 (5.97–16.99)	0.005
UC	14 (9.13–35.8)	11.07 (7.15–26.6)	0.011
Total	13.72 (8.17–35.8)	11.87 (5.97–26.6)	0.0003

Values are expressed as medians (range). Comparisons were performed using Mann–Whitney's test.

Serum homocysteine, folate and vitamin B_{12} levels in ulcerative colitis patients

In UC patients, the median serum levels of folate and vitamin B_{12} were 7.2 ng/mL (range 2.4-13.4 ng/mL) and 431 pg/mL (range 195-1 430 pg/mL) respectively. One patient had serum folate below the lower limit (2.4 ng/mL) and two others had normal folate near the lower limit (2.9 and 3.4 ng/mL respectively). All three had high levels of Hcys (the three highest values). One patient had vitamin B_{12} below the lower limit (195 pg/mL) and two others had normal B_{12} near the lower limit (226 and 237 pg/mL, respectively). The patient with low B_{12} and one of the two others had high levels of Hcys. These patients had no overlapping low values for both folate and B_{12} levels. The disease duration, activity, extent, endoscopic severity, medical treatment, and smoking status did not significantly influence Hcys, folate, and vitamin B_{12} levels. There were no significant differences in levels of folate and vitamin B_{12} between sexes.

Predictors of hyperhomocysteinemia in ulcerative colitis

Because the concentrations of Hcys, folate and B_{12} were not normally distributed, correlation and regression analysis were performed with log-transformed data. To directly assess the effect of age, folic acid and B_{12} on Hcys levels, the Pearson correlation coefficients between these variables were determined, as shown in Table 3. A relatively strong inverse correlation was observed between log-transformed serum levels of Hcys and log-transformed serum concentrations of folate (r = -0.466, P = 0.002). To further define the role of folic acid and B_{12} in determining Hcys levels, a multiple regression analysis was performed where log-Hcys was the dependent variable whereas age, gender, log-B_{12}, log-folic acid, smoking and history of thrombosis were the independent variables. Multiple linear regressions revealed the following variables to be significant independent predictors of Hcys levels in UC patients: male sex, folate, and B_{12} deficiency or lower serum values (r^2 = 0.4; P<0.001).

Table 3 Pearson coefficient analysis of variables within UC group

	log-Hcys	Age (yr)	log-folic acid	log-B_{12}
log-Hcys				
Coefficient	1.000	–0.016	–0.466	–0.163
P	0.000	0.920	0.002	0.314
Age (yr)				
Coefficient	–0.016	1.000	0.189	–0.039
P	0.920	0.000	0.244	0.811
log-folic acid				
Coefficient	–0.466	0.189	1.000	–0.193
P	0.002	0.244	0.000	0.234
log-B_{12}				
Coefficient	–0.163	–0.039	–0.193	1.000
P	0.314	0.811	0.234	0.000

Homocysteine metabolism in ulcerative colitis patients with previous thrombotic events

Two patients had a history of previous thrombotic events. hHcys was found in one of them. This patient had folate deficiency and the highest value of Hcys. The other one had vitamin B_{12} close to lower normal limit without hHcys.

[redacted]

This study showed that although Hcys levels were similar in UC patients and healthy control subjects, hHcys (serum Hcys ⩾15 μmol/L) was more common in UC patients than in healthy controls (adjusted odds ratio, 4.125; prevalence 30% *vs* 10%). Increased Hcys levels and high prevalence of hHcys in IBD patients have been reported in previous studies[31-36]. In our study, similar findings were observed in this cohort of UC patients with a slightly higher prevalence of hHcys (30%) than in other studies (10-26%)[31,32,35,36].

Our analysis showed that male sex and low serum levels of folic acid and vitamin B_{12} were correlated with high Hcys levels. Multiple regression analysis and Pearson's correlation coefficient showed that serum folic acid was the most significant predictor of Hcys levels. We did not find significant correlation between age, disease activity, medication, smoking status, and Hcys levels in this UC cohort. Chowers *et al*.[33], have observed similar findings in a group of patients with CD.

We did not study the frequency of MTHFR C677T variant in our study groups. In a previous study, Mahmud *et al*.[31], reported that the frequency of the homozygous C677T mutation, which results in slower synthesis of 5-methyltetrahydrofolate, is increased from 7.3% in controls to 17.5% in patients with UC and is related with high Hcys levels especially in folate deficiency status. However, in that study, Hcys levels were also elevated in patients with IBD with no mutation to MTHFR enzyme. The levels of Hcys decreased after folate supplementation, regardless of the fact that the genotype of the mutation was detected or not. It has been suggested that folate status should be addressed in all IBD patients and prophylactic folate supplementation has been recommended to all patients with IBD. In our study, the prevalence of hHcys in UC patients was much higher than the frequency of homozygous mutation of MTHFR as detected by Mahmud *et al*.[31]. The differences between prevalences of hHcys and MTHFR mutant can be explained by the existence of additional factors affecting Hcys levels. Vitamin deficiencies can be a significant

contributing factor as it has been supported by our study and previous reports. The suboptimal vitamin status in IBD patients can be due to a combination of several factors. Folate levels may be low due to either inadequate dietary intake, or increased utilization, or drug effects, mainly SASP[33]. In our study, one patient was receiving SASP and had low folate levels and hHcys. Other studies have conflicting conclusions about the significance of SASP antifolate effects[31,32]. Disease activity may contribute to increased demand for folate due to inflammation, but like Chowers *et al*.[33], we did not find any correlation between disease activity and folate or Hcys levels. Furthermore, Chowers *et al*.[33], found no change in Hcys levels, despite a significant improvement in the disease activity in a group of CD patients. These data point out that an inadequate intake of folate may be the most significant factor affecting folate levels in IBD patients.

The prevalence of thromboembolic complications in IBD patients is higher than that in the normal population, in large retrospective studies 1.3-8% of the patients develop these complications[1,2]. The pathogenesis of thromboembolism in IBD is unknown, but it seems to be multifactorial[37]. In our study we found a high prevalence (2/40; 5%) of thromboembolic events in this group of UC patients. hHcys was found in one of them. There are case reports that hHcys was noted in the test results in IBD patients with thrombosis[38,39]. In our study a correlation between hHcys and history of thrombosis was noted, but the number of patients is too small to supply safe conclusions. Nevertheless high Hcys levels may predispose IBD patients to thrombotic complications in combination with other existing circumstantial or permanent risk factors[37].

In conclusion, UC patients have a higher prevalence of hHcys than healthy controls. hHcys in these patients is related to low folate and B_{12} status but not to disease activity. All UC patients, irrespective of disease activity, are at risk for vitamin deficiencies. It is recommended that all patients should have an assessment of the nutritional status in order for the vitamin deficiencies to be detected and that they should also receive folate and vitamin B complex supplements for protection from complications of HHcys.

ACKNOWLEDGMENTS

The authors thank Associate Professor Rigas AG, Department of Electrical and Computer Engineering, School of Engineering of Democritus University of Thrace, and his associates Ms. Kotti VK and Mr. Vassiliadis VG, for their support in the detailed statistical analysis of data.

REFERENCES

1 **Talbot RW,** Heppell J, Dozois RR, Beart RW Jr. Vascular complications of inflammatory bowel disease. *Mayo Clin Proc* 1986; **61**: 140-145
2 **Vecchi M,** Cattaneo M, de Francis R, Mannucci PM. Risk of thromboembolic complications in patients with inflammatory bowel disease. Study of hemostasis measurements. *Int J Clin Lab Res* 1991; **21**: 165-170
3 **Graef V,** Baggenstoss AH, Sauer WG. Venous thrombosis occurring in non-specific ulcerative colitis. *Arch Intern Med* 1965; **117**: 377-382
4 **Hudson M,** Hutton RA, Wakefield AJ, Sawyerr AM, Pouder RE. Evidence for activation of coagulation in Crohn's disease. *Blood Coagul Fibrinolysis* 1992; **3**: 773-778
5 **Souto JC,** Martinez E, Roca M, Mateo J, Pujol J, Gonzalez D, Fontcuberta J. Prothrombotic state and signs of endothelial lesion in plasma of patients with inflammatory bowel disease. *Dig Dis Sci* 1995; **40**: 1883-1889
6 **Collins CE,** Cahill MR, Newland AC, Rampton DS. Platelets circulate in an activated state in inflammatory bowel disease. *Gastroenterology* 1994; **106**: 840-845
7 **Dhillon AP,** Anthony A, Sim R, Wakefield AJ, Sankey EA, Hudson M, Allison MC, Pounder RE. Mucosal capillary thrombi in rectal biopsies. *Histopathology* 1992; **21**: 127-133
8 **Wakefield AJ,** Sawyerr AM, Dhillon AP, Pittilo RM, Rowles PM, Lewis AA, Pounder RE. Pathogenesis of Crohn's disease: multifocal gastrointestinal infarction. *Lancet* 1989; **2**: 1057-1062
9 **Van Deventer SJ.** Tumor necrosis factor and Crohn's disease. *Gut* 1997; **40**: 443-448
10 **Nassif A,** Longo WE, Mazuski JE, Vernava AM, Kaminski DL. Role of cytokines and platelet-activating factor in inflammatory bowel disease. Implications for therapy. *Dis Colon Rectum* 1996; **39**: 217–223
11 **Bevilacqua MP,** Pober JS, Majeau GR, Fiers W, Cotran RS, Gimbrone MA Jr. Recombinant tumor necrosis factor induces procoagulant activity in cultured human vascular endothelium: characterization and comparison with the actions of interleukin 1. *Proc Natl Acad Sci USA* 1986; **83**: 4533–4537
12 **Nawroth PP,** Stern DM. Modulation of endothelial cell hemostatic properties by tumor necrosis factor. *J Exp Med* 1986; **163**: 740–745
13 **Dosquet C,** Weill D, Wautier JL. Cytokines and thrombosis. *J Cardiovasc Pharmacol* 1995; **25**(Suppl 2): S13-19
14 **Aadland E,** Odegaard OR, Roseth A, Try K. Free protein S deficiency in patients with chronic inflammatory bowel disease. *Scand J Gastroenterol* 1992; **27**: 957-960
15 **Aadland E,** Odegaard OR, Roseth A, Try K. Free protein S deficiency in patients with Crohn's disease. *Scand J Gastroenterol* 1994; **29**: 333-335
16 **Heneghan MA,** Cleary B, Murray M, O'Gorman TA, McCatrhy CF. Activated protein C resistance, thrombophilia, and inflammatory bowel disease. *Dig Dis Sci* 1998; **43**: 1356-1361
17 **Liebman HA,** Kashani N, Sutherland D, McGehee W, Kam AL. The factor V Leiden mutation increases the risk of venous thrombosis in patients with inflammatory bowel disease. *Gastroenterology* 1998; **115**: 830-834
18 **Koutroubakis IE,** Sfiridaki A, Mouzas IA, Maladaki A, Kapsoritakis A, Roussomoustakaki M, Kouroumalis EA, Manousos ON. Resistance to activated protein C and low levels of free protein S in Greek patients with inflammatory bowel disease. *Am J Gastroenterol* 2000; **95**: 190-194
19 **Novacek G,** Miehsler W, Kapiotis S, Katzenschlager R, Speiser W, Wogelsang H. Thromboembolism and resistance to activated protein C in patients with inflammatory bowel disease. *Am J Gastroenterol* 1999; **94**: 685-690
20 **Gallagher PM,** Meleady R, Shields DC, Tan KS, McMaster D, Rozen R, Evans A, Graham IM, Whitehead AS. Homocysteine and risk of premature coronary disease: Evidence for a common gene mutation. *Circulation* 1996; **94**: 2154-2158
21 **Ridker PM,** Hennekens CH, Selhub J, Miletich JP, Malinow MR, Stampfer MJ. Interrelation of hyperhomocyst(e)inemia, factor V Leiden, and risk of future venous thromboembolism. *Circulation* 1997; **95**: 1777-1782
22 **Cantu C,** Alonso E, Jara A, Martinez L, Rios C, Fernandez Mde L, Garcia I, Barinagarrementeria F. Hyperhomocysteinemia, low folate and vitamin B12 concentrations, and methylene tetrahydrofolate reductase mutation in cerebral venous thrombosis. *Stroke* 2004; **35**: 1790-1794
23 **den Heijer M,** Koster T, Blom HJ, Bos GM, Briet E, Reitsma PH, Vandenbroucke JP, Rosendaal FR. Hyperhomocysteinemia as a risk factor for deep-vein thrombosis. *N Engl J Med* 1996; **334**: 759-762
24 **Ray JG.** Meta-analysis of hyperhomocysteinemia as a risk

factor for venous thromboembolic disease. *Arch Intern Med* 1998; **158**: 2101-2106
25 **Langman LJ,** Ray JG, Evrovski J, Yeo E, Cole DE. Hyperhomocyst(e)inemia and the increased risk of venous thromboembolism: more evidence from a case-control study. *Arch Intern Med* 2000; **160**: 961-964
26 **McCully KS.** Homocysteine and vascular disease. *Nat Med* 1996; **2**: 386-389
27 **Seshadri N,** Robinson K. Homocysteine, B vitamins and coronary artery disease. *Med Clin North Am* 2000; **84**: 215-237
28 **Welch GN,** Loscalzo J. Homocysteine and atherothrombosis. *N Engl J Med* 1998; **338**: 1042-1050
29 **McCully KS.** Homocysteine, folate, vitamin B6, and cardiovascular disease. *JAMA* 1998; **279**: 392-393
30 **Loscalzo J.** The oxidant stress of hyperhomocyst(e)inemia. *J Clin Invest* 1996; **98**: 5-7
31 **Mahmud N,** Molloy A, McPartlin J, Corbally R, Whitehead AS, Scott JM, Weir DG. Increased prevalence of methylenetetrahydrofolate reductase C677T variant in patients with inflammatory bowel disease, and its clinical implications. *Gut* 1999; **45**: 389-394
32 **Oldenburg B,** Fijnheer R, van der Griend R, vanBerge-Henegouwen GP, Koningsberger JC. Homocysteine in inflammatory bowel disease: a risk factor for thromboembolic complications? *Am J Gastroenterol* 2000; **95**: 2825-2830
33 **Chowers Y,** Sela BA, Holland R, Fidder H, Simoni FB, Bar-Mier S. Increased levels of homocysteine in patients with Crohn's disease are related to folate levels. *Am J Gastroenterol* 2000; **95**: 3498-3502
34 **Koutroubakis IE,** Dilaveraki E, Vlachonikolis IG, Vardas E, Vrentzos G, Ganotakis E, Mouzas IA, Gravanis A, Emmanouel D, Kouroumalis EA. Hyperhomocysteinemia in Greek patients with inflammatory bowel disease. *Dig Dis Sci* 2000; **45**: 2347-2351
35 **Romagnuolo J,** Fedorak RN, Dias VC, Bamforth F, Teltscher M. Hyperhomocysteinemia and inflammatory bowel disease: prevalence and predictors in a cross-sectional study. *Am J Gastroenterol* 2001; **96**: 2143-2149
36 **Papa A,** De Stefano V, Danese S, Chiusolo P, Persichilli S, Casorelli I, Zappacosta B, Giardina B, Gasbarrini A, Leone G, Gasbarrini G. Hyperhomocysteinemia and prevalence of polymorphisms of homocysteine metabolism-related enzymes in patients with inflammatory bowel disease. *Am J Gastroenterol* 2001; **96**: 2677-26782
37 **Koutroubakis IE.** Unraveling the mechanisms of thrombosis in inflammatory bowel disease. *Am J Gastroenterol* 2001; **96**: 1325-1327
38 **Slot WB,** van Kasteel V, Coerkamp EG, Seelen PJ, van der Werf SD. Severe thrombotic complications in a postpartum patient with active Crohn's disease resulting in ischemic spinal cord injury. *Dig Dis Sci* 1996; **40**: 1395-1399
39 **Gonera RK,** Timmerhuis TP, Leyten AC, van der Heul C. Two thrombotic complications in a patient with active ulcerative colitis. *Neth J Med* 1997; **50**: 88-91

Science Editor Wang XL and Guo SY **Language Editor** Elsevier HK

PO Box 2345, Beijing 100023, China
www.wjgnet.com
wjg@wjgnet.com

ELSEVIER

World J Gastroenterol 2005;11(38):6043-6048
World Journal of Gastroenterology ISSN 1007-9327

• *BRIEF REPORTS* •

CD14 promoter polymorphism in Chinese alcoholic patients with cirrhosis of liver and acute pancreatitis

You-Chen Chao, Heng-Cheng Chu, Wei-Kuo Chang, Hsin-Hung Huang, Tsai-Yuan Hsieh

You-Chen Chao, Heng-Cheng Chu, Wei-Kuo Chang, Hsin-Hung Huang, Tsai-Yuan Hsieh, Division of Gastroenterology, Department of Internal Medicine, Tri-Service General Hospital, National Defense Medical Center, Taipei, Taiwan, China
Supported by grants from the Taiwan National Science Council (NSC- 91-2314-B-016-109) and from the ShuYuan Education and Academic Promotion Foundation
Co-first-authors: You-Chen Chao
Co-correspondents: You-Chen Chao
Correspondence to: You-Chen Chao, MD, No. 325, Section 2, Cheng-Kung Road, Neihu 114, Taipei, Taiwan, China. chaoycmd@ndmctsgh.edu.tw
Telephone: +886-2-87927008 Fax: +886-2-87927009
Received: 2004-12-28 Accepted: 2005-02-28

AIM: To investigate the relationship between genetic polymorphism of the CD14 promoter and the occurrence of alcoholic cirrhosis and alcoholic pancreatitis, and to challenge the conclusion made earlier that the patients with acute alcoholic pancreatitis and patients with alcoholic cirrhosis of liver are two different subpopulations.

METHODS: Using the polymerase chain reaction-restriction fragment length polymorphism (PCR-RFLP) method, we determined the polymorphism of CD14 gene and aldehyde dehydrogenase gene 2 (ALDH 2) in 335 alcoholic patients with different organ complications i.e., cirrhosis of liver (n = 100), acute pancreatitis (n = 100), esophageal cancer (n = 82) and avascular necrosis of hip joint (AVN) (n = 53) and 194 non-alcoholic controls in a Chinese group.

RESULTS: The results showed that the carriage of T allele was not different among alcoholic patients with cirrhosis of liver, alcoholic patients with other complication and non-alcoholic controls. On the other hand, the carriage of the C allele was significantly more prevalent for alcoholic pancreatitis than for esophageal cancer (0.79 *vs* 0.60, P<0.001), alcoholic AVN (0.79 *vs* 0.65, P<0.025) and non-alcoholic controls (0.79 *vs* 0.68, P<0.025). Furthermore, when only subjects with ALDH2 1-1 genotype were examined, the C allele frequency was significantly more prevalent for alcoholic pancreatitis than for alcoholic liver cirrhosis (0.82 *vs* 0.69, P<0.025), esophageal cancer (0.82 *vs* 0.61, P<0.01), alcoholic AVN (0.82 *vs* 0.64, P<0.01) and non-alcoholic controls (0.82 *vs* 0.69, P<0.05).

CONCLUSION: The C allele may be associated with some mechanism, which is important in the pathogenesis of alcoholic pancreatitis, and that alcoholic patients with acute pancreatitis and cirrhosis of liver are probably two different subpopulations.

Key words: CD14 promoter; Polymorphism; Alcoholic patients

Chao YC, Chu HC, Chang WK, Huang HH, Hsieh TY. CD14 promoter polymorphism in Chinese alcoholic patients with cirrhosis of liver and acute pancreatitis. *World J Gastroenterol* 2005; 11(38): 6043-6048
http://www.wjgnet.com/1007-9327/11/6043.asp

INTRODUCTION

It is well known that alcoholism causes numerous physical complications[1]. However, it is still a mystery why certain organ-specific complications occur only in some alcoholics. Twin concordance studies suggest a contribution by genetic factors. In a large study, consisting of 16 000 male twin pairs, the concordance rate of alcoholic cirrhosis was significantly greater among monozygous (14.6%) than dizygous (5.4%) twins[2]. Later, Reed *et al*., also confirmed the findings in 1996[3]. Based on the above findings, many studies were designed to search for candidate genes that contribute to the susceptibility to alcoholic liver disease (ALD)[4-8]. As we know, the alcohol metabolizing enzymes alcohol dehydrogenase (ADH), aldehyde dehydrogenase (ALDH) and cytochrome P4502E1 are polymorphic at the ADH2, ADH3, ALDH2 loci and the 5'-fling region of the P4502E1[9,10]. Many studies have investigated the differences in these alcohol-metabolizing enzymes to explain susceptibility to alcoholism and to alcohol-induced liver disease[9-12]. The studies have been inconclusive in the linkage of the susceptibility to ALD and polymorphism of alcohol-metabolizing enzymes[13-16].

More recently, accumulating clinical and experimental data indicate that inflammatory responses are involved in the pathogenesis of ALD. Elevated serum endotoxin levels are found in alcoholic patients and in alcohol-treated experimental animals[17,18], as a consequence of intestinal wall leakage, bacterial overgrowth, or reduced phagocytic clearance[19]. Circulating endotoxin is bound mainly to the lipopolysacchride binding protein. This complex has a high affinity for the CD14 receptor, which is expressed on monocytes and macrophages[20]. Binding of the lipopolysaccharide–lipopolysaccharide binding protein complex to CD14 initiates transcription and release of several proinflammatory cytokines, such as tumor necrosis factor-α and interleukin-1β[21].

A polymorphic C/T form at position-159 in the promoter region of the human CD14 gene was recently detected. The polymorphism is within the Spl transcription factor binding site, known to affect CD14 expression. The T variants of the -159 polymorphism promote CD14 gene transcription and cause higher expression of CD14 on monocytes, which seems to lead to an enhanced inflammatory response[22,23]. The T allele has a suggested association with myocardial infarction, which also is known to have an inflammatory component[23,24]. Later, Jarvelainen *et al*., investigated the allele frequency of the CD14 promoter genotype in a Finnish group and found that the T allele was associated with advanced ALD. The T allele confers increased risk of alcoholic liver damage. The TT homozygotes are at a high risk to develop cirrhosis[25]. On the other hand, Koppelman *et al*., reported the importance of the C allele influencing the expression and severity of the atopic phenotype in a Dutch group[26]. The CD14 genotype does not appear to represent a susceptibility gene for the development of atopy, yet it appears to produce a more severe atopic phenotype. Considering the ethnic variations, we conducted a study in a Chinese group to investigate the relationship between genetic polymorphism of the CD14 promoter and the occurrence of alcoholic cirrhosis and alcoholic pancreatitis, two common necro-inflammatory complications in alcoholic patients. Because the preliminary data revealed that the C allele was higher in alcoholic pancreatitis patients, we also included patients with non-alcoholic pancreatitis for comparison. By investigating the polymorphism of CD 14 gene, we also want to challenge the conclusion we made before that the Chinese alcoholic patients with cirrhosis of liver and acute pancreatitis are two different subpopulation[27].

[illegible]

Blood samples were obtained from 335 alcoholic and 194 non-alcoholic patients at the Tri-Service General Hospital in Taipei, from September 2002 to March 2004. Of the 335 alcoholic patients, 100 were diagnosed with cirrhosis of liver, 100 with acute pancreatitis, 82 with esophageal cancer, and 53 with avascular necrosis of the hip joint (AVN), with all instances of the respective diseases deemed to be alcohol-induced. Of the 194 non-alcoholic controls, 77 were diagnosed with gallstone pancreatitis and 117 were non-alcoholic controls that had been admitted to hospital during the same observation period (clinical diagnoses for the controls included peptic ulcer, inguinal hernia, acute appendicitis, bone fracture and acute gastroenteritis). All of the alcoholic patients had consumed in excess of 60 g alcohol per day, on average, for at least 6 years. None of the patients in the non-alcoholic subgroup had a history of alcoholism and consumption of alcoholic beverages was infrequent for these individuals. The 100 patients in the alcoholic cirrhosis subgroup were all negative for serum antinuclear and anti-mitochondrial antibodies, and negative for antibodies to the hepatitis C virus and its RNA (determined using a second-generation test kit, Abbott Laboratories, Chicago, IL, USA) and PCR, respectively. The hepatitis B surface antigen and HBV DNA were negative for all 100 of these patients. All the cirrhotic patients presented with typical sonographic signs suggestive of cirrhosis, and all had endoscopically proven esophageal varices. The distributions of these cirrhotic patients according to Child-Pugh score (A/B/C) were 4/70/26. Liver biopsy was not performed for most cases because of decompensated hepatic function or massive ascites. None of the patients in the alcoholic cirrhosis subgroup had a history of acute pancreatitis. The acute pancreatitis patients presented with typical symptoms and signs, with elevations of serum amylase and lipase at least three-fold normal levels. Abdominal sonography, computerized tomography (CT), and endoscopic retrograde cholangiopancreatography were used for patient evaluation. For the alcoholic pancreatitis subgroup (n = 100), risk factors for the pancreatitis, other than alcoholism, were carefully assessed before being ruled out. Of these 100 patients, 40 had experienced two or more episodes, with mild but persistent elevation for serum transaminases noted among 12 during a 6-mo follow-up period after discharge, indicating the possibility of a coexisting alcohol-induced liver disease. The serum albumin, total bilirubin, prothrombin time and peripheral platelet count for these 12 acute alcoholic pancreatitis patients were within normal limits. No evidence of esophageal varices or congestive gastropathy was noted for any of the 100 patients in this subgroup. All the patients in the alcoholic AVN subgroup had undergone total hip replacement, with diagnosis proven from pathology; for 11 of these, hip-joint involvement was bilateral. None of the 53 patients in alcoholic AVN subgroup had a history of acute pancreatitis. Eleven patients were diagnosed with alcoholic liver disease because of persistently abnormal transaminase levels; however, there was no clinical evidence of cirrhosis. The pathology diagnosis of the patients in esophageal cancer subgroup revealed that 72 of the 82 were squamous cell carcinoma and the other 10 were adenocarcinoma. The 82 patients showed no clinical evidence of liver cirrhosis on abdominal sonography, gastroscopy, and biochemical studies. However, seven of them had mildly elevated serum transaminase levels. None of them had any history of acute pancreatitis. Alcohol consumption histories were obtained using a standard questionnaire. The physician on duty ensured that the informed consent was obtained and the questionnaire was reliably completed by interviewing both the patient and a member of the family, usually the spouse or mother.

DNA isolation and CD14 genotyping

DNA was extracted from WBC pellets, obtained after lysis of the red cells with ammonium bicarbonate. The genotyping of a polymorphism in the promoter region of the CD14 receptor characterized by a C to T transition at -159 was accomplished by restriction fragment length polymorphism analyses. The genomic DNA was amplified using the following primer pair: forward, 5' GTGCCAACAGATGA-GGTTCAC 3'. And reverse, 5' GCCTCTGACAGTTTAT-GTAATC 3'. The PCR was carried out in a final volume of 50 μL, containing 1 mmol/L $MgCl_2$, 0.2 mmol/L of each deoxynucleotide triphosphate, 0.2 μmol/L of each primer, and 1 U Taq DNA polymerase. After an initial denaturation of 5 min at 94 ℃, the samples were subjected to 35 cycles at 94 ℃ for 30 s, 60 ℃ for 30 s, and 72 ℃ for

30 s, with a final extension of 7 min at 72 ℃. The 497-bp product was restricted with Eca 471 (Ava II; Fermentas, Amherst, NY) overnight at 37 ℃. The unrestricted 497-bp product represents the C allele, where a T allele was cut into 144- and 353-bp fragments. The three genotypes were scored after running on a 2.5 % agarose gel. A T/T homozygote was included in PCR as a positive control of digestion.

ALDH2 genotyping

ALDH2 genotyping was determined by our previously published method, using PCR-directed mutagenesis[14].

Statistical analysis

χ^2 analysis was performed to compare the allele frequencies between groups.

□□□□□□□

The patient's age, sex, and alcoholism history are listed in Table 1. The CD14 genotype and allele frequencies for alcoholic and non-alcoholic patients are presented in Table 2. Carriage of C allele was significantly more prevalent in alcoholic pancreatitis than in esophageal carcinoma ($P<0.001$), alcoholic AVN ($P<0.025$), non-alcoholic pancreatitis ($P<0.001$) and non-alcoholic controls ($P<0.025$). When the subjects with genotype CC compared with genotype TT, the CC genotype was more prevalent in alcoholic pancreatitis than in esophageal cancer ($P<0.005$), non-alcoholic pancreatitis ($P<0.005$), and non-alcoholic controls ($P<0.025$).

We also compared subjects with genotype CC *vs* CT and TT (T- *vs* T+). The CC genotype was more prevalent in alcoholic pancreatitis than in alcoholic esophageal cancer ($P<0.001$), alcoholic AVN ($P = 0.005$), non-alcoholic pancreatitis ($P<0.001$) and non-alcoholic controls ($P<0.002$). The CC genotype was more prevalent in alcoholic liver cirrhosis than in alcoholic esophageal cancer ($P<0.05$) (Table 2).

For further clarification of the role of C allele in the development of different alcohol-related complications, we checked the allele frequency of CD14 only in subjects with the ALDH2 1-1 genotype (Table 3). The C allele frequency was significantly more prevalent in alcoholic pancreatitis than in alcoholic liver cirrhosis ($P<0.025$), esophageal cancer ($P<0.01$), alcoholic AVN ($P<0.01$), non-alcoholic pancreatitis ($P<0.001$) and non-alcoholic controls ($P<0.05$). In a subgroup of subjects with genotype ALDH2 1-1, the genotype CC *vs*

Table 1 Age, sex, and alcohol consumption in the different groups

Groups (*n*)	Alcohol consumption			
	Age (yr)	Sex (M/F)	Daily (g)	Duration (yr)
Alcoholic cirrhosis (100)	50.5±12.9	97/3	189±119	25.8±11.6
Alcoholic pancreatitis (100)	40.2±11.7	95/5	143±93	15.8±8.8
Alcoholic esophageal Ca (82)	64.4±12.7	82/0	200±175	35.8±13.8
Alcoholic AVN (53)	44.7±9.7	53/0	197±139	19.6±8.2
Non-alcoholic pancreatitis (77)	53.2±17.5	38/39	-	-
Non-alcoholic controls (117)	60.6±18.3	75/32	-	-

Table 2 CD14 polymorphism

Groups (*n*)	CC	CT	TT	*C	*T
Alcoholic pancreatitis (100)	59[c,d,f,h,2,3]	39	2	0.79[a,b]	0.21
Alcoholic cirrhosis (100)	46[e]	49	5	0.71[1]	0.29
Alcoholic esophageal Ca. (82)	25	49	8	0.60	0.40
Alcoholic AVN (53)	18	33	2	0.65	0.35
Non-alcoholic pancreatitis (77)	25	43	9	0.60	0.40
Non-alcoholic controls (117)	49	62	6	0.68	0.32

C allele frequency, [a]$P<0.025$ *vs* alcoholic AVN and non-alcoholic controls; [b]$P<0.001$ *vs* esophageal carcinoma and non-alcoholic pancreatitis; [1]$P = 0.055$ *vs* esophageal carcinoma. Genotype CC *vs* TT, [c]$P<0.005$ *vs* esophageal cancer and non-alcoholic pancreatitis; [d]$P<0.001$ *vs* alcoholic AVN. Genotype CC *vs* CT and TT (T- *vs* T+), [f]$P<0.001$ *vs* alcoholic esophageal cancer; [h]$P<0.001$ *vs* non-alcoholic pancreatitis; [2]$P = 0.005$ *vs* alcoholic AVN; [3]$P = 0.017$ *vs* non-alcoholic controls. Genotype CC *vs* CT and TT (T- *vs* T+), [e]$P<0.05$ *vs* alcoholic esophageal cancer.

Table 3 CD14 polymorphism in ALDH2 1-1 homozygotes

Group (*n*)	CC	CT	TT	*C	*T
Alcoholic pancreatitis (65)	41[e,g,i,k]	24	0	0.82[a,b,c,d]	0.18
Alcoholic cirrhosis (77)	33	40	4	0.69	0.31
Alcoholic esophageal Ca (23)	8	12	3	0.61	0.39
Alcoholic AVN (42)	14	26	2	0.64	0.36
Non-alcoholic pancreatitis (40)	13	21	6	0.59	0.41
Non-alcoholic controls (54)	22	30	2	0.69	0.31

C allele frequency, [a]$P<0.025$ *vs* alcoholic cirrhosis; [b]$P<0.001$ *vs* non-alcoholic pancreatitis; [c]$P<0.05$ *vs* non-alcoholic controls; [d]$P<0.01$ *vs* esophageal cancer and alcoholic AVN. Genotype CC *vs* CT and TT, [e]$P<0.05$ *vs* alcoholic cirrhosis and alcoholic esophageal cancer; [g]$P<0.025$ *vs* alcoholic AVN; [i]$P<0.005$ *vs* non-alcoholic pancreatitis; [k]$P<0.05$ *vs* non-alcoholic controls.

Table 4 CD14 polymorphism in alcoholic patients with and without pancreatitis

Group (*n*)	CC	CT	TT	*C	*T
Alcoholics without pancreatitis (235)	89[b,c]	131	15	0.66[a]	0.34
Alcoholics with pancreatitis (100)	59	39	2	0.79	0.21
Alcoholics with genotype ALDH2 1-1					
Alcoholics without pancreatitis (142)	59[g,i]	78	9	0.66[e]	0.34
Alcoholics with pancreatitis (65)	41	24	0	0.82	0.18

C allele frequency, [a]$P<0.005$ *vs* alcoholics with pancreatitis. Genotype CC *vs* TT, [b]$P<0.001$ *vs* alcoholics with pancreatitis. [c]$P<0.05$ *vs* alcoholics with pancreatitis. Genotype CC *vs* CT and TT (T- *vs* T+), C allele frequency, [e]$P<0.005$ *vs* alcoholics with pancreatitis. Genotype CC *vs* TT, [g]$P<0.05$ *vs* alcoholics with pancreatitis. Genotype CC *vs* CT and TT (T- *vs* T+), [i]$P<0.005$ *vs* alcoholics with pancreatitis.

CT and TT (T- *vs* T+) was also more prevalent for the alcoholic pancreatitis than for the alcoholic liver cirrhosis ($P<0.05$), alcoholic esophageal cancer ($P<0.05$), alcoholic AVN ($P<0.01$), non-alcoholic pancreatitis ($P<0.005$) and non-alcoholic controls ($P<0.05$). We did not check CC *vs* TT, and TT *vs* CC and CT in subjects with ALDH2 1-1 genotype because there were no TT homozygous patients in alcoholic pancreatitis group. We also compared alcoholic patients with and without pancreatitis in Table 4. The frequency of C allele was more prevalent for the alcoholic patients with pancreatitis than for the alcoholic patients without pancreatitis ($P<0.005$). Genotype CC was more prevalent for alcoholic patients with pancreatitis than for patients without pancreatitis ($P<0.05$). The genotype CC *vs* CT and TT (T- *vs* T+) was also more prevalent in alcoholic patients with pancreatitis than patients without pancreatitis ($P<0.001$). In subjects with genotype ALDH2 1-1, the C allele frequency was significantly higher in alcoholic patients with pancreatitis than without pancreatitis ($P<0.005$). The CC genotype was more prevalent for alcoholic patients with pancreatitis than patients without pancreatitis ($P<0.05$). And, the genotype CC *vs* CT and TT (T- *vs* T+) was more prevalent in alcoholic patients with pancreatitis than patients without pancreatitis ($P<0.005$).

[illegible]

The genotype distribution of the CD14 promoter polymorphism was unique in that the TT genotype was less prevalent in the Chinese than in the Finnish group (4.8% in Chinese alcoholics *vs* 19.7% in Finnish alcoholics and 7.7% in Chinese non-alcoholics *vs* 16.4% in Finnish non-alcoholics)[25]. In this study, we investigated the genotype distribution of CD14 in alcoholic patients with necro-inflammatory complications, pancreatitis and liver cirrhosis and other complications i.e., esophageal cancer and avascular necrosis of hip joint. We did not confirm the results in Chinese alcoholic patients that the T allele confers increased risk of alcoholic liver damage, reported by Jarvelainen *et al*., in the Finnish group[25]. This indicates that this polymorphism is probably not, at least in the Chinese population, an important factor determining the severity of liver disease in alcoholic patients. But we found that the C allele frequency was significantly higher in alcoholic patients with pancreatitis than alcoholic patients with other complications.

The significant role of the T allele in CD14 promoter region was suggested by two findings: (1) it has been found to confer increased CD14 expression on monocytes[22,23] and (2) an increased risk for myocardial infarction has been observed among individuals who are CD14-promoter TT homozygotes[23,24]. The T allele seems to favor the inflammatory process. On the other hand, Ito *et al*., reported that no association between CD14 genotypes and serum CD14 levels was observed in the Japanese population[28]. Risley *et al*., suggested no significant differences in serum CD14 concentration between Caucasian healthy carriers and noncarriers of the T allele[29]. Furthermore, Fernandez-Real *et al*., also found that there was no difference in CD14 levels among healthy Spanish people with different CD14 genotypes[30]. However, the T/T homozygotes have higher levels of circulating CD14 in a subset of diabetic patients[27]. The CD14 genotype was associated with insulin sensitivity in both Caucasian healthy subjects and type 2 diabetic patients[29]. Taking these together, whether CD14 polymorphism was associated with circulating CD14 levels remains controversial. More functional studies are needed to study the effect of CD14/-159 on promoter activity.

Previous publications discuss the relationship between diseases and the CD14 genotypes and have revealed conflicting results. Hubacek *et al*., found the T allele and TT genotype elevated in Czech patients with myocardial infarction ($n = 178$) if compared with the control subjects, suggesting the -159 C/T nucleotide polymorphism to be a genetic risk factor[23]. In a large study which included 1 793 patients, conducted in Germany by Koch *et al*., data indicated that the -159 C/T polymorphism is not related to coronary artery disease or myocardial infarction[31]. In a Dutch population, Koppelman *et al*., found homozygotes for the C allele had a higher number of positive skin tests and higher total serum IgE levels and subsequently, more allergic symptoms including rhinitis and hay fever, compared with subjects with CT and TT alleles[26]. In our study, we found that the C allele frequency was significantly higher in alcoholic patients with pancreatitis than alcoholic patients with other complications. This difference persisted between alcoholic patients with pancreatitis and alcoholic patients with other complications when compared with CC to TT or T- to T+. This suggested that the C allele may be associated with some mechanism which is important and specific in the pathogenesis of alcoholic pancreatitis.

Previously, we reported that most Chinese alcoholic patients with liver cirrhosis never had an episode of acute alcohol-induced pancreatitis despite the fact that they are older and their daily alcohol consumption is larger than that of pancreatitis patients. Further analysis revealed that the ADH2*1 allele frequency is significantly different between Chinese alcoholic patients with cirrhosis and pancreatitis.

We also suggest that alcoholic patients with these two different complications are two different subpopulations[27]. In this study, we also want to investigate whether the CD14 allele frequency is different between alcoholic patients with liver cirrhosis and alcoholic pancreatitis. Initially when comparing the C allele frequency of CD14 in alcoholic patients with pancreatitis and liver cirrhosis, no significant difference was found in these two groups. As the alcohol-specific complications are considered to be influenced by multiple genes and also because the ALDH2 gene is one of the most important alcohol-metabolizing genes, we evaluated the relationship between CD14 genotypes and different complications only in alcoholic patients with genotype ALDH 2 1-1, the most common genotype in the Chinese alcoholic patients. The result showed that the C allele frequency is significantly different between alcoholic patients with cirrhosis of the liver and alcohol-induced pancreatitis. This further indicated that the C allele is associated with the development of alcoholic pancreatitis and alcoholic patients with cirrhosis and pancreatitis are of two different subpopulations.

Unlike alcoholic pancreatitis patients, those with gallstone pancreatitis share the similar frequency of C allele with general population. This indicates that the increased C allele frequency is specific for alcoholic, but not all types of pancreatitis.

The pathogenesis of alcoholic pancreatitis is not clear. There are several plausible explanations for a possible role of CD14 in alcoholic pancreatitis. CD14 is a multifunctional receptor and may play a role in different biological and pathophysiological processes such as: apoptosis, sepsis and inflammatory disease[32-35]. CD14 on monocytes and polymorphonuclear cells functions as a receptor for lipopolysaccharides, thereby inducing mediator and cytokine release. Thus, CD14 may be involved in a proinflammatory pathway through the release of cytokines.

The reason why alcoholic patients develop different organ complications is still unknown. It seems highly probable that the development of specific complications in alcoholic patients is determined by multiple genes, with most of these still not well understood.

REFERENCES

1 **Schuckit MA.** Alcohol and alcoholism. In Braunwald E, Isselbacher KJ, Eds. Harrison's principles of internal medicine, 13th Ed. *New York: McGraw-Hill* 1995: 2420-2425
2 **Hrubec Z,** Omenn GS. Evidence of genetic predisposition to alcoholic cirrhosis and psychosis: twin concordances for alcoholism and its biological end points by zygosity among male veterans. *Alcohol Clin Exp Res* 1981; **5**: 207-215
3 **Reed T,** Page WF, Viken RJ, Christian JC. Genetic predisposition to organ-specific endpoints of alcoholism. *Alcohol Clin Exp Res* 1996; **20**: 1528-1533
4 **Lieber CS.** Alcohol and the liver:1994 update. *Gastroenterology* 1994; **106**: 1085-1105
5 **Bosron WF,** Li TK. Genetic polymorphism of human liver alcohol and aldehyde dehydrogenase, and their relationship to alcohol metabolism and alcoholism. *Hepatology* 1986; **6**: 502-510
6 **Bosron WF,** Ehrig T, Li TK. Genetic factors in alcohol metabolism and alcoholism. *Semin Liver Dis* 1993; **13**: 126-135
7 **Goedde HW,** Agarwal DP. Acetaldehyde metabolism: genetic variation and physiological implications. In: Goedde HW, Agarwal DP, eds. Alcoholism: Biomedical and genetic aspects. *Elmsford: Pergamon Press* 1989: 21-56
8 **Smith M.** Genetics of human alcohol and aldehyde dehydrogenases. *Adv Hum Genet* 1986; **15**: 249-290
9 **Maezawa Y,** Yamauchi M, Toda G. Association between restriction fragment length polymorphism of the human cytochrome P450IIE1 gene and susceptibility to alcoholic liver cirrhosis. *Am J Gastroenterol* 1994; **89**: 561-565
10 **Tsutsumi M,** Takada A, Wang JS. Genetic polymorphisms of cytochrome P4502E1 related to the development of alcoholic liver disease. *Gastroenterology* 1994; **107**: 1430-1435
11 **Day CP,** James OF, Bassendine MF, Crabb DW, Li TK. Alcohol dehydrogenase polymorphisms and predisposition to alcoholic cirrhosis. *Hepatology* 1993; **18**: 230-232
12 **Crabb DW.** Ethanol oxidizing enzymes: roles in alcohol metabolism and alcoholic liver disease. *Prog Liver Dis* 1995; **13**: 151-172
13 **Enomoto N,** Takase S, Takada N. Alcoholic liver disease in heterozygotes of mutant and normal aldehyde dehydrogenase-2 genes. *Hepatology* 1991; **13**: 1071-1075
14 **Chao YC,** Liou SR, Chung YY, Tang HS, Hsu CT, Li TK, Yin SJ. Polymorphism of alcohol and aldehyde dehydrogenase genes and alcoholic cirrhosis in Chinese patients. *Hepatology* 1994; **19**: 360-366
15 **Chao YC,** Young TH, Chang WK, Tang HS, Hsu CT. An investigation of whether polymorphisms of cytochrome P4502E1 are genetic markers of susceptibility to alcoholic end-stage organ damage in a Chinese population. *Hepatology* 1995; **22**: 1409-1414
16 **Yamauchi M,** Maezawa Y, Mizuhara Y, Ohata M, Hirakawa J, Nakajima H, Toda G. Polymorphisms in alcohol metabolizing enzyme genes and alcoholic cirrhosis in Japanese patients: a multivariate analysis. *Hepatology* 1995; **22**: 1136-1142
17 **Bode C,** Kugler V, Bode JC. Endotoxemia in patients with alcoholic and non-alcoholic cirrhosis and in subjects with no evidence of chronic liver disease following acute alcohol excess. *J Hepatol* 1987; **4**: 8-14
18 **Nanji AA,** Khettry U, Sadrzadeh SM, Yamanaka T. Severity of liver injury in experimental alcoholic liver disease. Correlation with plasma endotoxin, prostaglandin E2, leukotriene B4, and thromboxane B2. *Am J Pathol* 1993; **142**: 367-373
19 **Schenker S,** Bay MK. Alcohol and endotoxin: another path to alcoholic liver injury? *Alcohol Clin Exp Res* 1995; **19**: 1364-1366
20 **Matsuura K,** Ishida T, Setoguchi M, Higuchi Y, Akizuki S, Yamamoto S. Upregulation of mouth CD14 expression in Kupffer cells by lipopolysaccharide. *J Exp Med* 1994; **179**: 1671-1676
21 **Kielian TL,** Blecha F. CD 14 and other recognition molecules for lipopolysaccharide: a review. *Immunopharmacology* 1995; **29**: 187-205
22 **Baldini M,** Lohman IC, Halonen M, Erickson RP, Holt PG, Martinez FD. Polymorphism in the 5′ flanking region of the CD 14 gene is associated with circulating soluble CD14 levels and with total serum immunoglobulin E. *Am J Respir Cell Mol Biol* 1999; **20**: 976-983
23 **Hubacek JA,** Rothe G, Pit'ha J, Skodova Z, Stanek V, Poledne R, Schmitz G. C(-260)T polymorphism in the promoter of the CD14 monocyte receptor gene as a risk factor for myocardial infarction. *Circulation* 1999; **99**: 3218-3220
24 **Unkelbach K,** Gardemann A, Kostrzewa M, Philipp M, Tillmanns H, Haberbosch W. A new promoter polymorphism in the gene of lipopolysaccharide receptor CD14 is associated with expired myocardial infarction in patients with low atherosclerotic risk profile. *Arterioscler Thromb Vasc Biol* 1999; **19**: 932-938
25 **Jarvelainen HA,** Orpana A, Perola M, Savolainen VT, Karhunen PJ, Lindros KO. Promoter polymorphism of the CD14 endotoxin receptor gene as a risk factor for alcoholic liver disease. *Hepatology* 2001; **33**: 1148-1153
26 **Koppelman GH,** Reijmerink NE, Colin Stine O, Howard TD, Whittaker PA, Meyers DA, Postma DS, Bleecker ER. Association of a promoter polymorphism of the CD14 gene and atopy. *Am J Respir Crit Care Med* 2001; **163**: 965-969
27 **Chao YC,** Young TH, Tang HS, Hsu CT. Alcoholism and alcoholic organ damage and genetic polymorphisms of alco-

hol metabolizing enzymes in Chinese patients. *Hepatology* 1997; **25**: 112-117

28 **Ito D,** Murata M, Tanahashi N, Sato H, Sonoda A, Saito I, Watanabe K, Fukuuchi Y. Polymorphism in the promoter of lipopolysaccharide receptor CD14 and ischemic cerebrovascular disease. *Stroke* 2000; **31**: 2661-2664

29 **Risley P,** Jerrard-Dunne P, Sitzer M, Buehler A, von Kegler S, Markus HS. Carotid Atherosclerosis Progression Study. Promoter polymorphism in the endotoxin receptor (CD14) is associated with increased carotid atherosclerosis only in smokers. The carotid atherosclerosis progression study (CAPS). *Stroke* 2003; **34**: 604-606

30 **Fernandez-Real JM,** Broch M, Richart C, Vendrell J, Lopez-Bermejo A, Ricart W. CD14 monocyte receptor, involved in the inflammatory cascade, and insulin sensitivity. *J Clin Endocrinol Metab* 2003; **88**: 1780-1784

31 **Koch W,** Kastrati A, Mehilli J, von Beckerath N, Schomig A. CD14 gene -159 C/T polymorphism is not associated with coronary artery disease and myocardial infarction. *Am Heart J* 2002; **143**: 971-976

32 **Schlegel RA,** Krahling S, Callahan MK, Williamson P. CD14 is a component of multiple recognition systems used by macrophages to phagocytose apoptotic lymphocytes. *Cell Death Differ* 1999; **6**: 583-592

33 **Gibot S,** Cariou A, Drouet L, Rossignol M, Ripoll L. Association between a genomic polymorphism within the CD14 locus and septic shock susceptibility and mortality rate. *Crit Care Med* 2002; **30**: 969-973

34 **Obana N,** Takahashi S, Kinouchi Y, Negoro K, Takagi S, Hiwatashi N, Shimosegawa T. Ulcerative colitis is associated with a promoter polymorphism of lipopolysaccharide receptor gene, CD14. *Scand J Gastroenterol* 2002; **37**: 699-704

35 **Klein W,** Tromm A, Griga T, Fricke H, Folwaczny C, Hocke M, Eitner K, Marx M, Duerig N, Epplen JT. A polymorphism in the CD14 gene is associated with Crohn disease. *Scand J Gastroenterol* 2002; **37**: 189-191

Science Editor Guo SY **Language Editor** Elsevier HK

PO Box 2345, Beijing 100023, China
www.wjgnet.com
wjg@wjgnet.com

ELSEVIER

World J Gastroenterol 2005;11(38):6049-6052
World Journal of Gastroenterology ISSN 1007-9327

• *BRIEF REPORTS* •

Balthazar computed tomography severity index is superior to Ranson criteria and APACHE II scoring system in predicting acute pancreatitis outcome

Ting-Kai Leung, Chi-Ming Lee, Shyr-Yi Lin, Hsin-Chi Chen, Hung-Jung Wang, Li-Kuo Shen, Ya-Yen Chen

Ting-Kai Leung, Chi-Ming Lee, Hsin-Chi Chen, Hung-Jung Wang, Li-Kuo Shen, Ya-Yen Chen, Department of Diagnostic Radiology, Taipei Medical University Hospital, Taipei, Taiwan, China
Shyr-Yi Lin, Department of Internal Medicine, Taipei Medical University Hospital, Taipei, Taiwan, China
Correspondence to: Chi-Ming Lee, MD, Department of Diagnostic Radiology, Taipei Medical University Hospital, 252, Wu Hsing Street, Taipei 110, Taiwan, China. yayen0220@yahoo.com.tw
Telephone: +886-2-27372181-1131 Fax: +886-2-23780943
Received: 2005-01-31 Accepted: 2005-04-18

Abstract

AIM: Acute pancreatitis (AP) is a process with variable involvement of regional tissues or organ systems. Multifactorial scales included the Ranson, Acute Physiology and Chronic Health Evaluation (APACHE II) systems and Balthazar computed tomography severity index (CTSI). The purpose of this review study was to assess the accuracy of CTSI, Ranson score, and APACHE II score in course and outcome prediction of AP.

METHODS: We reviewed 121 patients who underwent helical CT within 48 h after onset of symptoms of a first episode of AP between 1999 and 2003. Fourteen inappropriate subjects were excluded; we reviewed the 107 contrast-enhanced CT images to calculate the CTSI. We also reviewed their Ranson and APACHE II score. In addition, complications, duration of hospitalization, mortality rate, and other pathology history also were our comparison parameters.

RESULTS: We classified 85 patients (79%) as having mild AP (CTSI <5) and 22 patients (21%) as having severe AP (CTSI $\geqslant$5). In mild group, the mean APACHE II score and Ranson score was 8.6±1.9 and 2.4±1.2, and those of severe group was 10.2±2.1 and 3.1±0.8, respectively. The most common complication was pseudocyst and abscess and it presented in 21 (20%) patients and their CTSI was 5.9±1.4. A CTSI $\geqslant$5 significantly correlated with death, complication present, and prolonged length of stay. Patients with a CTSI $\geqslant$5 were 15 times to die than those CTSI <5, and the prolonged length of stay and complications present were 17 times and 8 times than that in CTSI <5, respectively.

CONCLUSION: CTSI is a useful tool in assessing the severity and outcome of AP and the CTSI $\geqslant$5 is an index in our study. Although Ranson score and APACHE II score also are choices to be the predictors for complications, mortality and the length of stay of AP, the sensitivity of them are lower than CTSI.

Key words: Acute pancreatitis; Ranson score; APACHE II score; Balthazar computed tomography severity index

Leung TK, Lee CM, Lin SY, Chen HC, Wang HJ, Shen LK, Chen YY. Balthazar computed tomography severity index is superior to Ranson criteria and APACHE II scoring system in predicting acute pancreatitis outcome. *World J Gastroenterol* 2005; 11(38): 6049-6052
http://www.wjgnet.com/1007-9327/11/6049.asp

INTRODUCTION

Acute pancreatitis (AP) is a process of acute inflammation of the pancreas, with variable involvement of regional tissues or organ systems. The clinical expression of AP varies from edematous mild AP to severe AP, and is frequently associated with necrosis of the pancreas, a protracted clinical course, organ failure, a high incidence of local complications, and a high mortality rate[1]. Multifactorial scales including the Ranson[2] and Acute Physiology and Chronic Health Evaluation (APACHE II) systems[3] have been used for AP since the 1970s. Balthazar computed tomography severity index (CTSI) was developed since 1990[4]. Computed tomography (CT) with intravenous contrast medium injection is accepted as the imaging procedure of choice: first to document the extent of pancreatic and extrapancreatic acute fluid collections and, second, to detect pancreatic necrosis. These two parameters have been identified as prognostic indicators of the severity of AP. CTSI, based on combined assessment of peripancreatic fluid collections, and the degree of pancreatic necrosis were developed to improve prognostic accuracy. The purpose of this review study was to assess the early predictability of a variety of parameters in AP, such as Ranson, APACHE II, and CTSI. We compared the accuracy of CTSI, Ranson score, and APACHE II score in course and outcome of AP prediction and the prognostic value of CT in the assessment of AP.

MATERIALS AND METHODS

We performed a retrospective review of all 121 patients who underwent helical CT within 48 h after onset of symptoms of a first episode of AP between 1999 and 2003.

Fourteen inappropriate subjects who did not meet criteria of clinical blood data for diagnosis of pancreatitis were excluded, CT was performed without contrast because of renal dysfunction and missing chart in medical records, and we reviewed the 107 contrast-enhanced CT images. Of these, there were 57 males, 50 females, with ages ranging from 21 to 87 years, mean age 56 years. The abdominopelvic CT scans were (HiSpeed CT/I; GE Medical Systems, Milwaukee, WI, USA) acquired from patients after oral administration of 4% iothalamate meglumine (Mallinckrodt, USA) 1 000 mL and intravenous administration of iohexol (Nycoveien, Norway) 100 mL (350 mg/mL); flow rate, 2 mL/s, with a section thickness of 10 mm and a pitch of 1.5. We reviewed the CTSI of their CT images. CTSI is a 10-point scoring system derived by assessing the degree of pancreatic and peripancreatic inflammation (0-4 points), and the presence and degree of pancreatic parenchymal nonenhancement or necrosis (0-6 points)[4]. In addition, we also collected the clinical chart records (temperature, heart rate, mean blood pressure, respiratory rate, etc.) to calculate the APACHE II and Ranson score. Complications, duration of hospitalization (according to Simchuk's study[5], we defined the prolonged length of stay as ≥20 d; short length of stay as <20 d), mortality rate, and other pathology history also were our comparison parameters.

RESULTS

According to Casas's study[6], we classified 85 patients (79%) as having mild AP (CTSI <5) and 22 patients (21%) as having severe AP (CTSI ≥5). We found that the CTSI in all patients was 0-8 points and mean score was 3.7. The mean CTSI in mild group was 1.9±0.4 and that in severe group was 6.1±0.5. In APACHE II score aspect, the mean score among all patients was 9.4±2.4. In CTSI mild AP group, the mean APACHE II score was 8.6±1.9 and that of CTSI severe AP was 10.2±2.1. In Ranson score aspect, the mean score in all patients was 2.7±1.4. In CTSI mild group, the mean Ranson score was 2.4±1.2 and that of CTSI severe group was 3.1±0.8. Complications included pseudocyst formation in 21 (20%) including abdominal abscess in two cases. The CTSI in these patients was 5-8, and the mean score was 5.9. Mean APACHE II score and Ranson score of them were 9.4 and 2.7 respectively. Four patients (3.7%) died because of multiorgan failure and sepsis. They died at 21st, 23rd, 19th, and 12th d after admission. The CTSI of them was 3, 5, 6, and 7 respectively. The APACHE II in these four patients was 6, 7, 7, and 9 and the Ranson score was 2, 2, 2, and 3. The APACHE II and Ranson score in the patient who died but with a CTSI of 3 were not significantly higher than other patients. In the length of stay aspect, 19 patients stayed for over 20 d and the mean CTSI was 5.6. Others stayed for 3-15 d and the mean CTSI was 2.7. By comparison, there is no significant difference of APACHE II and Ranson score in the short length of stay (<20 d) group and prolonged length of stay (≥20 d) group. Mean APACHE II score in short and prolonged length of stay was 8.9 and 9.8 and the mean Ranson score was 2.9 and 2.6, respectively. Comparison of CTSI, APACHE II score and Ranson score in our patients are listed in Table 1.

Table 2 shows the relationship between CTSI and outcomes. These data showed that the CTSI significantly correlated with all outcomes measured. Patients with a CTSI ≥5 was 15 times to die than those CTSI <5, and the prolonged length of stay and complications present were 17 times and 8 times than that in CTSI <5, respectively. AP was due to gallstone in 36 patients (34%), to alcohol consumption in 36 patients (34%), to both causes in 16 patients (15%) and to unknown reasons in 19 patients (18%). In other pathology history aspect, the most popular disease in our patients is diabetes mellitus (DM). Thirty-six patients (34%) were with DM and two of them underwent neuropathy. The mean CTSI in these DM patients was 5.3. Three of the DM patients died and their CTSI were 5, 6, and 7. In addition, AP relapse occurred in 17 patients (16%) and they all belonged to alcoholic type. The mean CTSI of them was 4.2.

Table 1 The comparison of severity, complication, mortality, and the length of stay in CTSI, Ranson score, and APACHE II score

		CTSI[1]	Ranson score	APACHE II score
Severity	Mild	1.9±0.4	2.4±1.2	8.6±1.9
	Severe	6.1±0.5	3.1±0.8	10.2±2.1
Complications	Present	5.9±1.4	2.7±0.9	9.4±2.4
	Absent	2.1±0.6[1]	2.5±1.1	8.7±1.6
Mortality	Present	5.3±1.7	2.3±0.5	7.3±1.3
	Absent	1.8±0.6[1]	2.5±0.7	8.5±0.9
Length of stay	≥20 d	5.6±1.6	2.6±1.1	9.8±0.9
	<20 d	2.7±1.1[1]	2.9±0.9	8.9±1.2

[1]Significant differences between two lines in the same parameter.

Table 2 CTSI and outcome prediction

		No. of patients	*P*	Odd's ratio
Death	CTSI ≥5	3	<0.05	15
	CTSI <5	103		
Prolonged length of stay (≥20 d)	CTSI ≥5	19	<0.05	17
	CTSI <5	88		
Complications	CTSI ≥5	21	<0.05	8
	CTSI <5	86		

DISCUSSION

Predicting the severity and outcome of AP still represents a challenge for the physician. Since the work of Ranson[2] establishing a scoring system of severity for patients with AP, there has been several other scoring systems: Imrie[7], APACHE II[3], and Balthazar CTSI[4] systems were used to assess the severity of disease that had a high sensitivity and positive predictive value (PPV). A milestone achievement in assessing the severity of AP occurred in 1974, when Ranson developed his prognostic signs. He examined the relationship of 43 different measurements made during the first 48 h of treatment, finding 11 variables that significantly correlated with overall morbidity and mortality. Imrie *et al*., later modified Ranson's criteria by removing serum transaminase and adding serum methemalbumin, albumin, and cyclic AMP to Ranson's prognostic variables. However, the Ranson and Imrie criteria cannot be calculated until data from admission and 48 h after admission are compared. Larvin and McMahon[3]

applied the APACHE II score in the setting of AP and found that those with scores >7 were likely to have a severe course. They defined a severe course as the development of major organ system failure and a pancreatic collection. An advantage of the APACHE II score was flexibility, as it could be recalculated at any time during a hospital stay. However, Larvin and McMahon also showed that the APACHE II score had just a 67% PPV at 24 h after admission. They also showed that the APACHE II score was even less accurate for identifying patients with specific complications including peripancreatic fluid collections or major organ failure. Thus, better prognostic tools are needed. The Balthazar CTSI was reported to be of value in identifying patients with severe and fatal outcome, only a few studies have investigated whether CTSI performance is superior to that of the APACHE II or Ranson score in predicting AP outcome. This is the major challenge of this study.

Robert *et al.*[8], demonstrated that the Ranson score in mild AP (defined as the course of the disease was uncomplicated) and in severe AP (defined as organ failure) were 1.9±0.9 and 2.2±0.5. The APACHE II score was 6.9±0.7 and 7.4±0.4 in mild and severe group. In Chatzicostas's study[9], the Ranson score in mild (defined as normal amylase and lipase level) and severe (defined as organ failure and complications) groups were 2.0±1.4 and 2.1±1.6. The APACHE II score was 10.1±0.2 and 9.8±0.6 in mild and severe group. There were no significant differences between these data. According to these data, Robert and Chatzicostas demonstrated that the Ranson score and APACHE II score are not absolute predictors for severity of AP. In our study, we also did not find significant differences of Ranson and APACHE II score in mild and severe groups. So we suppose that our results are similar to Robert's and Chatzicostas's. In addition, in Wilson's study[10], they demonstrated that the patients with Ranson score ⩾3 was always in a severe situation. On evaluation of mean Ranson score in our study, we found that in severe AP it was 3.1±0.8. However, only one-thirds of the patients with severe pancreatitis had Ranson score ⩾3. Compared to Wilson's results, there were still a lot of variability in Ranson score prediction.

Complications are often the major reasons that resulted in the death of AP patients. The management of complications is important to reduce the mortality rate. In our study, we found that the higher CTSI associated with higher complication rate and the CTSI ⩾5 is an index. However, we did not find the same situation in Ranson and APACHE II score. There were no significant differences between mild and severe groups of Ranson and APACHE II score. According to Nicolas[11], they found that complications occurred rarely in Ranson score <3 and APACHE II score <8. In our study, the mean Ranson score and APACHE II score in complications-occurred patients were 2.7 and 9.4. Our APACHE II score result was similar to Nicolas' but in Ranson score aspect, the results showed that the relationship between complications present and Ranson score appeared to involve multiple variables. In the length of stay aspect, we demonstrated that CTSI is a more sensitive predictor than APACHE II and Ranson score. The mean CTSI in short and in prolonged length of stay showed significant difference (2.7 *vs* 5.6). However, there is no significant difference of APACHE II and Ranson score in the short length of stay group and prolonged length of stay group. In Simchuk's study[5], they mentioned that the PPV of APACHE II and Ranson score for the length of stay were 31% and 38%, and the PPV of CTSI was 71%. However, in Fleszler's study[12], they mentioned that APACHE II score is the most appropriate index to predict the length of stay, but they also mentioned that this score requires an arterial blood gas level, which was not available on some patients, thus the practicality of APACHE II is lower than Ranson score and CTSI.

The reported mortality rates for patients with AP vary greatly from 15% to 56%[12]. In Casas's study[6], they demonstrated that CTSI ⩾5 is the index, if the patients are under the danger of death. In Bradley's study[13], their results showed that CTSI >8 is the index for death. In our study, three of the four died patients had a CTSI ⩾5. So we supposed that our results were more similar to Casas's. According to Simchuk *et al.*[5], they mentioned that the CTSI <3 had a 3% mortality rate, whereas patients with a CTSI >7 had a mortality rate of 17%, it is likely 5-6 times mortality rate in CTSI >7 group. From the CTSI definitional value described above, there was still a lot of variability in death prediction of CTSI. According to our results, we demonstrated that the reason resulted in the variability may be the different characteristics of patients. Age, chronic diseases such as DM present or not, alcohol consumption and organ dysfunction all may affect the mortality rate of AP. We found that three of our four died patients had DM and their CTSI were 5, 6, and 7, all of them were alcoholics, and the average age of the four died patients was 55 years. Mortality rate associated with higher CTSI and worse pathological rate, the different characteristics of individual should not be ignored.

In conclusion, the CTSI is a useful tool in assessing the severity and outcome of AP and the CTSI ⩾5 are likely to have a severe course in our study. Although Ranson and APACHE II scores also are choices to be the predictors for complications, mortality and the length of stay of AP, the sensitivity of them are lower than CTSI. In addition, we found that if we are using CTSI to be an indicator for mortality rate, the different characteristics of an individual should not be ignored.

REFERENCES

1 **Yousaf M**, McCallion K, Diamond T. Management of severe acute pancreatitis. *Br J Surg* 2003; **90**: 407-420

2 **Ranson JH**, Rifkind KM, Roses DF, Fink SD, Eng K, Spencer FC. Prognostic signs and the role of operative management in acute pancreatitis. *Surg Gynecol Obstet* 1974; **139**: 69-81

3 **Larvin M**, McMahon MJ. APACHE II score for assessment and monitoring of acute pancreatitis. *Lancet* 1989; **2**: 201-205

4 **Balthazar EJ**, Robinson DL, Megibow. Acute pancreatitis: value of CT in establishing prognosis. *Radiology* 1990; **174**: 331-336

5 **Simchuk EJ**, Traverso LW, Nukui Y, Kozarek RA. Computed tomography severity index is a predictor of outcomes for severe pancreatitis. *Am J Surg* 2000; **179**: 352-355

6 **Casas JD**, Diaz R, Valderas G, Mariscal A, Cuadras P. Prognostic value of CT in the early assessment of patients with acute pancreatitis. *Am J Roentgenol* 2004; **182**: 569-574

7 **Imrie CW**, Benjamin IS, Ferguson JC, McKay AJ, Mackenzie I, O'Neill J. A single-centre double-blind trial of Trasylol therapy in primary acute pancreatitis. *Br J Surg* 1978; **65**:

337-341
8 **Robert JH**, Frossard JL, Mermillod B. Early prediction of acute pancreatitis: prospective study comparing computed Tomography scans, Ranson, Glasgow, APACHE II scores, and various serum markers. *World J Surg* 2002; **26**: 612-619
9 **Chatzicostas C**, Roussomoustakaki M, Vardas E, Romanos J, Kouroumalis EA. Balthazar computed tomography severity index is superior to Ranson criteria and APACHE II scoring systems in predicting acute pancreatitis outcome. *J Clin Gastroenterol* 2003; **36**: 253-260
10 **Wilson C**, Heath DI, Imrie CW. Prediction of outcome in acute pancreatitis: a comparative study of APACHE II, clinical assessment and multiple factor scoring systems. *Br J Surg* 1990; **77**: 1260-1264
11 **Nicolas MB**, Panis Y, Soyer P, Riche F, Laisne MJ, Boudiaf M, Valleur P. Serial computed tomography is rarely necessary in patients with acute pancreatitis: a prospective study in 102 patients. *J Am Coll Surg* 2001; **193**: 146-152
12 **Fleszler F**, Friedenberg F, Krevsky B, Friedel D, Braitman LE. Abdominal computed tomography prolongs length of stay and is frequently unnecessary in the evaluation of acute pancreatitis. *Am J Med Sci* 2003; **325**: 251-255
13 **Bradley E 3rd**. A clinically based classification system for on acute pancreatitis. Summary of the international symposium on acute pancreatitis. *Arch Surg* 1993; **128**: 586-590

Science Editor Guo SY **Language Editor** Elsevier HK

PO Box 2345, Beijing 100023, China
www.wjgnet.com
wjg@wjgnet.com

ELSEVIER

World J Gastroenterol 2005;11(38):6053-6055
World Journal of Gastroenterology ISSN 1007-9327

• *BRIEF REPORTS* •

Downregulation of alpha-fetoprotein siRNA inhibits proliferation of SMMC-7721 cells

Yun-Shan Wang, Xiao-Li Ma, Tong-Gang Qi, Xiang-Dong Liu, Yue-Sheng Meng, Guang-Ju Guan

Yun-Shan Wang, Xiao-Li Ma, Central Laboratory, Jinan Central Hospital, Clinical Medical College of Shandong University, Jinan 250013, Shandong Province, China
Tong-Gang Qi, Yue-Sheng Meng, Guang-Ju Guan, Laboratory of Clinical Molecular Biology, The Second Hospital of Shandong University, Jinan 250015, Shandong Province, China
Xiang-Dong Liu, Shandong Provincial Hospital, Jinan 250020, Shandong Province, China
Supported by the Natural Science Foundation of Shandong Province, No. Z2003C01
Correspondence to: Professor Yun-Shan Wang, Jinan Central Hospital, 105# Jinan Jiefang Road, Jinan 250013, Shandong Province, China. sdjnwys@163.com
Telephone: +86-531-86557322 Fax: +86-531-86557322
Received: 2005-02-27 Accepted: 2005-04-11

AIM: To study the function of α-fetoprotein (AFP) in SMMC-7721 hepatoma cells.

METHODS: A hairpin siRNA expressing plasmid pSilencer3.0-H1-*afp* was constructed and transfected into SMMC-7721 cells with Lipofectamine 2000. The expression of AFP was monitored by real-time RT-PCR and immunoassays, its effect on SMMC-7721 cell proliferation and cell death was detected by MTT and fluorescence-activated cell sorter (FACS).

RESULTS: The AFP-siRNA expressing plasmid downregulated the expression of AFP obviously (about 34%), and inhibited SMMC-7721 cell proliferation, but did not induce apoptosis.

CONCLUSION: Downregulation of AFP siRNA inhibits proliferation of SMMC-7721 cells, but cannot cause apoptosis.

Key words: siRNAs; AFP; SMMC-7721 cell; Proliferation; Apoptosis

Wang YS, Ma XL, Qi TG, Liu XD, Meng YS, Guan GJ. Downregulation of alpha-fetoprotein siRNA inhibits proliferation of SMMC-7721 cells. *World J Gastroenterol* 2005; 11(38): 6053-6055
http://www.wjgnet.com/1007-9327/11/6053.asp

INTRODUCTION

Primary hepatocellular carcinoma (PHCC) is one of the most common malignancies in the world, with a high fatality rate and a short survival time[1].

α-fetoprotein (AFP) is a major serum protein produced by the liver or yolk sac in mammals and other vertebrates, and is not detectable in normal adults[2]. However, AFP is often elevated to a significant level in association with development of PHCC, and has been defined as an oncofetal antigen[3,4]. The biological role of AFP has been widely investigated. However, the relationship between AFP and PHCC is still unclear. Some recent investigations indicate that human AFP can enhance the proliferation of mouse hepatoma H-22 and human hepatoma SMMC-7721, BEL-7404, or QGY-7703 cells *in vitro*[5]. Similar growth stimulatory effect of AFP at low concentrations has also been found in human hepatoma Hep G_2 cells. These results have an important implication that AFP may function as a hepatoma growth stimulator, thus suppression of AFP gene expression and its biological activities may become a new strategy for the treatment of AFP-associated tumors such as PHCC.

RNA-mediated interference is the inhibition of expression of specific genes by double-stranded RNAs (dsRNAs)[6]. Since short dsRNAs can silence the expression of its homologous gene in mammalian cells, and do not induce nonspecific interferon response, it is widely used in genome and therapy study. Here we have designed a plasmid pSilencer3.0-H1-*afp*, which can express siRNAs in mammalian cells to study the function of AFP and its therapeutic effect on hepatoma cells *in vitro*.

MATERIALS AND METHODS

Plasmid construction

The plasmid pSilencer3.0-H1-*afp* was constructed as previously described[7]. The targeted sequence of AFP gene (GenBank accession no. NM_005030) is 5'-AACTCAGTG-AGGACAAACTAT-3'. Positive and negative technical controls were supplied by Ambion Incorporation, and the positive control plasmid was aimed at GAPDH gene.

Hepatoma cell culture and plasmid transfection

Human hepatoma SMMC-7721 cells were cultured in RPMI-1640 (Invitrogen) supplemented with 10% FCS. Transfection was done with Lipofectamine 2000 (Invitrogen). One day before transfection, SMMC-7721 cells were seeded in the wells of 24-well culture plates, about 7×10^4 cells/well. Before transfection, 1 μg plasmid and 2 μL Lipofectamine 2000 were diluted with 50 μL serum-free Opti-MEM I (Invitrogen) and incubated for 5 min. They were mixed and incubated for 20 min at room temperature,

added to the medium, mixed gently, and then incubated at 37 ℃ for 4 h. The medium was replaced with a new medium and incubated for 12, 24, and 48 h.

Quantitative real-time PCR

For validation of the silencing effect by quantitative PCR, cDNA was prepared from the SMMC-7721 cell line. RT-PCR was carried out using RT and SYBR Green PCR Master Mix (ABI) according to the manufacturer's instructions. RT reaction was performed at 48 ℃ for 30 min. The cDNA was analyzed by real-time quantitative PCR immediately and stored at -20 ℃ until use. Each PCR was carried out in triplicate in a 25 μL volume for 15 min at 95 ℃ for initial denaturing, followed by 40 cycles at 95 ℃ for 30 s and at 60 ℃ for 1 min in the ABI 7000 sequence detection system. Each primer set was first tested to determine optimal concentrations, and products were run out on a 3% agarose gel to confirm the appropriate size. Subsequently, the ABI dissociation curves software was used following a brief thermal protocol (95 ℃ for 15 s and 60 ℃ for 20 s, followed by a slow ramp to 95 ℃) to control their multiple species in each PCR amplification. cDNA from hepatoma cells was used to construct a standard curve for each gene. Values for each gene were normalized to expression levels of actin-β, and then a ratio comparing the expression in negative and positive control, and pSilencer3.0-H1-*afp*-transfected hepatoma cells was calculated. The sequences of the primers used for RT-PCR were as follows: actin-β forward: 5'-CGT ACC ACT GGC ATC GTG AT-3'; reverse: 5'-GTG TTG GCG TAC AGG TCT TTG-3'; GAPDH forward: 5'-CTT CAC CAC CAT GGA GAA GGC-3'; reverse primer: 5'-GGC ATG GAC TGT GGT CAT GAG-3'; AFP forward: 5'-AAA TAC ATC CAG GAG AGC CA-3'; reverse: 5'-CTG AGC TTG GCA CAG ATC CT-3'.

Immunoassay of AFP concentration in supernatant

AFP concentration in the supernatant in each well was determined by chemiluminescence immunoassay according to the manufacturer's instructions.

MTT assays

Eight hours after plasmid transfection, the cells were harvested and replated in 96-well microtiter plates in triplicate at 1×10^4 cells in 0.1 mL medium/well. Twenty microliters of MTT dye (5 mg/mL) was added and incubated for 0, 24, 48, and 72 h respectively. Following 4 h of incubation at 37 ℃, formazan crystals were dissolved in dimethyl sulfoxide (0.1 mL/well). The plates were mechanically agitated for 5 min and the optical density at 540 nm was determined on the microtiter plate reader. Each experiment was done thrice.

Fluorescence-activated cell sorter (FACS) analysis

Forty-eight hours after transfection, cells were harvested by trypsin digestion, washed twice with cold PBS, and resuspended in 1× binding buffer, regulated to the concentration 1×10^6/mL. Then 100 μL was extracted to a new tube, 5 μL PI and 5 μL annexin V-FITC were added, mixed gently, incubated at 25 ℃ for 15 min. Four hundred microliters of binding buffer was added and analyzed within 1 h with FACS.

RESULTS

SiRNAs expressing vector pSilencer3.0-H1-afp could silence the expression of AFP in hepatoma cells efficiently

To specifically deplete AFP in hepatoma cells, we took advantage of the recently developed vector-based siRNA technology. The targeting sequence of human AFP (GenBank accession no. NM_005030) is 5'-AACTCAGTG-AGGACAAACTAT-3'. The vector pSilencer3.0-H1-*afp*, pSilencer3.0-H1-*gapdh* (positive control) and negative control vector were transfected into SMMC-7721 cells, which were cultured for 48 h, then RT-PCR and AFP in supernatant fluid were assayed. Positive control vector pSilencer3.0-H1-*gapdh* could silence the GAPDH efficiently. The inhibition rate of the positive control plasmid and pSilencer3.0-H1-*afp* was 60% and 34% respectively. In order to confirm the inhibitory effect, we assayed the AFP concentration in the supernatant. The AFP level in the supernatant reduced about 40%, 48 h after transfection. These results showed that the expression of AFP in hepatoma cells was downregulated.

MTT assays and FACS

Figure 1A shows that vector pSilencer3.0-H1-*afp* inhibited the proliferation of SMMC-7721 cells obviously compared to the negative control plasmid, and that the suppression effect was most obvious at 32 h. The results of FACS showed no difference between the negative control and pSilencer3.0-H1-*afp*-treated cells (Figure 1B).

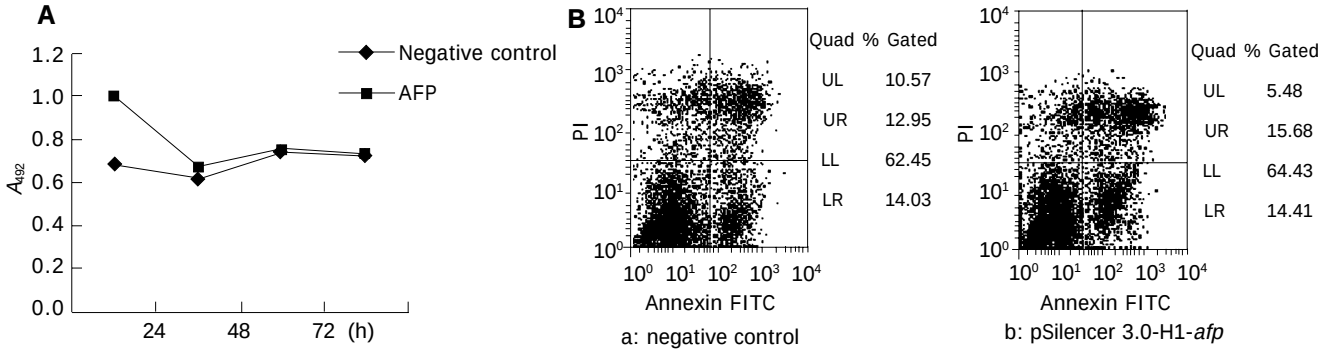

Figure 1 Proliferation (A) and apoptosis (B) of transfected cells. LR indicates the value of cell apoptosis.

DISCUSSION

Since AFP was found in the mid-1950s, this oncofetal protein has been used as a PHCC marker in clinical diagnosis[10]. But its biological activities in mammals still remain unclear. To date, only two functional roles of AFP have been ascertained[10]. In the last decade, the growth regulatory properties of AFP have aroused interests as a result of studies involving ontogenetic and oncogenic growth in both cell cultures and animal models. Particularly, the effect of AFP on the development of experimental tumors in mammals has been investigated *in vivo* with the use of carcinogens[11]. When AFP-treated mice develop larger tumors, they require a longer period for regression and have a significantly higher mortality[10]. Chicken AFP-treated quails develop tumors with shorter latent periods than the untreated quails[8]. The *in vivo* tumor growth stimulation by AFP can be explained by its immunosuppression. Cell-mediated immunity is an important mechanism of host resistance to malignant neoplasms. Recently, anonymous studies found that antihepatoma effects of AFP antisense S-ODNs are more significant in normal mice than in nude mice[10], suggesting that there exists a relationship between AFP and the susceptibility of hepatoma cells to immunity-mediated cytotoxicity. Recent studies indicate that AFP directly stimulates the proliferation of hepatoma cells *in vitro*, independent of its immunosuppression[11].

However, the precise relationship between AFP and PHCC is not clear. AFP is highly expressed in hepatic oval cells during the early stages of carcinogenesis, and high levels of AFP in the fully developed PHCC, or in the serum of the host, are associated with more aggressive behaviors, and increased anaplasia[9]. The present study also demonstrated that silencing the expression of AFP could effectively inhibit the growth of hepatoma cells *in vitro*, suggesting that AFP may play a role in the pathogenesis of PHCC.

The present results indicate that AFP siRNAs expressing plasmid exhibit significant antihepatoma activities *in vitro* by the sequence-specific silencing of AFP gene expression. But the results of FACS have no obvious difference between the negative control and the pSilencer3.0-H1-*afp* treated wells. Therefore, the mechanisms of antihepatoma action of AFP siRNAs expressing plasmid are not through the induction of hepatoma cell apoptosis.

ACKNOWLEDGMENTS

The authors express appreciation to Professor Bing-Yu Mao, Kunming Institute of Zoology, Chinese Academy of Sciences and Senior Lecturer Bin Yu, Sydney University, Australia for their critical revision of the manuscript.

REFERENCES

1 **Colleoni M,** Gaion F, Liessi G, Mastropasqua G, Nelli P, Manente P. Medical treatment of hepatocellular carcinoma: any progress? *Tumori* 1994; **80**: 315-326
2 **Wang W,** Alpert E. Downregulation of phorbol 12-myristate 13-acetate-induced tumor necrosis factor-alpha and interleukin-1beta production and gene expression in human monocytic cells by human alpha-fetoprotein. *Hepatology* 1995; **22**: 921-928
3 **Ogata A,** Yamashita T, Koyama Y, Sakai M, Nishi S. Suppression of experimental antigen-induced arthritis in transgenic mice producing human alpha-fetoprotein. *Biochem Biophys Res Commun* 1995; **213**: 362-366
4 **Jacobson HI,** Bennett JA, Mizejewski GJ. Inhibition of estrogen-dependent breast cancer growth by a reaction product of alpha-fetoprotein and estradiol. *Cancer Res* 1990; **50**: 415-420
5 **Wang XW,** Xie H. Effect of alpha-fetoprotein on the growth of human hepatoma cells *in vitro*. *Shiyan Shengwu Xuebao* 1999; **32**: 15-22
6 **Fire A,** Xu S, Montgomery MK, Kostas SA, Driver SE, Mello CC. Potent and specific genetic interference by double-stranded RNA in Caenorha-bditis elegans. *Nature* 1998; **391**: 806–810
7 **Qi TG,** Wang YS. Construction and identification of a plasmid expressing SiRNAs in mammalian cells aimed at AFP gene. *Shandong Daxue Xuebao* 2004; **42**: 107-109
8 **Yamada A,** Hayami M. Suppression of natural killer cell activity by chicken alpha-fetoprotein in Japanese quails. *J Natl Cancer Inst* 1983; **70**: 735-738
9 **Matsumoto Y,** Suzuki T, Asada I, Ozawa K, Tobe T, Honjo I. Clinical classification of hepatoma in Japan according to serial changes in serum alpha-fetoprotein levels. *Cancer* 1982; **49**: 354-360
10 Wang XW, Yuan JH, Zhang RG, Guo LX, Xie Y, Xie H. Antihepatoma effect of alpha-fetoprotein antisense phosphorothioate oligodeoxyribonucleotides *in vitro* and in mice. *World J Gastroenterol* 2001; **7**: 345-351
11 **Li MS,** Li PF, Chen Q, Du GG, Li G. Alpha-fetoprotein stimulated the expression of some oncogenes in human hepatocellular carcinoma Bel 7402 cells. *World J Gastroenterol* 2004; **15**: 819-824

Science Editor Wang XL and Guo SY **Language Editor** Elsevier HK

PO Box 2345, Beijing 100023, China
www.wjgnet.com
wjg@wjgnet.com

ELSEVIER

World J Gastroenterol 2005;11(38):6056-6060
World Journal of Gastroenterology ISSN 1007-9327

• *BRIEF REPORTS* •

Interaction models of *CYP1A1*, *GSTM1* polymorphisms and tobacco smoking in intestinal gastric cancer

Jing Shen, Run-Tian Wang, Yao-Chu Xu, Li-Wei Wang, Xin-Ru Wang

Jing Shen, Yao-Chu Xu, Xin-Ru Wang, Department of Epidemiology and Biostatistics, School of Public Health, Nanjing Medical University, Nanjing 210029, Jiangsu Province, China
Jing Shen, Department of Environmental Health Sciences, Mailman School of Public Health, Columbia University, New York, NY 10032, USA
Run-Tian Wang, Department of Epidemiology and Biostatistics, School of Public Health, Peking University, Beijing 100083, China
Li-Wei Wang, Yang Zhong Cancer Research Institute, Yang Zhong City Municipal Hospital, Yang Zhong 212200, China
Supported by the National Natural Science Foundation of China, No. 30170827 and 30070671
Correspondence to: Dr. Jing Shen, Department of Environmental Health Sciences, Mailman School of Public Health, Columbia University, 701 West 168th Street (Room 505), New York, NY 10032, USA. js2182@columbia.edu
Telephone: +1-212-3058158 Fax: +1-212-3055328
Received: 2005-01-07 Accepted: 2005-04-02

AIM: To explore the interaction models of the cytochrome P-450 (CYP) *1A1 Val* variant and glutathione S-transferase (GST) *M1* null polymorphisms with tobacco smoking in the occurrence of intestinal gastric cancer.

METHODS: A community-based case-control study was conducted in Yangzhong. Subjects included 114 intestinal types of gastric cancer with endoscopic and pathological diagnosis during January 1997 and December 1998, and 693 controls selected from their spouse, siblings or siblings-in-law who had no history of digestive system cancer. Logistic regression was used to estimate the interaction models.

RESULTS: The frequency of the *CYP1A1 Val* variant allele in cases did not differ from that in controls. The OR of *GSTM1* null genotype was 2.0 (95% confidence interval [95%CI]: 1.2-3.1, $P<0.01$). It showed a significant type 2 form of interaction model when both *CYP1A1 Val* variant allele and former tobacco smoking existed (i.e., among the multiplicative effects, the disease risk is increased by the tobacco exposure alone but not by the *CYP1A1* variant alone). The interaction index γ was 2.8, and OR_{eg} (95%CI) was 5.0 (1.9-13.4). *GSTM1* null genotype and former tobacco smoking were significant in a type 4 interaction model (i.e., the disease risk is increased by *GSTM1* null genotype or tobacco exposure alone among the multiplicative effects). The interaction index γ and OR_{eg} (95%CI) were 3.4 and 8.4 (3.4-20.9), respectively.

CONCLUSION: Different interaction models of *CYP1A1 Val* variant allele and *GSTM1* null genotype with tobacco smoking will contribute to understanding carcinogenic mechanism, but there is a need to further investigate in larger scale studies.

Key words: Interaction models; *CYP1A1*; *GSTM1*; Tobacco smoking; Intestinal gastric cancer

Shen J, Wang RT, Xu YC, Wang LW, Wang XR. Interaction models of *CYP1A1*, *GSTM1* polymorphisms and tobacco smoking in intestinal gastric cancer. *World J Gastroenterol* 2005; 11(38): 6056-6060
http://www.wjgnet.com/1007-9327/11/6056.asp

INTRODUCTION

Worldwide, gastric cancer is the second in rank overall (798 000 new cases per year), and ranks second in males, fourth in females. It remains the most common malignancy in many countries of the world[1,2], though the frequency of incidence and mortality is declining in almost all populations. Thirty-eight percent of gastric cancer cases occurred in China, where it remains to be most common and is the leading cause of cancer death in both sexes[1]. Yangzhong is among the areas with the highest gastric cancer mortality and incidence rate in south-east of China[3]. The crude mortality rate of gastric cancer changed from 96.9 to 110.9/100 000 during 1991 and 1997, and the average adjusted incidence rate in the same period was over 115/100 000 (unadjusted rate is 155.5/100 000). Previous studies have shown that high incidence rate of gastric cancer is associated with exposure to environmental factors (tobacco, alcohol consumption, and *H pylori* infection), and individual susceptibility[2,4].

Genetic polymorphisms in cytochrome P-450 (CYP) *1A1* and glutathione S-transferase (GST) *M1* genes that metabolize known and potentially carcinogenic environmental exposures may affect enzymatic activities and alter an individual's ability to metabolize pro-carcinogenic and related compounds, which may change the biologic effect of exposures[5]. A large number of studies have examined the role of polymorphisms in *CYP1A1*, *GSTM1*, and cancer risk, including gastric cancer[6-10], but the results are equivocal[11–14]. The interaction between *GSTM1* null genotype and tobacco smoking for the risk of gastric cancer has only been explored in three studies, with inconsistent evidence of departure from a

multiplicative model, possibly because of the small size (70, 91, and 136 gastric cancer cases, respectively), and the gene-environmental interaction (GEI) models best describing the risk of gastric cancer is not clear[6,11,14]. For this reason, we conducted a community-based case-control study in a Chinese population. Genetic polymorphisms in *CYP1A1* and *GSTM1* were analyzed to test the hypothesis that these genotypes have different interaction models with tobacco smoking in the development of intestinal gastric cancer.

[illegible]

Subjects

All gastric cancer patients and controls in this study are Han ethnic Chinese selected from Yangzhong County. Gastric cancer was prevalent in cases diagnosed according to International Classification of Diseases for Oncology IX, code = 151, and classified by the criteria of Laurén[15]. One hundred and fourteen intestinal gastric cancer patients (76 men and 38 women; mean age and SD 59.4±9.9 years) were identified by endoscopic and pathological diagnosis in Yangzhong City Municipal Hospital from January 1997 to December 1998. To reduce misclassification of the histological types, two pathologists reviewed and confirmed all diagnosed cases. Controls were selected from case's siblings (150 male and 140 female) and non-blood relatives (403 spouses and the siblings-in-law, 160 male and 243 female) without digestive tract cancers. Both kinds of controls differed slightly in demographic features, and their results were combined to increase the sample size and decrease type I error. The study was approved by the regional ethics committees of Yangzhong. All participants were given an explanation of the study and informed consent was obtained. Study subjects completed a questionnaire administered by specially trained interviewers through a face-to-face interview. The questionnaire was designed to elicit detailed information on tobacco smoking habit, alcohol drinking habit, family history of cancer, and occupational exposures. Cigarette smokers were defined as subjects who reported smoking of at least one cigarette per day for 1 year or more, or whose accumulated tobacco cigarette consumption was over 18 packs per year. Former smokers were those who had stopped smoking for one or more years before the interview. Cumulative smoking exposure (pack years) was defined as one pack per day for 1 year equals 1 pack years.

CYP1A1 and GSTM1 genotypes

DNA extraction was performed using Puregene DNA isolation kits (Gentra Systems, Minneapolis, MN, USA). PCR-RFLP approach was used to detect the 7th *CYP1A1 Ile/Val* variant at position 4 889. PCR was used to amplify the transcription regulatory region of *CYP1A1* that includes the restriction enzyme recognition site for *Hin*cII. The two allele-specific primers are respectively F5'-TCCT ACCTG-AACGGTTTCTCACCC-3' (T_m = 63.0) and R5'-TTTTTT-TTTTTGAAAGACCTCCCAGG GGTCA-3' (T_m = 65.1) modified from those previously reported[16]. The homozygous null polymorphism of *GSTM1* was determined using a PCR approach as previously reported[16].

Statistical analysis

The relative associations between cases and controls were assessed by crude odds ratio (OR), interaction OR_{eg} and the corresponding 95%CI. Unconditional logistic regression analysis was performed to assess the association between the *CYP1A1 Ile/Val* and *GSTM1* null polymorphism and intestinal gastric cancer after adjusting for confounding factors. All models included as co-variables: gender, age (entered as a continuous variable), living areas (relative lower or higher incidence areas in Yangzhong), education level (years), former tobacco smoking, former alcohol drinking, BMI (weight [kg]/height [m^2]) and family history of cancer. Test of trend was calculated through logistic models based on semi-continuous and dummy variables. A common way to describe the interaction between the effect of an environmental agent and a genetic risk factor is to use a term called interaction index (γ), which is determined by coefficient (β) in a multiple logistic regression model. The coefficient of this interactive term was calculated according to the method of Taioli *et al*.[17]. If the types of interaction belong to multiplicative effects suggested by Khoury and Ottman[18-20], it included several types of interactions. Such as type 1 interaction which means that the disease risk is increased only in the presence of the genotype and the environmental exposure. Type 2 interaction: the disease risk is increased by the environmental exposure alone but not by the genotype alone. Type 3 interaction: the disease risk is increased by the genotype in the absence of the environmental exposure but not by the environment alone. Type 4 interaction means that the disease risk is increased by genotype or environmental exposure alone[18-20]. False positive report probability (FPRP) was used as an index for judging the noteworthy or not noteworthy results at the 0.5 FPRP level among significant GEI results[21]. All data analysis was performed with the SAS package Genmod (SAS Institute, Cary, NC, USA) for the personal computer.

[illegible]

CYP1A1, GSTM1 polymorphisms and risk of intestinal gastric cancer

Compared with controls, patients were significantly older (median age 59 years for cases and 53 years for controls) and with a BMI less than 20. Former tobacco smoking is significantly associated with the risk of intestinal gastric cancer (OR = 2.4, 95%CI: 1.0-5.8). A significant dose-response was observed in relation to increasing gastric cancer risk, especially in 20 pack-years or more smokers (Table 1). The frequencies of *CYP1A1 Ile/Val* and *Val/Val* genotypes in controls were 33.4% and 5.6%, respectively, which showed no significant difference from that in cases (32.1% and 5.4%, respectively). The homozygote null *GSTM1* genotype was observed in 63.4% of cases, which was significantly higher than that in controls (53.5%). The adjusted OR was 2.0 (95%CI: 1.2-3.1).

Interaction models of CYP1A1 and GSTM1 polymorphisms with former tobacco smoking

Among former tobacco smokers with *CYP1A1 Ile* or *GSTM1* present genotypes, the OR_{eg} of intestinal gastric

Table 1 Characteristics of the interviewed subjects

	Characteristics	Gastric cancer cases (114)	Control subjects (693)	OR (95%CI)
Median age	yr±SD	59±10	53±10	1.1 (1.0-1.1) [1]
	Min (yr)	35	30	
	Max (yr)	82	78	
Gender	Female (%)	38 (33)	383 (55)	1.0 (Ref.)
	Male (%)	76 (67)	310 (45)	1.2 (0.7-2.1)
	F/M ratio	1:2	1:0.8	
Educational level	>5 yr	44 (38.6)	246 (35.5)	1.0 (Ref.)
	≤5 yr	70 (61.4)	447 (64.5)	1.0 (0.6-1.7)
Occupation				
	Manual	51 (44.7)	375 (54.1)	1.0 (Ref.)
	Office	9 (7.9)	87 (12.6)	0.6 (0.2-1.3)
	Retired	54 (47.4)	231 (33.3)	1.2 (0.7-1.9)
Marriage status				
	Married	100 (87.7)	649 (94.7)	1.0 (Ref.)
	Divorce or bereft spouse	14 (12.3)	36 (5.3)	1.4 (0.6-3.0)
Family history of cancer				
	No	84 (76.4)	613 (90.3)	1.0 (Ref.)
	Yes	26 (23.6)	66 (9.7)	3.9 (2.1-7.3) [1]
BMI (kg/m^2)				
	<20	56 (49.1)	95 (13.7)	1.0 (Ref.)
	20-	44 (38.6)	254 (36.7)	0.3 (0.2-0.5)[1]
	23-	14 (12.3)	344 (49.6)	0.1 (0.03-0.12)[1]
Tobacco smoking habits				
	Never	51 (44.7)	437 (63.0)	1.0 (Ref.)
	Current	36 (31.6)	225 (32.5)	0.6 (0.3-1.3)
	Former	27 (23.7)	31 (4.5)	2.4 (1.0-5.8)[1]
Amount of former smoking (pack years)				
	No	87 (76.4)	662 (95.6)	1.0 (Ref.)
	1-19	7 (6.1)	10 (1.4)	2.6 (0.8-8.6)
	20-29	8 (7.0)	11 (1.6)	3.1 (1.1-9.0)[1]
	≥30	12 (10.5)	10 (1.4)	4.4 (1.7-11.9)[1]
Alcohol drinking habits				
	Never	78 (68.5)	505 (72.9)	1.0 (Ref.)
	Current	11 (9.6)	156 (22.5)	0.2 (0.1-0.5)[1]
	Former	25 (21.9)	32 (4.6)	2.3 (1.2-4.7)[1]
Plasma *H pylori* CagA antibody				
	Negative	136 (82.4)	107 (49.3)	1.0 (Ref.)
	Positive	29 (17.6)	110 (50.7)	0.2 (0.1-0.3)[1]
CYP1A1 genotype				
	Ile/Ile	70 (62.5)	412 (61.0)	1.0 (Ref.)
	Ile/Val	36 (32.1)	226 (33.4)	0.9 (0.5-1.4)
	Val/Val	6 (5.4)	38 (5.6)	0.7 (0.2-1.8)
GSTM1 genotype				
	Present	41 (36.6)	314 (46.5)	1.0 (Ref.)
	Null	71 (63.4)	361 (53.5)	2.0 (1.2-3.1) [1]

[1]Showed significant difference after adjusting co-variables.

cancer were 1.8 and 3.5, respectively. With both exposure to tobacco smoking and the *CYP1A1 Val* allele or *GSTM1* null genotype, the OR_{eg} of suffering intestinal gastric cancer increased sharply, 5.0 (95%CI: 1.9-13.4) and 8.4 (95%CI: 3.4-20.9), respectively. The γ were 2.8 and 3.4, respectively, which showed multiplicative effects of type 2 GEI model for *CYP1A1* and type 4 model for *GSTM1* (Table 2).

Assessment of the probability of a potential positive result

A high FPRP (e.g., >0.5) could be a consequence of any combination of a low prior probability, low statistical power, or a relatively high *P* value[21]. We calculated FPRP to assess the probability that a positive result might be false using the observed *P* value or CI for the observed ORs, and to determine whether to consider a significant finding to be noteworthy with the specific prior probability (Table 3). The results showed that the FPRP was less than 0.5 for *GSTM1* null and former smokers, which indicated the most noteworthy finding in the present study even with a prior probability between 0.0001 and 0.00001.

□□□□□□□□□□

A large number of molecular epidemiological studies completed in the past decade have identified the relative etiologic roles of the *CYP1A1 Val* variant allele and *GSTM1* null genotype for cancer risk (including gastric cancer), although some results indicate no overall associations, only specific relationships were found in subgroups, such as in smokers, *H pylori*-infected patients or low consumption of

Table 2 Interaction models of *CYP1A1* and *GSTM1* polymorphism with former smoker in intestinal gastric cancer

Genotype	Former smoker	Cases	Controls	OR_{eg}	95%CI
Ile[1]	No	57	391	1.0	Ref.
Val[2]	No	29	254	0.7	0.4-1.1
Ile	Yes	13	21	1.8	0.7-4.3
Val	Yes	13	10	5.0[5]	1.9-13.4
Present[3]	No	31	302	1.0	Ref.
Null[4]	No	54	345	1.9	1.1-3.1
Present	Yes	10	12	3.5	1.2-10.1
Null	Yes	17	16	8.4[6]	3.4-20.9

[1][*Ile*]: *CYP1A1* homozygous (*Ile*/*Ile*) genotype; [2][*Val*]: *CYP1A1* heterozygous (*Ile*/*Val*)+homozygous (*Val*/*Val*) genotypes; [3][present]: present genotype for *GSTM1*; [4][null]: null genotype for *GSTM1*; [5]adjusted by age, gender, living areas, family history of cancer, and former alcohol drinking; $\chi^2_{trend} = 24.0$, df = 1, $P = 0.00$; $\gamma = 1.61/0.57 = 2.8$; [6]adjusted by age, gender, living areas, family history of cancer, and former alcohol drinking; $\chi^2_{trend} = 45.7$, df = 1, $P = 0.00$; $\gamma = 2.13/0.63 = 3.4$.

Table 3 FPRP values for interactions between GSTM1 and former tobacco smoking in intestinal gastric cancer

GSTM1	Former	Observed	Assuming	Prior probability					
genotype	Smoking	OR	OR	0.25	0.1	0.01	0.001	0.0001	0.00001
GSTM1 null	No	1.9	1.2	0.481[1]	0.736[2]	0.968	0.997	1.000	1.000
			1.5	0.151	0.348	0.854	0.983	0.998	1.000
			2.0	0.050	0.136	0.634	0.946	0.994	0.999
GSTM1 present	Yes	3.5	2.4	0.202	0.432	0.893	0.988	0.999	1.000
			3.0	0.137	0.322	0.840	0.981	0.998	1.000
			4.0	0.093	0.236	0.773	0.972	0.997	1.000
GSTM1 null	Yes	8.4	4.8	0.000	0.000	0.004	0.040	0.293	0.805
			6.0	0.000	0.000	0.002	0.020	0.168	0.669
			8.4	0.000	0.000	0.001	0.009	0.087	0.487

[1]Bold with gray fill color indicate "noteworthy at the 0.5 FPRP level"; [2]with no fill color indicate "not noteworthy at the 0.5 FPRP level".

fruit[6-10]. Other studies have reported contrary findings[11-14]. These inconsistent results might be contributed to ethnically diverse populations involved in studies, different histological subtypes of cases used, and different co-variables categorized the sub-population. Until now, only a few studies discussed interactions between tobacco smoking and the polymorphisms in the occurrence of gastric cancer[6,11,14]. In the present study, we observed some evidence of a relationship between *GSTM1* null genotype and a risk of gastric cancer. Both the *CYP1A1 Val* variant allele and *GSTM1* null polymorphism have statistically significant interactions with former tobacco smoking. The GEI model of *CYP1A1* with smoking belongs to type 2, and *GSTM1* with smoking belongs to type 4 as Khoury and Ottman described. Present study as most molecular epidemiology studies based on multiple comparison corrective procedures is relied on the standard *P* value criterion of 0.05 to define statistical significance without consideration of power or prior probability, which may create a lot of false positives[21]. We further calculated FPRP as one of indices to decide about whether a positive finding in association study can be called "a noteworthy finding" or "deserve of more attention". We confirmed that the interaction between *GSTM1* null and former smokers was the most noteworthy positive finding in the present study even with a prior probability less than 0.0001. The interaction between *CYP1A1 Val* variant allele and former smokers was also a possible noteworthy positive finding with a prior probability less than 0.01 (data not shown). These results suggest that the risk of intestinal gastric cancer was greatly dependent upon both tobacco smoking exposures and susceptibility genes. Only complete smoking cessation may decrease susceptibility to gastric cancer in persons carrying the *CYP1A1 Val* variant allele or *GSTM1* null genotype. The different types of GEI models indicated that the interactions between genes and environmental factors are neither simply gene specific, nor exposure specific, and must be related to the mechanism of action of the gene product and features of exposure leading to gastric cancer.

Although the mechanism for tobacco-related gastric cancer risk is not well understood, tobacco-specific nitrosamines and other nitroso-compounds, plus other carcinogens contained in tobacco and tobacco smoke, are swallowed and may thus be involved in the process of gastric carcinogenesis[22,23]. Among gastric cancer cases, smoking-related DNA-adduct levels were higher in smokers than in non-smokers[24], and a study in China found smoking to be a risk factor for intestinal metaplasia and gastric dysplasia arising from chronic atrophic gastritis[25]. The biological mechanisms responsible for different interaction models observed in our study were not known, but it was possible to speculate that these interaction effects might be a reflection for individuals with and without environmental susceptible genotypes. This analytical approach may be used to determine higher risk individuals and take further preventive measures to decrease cancer risks in these susceptible individuals.

One limit of the study is the small number of subjects in some cells when GEI models were analyzed. The models resulting from the present study might be affected by chance, and need to be identified by more large-scale molecular epidemiological studies. Another potential limit was the

selection of controls, which include case's siblings. This kind of selection might create over-matching because siblings were more likely to have the same genotypes as cases than non-related controls, therefore leading to some loss of statistical efficiency, i.e. larger sample sizes required to attain the same statistical precision[26]. But others consider that the use of sibling controls generally improves efficiency for GEI evaluations[27,28].

In conclusion, our studies identified two kinds of GEI models between the *CYP1A1 Val* variant allele, *GSTM1* null genotype and tobacco smoking. Although the proposed carcinogen metabolism pathway seems a plausible explanation of our findings, further large studies are required to replicate these observations.

ACKNOWLEDGMENTS

We thank Zhaoxi Wang for his excellent technical assistance; thank Professor Regina M Santella for editing the manuscript. We also thank all the doctors for their kind help in collecting the biological samples and epidemiological data. We thank all participants in our study for their cooperation.

REFERENCES

1 **Parkin DM**. The global burden of cancer. *Seminars Cancer Biol* 1998; **8**: 219-235
2 **Stadtlander CT**, Waterbor JW. Molecular epidemiology, pathology and prevention of gastric cancer. *Carcinogenesis* 1999; **20**: 2195-2207
3 **Setiawan VW**, Zhang ZF, Yu GP, Lu QY, Li YL, Lu ML, Wang MR, Guo CH, Yu SZ, Kurtz RC, Hsieh CC. GSTP1 polymorphisms and gastric cancer in a high-risk Chinese population. *Cancer Causes Control* 2001; **12**: 673-681
4 **Zhang ZF**, Kurtz RC, Klimstra DS, Yu GP, Sun M, Harlap S, Marshall JR. *Helicobacter pylori* infection on the risk of stomach cancer and chronic atrophic gastritis. *Cancer Detect Prev* 1999; **23**: 357-367
5 **Nebert DW**, Ingelman-Sundberg M, Daly AK. Genetic epidemiology of environmental toxicity and cancer susceptibility: human allelic polymorphisms in drug-metabolizing enzyme genes, their functional importance, and nomenclature issues. *Drug Metab Rev* 1999; **31**: 467-487
6 **Tamer L**, Ates NA, Ates C, Ercan B, Elipek T, Yildirim H, Camdeviren H, Atik U, Aydin S. Glutathione S-transferase M1, T1 and P1 genetic polymorphisms, cigarette smoking and gastric cancer risk. *Cell Biochem Funct* 2005; 23: 267-272
7 **Gonzalez CA**, Sala N, Capella G. Genetic susceptibility and gastric cancer risk. *Int J Cancer* 2002; **100**: 249-260
8 **Parl FF**. Glutathione S-transferase genotypes and cancer risk. *Cancer Lett* 2005; **221**: 123-129
9 **Agundez JA**. Cytochrome P450 gene polymorphism and cancer. *Curr Drug Metab* 2004; **5**: 211-224
10 **Ng EK**, Sung JJ, Ling TK, Ip SM, Lau JY, Chan AC, Liew CT, Chung SC. *Helicobacter pylori* and the null genotype of glutathione-S-transferase-mu in patients with gastric adenocarcinoma. *Cancer* 1998; **82**: 268-273
11 **Deakin M**, Elder J, Hendrickse C. Glutathione S-transferase GSTT1 genotypes and susceptibility to cancer: studies of interactions with GSTM1 in lung, oral, gastric and colorectal cancers. *Carcinogenesis* 1996; **17**: 881-884
12 **Suzuki S**, Muroishi Y, Nakanishi I, Oda Y. Relationship between genetic polymorphisms of drug-metabolizing enzymes (CYP1A1, CYP2E1, GSTM1, and NAT2), drinking habits, histological subtypes, and p53 gene point mutations in Japanese patients with gastric cancer. *J Gastroenterol* 2004; **39**: 220-230
13 **Wu MS**, Chen CJ, Lin MT, Wang HP, Shun CT, Sheu JC, Lin JT. Genetic polymorphisms of cytochrome p450 2E1, glutathione S-transferase M1 and T1, and susceptibility to gastric carcinoma in Taiwan. *Int J Colorectal Dis* 2002; **17**: 338-343
14 **Setiawan VW**, Zhang ZF, Yu GP, Li YL, Lu ML, Tsai CJ, Cordova D, Wang MR, Guo CH, Yu SZ, Kurtz RC. GSTT1 and GSTM1 null genotypes and the risk of gastric cancer: a case-control study in a Chinese population. *Cancer Epidemiol Biomarkers Prev* 2000; **9**: 73-80
15 **Lauren P**. The two histological main types of gastric carcinoma: diffuse and so-called intestinal-type carcinoma. An attempt at a histoclinical classification. *Acta Pathol Microbiol Scand* 1965; **64**: 31-49
16 **Morita S**, Yano M, Shiozaki H, Tsujinaka T, Ebisui C, Morimoto T, Kishibuti M, Fujita J, Ogawa A, Taniguchi M, Inoue M, Tamura S, Yamazaki S, Kikkawa N, Mizunoya S, Monden M. CYP1A1, CYP2E1 and GSTM1 polymorphisms are not associated with susceptibility to squamous-cell carcinoma of the esophagus. *Int J Cancer* 1997; **71**: 192-195
17 **Taioli E**, Zocchetti C, Garte S. Models of interaction between metabolic genes and environmental exposure in cancer susceptibility. *Environ Health Perspect* 1998; **106**: 67-70
18 **Khoury MJ**, James LM. Population and familial relative risks of disease associated with environmental factors in the presence of gene-environment interaction. *Am J Epidemiol* 1993; **137**: 1241-1250
19 **Khoury MJ**, Wagener DK. Epidemiological evalution of the use of genetics to improve the predictive value of disease risk factors. *Am J Hum Genet* 1995; **56**: 835-844
20 **Ottman R**. An epidemiologic approach to gene-environment interaction. *Genet Epidemiol* 1990; **7**: 177-185
21 **Wacholder S**, Chanock S, Garcia-Closas M, El Ghormli L, Rothman N. Assessing the probability that a positive report is false: an approach for molecular epidemiology studies. *J Natl Cancer Inst* 2004; **96**: 434-442
22 **Hecht SS**, Hoffmann D. The relevance of tobacco-specific nitrosamines to human cancer. *Cancer Surv* 1989; **8**: 273-294
23 **Hecht SS**. Tobacco smoke carcinogens and lung cancer. *J Natl Cancer Inst* 1999; **91**: 1194-1210
24 **Dyke GW**, Craven JL, Hall R, Garner RC. Smoking-related DNA adducts in human gastric cancers. *Int J Cancer* 1992; **52**: 847-850
25 **Kneller RW**, You WC, Chang YS, Liu WD, Zhang L, Xu GW, Fraumeni JF, Blot WJ. Cigarette smoking and other risk factors for progression of precancerous stomach lesion. *J Natl Cancer Inst* 1992; **84**: 1261-1266
26 **Thomas DC**, Witte JS. Point: population stratification: a problem for case-control studies of candidate-gene associations? *Cancer Epidemiol Biomarkers Prev* 2002; **11**: 505-512
27 **Gauderman W**, Witte J, Thomas D. Family-based association studies. *Monogr Natl Cancer Inst* 1999; **26**: 31-37
28 **Witte JS**, Gauderman WJ, Thomas DC. Asymptotic bias and efficiency in case-control studies of candidate genes and gene-environment interactions: basic family designs. *Am J Epidemiol* 1999; **148**: 693-705

Science Editor Guo SY **Language Editor** Elsevier HK

PO Box 2345, Beijing 100023, China
www.wjgnet.com
wjg@wjgnet.com

ELSEVIER

World J Gastroenterol 2005;11(38):6061-6065
World Journal of Gastroenterology ISSN 1007-9327

• *BRIEF REPORTS* •

Effect of peroxisome proliferator-activated receptor-gamma ligand on inflammation of human gallbladder epithelial cells

Guang-Dong Pan, Hong Wu, Jiang-Wen Liu, Nan-Sheng Cheng, Xian-Ze Xiong, Sheng-Fu Li, Guo-Fu Zhang, Lu-Nan Yan

Guang-Dong Pan, Hong Wu, Jiang-Wen Liu, Nan-Sheng Cheng, Xian-Ze Xiong, Lu-Nan Yan, Department of General Surgery, West China Hospital, Sichuan University, Chengdu 610041, Sichuan Province, China
Sheng-Fu Li, Laboratory of Transplant and Immunology, West China Hospital, Sichuan University, Chengdu 610041, Sichuan Province, China
Guo-Fu Zhang, Laboratory of Isotope, West China Hospital, Sichuan University, Chengdu 610041, Sichuan Province, China
Supported by the Grants From the Scientific Research Foundation for Returned Overseas Chinese Scholars, Education Ministry of China, No. 2001-345
Co-first-authors: Guang-Dong Pan and Hong Wu
Correspondence to: Dr. Guang-Dong Pan, PO Box 119, West China Medical University, Chengdu 610041, Sichuan Province, China. pgdhx@126.com
Telephone: +86-28-88054973
Received: 2004-08-30 Accepted: 2005-01-14

ABSTRACT

AIM: To investigate the effect of peroxisome proliferator-activated receptor gamma (PPAR-γ) and its ligand, ciglitazone, on inflammatory regulation of human gallbladder epithelial cells (HGBECs) and to assess the effect of human epithelial growth factor (hEGF) on growth of HGBECs.

METHODS: HGBECs were cultured in media containing hEGF or in hEGF-free media. HGBECs were divided into normal control group, inflammatory control group and ciglitazone group (test group). Inflammatory control group and ciglitazone group were treated with 5 μg/L of human interleukin-1β (hIL-1β) to make inflammatory model of HGBECs. The ciglitazone group was treated with various concentrations of ciglitazone, a potent ligand of PPAR-γ. Subsequently, interleukin-8 (IL-8), IL-6, and tumor necrosis factor-α (TNF-α) concentrations in all groups were measured. The data were analyzed statistically.

RESULTS: HGBECs were cultured in medium successfully. The longevity of HGBECs in groups containing hEGF was longer than that in hEGF-free groups. So was the number of HGBECs. The longest survival time of HGBEC was 25 d. The inflammatory model of HGBECs was obtained by treating with hIL-1β. The concentrations of IL-6 and IL-8 in ciglitazone group were lower than those in inflammatory control group ($P<0.05$). The secretion of IL-6 in inflammatory control group was higher (350.31±37.05 μg/L) than that in normal control group (50.0±0.00 μg/L, $P<0.001$). Compared to normal control group, IL-8 concentration in inflammatory control was higher ($P<0.05$).

CONCLUSION: hEGF improves the growth of HGBECs *in vitro*. Ciglitazone inhibits the inflammation of HGBECs *in vitro* and has potential therapeutic effect on cholecystitis *in vivo*.

Key words: PPAR-γ; Human gallbladder epithelial cells; Inflammation; Effect

Pan GD, Wu H, Liu JW, Cheng NS, Xiong XZ, Li SF, Zhang GF, Yan LN. Effect of peroxisome proliferator-activated receptor-gamma ligand on inflammation of human gallbladder epithelial cells. *World J Gastroenterol* 2005; 11(38): 6061-6065
http://www.wjgnet.com/1007-9327/11/6061.asp

INTRODUCTION

The peroxisome proliferator-activated receptor-γ (PPAR-γ) is a member of the nuclear receptor superfamily of ligand-dependent transcription factors[1]. With ligand binding, PPAR-γ forms a heterodimer with the retinoid X receptor-α (RXR-α) and joins to the PPAR response element in promoters of target genes, thus directly regulating their expressions[2]. PPAR-γ plays an important role in cell growth, differentiation, inflammation, and apoptosis. Binding to its ligand, PPAR-γ is associated with the regulation of cardiovascular disease, diabetes, and carcinogenesis[3]. Expression in many kinds of cells such as colon epithelial cells, monocytes, hepatic stellate cells, aortic smooth-muscle cells, thyrocytes, and airway epithelial cells, PPAR-γ gene can regulate their inflammation[4-8].

The commonly used method to elucidate the physiological role of PPAR-γ is to investigate the effects of its well-characterized ligands. The most specific PPAR-γ agonists are thiazolidinediones (TZDs)-insulin-sensitizing drugs including pioglitazone, rosiglitazone, troglitazone, and ciglitazone[9]. Previously, cyclopentenone prostanoids were thought to be the most potent one among the naturally occurring PPAR-γ activators[10]. However, 15d-PGJ2 is proved to be a potent inducer of interleukin-6 (IL-6) and IL-8 production and can be a mediator of inflammatory response recently, but this effect is independent of PPAR-γ activation[11].

In activated macrophages and vascular smooth muscle cells, the agonists of PPAR-γ inhibit the expression of many proinflammatory genes, like inducible nitric oxide synthase (iNOS), tumor necrosis factor-α (TNF-α), IL-6 or metalloproteinase-9. Endothelium lines, the inner surface of blood vessels, and is a primary target for inflammatory

agents. Exposure of endothelial cells to cytokines or bacterial lipopolysaccharide (LPS) induces the secretion of proinflammatory mediators, among them both IL-6 and IL-8 are crucial to acute inflammation[12,13]. IL-6 and IL-8 are produced either by endothelial cells directly or by endothelial cells activated by human interleukin-1β (hIL-1β) and TNF-α[14].

The present study was to investigate whether and how the PPAR-γ agonist, ciglitazone, one of the TZDs, affected the inflammatory regulation of human gallbladder epithelial cells (HGBECs). The effect was assessed by changes of IL-6, IL-8, and TNF-α in media after being treated with ciglitazone and IL-1β in order to determine the potential therapeutic function of PPAR-γ agonists for cholecystitis.

[illegible]

Materials

Dulbecco's modified Eagle's medium (DMEM), antibiotic-antimycotic solution, trypsin-ethylenediaminetetraacetic acid (EDTA) were purchased from Gibco BRL Life Technologies. Epidermal growth factor (EGF), type IV collagenase were purchased from Sigma Chemical Co. hIL-1β was purchased from Roche Biology Co. Ciglitazone was purchased from Cayman Chemical Co. IL-8, IL-6 RIA kit and TNF-α RIA kit were purchased from East Asia Radio-immunology Institution, Beijing, China. The lower detection limit of the assay was 0.3 μg/L for TNF-α, 50 μg/L for IL-6, and 0.2 μg/L for IL-8.

Cell isolation and primary culture

The isolation of HGBECs was processed immediately after its surgical removal. Bile was aspirated through a cannula placed in the cystic duct and the mucosal cavity was washed repeatedly with cold PBS containing 10^5 U/L penicillin and 100 mg/L streptomycin. Subsequently, 15 mL of 2.5 g/L trypsin-EDTA was introduced into the gallbladder and then placed in a sterile glass container immersed in a water bath at 37 ℃ for 20 min. Trypsin treatment led to a clear separation of the lining columnar epithelial cells from the underlying fibrous connective tissue. The cells were further dissociated by agitating in a turbulent stream of culture medium containing the pepsin for 5-10 min. The cell suspension was then centrifuged at 4 000 r/min for 5 min and the pellet was washed twice with DMEM containing 100 mL/L FCS. Subsequently, the cells were counted and tested for viability using concentrated trypan blue solution. In a typical study, >95% of cells would exclude trypan blue. Cells were placed on the Vitrogen-100 coated 24-well culture plate with DMEM containing 100 mL/L FCS, 10 μg/L human epithelial growth factor (hEGF) as test groups. Another 24-well cells were cultured in media without hEGF as control groups. Cell concentration was $(5\text{-}10)\times10^5$/mL. After being incubated for 2 h, media were changed to exclude non-epithelial cells. Media were changed after 48 h and subsequently, the cells were fed every 3 d.

Cells in three wells were digested by 2.5 g/L trypsin/0.1 g/L EDTA and counted every 24 h for 3 d to protract cell growth curve. Cells were studied serially by inverted phase microscopy and immunohistochemical reaction with epithelial keratins.

Cell group and treatment

HGBECs obtained through the above procedure were incubated in DMEM supplemented with 100 mL/L FCS, 10 μg/L hEGF, 10^5 U/L of penicillin, 10 mg/L of streptomycin at 37 ℃ in 50 mL/L CO_2. They were placed into 48-well culture plates in 5×10^5/mL of cell density. Then, they were randomly divided into normal control group, inflammatory control group, test group 1, test group 2, test group 3, and test group 4, among which each group had 8 wells containing 2 mL of media in a well. On the 5th d of culture, media were changed to DMEM without hEGF. Various final concentrations including 10, 20, 30, 50 mmol/L of ciglitazone were added into test groups 1-4, respectively. Cells were incubated in DMEM at 37 ℃ in 50 mL/L CO_2. The cells were treated with ciglitazone and incubated for 24 h, then inflammatory control group and all test groups were treated with the final concentration 5 μg/L of hIL-1β. Media were collected after 2-h incubation for measuring concentration of IL-6, TNF-α, and IL-8 by radioimmunoassay. Cell morphology was studied serially by inverted phase contrast microscopy.

Statistical analysis

The data were analyzed by Student's *t*-test for paired sample, by ANOVA for multiple comparison between groups. The statistical significance of the difference between mean values was determined by the *P* value less than 0.05.

[illegible]

Growth and conformation of cultured cells

HGBECs were cultured successfully in DMEM containing hEGF or without hEGF. In groups containing hEGF, the number of HGBECs reached the peak on the 5th d of culture and maintained for 10-12 d. After 20 d, apoptosis of HGBECs was noted. The longest longevity of HGBECs was 25 d. Compared to hEGF-free group, the growth and number of HGBECs were increased by hEGF (Figure 1).

After 6 h of culture, HGBECs attached to the monolayer were flat and multiangular in morphology. Some of the HGBECs were columnar with vigorous growth (Figure 2A). After 20 d of culture, vacuoles and drawbenches were found in cytoplast.

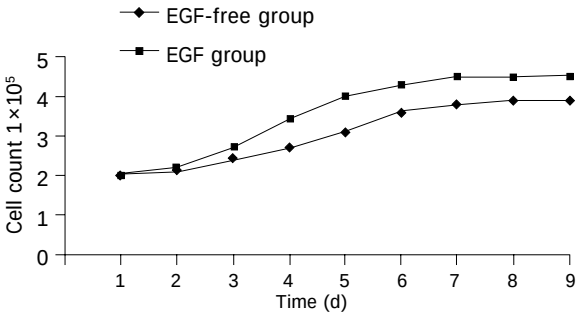

Figure 1 Growth curve of HGBECs.

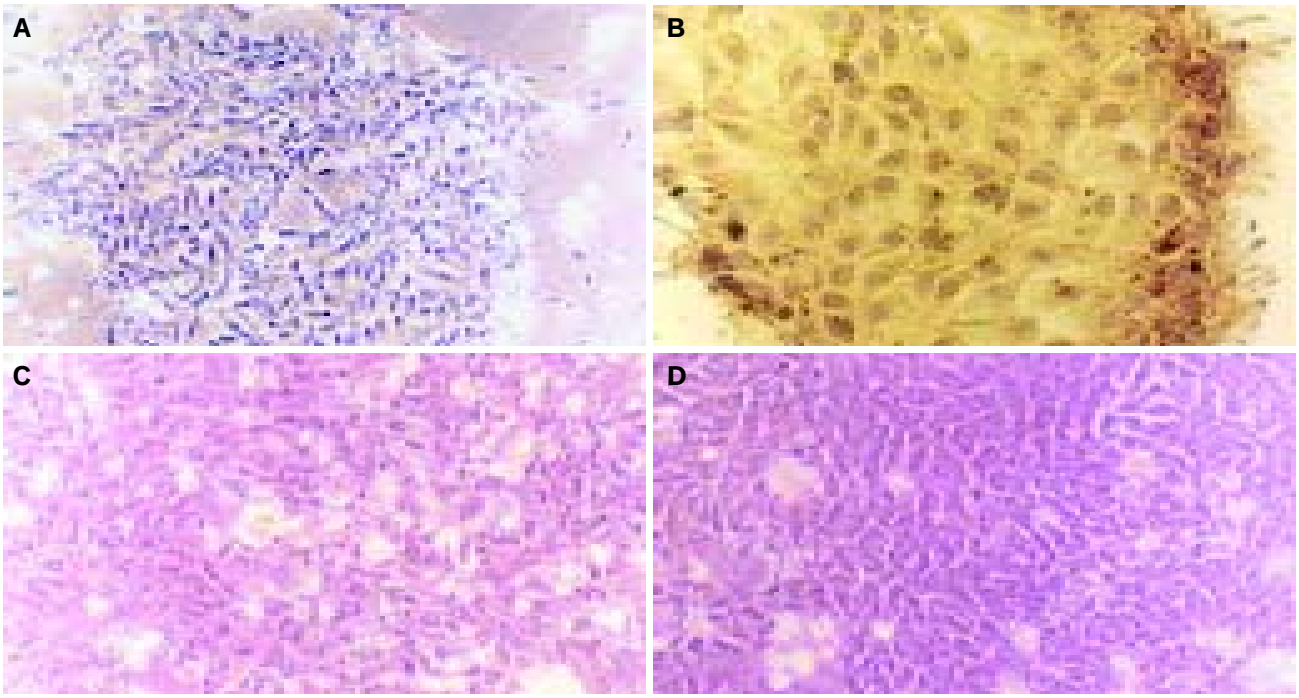

Figure 2 Attachment to monolayer (A), positive response (B), normal shape and structure (C) and edema (D) of HGBEC.

Identification of HGBECs

The cultured cells were identified by immunohistochemistry as keratin CK19. Specific positive reaction that could identify HGBECs was found in the cultured cells (Figure 2B).

Morphology of inflammatory HGBECs and inflammatory model of HGBECs

After HGBECs were treated with hIL-1β for 2 h, inflammatory changes of HGBECs such as swelling, unclear edge and irregular shape were found in test groups and inflammatory control group compared to normal control groups (Figures 2C and D).

Concentration of IL-6, IL-8 and TNF-α

Concentration of IL-6, IL-8 and TNF-α was measured by radioimmunoassay (Table 1). The data of TNF-α concentration were not shown because of its error and dispersion.

Table 1 IL-6 and IL-8 concentration in all groups (mean±SE)

Group	IL-6 (μg/L)	IL-8 (μg/L)
Normal control	50.0±0.00	0.20±0.00
Inflammatory control	350.31±37.05[b]	13.97±0.63[b]
Ciglitazone 10 mmol/L	231.46±39.41[a]	10.94±1.59[a]
20 mmol/L	207.22±26.72[a]	11.74±2.01[a]
30 mmol/L	188.89±29.33[a,d]	9.62±1.71[a]
50 mmol/L	170.46±20.24[a,e]	9.34±2.91[a,e]

[a]P<0.05 *vs* inflammatory control group; [b]P<0.001 *vs* normal control group; [d]P<0.001, [e]P<0.025 *vs* 10 mmol/L group.

[redacted]

The isolation and culture of HGBECs play a crucial role in studying biliary tract and liver disease. HGBECs have been cultured successfully since 1993[15], but its short duration limits the related research about the pathophysiology of biliary tract and liver. hEGF is a potent proliferation-activated factor of epithelial cells[16]. The first part of this study was performed to determine the hypothesis that hEGF could improve the growth of HGBECs. The proliferative activity of HGBECs promoted by hEGF was assessed by calculating the number and the life span of HGBECs, and compared to those in hEGF-free group. Results are in agreement with the hypothesis because hEGF increased the number of HGBECs and prolonged the longevity of HGBECs in which the longest was 25 d (8.2 d in EGF-free group). Also, the effect of hEGF on the growth of HGBECs is in agreement with the light microscopic findings. Thus, HGBECs cultured in medium containing hEGF are beneficial to the biological study of HGBECs.

The discovery that the insulin-sensitizing TZDs-specific PPAR-γ agonists have antiproliferative, anti-inflammatory and immunomodulatory effects has led to the evaluation of their potential use in the treatment of diabetic complications and inflammatory, proliferative diseases in non-insulin-resistant, euglycemic individuals. Apart from improving insulin resistance, plasma lipids and systemic inflammatory markers, ameliorating atherosclerosis and preventing coronary artery restenosis in diabetic subjects, currently approved TZDs that have been shown to improve psoriasis and ulcerative colitis in euglycemic human subjects[17]. In endothelial cells, troglitazone reduces expression of vascular cell adhesion molecule-1 and intercellular adhesion molecule-1, which are adhesion molecules that facilitate monocyte attachment and migration[18].

In addition to their impact on TNF-α and IL-6, IL -8, PPAR-γ agonists have also been reported by Pasceri *et al*.[18], to inhibit other macrophage proinflammatory mediators, including iNOS, gelatinase B, and the macrophage scavenger

receptor-A. PPAR-γ activation suppresses gastric mucosal inflammatory responses to *Helicobacter pylori* (*H pylori*) LPSs, suggesting that pharmacological manipulation of PPAR-γ activation may provide therapeutic benefits in the resolution of inflammation associated with *H pylori* infection[19]. In airway, PPAR-α and -γ (co) agonists might be of therapeutic interest for the regulation of allergic or inflammatory reactions by targeting both regulatory and effector cells involved in the immune response[20,21]. An important step in the monthly turnover of the endometrial lining during the menstrual cycle is the cyclical recruitment and activation of inflammatory cells. The use of PPAR-γ ligands to reduce chemokine production and inflammation may be a productive strategy for future therapy of endometrial disorders, such as endometriosis[22,23].

The mechanism of PPAR-γ and its ligand to regulate cellular inflammation may involve multiple pathways in different kinds of cells and the state of differentiation/ activation of the same source of cells. In macrophages and epithelial cells, the effect of 15 d-PGJ2 is targeted to the NF-κB/I-κB pathway and to the mitogen-activated protein kinase ERK1/2. The role of PPAR-γ activation in tissue factor inhibition by 15 d-PGJ2 is excluded[24]. 15 d-PGJ2 and rosiglitazone rapidly induce the transcription of suppressor of cytokine signalings 1 and 3, which in turn inhibit Janus kinase (JAK) activity in activated glial cells. In addition, Src homology 2 domain-containing protein phosphatase 2, another negative regulator of JAK activity, is also involved in their anti-inflammatory action[25]. Although it is not a direct causal effect, the insufficient PPAR-γ activity contributes to ongoing dysregulated inflammation in pulmonary sarcoidosis by failing to suppress NF-κB[26]. Dendritic cells (DCs), the most potent antigen-presenting cells, involve the anti-inflammatory activation of PPAR-γ. Recent reports showed that activation of PPAR-γ alters the maturation process of DCs, prevents induction of Th2-dependent eosinophilic airway inflammation and contributes to immune homeostasis in the lung[27]. However, conflicting findings on the consequences of PPAR-γ activation on inflammatory responses have led to a confusion regarding the role of the transcription factor in inflammation. Cyclopentenone prostaglandins, synthetic ligand of PPAR-γ, induce apoptosis of human DCs in a PPAR-γ-independent manner. Since these compounds are released during an inflammatory event and show anti-inflammatory properties, they may contribute to the downregulation of DC function through apoptotic cell death[28]. In a murine model of asthma, IL-8 release and activation of NF-κB-responsive reporter gene are inhibited only at micromolar concentrations, suggesting that these effects are not mediated by PPAR[29].

Based on the hypothesis that PPAR-γ expresses in HGBECs and inhibits inflammation of HGBECs, the following part of this study was designed to investigate whether the activation of PPAR-γ inhibited inflammation of HGBECs. IL-1β is a potent proinflammation factor that can induce multiple inflammatory mediators. After being treated with IL-1β for 2 h, HGBECs secreted a higher concentration of IL-6 and IL-8 in media ($P<0.001$). An inflammatory model of HGBECs was achieved successfully and showed a higher concentration of IL-6 and IL-8 in media, and inflammatory morphological changes such as edema and unclear edge in cellular formation. TNF-α, a potent inflammatory mediator, is often produced by white blood cells and smooth muscle cells in the early stage of inflammation. TNF-α could not be detected in the present study because HGBECs did not secrete it.

In vivo, IL-1β, TNF-α, and LPS initiate the secretion of cytokines including IL-6, IL-8, and IL-2. IL-1 can induce inflammation of gallbladder epithelial cells and biliary epithelial cells. Gallbladder inflammation is an early feature of gallstone formation[30]. These findings have been proved by molecular biology at mRNA level[31,32]. Also, these cytokines interact to form a network, which is named as cytokine storm[33]. The storm activates inflammatory cells and mediates inflammatory cell chemotaxis, then causes systemic inflammation. This process is defined as systemic inflammation response syndrome by the Association of American Physician and Critical Care in 1992[34].

PPAR-γ is a nuclear hormone receptor, with a well-established role in adipogenesis and glucose metabolism. Over the past 3 years several laboratories have reported that this protein can influence macrophage responses to a variety of inflammatory stimuli[32]. Immunolocalization of PPAR-γ primarily to colonocytes, especially in the presence of inflammation, strongly suggests that these epithelial cells are the target of PPAR-γ ligands[35-37]. In order to verify that HGBECs could express PPAR-γ and that PPAR-γ could affect the inflammation of HGBECs after binding to the ligand, we investigated the characteristics of PPAR-γ receptor using traditional endocrinological technique to study unknown receptor by binding to known ligand. We noted that ciglitazone with a final concentration of 10-50 mmol/L could suppress the IL-6 and IL-8 gene expression induced by IL-1β in a dose-dependent manner. This is consistent with our experimental hypothesis. Our results suggest that activation of PPAR-γ downregulates inflammation of HGBECs *in vitro*.

PPARs are nuclear receptor isoforms with key roles in the regulation of lipid and glucose metabolism. Synthetic ligands for PPAR-γ promote insulin sensitization in the context of obesity. In this study, ciglitazone showed potential therapeutic effects on inflammation of HGBECs *in vivo*.

REFERENCES

1 **Lemberger T,** Desvergne B, Wahli W. Peroxisome proliferator-activated receptors: a nuclear receptor signaling pathway in lipid physiology. *Annu Rev Cell Dev Biol* 1996; **12**: 335-363

2 **Michalik L,** Wahli W. Peroxisome proliferator-activated receptors: three isotypes for a multitude of functions. *Current Opin Biotechnol* 1999; **10**: 564-570

3 **Dalei S,** Rangwala SM, Bailey ST, Krakow SL, Reginato MJ. Interdomain comunication regulating ligand binding by PPAR-gamma. *Nature* 1998; **396**: 377-380

4 **Marra F,** Efsen E, Romanelli RG, Caligiuri A, Pastacaldi S, Batignani G, Bonacchi A, Caporale R, Laffi G, Pinzani M, Gentilini P. Ligands of peroxisome proliferator-activated receptors-gamma modulate profibrogenic and proinflammatory actions in hepatic stellate cells. *Gastroenterology* 2000; **119**: 466-478

5 **Staels B**, Koenig W, Habib A, Merval R, Lebret M, Torra IP, Delerive P, Fadel A, Chinetti G, Fruchart JC, Najib J, Maclouf J, Tedgui A. Activation of human aortic smooth-muscle cells is inhibited by PPAR-αbut not by PPAR-gamma activators.

Nature 1998; **393**: 790-793
6 **Hsueh WA,** Jackson S, Law RE. Control of vascular cell proliferation and migration by PPAR-gamma: a new approach to the macrovascular complications of diabetes. *Diabetescare* 2001; **24**: 392-397
7 **Wang AC,** Dai X, Liu B, Conrad DJ. Peroxisome proliferator-activated receptor-gamma regulates airway epithelial cell activation. *Am J Res Cell Mol Bilo* 2001; **24**; 688-693
8 **Kasai K,** Banba N, Hishinuma A, Matsumura M. Kakishita H, Matsumura M, Motohashi S, Sato N, Hattori Y. 15-Deoxy-Delta(12,14)-Prostaglandin J(2) facilitates thyroglobulin prodution by cultured human thyroicytes. *Am J Physiol Cell Physiol* 2000; **279**: 1859-1869
9 **Lehmann JM,** Moore LB, Smith-Olivier TA, Wilkison WO, Willson TM, Kliewer SA. An antidiabetic thiazolidinedione is a high affinity ligand for peroxisome proliferator-activated receptor-γ(PPAR-γ). *J Biol Chem* 1995; **270**: 12953-12956
10 **Kliewer SA,** Lenhard JM, Willson TM, Patei I, Morris DC, Lehmann JM. A prostaglandin-J_2 metabolite binds peroxisome proliferator-activated receptor γ and promotes adipocyte differentiation. *Cell* 1995; **83**: 813-817
11 **Jozkowicz A,** Dulak J, Proger M, Nanobashvili J, Nigisch A, Winter B, Weigel G, Huk I. Prostaglandin-J2 induces synthesis of interleukin-8 by endothelial cells in a PPAR-gamma independent manner. *Prostagl Other Lipid Med* 2001; **165**: 165-177
12 **Jiang C,** Ting AT, Seed B. PPAR-γ agonists inhibits production of monocyte inflammatory cytokines. *Nature* 1998; **391**: 82-86
13 **Kawahito Y,** Kondo M, Tsubouchi Y, Hashiramoto A, Bishop-Bailey D, Inoue KI, Kohno M, Yamada R, Hla T, Sano H. 15-deoxy-Ä^{12,14}–PGJ_2 induces synviocyte apoptosis and suppreses adjuvant-induced arthritis in rats. *J Clin Invest* 2000; **106**: 189
14 **Fitzegerald DJ,** Cecere G. Hemofiltration and inflammatory mediators. *Perfusion* 2002; **17**(Suppl): 23-28
15 **Purdum PP**, Ulissi A, Hylemon PB, Shiffman ML, Moore EW. Cultured human gallbladder epithelia. *Lab Invest* 1993; **68**: 345-353
16 **Liu HB,** Wang BS. Culture *in vitro* and biological feature of human bile duct epithelial cells. *Gandanyi Waike Zazhi* 1998; **10**: 165-166
17 **Pershadsingh HA.** Peroxisome proliferator-activated receptor-gamma: therapeutic target for diseases beyond diabetes: quo vadis?. *Expert Opinion on Investigational Drugs* 2004; **13**: 215-228
18 **Pasceri V,** Wu HD, Willerson JT, Yeh ETH. Modulation of vascular inflammation *in vitro* and *in vivo* by peroxisome proliferator-activated receptor-gamma activators. *Circulation* 2000; **101**: 235-238
19 **Slomiany BL,** Slomiany A. Suppression of gastric mucosal inflammatory responses to *Helicobacter pylori* lipopolysaccharide by peroxisome proliferator-activated receptor gamma activation. *IUBMB Life* 2002; **53**: 303-308
20 **Su CG,** Wen X, Bailey ST, Jiang W, Rangwala SM, Keilbaugh SA, Flanigan A, Murthy S, Lazar MA, Wu GD. A novel therapy for colitis utilizing PPAR-gamma ligands to inhibit the epithelial inflammatory response. *J Clin Invest* 1999; **104**: 383-389
21 **Mueller C,** Weaver V, Vanden Heuvel JP, August A, Cantorna MT. Peroxisome proliferator-activated receptor gamma ligands attenuate immunological symptoms of experimental allergic asthma. *Arch Biochem Biophys* 2003; **418**: 186-196
22 **Woerly G,** Honda K, Loyens M, Papin JP, Auwerx J, Staels B, Capron M, Dombrowicz D. Peroxisome proliferator-activated receptors alpha and gamma down-regulate allergic inflammation and eosinophil activation. *J Exp Med* 2003; **198**: 411-421
23 **Pritts EA,** Zhao D, Ricke E, Waite L, Taylor RN. PPAR-gamma decreases endometrial stromal cell transcription and translation of RANTES *in vitro*. *J Clin Endocrinol Metab* 2002; **87**: 1841-1844
24 **Hornung D,** Waite LL, Ricke EA, Bentzien F, Wallwiener D, Taylor RN. Nuclear peroxisome proliferator-activated receptors alpha and gamma have opposing effects on monocyte chemotaxis in endometriosis. *J Clin Endocrinol Metab* 2001; **86**: 3108-3114
25 **Eligini S,** Banfi C, Brambilla M, Camera M, Barbieri SS, Poma F, Tremoli E, Colli S. 15-deoxy-delta12,14-Prostaglandin J2 inhibits tissue factor expression in human macrophages and endothelial cells: evidence for ERK1/2 signaling pathway blockade. *Thromb Haemost* 2002; **88**: 524-532
26 **Park EJ,** Park SY, Joe EH, Jou I. 15d-PGJ2 and rosiglitazone suppress Janus kinase-STAT inflammatory signaling through induction of suppressor of cytokine signaling 1 (SOCS1) and SOCS3 in glia. *J Biol Chem* 2003; **278**: 14747-14752
27 **Trifilieff A,** Bench A, Hanley M, Bayley D, Campbell E, Whittaker P. PPAR-alpha and -gamma but not -delta agonists inhibit airway inflammation in a murine model of asthma: *in vitro* evidence for an NF-kappaB-independent effect. *Br J Pharmacol* 2003; **139**: 163-171
28 **Hammad H,** de Heer HJ, Soullie T, Angeli V, Trottein F, Hoogsteden HC, Lambrecht BN. Activation of peroxisome proliferator-activated receptor-gamma in dendritic cells inhibits the development of eosinophilic airway inflammation in a mouse model of asthma. *Am J Pathol* 2004; **164**: 263-271
29 **Nencioni A,** Lauber K, Grunebach F, Brugger W, Denzlinger C, Wesselborg S, Brossart P. Cyclopentenone prostaglandins induce caspase activation and apoptosis in dendritic cells by a PPAR-gamma-independent mechanism: regulation by inflammatory and T cell-derived stimuli. *Exp Hematol* 2002; **30**: 1020-1028
30 **Rege RV.** Inflammatory cytokines alter human gallbladder epithelial cell absorption/secretion. *J Gastrointest Surg* 2000; **4**: 185-192
31 **Morland CM,** Fear J, Joplin R, Adams DH. Inflammatory cytokines stimulate human biliary epithelial cells to express interleukin-8 and monocyte chemotactic protein-1. *Biochem Soc Trans* 1997; **25**: 232S
32 **Savard CE,** Blinman TA, Choi HS, Lee SK, Pandol SJ, Lee SP. Expression of cytokine and chemokine mRNA and secretion of tumor necrosis factor-alpha by gallbladder epithelial cells: response to bacterial lipopolysaccharides. *BMC Gastroenterol* 2002; **2**: 23
33 **Yoon JH,** Kim KS, Kim HU, Linton JA, Lee JG. Effects of TNF-alpha and IL-1 beta on mucin, lysozyme, IL-6 and IL-8 in passage-2 normal human nasal epithelial cells. *Acta Oto-Laryngol* 1999; **119**: 905-910
34 **Bone RC,** Balk RA, Cerra FB, Dellinger RP, Fein AM, Knaus WA, Schein RM, Sibbald WJ. Definitions for sepsis and organ failure and guidelines for the use of innovative therapies in sepsis. *Chest* 1992; **101**: 1644-1655
35 **Moore KJ,** Fitzgerald ML, Freeman MW. Peroxisome proliferator-activated receptors in macrophage biology: friend or foe? *Curr Opin Lipidol* 2001; **12**: 519-527
36 **Hinz B,** Brune K, Pahl A. 15-Deoxy-Delta(12,14)-prostaglandin J2 inhibits the expression of proinflammatory genes in human blood monocytes via a PPAR-gamma-independent mechanism. *Biochem Biophys Res Commun* 2003; **302**: 415-420
37 **Takagi T,** Naito Y, Tomatsuri N, Handa O, Ichikawa H, Yoshida N, Yoshikawa T. Pioglitazone, a PPAR-gamma ligand, provides protection from dextran sulfate sodium-induced colitis in mice in association with inhibition of the NF-kappaB-cytokine cascade. *Redox Report* 2002; **7**: 283-289

Science Editor Wang XL and Guo SY **Language Editor** Elsevier HK

PO Box 2345, Beijing 100023, China
www.wjgnet.com
wjg@wjgnet.com

ELSEVIER

World J Gastroenterol 2005;11(38):6066-6068
World Journal of Gastroenterology ISSN 1007-9327

• *CASE REPORT* •

Multiseptate gallbladder with anomalous pancreaticobiliary ductal union: A case report

Takafumi Yamamoto, Jun Matsumoto, Shinya Hashiguchi, Atsumasa Yamaguchi, Koro Sakoda, Chiaki Taki

Takafumi Yamamoto, Jun Matsumoto, Shinya Hashiguchi, Atsumasa Yamaguchi, Koro Sakoda, Chiaki Taki, Department of Endoscopy, Kagoshima University Hospital, Kagoshima 890-8520, Japan; Departments of Internal Medicine, Surgery, and Pathology, Kagoshima Medical Association Hospital, Kagoshima 890-0081, Japan
Correspondence to: Dr. Takafumi Yamamoto, Department of Endoscopy, Kagoshima University Hospital, 8-35-1 Sakuragaoka Kagoshima City, Kagoshima 890-8520, Japan. tyama@m2.kufm.kagoshima-u.ac.jp
Telephone: +81-99-275-5325 Fax: +81-99-275-3504
Received: 2005-02-15 Accepted: 2005-04-09

Abstract

Multiseptate gallbladder, characterized by the presence of multiple septa dividing the gallbladder lumen, is a very extremely rare congenital anomaly of the gallbladder. On the other hand, anomalous pancreaticobiliary ductal union is also one of the congenital anomalous biliary diseases and thought to be related with choledochal cyst or biliary tract malignancies. In this paper, we describe a unique and first patient of multiseptate gallbladder with anomalous pancreaticobiliary ductal union and a review of the literature. To clarify more characters of the multiseptate gallbladder, examination of a larger patient population will be needed and further studies will be required.

Key words: Multiseptate gallbladder; Anomalous pancreaticobiliary ductal union; Congenital anomaly

Yamamoto T, Matsumoto J, Hashiguchi S, Yamaguchi A, Sakoda K, Taki C. Multiseptate gallbladder with anomalous pancreaticobiliary ductal union: A case report. *World J Gastroenterol* 2005; 11(38): 6066-6068
http://www.wjgnet.com/1007-9327/11/6066.asp

INTRODUCTION

Multiseptate gallbladder is a very extremely rare congenital anomaly of the gallbladder. In the published cases, concomitant biliary diseases of the multiseptate gallbladder were reported as cholecystolithiasis, choledochal cyst, and hypoplasia. On the other hand, anomalous pancreaticobiliary ductal union is also one of the congenital anomalous biliary diseases and thought to be related with choledochal cyst or biliary tract malignancies. Along with the review of literature, reported here is a first patient of multiseptate gallbladder with anomalous pancreaticobiliary ductal union.

CASE REPORT

A 46-year-old Japanese female with gastric carcinoma underwent preoperative examinations at our institution. She had no complaints and her past history and family history were noncontributory. She reported no history of smoking and alcohol. Neither anemia nor jaundice was present. The abdomen was flat and soft. Liver, spleen, and mass could not be palpable. No lymph node swelling was palpated. Plain abdominal X-ray was normal. Laboratory data including tumor makers showed within normal range. Abdominal US and CT suspected septa in the gallbladder and showed neither cholecystolithiasis nor tumor lesion in the gallbladder. EUS demonstrated clearly multiple thin septa of the gallbladder (Figure 1A). ERCP revealed multiple faint septation in the neck portion of the gallbladder and combined with anomalous pancreaticobiliary ductal union. The common bile duct was not significantly dilated (Figures 1B and C).

Total gastrectomy and cholecystectomy were performed. In the macroscopic findings, the resected gallbladder was of normal size with smooth surface. Multiple thin septa were present only at the neck of the gallbladder. Neither tumor nor cholelithiasis was observed (Figure 1D). Microscopically, the septa were lined by typical columnar epithelium containing normal muscular layer of the gallbladder. There were mild chronic inflammation changes with the gallbladder. Pathological findings were consistent with multiseptate gallbladder (Figure 1E).

DISCUSSION

In recent years, congenital malformations of the gallbladder are increasingly diagnosed according to the rapid improvement of the imaging. The congenital malformations of the gallbladder are classified as anomalous forms, abnormal position, and absence. Multiseptate gallbladder is a very rare congenital anomaly form, which was first described by Simon and Tandon[1]. To our knowledge, only 30 cases including our case have been reported in the literature. A review of the cases described a female predominance; 21 of the patients were females. A mean age showed 29.4 years (range 3-70 years), and pediatric patients in four cases[2-5].

Most patients usually present with right upper abdominal pain, epigastralgia, and back pain, only six cases including our case were asymptomatic. Though the symptoms of multiseptate gallbladder patients were relieved after cholecystectomy, histological findings of the resected gallbladder in patients were usually of normal size with smooth surface and not

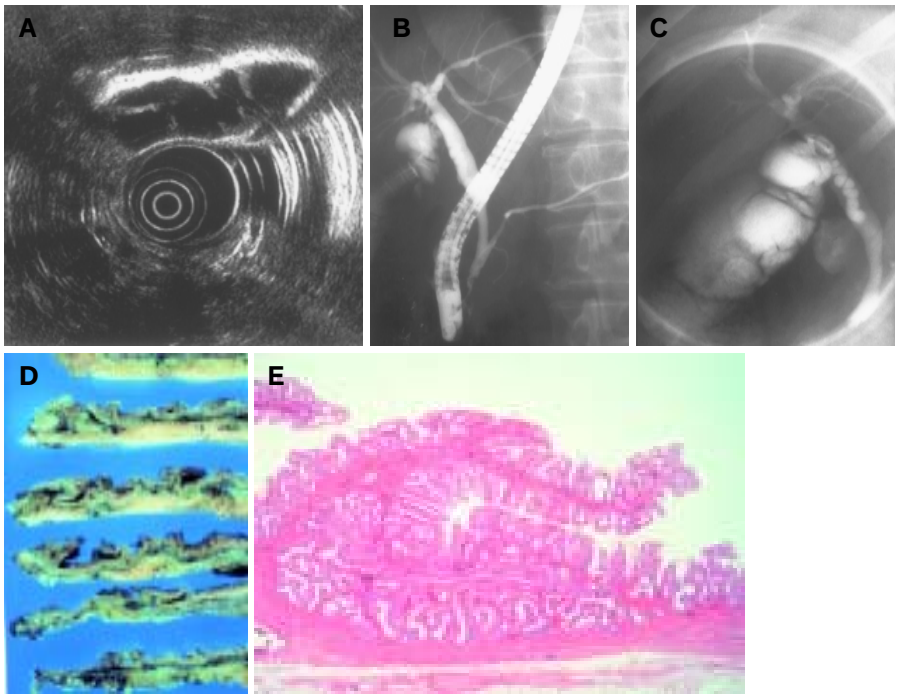

Figure 1 A: Endoscopic ultrasonography of the gallbladder showing multiple thin septa in the neck portion. B: Endoscopic retrograde cholangiopancreatography showing anomalous pancreaticobiliary ductal union. The common bile duct was not dilated. C: Endoscopic retrograde cholangiopancreatography showing multiple faint septation in the neck of the gallbladder. D: Longitudinal resected gallbladder shows multiple thin septa appearance at the neck portion. E: Microscopic findings of the resected gallbladder demonstrate the septa lined by normal typical columnar epithelium containing normal muscular layer (H&E stain, original magnification ×40).

always recognized as acute cholecystitis or cholecystolithiasis, and the exact mechanism of the biliary symptoms of multiseptate gallbladder is unknown. Saimura and co-workers investigated the mechanism of the symptoms of the patients with multiseptate gallbladder using biliary manometry and scintigraphy[6]. According to their study, both biliary manometry and scintigraphy indicated the impairment of the bile flow between the common bile duct and the gallbladder. One of the mechanism of the symptoms of multiseptate gallbladder is considered to be the impairment of the bile flow.

In nearly all literatures, pathological findings of multiseptate gallbladder reveal numerous septa, which consisted of a normal muscularis layer of the gallbladder wall, like a honeycomb appearance. Though the septa usually existed in the whole of the gallbladder, in some cases, the septations were confined to the neck, the body and the fundus alone[2,7,8]. This case presented the multiple septa in the neck portion of the gallbladder.

To make a diagnosis of multiseptate gallbladder exactly, it is important to detect clearly the septa in the gallbladder. Diagnostic imaging modalities for this disease were reported as abdominal US, abdominal CT[9], ERCP[7,10], oral cholecystography, and 99mTc hepatobiliary imaging[11]. In some asymptomatic cases, the diagnosis were made incidentally by abdominal US[3,4,8,12]. This case presented more clearly multiple thin septa in the neck portion of the gallbladder on EUS rather than other imagings. EUS is considered to be a very useful modality for the diagnosis of the cases with partial multiseptation.

Concomitant biliary disease of the patients with multiseptate gallbladder besides our case was reported in six patients; cholelithiasis in two patients[3,13], choledochal cyst in two[5,14], and hypoplasia of the gallbladder in two[15,16]. No cases that coexisted with malignancies were reported in the literature. On the other hand, anomalous pancreaticobiliary ductal union is also known as the congenital malformation of the pancreaticobiliary duct system and is thought to be related to choledochal cyst and biliary tract carcinoma. Though anomalous pancreaticobiliary ductal union is frequently observed in patients with congenital choledochal cyst, the cases without choledochal cyst are recognized to have great malignant potential of the gallbladder[17,18]. In this case, ERCP demonstrated anomalous pancreaticobiliary ductal union without choledochal cyst.

Our case is asymptomatic and has the septations at the only neck of the gallbladder. Besides these unique findings, this present case is the first report of multiseptate gallbladder associated with anomalous pancreaticobiliary ductal union in the world literature. To clarify more characters of the multiseptate gallbladder, examination of a larger patient population will be needed and further studies will be required.

REFERENCES

1 **Simon M**, Tandon BN. Multiseptate gallbladder: A case report. *Radiology* 1963; **80**: 84-86
2 **Strauss S**, Starinsky R, Alon Z. Partial multiseptate gallbladder: sonographic appearance. *J Ultrasound Med* 1993; **12**: 201-203
3 **Miwa W**, Toyama K, Kitamura Y, Murakami K, Kamata K, Takada T, Tanabe H, Kanayama M. Multiseptate gallbladder with cholelithiasis diagnosed incidentally in an elderly patient. *Intern Med* 2000; **39**: 1054-1059
4 **Saddik D**. Multiseptate gall-bladder: incidental diagnosis on ultrasound. *Australas Radiol* 1998; **42**: 374-376
5 **Pery M**, Kaftori JK, Marvan H, Sweed Y, Kerner H. Ultrasonographic appearance of multiseptate gallbladder:

report a case with coexisting choledochal cyst. *J Clin Ultrasound* 1985; **13**: 570-573
6 **Saimura M**, Ichimiya H, Naritomi G, Ogawa Y, Chijiiwa K, Yamaguchi K. Multiseptate gallbladder: biliary manometry and scintigraphy. *J Gastroenterol* 1996; **31**: 133-136
7 **Naritomi G**, Kimura H, Konomi H, Takeda T, Ogawa Y, Chijiiwa K. Multiseptate gallbladder as a cause of biliary pain. *Am J Gastroenterol* 1994; **89**: 1891-1892
8 **Adear H**, Barki Y. Mutiseptate gallbladder in a child: incidental diagnosis on sonography. *Pediatr Radiol* 1990; **20**: 192
9 **Isomoto I**, Matsunaga N, Ochi M, Hayashi K, Amamoto Y, Tachibana K, Furukawa M. Multiseptate gallbladder: computed tomographic appearance. *Radiat Med* 1990; **8**: 55-57
10 **Hahm KB**, Yim DS, Kang JK, Park IS. Cholangiographic appearance of multiseptate gallbladder: case report and a review of the literature. *J Gastroenterol* 1994; **29**: 665-668
11 **Vasinrapee P**, Linden K, Cook RE. Multiseptate gallbladder demonstrated on Tc-99m hepatobiliary imaging. *Clin Nucl Med* 1990; **15**: 272
12 **Lev-Toaff AS**, Friedman AC, Rindsberg SN, Caroline DF, Maurer AH, Radecki PD. Multiseptate gallbladder: incidental diagnosis on sonography. *Am J Roentgenol* 1987; **148**: 1119-1120
13 **Croce EJ**. The multiseptate gallbladder. *Arch Surg* 1973; **107**: 104-105
14 **Tan CE**, Howard ER, Driver M, Murray-Lyon IM. Non-communicating Multiseptate gallbladder and choledochal cyst: a case report and review of publications. *Gut* 1993; **34**: 853-856
15 **Bhagavan BS**, Amin PB, Land AS, Weinberg T. Multiseptate gallbladder. Embryogenetic hypotheses. *Arch Pathol* 1970; **89**: 382-385
16 **Jena PK**, Hardie RA, Hobsley M. Multiseptate hypoplastic gallbladder. *Br J Surg* 1977; **64**: 192-193
17 **Yamauchi S**, Koga A, Matsumoto S, Tanaka M, Nakayama F. Anomalous junction of pancreaticobiliary duct without congenital choledochal cyst: a possible risk factor for gallbladder cancer. *Am J gastroenterol* 1987; **82**: 20-24
18 **Chijiiwa K**, Kimura H, Tanaka M. Malignant potential of the gallbladder in patients with anomalous pancreaticobiliary ductal junction. The difference in risk between patients with and without choledochal cyst. *Int Surg* 1995; **80**: 61-64

Science Editor Guo SY **Language Editor** Elsevier HK

PO Box 2345, Beijing 100023, China
www.wjgnet.com
wjg@wjgnet.com

ELSEVIER

World J Gastroenterol 2005;11(38):6069-6071
World Journal of Gastroenterology ISSN 1007-9327

• *CASE REPORT* •

Autoimmune hepatitis triggered by acute hepatitis A

Hiroto Tanaka, Hiroto Tujioka, Hiroki Ueda, Hiroko Hamagami, Youhei Kida, Masakazu Ichinose

Hiroto Tanaka, Hiroto Tujioka, Hiroki Ueda, Hiroko Hamagami, Youhei Kida, Masakazu Ichinose, 3rd Department of Internal Medicine, Wakayama Medical University, Japan
Correspondence to: Masakazu Ichinose, MD, PhD, 3rd Department of Internal Medicine, Wakayama Medical University, 811-1 Kimiidera, Wakayama 641-0015, Japan. h-tana@yf6.so-net.ne.jp
Telephone: +81-73-441-0619 Fax: +81-73-446-2877
Received: 2005-02-17 Accepted: 2005-05-12

Abstract

The patient was a 57-year-old woman presenting with jaundice as the chief complaint. She began vomiting on July 10, 2003. Jaundice was noted and admitted to our hospital for thorough testing. Tests on admission indicated severe hepatitis, based on: aspartate aminotransferase (AST), 1 076 IU/L; alanine aminotransferase (ALT), 1 400 IU/L; total bilirubin (TB), 20.9 mg/dL; and prothrombin time rate (PT%), 46.9%. Acute hepatitis A (HA) was diagnosed based on negative hepatitis B surface antigen and hepatitis C virus RNA and positive immunoglobulin (Ig) M HA antibody, but elevation of anti-nuclear antigen (×320) and IgG (3 112 mg/dL) led to suspicion of autoimmune hepatitis (AIH). Plasma exchange was performed for 3 d from July 17, and steroid pulse therapy was performed for 3 d starting on July 18, followed by oral steroid therapy. Liver biopsy was performed on August 5, and the results confirmed acute hepatitis and mild chronic inflammation. Levels of AST and ALT normalized, so dose of oral steroid was markedly reduced. Steroid therapy was terminated after 4 mo, as the patient had glaucoma. Starting 3 mo after cessation of steroid therapy, levels of AST and ALT began to increase again. Another liver biopsy was performed and AIH was diagnosed based on serum data and biopsy specimen. Oral steroid therapy was reinitiated. Levels of AST and ALT again normalized. The present case was thus considered to represent AIH triggered by acute HA.

Key words: Acute hepatitis A; Autoimmune hepatitis; International criteria for AIH; HLA

Tanaka H, Tujioka H, Ueda H, Hamagami H, Kida Y, Ichinose M. Autoimmune hepatitis triggered by acute hepatitis A. *World J Gastroenterol* 2005; 11(38): 6069-6071
http://www.wjgnet.com/1007-9327/11/6069.asp

INTRODUCTION

Autoimmune hepatitis (AIH) is a chronic progressive hepatitis characterized clinically by positive anti-nuclear antibody (ANA) and hypergammaglobulinemia, and histologically by portal inflammatory cell infiltration (plasmacyte dominant) and piecemeal necrosis. However, the exact mechanisms of onset are unknown. Based on past reports, AIH appears to be induced by antibody-dependent cell-mediated cytotoxicity, which involves both antibody-mediated and cellular immunity against specific liver antigens on hepatocyte membranes[1]. Several studies have documented the involvement of genetic factors, including human lymphocyte antigen (HLA) types such as DR3 and DR4[2]. Furthermore, cases of AIH have been reported in which viruses causing acute hepatitis such as hepatitis A (HA) virus[3-7], HBV[8] and Epstein-Barr virus[9] have acted as a trigger. We report herein the case of a patient with AIH that appears to have been triggered by acute HA.

CASE REPORT

The patient was a 57-year-old woman with jaundice as the chief complaint.

History of present illness

The patient had been seeing a local doctor for hypertension, with no sign of hepatic pathology. On July 2, 2003, she developed hives and was given fexofenadine hydrochloride. Around this time, she began to feel sick. While she had eaten raw foods within the previous month, she had not eaten raw oysters. Starting on July 10, she began vomiting and visited the local doctor on July 14. Jaundice was noted, and the patient was referred and admitted to our hospital for thorough testing.

Physical findings on admission

The patient was 163 cm tall and weighed 100 kg. She was thus very obese, and although yellowing of the bulbar conjunctiva was noted, no other abnormalities were identified.

Test findings on admission (Table 1)

Aspartate aminotransferase (AST), 1 076 IU/L; alanine aminotransferase (ALT), 1 400 IU/L; total bilirubin (TB), 20.9 mg/dL; prothrombin time rate (PT%), 46.9%; hepatitis B surface antigen (HBsAg) negative; hepatitis C virus (HCV) RNA negative; and immunoglobulin (Ig) M HA antibody positive (titer, 1.9 cut of index). Acute HA was therefore diagnosed. Furthermore, as levels of ANA (×320) and IgG (3 112 mg/dL) were elevated, AIH was suspected. Drug lymphocyte stimulation test (DLST) yielded negative results for fexofenadine hydrochloride. The patient scored 1 point according to the diagnostic criteria for acute drug-induced

hepatic injury established by the International Consensus Meeting (ICM)[10], excluding the possibility of drug-induced hepatic injury. Computed tomography showed no hepatic atrophy, but thickening of the gallbladder wall was apparent, suggesting acute hepatitis (Figure 1). HLA assessment conducted after admission revealed: A24(9); B52(5); B61 (40); DR15(2); and DR9.

Table 1 Labo data on admission

WBC	6900/uL	BS	129 mg/dL
Neutro	60.9%	HbA1c	6.4%
Eosin	3.6%	CRP	1.59 mg/dL
Baso	0.5%	Na	137 mEq/L
Mono	9.1%	K	3.6 mEq/L
Lympho	25.9%	Cl	99 mEq/L
RBC	502×10⁴/uL		
Hb	15.2 g/dL		
Ht	44.7%		
Plt	16.5×10⁴/uL	ANA	320 times
		AMA	-
TP	8.5 g/dL	IgG	3 112 mg/dL
Alb	3.4 g/dL	IgM	234 mg/dL
BUN	11 mg/dL	IgA	631 mg/dL
Cr	0.9 mg/dL		
T-Bil	20.9 mg/dL	IgM HA	+
D-Bil	16.9 mg/dL	HBsAg	-
AST	1 076 IU/L	HCV Ab	-
ALT	1 400 IU/L	CMV IgM	-
PT%	46.9%	EBV IgM	-
LDH	498 U/L		
Γ-GTP	129 IU/L		
ChE	242 U/L	DLST	-

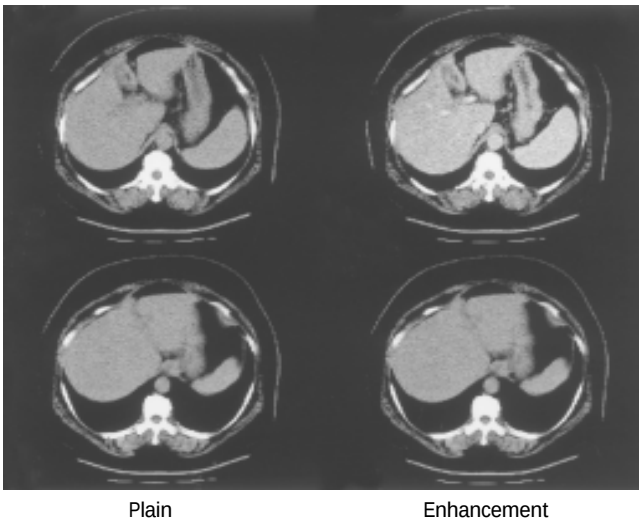

Figure 1 Liver parenchyma is not atrophic. Thickening of the gall bladder wall is also seen. This finding is compatible with acute hepatitis.

Clinical course following admission

Although AST and ALT levels started to improve, TB and PT% deteriorated to 27.5 mg/dL and 40.8%, respectively. To avoid onset of fulminant hepatitis, plasma exchange was performed for 3 d starting on July 17. From July 18, steroid pulse therapy was performed for 3 d, followed by oral steroid therapy. Levels of AST, ALT, TB, and PT% improved. Results of liver biopsy on August 5 confirmed acute hepatitis and mild chronic inflammation (mild fibrous enlargement of portal area was shown in two of eight portal areas and marked inflammatory cell infiltration of liver parenchyma was identified). The patient scored seven points according to international diagnostic criteria for AIH[11], which was thus excluded at this time. Acute HA was therefore diagnosed. At first, 50 mg/d of oral steroid (prednisolone) was administered, with dose reduced by 10 mg/d every week. Levels of AST, ALT, and TB gradually improved, and the patient was discharged while receiving 20 mg/d of steroid. After discharge, dose of oral steroid was reduced by 5 mg/d every week. As the patient also had glaucoma, oral steroid therapy was terminated after 4 mo. Levels of AST and ALT remained low, but began to increase around 3 mo after cessation of therapy. Since IgM HA antibody was negative at this time, AIH was suspected to be based on serum data such as ANA and IgG levels, and liver biopsy was performed on April 13 (Figure 2). AIH was diagnosed, and 600 mg/d of ursodeoxycholic acid was administered. This therapy proved ineffective, and oral steroid therapy (40 mg/d) was reinstated. AST and ALT levels normalized, and dose of oral steroid was gradually reduced. The patient is currently undergoing treatment in an outpatient basis with oral steroid therapy 1 mg/d, and no further elevation of AST or ALT levels has been seen.

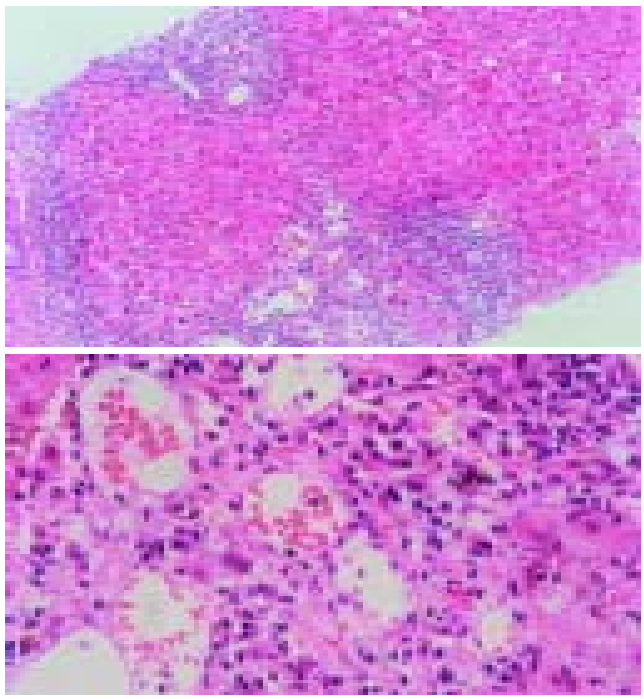

Figure 2 This liver biopsy specimen show the histopathologic appearance of chronic hepatitis. Interface hepatitis is present with bridging fibrosis, which fibrosis connects portal and cetral arreas. However, dominant plasmacyte infiltrates and rossete formation are not present.

[illegible]

On admission, although drug-induced hepatic injury was suspected in the present patient, acute HA was diagnosed due to positive IgM HA antibody. However, since ANA

was ×320 and IgG was 3 110 mg/dL, AIH could not be excluded as a possibility, and we could not be certain that the acute hepatic injury was caused by HA alone. DLST for the prescribed drug was negative, and the patient scored one point according to the diagnostic criteria for acute drug-induced hepatic injury established by the ICM [9]. Drug-induced hepatic injury thus seemed unlikely.

In the present patient, AIH was suspected at the onset of acute hepatitis, and assessment was performed in accordance with the international diagnostic criteria for AIH[11]. However, as the patient scored seven points, AIH was not initially diagnosed. Oral steroid therapy was terminated after 4 mo because transaminase levels remained normal and the patient also had glaucoma. However, transaminase levels again increased 3 mo after terminating oral steroid therapy. Since AIH had been suspected based on serum data such as ANA and IgG, liver biopsy was performed again. At this time, the patient scored 21 points according to international diagnostic criteria for AIH[11], and AIH was thus diagnosed.

While viral infection has been known to trigger AIH, few cases of AIH following acute HA have been described[3-7]. In most of these cases, AIH did not occur at the same time as acute hepatitis, with AIH often occurring several months after the onset of acute HA. According to international diagnostic criteria, the present patient did not display AIH at the time of acute hepatitis. However, since levels of ANA and IgG were high, excessive immune reactions were present. We suspect that these excessive immune reactions may lead to onset of AIH. No studies have investigated AIH during the early stages of acute hepatitis, and excessive immune reactions during acute HA have not been documented. One report documented a case of AIH that occurred after several months of abnormal liver function following acute HA[5]. While immune reactions are not often assessed in acute HA, as was the case with the present patient, excessive immune reactions may occur during acute HA.

Vento and colleagues[3] reported a patient with a deficiency of specific suppressor T cells for asialoglycoprotein receptor who developed type I AIH following subclinical HA, suggesting the possibility that immunological abnormalities including antigen presentations were involved in the onset of AIH following acute HA. HLA typings of patients with AIH triggered by acute HA were compared, but no specific tendencies were identified (Table 2). Since the sample of patients was small, larger subject populations need to be studied in future.

Herein, we presented the case of a patient with AIH that appears to have been triggered by acute HA. Given the existence of such patients and the need for careful follow-up of patients with acute HA, the clinical features of AIH patients after acute hepatitis need to be investigated for early diagnosis of AIH.

Table 2 Sample of patients

Author	Age (yr)	Sex Male/Female	Term (wk)	HLA
Vento S *et al.*	18	M	16	A2, B15, B40, DR7, DR4
Vento S *et al.*	13	F	15	A1, A19, B8, B44, DR7, DR3
Rahaman SM *et al.*	55	F	10	NT
Huppertz HI *et al.*	7	M	10	A1, A2, Bw52, Bw62, Cw3, Cw6, DR7, DRw8, DQw2
Hilzenrat N *et al.*	55	F	7	A26, B38, DRB1*0401, DRB44*01, DQB1*02
Bertran EM *et al.*	27	M	10	NT
Our case	57	F	28	A24, B52, B61, DR15, DR9

1 **Eggink HF,** Houthoff HJ, Huitema S, Gips CH, Poppema S. Cellular and humoral immune reactions in chronic liver disease. I. Lymphocyte subsets in liver biopsies of patients with untreated idiopathic autoimmune hepatitis, chronic active hepatitis B and primary biliary cirrhosis. *Clin Exp Immunol* 1982; **50**: 17-24

2 **Czaja AJ,** Carpenter HA, Santrach PJ, Moore SB. DR human leukocyte antigens and disease severity in chronic hepatitis C. *J Hepatol* 1996; **24**: 666-673

3 **Vento S,** Garofano T, Di Perri G, Dolci L, Concia E, Bassetti D. Identification of hepatitis A virus as a trigger for autoimmune chronic hepatitis type I in susceptible individuals. *Lancet* 1991; **337**: 1183-1187

4 **Huppertz HI,** Treichel U, Gassel AM, Jeschke R, Meyer KH. Autoimmune hepatitis following hepatitis A virus infection. *J Hepatol* 1995; **23**: 240-248

5 **Rahaman SM,** Chira P, Koff RS. Idiopathic autoimmune chronic hepatitis triggered by hepatitis A. *Am J Gastroenterl* 1994; **89**: 106-108

6 **Hilzenrat N,** Zilberman D, Klein T, Zur B, Sikuler E. Autoimmune hepatitis in a genetically susceptible patient. Is it triggered by acute viral hepatitis A? *Dig Dis Sci* 1999; **44**: 1950-1952

7 **Munoz Bertran E,** Rosa Salazar V, Hostalet Robles F, Correa Estan JA, Belda Abad G, Munoz Ramirez E. autoimmune hepatitis caused by acute hepatitis due to hepatitis A virus. *Gastroenterol Hepatol* 2002; **25**: 501-504

8 **Laskus T,** Slusarczyk J. Autoimmune chronic active hepatitis developing after acute type B hepatitis. *Dig Dis Sci* 1989; **34**: 1294-1297

9 **Vento S,** Guella L, Mirandola F, Cainelli F, Di Perri G, Solbiati M, Ferraro T, Concia E. Epstein-Barr virus as a trigger for autoimmune hepatitis in susceptible individuals. *Lancet* 1995; **346**: 608-609

10 **Danan G,** Benichou C. Causality assessment of adverse reactions to drugs. I. A novel method based on the conclusions of international consensus meeting: application to drug-induced liver injuries. *J Clin Epidemiol* 1993; **46**: 1323-1330

11 **Alvarez F,** Berg PA, Bianchi FB, Bianchi L, Burroughs AK, Cancado EL, Chapman RW, Cooksley WG, Czaja AJ, Desmet VJ, Donaldson PT, Eddleston AL, Fainboim L, Heathcote J, Homberg JC, Hoofnagle JH, Kakumu S, Krawitt EL, Mackay IR, MacSween RN, Maddrey WC, Manns MP, McFarlane IG, Meyer zum Buschenfelde KH, Zeniya M. International Autoimmune Hepatitis Group Report: review of criteria for diagnosis of autoimmune hepatitis. *J Hepatol* 1999; **31**: 929-938

Science Editor Guo SY **Language Editor** Elsevier HK

PO Box 2345, Beijing 100023, China
www.wjgnet.com
wjg@wjgnet.com

ELSEVIER

World J Gastroenterol 2005;11(38):6072-6073
World Journal of Gastroenterology ISSN 1007-9327

• *LETTERS TO THE EDITOR* •

Role of von Willebrand factor levels in the prognosis of stage IV colorectal cancer: Do we have enough evidence?

I. Gil-Bazo, J.A Díaz González, J. Rodríguez, J. Cortés, E. Calvo, J.A. Páramo, J. García-Foncillas

I. Gil-Bazo, J.A Díaz González, J. García-Foncillas, Department of Medical Oncology, University Clinic, University of Navarra, Pío XII, 36. 31008 Pamplona, Spain
J.A. Páramo, Service of Haematology, University Clinic, University of Navarra, Pío XII, 36. 31008 Pamplona, Spain
J. Cortés, Department of Medical Oncology, Vall d'Hebron, University Hospital, Pg Vall d'Hebron, 119-129, E-08035 Barcelona, Spain
E. Calvo, Institute for Drug Development, Cancer Therapy and Research Center. University of Texas Health Science Center at San Antonio, 7979 Wurzbach Road, Zeller Building, San Antonio, TX 78229, United States
Correspondence to: I. Gil-Bazo, MD, PhD, Cancer Biology and Genetics Program, Memorial Sloan-Kettering Cancer Center, 1275 York Avenue, Box 241, New York, NY 10021, United States. gilbazoi@mskcc.org
Telephone: +1-21-26392390 Fax: +1-646-4222063
Received: 2005-04-30 Accepted: 2005-06-09

Key words: Von Willebrand factor; Colorectal cancer; Prognosis

Gil-Bazo I, Diaz-Gonzalez JA, Rodríguez J, Cortés J, Calvo E, Páramo JA, García-Foncillas J. Role of von Willebrand factor levels in the prognosis of stage IV colorectal cancer: Do we have enough evidence? *World J Gastroenterol* 2005; 11 (38): 6072-6073
http://www.wjgnet.com/1007-9327/11/6072.asp

[illegible]

Cancer patients usually present a prothrombotic condition. Several clotting-related proteins, such as von Willebrand factor (vWF), presenting higher plasma concentrations in these patients, may play a key role in this process. Moreover, some of those proteins are currently being characterized as response rate and overall survival markers in metastatic colorectal cancer (MCRC). In this comment article, we discuss the last piece of evidence that supports the use of vWF as a prognostic indicator in MCRC patients, provided by a paper recently published by Wang *et al*., in the *World Journal of Gastroenterology*. Summarizing, although vWF should be seriously considered as potential future prognostic and predictive indicator in colorectal cancer, more dynamic and better designed studies in longer series of patients should be conducted before standardizing its universal use among these patients.

Wang *et al*.[1], have recently published an encouraging paper in the World Journal of Gastroenterology regarding the possible and novel use, as a prognostic factor, of vWF plasma levels in MCRC.

As the authors expose, cancer patients often show an imbalance between coagulation and fibrinolysis systems, which results in their prothrombotic condition[2-6]. Several clotting-related proteins, such as vWF, presenting higher plasma concentrations in these patients[7-11], may play a key role in this process. Moreover, some of those proteins are currently being characterized as response rate and overall survival markers in MCRC[12-16].

Accordingly, the data shown by Wang *et al*.[1], seem to indicate that plasma vWF concentrations are increased among colorectal cancer patients and correlate with tumor stage. In addition, those vWF higher levels may be related to significantly poor prognosis of subjects presenting metastasis.

However, although authors are aware of the important variability of vWF levels in humans due to the presence of a variety of diseases like diabetes mellitus, connective tissue disease, cardiovascular dysfunctions, thrombo-embolic events, acute infections, and other conditions like age or gender[17-20], patients suffering any of those illnesses were not apparently excluded from the study nor controlled by those factors in the multivariate analysis.

More strikingly, even though platelets are partially responsible for vascular endothelial growth factor (VEGF) levels[21-25], and VEGF is considered the most potent activator of the endothelium (main vWF producer), neither platelet count nor VEGF levels were measured and included in the statistical analysis.

Other issue that remains unclear in this article is whether the chemotherapy (CMT) regime used (5-fluorouracil alone or in combination with irinotecan, oxaliplatin or capecitabine) in each group of patients could have accounted for the differences observed between the survival curves for individuals presenting vWF$\geqslant$160% and those with levels below that threshold. Thus, in order to avoid the possible bias, the CMT regime administered to each patient should have also been taken into account in the multivariate statistical analysis.

Finally, given the fact that the CMT could catalyze the original risk for progression and death in these patients due to its alleged antiangiogenic effect, measuring vWF concentrations during treatment may modify the prognostic value of this protein.

According to this, in the University Clinic of the University of Navarra, 64 colorectal cancer patients were enrolled from 2002 and 2004. Blood samples were taken dynamically before and after fluoropirimidine-based CMT in 32 patients presenting metastasis, and stored until further

processing. vWF, VEGF, plasminogen activator inhibitor (PAI) 1, D-dimer, fibrinogen levels and platelet count were measured before and after CMT using standardized techniques. Gender, age, ECOG performance status, tumor burden, CMT course, and regime and CEA/CA 19.9 levels were also considered for the statistical analysis. Patients received a median of 3 cycles of CMT (range: 2-10) between both blood samples. After a median follow-up of 10 mo, baseline levels of vWF >202% showed an associated hazard ratio (HR), for death higher than patients with vWF ≤202%, with tendency to the statistical significance ($P = 0.08$). Meanwhile, post-CMT vWF levels above 189% were related to a fourfold HR for progression with respect to those subjects showing concentrations ≤189% after CMT treatment. These results were adjusted for the rest of the different protein levels measured, age, gender, ECOG performance status, tumor burden, and CMT course and regime.

In conclusion, although vWF and other coagulation/fibrinolysis factors should be seriously considered as potential future prognostic and predictive indicators in colorectal cancer, more dynamic and better designed studies in longer series of patients should be conducted before standardizing their universal use among these patients.

REFERENCES

1 **Wang WS**, Lin JK, Lin TC, Chiou TJ, Liu JH, Yen CC, Chen PM. Plasma von Willebrand factor level as a prognostic indicator of patients with metastatic colorectal carcinoma. *World J Gastroenterol* 2005; **11**: 2166-2170

2 **Bick RL.** Alterations of hemostasis associated with malignancy: etiology, pathophysiology, diagnosis and management. *Semin Thromb Hemost* 1978; **5**: 1-26

3 **Ho CH,** Yuan CC, Liu SM. Diagnostic and prognostic values of plasma levels of fibrinolytic markers in ovarian cancer. *Gynecol Oncol* 1999; **75**: 397-400

4 **Lip GY,** Chin BS, Blann AD. Cancer and the prothrombotic state. *Lancet Oncol* 2002; **3**: 27-34

5 **Lykke J,** Nielsen HJ. Haemostatic alterations in colorectal cancer: perspectives for future treatment. *J Surg Oncol* 2004; **88**: 269-275

6 **Paramo JA,** Cuesta B, Hernandez M, Fernandez J, Paloma MJ, Rifon J, Rocha E. Coagulation inhibitors in patients with neoplasms. *Med Clin* 1989; **92**: 164-166

7 **Gadducci A,** Baicchi U, Marrai R, Del Bravo B, Fosella PV, Facchini V. Pretreatment plasma levels of fibrinopeptide-A (FPA), D-dimer (DD), and von Willebrand factor (vWF) in patients with ovarian carcinoma. *Gynecol Oncol* 1994; **53**: 352-356

8 **Gil-Bazo I,** Páramo Fernández JA, García-Foncillas J. Hemostasis, angiogenesis and cancer: role of the von Willebrand factor. *Rev Clin Esp* 2003; **203**: 199-201

9 **Rohsig LM,** Damin DC, Stefani SD, Castro CG Jr, Roisenberg I, Schwartsmann G. von Willebrand factor antigen levels in plasma of patients with malignant breast disease. *Br J Med Biol Res* 2001; **34**: 1125-1129

10 **Schwartsmann G,** Damin DC, Roisemberg I. Malignant disease and von Willebrand factor. *Lancet Oncol* 2001; **2**: 716-717

11 **Zietek Z,** Iwan-Zietek I, Paczulski R, Kotschy M, Wolski Z. von Willebrand factor antigen in blood plasma of patients with urinary bladder carcinoma. *Thromb Res* 1996; **83**: 399-402

12 **Blackwell K,** Hurwitz H, Lieberman G, Novotny W, Snyder S, Dewhirst M, Greenberg C. Circulating D-dimer levels are better predictors of overall survival and disease progression than carcinoembryonic antigen levels in patients with metastatic colorectal carcinoma. *Cancer* 2004; **101**: 77-82

13 **Hogdall CK,** Christensen IJ, Stephens RW, Sorensen S, Norgaard-Pedersen B, Nielsen HJ. Serum tetranectin is an independent prognostic marker in colorectal cancer and weakly correlated with plasma suPAR, plasma PAI-1 and serum CEA. *APMIS* 2002; **110**: 630-638

14 **Loktionov A,** Watson MA, Stebbings WS, Speakman CT, Bingham SA. Plasminogen activator inhibitor-1 gene polymorphism and colorectal cancer risk and prognosis. *Cancer Lett* 2003; **189**: 189-196

15 **Seetoo DQ,** Crowe PJ, Russell PJ, Yang JL. Quantitative expression of protein markers of plasminogen activation system in prognosis of colorectal cancer. *J Surg Oncol* 2003; **82**: 184-193

16 **Gil Bazo I,** Catalan Gonzalez V, Alonso Gutierrez A, Rodriguez Rodriguez J, Paramo Fernandez JA, de la Camara Gomez J, Hernandez-Lizoain JL, Garcia-Foncillas Lopez J. Impact of surgery and chemotherapy on von Willebrand factor and vascular endothelial growth factor levels in colorectal cancer. *Clin Transl Oncol* 2005; **7**: 150-155

17 **Gordon JL,** Pottinger BE, Woo P, Rosenbaum J, Black CM. Plasma von Willebrand factor in connective tissue disease. *Ann Rheum Dis* 1987; **46**: 491-492

18 **Kadir RA,** Economides DL, Sabin CA, Owens D, Lee CA. Variations in coagulation factors in women: effects of age, ethnicity, menstrual cycle and combined oral contraceptive. *Thromb Haemost* 1999; **82**: 1456-1461

19 **Lufkin EG,** Fass DN, O'Fallon WM, Bowie EJ. Increased von Willebrand factor in diabetes mellitus. *Metabolism* 1979; **28**: 63-66

20 **Pottinger BE,** Read RC, Paleolog EM, Higgins PG, Pearson JD. von Willebrand factor is an acute phase reactant in man. *Thromb Res* 1989; **53**: 387-394

21 **George ML,** Eccles SA, Tutton MG, Abulafi AM, Swift RI. Correlation of plasma and serum vascular endothelial growth factor levels with platelet count in colorectal cancer: clinical evidence of platelet scavenging? *Clin Cancer Res* 2000; **6**: 3147-3152

22 **Verheul HM,** Hoekman K, Luykx-de Bakker S, Eekman CA, Folman CC, Broxterman HJ, Pinedo HM. Platelet: transporter of vascular endothelial growth factor. *Clin Cancer Res* 1997; **3**: 2187-2190

23 **Verheul HM,** Pinedo HM. Tumor growth: A putative role for platelets? *Oncologist* 1998; **3**: 2

24 **Verheul HM,** Pinedo HM. The importance of platelet counts and their contents in cancer. *Clin Cancer Res* 2003; **9**: 3219-3221

25 **Werther K,** Christensen IJ, Nielsen HJ. Determination of vascular endothelial growth factor (VEGF) in circulating blood: significance of VEGF in various leucocytes and platelets. *Scand J Clin Lab Invest* 2002; **62**: 343-350

Science Editor Guo SY **Language Editor** Elsevier HK

PO Box 2345, Beijing 100023, China
www.wjgnet.com
wjg@wjgnet.com

ELSEVIER

World J Gastroenterol 2005;11(38):6074
World Journal of Gastroenterology ISSN 1007-9327

Acknowledgments to Reviewers of *World Journal of Gastroenterology*

Many reviewers have contributed their expertise and time to the peer review, a critical process to ensure the quality of *World Journal of Gastroenterology*. The editors and authors of the articles submitted to the journal are grateful to the following reviewers for evaluating the articles (including those were published and those were rejected in this issue) during the last editing period of time.

Trond Berg, Professor
Department of Molecular Biosciences, University of Oslo, PO Box 1041 Blindern, Oslo 0316, Norway

Bruno Clement, Professor
INSERM U-620, University of Rennes I, Faculty of Medicine, 2 ave. L. Bernard, Rennes 35043, France

Xue-Gong Fan, Professor
Xiangya Hospital, Changsha 410008, China

Edoardo G Giannini, Assistant Professor
Department of Internal Medicine, Gastroenterology Unit, Viale Benedetto XV, no. 6, Genoa, 16132, Italy

Hans Gregersen, Professor
The Research Administration, Aalborg Hospital, Hobrovej 42 A, Aalborg 9000, Denmark

Anna S Gukovskaya, Professor
Department of Medicine, UCLA, 11301 Wilshire Blvd, Los Angeles 91301, United States

Werner Hohenberger, Professor
Chirurgische Klinik und Poliklinik, Krankenhausstrasse 12, Erlangen D-91054, Germany

Masayoshi Ito, M.D.
Department of Endoscopy, Yotsuya Medical Cube, 5-5-27-701 Kitashinagawa, Shinagawa-ku, Tokyo 1410001, Japan

Hiroaki Itoh, M.D.
First Department of Internal Medicine, Akita University Scool of Medicine, 1-1-1, Hondou, Akita City 010-8543, Japan

Tsuneo Kitamura, Associate Professor
Department of Gastroenterology, Juntendo University Urayasu Hospital, Juntendo University School of Medicine, 2-1-1 Tomioka, Urayasu-shi, Chiba 279-0021, Japan

Zahariy Krastev, Professor
Department of Gastroneterology, Universiti Hospital "St. Ivan Rilski", #15, blvd "Acad. Ivan Geshov", Sofia 1431, Bulgaria

Shoji Kubo, M.D.
Hepato-Billiary-Pancreatic Surgery, Osaka City University Graduate School of Medicine, 1-4-3 Asahimachi, Abeno-ku, Osaka 545-8585, Japan

Fin Stolze Larsen, Associate Professor
Hepatology A-2121, Rigshospitalet Univ. Hospital of Copenhagen, Blegdamsvej 9, Copenhagen 2100, Denmark

James Neuberger, Professor
Liver Unit, Queen Elizabeth Hospital, Birmingham B15 2TH, United Kingdom

Mikio Nishioka, M.D.
Ehime Rosai Hospital, 13-27 Minami Komatsubara, Niihama 792-8550, Japan

Gustav Paumgartner, Professor
University of Munich, Klinikum Grosshadern, Marchioninistr. 15, Munich D-81377, Germany

Zhiheng Pei, Assistant Professor
Department of Pathology and Medicine, New York University School of Medicine, Department of Veterans Affairs, New York Harbor Healthcare System, 6001W, 423 East 23rd street, New York NY 10010, United States

Lun-Xiu Qin, Professor
Liver Cancer Institute and Zhongshan Hospital, Fudan University, 180 Feng Lin Road, Shanghai 200032, China

Manfred Stolte, Professor
Institute of Pathology, Klinikum Bayreuth, Preuschwitzer Str. 101, Bayreuth 95445, Germany

Michael Trauner, Professor
Medical University Graz, Auenbruggerplatz 15, Graz A-8036, Austria

Takato Ueno, Professor
Research Center for Innovative Cancer Therapy, Kurume University, 67 Asahi-machi, Kurume 830-0011, Japan

Toshio Watanabe, Associate Professor
Department of Gastroenterology, Osaka City University, Graduate School of Medicine, 1-4-3 Asahimachi, Abenoku-ku, Osaka 545-8585, Japan

Harry H-X Xia, M.D.
Department of Medicine, The University of Hong Kong, Pokfulam Road, Hong Kong, China